Seventh Edition

Peters' Atlas of TROPICAL MEDICINE AND PARASITOLOGY



Laura Nabarro
Stephen Morris-Jones
David A. J. Moore

ELSEVIER

Peters' Atlas of Tropical Medicine and Parasitology

Seventh Edition

Laura Nabarro MBBS BSc MRCP FRCPath DTM&H
Specialist Registrar in Infectious Diseases and Microbiology
Hospital for Tropical Diseases, University College London Hospitals NHS Foundation Trust
London, UK

Stephen Morris-Jones MA MBBS MSc MRCP FRCPath DTM&H
Consultant in Clinical Microbiology and Infectious Diseases
University College London Hospitals NHS Foundation Trust
London, UK

David A.J. Moore MBChB MRCP MD MSc DTM&H
Professor of Infectious Diseases and Tropical Medicine
Hospital for Tropical Diseases,
University College London Hospitals NHS Foundation Trust
and
Department of Clinical Research
London School of Hygiene and Tropical Medicine
London, UK

ELSEVIER

Downloaded From Vet-eBooks.com

ELSEVIER

© 2019, Elsevier Limited. All rights reserved.

First edition 1977
Second edition 1981
Third edition 1989
Fourth edition 1995
Fifth edition 2001
Sixth edition 2007

The right of Laura Nabarro, Stephen Morris-Jones and David A.J. Moore to be identified as authors of this work has been asserted by them in accordance with the Copyright, Designs and Patents Act 1988.

No part of this publication may be reproduced or transmitted in any form or by any means, electronic or mechanical, including photocopying, recording, or any information storage and retrieval system, without permission in writing from the publisher. Details on how to seek permission, further information about the Publisher's permissions policies and our arrangements with organizations such as the Copyright Clearance Center and the Copyright Licensing Agency, can be found at our website: www.elsevier.com/permissions.

This book and the individual contributions contained in it are protected under copyright by the Publisher (other than as may be noted herein).

Notices

Practitioners and researchers must always rely on their own experience and knowledge in evaluating and using any information, methods, compounds or experiments described herein. Because of rapid advances in the medical sciences, in particular, independent verification of diagnoses and drug dosages should be made. To the fullest extent of the law, no responsibility is assumed by Elsevier, authors, editors or contributors for any injury and/or damage to persons or property as a matter of products liability, negligence or otherwise, or from any use or operation of any methods, products, instructions, or ideas contained in the material herein.

ISBN: 978-0-7020-4061-0
E-ISBN: 978-0-7020-5040-4

Content Strategists: **Belinda Kuhn, Charlotta Kryhl**
Content Development Specialist: **Joanne Scott**
Project Manager: **Beula Christopher**
Design: **Christian Bilbow**
Illustration Manager: **Karen Giacomucci**
Illustrators: **Oxford Illustrators, Wendy B. Jackelow, Jade Myers**
Marketing Manager: **Michele Milano**

Printed in the United Kingdom

Last digit is the print number: 9 8 7 6 5 4 3 2 1

ELSEVIER Book Aid International Working together to grow libraries in developing countries
www.elsevier.com • www.bookaid.org

Downloaded From Vet-eBooks.com

Dedication

This book is dedicated to the patients, past, present and future, whose suffering still makes this book relevant; to the clinicians, whose commitment to diagnose and manage these conditions to the best of their abilities and resources provides the purpose for the book; and to the readers, whose interest defines the book.

Downloaded From Vet-eBooks.com

Foreword

Whereas the opening of extensive colonisation towards the end of the18th century gave rise to the birth of 'tropical medicine', the ensuing outbreaks of disastrous wars that followed spawned an international blossoming of this discipline in a succession of newly opened areas of the tropics and subtropics. The rapidly increasing volume of medical and scientific literature that described the multitude of previously unfamiliar diseases that were encountered was gradually assembled in various languages in the form of textbooks. One of the oldest of these was *Manson's Tropical Diseases – A manual of the diseases of warm climates*, the 1st edition of which was published in May 1898 and contained very few illustrations. The 23rd edition, which appeared in 2013, includes a number of important illustrations; however, the majority of these are in black and white.

The original version of the *Atlas of tropical medicine and parasitology* saw the light of day in 1977 as one of a large series of colour atlases on medical topics that were produced from 1969 onwards by a foresighted publisher named Peter Wolfe, under the general medical editorship of G. Barry Caruthers. It is curious to reflect that, up to that period, in the light of the evident value of high-quality illustrations in medical books of any kind, very few such books were available. *Wolfe publishers* was by then a small London-based company that had produced a modest number of books on a wide variety of popular topics, such as one describing wine production for the home (a copy of which I have made good use of). The first of the medical series, a work on haematological cytology that appeared originally in 1969, was succeeded by a stream of atlases on other topics. Before long, new editions were produced by Wolfe and other publishers, the greatest success proving to be one on human anatomy by Robert McMinn and Ralph Hutchings of which several million copies had been published in some 30 languages by the time of McMinn's death in 2014.

In the late 1960s *Wolfe Medical Publications* approached the Liverpool School of Tropical Medicine to seek the collaboration of the late Brian Maegraith, who was at that time the Dean, in the development of an Atlas of Tropical Medicine. Brian (author of a seminal 1963 *Lancet* paper entitled *Unde venis*) recommended that the task should go to my colleague Herbert M. Gilles, then one of his most senior staff who, in turn, sought my collaboration as his co-author. During the early 1970s Herbert and I devoted our efforts to this task. He constructed the overall framework and content of the manuscript and I assembled the majority of the 763 figures and 15 tables. Following the success of our original *Atlas* in 1977, a further three editions had appeared by 1995, some of which also appeared as French, Spanish, Italian and Indonesian translations. A special cheap, unadorned, English-language version of the 3rd edition for readers in developing countries was published in 1985 with the support of the English Language Book Society funded by the British government. Later that year after the 4th edition was completed, Herbert retired from his role. Geoffrey Pasvol of Imperial College London joined me as co-author for the 5th edition, which was also translated into French and Mandarin, as well as the 6th edition, which also appeared in a Spanish version. When the need for a 7th edition was evident, I decided that the moment was ripe for

Downloaded From Vet-eBooks.com

me to pass on the baton to Geoffrey who, having devoted much time to his new task, unfortunately was obliged, in his turn, to retire. All three of us, Herbert, Geoffrey and I are delighted that the current publishers, Elsevier, have been able to pass this latest edition into the hands of David Moore, Laura Nabarro and Stephen Morris-Jones of the London School of Hygiene and Tropical Medicine and the Hospital for Tropical Diseases in London.

The invitation to write a Foreword to this work caused me to reflect on the major changes in the fields of tropical medicine and parasitology that have emerged since we worked on the original edition, ie, the late 1960s and early 1970s, a period of a little less than 50 years that seemed to pass like the wind. With the wisdom of hindsight, it is clear that major changes, some imposed by nature, others created by man, are inducing radical changes in our environment that, in their wake, are responsible for significant modifications in the global patterns of human and animal health, and disease. It is particularly important that those of us whose interests are focussed on the conditions with which this atlas deals, bear such changes in mind since they impinge radically on the problems included in *Tropical medicine and parasitology*. Global warming, human conflict, ever-expanding international travel (see *Frontispiece* of 5th edition), population size management and the use and misuse of potent therapeutic agents are among the areas that pose some of our greatest challenges.

In addition, we have been faced during the past 50 years with the appearance and global spread of HIV, the threat of dissemination from the Far East of a viral disease SARS (severe acute respiratory syndrome) caused by an enzootic corona virus and, more recently, another enzootic corona virus causing MERS-CoV (Middle East respiratory syndrome). A massive increase in global travel and (in the latter case) short-term but large-scale human assemblies, such as the Haj, which is followed by the return of the pilgrims to a global network of their home countries, present a constant challenge. In other areas, religious beliefs on the origin of locally endemic diseases, some of which are a potential threat on a much wider scale, can seriously impede efforts to overcome them using the currently available tools, such as the administration of vaccines.

On the positive side, the past half century in particular has seen formerly unimaginable advances in biotechnology, a number of which have already enabled us to make serious reductions in the burden imposed by such conditions as malaria, leishmaniasis and dracunculiasis. Molecular biologists and immunologists have opened up dramatic possibilities for the diagnosis and prevention of an increasing range of infections such as malaria that have consistently threatened the populations of a large proportion of the tropics and subtropics, as well as being a constant threat to international travellers.

Advances in the development of invaluable and novel drugs have, however, been offset by the emergence of drug resistance through their gross misuse and especially by the reluctance to deploy rationally selected drug combinations. This has been particularly evident in the field of malaria prevention and control, yet it is still grossly ignored. As I write, an encouraging example of how currently available technical and logistic problems can be resolved is the manner and relative rapidity with which another recently extended viral infection, namely haemorrhagic Ebola fever in tropical Africa, can be held at bay by the application of internationally funded collaboration in the laboratory and on the ground. This deadly infection was not recognised until 1976, just too late for its inclusion in the 1st edition of this *Atlas* in 1977, but it was well documented in the 2nd edition that appeared in 1981.

Wallace Peters
Emeritus Professor of Medical Protozoology
Faculty of Infectious and Tropical Diseases
London School of Hygiene and Tropical Medicine

Downloaded From Vet-eBooks.com

Preface

For the 7th Edition of the *Atlas* we have introduced several hundred new images, updated and significantly streamlined text, revised life cycles and epidemiological maps, and tweaked the chapter themes.

The organisation of earlier editions of the book based upon the primary mode of disease transmission has been extended to define disease more strictly according to the route of acquisition; thus, for example, conditions are grouped separately that are vector-borne or percutaneously acquired, inhaled or ingested. Though we settled on this structure after consideration of a range of alternatives, there remain instances when this works less well – the disadvantage of bringing relevant opportunistic infections into the same chapter as HIV is that some of them are not acquired by the same percutaneous route. On balance, however, we think this approach is the most logical and reflects the principles applied to control measures for most infections, so we hope the reader shares our view and enjoys the depth and diversity of this book. We have all fondly enjoyed previous editions of the *Atlas* and are sincerely grateful to 'Pete' and to Geoff Pasvol for entrusting this much-loved work to us. We really hope that we have done justice to this next incarnation.

David Hill, Nick Beeching and Sebastian Lucas are thanked for their early work towards this edition.

Laura Nabarro
Stephen Morris-Jones
David A.J. Moore
London 2018

Downloaded From Vet-eBooks.com

1. Arthropod-Borne Diseases

Arthropods can transmit viruses, bacteria and parasites. To date, there is no known arthropod-borne fungal infection.

Mosquitoes transmit more disease, and a greater variety of disease, than any other arthropod. However, other biting flies, fleas, ticks, lice and mites are also responsible for transmission of some infections. Most of these infections are zoonotic; animal and human hosts may exhibit disparate behaviour and inhabit differing environments, thus the arthropod vector is essential at bridging the ecological gap between the two. Arthropod-borne animal infections may adapt to transmit to humans and directly from human to human, making arthropods important contributors to the emergence of some infectious diseases.

Some mosquito species, such as *Aedes (Stegomyia) aegypti*, are increasingly cosmopolitan and are found throughout the tropical world. The ability of *Ae. (Stg.) aegypti* to breed in dirty urban water containers has resulted in large outbreaks of dengue in tropical metropolises. Rapid airline transport of mosquitoes or infective human hosts may result in large outbreaks of disease in areas previously free of infection but with competent arthropod vectors. South America has been afflicted by this twice in the last 5 years; chikungunya arrived in 2013 and Zika virus in 2015.

Some pathogens, particularly parasites, are dependent upon arthropod host physiology to complete their life cycle. Most pathogens can multiply within the arthropod vector and some, particularly viruses, may mutate to more virulent or transmissible forms of disease. A single nucleotide polymorphism in Venezuelan equine encephalitis virus increased its infectivity to *Culex*, resulting in an outbreak of disease in Mexico in 1996.

With the exception of Japanese encephalitis and yellow fever, there are few effective vaccines for arthropod-borne diseases. At the community level, prevention relies upon vector control through environmental management and chemical agents. In recent years, there has been increasing insecticide resistance worldwide, threatening control programmes. There is also increasing resistance to essential drugs used to treat these diseases, such as artemisinin which is used to treat malaria.

This chapter is divided into four sections. The first describes the main mosquito vectors of infection and the following three sections describe arthropod-borne viral, bacterial and parasitic infections.

MOSQUITO VECTORS

The main characteristics of the principal mosquito vectors of infection are presented in the following figures.

Downloaded From Vet-eBooks.com

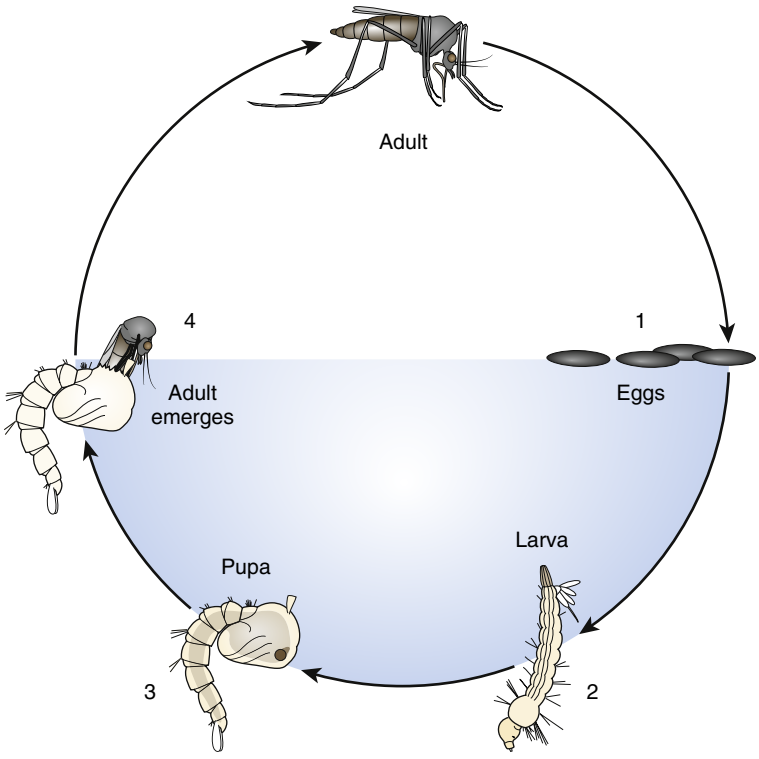


Fig. 1.01 Mosquito life cycle.
The adult female mosquito lays her eggs on water (1). Eggs hatch into larvae (2) which feed on micro-organisms and organic matter under water. After several days and skin sheds they transform into comma-shaped pupae (3) from which the adult mosquito emerges (4).



Fig. 1.02 Female *Anopheles gambiae* probing.
Anopheles mosquitoes transmit malaria but can also transmit lymphatic filariasis and o'nyong'nyong virus. In their resting position, the abdomen points upwards in line with their head and thorax.



Fig. 1.03 *Aedes (Stegomyia) aegypti* taking a blood meal.
Aedes and *Culex* are both members of the *Culicinae* subfamily. The adult's body lies parallel to the surface on which it stands, or points slightly downwards. *Ae. (Stg.) aegypti* is the principal vector of dengue, chikungunya, yellow fever and Zika viruses. Note the lyre-shaped markings on the dorsal thorax and the white bands on the legs. (From The United States Centers for Disease Control and Prevention (CDC) Public Health Image Library (PHIL), PHIL ID# 9253, Professor Frank Hadley Collins, Director, Center for Global Health and Infectious Diseases, University of Notre Dame. Photographer: James Gathany, Biomedical Photographer, CDC.)

Downloaded From Vet-eBooks.com



Fig. 1.04 *Aedes (Stegomyia) albopictus* taking a blood meal.
Ae. (Stg.) albopictus also has white bands on its legs but can be distinguished from *Ae. (Stg.) aegypti* by a longitudinal white line on its thorax. (From The United States Centers for Disease Control and Prevention (CDC) Public Health Image Library (PHIL), PHIL ID# 1864, Professor Frank Hadley Collins, Director, Center for Global Health and Infectious Diseases, University of Notre Dame. Photographer: James Gathany, Biomedical Photographer, CDC.)

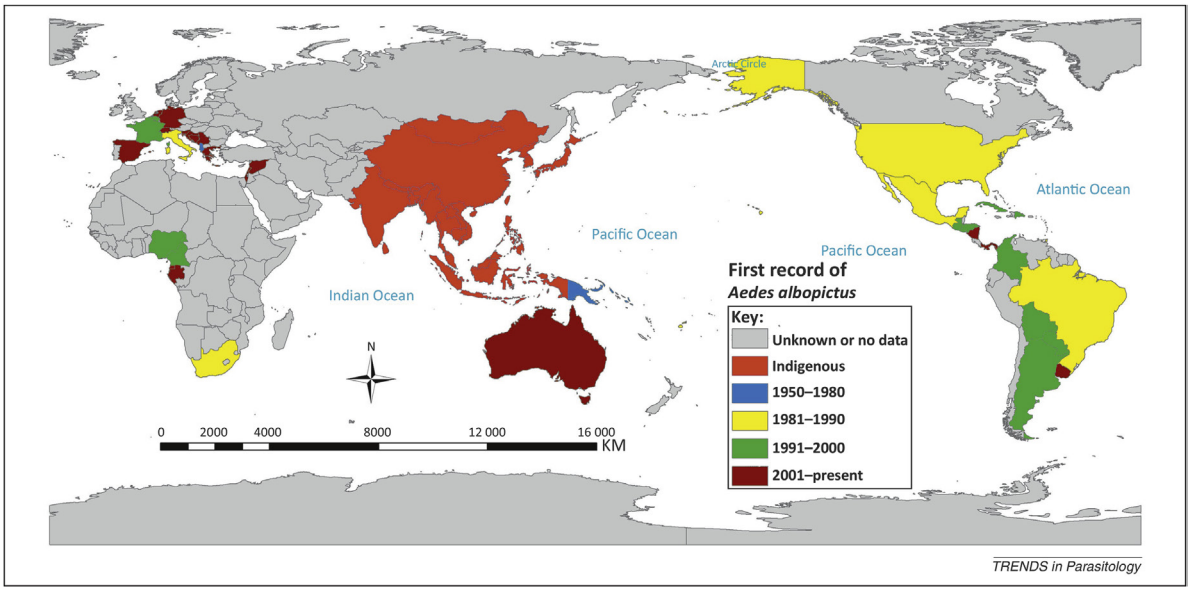


Fig. 1.05 The expanding geographical range of *Aedes (Stegomyia) albopictus*.
This figure shows the expansion of *Ae. (Stg.) albopictus* from its native range over the last 30 years. International trade in used tyres and plants has assisted its dispersal. It exhibits opportunistic feeding and breeding behaviour, can survive in temperate climates and can competently transmit multiple pathogens including dengue and chikungunya. It was responsible for the first autochthonous transmission of dengue in Europe in 2010. (From Bonizzoni M, Gasperi G, Chen X et al. The invasive mosquito species *Aedes albopictus*: current knowledge and future perspectives. Trends in Parasitology, 2013-09-01, Volume 29, Issue 9, Pages 460–468, Figure 2.)



Fig. 1.06 Feeding *Culex pipiens*.
This common culicine, which is one of the most widely distributed in the world, will feed on both human and avian blood. Some subspecies (e.g. *Cx. pipiens molestus*) breed in peridomestic collections of polluted water even in total darkness, as well as in cleaner, open sites. (From Reiter N, Reiter M, Altrichter S, et al. Anaphylaxis caused by mosquito allergy in systemic mastocytosis. The Lancet, 2013-10-19, Volume 382, Issue 9901, Pages 1380–1380.)

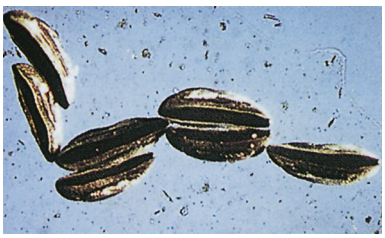


Fig. 1.07 *Anopheles* eggs.
Anopheles spp. eggs have lateral floats and aggregate on the water into 'Chinese figure' patterns.

Downloaded From Vet-eBooks.com

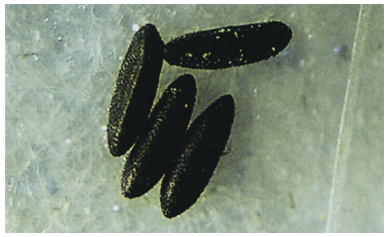


Fig. 1.08 *Aedes (Stegomyia)* eggs.
Aedes (*Stg.*) spp. eggs are laid singly on the water surface and are resistant to desiccation.

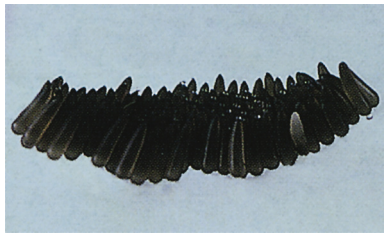


Fig. 1.09 *Culex* eggs.
Culex spp. eggs are laid on the water surface in rafts and cannot withstand desiccation.



Fig. 1.10 Third-stage larva of *Anopheles* spp.
Anopheles spp. larvae lie parallel to the water surface. They breathe through spiracles found on abdominal segments.



Fig. 1.11 Third-stage larvae of *Culex quinquefasciatus* and *Aedes (Stegomyia) aegypti*.
In contrast to anopheline larvae, the larvae of *Culex* spp. and *Aedes* (*Stg.*) spp. lie perpendicular to the water surface, suspended by a siphon which acts as a breathing tube. *Aedes (Stg.)* spp. (right) have a short siphon and a single hair tuft. *Culex* spp. (left) have a longer siphon and several tufts of lateral siphon hairs. (Courtesy, L. Oke.)



Fig. 1.12 Pupae of *Anopheles* spp.
The comma-shaped pupae of all three species are similar. They obtain air through siphons on the cephalothorax.

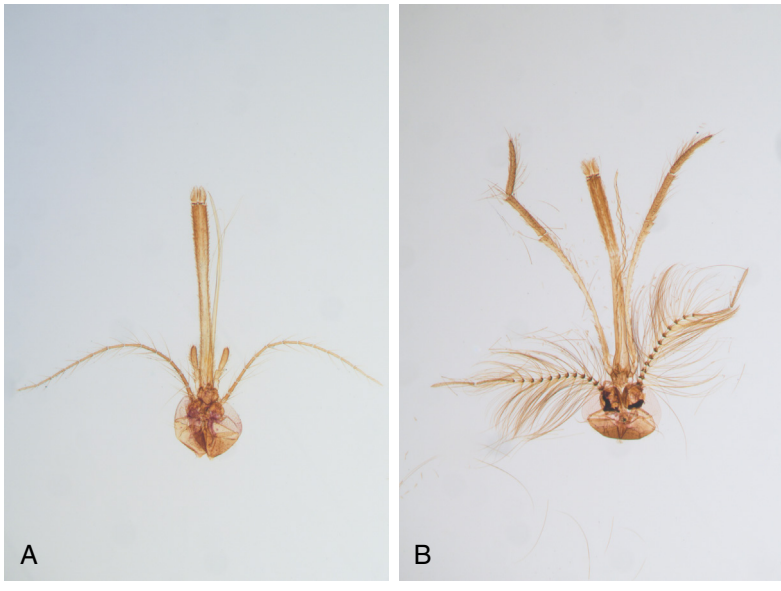


Fig. 1.13 Heads of adult culicine mosquitoes.
Anopheline and culicine mosquitoes can be distinguished and sexed by the shape of their antennae and palps. Female culicines have short palps, less than one-quarter the length of the proboscis (A), whilst males have long, pointed palps, which are usually quite hairy (B). The antennae of the male are also much more hairy than those of the female. Compare these with the heads of the anopheline mosquitoes in 1.14. (Courtesy, S. McIntyre.)

Downloaded From Vet-eBooks.com



Fig. 1.14 Heads of adult *Anopheles* mosquitoes.
Female *Anopheles* mosquitoes have palps that are the same length as their proboscis (A). Male *Anopheles* have club-shaped palps (B). Once again, the antennae of the male are much more hairy than those of the female. Compare these with the heads of the culicine mosquitoes in 1.13. (Courtesy, S. McIntyre.)

THE ARBOVIRUSES: ARTHROPOD-BORNE VIRAL INFECTIONS

The arboviruses are a diverse group of viral infections spread by arthropods. Following a blood meal from an infected vertebrate host, the virus multiplies within the arthropod, before being transmitted to a vertebrate host.

Most arboviruses are zoonotic; the exceptions are dengue and o'nyong'nyong where humans are the primary vertebrate host. Mosquitoes are the most common vectors, but ticks and sandflies are also implicated in the transmission of some viruses. The global distribution of some mosquito vectors and the rapidity of international travel has allowed certain viruses to become endemic in areas previously free of disease following movement of viraemic hosts or mosquitoes. Gene mutation may also have an effect on transmission; chikungunya moved rapidly through Asia following a single amino acid change in its envelope protein, which greatly increased transmissibility by a secondary mosquito vector, *Aedes (Stegomyia) albopictus*.

Although arboviruses cause a wide range of clinical symptoms, it is conceptually simpler to consider them in syndromic groups. Some, such as dengue and chikungunya virus, cause a fever, arthralgia and rash syndrome. Others, such as West Nile virus and St Louis encephalitis virus, cause an encephalitic syndrome. Viruses such as Crimean-Congo haemorrhagic fever and yellow fever may cause a haemorrhagic syndrome. There is some overlap between these syndromic groups; West Nile virus causes fever, arthralgia and rash in mild infection and encephalitis in severe infection. Table 1.1 summarises current arboviruses of clinical significance, updated to December 2016.

Downloaded from Vet-eBooks.com

Table 1.1 Arboviruses of clinical significance, updated to December 2016

Virus or disease	Main vector(s)	Main reservoirs/ amplifying hosts	Geographical distribution	Clinical syndrome
Family: Togaviridae				
Genus: Alphavirus				
Chikungunya	Aedes	Monkeys, ? rodents	Africa, Asia, South America	FAR
Mayaro	Aedes, Anopheles	Wild vertebrates	South America	FAR
O'nyong'nyong	Anopheles	Humans	Africa	FAR
Ross River	Aedes	? Wallabies	Australia	FAR
Sindbis	Culex	Birds	Africa, Asia, Australia, Europe	FAR
Venezuelan equine encephalitis	Aedes, Culex	Rodents/horses	North/South America	Encephalitis
Western equine encephalitis	Culex	Birds/horses	North/South America	Encephalitis
Eastern equine encephalitis	Culiseta	Birds/horses	North/South America	Encephalitis
Family: Flaviviridae				
Genus: Flavivirus				
Dengue 1, 2, 3, 4	Aedes	Aedes/humans	Worldwide tropics	FAR
Zika	Aedes	Humans/ non human primates	Africa, South America, Asia, Pacific	FAR, congenital syndrome
Kunjin	Culex	Birds	Australia, Indonesia	FAR/encephalitis
Japanese encephalitis	Culex	Birds/pigs	East Asia/Australasia	Encephalitis
Murray Valley encephalitis	Culex	Birds	Australia	Encephalitis
Rocio	Culex	Birds	Brazil	Encephalitis
St Louis encephalitis	Culex	Mosquitoes, birds	North/South America	Encephalitis
West Nile	Culex	Birds, bats, horses,	Africa, Europe, North America, Middle East	Encephalitis
Louping ill	Ixodidae	Rodents, birds	UK	Encephalitis
Powassan	Ixodidae	Rodents	North America	Encephalitis
Tick-borne encephalitis	Ixodidae	Small mammals/ ruminants	Europe	Encephalitis
Russian spring-summer encephalitis	Ixodidae	Rodents, birds	Russia	Encephalitis
Kyasanur forest disease	Ixodidae	Forest rodents/monkeys	India	Haemorrhagic
Omsk haemorrhagic fever	Ixodidae	Ticks, rodents	Russia	Haemorrhagic
Yellow fever	Aedes Haemagogus	Mosquitoes/monkeys	South America, Africa	Haemorrhagic
Family: Reoviridae				
Genus: Coltiviridae				
Colorado tick fever	Ixodidae	Rodents	North America	FAR/encephalitis/ haemorrhagic

Downloaded From Vet-eBooks.com

Table 1.1 Arboviruses of clinical significance, updated to december 2016—cont'd				
Family: Bunyaviridae				
Genus: Nairovirus				
Crimean-Congo haemorrhagic fever	Ixodidae	Ticks, sheep, goats, cattle, rodents, birds	Parts of Africa, Asia, Europe, Middle East,	Haemorrhagic
Genus: Bunyavirus				
California encephalitis group	Aedes	Rabbits, rodents	North America	Encephalitis
La Crosse	Aedes	Chipmunks, squirrels	North America	Encephalitis
Oropouche	Culicoides	Monkeys, sloths	South America	FAR, encephalitis
Genus: Phlebovirus				
Rift Valley fever	Anopheles, Aedes, Culex	Cattle, sheep, goats	Africa, Middle East	Fever, encephalitis, haemorrhagic
Sandfly fever (Naples, Sicily)	Phlebotomus	Unknown	Africa, Asia, Europe	FAR
Sandfly fever (Toscana)	Phlebotomus	Unknown	Countries bordering Mediterranean Sea	FAR, encephalitis

FAR: fever, arthralgia, rash syndrome

Dengue

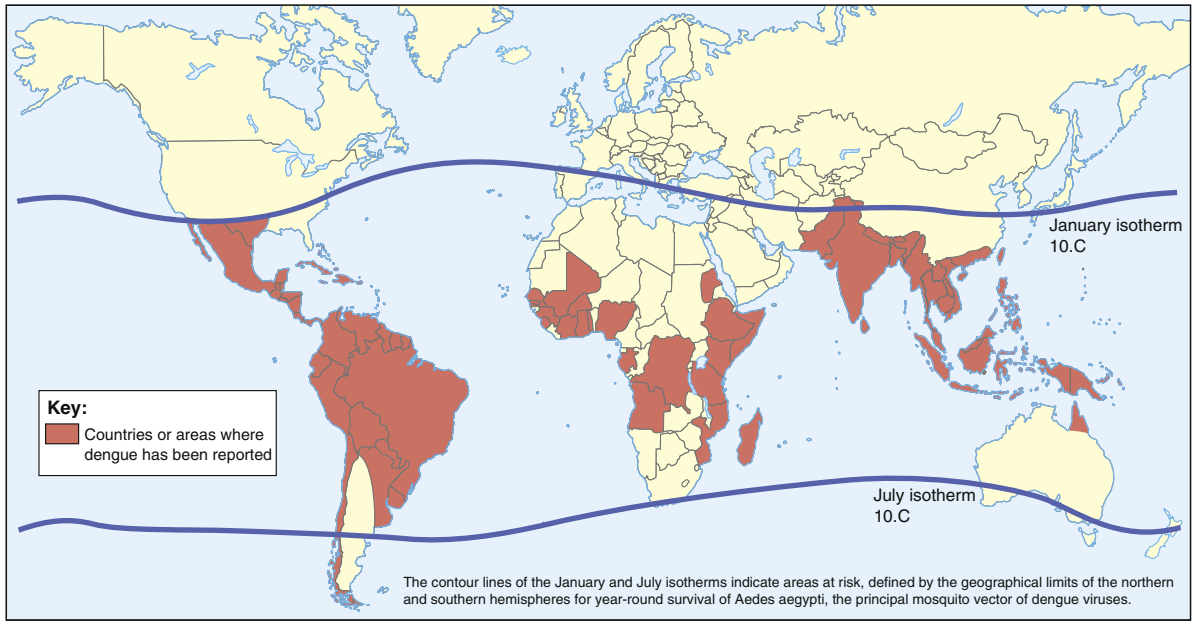
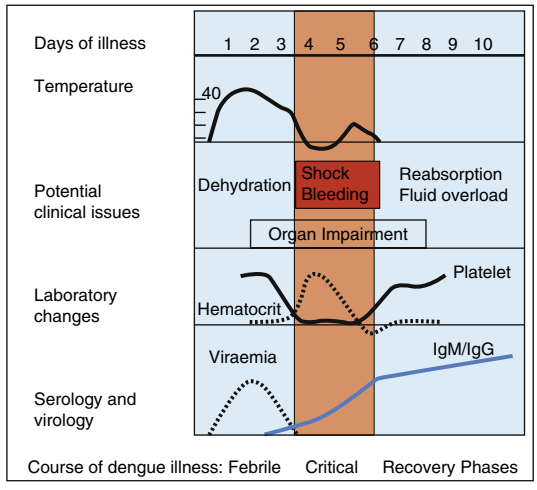


Fig. 1.15 Worldwide distribution of dengue.
In recent years, both the incidence and geographical range of dengue has increased. As of 2015, there are 3.9 billion people in 128 countries worldwide at risk of infection with an estimated 390 million infections each year. Climate change, overcrowding and haphazard urban growth have fuelled this, resulting in large parts of the tropics where dengue is hyperendemic with continuous circulation of multiple dengue serotypes. Airplane travel, allowing rapid transport of viraemic people, has made dengue a common imported infection in areas previously free of the disease and triggered local outbreaks with autochthonous transmission in Europe and the United States. (Courtesy, WHO.)

Downloaded From Vet-eBooks.com



Fig. 1.16 Breeding site of *Aedes (Stegomyia) aegypti* in a Thai cemetery.
Ae. (Stg.) aegypti is the principal vector of dengue and thrives in urban areas by breeding in man-made containers. Numerous *Ae. (Stg.) aegypti* larvae were found in the flowerpots decorating this altar in a Thai cemetery during a dengue outbreak.



IgM = immunoglobulin M; IgG = immunoglobulin G. Temperature is given in degrees Celsius (°C)

Fig. 1.17 Clinical course of dengue infection.
After the initial febrile stage, most patients will improve. Patients with increased plasma leak will enter the critical phase and can then become severely unwell. Warning signs include abdominal pain, persistent vomiting, peripheral oedema, hepatomegaly and mucosal bleeding. A rising haematocrit with falling platelet count is a sinister sign that precedes onset of shock, organ failure and haemorrhage. Rapid restoration of plasma volume is essential, and case fatality may be as high as 15% in the absence of optimal medical management. (From WHO Handbook for clinical management of dengue.)

Downloaded From Vet-eBooks.com



Fig. 1.18 Typical dengue rash.
Dengue typically presents with fever, headache and retro-orbital pain. Severe muscle and joint pain is common leading to the colloquial name of 'break-bone fever'. The classic blanching rash pictured here usually occurs on day 2 to 5 of illness. (Courtesy, Professor D. A. J. Moore.)



Fig. 1.19 Confluent rash with islands of sparing.
The confluent erythematous rash with pale areas is sometimes described as 'white islands in a red sea'. (Courtesy, Dr S. Yacoub.)

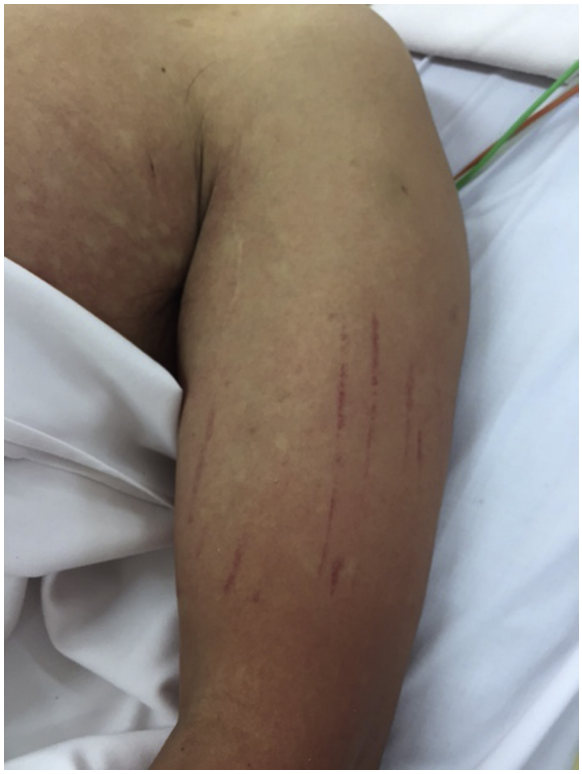


Fig. 1.20 Linear petechiae in a patient with dengue.
Note the linear petechiae seen here, caused by a combination of low platelets and capillary fragility. (Courtesy, Dr S. Yacoub.)



Fig. 1.21 Subcutaneous haemorrhage in dengue haemorrhagic fever.
This Thai patient had a large haemorrhagic lesion on his upper arm. (Courtesy, Wellcome Trust and WHO.)

Downloaded from Vet-eBooks.com



Fig. 1.22 Intracranial haemorrhage in severe dengue.
This patient with severe dengue, low platelets and abnormal clotting developed a left basal ganglia bleed with intraventricular extension. There was no preceding trauma. He later died of this complication. (From Kumar, R., Prakash, O., Sharma, B. Intracranial hemorrhage in dengue fever: management and outcome. Surgical Neurology, 2009-10-01, Volume 72, Issue 4, Pages 429–433, Figure 1. Copyright © 2009 Elsevier Inc.)

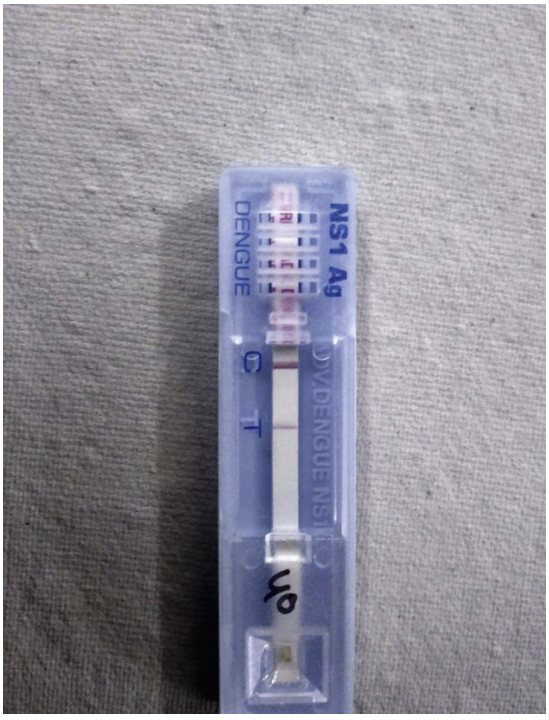


Fig. 1.23 Dengue point-of-care test.
Point-of-care tests targeting the NS1 antigen are increasingly used in diagnosis and are usually positive for the first 5 days of clinical illness. They are easy to use, require little laboratory expertise and have high positive predictive values.



Fig. 1.24 Guppy fish used for vector control in South East Asia.
In areas with high levels of dengue transmission the local environment needs to be carefully managed to reduce mosquito breeding sites. The introduction of larvivorous guppy fish (*Poecilia reticulata*) into freshwater wells and irrigation ditches has proved successful in some areas but is reliant on community participation and adequate organization to distribute the fish effectively.

Downloaded from Vet-eBooks.com

Yellow Fever



Fig. 1.25 The distribution of yellow fever.
Yellow fever is found in tropical areas of sub-Saharan Africa and South America. Ninety per cent of infections occur in the former region with an estimated 130,000 cases and 78,000 deaths in 2013. There have been no autochthonous cases in Asia, despite the presence of *Aedes (Stegomyia) aegypti* and extensive travel between the two continents. The reason for this is unclear but may be due to cross-protection afforded by previous infection with other flaviviruses such as dengue or Japanese encephalitis or reduced vector competency of Asian *Ae. (Stg.) aegypti* compared with its African counterpart. However, Asia is still at risk of a large yellow fever outbreak as highlighted by the repatriation of 11 viraemic workers to mainland China during the Angolan yellow fever outbreak of 2016. (From International Travel and Health. Geneva: WHO; 2009:96, with permission.)

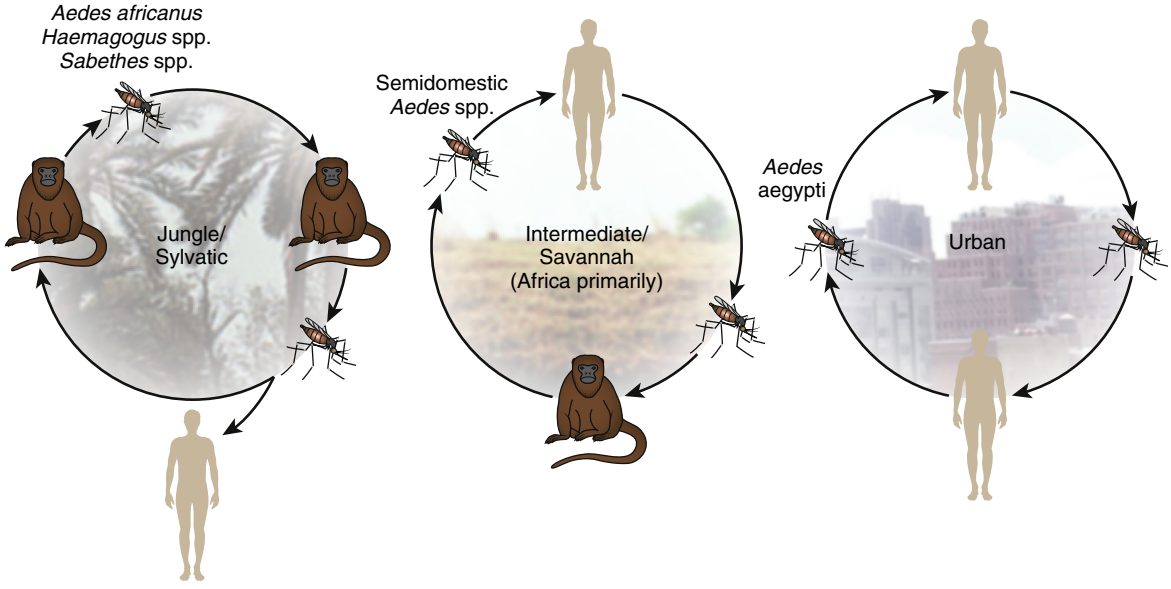


Fig. 1.26 Transmission cycles of yellow fever.
Yellow fever exists in three inter-related transmission cycles. In the sylvatic (jungle) cycle, yellow fever is passed between monkeys by mosquito vectors. Sporadic human infections occur in people living or working in forested areas. An intermediate cycle occurs, primarily in Africa, where semi-domestic mosquitoes feed on both humans and monkeys in areas of rural savannah. Infection is passed between the two, resulting in small outbreaks. Explosive epidemics occur when viraemic individuals introduce the virus into densely populated areas with low vaccine coverage. *Ae. (Stg.) aegypti* becomes the dominant mosquito vector and is able to rapidly transmit virus from person to person (urban transmission cycle). In South America, most cases are sporadic and result from the sylvatic cycle. In Africa, there are frequent urban epidemics such as that experienced in Angola and the Democratic Republic of Congo in 2016.

Downloaded From Vet-eBooks.com

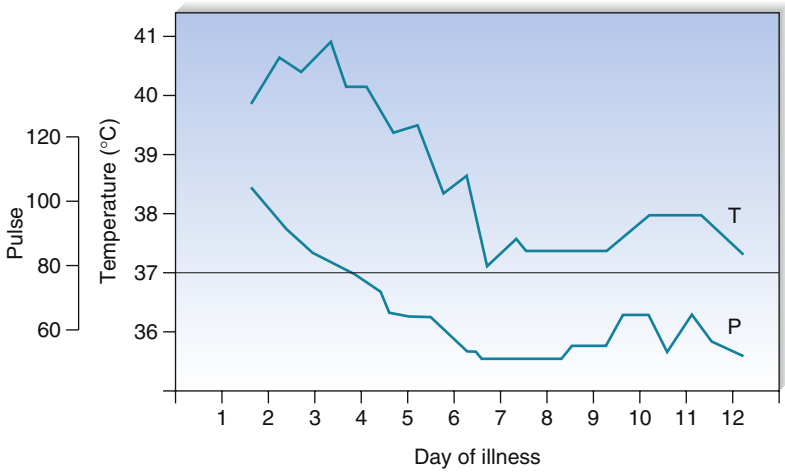


Fig. 1.27 Temperature chart of a patient with yellow fever.
Initially, yellow fever presents as an acute febrile illness with non-specific symptoms including malaise, headache, anorexia, lumbosacral and lower limb pain. Physical examination is often unremarkable but conjunctivitis, hepatomegaly and epigastric tenderness may be present. The often-cited Faget's sign—relative bradycardia in a febrile patient—may occur, but it is not specific to yellow fever and may also be a feature of enteric fever and brucellosis.



Fig. 1.28 Upper gastrointestinal bleeding in the terminal phase of yellow fever.
Following the initial febrile period, most patients recover. Around 15% enter a period of intoxication with fever, vomiting, jaundice and prostration. Liver failure, renal failure and haemorrhage ensue, with death in 20% to 50% of patients. This Costa Rican patient with severe jaundice had coffee ground vomiting just before he died. (Courtesy, Dr H. Lieske.)

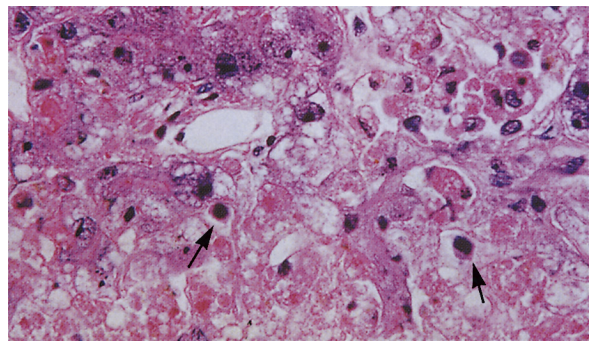


Fig. 1.29 Section of liver from a fatal case of yellow fever.
Viral antigen localizes in the midzone of the liver causing necrosis which spares cells bordering the central vein and portal tract. Eosinophilic intranuclear inclusions, known as Councilman bodies (arrowed), are a characteristic histological feature. In patients who survive the acute infection, the liver usually recovers completely with no post necrotic fibrosis (Giemsa x 800) (AFIP No.71-1981). (Courtesy, The Director, Armed Forces Institute of Pathology, Washington, DC.)



Fig. 1.30 Angolan child vaccinated during the 2016 yellow fever outbreak.
Despite the existence of a single-dose vaccine which confers lifelong protection against infection, many people living in areas at risk of yellow fever are not vaccinated. Shortages in vaccine during the Angolan outbreak in 2016 led to fractional dosing of vaccine (at one-fifth the standard dose) to maximize the number of people vaccinated. (From Green, A. Yellow fever continues to spread in Angola. The Lancet, Volume 387, Issue 10037, Pages 2493–2493. Copyright © 2016 Elsevier Ltd.)

Downloaded from Vet-eBooks.com

Chikungunya and Other Alphaviruses



Fig. 1.31 Acute arthritis of the interphalangeal joints in a patient with chikungunya.
Chikungunya causes a febrile illness often accompanied by rash and a symmetrical distal arthralgia. The unusual name derives from the Makonde language of Tanzania, meaning 'that which bends up'. Joint symptoms may persist after acute infection, resulting in persistent arthralgia and arthritis. It is unclear whether this is due to viral persistence or an immune phenomenon. (From Khasnis, A. A., Schoen, R. T. Calabrese, L. H. Emerging viral infections in rheumatic diseases. Seminars in Arthritis and Rheumatism, 2011-10-01, Volume 41, Issue 2, Pages 236–246. Copyright © 2011 Elsevier Inc.)



Fig. 1.32 Eastern grey kangaroos, vertebrate host of Ross River virus.
Ross River virus causes a similar clinical syndrome to chikungunya in Australia, Papua New Guinea and the Pacific. Native macropods, including this eastern grey kangaroo, are the vertebrate hosts. Other alpha viruses including o'nyong'nyong in East Africa and Mayaro in South America cause a similar clinical syndrome. (Courtesy, L. Halsey.)

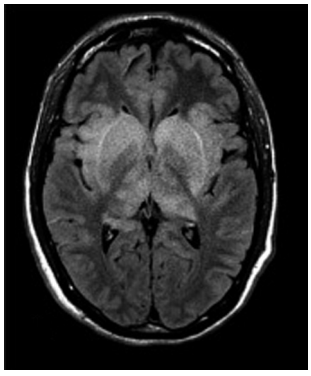


Fig. 1.33 MRI changes in a fatal case of eastern equine encephalitis.
With the exception of Mayaro and chikungunya, alphaviruses found in the Americas tend to cause encephalitic syndromes. Eastern equine encephalitis occurs on the eastern coast of the United States, through Central America and southwards into Brazil and Argentina. It is maintained in a bird-mosquito cycle with incidental infection in horses and humans. It is rapidly fatal in horses and is the most severe of the arboviral encephalitides in humans with an encephalitic rate of 5% and, in those, a mortality rate of 30–50%. This middle-aged man developed an acute encephalitis and died within a week. Note the increased T2 flair signal in the thalami, the basal ganglia and the midbrain. Western equine encephalitis and Venezuelan equine encephalitis cause similar but less severe clinical syndromes. (From Nickerson, J. P. MRI findings in eastern equine encephalitis: the "parenthesis" sign. Clinical Imaging, 2016-03-01, Volume 40, Issue 2, Pages 222–223, Figure 2.)

Zika

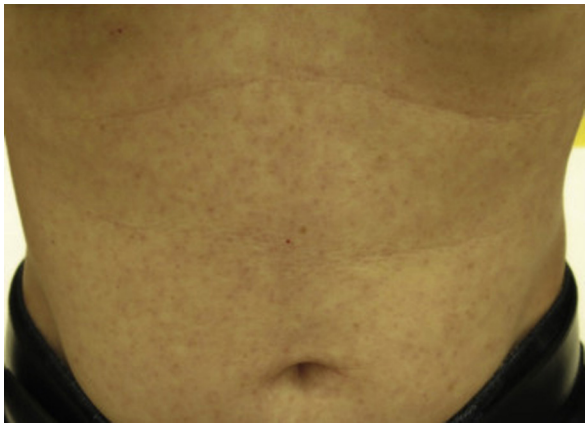


Fig. 1.34 Rash of Zika virus.
Since its discovery in Uganda in 1947, there have been outbreaks of Zika in Africa, South East Asia and the Pacific. Many infections are asymptomatic but 20% of people experience mild fever, arthralgia and non-purulent conjunctivitis. The typical rash associated with Zika is maculopapular and pruritic but is difficult to distinguish clinically from other viral exanthems. (From Ginier, M., Neumayr, A., Günther S., et al. Zika without symptoms in returning travellers: What are the implications? Travel Medicine and Infectious Disease, 2016-01-01, Volume 14, Issue 1, Pages 16–20, Figure 1.)

Downloaded From Vet-eBooks.com



Fig. 1.35 Brazilian infant with microcephaly.
In May 2015, Zika was first detected in Brazil. Soon afterwards, a large number of cases of microcephaly were noted in areas experiencing the Zika outbreak. Zika is now known to cause microcephaly with characteristic craniofacial disproportion, ventriculomegaly and intracranial calcifications in the babies of mothers infected during pregnancy. The long-term outcome of children born with these disabilities and of children without structural abnormalities born to mothers infected during pregnancy is yet to be seen. (Courtesy, Dr A. Kumar.)

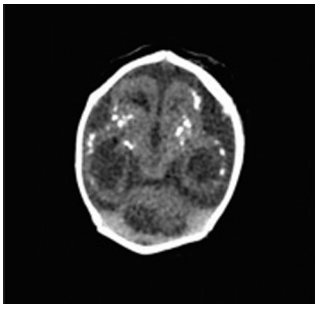


Fig. 1.36 CT scan abnormalities in congenital Zika virus syndrome.
Note the microcephaly, simplified gyral pattern and cortical and subcortical calcification in this child with congenital Zika virus syndrome. (From de Araújo, T., Rodrigues, L., de Alencar Ximenes R. Association between Zika virus infection and microcephaly in Brazil, January to May, 2016: preliminary report of a case-control study. Lancet Infectious Diseases, 2016. Volume 16, No. 12, pages 1356-1363.)

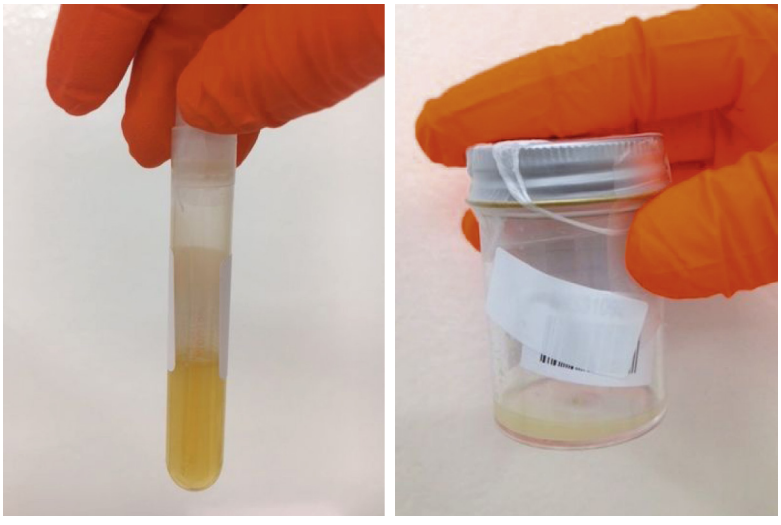


Fig. 1.37 Urine and semen; diagnostic specimens for Zika virus polymerase chain reaction.
Although the viraemic period in blood is usually between three and seven days, Zika may continue to be excreted in the urine for up to 14 days and for more than three months in the semen (2016 data). Male-to-female sexual transmission is well documented, although the reverse is rare. Because the specificity of serological testing is compromised by cross-reactivity with other flaviviruses such as dengue, urine and occasionally semen can be useful diagnostic specimens for molecular tests to detect recent infection.

Downloaded from Vet-eBooks.com

Japanese Encephalitis and West Nile

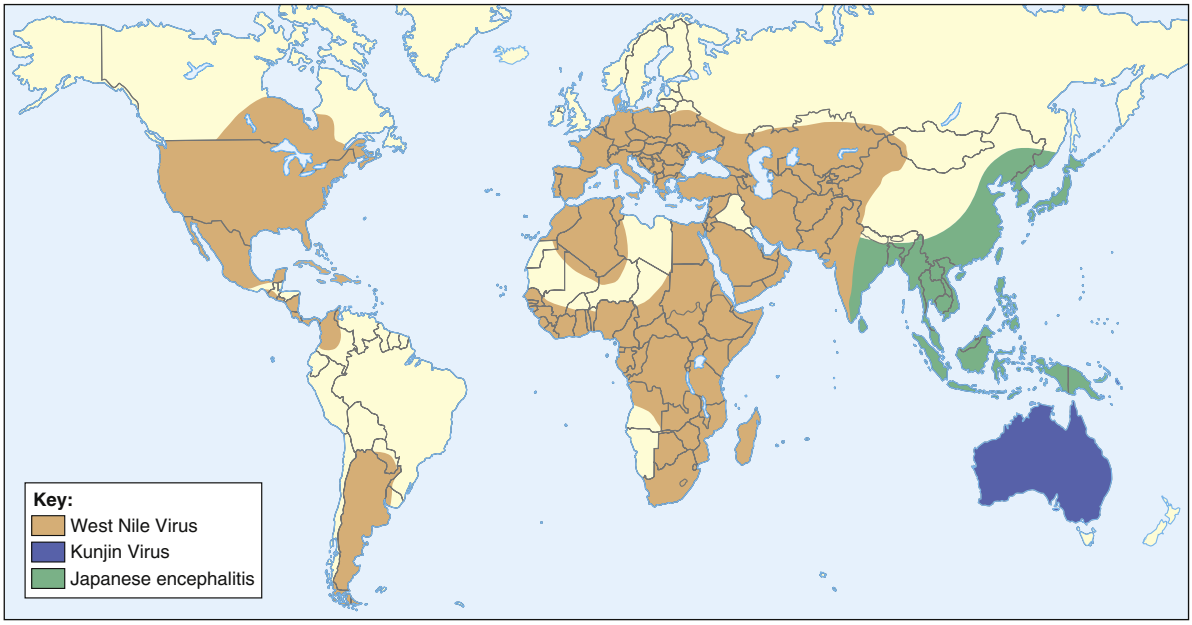


Fig. 1.38 Geographical distribution of the West Nile and Japanese encephalitis viruses.
Japanese encephalitis virus (JEV) and West Nile virus (WNV) are both members of the JE antigenic complex of flaviviruses and share similar clinical syndromes and transmission cycles. WNV is endemic in Africa, Asia and Europe. In 1999, it was imported to the United States where it caused a large outbreak and became endemic, spreading south through Central America to encroach on South America. A subtype of this virus, Kunjin virus, is endemic in Australasia. Japanese encephalitis is found in Asia west of the Pakistan/Indian border and extends south through South East Asia and into northern Australia.



Fig. 1.39 Grey heron, a potential carrier of West Nile virus (WNV).
This is one of a number of species of water birds that migrate seasonally from endemic areas and can carry WNV. *Culex pipiens*, which feeds on both avian and human blood, is the main vector.

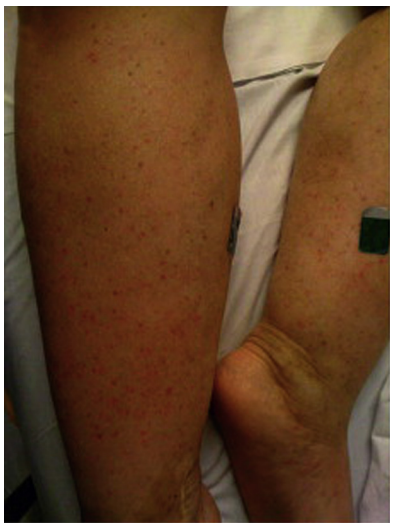


Fig. 1.40 Maculopapular rash in West Nile virus (WNV).
Many patients with WNV have an asymptomatic infection. Others develop an acute viral illness with fever, headache and myalgia, similar to dengue. Between 25 and 50% develop a rash that may be maculopapular, as seen here, or morbilliform and may be accompanied by pruritus or dysaesthesia. This usually presents around defervescence and is associated with reduced risk of encephalitis. (From Martindale, J. L. Locally acquired West Nile encephalitis. Journal of Emergency Medicine, 2012-12-01, Volume 43, Issue 6, Pages e435–e438, Figure 1.)

Downloaded from Vet-eBooks.com

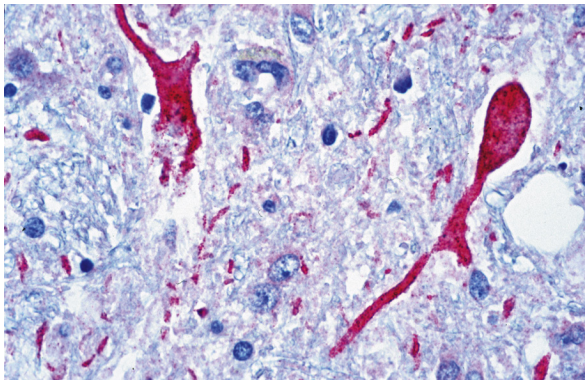


Fig. 1.41 A section of human brain from a fatal case of encephalitis caused by West Nile virus (WNV).
Only 1% of people infected with WNV develop neuroinvasive disease. Manifestations of this include meningitis, encephalitis and acute flaccid paralysis. Mortality rate can reach 10%. This section, from a fatal case of WNV encephalitis, is stained to demonstrate viral antigen in neurones and neuronal processes. (Methylene blue x 200.) (Courtesy, Dr W. Shieh and Dr S. Zaki.)

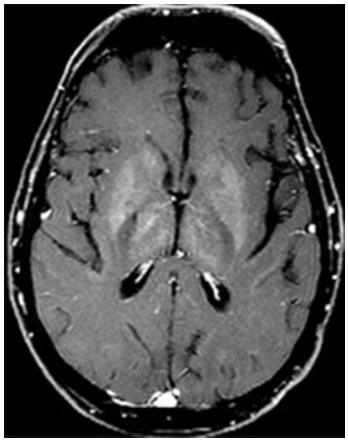


Fig. 1.42 MRI of an immunocompromised patient with West Nile virus (WNV).
This man, who had previously received a renal transplant, developed fever and tremor and was diagnosed with WNV. Note the enhancement in the basal ganglia and thalamus. Neuroinvasion is both more frequent and more severe in immunocompromised patients. (From Moritani, T., Ekholm, S. E., Westesson, P. L. Diffusion-weighted MR imaging of the brain. 2nd edition. Berlin, Heidelberg (Germany): Springer-Verlag; 2009, Page 218; with permission.)



Fig. 1.43 Control of culicine vectors of West Nile virus (WNV).
In urban areas where peridomestic culicine mosquitoes transmit WNV, the distribution of insecticides by fogging machines is a valuable method of vector control. (Courtesy, Dr J. Lucas.)



Fig. 1.44 Blood transfusion.
West Nile virus (WNV) can be transmitted by transfusion of viraemic blood products or organs. In endemic areas, donor blood should be screened for the virus, although many endemic countries lack the infrastructure to do this. (From Hoffbrand, A. V. Blood transfusion. Color Atlas of Clinical Hematology, 4th edition. Elsevier. Pages 509–518, Figure 29.7.)

Downloaded from Vet-eBooks.com

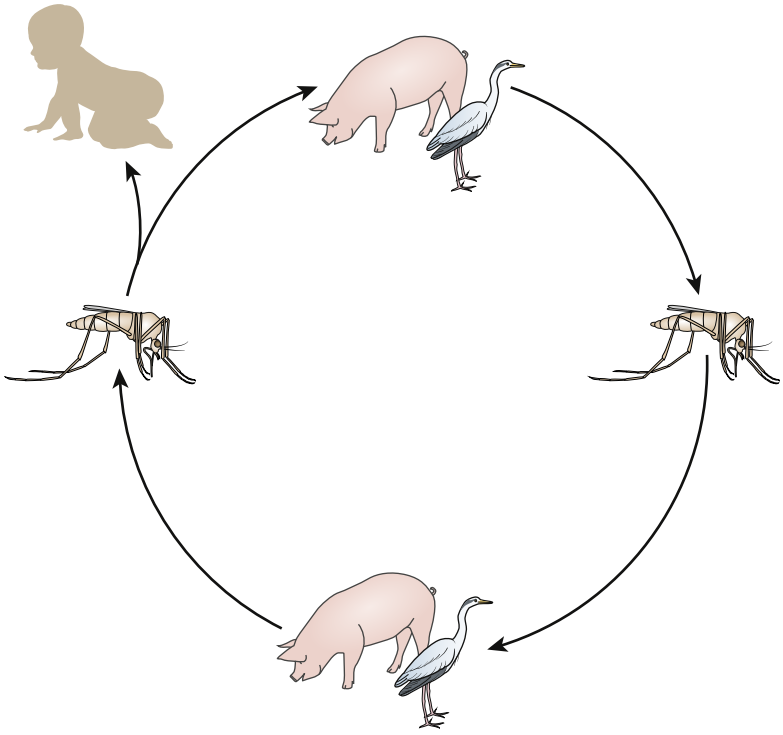


Fig. 1.45 Cycle of transmission of Japanese encephalitis virus (JEV).
JEV is transmitted by mosquitoes, primarily *Culex tritaeniorhynchus*, between amplifying mammalian hosts, principally pigs and wading birds. Pigs develop extremely high viraemias but do not become unwell, rendering them a very effective reservoir of infection. Wading birds facilitate transmission of the virus both to and within areas without pigs. Humans are incidentally infected and do not develop sufficiently high viraemia to transmit infection.



Fig. 1.46 *Culex tritaeniorhynchus*.
Cx. tritaeniorhynchus is the principal vector of Japanese encephalitis. Note the pale band on the proboscis. (Courtesy, S. McIntyre.)



Fig. 1.47 Rice paddy fields in South India.
Rice paddy fields are important breeding grounds for *Cx. tritaeniorhynchus*. They also serve as feeding grounds for migratory birds, such as the cattle egret, which serve as reservoir hosts. (Courtesy, Dr L. Nabarro.)

Downloaded From Vet-eBooks.com



Fig. 1.48 Acute Japanese encephalitis.
Following non-specific symptoms of fever, headache and lethargy, patients may develop an encephalitis or aseptic meningitis. Seizures are common, especially in children, but may be subtle and difficult to identify without EEG. Focal neurological symptoms may include movement disorders, hemiplegia, cranial nerve abnormalities or parkinsonian symptoms due to extrapyramidal involvement. The encephalitis seen in this Sri Lankan infant is severe. He was comatose and had spasms and choreoathetotic movements of all four limbs. The sequelae are serious and include learning difficulties. (Courtesy, Professor D. A. Warrell.)



Fig. 1.49 Wasting following acute flaccid paralysis secondary to Japanese encephalitis virus (JEV).
This patient developed an acute flaccid paralysis secondary to JEV. Note the severe wasting with residual weakness evident 1 year following infection. (Photo courtesy of T. Solomon, reproduced from Solomon T, Kneen R, Dung NM, et al. Poliomyelitis-like illness due to Japanese encephalitis virus. Lancet 1998;351:1094–7.)

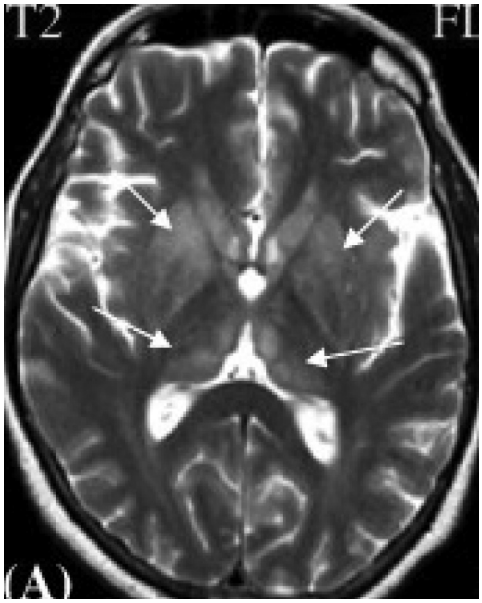


Fig. 1.50 MRI changes in acute Japanese encephalitis virus (JEV).
This axial T2 weighted MRI was performed 4 days after presentation. Note the bilateral thalamic and basal ganglia involvement (arrowed), which is typical of JEV. (From Sawlani, V. Diffusion-weighted imaging and apparent diffusion coefficient evaluation of herpes simplex encephalitis and Japanese encephalitis. Journal of the Neurological Sciences, 2009-12-15. Volume 287, Issue 1, Pages 221–226. Figure 2, panel A. Copyright © 2009 Elsevier.)

Downloaded From Vet-eBooks.com

Rift Valley Fever and Crimean-Congo Haemorrhagic Fever

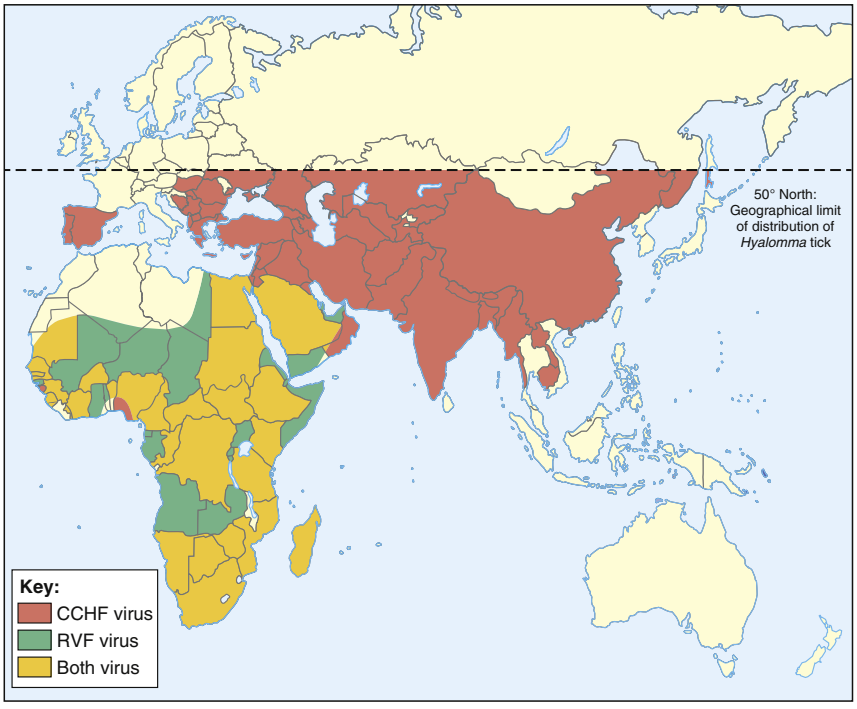


Fig. 1.51 Distribution of Rift Valley fever virus (RVFV) and Crimean-Congo haemorrhagic fever (CCHF).
RVFV is a major mosquito-borne infection of livestock in Africa. Movement of infected animals from the Horn of Africa in 2000 spread the disease to the Arabian Peninsula. Although in humans it usually causes a self-limiting acute febrile illness, 1% of cases develop haemorrhagic manifestations. CCHF is a tick-borne bunyavirus that causes a severe haemorrhagic illness. Its wide distribution is increasingly evident with cases described through Africa, Asia and eastern Europe. A recently described case in Spain suggests that CCHF probably occurs throughout the distribution of its *Hyalomma* tick vector.

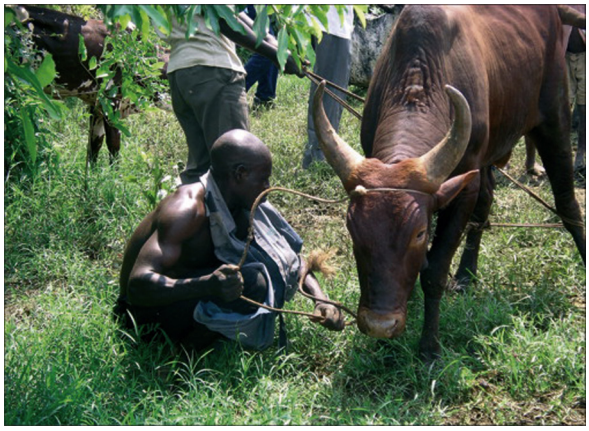


Fig. 1.52 Farmer with cattle in East Africa.
Rift Valley fever virus causes high mortality in young domestic ruminants with spontaneous abortion in pregnant animals. The disease is passed between ruminants by *Aedes (Stegomyia)* mosquitoes, which transmit the virus to their offspring transovarially. Humans become infected through mosquito bites or by contact with the blood or tissues of infected animals. Outbreaks occur every 5 to 15 years, often after flooding or coinciding with the warm phase of the El Niño – Southern Oscillation. (From Senior, K. Is the end in sight for sleeping sickness in Africa? The Lancet Infectious Diseases, 2009-10-01. Volume 9, Issue 10, Pages 595–595. Copyright © 2009 Elsevier. Copyright © 2009 Sue Welburn.)

Downloaded From Vet-eBooks.com

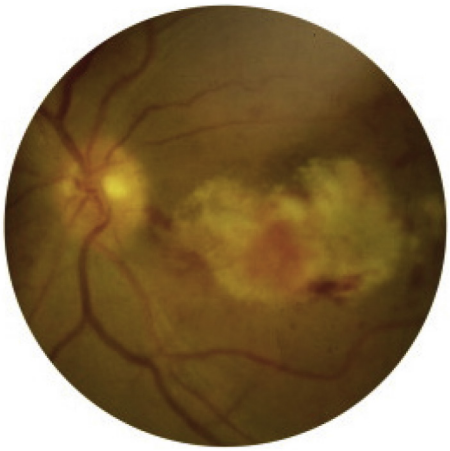


Fig. 1.53 Retinitis in a patient with Rift Valley fever virus (RFVF).
Most human infections cause a mild viral illness or are asymptomatic. Severe infection is unusual but may manifest as a hepatitis, encephalitis or haemorrhagic fever. Retinitis is a late complication, occurring 4 to 15 days after onset of symptoms. Note the creamy full thickness retinitis seen here with adjacent retinal haemorrhages. Macular involvement and scarring may result in permanent visual loss. (From Al-Hazmi, A., Al-Rajhi, A. A., Abboud, E. B., et al. Ocular complications of Rift Valley fever outbreak in Saudi Arabia. Ophthalmology, 2005, Volume 112, Pages 313–318.)



Fig. 1.55 Immature *Hyalomma marginatum rufipes* feeding on an African dove, *Streptopelia senegalensis*.
H. marginatum rufipes, which often lives on birds, is another vector of this virus. The bird tick is widely distributed from Africa to eastern Europe, Russia and Central Asia. (Courtesy, Dr M. L. Wilson.)



Fig. 1.54 *Hyalomma marginatum*.
Hard-bodied *Hyalomma* ticks have a life span of around 2 years and are the principal vector of Crimean-Congo haemorrhagic fever (CCHF). As larvae, they feed on small mammals, including rodents and ground-dwelling birds, which serve as amplifying hosts for CCHF. As adults, they feed on domestic livestock including sheep and goats, which act as viral reservoirs. Transmission to humans occurs following tick bite or by exposure to the bodily fluids of viraemic animals, primarily during animal slaughter. (Courtesy, S. McIntyre.)



Fig. 1.56 Ecchymoses in a patient with Crimean-Congo haemorrhagic fever.
Although some infections may be subclinical, illness typically begins with acute onset fever, headache and back pain. The patient may appear flushed or develop a maculopapular rash with conjunctivitis. Bruising may occur due to low platelets and deranged clotting. Around 20% of patients develop haemorrhagic manifestations.

Downloaded from Vet-eBooks.com



Fig. 1.57 Bilateral subconjunctival haemorrhage.
Note the bilateral spontaneous subconjunctival haemorrhages seen in this patient with Crimean-Congo haemorrhagic fever. (From Engin, A., Erdogan, H., Ozec, A. Ocular findings in patients with Crimean-Congo hemorrhagic fever. American Journal of Ophthalmology, 2009-04-01, Volume 147, Issue 4, Pages 634–638, Figure 1.)

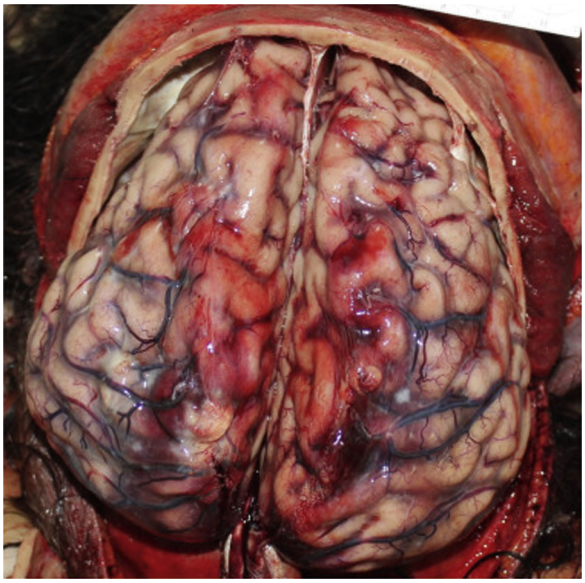


Fig. 1.58 Subarachnoid haemorrhage in a patient who died of Crimean-Congo haemorrhagic fever.
Patients with severe disease develop disseminated intravascular coagulation and a cytokine storm resulting in multiple organ dysfunction syndrome with haemorrhage and death. (From Ozsoy, S., Gokmen, A., Ozdemir M. et al. Medical examiners and Crimean-Congo hemorrhagic fever contamination risk. Journal of Forensic and Legal Medicine, 2015-11-01, Volume 36, Pages 32–36, Figure 10.)

ARTHROPOD-BORNE BACTERIAL INFECTIONS

Arthropod-borne bacterial infections are predominantly transmitted by ticks, lice, mites and fleas. The exception to this is *Francisella tularensis,* which can be transmitted by mosquitoes, and *Bartonella bacilliformis,* which is believed to be transmitted by sandflies.

Rickettsiae multiply within vascular endothelial cells resulting in a vasculitis-like systemic disease of varying severity. These infections are summarized in Table 1.2. *Borrelia* species are expert at evading the immune system; *B. burgdorferi* is one of medicine's great imitators whilst episodic antigen variation in other *Borrelia* species gives rise to periodic fever relapses. *Yersinia pestis* has caused some of the greatest plagues in history, including the Black Death, which killed up to 200 million people between 1346 and 1353.

All of these bacteria are capable of causing severe disease, requiring antibiotics for resolution. Most respond to doxycycline, although the addition of further agents including aminoglycosides or chloramphenicol is often beneficial.

Downloaded from Vet-eBooks.com

Table 1.2 Clinically relevant rickettsial diseases, updated to 2016

Disease	Causative agent	Vector	Animal reservoir	Geographical distribution
Typhus				
Epidemic typhus	*Rickettsia prowazekii*	*Pediculus humanus corporis*	Humans Flying squirrels–New World Unclear elsewhere	Ethiopia/Rwanda/Burundi Rural South/Central America
Endemic (murine) typhus	*Rickettsia typhi*	*Xenopsylla cheopis** *Ctenocephalides felis*	Rat (cat, opossum-USA)	Worldwide
Spotted fevers				
Rocky Mountain spotted fever	*Rickettsia rickettsii*	Various tick spp.*	Many small mammals	North America, patchy distribution in Central and South America
Mediterranean spotted fever/Fièvre boutonneuse	*Rickettsia conorii*	*Rhipicephalus sanguineus**	Dogs, small mammals	Mediterranean, sub-Saharan Africa
African tick typhus	*Rickettsia africae*	*Amblyomma spp.**	? Rodents	Sub-Saharan Africa, Eastern Caribbean
Lymphangitis associated rickettsiosis	*Rickettsia sibirica subsp mongolotimonae*	*Dermacentor spp.**	Farm and wild animals	France, Portugal, South Africa
Transitional group rickettsiae				
Queensland tick typhus	*Rickettsia australis*	*Ixodes holocyclus**	Rodents	Australia
Rickettsial pox	*Rickettsia akari*	Mites* *Liponyssoides sanguineus*	Mice	Korea, central and southern Africa, Ukraine, eastern USA
Scrub typhus				
Scrub typhus	*Orientia tsutsugamushi*	Trombiculid mites	Small mammals, rodents, birds	South and South East Asia, Australia, Pacific
Anaplasmosis				
Human monocytic ehrlichiosis	*Ehrlichia chaffeensis*	*Amblyomma americana*	White tailed deer, raccoon, opossum	Unclear – cases reported from North America, Europe, Asia, Africa
Human granulocytic anaplasmosis	*Anaplasma phagocytophila*	*Ixodes scapularis*	White-footed mouse, other rodents, cattle, sheep, horses	North America, North and Central Europe, China, Russia

*Vertical transmission can occur in vectors.

Downloaded From Vet-eBooks.com

Typhus



Fig. 1.59 Refugees in the Ethiopian Highlands.
The body louse, *Pediculus humanus corporis*, thrives in poor, overcrowded areas where hygiene standards are difficult to maintain. Typically this includes refugee camps and prisons where they are capable of causing epidemics of disease. Ethiopia is one of the few remaining places in the world where outbreaks of epidemic typhus occur. (From Shears, P. Poverty and infection in the developing world: Healthcare-related infections and infection control in the tropics. Journal of Hospital Infection, 2007-11-01, Volume 67, Issue 3, Pages 217–224, Figure 3.)

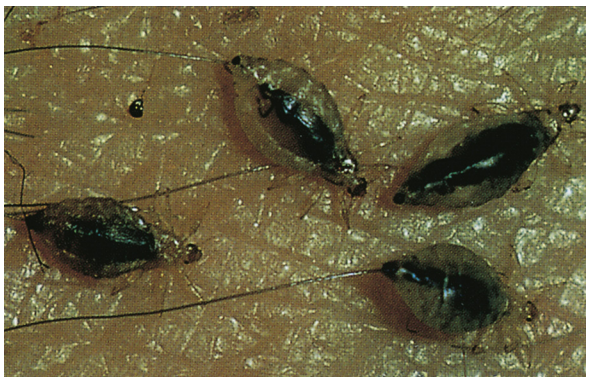


Fig. 1.60 Feeding body lice (*Pediculus humanus corporis*).
Aside from causing considerable discomfort through itching, body lice can also transmit *Rickettsia prowazekii* (epidemic typhus), *Bartonella quintana* (trench fever) and *Borrelia recurrentis* (relapsing fever). The lice live on the skin or in clothes and defecate highly infective faeces whilst feeding. Pruritus provokes the human host to scratch, inadvertently introducing the pathogens into abraded skin. The use of DDT for disinfection of louse-infested communities is a primary control measure in epidemic situations. (x 4). (Courtesy, Dr H. Lieske.)



Fig. 1.61 Rash of epidemic, louse-borne typhus *(R. prowazekii)*.
The illness usually starts abruptly with fever, headache and sometimes cough or abdominal pain. After several days, 60% of patients develop a non-specific macular or maculopapular rash. Most patients experience some neurological symptoms including confusion, seizures or focal neurological signs. This woman had a fine, macular erythematous rash on the face and the extremities that appeared several days into illness. (Courtesy, Professor W. E. Farrar.)



Fig. 1.62 Peripheral gangrene in severe epidemic typhus.
One of the characteristic features of typhus is the severe toxicity of the infection. Gangrene of feet and hands, as seen in this Ethiopian patient, occasionally occurs. (Courtesy, Dr P. L. Perine.)

Downloaded From Vet-eBooks.com



Fig. 1.63 *Rattus norvegicus*, a host of *Rickettsia typhi* (murine typhus).
Murine typhus is a cosmopolitan rickettsial illness which occurs sporadically on all inhabited continents. The main hosts are rats, which can develop quite high rickettsaemias allowing onward transmission to feeding fleas. Humans are incidentally infected when infected flea faeces is introduced into bite sites. The resultant clinical illness is usually mild with fever, myalgia, headache and sometimes rash. (From Weber WR., On The Cover – Brown Rat. Annals of Allergy, Asthma & Immunology, 2011. Volume 107, Issue 4, Page A6.)



Fig. 1.65 Eschar of African tick typhus.
This patient presented with fever, myalgia and an eschar following a safari holiday in South Africa. The clinical presentation is typical of *R. africae* infection, a mild spotted fever which often resolves without treatment. The diagnosis can be confirmed by polymerase chain reaction of the eschar or by serological testing. (Courtesy, Dr L. Nabarro.)

Spotted Fevers

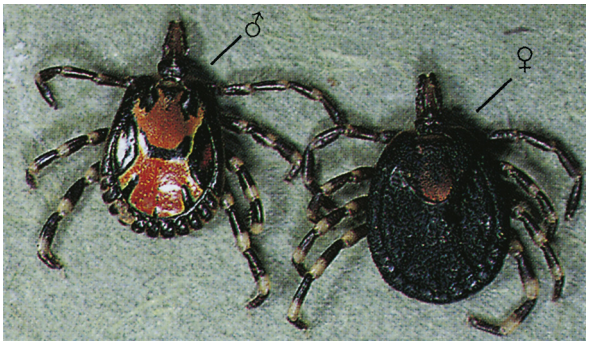


Fig. 1.64 Male and female *Amblyomma variegatum*, a vector of *Rickettsia africae* in sub-Saharan Africa (M - left, F - right).
Various species of hard tick transmit a spectrum of rickettsial pathogens. In sub-Saharan Africa, *R. africae* is transmitted by *Amblyomma variegatum*. Note the characteristic properties of hard ticks; the mouthparts which are visible from above and the hard scutum (Latin for 'shield') which covers the whole dorsal surface in males and part of the dorsal surface in females. (x5.5.)



Fig. 1.66 Petechial rash of Rocky Mountain spotted fever (RMSF).
Rickettsia rickettsii is transmitted by hard ticks with various small rodents including gophers and woodchucks as mammalian hosts. The illness can be very severe, with complications including acute respiratory distress syndrome, encephalitis and disseminated intravascular coagulation and an untreated mortality rate up to 30%. The 4-year-old child seen here was comatose on day 8 of illness but went on to make a full recovery. An eschar marked the site of the bite. The application of a tourniquet, as seen here, accentuates the haemorrhagic nature of the rash distal to the site of the pressure (Hess test).

Downloaded from Vet-eBooks.com



Fig. 1.67 *Rickettsia sibirica.*
Despite its name, *R. sibirica* subspecies *mongolotimonae*, is most commonly reported from France and Portugal. It often presents with an eschar associated with lymphangitis or regional lymph nodes lending it the name 'lymphangitis associated rickettsia'. (From Faccini-Martinez, A., Garcia-Alvarez, L., Hidalgo, M., et al. Syndromic classification of rickettsioses: an approach for clinical practice. International Journal of Infectious Diseases, 2014-11-01, Volume 28, Pages 126–139, Figure 11. Courtesy of Dr R. de Sousa.)

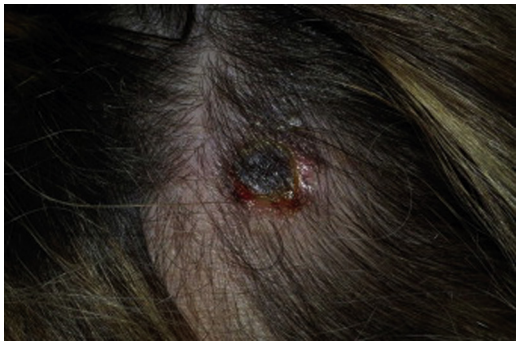


Fig. 1.68 Scalp eschar in a patient with *Rickettsia slovaca* infection.
R. slovaca classically causes a scalp eschar with localized lymphadenopathy following the bite of a *Dermacentor* tick. This syndrome is known as SENLAT —Scalp Eschar and Neck Lymphadenopathy After Tick bite—and typically occurs in European countries in early spring and autumn. (From Faccini-Martinez, A., Garcia-Alvarez, L., Hidalgo, M., et al. Syndromic classification of rickettsioses: an approach for clinical practice. International Journal of Infectious Diseases, 2014-11-01, Volume 28, Pages 126–139, Figure 9.)



Fig. 1.69 Eschar and vesicular rash of *Rickettsia akari.*
Note the eschar, vesicular lesion and lymphangitis in this patient with *R. akari*, one of the few rickettsiae to cause a vesicular rash, hence the name rickettsial pox. Although rarely diagnosed, it is thought to have a worldwide distribution due to the ubiquity of its house mouse host, *Mus musculus*, and main vector, the mouse mite *Liponyssoides sanguineus*. (From Renvoisé, A., van't Wout, J., van der Schroeff, J., et al. A case of rickettsialpox in Northern Europe. International Journal of Infectious Diseases, 2012-03-01, Volume 16, Issue 3, Pages e221–e222, Figure 1.)

Downloaded From Vet-eBooks.com



Fig. 1.70 *Liponyssoides sanguineus.*
The mouse mite *Liponyssoides sanguineus* transmits *R. akari.* (From Paddock, C. D. Rickettsialpox. In: Hunter's Tropical Medicine and Emerging Infectious Diseases. 9th edition. New York: Elsevier Inc.; 2000, Pages 553–557, Figure 65.2A.)

Scrub Typhus

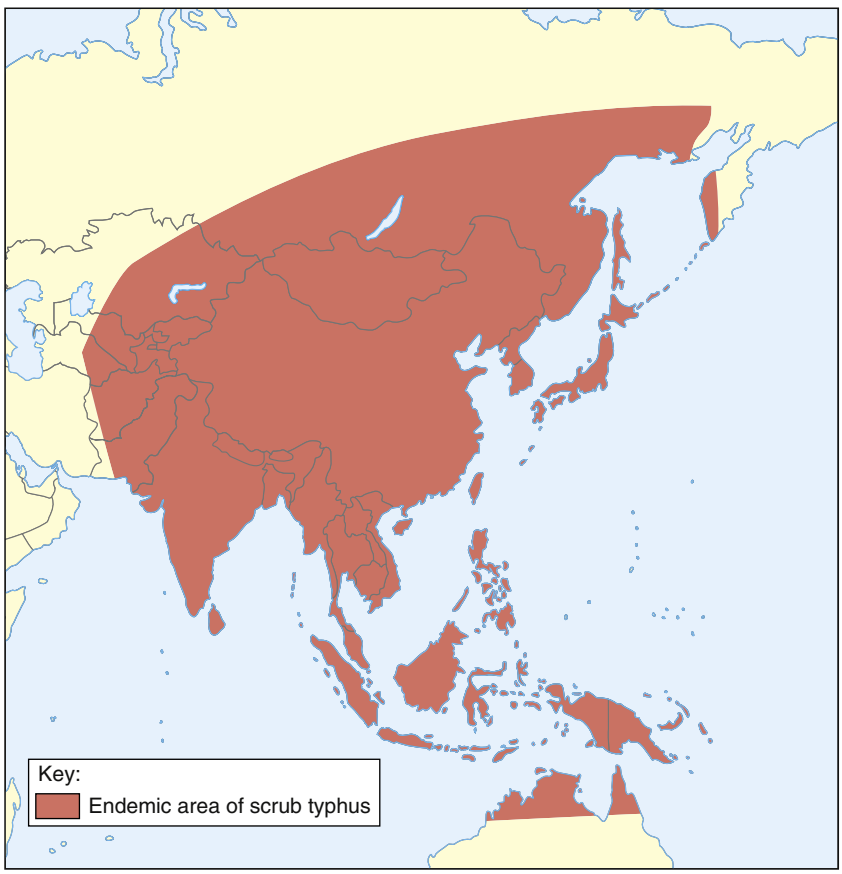


Fig. 1.71 Distribution of scrub typhus. Scrub typhus results from infection with *Orientia tsutsugamushi*, a rickettsial organism transmitted by larval trombiculid mites. The disease classically occurs in the tsutsugamushi triangle, which stretches from the Indian subcontinent to the far east of Russia and southwards to the northern tip of Australia. However, infection is increasingly described outside this area, most recently from Chiloé Island off the coast of Chile.

Downloaded from Vet-eBooks.com



Fig. 1.72 Larva of *Leptotrombidium*.
Leptotrombidium mites live in 'mite islands' in variable vegetation types. They pass *Orientia tsutsugamushi* to subsequent mite generations transovarially. The mite is thus the main reservoir. Rodents may also become infected when parasitized by larval mite stages (chiggers) and may spread infection between mite islands. Humans are dead-end hosts, infected accidentally when walking through mite islands. (x80.)

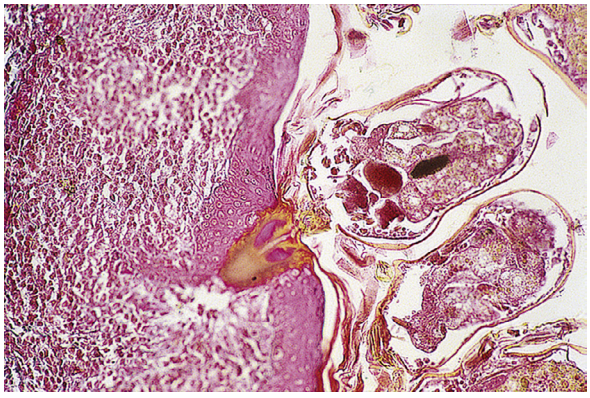


Fig. 1.73 Longitudinal section through a feeding trombiculid larva to show the stylostome.
When the larvae feed they penetrate the upper dermis of the host with their chelicerae, then inject a histiolytic salivary secretion that dissolves the underlying tissue. This hardens to form an attachment to the chelicerae known as a 'stylostome'; a central tubular cavity through which saliva can pass. Saliva contains digestive enzymes that render the host tissue liquid enough to be taken up through the stylostome. Thus the larvae feed on partially digested host tissues rather than blood (Haematoxylin and eosin (H&E) x100). (Courtesy, J. Williams.)



Fig. 1.74 Eschar at site of mite bite.
An eschar may form at the site of trombiculid bite. They are often found in the skin creases around the groin and breasts; a thorough clinical examination is essential if this diagnostic clue is to be identified. (Courtesy, Professor D. A. Warrell.)

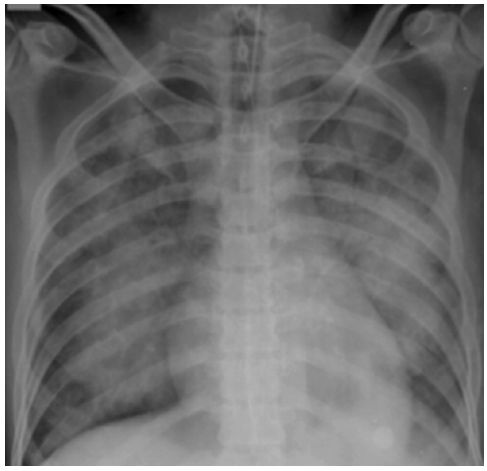


Fig. 1.75 Acute respiratory distress syndrome (ARDS) in a patient with severe scrub typhus.
Scrub typhus classically presents with fever, headache and myalgia, with or without an eschar and maculopapular rash. It causes a systemic vasculitis which, untreated, may progress to severe disease with ARDS, renal failure or meningoencephalitis. This patient presented severely unwell with a fever, eschar and shortness of breath. Chest radiograph showed ARDS. The patient was treated with doxycycline and defervesced at 48 hours. Azithromycin and chloramphenicol are alternative antibiotics that can be used to treat this disease. (Courtesy, Professor G. Varghese.)

Downloaded From Vet-eBooks.com

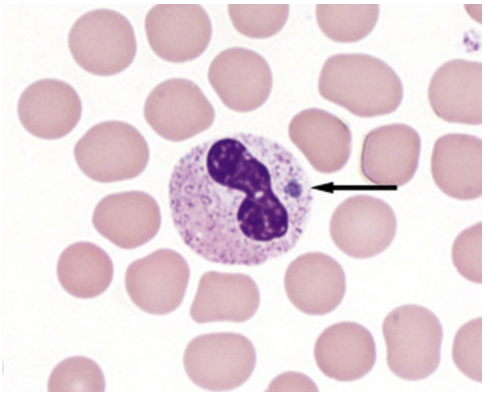


Fig. 1.76 Intraleukocytic inclusion body (morula) of *Anaplasma phagocytophilum* causing human granulocytic anaplasmosis.
This tick-borne infection causes fever, myalgia and fatigue and may be fatal in people with co-morbidities. The worldwide distribution is unclear but it is primarily identified, albeit uncommonly, in North America and Europe. Note the characteristic inclusion body in this neutrophil. (Wright Giemsa stain, x1000.) (From Caulfield, A. J., Pritt, B. Lyme disease coinfections in the United States. Clinics in Laboratory Medicine, 2015-12-01, Volume 35, Issue 4, Pages 827–846, Figure 3.)



Fig. 1.78 Lesions of 'verruga peruana'.
Following acute infection, whether symptomatic or not, an eruptive or 'verruga' phase may occur. *B. bacilliformis* invades capillary endothelial cells resulting in cellular proliferation and angiomatous lesions on the skin and mucosa. (Courtesy, Professor P. Garcia.)

Bartonella

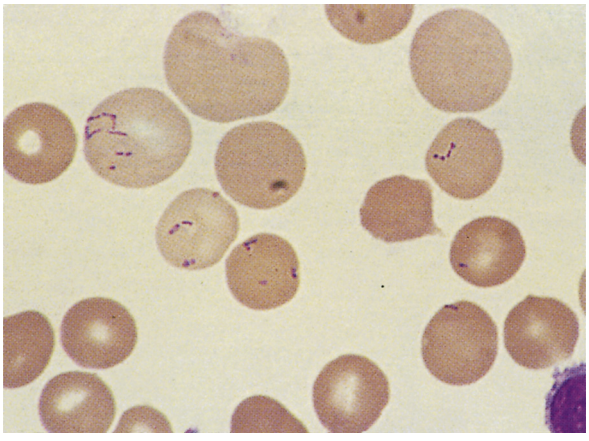


Fig. 1.77 Blood film showing *Bartonella bacilliformis* in Carrión's disease.
B. bacilliformis is a Gram-negative organism believed to be transmitted by sandflies in high-altitude regions of the Andes in Peru, Colombia and Ecuador. The acute stage presents with fever, headache and malaise (Oroya fever). Invasion of red blood cells, as seen here, causes an acute haemolytic anaemia. A transient immunosuppression predisposes patients to secondary opportunistic infections including non-typhoidal salmonella sepsis and toxoplasmosis. Untreated the mortality rate is high. (Giemsa x 1300.)

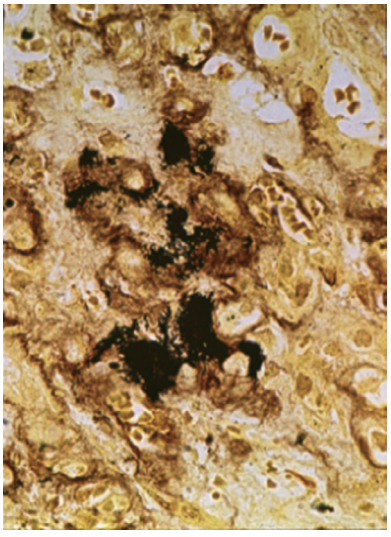


Fig. 1.79 Bacillary angiomatosis.
Note the small dark Warthin-Starry stained bacteria in this section taken from the skin of an HIV-positive patient with *Bartonella henselae* infection. (Courtesy, Professor S. Lucas.)

Downloaded from Vet-eBooks.com

Plague

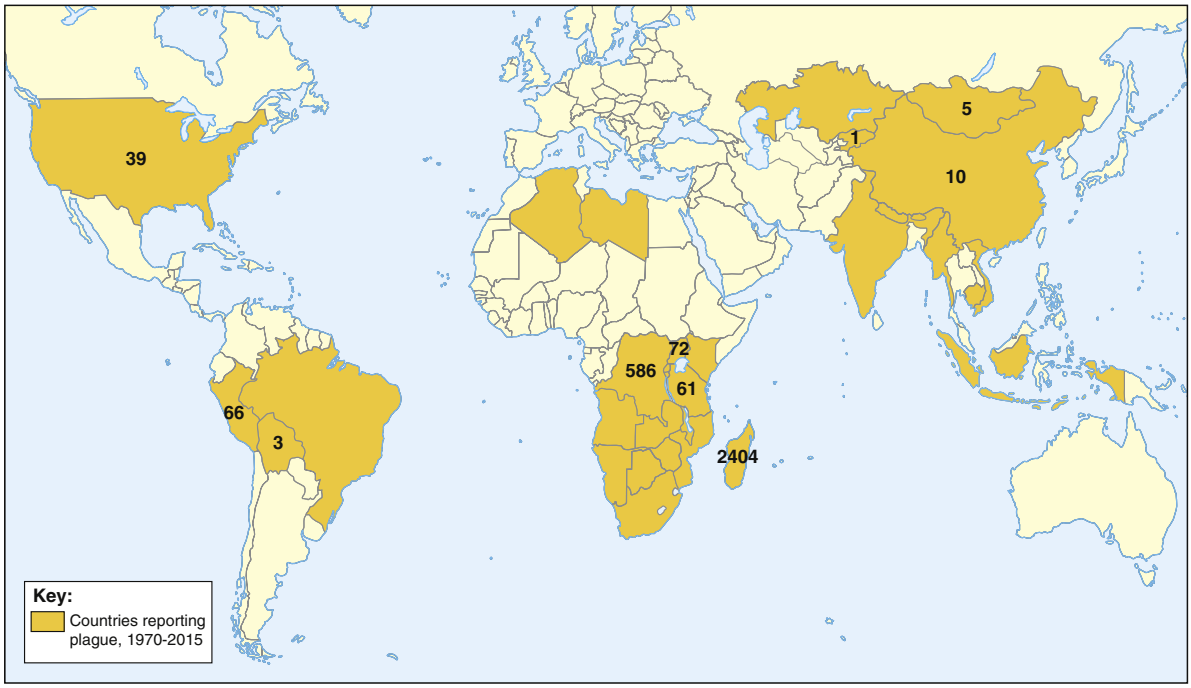


Fig. 1.80 Distribution of plague.
Plague is the colloquial name for infection caused by the Gram-negative bacterium *Yersinia pestis*. It is usually spread to humans by the bites of infected rat fleas and causes a suppurative lymphadenitis ('bubonic plague'). Less commonly, it can be transmitted by aerosol from human to human, causing 'pneumonic plague', which has a much higher mortality rate. Plague has previously been responsible for devastating pandemics, such as the Black Death, which killed 75–200 million people between 1346 and 1353, including over a third of the population of Europe. Nowadays, there are a few sporadic cases of bubonic plague occurring in focal areas in a small number of countries and occasional small outbreaks of pneumonic plague. The figures on this map are the total number of reported cases in each country between 2010 and 2015.



Fig. 1.81 *Xenopsylla cheopis*.
Xenopsylla cheopis, the oriental rat flea, is the most efficient and cosmopolitan vector of *Yersinia pestis*, although other fleas are responsible for transmission in localized geographical areas. The flea is 1–3 mm in length with an oval body. It does not possess genal or pronotal combs. The presence of a mesopleural rod and the absence of sclerotized antennal fossae distinguishes it from *Pulex irritans*, the human flea. (Courtesy, S. McIntyre.)

Downloaded From Vet-eBooks.com



Fig. 1.82 Proventriculus of *Xenopsylla cheopis* blocked by plague bacilli.
Hungry fleas abandon dying domestic rats (*R. norvegicus, R. rattus*). The fleas often have their foreguts blocked by bacilli and, in this condition, they will attempt to feed on any animal. If they bite humans, they may transmit the disease. (x 215.)



Fig. 1.83 The California ground squirrel, host of *Oropsylla montana*.
In the United States most human cases of plague are acquired following bites from *Oropsylla montana* fleas, which normally feed on ground squirrels. (Copyright © 2013 Wikicommons/Brocken Inaglory. From Hayward, P. Rare zoonoses in the USA. The Lancet Infectious Diseases, 2013-09-01, Volume 13, Issue 9, Pages 740–741.)



Fig. 1.84 Bubonic plague.
Following a flea bite, the organisms pass from the bite site to the local lymphatics. Within a week, there is acute onset of fever, headache and malaise, followed by the development of painful suppurative lymphadenopathy in the lymph nodes draining the initial bite site. Untreated, infection proceeds to septicaemia with disseminated intravascular coagulation and death.

Downloaded from Vet-eBooks.com



Fig. 1.85 Septicaemic plague.
This patient with disseminated intravascular coagulation showed cutaneous bleeding and gangrene of the terminal phalanges in a systemic inflammatory response to *Y. pestis* septicaemia. (Courtesy, Dr D. Dennis.)

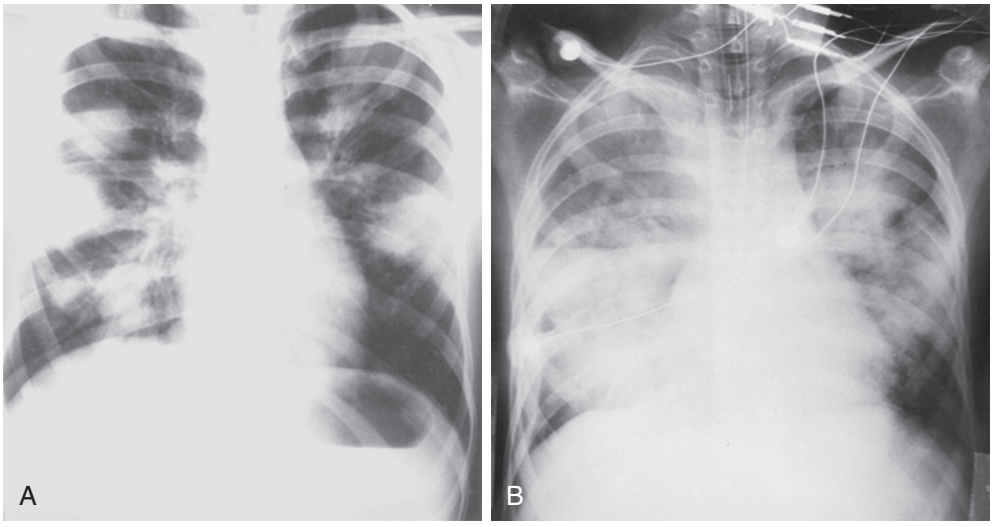


Fig. 1.86 Secondary pneumonic plague.
Haematogenous dissemination of *Y. pestis* to the lungs results in secondary plague pneumonia. Typically this is a perimortem sign. The first radiograph shows bilateral nodular opacities (A) which progressed to confluent airspace shadowing within 24 hours (B). (From Alsofrom, D. J., Mettler, F. A., Mann, J. M. Radiographic manifestations of plague in New Mexico 1975–1980. Radiology, 1981 Volume 139, Pages 561–565.)

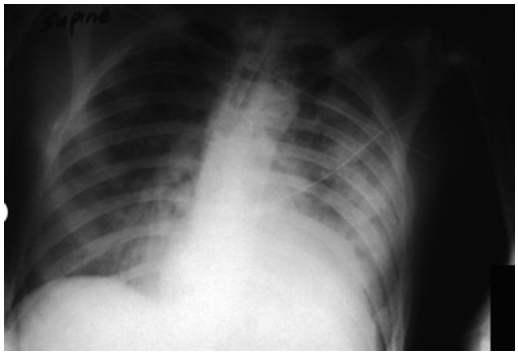


Fig. 1.87 Primary pneumonic plague.
Inhalation of *Y. pestis*, following exposure to a patient with pneumonic plague or aerosolization of the bacillus, results in primary pneumonic plague. It presents within a few days of exposure with a lobar pneumonia that rapidly progresses to be bilateral and multilobar. Mucoid sputum becomes foamy and blood stained and is packed with *Y. pestis*, making it highly infectious. Even with treatment, mortality exceeds 50%. (Courtesy of CDC and Dr J. Poland. From Artenstein, A. Bioterrorism and biodefense. In: Cohen, J. et al. (eds) Infectious Diseases, Pages 747–758, Figure 71.8. Copyright © 2010 Elsevier Ltd. All rights reserved.)

Downloaded From Vet-eBooks.com



Fig. 1.88 Lung from a fatal case of pneumonic plague.
Pneumonic infection, which allows direct human-to-human spread of bacteria via aerosol, is the least common form of plague. In late 2004, over 60 workers died of pneumonic plague among some 7000 employed in a diamond mine in the northern part of the Democratic Republic of the Congo. The lower lobe of the lung seen here shows intense hyperaemia and haemorrhage with necrotic nodules. The upper lobe contains only necrotic nodules with compensatory emphysematous changes. (AFIP No. 40657.)

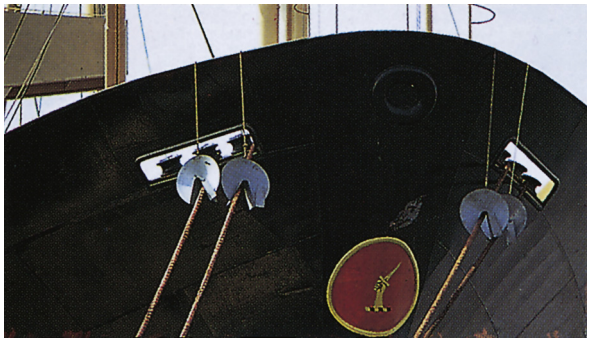


Fig. 1.89 Metal guards preventing access of rats along ships' hawsers.
Plague control demands strictly enforced rodent-control measures and international quarantine regulations, particularly for shipping.

Tularaemia



Fig. 1.90 Primary ulcer of tularaemia.
Francisella tularensis is a Gram-negative coccobacillus that affects a wide range of wild rodents and rabbits. Zoonotic infection in humans is usually acquired by contact with infected animals—typically hunters who prepare animal carcasses—or from the bites of infected mosquitoes or ixodid ticks. The disease occurs sporadically in Europe, North Africa, North America and the Middle and Far East. Ulceroglandular disease is the commonest manifestation of disease and presents with an ulcerative lesion with central eschar at the site of tick bite and localized lymphadenopathy. (Courtesy, Professor W. E. Farrar.)



Fig. 1.91 Oropharyngeal tularemia with cervical lymphadenopathy.
Oropharyngeal tularemia occurs following consumption of contaminated food or water. (From Ulu-Kilic, A. and Doganay, M. An overview: Tularemia and travel medicine. Travel Medicine and Infectious Disease, 2014-11-01, Volume 12, Issue 6, Pages 609–616, Figure 3. Copyright © 2014 Elsevier Ltd.)

Downloaded from Vet-eBooks.com

THE RELAPSING FEVERS

Tick-Borne Relapsing Fever

Tick-borne relapsing fever is enzootic in many countries, but human infections are uncommon. The *Borrelia* species, tick vector and animal host vary geographically; *B. duttoni* is the commonest species in Africa and is transmitted by the soft tick *Ornithodoros moubata*, while *B. hermsii* is found in North Africa and is transmitted by *O. hermsii*. All cause a similar clinical syndrome consisting of high fever, headache and malaise for 1–3 days followed by a 4–14 day fever-free interval and a variable number of relapses. The first febrile period tends to be the most severe but localized neurological complications may be more common in later episodes.

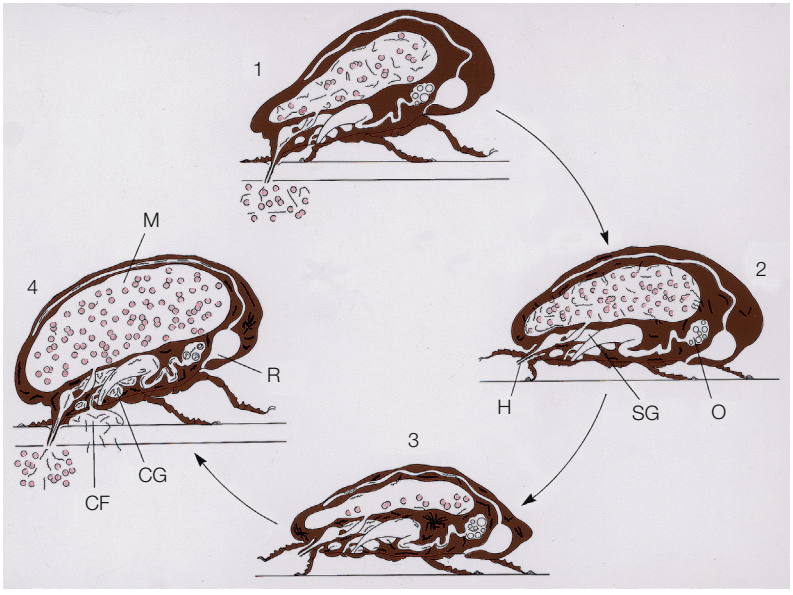


Fig. 1.92 Transmission of *Borrelia* spp. through *Ornithodoros moubata*.
Organisms enter the midgut with a blood meal (1). They invade the haemocoele (2), where they reproduce and enter all body organs, including ovaries, salivary glands and coxal glands (3). At the next blood meal the *Borrelia* pass into the new host through the saliva or coxal fluid (4). Transovarial transmission occurs via ova. H, hypostome; M, midgut; R, rectum; O, ovary; SG, salivary glands; CG, coxal glands; CF, coxal fluid. (Adapted from Geigy and Herbig, 1955 Erreger und Überträger tropischer krakheiten. Acta Tropica Supplement 6. Verlag für Recht und Gesellschaft, Basel.)



Fig. 1.93 Fully engorged *Ornithodoros moubata*.
Soft ticks, such as *O. moubata*, transmit *B. duttoni* from rodents to humans and from human to human. They have ventrally placed mouthparts, which are not visible from above, and do not have a hard scutum. They live in soft earth at the base of mud-walled huts and feed on the inhabitants. (x 8.1)

Downloaded From Vet-eBooks.com



Fig. 1.94 Site of bite of *Ornithodoros moubata*.
Tick saliva contains an anticoagulant component, which results in bleeding at the site of bite. *B. duttoni* is passed into the skin with tick saliva but is also released in coxal fluid which can contaminate the bite site after the fully engorged tick has detached.

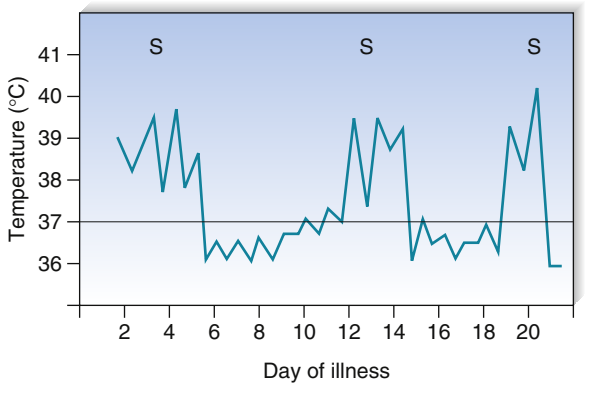


Fig. 1.95 Temperature chart of tick-borne relapsing fever.
The infection acquires its name from the typical relapsing nature of the fever. *Borrelia* species periodically change a major surface antigen allowing them to temporarily evade the immune response. When the antigen changes, the host develops fever and spirochaetes become visible in the blood on dark field microscopy (S). As the immune system responds to the new antigen, the fever wanes but then returns when the surface antigen changes again.

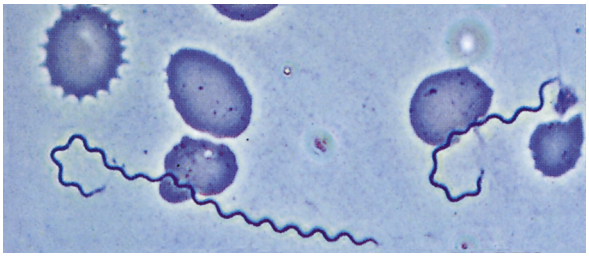


Fig. 1.96 *Borrelia duttoni* in a human blood film from Tanzania.
Spirochaetes can be visualized in the blood at the peak of fever. (Giemsa – phase contrast x 1300.)

Louse-Borne Relapsing Fever



Fig. 1.97 Louse-borne relapsing fever in an Ethiopian man.
B. recurrentis transmitted by body lice occurs in epidemic form in Ethiopia, Eritrea and Sudan. The febrile periods usually only recur once or twice, occasionally up to five times. This patient, who presented with fever, jaundice and large petechial haemorrhages on the trunk, was severely emaciated. Mortality in untreated patients may be as high as 40% during epidemics. Jarisch-Herxheimer reactions are almost universal when antibiotic therapy is instituted. (Courtesy, Professor D. A. Warrell.)



Fig. 1.98 Conjunctival haemorrhages in a patient with *B. recurrentis* infection.
This sign is commonly associated with severe louse-borne relapsing fever. (Courtesy, Professor D. A. Warrell.)

Downloaded from Vet-eBooks.com

Lyme Disease

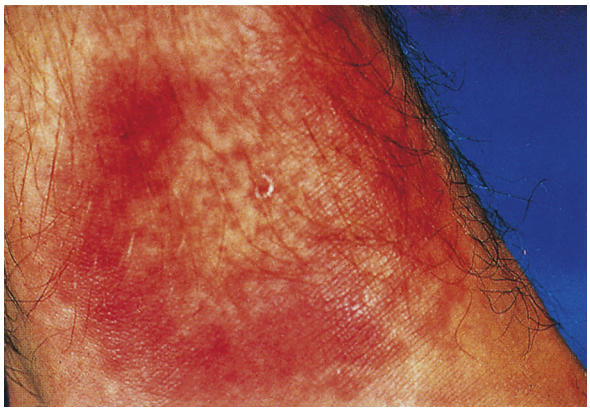


Fig. 1.99 Erythema chronicum migrans.
Lyme disease is caused by three closely related spirochaetes *Borrelia burgdorferi*, *B. afzelii* and *B garinii* and occurs in North America, Europe and Asia. It is transmitted by ixodid ticks with geographically variable mammalian hosts including rodents, birds and deer. Erythema chronicum migrans, the first sign of infection, manifests as a bull's eye rash that spreads slowly outwards from the site of tick bite. At this early stage in disease, serology is often negative, thus the patient should be treated empirically with doxycycline.



Fig. 1.100 Acrodermatitis chronica atrophicans.
This chronic cutaneous manifestation of Lyme is most common in Europe secondary to *B. afzelii* infection. The typical bluish-red inflammatory lesions with surrounding oedema are usually found on the extensor surfaces of the hands or feet and enlarge slowly over months or years. (Courtesy, Dr E. Asbrink. From Sivadas, R., Rahn, D. W., Luft, B. J. Lyme disease. In: Cohen, J., Powderly, W., eds. Infectious Diseases, 2nd edition. Edinburgh: Mosby; 2004, Pages 591–604.)

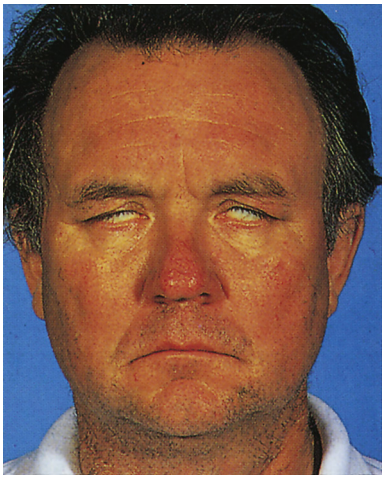


Fig. 1.101 Bilateral Bell's palsy lesion in Lyme disease.
Early disseminated Lyme disease can result in various neurological manifestations including a lymphocytic meningitis, radiculopathy or peripheral neuropathy. Unilateral facial nerve palsy is common but bilateral disease also occurs, such as in this 50-year-old German man. The differential diagnosis of bilateral facial nerve palsy further includes tuberculosis and sarcoid.

ARTHROPOD-BORNE PARASITIC INFECTIONS

Arthropods are also capable of transmitting various pathogenic protozoa and nematode infections. Many of these are on the WHO list of neglected tropical diseases and are subject to control or elimination programmes.

Malaria, transmitted by anopheline mosquitoes, remains endemic in 91 countries and responsible for more than 400,000 deaths per year. Babesia, a closely related parasite of red blood cells, occasionally causes tick-borne infection in temperate zones of the northern hemisphere.

Human African trypanosomiasis, or sleeping sickness, continues to cause disease in remote rural sub-Saharan Africa, but cases have significantly declined since the turn of this century. Cases of Chagas disease and leishmaniasis have also declined

Downloaded from Vet-eBooks.com

but their epidemiology is changing with international migration, HIV-AIDS and the increased use of immunosuppressive drugs.

Arthropod-transmitted nematode infections—lymphatic filariasis, onchocerciasis and loiasis—are diseases of the rural poor, predominantly in sub-Saharan Africa. Mass drug administration of preventative chemotherapy is significantly reducing their incidence and improving the economic and social prospects for people living in highly endemic areas.

Malaria

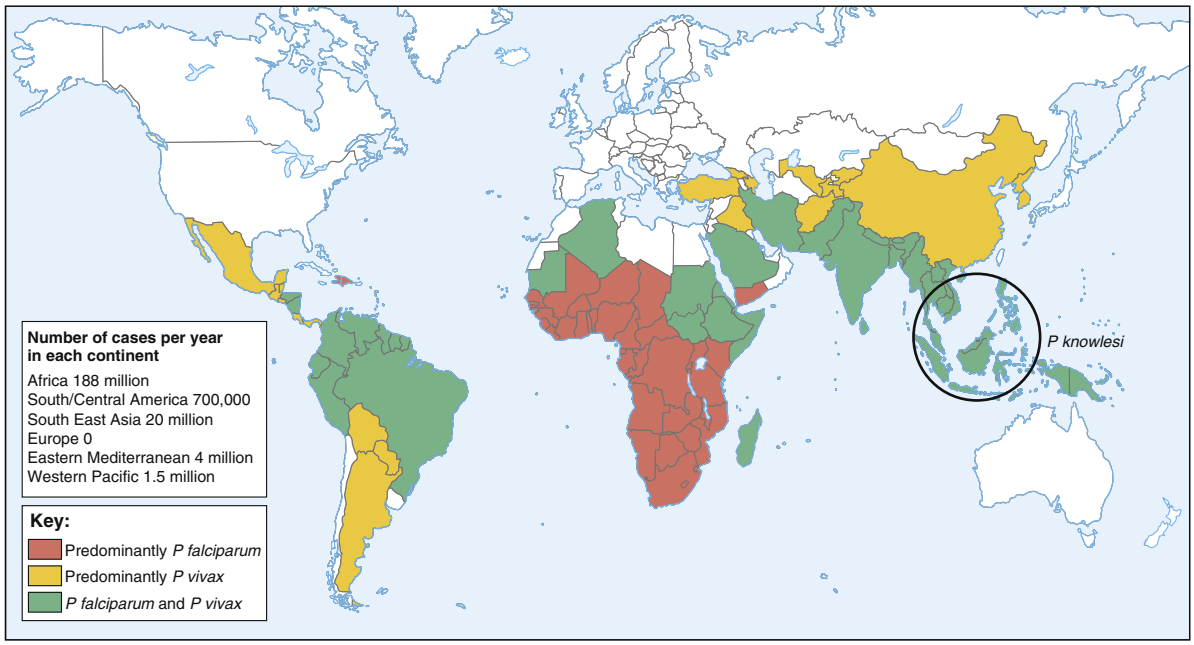


Fig. 1.102 The distribution of malaria.
Malaria is still widely distributed across the tropics, with an estimated 214 million cases and 438,000 deaths in 2015 alone. However, the global burden of malaria is falling. Since 2000, estimated cases and deaths worldwide have fallen by 18% and 48%, respectively. Eleven countries have eliminated the disease and 57 have reduced malaria by more than 75%. The majority of cases and deaths worldwide are caused by *P. falciparum*. *P. vivax* is the next most prevalent and, although often considered benign, can cause severe disease and death. *P. ovale* and *P. malariae*, endemic to Africa, Asia, Oceania and South America, are less common and cause a mild disease with low parasitaemia. *P. knowlesi* is a non-human primate parasite which has recently been identified as causing severe disease amongst human populations in Malaysian Borneo and the surrounding regions. (Adapted from RGA Feachem, AA Phillips, GA Targett (Eds.), Shrinking the Malaria Map: A Prospectus on Malaria Elimination, The Global Health Group, Global Health Sciences, University of California, San Francisco, San Francisco (2009) Fig_1.314.)

Downloaded from Vet-eBooks.com

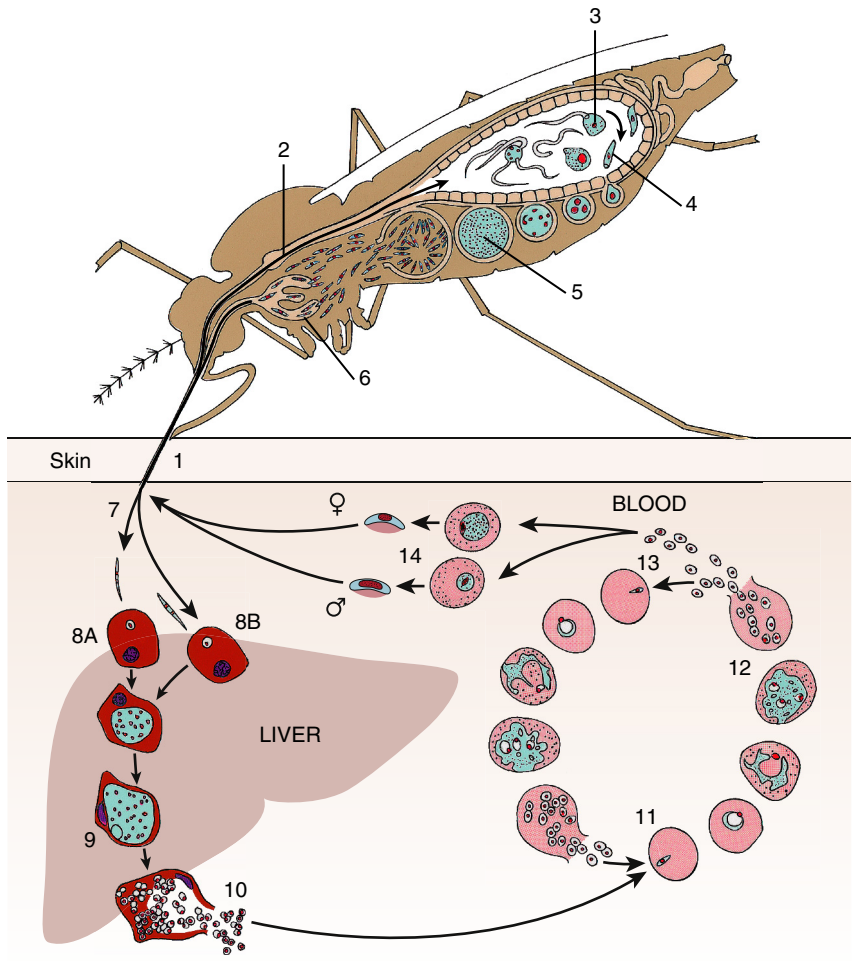


Fig. 1.103 Life cycle of malaria.
The female *Anopheles* mosquito takes a blood meal (1), ingesting male microgametocytes and female macrogametocytes into her stomach (2). The microgamete penetrates the macrogamete forming a zygote (3) which elongates to become a motile ookinete (4). This penetrates the mosquito midgut wall and develops into an oocyst containing several thousand sporozoites (5). After 7 to 20 days, the oocyst wall ruptures, releasing sporozoites which migrate into the mosquito's salivary ducts to be transmitted during the next feed (6).

Once injected into a human, the sporozoites (7) rapidly migrate to the parenchymal cells of the liver (8A) where they develop into large pre-erythrocytic schizonts over 6 to 14 days (9). The schizont then ruptures, releasing merozoites (10) which infect erythrocytes within the hepatic sinusoids. Within the erythrocyte, the merozoites become trophozoites (11) and then schizonts, (12) eventually rupturing to release further merozoites capable of infecting further erythrocytes (13). It is this erythrocytic stage of the cycle that causes clinical symptoms. Some parasites will differentiate into gametocytes, which pass the infection to mosquitos during a blood meal, thus perpetuating the cycle (14).

Note: In infections caused by *P. vivax* and *P. ovale*, some sporozoites remain latent in the liver as unicellular hypnozoites, capable of starting the process of pre-erythrocytic schizogony months or even years later (8B).

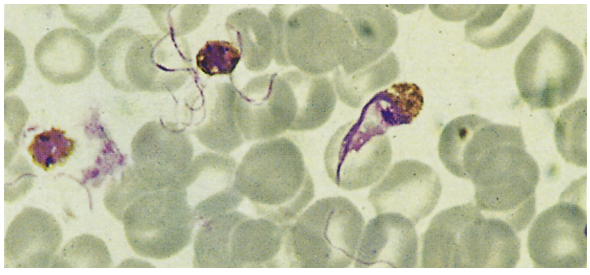


Fig. 1.104 Development of male gametes.
Male gametes develop in the midgut of the female anopheline by a process of flagellar extrusion (exflagellation), from microgametocytes contained in the blood meal. (x950.) (See stage 2, Fig. 1.103.)

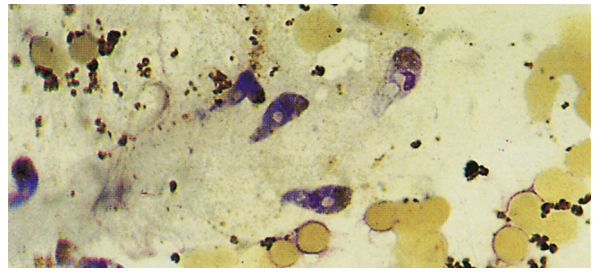


Fig. 1.105 Ookinetes in mosquito midgut.
Male and female gametes fuse to produce motile ookinetes, which enter midgut epithelial cells. (x950.) (See stages 3 and 4, Fig. 1.103.)

Downloaded from Vet-eBooks.com

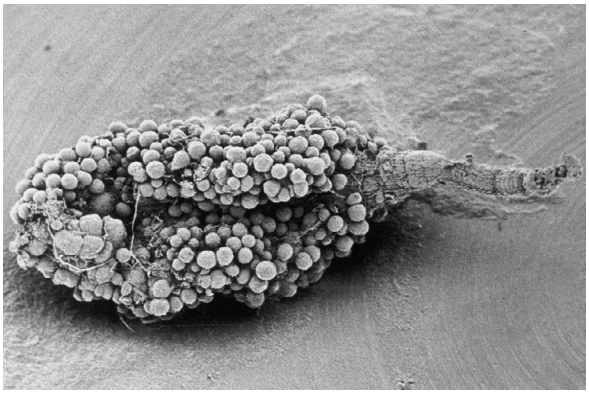


Fig. 1.106 Scanning electron micrograph of oocysts outside anopheline midgut.
Infective stages (sporozoites) develop in oocysts that lie on the outside of the mosquito midgut. (x65.) (See stage 5, Fig. 1.103.)

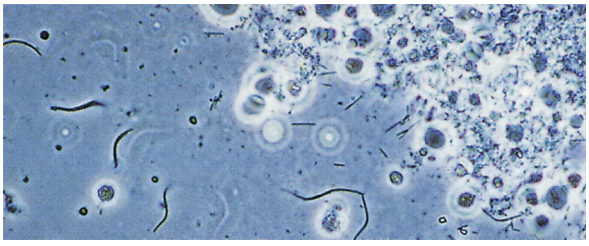


Fig. 1.107 Living infective sporozoites.
Bow-shaped sporozoites emerge from the oocyst and migrate to the salivary glands of the insect, ready for transmission to a human next time the mosquito takes a blood meal. (x370.) (See stage 6, Fig. 1.103.)

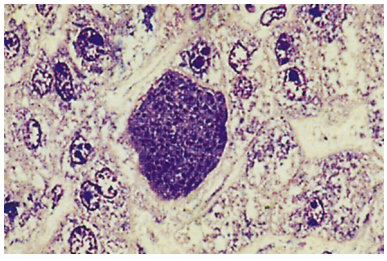


Fig. 1.108 Exoerythrocytic schizont of *Plasmodium malariae* in liver.
Within 30 minutes, the sporozoites enter the parenchymal cells of the host's liver. Here they develop into large pre-erythrocytic schizonts over 6–14 days before rupturing to release merozoites into the hepatic circulation. (Giemsa–colophonium technique x 350.) (See stages 8–10, Fig. 1.103.)

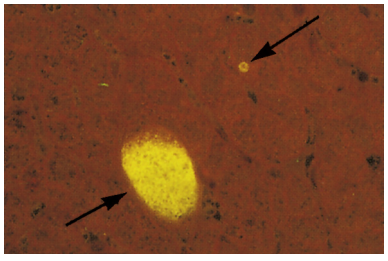


Fig. 1.109 Hypnozoite and preerythrocytic schizont in liver biopsy.
The unicellular, dormant hypnozoite (arrowed, right) stands in sharp contrast to the maturing pre-erythrocytic schizont (left) in this fluorescent-antibody-stained section of Rhesus monkey liver containing *Plasmodium cynomolgi*—a relapsing species of monkey malaria used as a model for human *P. vivax* infection. (x270.) (Courtesy, Dr W. A. Krotoski.)

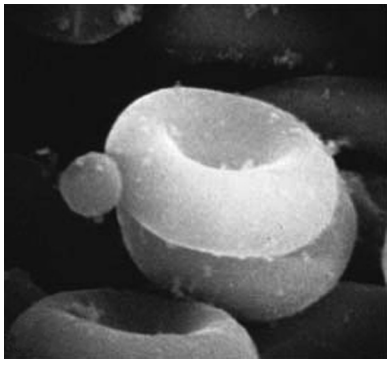


Fig. 1.110 A merozoite of *P. falciparum* attaches to an uninfected erythrocyte.
This scanning electron micrograph shows a merozoite of *P. falciparum* attaching to an uninfected erythrocyte. (See stages 10 and 11, Fig. 1.103.) (Courtesy, L. H. Bannister, Wellcome Trust International Health Image Collection.)

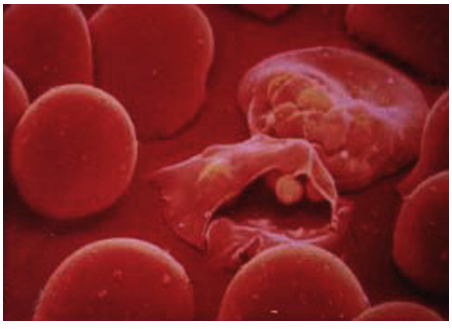


Fig. 1.111 Scanning electron micrograph of schizont rupture.
Here, a schizont of *P. falciparum* ruptures to release merozoites, which will then infect further erythrocytes. (See stage 13, Fig. 1.103.) (From Hoffman, S. et al. Malaria. In: Guerrant, R. L. (ed). Tropical Infectious Diseases: Principles, Pathogens and Practice, 3rd edition. © 2011, Elsevier Inc. All rights reserved. Figure 96.3.rd)

Downloaded From Vet-eBooks.com

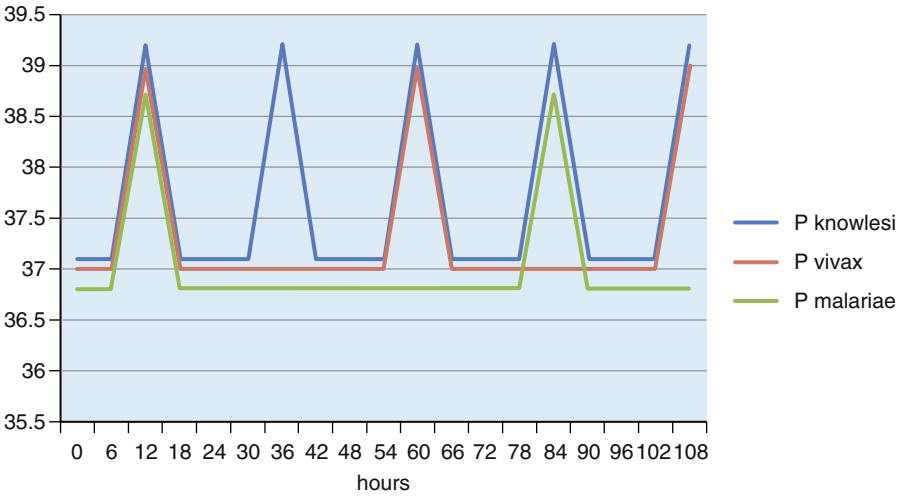


Fig. 1.112 Classic fever pattern in various malaria species.
Within the host, the intra-erythrocytic life cycle of the parasite shows some synchrony, with parasites maturing at roughly the same time. As fever occurs when schizonts mature, this results in characteristic fever patterns. *P. falciparum*, *P. vivax* and *P. ovale* require 48 hours to complete schizogony resulting in tertian periodicity. *P malariae* requires 72 hours giving a quartan fever (72 hours between paroxysms) while *P. knowlesi* requires 24 hours resulting in a quotidian fever (24 hours between paroxysms).

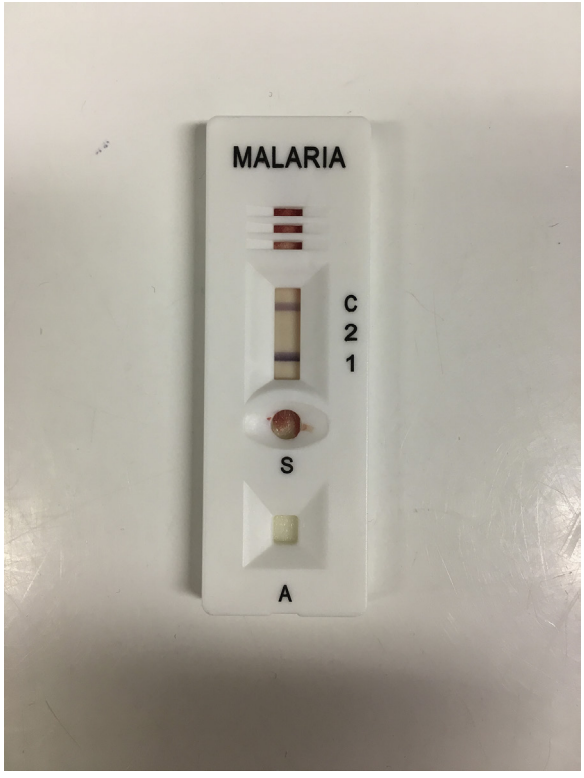


Fig. 1.113 Rapid diagnostic test (RDT) for malaria.
RDTs are increasingly used for the diagnosis of malaria in endemic and non-endemic areas. They are quick, easy to use, sensitive and require minimal laboratory infrastructure and operator training. RDTs are based on the detection of malarial antigens, usually histidine-rich protein 2 (HRP2), Plasmodium lactate dehydrogenase (pLDH) or aldolase. RDTs that are HRP2-based will only detect *P. falciparum* as the non-falciparum species do not produce this antigen; tests based on pLDH or aldolase will detect falciparum and non-falciparum species but are less sensitive than HRP2-based tests.

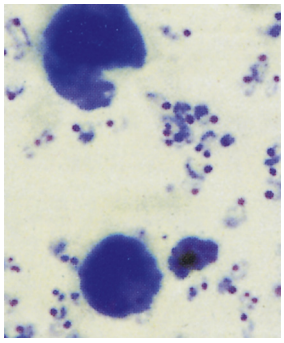


Fig. 1.114 Thick blood film.
Malaria films, stained with Giemsa, are still the gold standard of malaria diagnosis. Thick films, in which red cells are lysed, are more sensitive at detecting low parasitaemias but do not allow reliable speciation of the parasite or an estimate of parasite density to be made.

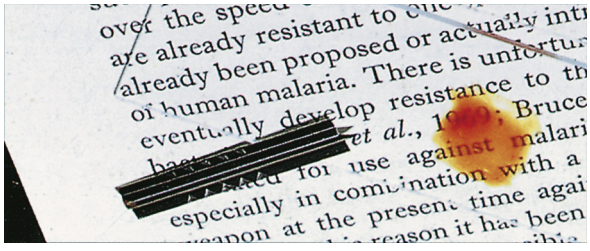


Fig. 1.115 Preparation of thick blood film for malaria.
Thick films are made by spreading two or three large drops of blood on a slide, then spreading them out with the corner of a second slide. The thick smear should still be sufficiently transparent to see print through it, as shown here. They are then dried and stained with Giemsa without fixation.

Downloaded from Vet-eBooks.com

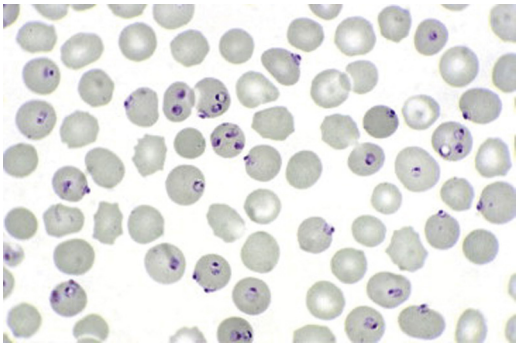


Fig. 1.116 Thin blood film.
The thin film is less sensitive at detecting low parasitaemias but allows reliable speciation of the parasite and estimation of parasitaemia. (From Gkrania-Klotsas, E. and Lever, A. An update on malaria prevention, diagnosis and treatment for the returning traveller. Blood Reviews, 2007-03-01, Volume 21, Issue 2, Pages 73–87. Copyright © 2006 Elsevier Ltd.)

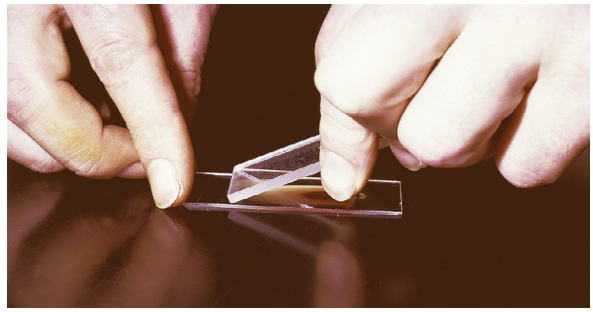


Fig. 1.117 Preparation of a thin blood film.
Thin films are made by placing a small drop of blood on a clean slide and pulling a second slide away from the drop. They are then air-dried, methanol-fixed and stained with Giemsa.

Plasmodium falciparum

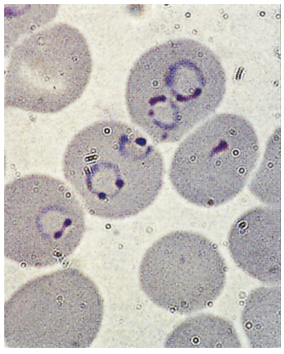


Fig. 1.118 Trophozoites of *P. falciparum*.

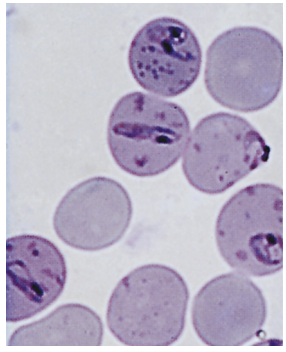


Fig. 1.119 Maurer's clefts and dots in *P. falciparum*.

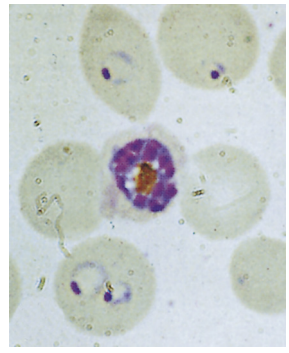


Fig. 1.120 Schizont of *P. falciparum*.

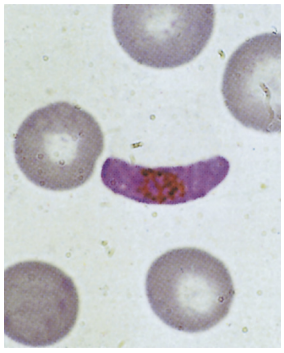


Fig. 1.121 Macrogametocyte of *P. falciparum*.
The red cell is of normal size but may contain multiple parasites. Trophozoites are fine and delicate and may have a double chromatin dot (Fig. 1.118). Basophilic clefts and spots of irregular shape and size (Maurer's clefts and dots) may be seen in erythrocytes containing more mature parasites (Fig. 1.119). Schizonts are uncommon in the peripheral circulation as they sequester to the post-capillary venules of internal organs. When seen, they are an ominous sign, indicating severe malaria. They are small, containing 8 to 32 merozoites and a single clump of dark pigment (Fig. 1.120). Gametocytes are a distinctive crescent shape with round or pointed ends, although oval forms are sometimes seen (Fig. 1.121).

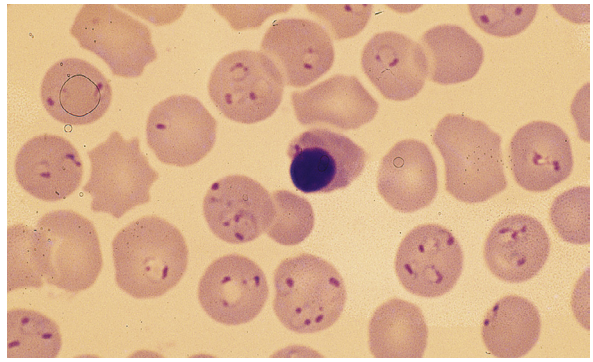


Fig. 1.122 Blood film from a patient with hyperparasitaemia in acute falciparum malaria.
This patient presented with jaundice and was initially mistakenly thought to have hepatitis. The blood films show 80% parasitaemia. Included is a late erythroblast, which has emerged from the bone marrow and is also interestingly infected with a ring form of *P. falciparum*. The patient died within half an hour of this blood film being made. (Leishman x 900.)

Downloaded From Vet-eBooks.com



Fig. 1.123 Malarial anaemia.
Malarial anaemia can cause severe morbidity and mortality in children and pregnant women. Its pathogenesis is multifactorial, involving destruction of parasitized cells, haemolysis of uninfected cells, splenic and hepatic sequestration and dyserythropoiesis. This young Kenyan boy with *P. falciparum* parasitaemia had profound anaemia. (Courtesy, Professor D. A. Warrell.)

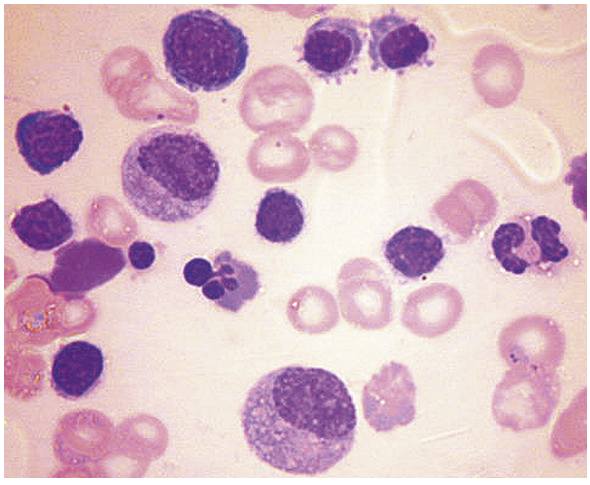


Fig. 1.124 Spleen smear showing association of dyserythropoiesis with malaria.
Although erythropoiesis is usually normoblastic in individuals with acute or chronic malaria, the examination of bone marrow frequently shows changes reflecting dyserythropoiesis such as the irregular nuclei and cytoplasmic bridges in erythroblasts seen in this figure. Two young rings of *P. falciparum* can be seen in an erythrocyte in this spleen. (Giemsa stain x 900.) (Courtesy, Dr S. Abdalla.)

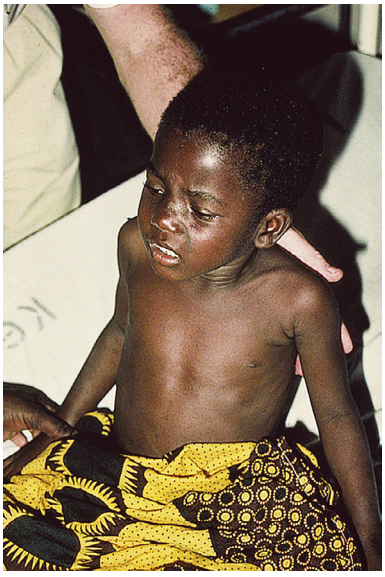


Fig. 1.125 Prostration in malaria.
A common manifestation of severe malaria in children is the inability to sit up and take fluid by mouth. Here a child with falciparum malaria, while fully conscious, is being supported to take water.



Fig. 1.126 Cerebral malaria in a comatose Malawian child.
Cerebral malaria commonly occurs in children between 6 months and 3 years of age in holoendemic areas. It may present with impaired consciousness, delirium or seizures. Hypoglycaemia may also cause seizures in malaria and should always be sought as it is rapidly treatable. The pathogenesis is multifactorial and includes impaired hepatic gluconeogenesis. (Courtesy, Professor M. Molyneux.)

Downloaded From Vet-eBooks.com

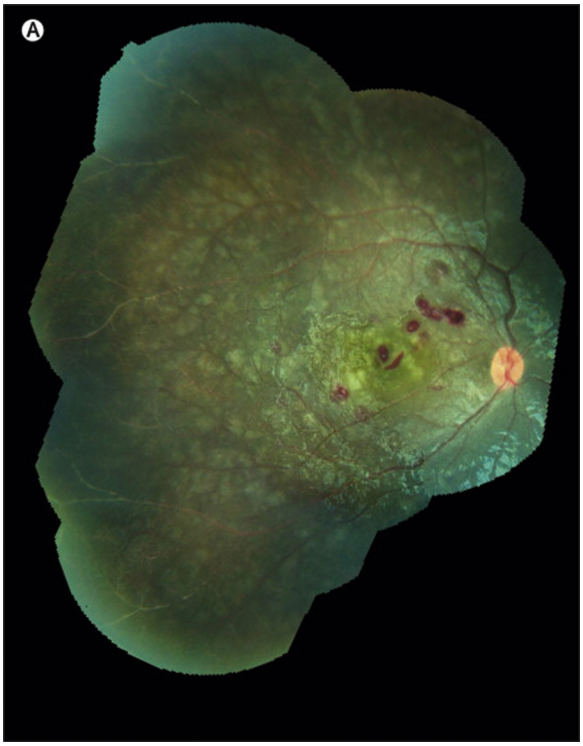


Fig. 1.127 Malarial retinopathy in a child with cerebral malaria.
This composite retinal photograph from a child with cerebral malaria shows the distinctive changes of malarial retinopathy, providing a window on disease effects upon the brain vasculature. Parasite sequestration and cytoadherence to the microvascular endothelium result in white-centred retinal haemorrhages. Poor capillary perfusion causes orange-white discoloration of the retinal vessels and macular and peripheral whitening from ischemia. Although the severity of malarial retinopathy is associated with increased length of coma and death, there is no residual effect on visual acuity or persistent retinal abnormalities in children who survive. (From Glover, S., Maude, R., Taylor, T., et al. Malarial retinopathy and fluorescein angiography findings in a Malawian child with cerebral malaria. Lancet Infectious Diseases, 2010, Volume 10, Issue 6, Pages 440–444, Panel A.)

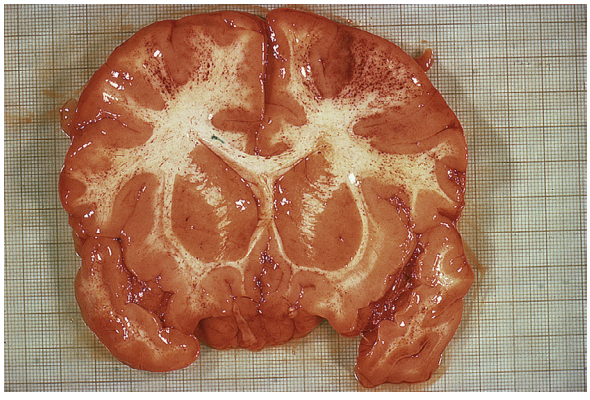


Fig. 1.128 Cross section of brain in cerebral malaria.
Many of the complications of malaria are due to cytoadherence of parasitized and non-parasitized erythrocytes to post-capillary venules in various organs. The resultant micro-infarcts, haemorrhage and capillary leak results in organ dysfunction. Petechial haemorrhages are clearly visible in this post mortem brain. (Courtesy, Dr R. Cooke.)

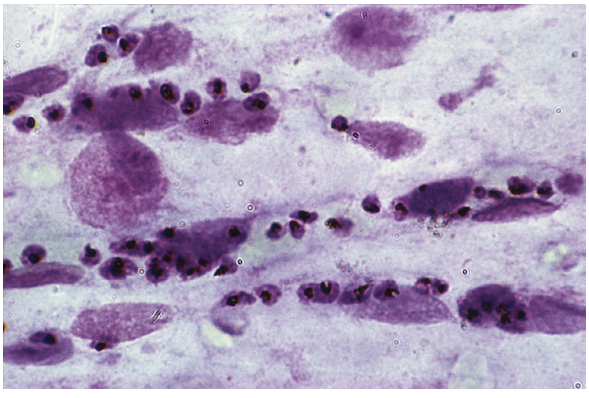


Fig. 1.129 Brain smear from a fatal case of cerebral malaria.
This brain smear was taken from a patient who died of cerebral malaria. The capillaries are full of erythrocytes containing maturing trophozoites and schizonts of *P. falciparum*. (Giemsa x 350.)

Downloaded from Vet-e-Books.com



Fig. 1.130 Severe malarial jaundice.
Jaundice, as seen in this Vietnamese man with falciparum malaria, occurs more commonly in adults than children. The aetiology is multifactorial and includes haemolysis with concurrent hepatocyte injury and cholestasis. However, fulminant liver failure, as seen in viral hepatitis, does not occur in malaria. (Courtesy, Professor D. A. Warrell.)

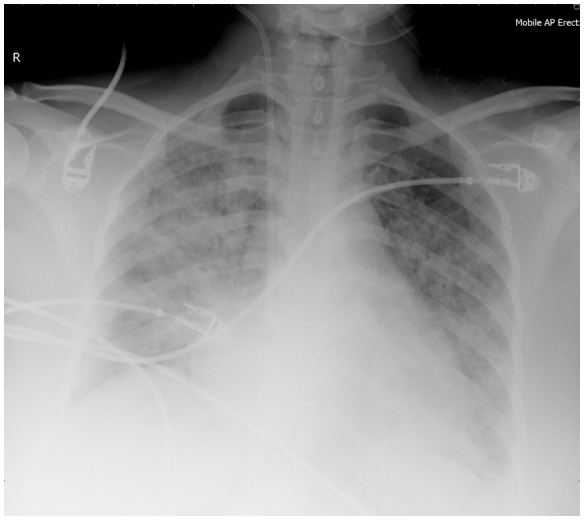


Fig. 1.131 Acute respiratory distress syndrome (ARDS) in a patient with severe malaria.
This patient with severe falciparum malaria developed acute pulmonary oedema on day 3 of presentation. Malarial ARDS occurs predominantly in adults and usually occurs after day 2 of presentation. It probably results from increased capillary permeability, but this is often exacerbated by overzealous fluid resuscitation. (Courtesy, Dr L. Nabarro.)



Fig. 1.132 Disseminated intravascular coagulation in falciparum malaria.
Bleeding into the skin is seen in this patient with disseminated intravascular coagulation secondary to severe malaria. He was thrombocytopenic with a prolonged prothrombin time, increased fibrinogen degradation products and hypofibrinogenaemia. He had no signs of cerebral malaria.



Fig. 1.133 Malarial haemoglobinuria 'blackwater fever'.
Massive haemolysis resulting in very dark urine may occur in severe malaria or in patients with G6PD deficiency exposed to oxidant drugs such as primaquine. Note the pale conjunctivae and the small volume of very dark urine passed by this Thai man with severe malaria. (Courtesy, Professor D. A. Warrell.)

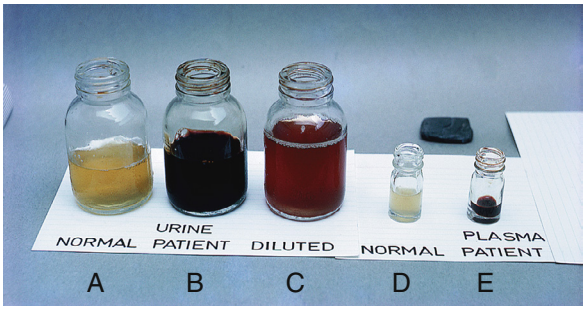


Fig. 1.134 Urine and plasma in blackwater fever.
The figure shows normal urine (A) compared with a specimen of urine from a patient with blackwater fever undiluted (B) and diluted (C). Also shown is a normal plasma sample (D) compared with that from a patient with blackwater fever (E).

Downloaded from Vet-eBooks.com

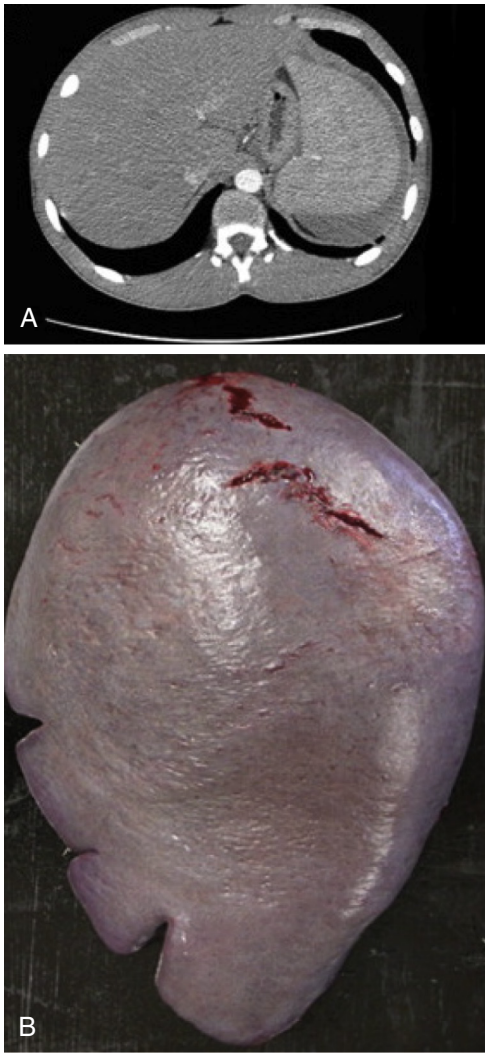


Fig. 1.135 Splenic rupture in a patient with falciparum malaria.
Splenic rupture is an unusual complication which may occur with all species of malaria. This Gabonese man presented with uncomplicated falciparum malaria. Abdominal CT showed splenomegaly with a perisplenic haematoma (A). The removed spleen was five times its normal weight with posterior and superior pole tears (B). (From Imbert, P., Rapp, C. and Buffet, P. Pathological rupture of the spleen in malaria: analysis of 55 cases (1958–2008). Travel Medicine and Infectious Disease, 2009-05-01, Volume 7, Issue 3, Pages 147–159, Figure 1. Copyright © 2009 Elsevier Ltd.)

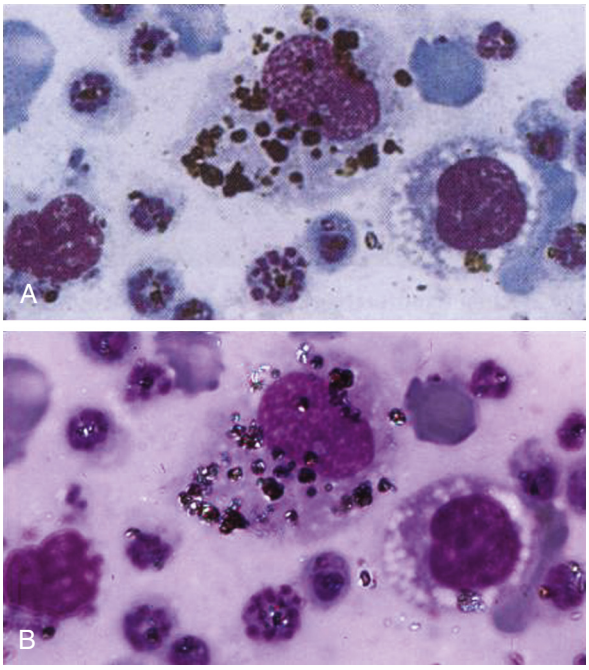


Fig. 1.136 A & B: Macrophage from the spleen of a patient with acute falciparum malaria.
Parasitized erythrocytes are removed from the peripheral circulation by macrophages in the reticuloendothelial tissues. Panel A shows a large monocyte/macrophage, which contains large quantities of malaria pigment (haemozoin), the residue from the digestion of infected red cells. The use of a polarizing filter (B) clearly reveals the haemozoin, which is birefringent, a technique particularly useful in material that contains only scarce parasites. (Giemsa x1500.)

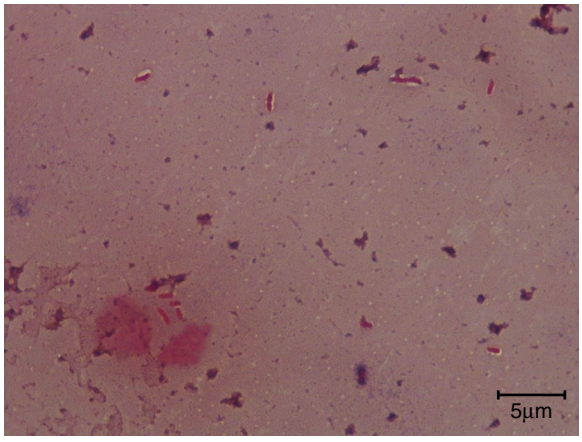


Fig. 1.137 Non-typhoidal *Salmonella* co-infection.
Co-infection with non-typhoidal *Salmonella* bacteraemia is a complication of severe malaria particularly occurring in children in sub-Saharan Africa. Note the Gram-negative rods in this blood culture isolate. Lack of blood culture facilities in many places mean that this diagnosis is often missed. (Courtesy, Dr S. De.)

Downloaded from Vet-eBooks.com

Plasmodium vivax

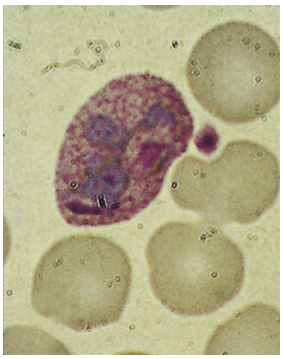


Fig. 1.138 Trophozoite of *P. vivax*.

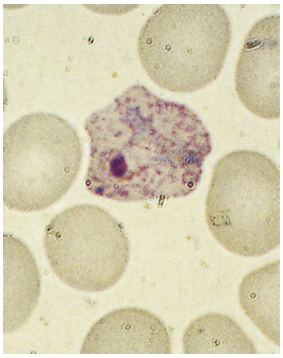


Fig. 1.139 Trophozoite of *P. vivax*.

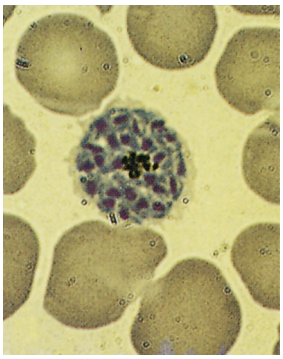


Fig. 1.140 Schizont of *P. vivax*.

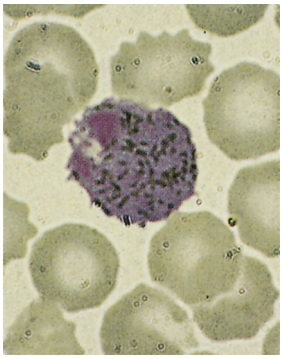


Fig. 1.141 Macrogametocyte of *P. vivax*.
P. vivax preferentially infects young erythrocytes so the host cell is usually enlarged. Uniform fine eosinophilic stippling (Schüffner's dots) is seen throughout the cell (Fig. 1.138). The trophozoites are large and messy (amoeboid) (Fig. 1.139). Schizonts may be seen in the peripheral circulation and are large, round or irregular. When mature, they contain 12–18 merozoites with a small amount of pigment (Fig. 1.140). Gametocytes are large and may be round or irregular in shape with Schüffner's dots and scattered pigment granules (Fig. 1.141). All stages of parasite appear in the peripheral circulation from young trophozoites to schizonts and gametocytes and parasitaemia rarely exceeds 2%.

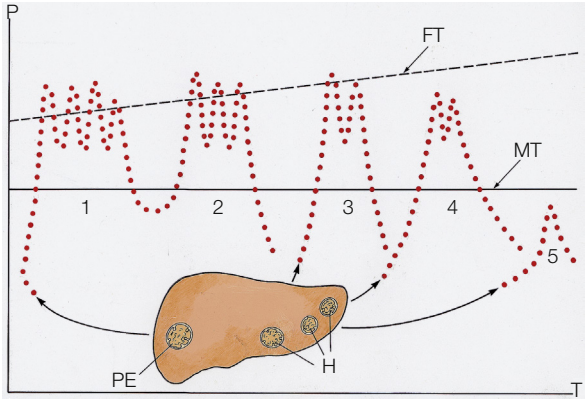


Fig. 1.142 Diagram of relapse patterns in vivax malaria.
Variations in parasitaemia (P) over time (T) after inoculation are shown. The primary attack (1) arises from the first generation of schizonts in the hepatocytes (pre-erythrocytic schizogony). One or more recrudescences (2) arise when subpatent intraerythrocytic asexual parasites escape the host immunity. True relapses (3, 4, 5, etc.), as opposed to recrudescences, occur when new generations of merozoites are later released from previously dormant hypnozoites (H) that undergo secondary schizogony in hepatocytes. In tropical areas, the first relapses may arise within 3–4 months of a primary attack but in subtropical areas, usually only after 9 months or more. The fever threshold (FT) rises with increasing immunity, i.e. the host tolerates the parasitaemia. Also, with increasing immunity, smaller numbers of merozoites survive in the erythrocytes and the infection may become subpatent (i.e. below the microscopic threshold—MT), although still present. Most *P. vivax* infections will die out within 1–3 years, even if untreated.

Downloaded from Vet-eBooks.com

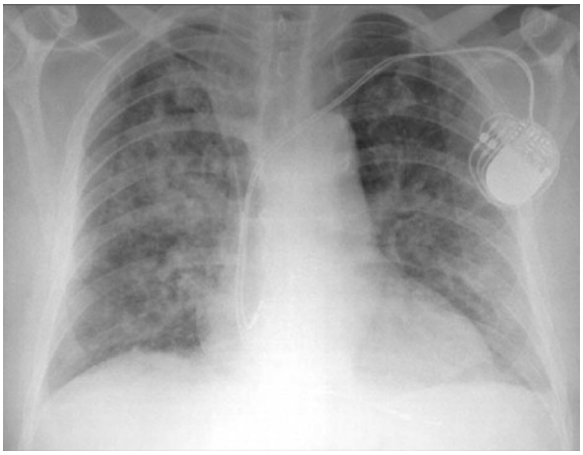


Fig. 1.143 Acute respiratory distress syndrome (ARDS) in a traveller with *P. vivax* infection.
Although non-falciparum malarias are historically referred to as benign, life-threatening infection can occur with *P. vivax*. This man developed ARDS on day 3 of treatment with chloroquine. Other (uncommon) complications of *P. vivax* include severe anaemia, haemophagocytosis and renal failure. (From Tan, L., Yacoub, S., Scott, S., et al. Acute lung injury and other serious complications of *Plasmodium vivax* malaria. Lancet Infectious Diseases, 2008-07-01, Volume 8, Issue 7, Pages 449–454, Figure 1. Copyright © 2008 Elsevier Ltd.)

Plasmodium ovale

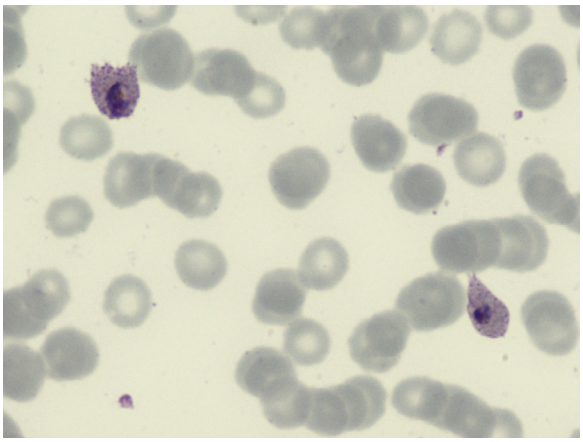


Fig. 1.144 Oval and fimbriated cells containing trophozoites of *P. ovale*. (Courtesy, H. Edwards.)

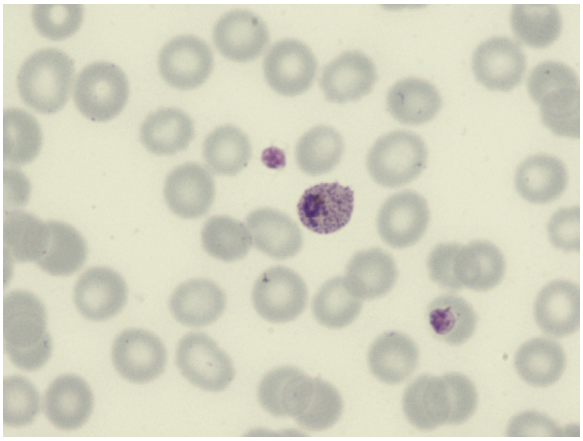


Fig. 1.145 Trophozoite of *P. ovale*. (Courtesy, H. Edwards.)

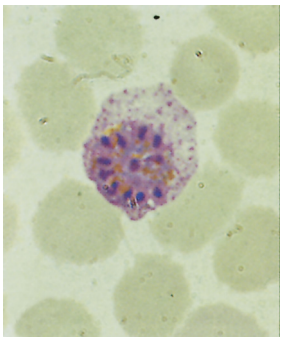


Fig. 1.146 Schizont of *P. ovale*.

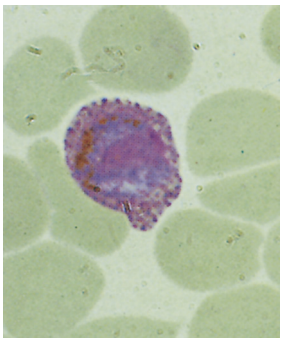


Fig. 1.147 Microgametocyte of *P. ovale*.
The host red cell, usually younger and enlarged as with *P. vivax*, may be oval (hence the name) but can also appear irregular with ragged (fimbriated) ends (Fig. 1.144). Schüffner's dots, known here as James' stippling, may be seen in the cytoplasm (Fig. 1.144/5). The trophozoites are small, neat and compact with a prominent nucleus (Fig. 1.145). They are similar to those of *P. malariae* but contain less pigment. Parasitaemia rarely exceeds 2%. Schizonts may appear in the peripheral circulation and are small, containing 8–14 merozoites (Fig. 1.146). Gametocytes are small and round with a nucleus that may lie to one side. They are difficult to distinguish from late stage trophozoites (Fig. 1.147).

Downloaded From Vet-eBooks.com

Plasmodium malariae

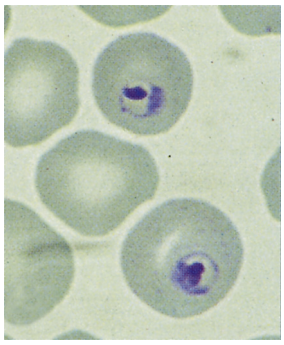


Fig. 1.148 Trophozoites of *P. malariae*.

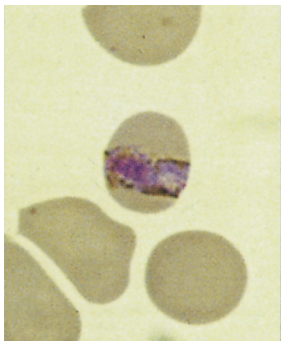


Fig. 1.149 Band form trophozoite of *P. malariae*.

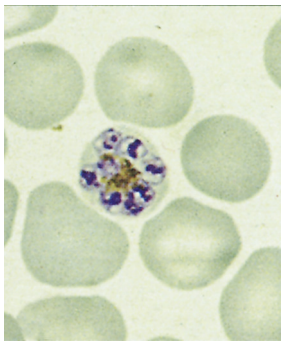


Fig. 1.150 Schizont of *P. malariae*.

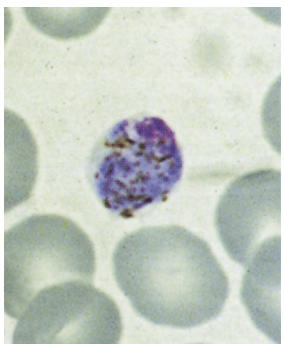


Fig. 1.151 Macrogametocyte of *P. malariae*.
The host red cell is of normal or reduced size with no Schüffner's dots or Maurer's clefts. Trophozoites are thick and compact with lots of yellow-brown pigment (Fig. 1.148). Band forms and bird's eye forms may be present (Fig. 1.148/9). Parasitaemia rarely exceeds 1%. Schizonts, which may be seen in the peripheral circulation, are neat, fill the host red cell and have up to 10 merozoites when mature. They contain copious pigment (Fig. 1.150). Gametocytes are small, round and compact, containing a blackish pigment. They are difficult to distinguish from late-stage trophozoites (Fig. 1.151).



Fig. 1.152 Child with nephrotic syndrome due to *P. malariae* infection (Quartan nephropathy).
Children repeatedly or continuously infected with *P. malariae* may develop a chronic immune complex nephropathy. This West African child has full-blown nephrotic syndrome with pallor, peripheral oedema and an abdomen distended by ascites. Treatment with antimalarials does not prevent progression.

Downloaded from Vet-eBooks.com

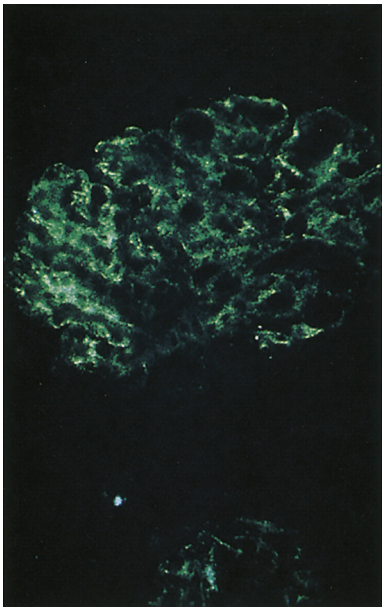


Fig. 1.153 Immune complex deposition in Quartan nephropathy.
Immunofluorescent antibody staining demonstrates the deposition of immune complexes on the basement membrane of the glomeruli in quartan malarial nephrosis. (x 350.)

Plasmodium knowlesi

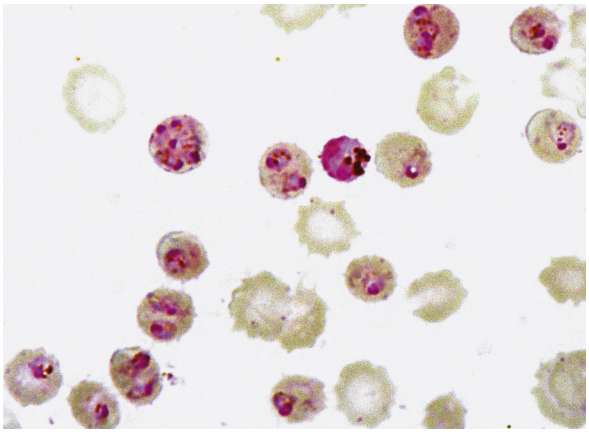


Fig. 1.154 A heavy infection with *P. knowlesi*.
P. knowlesi is morphologically similar to *P. malariae* and is difficult to distinguish on thin film examination alone. However, as *P. knowlesi* only requires 24 hours to complete schizogony, infections can be severe and parasitaemia may exceed 2%. The heavy infection in this thin blood film in a patient from Sarawak shows a typically asynchronous infection containing most of the asexual stages and a macrogametocyte. (Courtesy, Dr D. Sung.)



Fig. 1.155 *Macaca fascicularis*, the normal host of *P. knowlesi*.
P. knowlesi is principally a parasite of macaques found in Southeast Asia. However, deforestation and environmental change have resulted in increasing numbers of cases in humans. It is now the most common species of malaria in Malaysian Borneo.

Chronic Complications of Malaria



Fig. 1.156 New Guinea child with grossly enlarged spleen.
The highlands of Papua New Guinea have the highest global incidence of hyper-reactive malarial splenomegaly (HMS), previously known as tropical splenomegaly syndrome. Repeated or persistent malaria infection, usually with *P. vivax* or *P. malariae*, result in overproduction of polyclonal IgM, immune complex formation and progressive splenic hyperplasia. Patients develop abdominal distension, hypersplenism and increased susceptibility to bacterial infections. HMS may also be associated with lymphoma.

Downloaded from Vet-eBooks.com

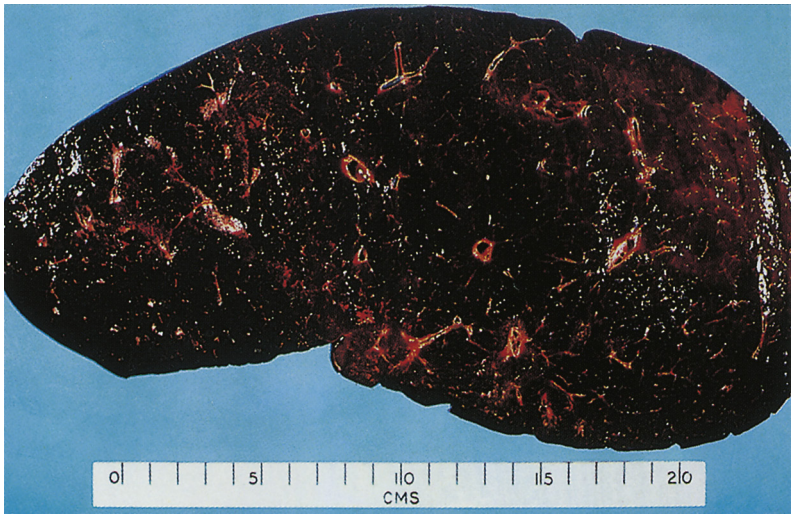


Fig. 1.157 Massive spleen in hyper-reactive malarial splenomegaly.
Regression of the enlarged spleen may occur with long-term antimalarial prophylaxis. Splenectomy should be considered if treatment fails or in cases of severe hypersplenism. (Courtesy, Professor M. S. R. Hutt.)



Fig. 1.158 Liver in chronic malaria.
In chronic infection, accumulation of malaria pigment (haemozoin) in the macrophages produces a dark brown discolouration of the liver and spleen. (Courtesy, Professor S. Lucas.)



Fig. 1.159 Malaria in pregnancy.
Pregnant women are at increased risk of malaria and are more likely to develop complications including anaemia, pulmonary oedema and hypoglycaemia. Premature and low birth weight neonates are common, particularly in first pregnancies. The WHO recommends intermittent preventive treatment in pregnancy (IPTp) for all pregnant women in holoendemic regions, but uptake is poor in many sub-Saharan African countries. (From Chico R.M., Moss, W.J. Prevention of malaria in pregnancy: a fork in the road? Lancet 386 (10012) Pages 2454-2456. Copyright Elsevier 2015.)

Downloaded From Vet-eBooks.com

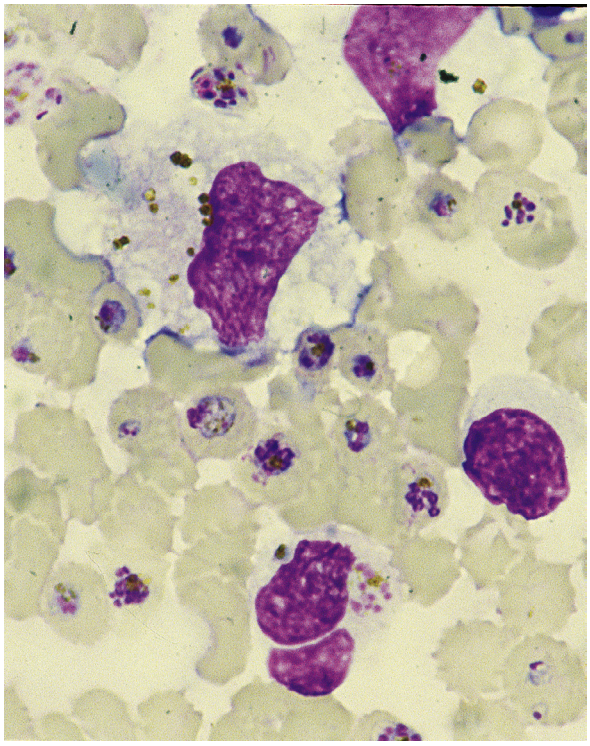


Fig. 1.160 Placental smear with *P. falciparum* schizonts and macrophage.
Placental sequestration of parasites results in placental insufficiency and foetal growth retardation. Note the presence of haemozoin granules in the macrophage. Pigment-loaded macrophages and neutrophils in the peripheral circulation usually indicate that the blood infection has been present for some days. (Giemsa x 900.)

Malaria Treatment



Fig. 1.161 Flowers of *Cinchona ledgeriana*, the source of quinine.
A young plant growing in a plantation in Madagascar. Quinine and related alkaloids are harvested from the bark of the Cinchona tree. Until the introduction of artesunate, quinine was the most effective and widely used antimalarial worldwide. Treatment is associated with hypoglycaemia and cinchonism, a complex of symptoms including tinnitus, disturbed vision and dizziness.

Downloaded From Vet-eBooks.com



Fig. 1.162 *Artemisia annua*.
The leaves of the sweet wormwood plant *Artemisia annua* have been used in China for thousands of years for treatment of fever. Derivatives of this are now used parenterally to treat severe malaria and are superior to quinine with more rapid parasite clearance and reduced mortality in adults and children. Oral artemisinin-based combination therapies can be used in uncomplicated malaria but should be used in combination with a second drug such as lumefantrine or amodiaquine to prevent the emergence of resistance. Delayed parasite clearance time is increasingly seen in South East Asia associated with point mutations in the Kelch 13 protein. (Copyright © 2010 Science Photo Library.)

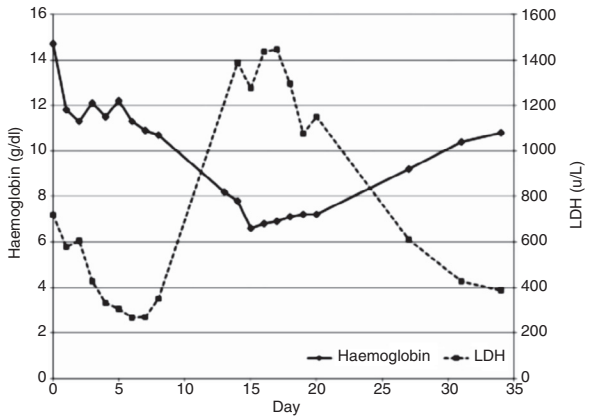


Fig. 1.163 Delayed haemolysis, a late complication of artemisinin drugs.
Artemisinin drugs are usually well tolerated, with none of the unpleasant side effects of parenteral quinine. However, there is increasing recognition of an association with delayed haemolysis, which occurs in 7% to 23% of people following treatment of severe malaria. This typically occurs two to three weeks after treatment, and anaemia is associated with a concurrent rise in lactate dehydrogenase. (From Rolling, T., Agbenyega, T., Krishna, S., et al. Delayed haemolysis after artesunate treatment of severe malaria- review of the literature and persepective. Travel Medicine and Infectious Disease, 2015, Volume 13, 2, Pages 143–149, Figure 1.)



Fig. 1.164 Long-lasting insecticide-treated nets.
Insecticide-treated bed nets have been the greatest contributor to the rapid reduction in malaria incidence seen in recent years. The insecticide-treated net around a sleeping human works as a baited trap. Contact with the insecticide shortens the life span of mosquitoes attracted to attempt a blood meal. This reduces the likelihood that mosquitoes will survive the requisite time to complete the *Plasmodium* life cycle. Thus bed nets directly protect individuals sleeping under them and indirectly protect other members of the community in which bed nets are deployed. (Courtesy, Dr J. R. Lucas.)

Downloaded from Vet-eBooks.com

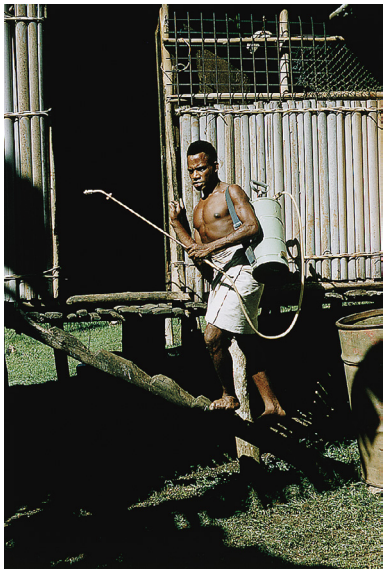


Fig. 1.165 Indoor residual spraying (IRS) in malaria control.
The ambitious global programme that started in the 1950s to eradicate malaria by spraying the inside of all dwellings in endemic areas with long-lasting insecticides such as DDT failed to meet its objective in all but a few areas. IRS is still an effective way to control malaria, but the high level of coverage required to confer community protection comes with considerable logistical difficulties.



Fig. 1.166 Insecticide resistance in Africa.
All major malaria vector species now exhibit some resistance to insecticides with less than 90% mosquito mortality after exposure to a discriminating dose. The epidemiological scale of this problem is unclear, as many countries do not routinely test for insecticide resistance. Here, red dots show pyrethroid-resistant populations of *Anopheles* whilst green dots show susceptible populations. (Reproduced from IR Mapper (www.irmapper.com), by permission of IR Mapper, October, 2014.)

Babesiosis

Babesiosis is a tick-borne mammalian parasite that infects erythrocytes. Humans are dead-end hosts and acquire infection from the bite of an infected tick. Sporozoites are injected by the infected tick during a blood meal. These directly invade erythrocytes producing ring forms and then undergo multiplication by budding to form merozoites. Ring forms may look much like malaria except that pigment is not formed in *Babesia*-infected cells and there is no change in erythrocyte morphology or staining.

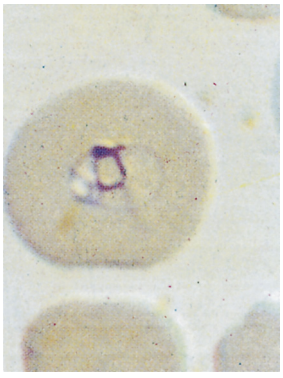


Fig. 1.167 Thin film of *Babesia microti*.
Babesia microti is the principal species found in the United States. It can cause clinical infection in patients with normal spleens, and co-infection with *Borrelia burgdorferi* (which shares the same tick vector) has also been described. Note the small, neat, round parasites and the absence of haemozoin pigment. Exo-erythrocytic parasites may be seen in high parasitaemias. (Courtesy, Professor G. Wernsdorfer.)

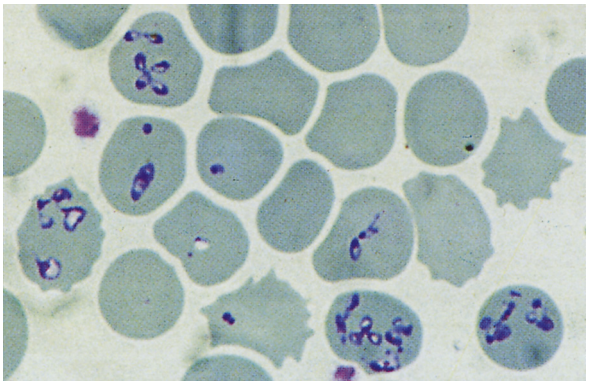


Fig. 1.168 Thin film of *Babesia divergens*.
Babesia divergens is the commonest *Babesia* species in Europe. Most identified infections occur in splenectomized individuals who may become severely unwell with parasitaemias over 50% in some cases. Note the presence of multiparasitized erythrocytes. The 'Maltese cross' in the upper left corner occurs when ring forms divide into merozoites which are arranged in tetrads.

Downloaded from Vet-e-Books.com



Fig. 1.169 *Ixodes scapularis.*
Ixodes scapularis is the principal vector of *B. microti* in the USA. They feed on the white-footed mouse and white-tailed deer. Most human infections occur in summer months from the bite of infected nymphs. (Courtesy, S. McIntyre.)

Human African Trypanosomiasis

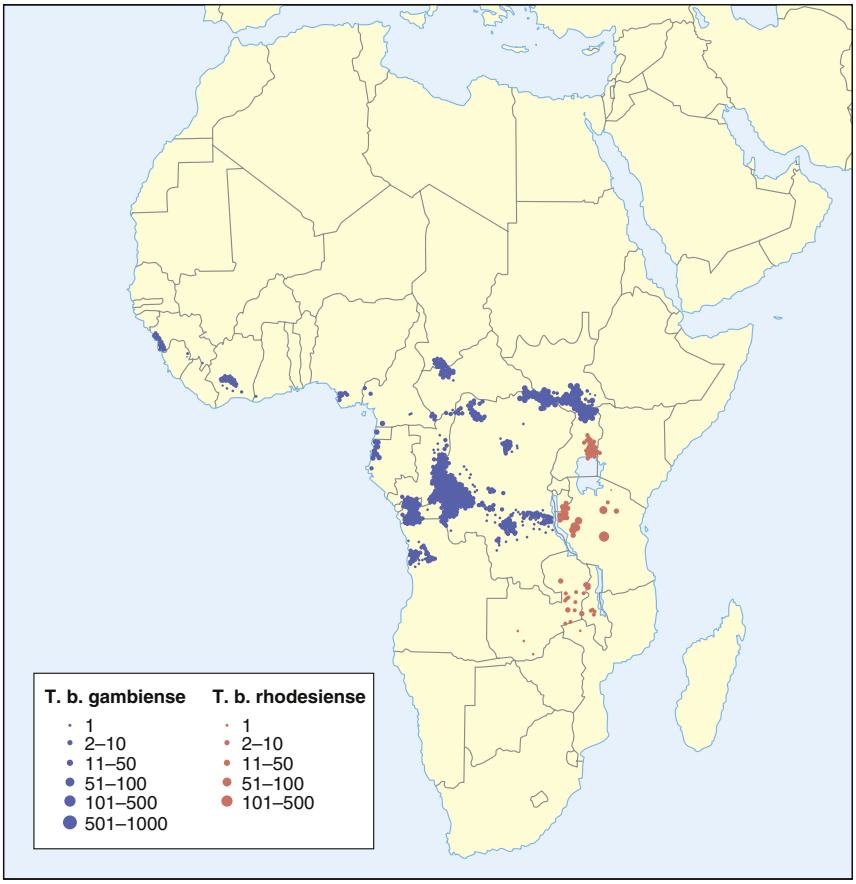


Fig. 1.170 Distribution of human African trypanosomiasis (HAT) infection.
HAT transmission is confined to equatorial Africa and has a patchy distribution. It is caused by two subspecies of *Trypanosoma brucei* which cause different clinical syndromes. Ninety-eight per cent of reported cases are due to *T. b. gambiense* infection which occurs in West and Central Africa and is transmitted by riverine species of tsetse fly (*Glossina spp.*). Seventy per cent of *T. b. gambiense* cases occur in the Democratic Republic of the Congo (DRC). The remaining 2% cases are caused by *T. b. rhodesiense* in East Africa and are transmitted by savannah species of tsetse fly. Uganda is the only country with human cases of both species, although (as of 2016) these occur in geographically distinct zones. (From Krisha, S., Stitch, A. African Trypanosomiasis. In: Hunter's Tropical Medicine and Emerging Infectious Diseases. Pages 718–724, Figure 97.2. Copyright © 2013 Elsevier Inc. All rights reserved.)

Downloaded From Vet-eBooks.com

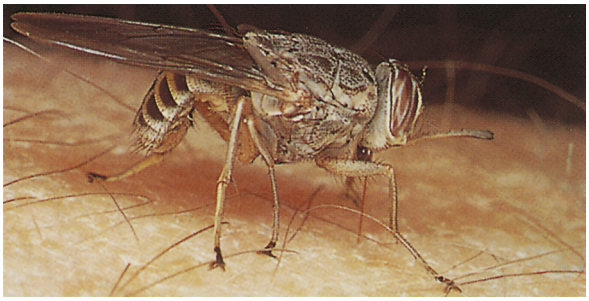


Fig. 1.171 Tsetse fly feeding.
Glossina palpalis is the major vector of *T. b. gambiense*. Although both anthropophilic and zoophilic, it prefers to feed on humans. It inhabits humid, riverine environments and typically bites humans when bathing in small rural rivers. *Glossina morsitans* is the main vector of *T. b. rhodesiense*. It inhabits the savannahs of East Africa and is mainly zoophilic, feeding on wild and domestic mammals.



Fig. 1.172 Larva (white), pre-pupa (red) and pupa (black) of *Glossina morsitans*.
Tsetse flies have an unusual lifecycle. The female tsetse fly mates only once. The larva develops within the uterus of the fly and is then released to pupate underground. After 30 days the adult fly emerges from the pupa. Despite only mating once, the mother continues to produce larvae every 9 days or so producing three to five in her 3-month life span. The whole life cycle takes around 50 days in total, and so tsetse populations grow slowly. As a result, and importantly for vector control, even a small increase in tsetse mortality rate may have a large effect on tsetse population size.



Fig. 1.173 Tsetse fly emerging from its pupa.
Larvae pupate underground. The adult fly emerges from the pupa after 30 days. (© IRD-Cirad Luc Riolon.)



Fig. 1.174 Domestic cattle infected with *Trypanosoma brucei rhodesiense*.
Chronic infection with trypanosomes of the *T. brucei* complex results in progressive emaciation, as seen in these cattle on a central African farm. This places a serious burden on the rural economy and increases the problem of protein malnutrition in many communities.



Fig. 1.175 *Trypanosoma brucei gambiense* transmission site.
Transmission of *T. b. gambiense* to humans typically occurs around rivers during bathing, washing and other daily tasks. (From Burri, C. Human African trypanosomiasis. Manson's Tropical Diseases, Volume 45, 606–621, Figure 45.5.)

Downloaded from Vet-eBooks.com

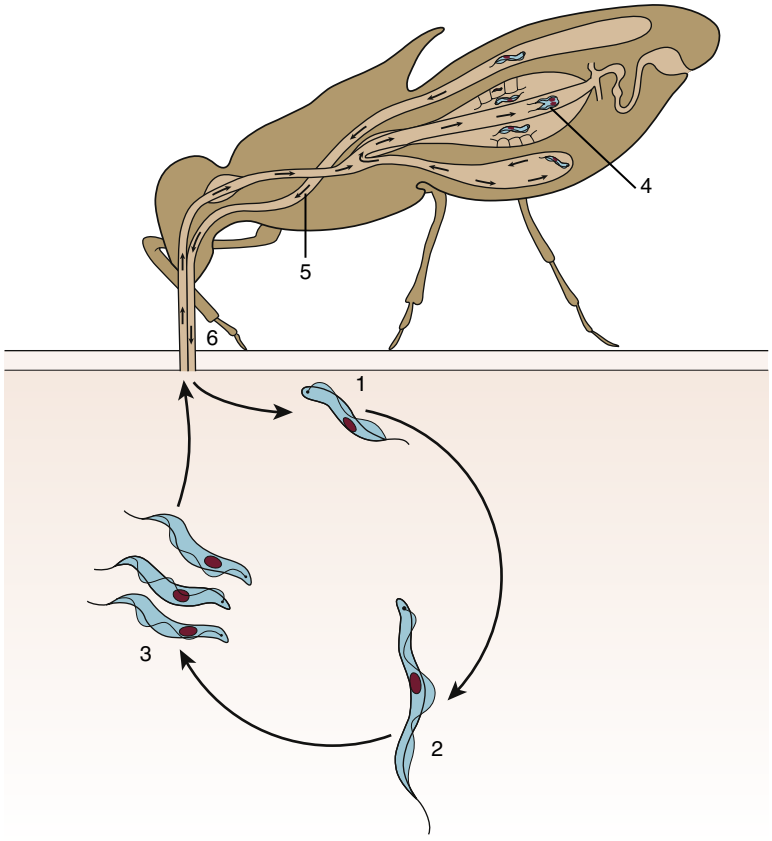


Fig. 1.176 Life cycle of African trypanosomiasis in humans and reservoir hosts.
The tsetse fly injects metacyclic trypomastigotes into the skin during a blood meal (1). These transform into bloodstream trypomastigotes and spread via the bloodstream and lymphatics to various organs (2). Multiplication by binary fission occurs in the blood, the lymphatics and extravascular tissues (3). A feeding tsetse fly ingests bloodstream trypomastigotes. Over a period of three weeks, these first transform into procyclic trypomastigotes in the tsetse midgut and multiply by binary fission (4). They then transform into epimastigotes, which migrate to the salivary glands (5), multiply again then convert back to metacyclic trypomastigotes to be injected during a blood meal (6).

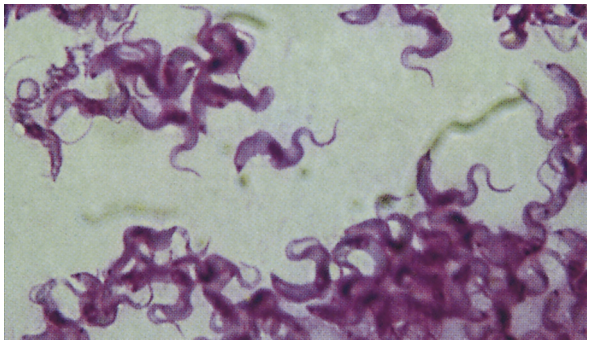


Fig. 1.177 Metacyclic trypomastigotes in salivary probe.
Metacyclic trypomastigotes, the infective stage, are passed with saliva into the skin when the tsetse fly feeds. (x900.)

Downloaded From Vet-eBooks.com



Fig. 1.178 Original illustration of *Trypanosoma (Trypanozoon) brucei gambiense* in human blood stained with Romanowsky stain by J. Everett Dutton.
Polymorphic trypanosomes were first discovered more than a century ago, in 1895, by Sir D. Bruce in the blood of domestic cattle suffering from the wasting disease nagana in South Africa. The first observation of these protozoa in humans was by R. M. Forde, who noted, in 1902, 'small worm-like, extremely active bodies' in the blood of a sick European seaman in the Gambia. Note the central nucleus, the grainy cytoplasm and the small posterior kinetoplast from which a single flagellum extends forward, along the undulating membrane, to form a free anterior flagellum. Trypanosomes are characteristically pleomorphic, measuring between 18 and 35 μm. (Courtesy, Director, Liverpool School of Tropical Medicine.)



Fig. 1.179 Chancre of *Trypanosoma brucei rhodesiense*.
A trypanosomal chancre may develop at the site of tsetse bite due to multiplication of the parasite within the skin. It is more commonly seen in *T. b. rhodesiense* than in *T. b. gambiense*. It may be mistaken for a furuncle or cellulitis but is usually painless and may be associated with regional lymphadenopathy. This man returned to the UK from a safari holiday in the Serengeti in Tanzania and recalled painful bites from persistent flies that were hard to kill. (Courtesy, Professor D. A. J. Moore)



Fig. 1.180 Trypanosomal rash.
T. b. rhodesiense presents as an acute febrile illness which untreated will progress rapidly to neurological impairment and death. In fair-skinned individuals, a rash may be visible during fever spikes as seen in this patient who had been febrile for 6 days. Other early symptoms include headache and muscle pain. Patients may develop a severe perimyocarditis which can be fatal before the neuropsychiatric features of the second stage develop. (Courtesy, Professor A. Bryceson.)

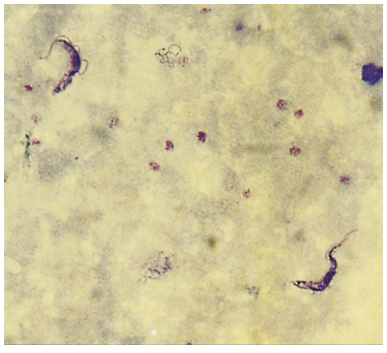


Fig. 1.181 *Trypanosoma brucei rhodesiense* in human blood.
Thick films stained with Giemsa or direct thin films may reveal the presence of trypanosomes in the blood. They are most commonly seen in the early stages of infection with *T. b. rhodesiense* as this subspecies is associated with acute disease and higher parasitaemias. The two subspecies are virtually indistinguishable on blood smear. Epidemiological exposure and clinical history may suggest one subspecies or other and molecular techniques can provide definitive identification. (Courtesy, Dr D. A. T. Baldry.)

Downloaded from Vet-eBooks.com

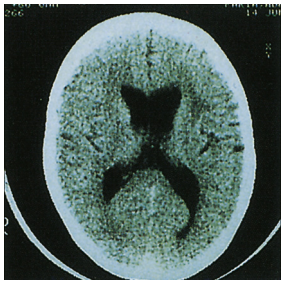


Fig. 1.182 Cerebral changes in *Trypanosoma brucei rhodesiense* infection.
Computed tomography may show evidence of cerebral involvement prior to treatment. Atrophic changes with hydrocephalus are seen in the scan of this young child 9 months after clinical cure. (Courtesy, Dr J. L. Champalimaud.)



Fig. 1.183 Cervical lymphadenopathy in a patient with *Trypanosoma brucei gambiense*.
T. b. gambiense is associated with a more chronic and indolent course with a mean first-stage duration of 526 days and second-stage duration of 252 days. Enlargement of lymphatic glands, especially in the posterior triangle of the neck (the notorious 'Winterbottom's sign'), is an important clinical feature of infection and calls for diagnostic lymph node aspirate.



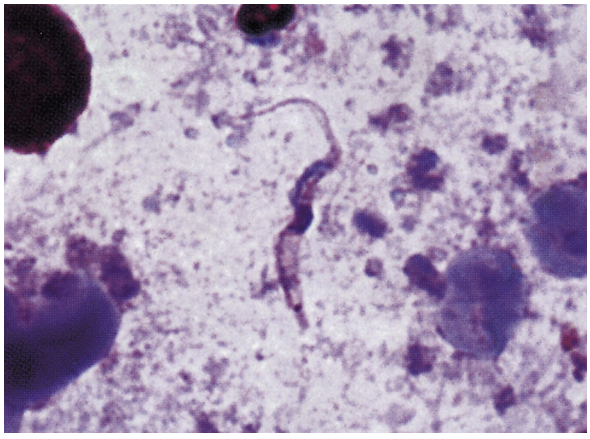


Fig. 1.184 Trypanosome in lymph node fluid.
The trypanosomes are easily identified as actively motile organisms in the wet preparation of aspirated gland fluid. (Giemsa x 1650.)

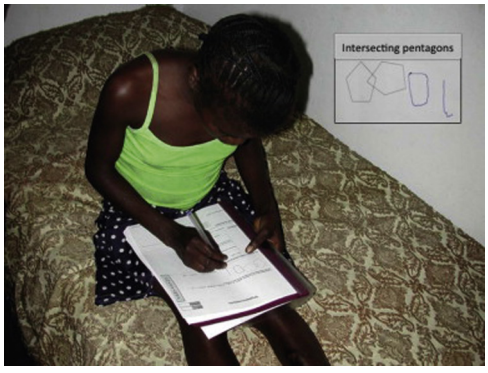


Fig. 1.185 Neurological dysfunction in late-stage trypanosomiasis.
The meningoencephalitic stage of West African trypanosomiasis is insidious in onset. Some patients present with mood disorders which may be misdiagnosed as psychiatric illness. Patients may become agitated and have difficulty in completing simple tasks. Seizures, motor weakness and abnormal movements are common in late disease. This child with late-stage human African trypanosomiasis was unable to copy intersecting pentagons (inset). (From Krishna, S., Stich, A. African trypanosomiasis. In Hunter's Tropical Medicine and Emerging Infectious Diseases, 9th edition. Pages 718–724, Figure 97.8. Copyright © 2013 Elsevier Inc. All rights reserved.th)

Fig. 1.186 Somnolent Nigerian child with *Trypanosoma brucei gambiense*.
Inflammation within the hypothalamus may result in disordered, fragmented sleep patterns with daytime somnolence. Finally the patient slips into a comatose state. It is this which gives the disease its common name, African sleeping sickness.

Downloaded From Vet-eBooks.com



Fig. 1.187 Cachectic man with late-stage trypanosomiasis.
In the absence of treatment, this patient with *T. b. gambiense* became progressively more wasted and comatose. Note the prominent cachexia caused by the burden of infection and food apathy. (Courtesy, Dr M. P. Hutchinson.)

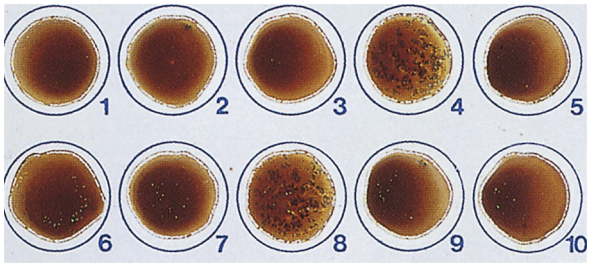


Fig. 1.188 Card agglutination test for *Trypanosoma brucei gambiense*.
This card agglutination test can be used in the field to screen patients for *T. b. gambiense*. A drop of whole heparinized blood is added to the reagent which contains a mixture of freeze-dried trypanosomes of specific variable antigen types. If specific trypanosomal antibodies are present, agglutination will occur (wells 4 and 8). Serological evidence of infection does not alone justify treatment but should be considered in conjunction with exposure history, clinical syndrome and other techniques which directly visualize or detect DNA of the parasite. (Courtesy, Mr A. R. Chandler and Smith Kline & French Laboratories.)

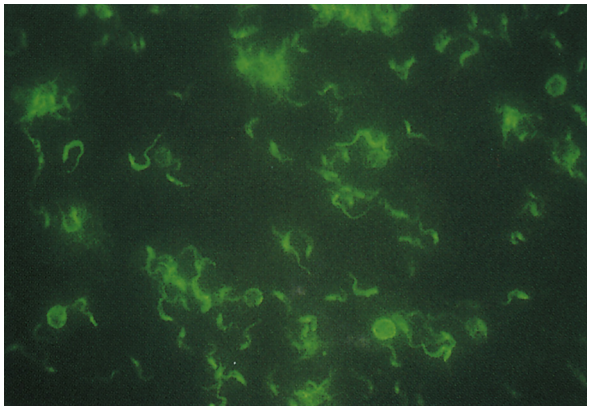


Fig. 1.189 Acridine-orange-stained *Trypanosoma brucei rhodesiense* in centrifuged blood.
The examination of centrifuged blood to detect trypanosomes is facilitated by the use of the quantitative buffy coat technique with fluorescent staining, as seen here. The method is highly sensitive and simple to use. (x200.) (Courtesy, Dr D. Smith.)

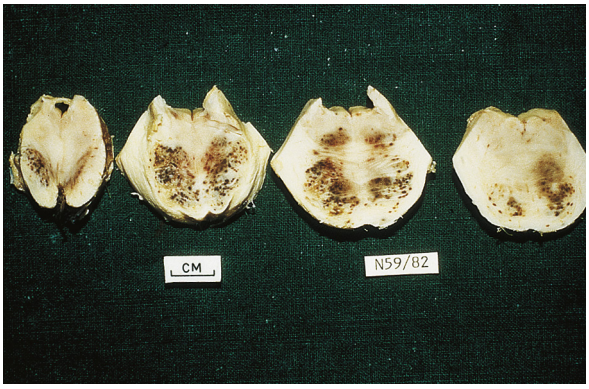


Fig. 1.190 Acute haemorrhagic leukoencephalopathy.
Numerous small haemorrhagic foci, some of them confluent, are seen in these sections of the brainstem from a fatal case of African trypanosomiasis. (Courtesy, Department of Neuropathology, Southern General Hospital, Glasgow, reproduced by courtesy of WHO. ID: 9204178, WHO/TDR.)

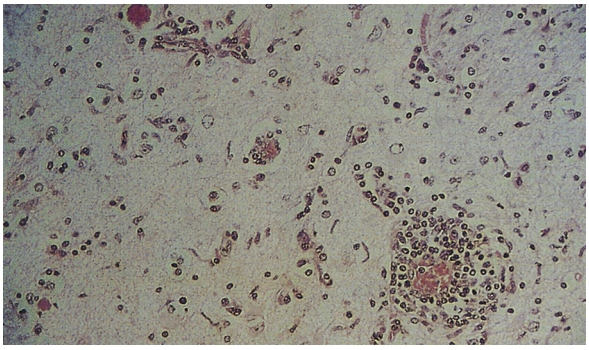


Fig. 1.191 Microscopic changes in brain.
The leptomeninges are congested and there may be oedema. Small haemorrhages are commonly present. The basic pathological change is a meningoencephalitis in which perivascular cuffing with round cells is often pronounced. (H&E x 200.) (Courtesy, Professor S. Lucas.)

Downloaded From Vet-eBooks.com

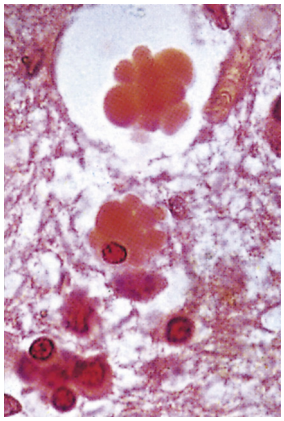


Fig. 1.192 Morula cells in brain.
Scattered irregularly through the brain substance in late disease are large eosinophilic mononuclear cells known as morula cells of Mott. They have an eccentric nucleus and characteristic vacuoles may be seen in the cytoplasm. (H&E x1500.)

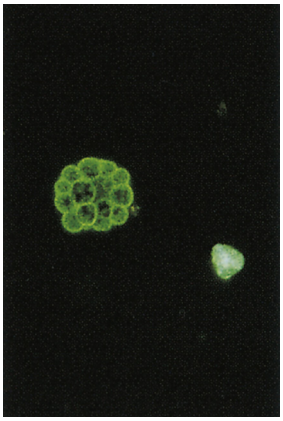


Fig. 1.193 Morula cells treated with anti-IgM antibody.
Morula cells are IgM-producing plasma cells. In this preparation, they have been treated with anti-IgM antibody. (x1500.) (Courtesy, Professor B. M. Greenwood.)

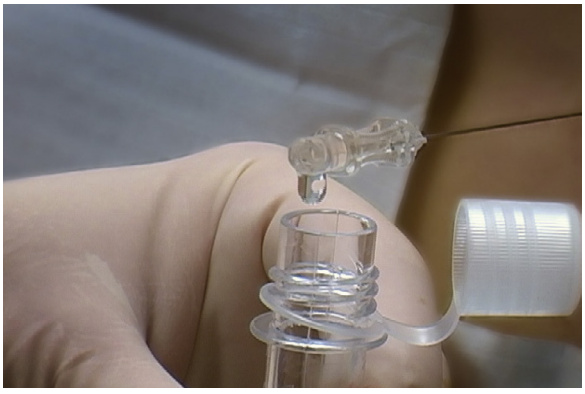


Fig. 1.194 Lumbar puncture.
The specific drug therapy chosen for treatment of human African trypanosomiasis is dependent upon the subspecies and stage of disease. It is not possible to clinically distinguish first- from second-stage disease without examination of the cerebrospinal fluid (CSF). An elevated CSF white cell count >5 cells/mm^3 or the presence of parasites within the CSF indicates second-stage disease. (From Rivers, M. Lumbar puncture (procedures consult). 2007, Figure 2.)



Fig. 1.195 Preparation of eflornithine.
Eflornithine is used in the treatment of second-stage *T. b. gambiense*. The 2-week parenteral treatment course can be shortened to 7 days by combining it with 10 days of oral nifurtimox. Nifurtimox-Eflornithine Combination Treatment (NECT) has less drug-related adverse effects than eflornithine monotherapy and is easier to administer in the field. [From François Chappuis (Médecins sans Frontières Switzerland); Banda, Democratic Republic of the Congo.]

Downloaded From Vet-eBooks.com

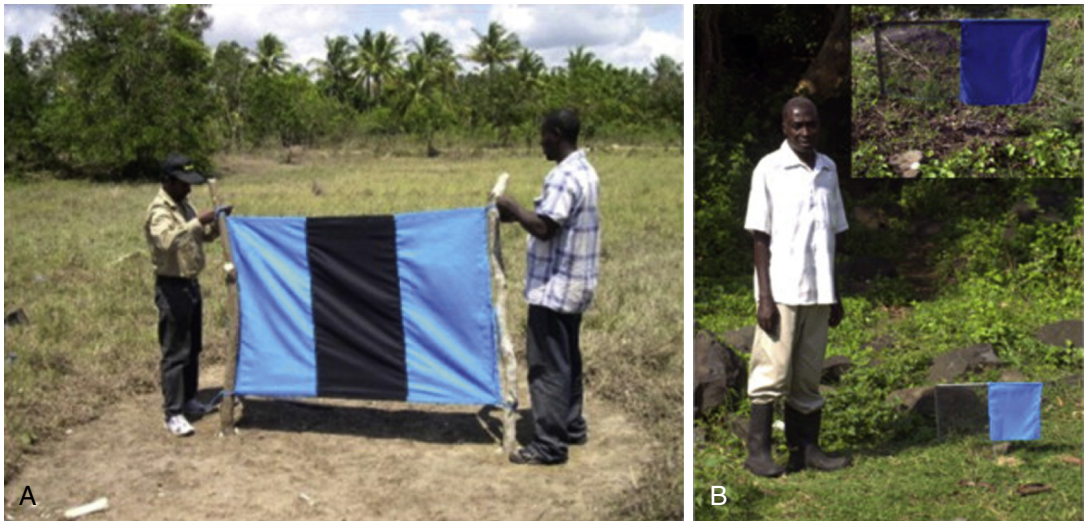


Fig. 1.196 Tsetse target with odour attractant.
The control of African trypanosomiasis is based mainly on the destruction of vectors. One of the most successful methods is the use of targets treated with insecticides. Tsetses are attracted to the target by its blue colour but preferentially land on the black area which is impregnated with insecticide. Chemoattractants, which imitate animal odour, can also be used to attract the flies. Savannah tsetses are most attracted to strongly scented, large target traps (A), whilst riverine species are less attracted by odour and more effectively caught by a larger number of smaller traps (B). (From Torr, S. J. and Vale, G.A. Know your foe: lessons from the analysis of tsetse fly behavior. Trends in Parasitology, 2015-03-01, Volume 31, Issue 3, Pages 95–99.)

Chagas Disease



Fig. 1.197 Distribution of Chagas disease.
Trypanosoma cruzi, the causative agent of American trypanosomiasis, is endemic in South and Central America. It is typically an infection of the rural poor, but rural-to-urban migration together with emigration to North America and Europe have contributed to a change in the epidemiology of disease. Co-ordinated multinational control programmes aimed at eradicating vectors together with screening of transfusion blood have resulted in a massive reduction in cases from 17 million in the 1980s to an estimated 8 million in 2016. Between 2% and 5% of pregnancies in infected mothers result in vertical transmission, a risk which can be reduced by pre-conception anti-trypanosomal treatment. Treatment of infants is highly effective, so identification of infected women of childbearing age is a growing focus of attention in Latin American migrant populations in non-endemic regions.

Downloaded from Vet-eBooks.com



Fig. 1.198 *Triatoma infestans* nymph.
Reduviid bugs (also known as 'assassin' or 'kissing' bugs), particularly the genera *Triatoma*, *Rhodnius* and *Panstrongylus*, transmit *T. cruzi* while feeding, not by inoculation but by faecal contamination of bite sites. (Courtesy, C. Whitehorn.)



Fig. 1.199 *Triatoma infestans* feeding on a human arm.
T. infestans is one of the most widely distributed species and can be distinguished from *Rhodnius* and *Panstrongylus* by the position of the proboscis.



Fig. 1.200 Ecology of triatomine vectors.
The favourite habitats of the reduviid bugs are cracks in the walls of mud huts in poor rural areas. They hide here during the day and emerge after dark to feed on sleeping inhabitants. The bite is remarkably painless, hence the name 'assassin bugs', even though the bug may take 10–20 minutes to become fully engorged. Note the adults and clusters of eggs seen here. (Courtesy, Professor H. Schenone.)

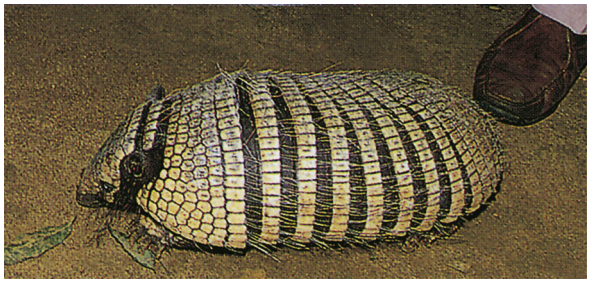


Fig. 1.201 *Dasypus novemcinctus*, a reservoir host of *Trypanosoma cruzi*.
Chagas disease is a zoonosis. *T. cruzi* has an extensive mammalian reservoir in wild hosts such as the nine-banded armadillos (*Dasypus novemcinctus*).



Fig. 1.202 *Didelphis* species, reservoir host of *Trypanosoma cruzi*.
Opossums (*Didelphis* species) are another wild host. Some domestic animals are similarly believed to be important reservoirs.



Fig. 1.203 Sugarcane juice: a risk factor for Chagas acquisition.
Chagas can also be transmitted by ingestion of food or drink contaminated by *T. cruzi*–infected triatomine bugs or their faeces during preparation. This is becoming an increasingly prominent mode of transmission in areas where domestic vector control has been effective. Classically outbreaks occur following consumption of sugar cane juice. Of the 1252 acute cases of Chagas reported in Brazil between 2001 and 2011, 70% were associated with oral transmission. These infections tend to have a more severe acute phase with higher rates of acute myocarditis, fulminant heart failure and death, probably due to the larger infecting dose and direct mucosal inoculation. (Courtesy of Shriners Hospital for Children, Philadelphia Unit. From Kozin, S. H. and Zlotolow, D. A. Sugar cane juice – nerve injury and repair in children. In Green's Skeletal Trauma in Children. Pages 631–643, Figure 22.2. Copyright © 2015 Saunders, an imprint of Elsevier Inc.)

Downloaded From Vet-eBooks.com

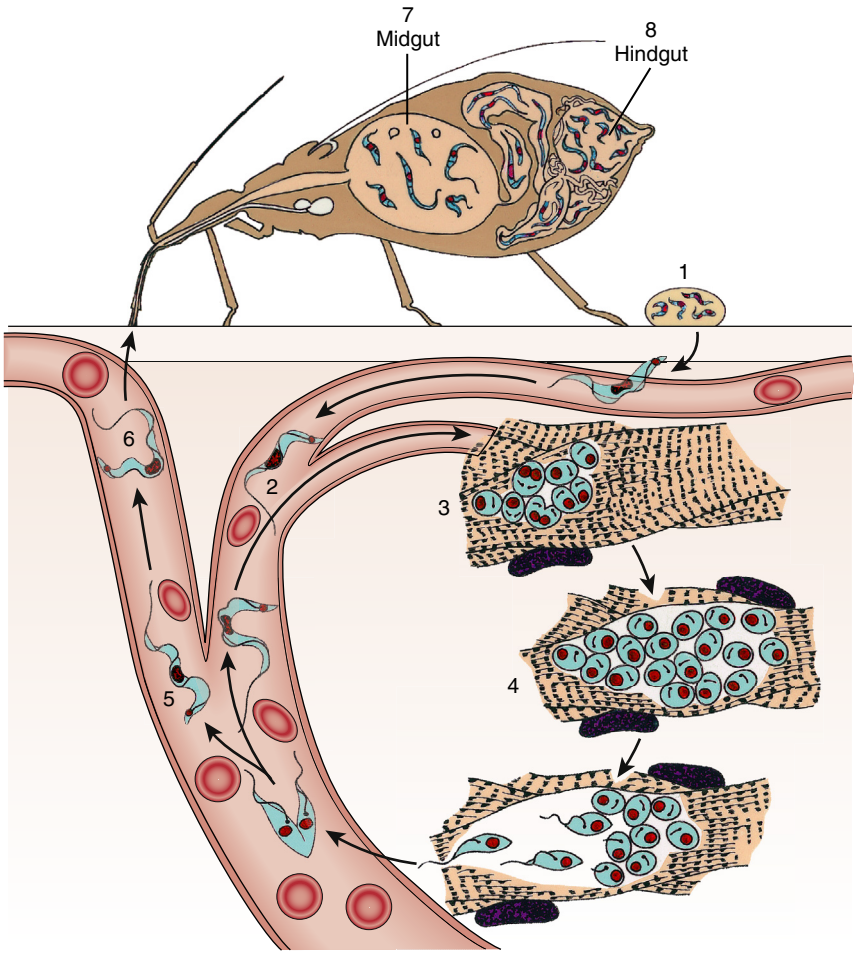


Fig. 1.204 Life cycle of *Trypanosoma cruzi* in humans and triatomine bugs.
Whilst feeding, the triatomine defaecates onto the skin or mucous membrane (1). Infective metacyclic trypomastigotes pass through the skin at site of bite and into the blood (2). A local inflammatory reaction may occur known as a chagoma. From there, the trypomastigotes penetrate smooth muscle in organs such as the heart, gastrointestinal tract wall or skeletal muscle (3). Within the muscle they convert to amastigotes which reproduce by binary fission to form pseudocysts (4). Some amastigotes will form trypomastigotes and re-enter the circulation (5). These circulating trypomastigotes are taken up when another triatomine feeds (6). They enter the midgut of the bug where they become short epimastigotes and multiply by binary fission (7). After 1–2 weeks they enter the rectum where they form metacyclic trypomastigotes that are passed when the bug defaecates again (8).

Downloaded from Vet-eBooks.com



Fig. 1.205 Metacyclic stage in bug faeces.
Parasites are defaecated by the bug onto the skin during feeding. These may invade the site of the bite or adjacent mucosa, such as the conjunctiva. (Giemsa x1500.)

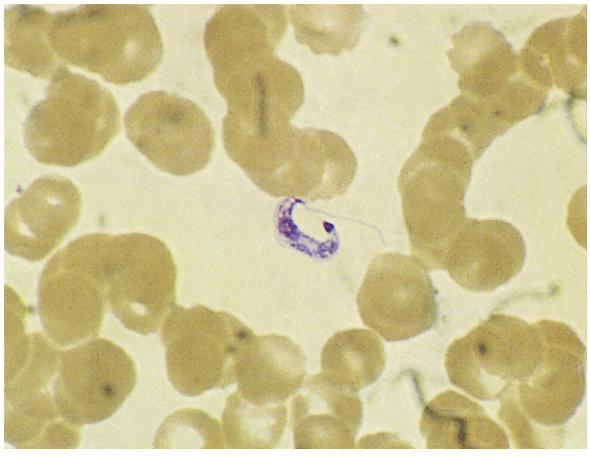


Fig. 1.206 *Trypanosoma cruzi* in human blood film.
T. cruzi trypomastigotes may be seen on blood films during acute infection. Note the very prominent kinetoplast (larger than that of *T. brucei*) at the posterior end, the central nucleus and the anterior flagellum. Trypanosomes measure between 12 and 30 μm and are monomorphic. (Giemsa x 950.)

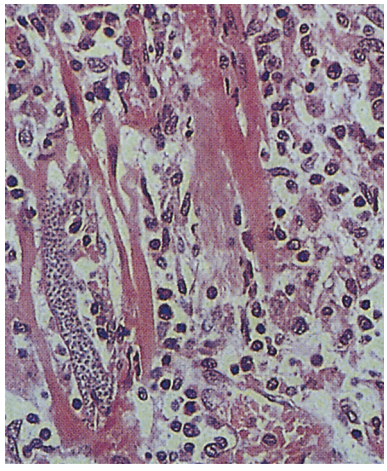


Fig. 1.207 Amastigotes in heart muscle.
After the initial parasitaemia, trypomastigotes pass to the cardiac muscle and the smooth muscle lining the intestinal tract. Here, they transform to the amastigote stage (Leishman–Donovan bodies) in which they multiply to form pseudocysts. (Giemsa x 350.) (Courtesy, Professor S. Lucas.)



Fig. 1.208 Romaña's sign.
Most patients with acute infection are asymptomatic or have non-specific symptoms with fever and malaise. A few develop an inflammatory lesion at the site of inoculation known as a chagoma. Romaña's sign, unilateral swelling of the eyelid with chemosis seen here, may occur if there is conjunctival inoculation. During the acute phase, trypomastigotes may be visualized on microscopy of fresh blood or buffy coat. (Courtesy, Professor H. Schenone.)

Downloaded From Vet-eBooks.com

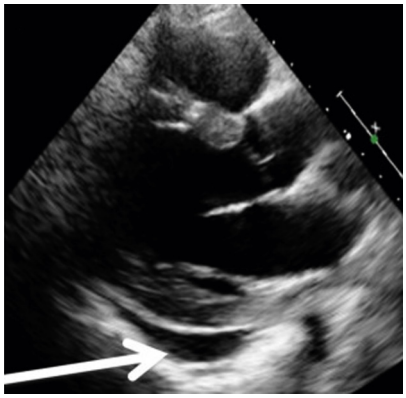


Fig. 1.209 Pericardial effusion in acute Chagas disease.
This patient with acute infection developed pericarditis with a small pericardial effusion (arrowed). Although most patients have a mild acute illness, severe infections do occasionally occur and carry a significant risk of mortality. (From Villamil-Gómez, W., Echeverria, L., Ayala, M., et al. Orally transmitted acute Chagas disease in domestic travelers in Colombia. Journal of Infection and Public Health, Volume 10, Issue 2, 244-246. Figure 1.)

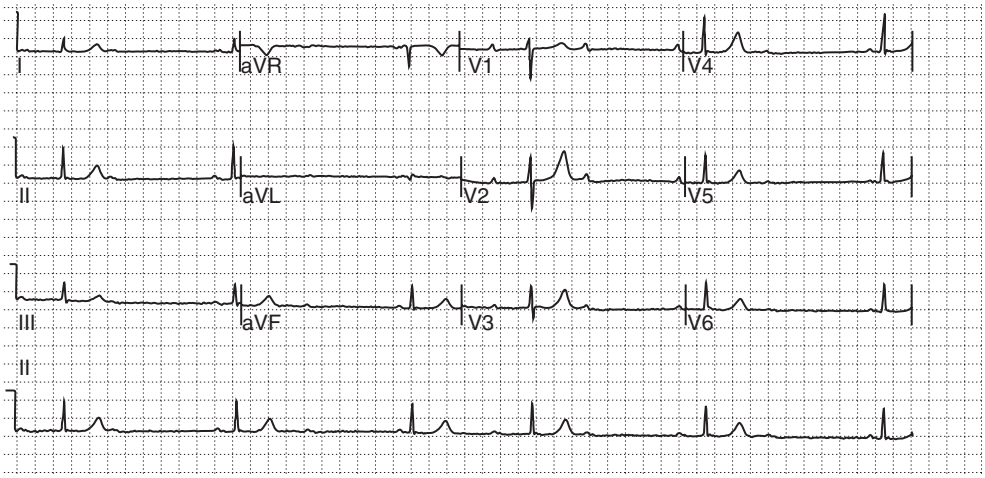


Fig. 1.210 Electrocardiogram showing heart block.
Sudden arrhythmic cardiac death is the commonest cause of mortality in patients with Chagas disease. Conduction defects and almost any type of atrial or ventricular arrhythmia may occur. (Courtesy, Dr B. Dyer.)

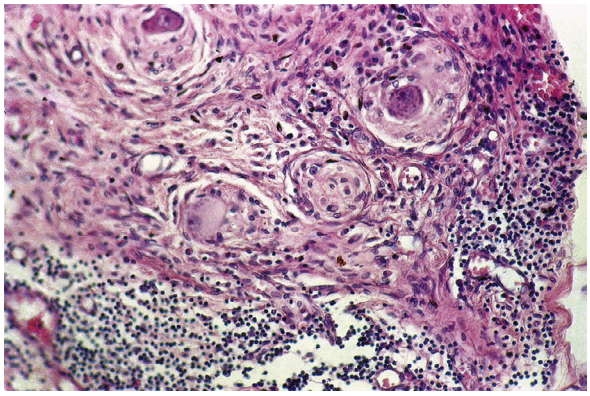


Fig. 1.211 Sympathetic ganglion in wall of atrium.
This patient with Chagas died of sudden cardiac failure. Note the degenerative changes in neuronal cells and the conspicuous mononuclear cell infiltration, especially round the capsule of the ganglion. (H&E x130.) (Courtesy, Professor H. de Oliveira Almeida.)

Downloaded from Vet-eBooks.com

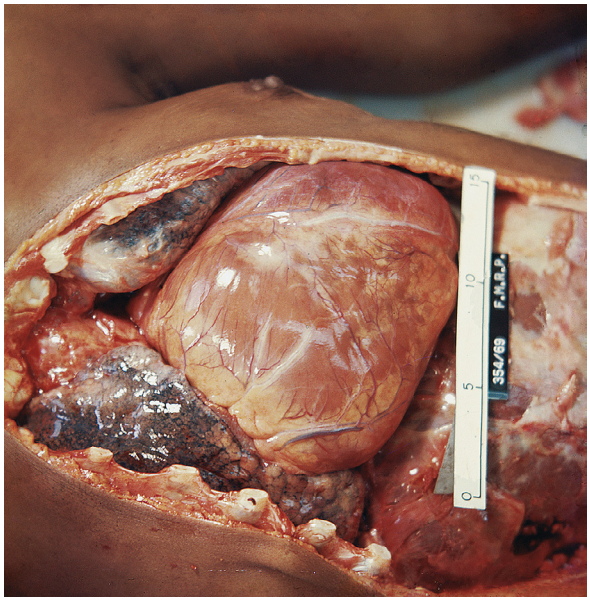


Fig. 1.212 Cardiomegaly.
Left ventricular dysfunction is an independent predictor of mortality in patients with chronic cardiac Chagas disease. Heart failure in Chagas should be managed in the same way as other causes of heart failure. This post mortem specimen shows gross enlargement and dilatation of the right atrium and both ventricles. (Courtesy, Professor F. Köberle.)

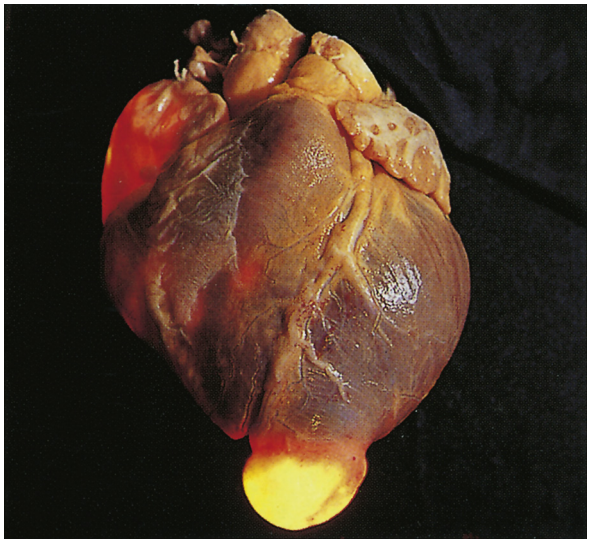


Fig. 1.213 Apical aneurysm of the heart.
Apical aneurysms are commonly seen in advanced disease and may give rise to thromboemboli. (Courtesy, Professor F. Köberle.)



Fig. 1.214 Dilated oesophagus.
The gastrointestinal manifestations of Chagas are rarely fatal but can significantly reduce quality of life. They are more common in the Southern Cone countries and are rarely seen in Central America or Mexico, which may reflect strain differences. Oesophageal involvement ranges from achalasia to severe megaoesophagus as shown here. Progressive dysphagia may be complicated by aspiration, oesophageal ulceration and oesophageal cancer. (From Lamps, L. W. Infectious disorders of the gastrointestinal tract. In Odze and Goldblum Surgical Pathology of the GI Tract, Liver, Biliary Tract and Pancreas. Chapter 4. Pages 55–93.e5, Figure 4.35. Copyright © 2015, 2009, 2004 Saunders, an imprint of Elsevier Inc. Courtesy, Dr D. Baroni-Cruz, University of Santa Cruz.)

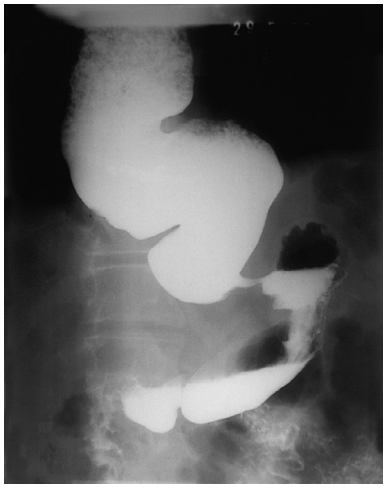


Fig. 1.215 Radiograph of megaoesophagus.
Muscular degeneration and denervation of segments of the alimentary tract through destruction of the cells of Auerbach's plexus cause megaoesophagus, megastomach and megacolon. This can be detected radiographically as in this barium swallow showing megaoesophagus.

Downloaded from Vet-eBooks.com

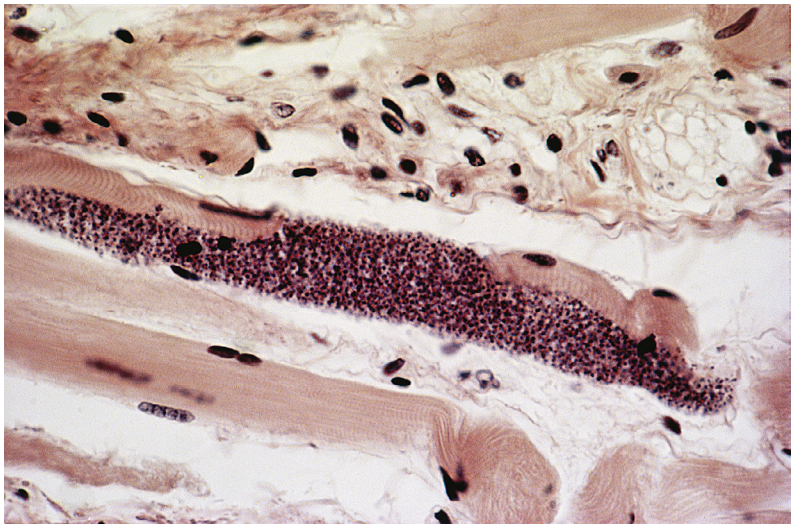


Fig. 1.216 Amastigotes in oesophageal muscle.
Pseudocysts containing amastigotes of *T. cruzi* can rarely be demonstrated in ganglion cells of the intestinal tract, although the smooth muscle is often invaded. (x480.) (Courtesy, Dr W. Petana.)

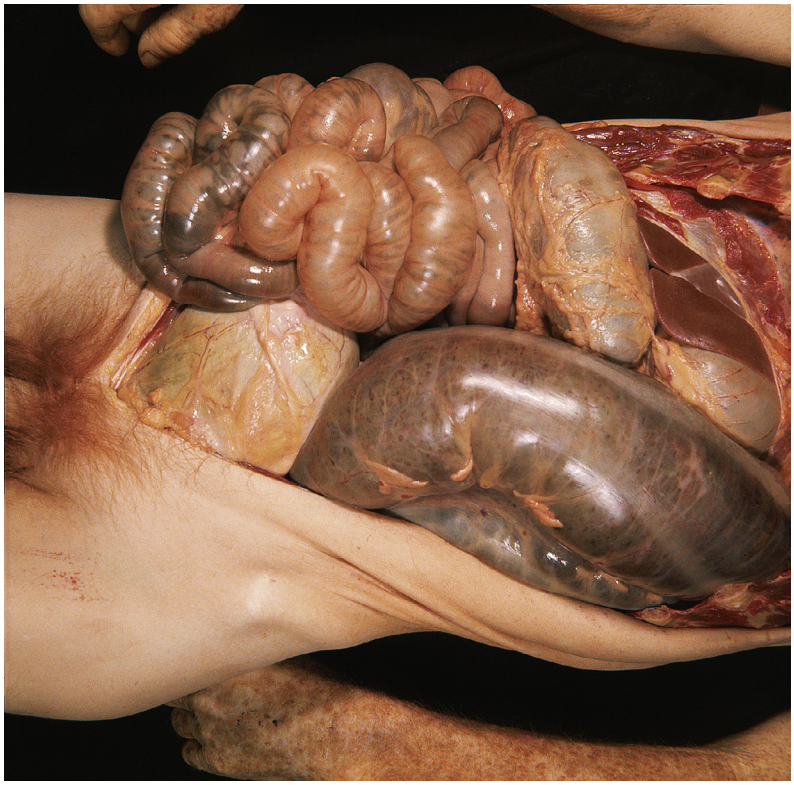


Fig. 1.217 Post-mortem of patient with megacolon.
Megacolon may be asymptomatic or present with worsening constipation. Recurrent volvulus may also occur. Note the grossly distended colon in this patient who died of complications of Chagas disease. (Courtesy, Professor F. Köberle.)

Downloaded From Vet-eBooks.com

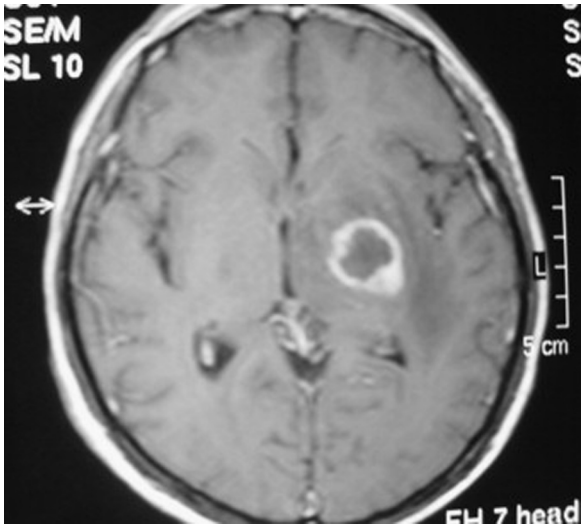


Fig. 1.218 Cerebral chagoma in a patient with HIV.
Chronic *T. cruzi* infection may reactivate in people who become immunocompromised due to chemotherapy, transplant immunosuppressants or HIV infection. Patients with advanced HIV may develop a cerebral chagoma—a *T. cruzi* brain abscess—which is easily confused with cerebral toxoplasmosis on imaging, as it may appear ring enhancing with perilesional oedema. (From Cordova, E., Boschi, A., Ambrosioni, J., et al. Reactivation of Chagas disease with central nervous system involvement in HIV-infected patients in Argentina, 1992–2007. International Journal of Infectious Diseases, 2008-11-01, Volume 12, Issue 6, Pages 587–592, Figure 2. Copyright © 2008 International Society for Infectious Diseases.)



Fig. 1.219 Xenodiagnosis.
After the acute phase, when *T. cruzi* trypomastigotes can be identified in blood, detection of the organism is challenging. Two serological tests, usually an enzyme-linked immunosorbent assay and indirect fluorescent antibody targeting different antigens, are used in combination, as neither test has sufficient sensitivity or specificity to establish the diagnosis alone. Molecular assays have variable sensitivities in chronic disease but are very useful in the screening of blood for transfusion. Polymerase chain reaction for *T. cruzi* DNA is increasingly being used for the testing of infants born to *T. cruzi* infected mothers. Historically, absolute confirmation of active infection was obtained by demonstrating that blood from the patient could infect the vector (xenodiagnosis). Laboratory-bred, starved and clean triatomine bugs were fed on patients. Two weeks later the hindgut was dissected out and examined for metacyclic trypomastigotes. (Courtesy, Professor A. Bryceson.)



Fig. 1.220 The unfinished brick walls of a new house are sprayed with a long-lasting insecticide in Peru.
The move from mud-walled huts to bricked housing together with application of long-lasting insecticides is key to reducing the transmission of Chagas disease. (From Fraser, B. Controlling Chagas' disease in urban Peru. The Lancet, 2008-07-05, Volume 372, Issue 9632, Pages 16–17.)

Downloaded from Vet-eBooks.com

Leishmaniasis

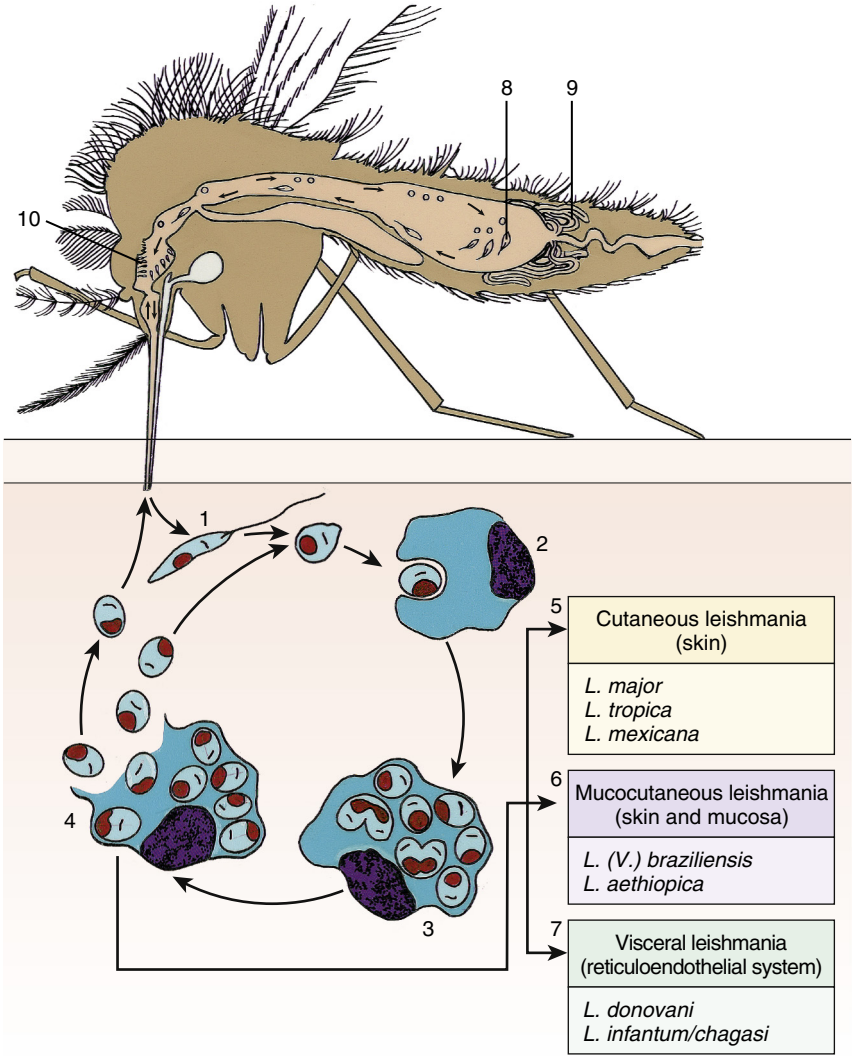


Fig. 1.221 Life cycle of *Leishmania*.
Infective, flagellated promastigotes pass during feeding from the sandfly proboscis into the subcutaneous tissues (1). Promastigotes penetrate local tissue macrophages, losing their flagella to become rounded amastigotes, known as Leishman–Donovan bodies (2). Amastigotes multiply by asexual binary fission to form 'cell nests' (3) which rupture the host cell (4). The progeny are taken up by other local or circulating macrophages. Depending on the species of parasite, amastigotes may remain in the superficial tissues and continue the reproductive cycle (5). Others may be transported to mucosa (6) or to the reticuloendothelial system including the bone marrow, spleen and liver (7). When another sandfly takes a blood meal, amastigotes in macrophages (either in the skin or in the peripheral circulation) are taken into the midgut, where they become promastigotes and divide by binary fission (8). Species of *Leishmania* (*Viannia*) also undergo binary fission in the sandfly hindgut (9). Promastigotes then move anteriorly to the proboscis where they pass into the host during feeding (10).

Downloaded From Vet-eBooks.com



Fig. 1.222 Adult female *Lutzomyia longipalpis* biting.
Leishmaniasis is transmitted by sandflies of the genus *Phlebotomus* in the Old World and Far East, and by *Lutzomyia* in the New World (Latin America). This figure gives an impression of the small size of these flies. (x2.)



Fig. 1.223 Larva of *Lutzomyia*.
Note the encapsulated head, matchstick hairs that protrude from the body and long caudal setae of this *Lutzomyia* larva. (Courtesy, S. McIntyre.)



Fig. 1.224 Pupa of *Lutzomyia*.
Note the shed skin of the larva at the caudal end of this pupa. Matchstick hairs and long caudal setae are also visible. (Courtesy, S. McIntyre.)

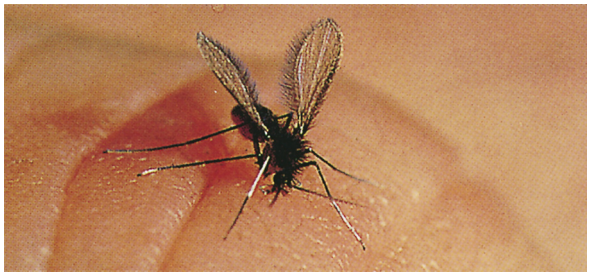


Fig. 1.225 Close-up view of *Lutzomyia longipalpis*.
The female sandfly has a 'blunt' end to her abdomen. (x10.) (Courtesy, Professor R. Lainson.)

Downloaded from Vet-eBooks.com



Fig. 1.226 Male *Lutzomyia longipalpis*.
The claspers of the male genitalia as seen in this figure readily distinguish the male from the female. (x10.) (Courtesy, Professor R. Lainson.)

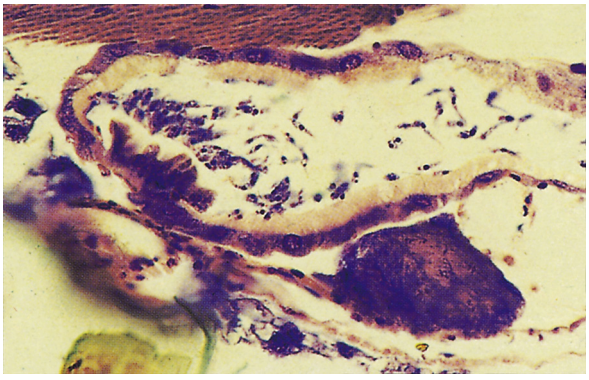


Fig. 1.228 Promastigotes in vector midgut.
In the midgut of the vector, amastigotes transform to promastigotes, which then divide asexually. (Giemsa x 1150.)



Fig. 1.227 Cross section through *Phlebotomus argentipes* in the process of feeding.
The female feeds from the pool of capillary blood that accumulates at the tip of the proboscis. (Haematoxylin x 100.) (Courtesy, Colonel H. E. Shortt.)

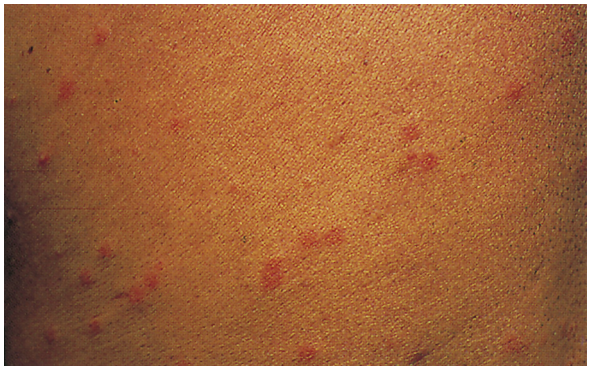


Fig. 1.229 Reaction to sandfly bites.
A persistent macule appears at the site of each bite, even from an uninfected fly; this may be the starting point of the lesion in simple cutaneous leishmaniasis. Multiple primary lesions occur when the sandfly probes repeatedly in the course of feeding. (Courtesy, Dr C. F. Farthing.)

Downloaded from Vet-eBooks.com

Visceral Leishmaniasis

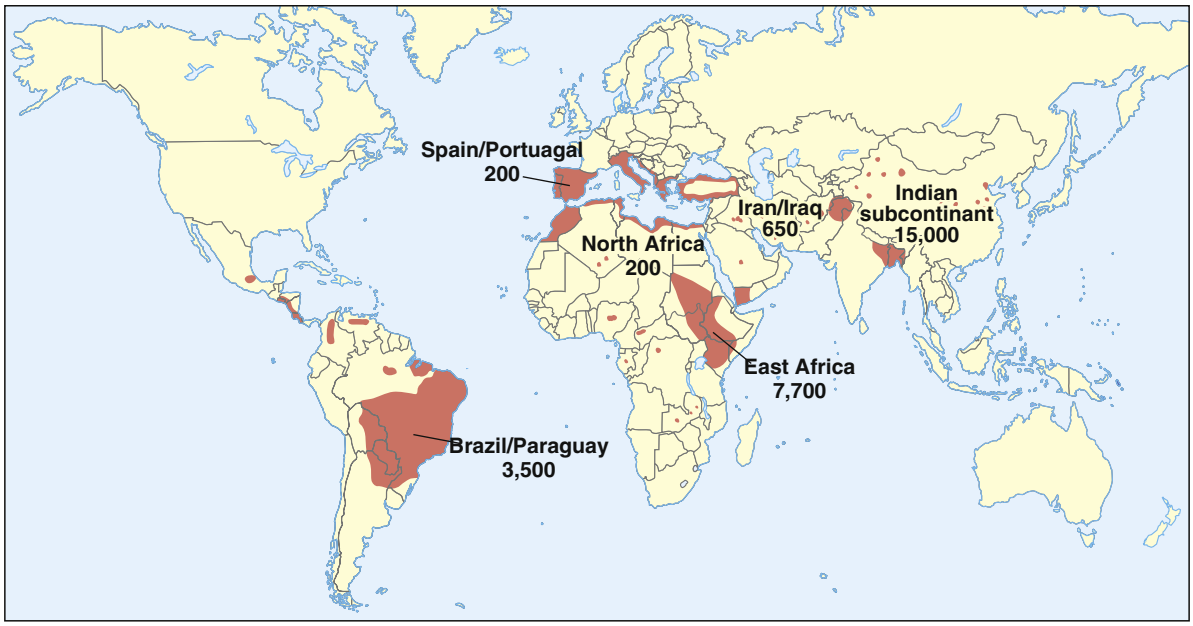


Fig. 1.230 Distribution of visceral leishmaniasis (VL, kala-azar).
Almost 90% of VL is found in just three regions: the Indian subcontinent, East Africa and Brazil. In the Indian subcontinent and East Africa, *L. donovani* occurs in discrete foci principally in the rural poor causing recurring outbreak cycles. It is predominantly anthroponotic, although dogs and rodents may act as reservoirs in East Africa. By contrast, *L. infantum*, which occurs sporadically around the Mediterranean, the Middle East and South America, is a zoonosis with dogs as the principal reservoir. The figures given here are the number of reported cases in 2013 but likely underestimate the true scale of the disease. (Data from WHO 2013.)



Fig. 1.231 Village in the visceral leishmaniasis (VL) endemic area of Bihar, India.
The close association between humans and domestic animals in this village favours the growth of populations of the local vector, *Phlebotomus argentipes*. They are synanthropic but zoophilic, feeding readily on cattle that are sheltered in or adjacent to human dwellings in such villages, and rest indoors after taking a meal. (Courtesy, Dr M. Gonzáles Sanz.)



Fig. 1.232 Educating people in endemic areas about the symptoms of visceral leishmaniasis (VL).
A co-ordinated effort to eliminate VL as a public health problem in East India resulted in a 72% reduction in cases and 85% reduction in deaths between 2011 and 2014. This has been achieved through a combination of education, early diagnosis, improved case management, passive and active case detection and vector control. (Courtesy, Dr M. Gonzáles Sanz.)

Downloaded from Vet-eBooks.com



Fig. 1.233 Refugees in South Sudan.
In South Sudan, a large, prolonged outbreak of VL was ongoing as of 2016. The forcible displacement of malnourished refugees with low VL immunity into VL endemic areas has exacerbated this. (Courtesy of UN photo (#476122) by Paul Banks.)



Fig. 1.234 Reservoirs of zoonotic *Leishmania infantum*.
The loss of hair, overgrowth of nails and generally poor condition of this dog seen in southern France are typical of chronic infection with *L. infantum*. The nails are commonly infested with *Demodex* mites and grossly overgrown. Wild carnivores and various species of rodent may also serve as reservoirs.

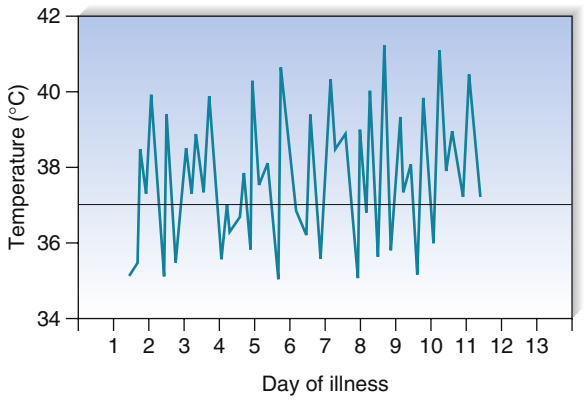


Fig. 1.235 Temperature chart in visceral leishmaniasis.
The temperature chart often shows a double peak every 24 hours. Despite the high temperature, the patient may look remarkably well and have a good appetite.

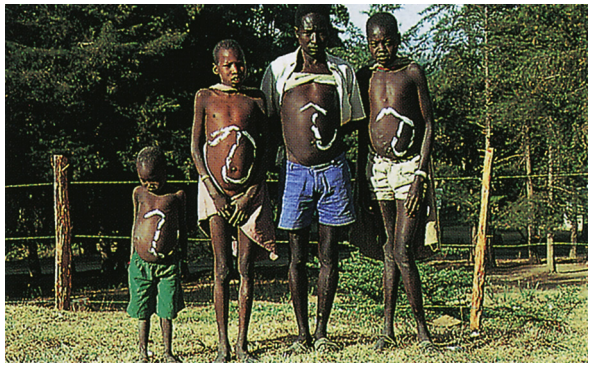


Fig. 1.236 Hepatosplenomegaly due to visceral leishmaniasis (VL).
The presentation of VL is usually insidious in onset with slowly worsening malaise, weight loss and fever. Over a period of months, abdominal discomfort may develop secondary to splenomegaly. Lymphadenopathy may be seen along with darkening of the skin; it is this sign that gives VL its common name kala-azar, Hindi for 'black fever'.



Fig. 1.237 Infantile visceral leishmaniasis.
This infant was infected with *L. infantum* in the north-east of Brazil. This species is more common in children and immunocompromised adults. Children present with chronic, irregular fever, a moderately enlarged, non-tender liver and a greatly enlarged, firm spleen. If left untreated, the disease may be fatal, often as a result of secondary bacterial infection.

Downloaded from Vet-eBooks.com



Fig. 1.238 Purpura in visceral leishmaniasis (VL).
The combination of pancytopenia, fever and splenomegaly in a patient with epidemiological exposure should prompt investigation for VL. Pancytopenia is due to parasite invasion into the bone marrow, which may also result in anaemia or recurrent or severe infections. This Indian boy developed a petechial rash as a result of thrombocytopenia.

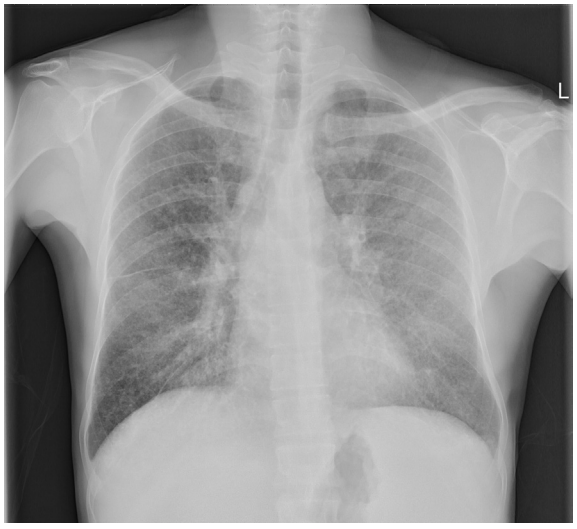


Fig. 1.239 Chest radiograph in an HIV-positive patient with disseminated visceral leishmaniasis (VL).
HIV–VL co-infection is increasingly common and very difficult to treat. Whilst HIV infection increases the risk of acquiring VL, VL hastens the progression of HIV. These patients may also develop disseminated VL with involvement of unusually affected organs. This Ethiopian man with AIDS had previously been treated for VL and was on prophylactic pentamidine when he developed worsening cough and shortness of breath. He was initially treated for *Pneumocystis* pneumonia, but bronchoalveolar lavage was found to be positive for *L. donovani* by both culture and molecular detection. (Courtesy, UCL Hospitals Radiology.)



Fig. 1.240 Post kala-azar dermal leishmaniasis (PKDL).
This syndrome is a sequela of visceral leishmaniasis that may arise several years following successful treatment of primary *L. donovani* infection. It is most common in East Africa following treatment with antimonials and is uncommon following treatment with amphotericin B. Dermal lesions vary greatly in appearance and may contain large numbers of infectious amastigotes, thus patients with PKDL may constitute an important reservoir. Note the small inflammatory nodules on the face of this Indian woman.



Fig. 1.241 Post kala-azar dermal leishmaniasis nodules in an Indian patient.
Nodules of various sizes, some pedunculated, are seen in this patient, who had been treated for visceral leishmaniasis over a period of 6 months, 20 years previously.

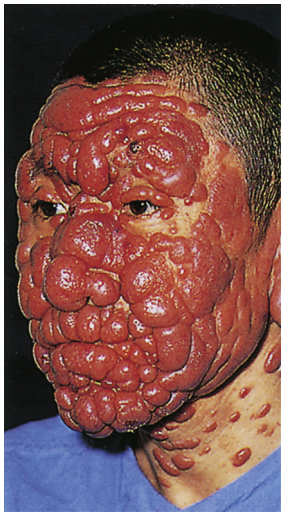


Fig. 1.242 Post kala-azar dermal leishmaniasis in a Chinese patient.
The patient was completely cured by chemotherapy. This response differentiates the condition from the anergic diffuse cutaneous type of leishmaniasis (see Figs. 1.268/9).

Downloaded from Vet-eBooks.com



Fig. 1.243 Hypopigmented macules of post kala-azar dermal leishmaniasis.
This patient had been treated for visceral leishmaniasis 15 years previously. Note the hypopigmented patches that could be mistaken for leprosy but have no associated sensorineural change. A punch biopsy has been performed at the edge of the lesion to maximize the chance of obtaining a parasitological diagnosis. (Courtesy, Professor G. Varghese.)

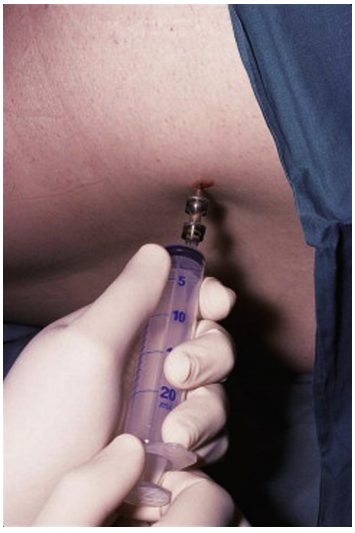


Fig. 1.244 Bone marrow aspirate.
Visualization of amastigotes, or molecular detection of leishmania by polymerase chain reaction, is essential to make a definite diagnosis of visceral leishmaniasis. In a patient with splenomegaly, direct smear microscopy from a splenic aspirate has the highest sensitivity but carries a small risk of life-threating haemorrhage. This patient is undergoing a bone marrow biopsy from the iliac crest, which is a safer procedure but significantly more painful. Lymph node aspirate can also be performed in patients with palpable lymphadenopathy but has a lower diagnostic yield. (From Howard, M. and Hamilton, P. Bone marrow aspiration and trephine biopsy. In Haematology: an illustrated colour text. 4th edition. 106-107. Figure 53.3. Copyright © 2013 Elsevier Ltd.)

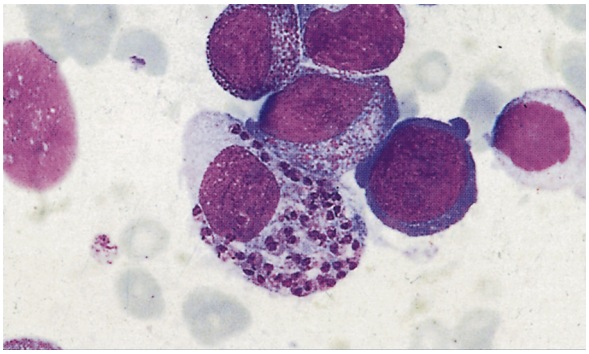


Fig. 1.245 *Leishmania infantum* in macrophage from bone marrow.
Amastigotes are typically found in macrophages and can be identified by the dark red staining nucleus and kinetoplast. Isolated extracellular amastigotes from disrupted host cells may also be seen. Polymerase chain reaction can be used to speciate the parasite. (Giemsa x 810.)

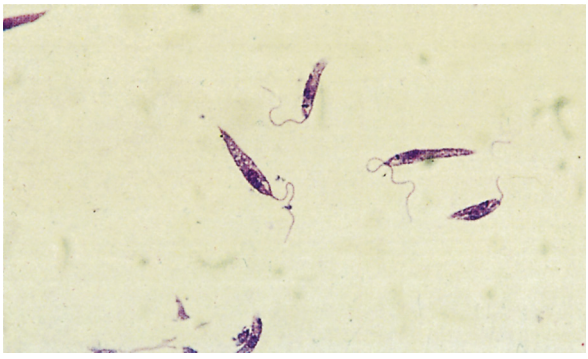


Fig. 1.246 Promastigotes on Novy-MacNeal-Nicolle (NNN) medium.
Culture of aspirate material on NNN media at 24 to 26 °C yields motile promastigotes at 1–4 weeks. (Giemsa x 950.)

Downloaded From Vet-eBooks.com

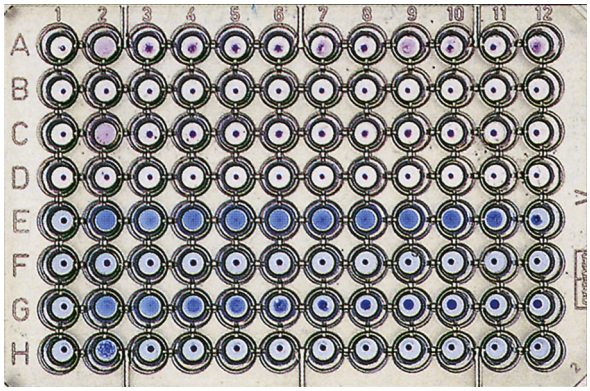


Fig. 1.247 The Direct Agglutination Test (DAT) for visceral leishmaniasis (VL).
DAT is a semi-quantitative method that detects antibodies to *L. donovani*. Stained dead *L. donovani* promastigotes are mixed with patient serum in increasing dilutions on a microtitre plate. In the presence of specific leishmania antibodies, agglutination that prevents pelleting will occur by 18 hours as seen in samples E and G on this plate, both of which are strongly positive. Serological tests for leishmaniasis are limited by the fact that many healthy individuals in endemic areas have asymptomatic VL infection or previous VL exposure, thus the result should always be interpreted in conjunction with the clinical syndrome. (Courtesy, S. N. McDermott.)



Fig. 1.248 K39 rapid diagnostic test for visceral leishmaniasis.
This rapid diagnostic test detects rK39, a protein found in *L. infantum* and *L. donovani*. It is highly sensitive, cheap and takes less than 20 minutes to perform. Here, a negative control is seen on the left and a positive test on the right.

Old World Cutaneous Leishmaniasis

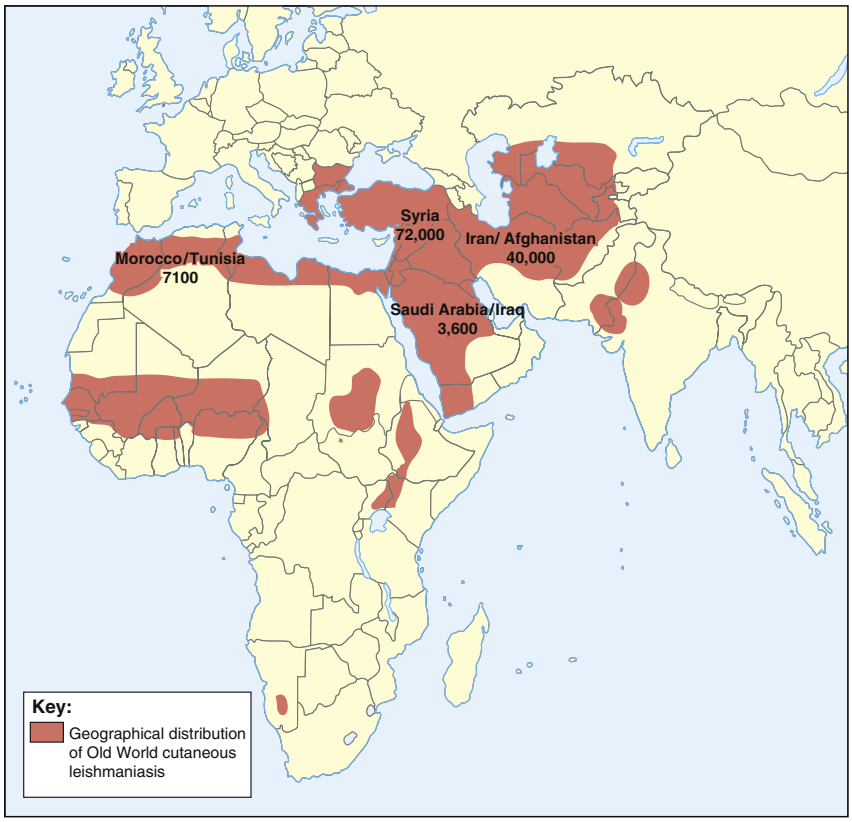


Fig. 1.249 The distribution of Old World cutaneous leishmaniasis (CL).
Old World CL is a zoonotic infection caused by *L. major*, *L. tropica* and *L. aethiopica*. *L. donovani* and *L. infantum*, which principally cause visceral leishmaniasis, can occasionally cause localized cutaneous lesions. Local names for CL include Oriental sore, Aleppo button and Baghdad boil. Outbreaks may occur when people are displaced and sandfly habitats disrupted as has been seen in Syria, where numbers of reported cases have more than doubled since the beginning of the civil war. The figures on this map are the number of reported cases in 2013. These are likely to underestimate the true incidence of CL.

Downloaded from Vet-eBooks.com



Fig. 1.250 Male and female *Phlebotomus papatasi*.
This is the most important vector of *L. major* from North Africa, through the Middle East to Mongolia. The female (upper figure) has a fully engorged midgut. Note the blunted terminal abdominal segment of the female and the claspers on the terminal abdomen of the male. (x 9.) (Courtesy, Dr A. Warburg.)



Fig. 1.251 Animal reservoirs of *Leishmania major*.
Various rodent species such as this 'great gerbil', *Rhombomys opimus*, of eastern Iran and neighbouring parts of the former Soviet Union, and the 'fat-tailed sand rat', *Psammomys obesus* (Fig. 1.252) in Libya, Israel and Saudi Arabia, are important reservoirs of *L. major*. (Courtesy, Professor V. Sěry.)

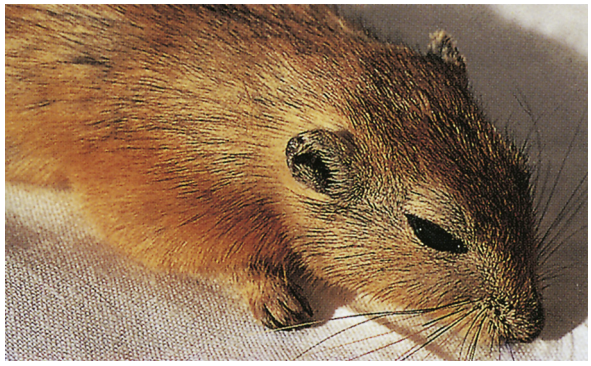


Fig. 1.252 Ear lesion on *Psammomys obesus*.
These rodents, and the sandflies that rest in their burrows, are responsible for outbreaks of cutaneous leishmania in newly urbanized areas that intrude into their natural habitat of arid or semi-desert terrain. The burrows provide ideal breeding and resting sites for sandfly vectors such as *Phlebotomus papatasi* that transmit *L. major*. Sandflies also rest during the day in cool deep crevices in the ground, between rocks, in caves, cellars and house walls. Although the eroded ear seen here is typical of *L. major* in its natural host, many infected animals have no obvious skin lesions. (Courtesy, Dr R. Ben-Ismail.)



Fig. 1.253 Nodulo-ulcerative lesion of *Leishmania major*.
Lesions typically begin as a papule which enlarges to a nodule or plaque and then becomes a painless ulcer. Note the well-defined central ulcer and typical rolled edge which is sometimes said to resemble the crater of a volcano. Superadded bacterial infection may result in the lesion becoming painful.

Downloaded from Vet-eBooks.com



Fig. 1.254 'Wet' lesion of mouth.
L. major occurs most commonly in rural areas, causing moist, ulcerative lesions that may be extensive and sometimes involve the epithelium of lips and nose. (Courtesy, Dr W. A. D. Griffiths.)



Fig. 1.255 Spontaneous cure in *L. major*.
L. major has a spontaneous cure rate of around 50% at 8 weeks. This patient had three lesions of *L. major* all of which healed without treatment within 4 weeks. The photo on the left was taken at presentation whilst the one on the right was taken 4 weeks later. (Courtesy, Dr L. Nabarro.)

Downloaded from Vet-eBooks.com



Fig. 1.256 Invasive ulcerative lesion of *L. major*.
The extensive lesion on the lower leg of this Sudanese woman near Khartoum has exposed deep tissues, including a tendon sheath. (Courtesy, Dr S. El-Safi.)



Fig. 1.257 Multiple lesions of *L. major* in a non-immune man.
This Thai builder received multiple bites by infected *P. papatasi* when sleeping outdoors without protection in a highly endemic area of eastern Saudi Arabia. Each bite has developed into a separate focus of cutaneous leishmaniasis.



Fig. 1.258 Lymphatic spread of *L. major*.
In this patient, there is sporotrichoid spread from the primary lesion up the lymphatics of the arm. The subcutaneous nodules have been marked with ink and are often more readily felt than seen. They give the lymphatics a 'beaded cord' property on palpation. Other pathogens that cause sporotrichoid spread include *Sporothrix schenckii*, *Mycobacterium marinum* and *Nocardia*.



Fig. 1.259 Infant with mucocutaneous lesions caused by *L. major*.
Although mucocutaneous leishmaniasis (MCL) is classically associated with New World species, it occasionally occurs in individuals with Old World CL who have impaired cellular immunity. This infant with *L. major* was seen in eastern Saudi Arabia.



Fig. 1.260 Punch biopsy of skin lesion.
A piece of tissue is removed under local anaesthetic with a disposable skin punch for histology, culture and direct demonstration of amastigotes. The punch should be taken from the edge of the lesion where amastigotes are most plentiful. (From Tuggy, M., Garcia, G. Punch biopsy. In: Atlas of Essential Procedures, Pages 3–5, Figure 1.5. Copyright © 2011 Elsevier Inc. All rights reserved.)

Downloaded from Vet-eBooks.com

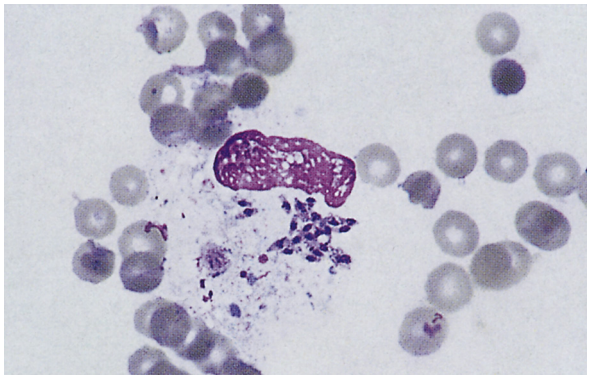


Fig. 1.261 Amastigotes in macrophages from skin.
The diagnosis is confirmed by demonstrating amastigotes in smears from biopsy of the cutaneous lesions. (Giemsa x 950.)

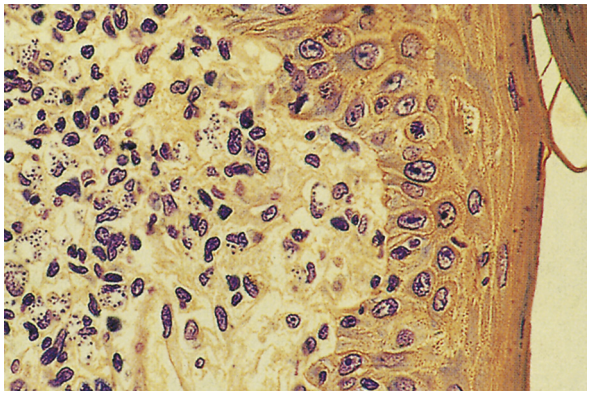


Fig. 1.262 Parasitized macrophages in skin section.
Note the numerous amastigotes seen in macrophages in this section from an acute lesion caused by *L. major*. (H&E x 220.) (Courtesy, Dr D. A. Evans.)

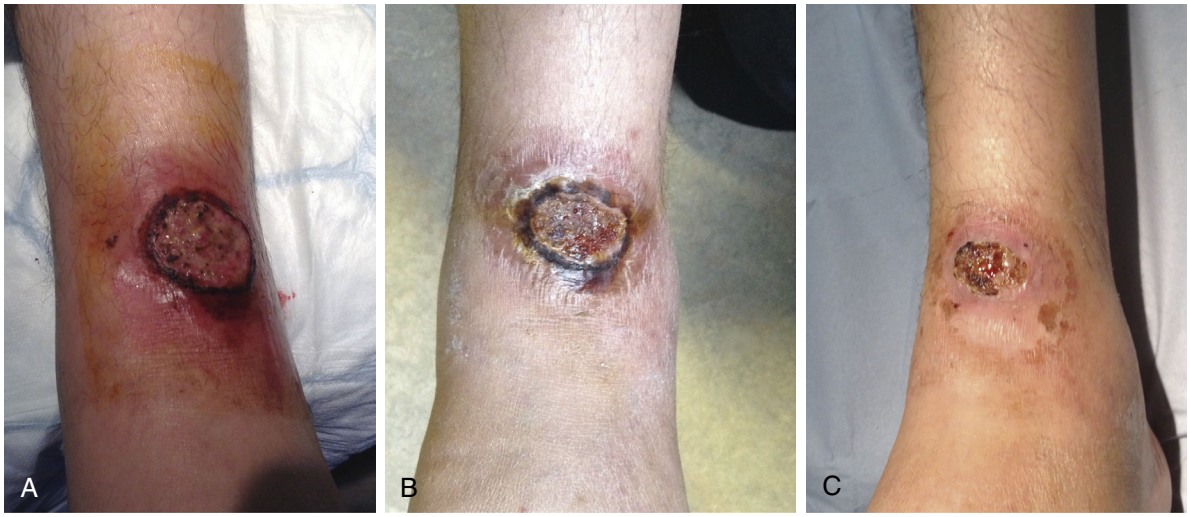


Fig. 1.263 Cutaneous leishmaniasis treated with intralesional sodium stibogluconate.
This lesion was treated with weekly infiltration of sodium stibogluconate. Panel A shows the lesion at initiation of treatment, the brown pigment is iodine used as a disinfecting agent. Panel B shows the lesion at week 1; it has dried out and is marginally smaller. Panel C shows the lesion at week 3 by which time it has shrunk considerably. The lesion was infiltrated twice more before it disappeared completely (not shown). Heat treatment or paromomycin ointment can also be used for localized treatment of Old World cutaneous leishmaniasis, although systemic treatment with miltefosine, liposomal amphotericin or pentavalent antimonials may be necessary to treat large or multiple lesions. (Courtesy, Dr L. Nabarro.)

Downloaded from Vet-e-Books.com



Fig. 1.264 *L. tropica* in an Arabian child.
L. tropica usually produces a single dry lesion on the head or neck. It is commonly seen in and around towns in the Middle East, Iran and Afghanistan. Although predominantly a zoonosis, anthroponotic transmission may occur in certain environments as was seen in Kabul, Afghanistan, in 2004, when, after 20 years of war, 67,500 residents were found to be suffering from the disease.



Fig. 1.265 Leishmaniasis recidivans.
Rarely, infection with *L. tropica* may result in leishmaniasis recidivans. After the primary lesion has healed, a few persistent organisms remain which provoke a vigorous cell-mediated immune response. Clinically this manifests as papules and nodules which appear at the edge of the scar some time after the primary lesion has healed. Slowly, the edge enlarges leaving a clear and well-healed centre. It is often misdiagnosed as lupus vulgaris, particularly as amastigotes are scarce in skin biopsy due to the robust immune response. The history of initial cutaneous ulceration is crucial in clinching the diagnosis. (From Handler, M., Patel, P., Kapila, R., et al. Cutaneous and mucocutaneous leishmaniasis. Journal of American Academy of Dermatology, 2015-12-01, Volume 73, Issue 6, Pages 897-908, Fig. 7.)



Fig. 1.266 Mucocutaneous leishmaniasis in Ethiopia.
L. aethiopica is the main cause of cutaneous leishmaniasis (CL) in the Ethiopian highlands where rock hyraxes are the reservoir. In addition to simple cutaneous lesions, mucocutaneous and diffuse CL may occur.



Fig. 1.267 *Procavia capensis*; the rock hyrax.
Widely distributed in Africa and Arabia, this hyrax is the reservoir of cutaneous leishmaniasis in Ethiopia. (Courtesy, Dr I. Davidson.)



Fig. 1.268 Diffuse cutaneous leishmaniasis (DCL) of face and hand.
Note the nodules, plaques and indurated tissue in the absence of ulceration seen in this patient with DCL secondary to *L. aethiopica*. A defect in cell-mediated immunity allows the parasite to multiply uncontrollably in this anergic variant of CL which may spread to cover large areas of skin. (Courtesy, Professor K. F. Schaller.)

Downloaded From Vet-eBooks.com



Fig. 1.269 Diffuse cutaneous leishmaniasis (DCL) mistaken for lepromatous leprosy.
This Ethiopian man with DCL secondary to *L. aethiopica* was treated for years in a leprosarium with no improvement in the mistaken belief that he was suffering from lepromatous leprosy. (Courtesy, Professor A. Bryceson.)

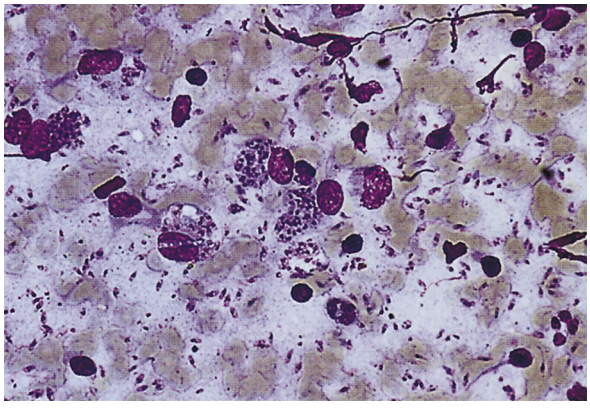


Fig. 1.270 Skin smear in diffuse cutaneous leishmaniasis (DCL).
This smear from a skin biopsy of another Ethiopian patient with DCL shows large numbers of amastigotes. Parasites are rarely so numerous in biopsies from patients with other forms of CL. (Giemsa x 390.)

New World Cutaneous Leishmaniasis



Fig. 1.271 Distribution of New World cutaneous leishmaniasis (CL).
New World CL occurs focally from Texas (USA) and Mexico southwards throughout Central America and South America as far south as São Paulo State in Brazil. The disease is limited by the Andean chain to the west except in Peru where a focus of disease is found on the western slopes of the Andes. The figures give the reported cases in 2013 but likely underestimate the true incidence of disease.

Downloaded From Vet-eBooks.com

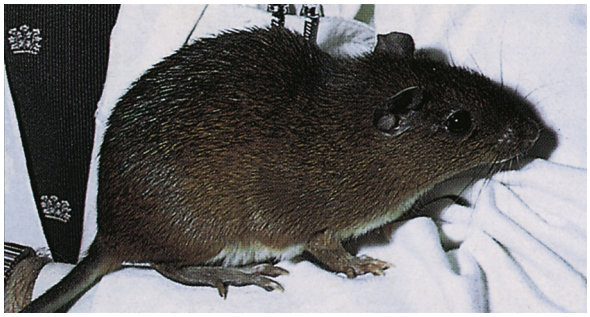


Fig. 1.272 Rodent reservoir of *L. amazonensis* in the Brazilian rainforest.
Most CL in the New World are zoonoses associated with rodents of the rainforest. *L. amazonensis* has been isolated from this species, *Proechimys guyanensis*, in the Amazon basin of Brazil. A number of ground-loving mammals including rodents are primary reservoirs for *L. (V.) braziliensis*.



Fig. 1.273 Lesion of *L. mexicana*.
An early lesion caused by *L. mexicana* is seen on the ear of this man infected in the jungle of Belize. *L mexicana* typically causes small single ulcers which may heal spontaneously. The *L. mexicana* species complex, which includes *L. mexicana* and *L. venezuelensis*, do not cause mucocutaneous leishmaniasis. The exception in this complex is *L. amazonensis*, which may occasionally develop mucosal involvement. (Courtesy, Professor R. Lainson.)



Fig. 1.274 Chiclero's ulcer.
Forest workers collecting gum from wild chicle trees commonly sleep near the forest floor and are bitten on exposed parts of the head by vectors that normally maintain transmission of *L. mexicana* among forest rodents. Ulcers leading to erosion of the auricular cartilage are known as 'Chiclero's ulcer'.



Fig. 1.275 'Sporotrichoid' dissemination.
As noted for *L. major* (Fig. 1.258) lymphatic spread may also occur with New World species. This patient was infected with *L. guyanensis*, the agent of 'pian-bois'. In such infections the lymphatic nodules may ulcerate, resulting in chains of 'sporotrichoid' lesions. *L. guyanensis* may also cause mucocutaneous leishmaniasis. (Courtesy, Professor J.-P. Dedet.)

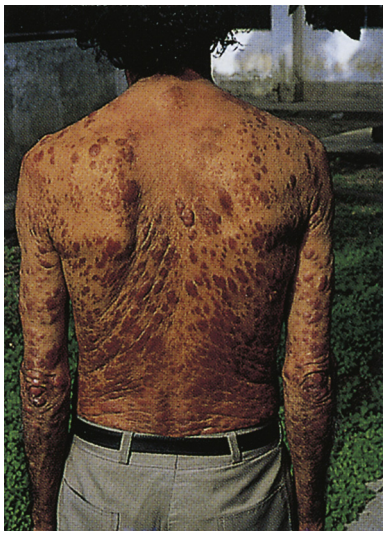


Fig. 1.276 Diffuse cutaneous leishmaniasis (DCL) in the New World.
In rare individuals, a failure of specific cell-mediated immunity may result in the development of diffuse CL, usually in patients infected with *L. amazonensis* or *L. mexicana*. DCL does not affect the mucosae and is often misdiagnosed as lepromatous leprosy.

Downloaded from Vet-eBooks.com

Mucocutaneous Leishmaniasis

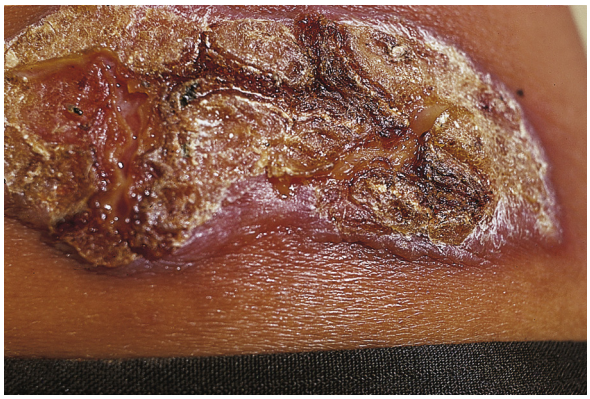


Fig. 1.277 Cutaneous lesion caused by *L. braziliensis*.
Mucocutaneous leishmaniasis (MCL) is caused by the *Viannia* subgenus which includes *L.V. braziliensis*, *L.V. guyanensis* and *L.V. panamensis*. *L.V. braziliensis* typically causes large lesions which may take a long time to heal. Less than 5% of cases go on to develop MCL after a variable period of latency. The risk is negligible if the primary lesion is adequately treated. Here, a primary lesion of *L.V. braziliensis* is seen on the lower abdomen of this man living in the town of Coarí on the Amazon river.



Fig. 1.278 Early nasal lesion.
Mucosal disease often starts in the nasal mucosa. Patients complain of nasal stuffiness or bleeding. An ulcer forms which may subsequently perforate the nasal septum. (From Nelson, S. A. Protozoa and worms. In Dermatology, 3rd edition. Pages 1391–1421, Figure 83.9. Copyright © 2012, Elsevier Limited. All rights reserved. Courtesy, K. Watsky.)

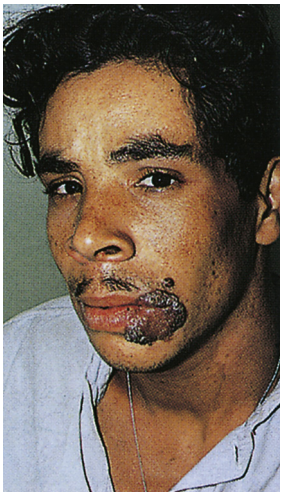


Fig. 1.279 Early lesion of mucocutaneous leishmaniasis.
The oral mucosa may be affected with inflamed and ulcerated lip lesions and tissue destruction. Lesions are painless in contrast to paracoccidioidomycosis and oral cancers which may cause lesions of similar appearance.



Fig. 1.280 Early destruction of the nasal septum.
The progress of the disease in this man, seen in Belo Horizonte, Brazil, was arrested by intensive chemotherapy, leaving him with the need for reconstructive surgery.

Downloaded from Vet-eBooks.com



Fig. 1.281 Pharyngeal involvement.
Ulceration may extend to the pharynx and soft palate, and the first symptoms may be related to tissue destruction in this area. This man from Pará, Brazil, had a large, destructive lesion of the hard palate. (Courtesy, Professor R. Lainson.)



Fig. 1.282 Destructive mucocutaneous leishmaniasis.
Gross destruction of the nose, including the septum and palate, may follow inadequate treatment of *L.V. braziliensis* infection. Many patients with this disease, known locally as *espundia*, respond very poorly if at all to any form of chemotherapy and require reconstructive plastic surgery.

NEMATODES: FILARIAL DISEASES

Table 1.3 The filarial diseases

Species	Clinical disease	Location of MF (periodicity)	Sheath	Main characteristcs	Distribution
Wuchereria bancrofti	LF	Blood (nocturnal*)	+	Tail - pointed tail, nuclei not to tip. Body - 275-300 x 9µm, smooth curves. Sheath - stains pale mauve with Giemsa.	All tropics
Brugia malayi	LF	Blood (nocturnal**)	+	Tail - tapers irregularly, 2 nuclei at tip. Body - 200-275 x 6µm, kinked. Sheath - stains bright pink with Giemsa.	Southeast Asia
Brugia timori	LF	Blood (nocturnal)	+	Tail - tapers irregularly, 2 nuclei at tip. Body - 290-325 x 6µm, kinked. Sheath - stains poorly with Giemsa.	Timor-Leste
Loa loa	Eye worm	Blood (diurnal)	+	Tail - rounded tip, nuclei to tip. Body - 250-300 x 9µm, kinked. Sheath - does not stain with Giemsa.	West Africa, forested areas
Onchocerca volvulus	River blindness	Skin (no periodicity)	–	Tail - long and pointed, nuclei not to tip, crooked. Body - 240-360 x 8µm. Head - spatulate. No sheath.	Africa, Central and South America, Yemen
Mansonella perstans	Most asymptomatic	Blood (no periodicity)	–	Tail - nuclei extend to tip of rounded tail, large nucleus at tip. Body - 190-240 x 5µm. No sheath.	Sub-Saharan Africa, Central and South America

Downloaded from Vet-eBooks.com

Table 1.3 The filarial diseases—cont'd

Species	Clinical disease	Location of MF (periodicity)	Sheath	Main characteristcs	Distribution
Mansonella ozzardi	Most asymp-tomatic	Blood/Skin (no periodicity)	–	Tail - long pointed tail with no nuclei. Body - 150-200 x 5 µm, anterior nuclei positioned side by side. No sheath.	Central and South America, Caribbean
Mansonella streptocerca	Asymptom-atic Dermatitis	Skin (no periodicity)	–	Tail - nuclei extend to tip of rounded, hooked tail. Body - 180-240 x 5µm. Single file anterior nuclei. No sheath.	Central and West Africa

*In the South Pacific, microfilariae may be diurnally sub-periodic.
**In the Philippines, microfilariae may be nocturnally sub-periodic.
LF, lymphatic filariasis.

Lymphatic Filariasis

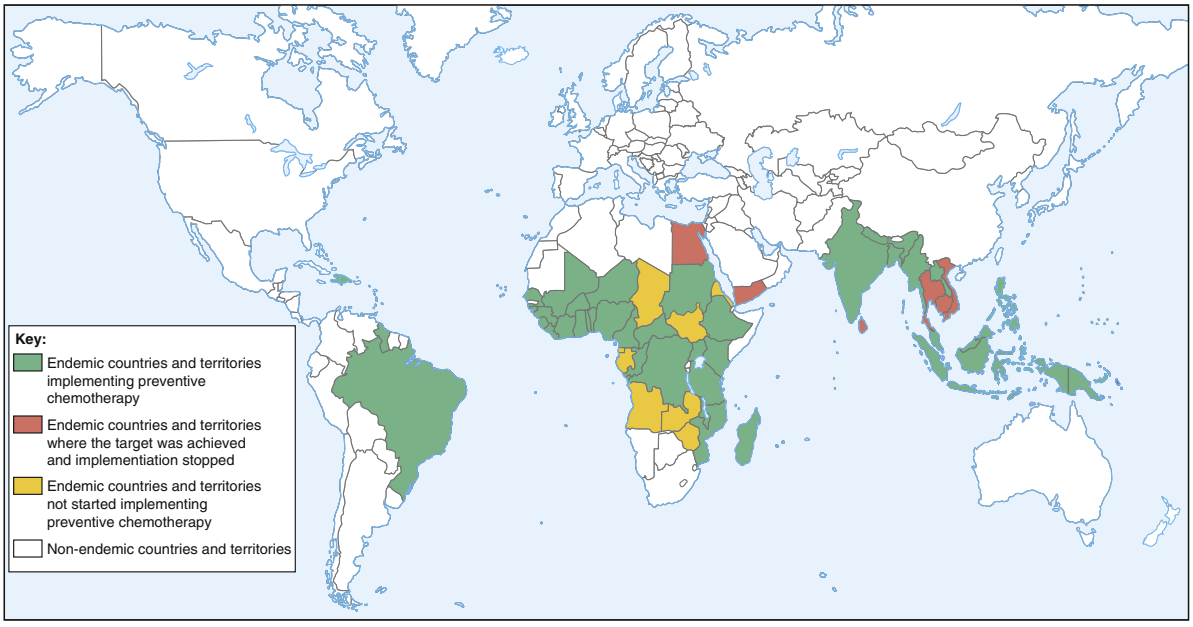


Fig. 1.283 Distribution of lymphatic filariasis (2014).
Worldwide, 947 million people in 54 endemic countries remain at risk of lymphatic filariasis. Of the three causative parasites, *Wuchereria bancrofti* accounts for more than 90% of disease and is endemic through tropical Africa as well as parts of Asia and South America. It is widespread and occurs in both urban and rural areas. *B. malayi* is predominantly a rural disease occurring in focal spots in Malaysia, the Philippines, Indonesia and parts of India. It accounts for most of the remaining 10%. *B. timori* affects a small number of people in Timor-Leste. Since 2000, the Global Program to Eliminate Lymphatic Filariasis (GPELF) has administered 6.2 billion treatments to 820 million people in 62 countries resulting in a 43% reduction in transmission. This map illustrates the status of the programme as of 2014. Note the few countries which have yet to implement preventative chemotherapy, all of which are in sub-Saharan Africa. The aim is for elimination of transmission by 2020. (Courtesy, WHO.)

Downloaded from Vet-eBooks.com

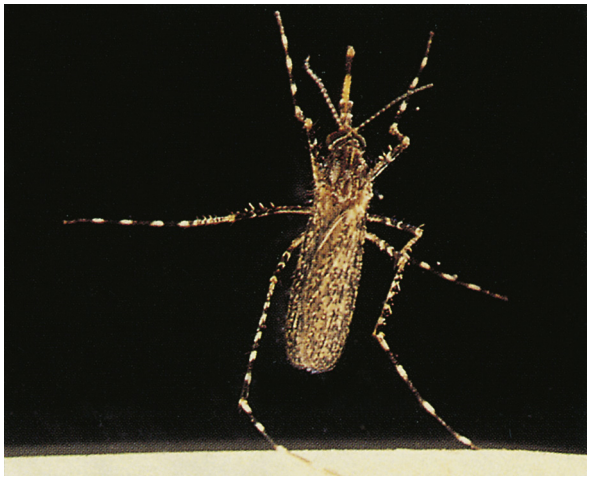


Fig. 1.284 Female *Mansonia* spp.
Mosquito vectors of *Wuchereria* and *Brugia* vary geographically but include *Aedes*, *Anopheles*, *Culex*, *Coquillettidia* and *Mansonia*. In the Far East and south-west Pacific, several species of *Mansonia* (all of which are common swamp breeders) are the main vectors of *B. malayi*. (x 6) (Courtesy, L Oke.)

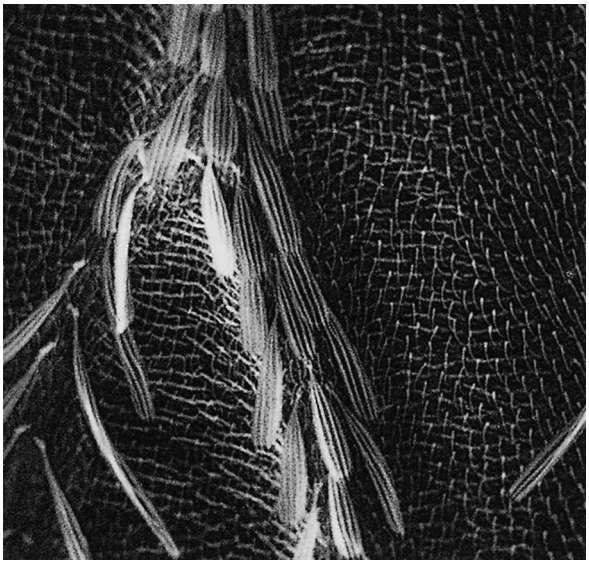


Fig. 1.286 Wing scales of *Culex*.
Note the smaller wing scales of *Culex*. (x 370.) (Courtesy, Professor H. Townson.)

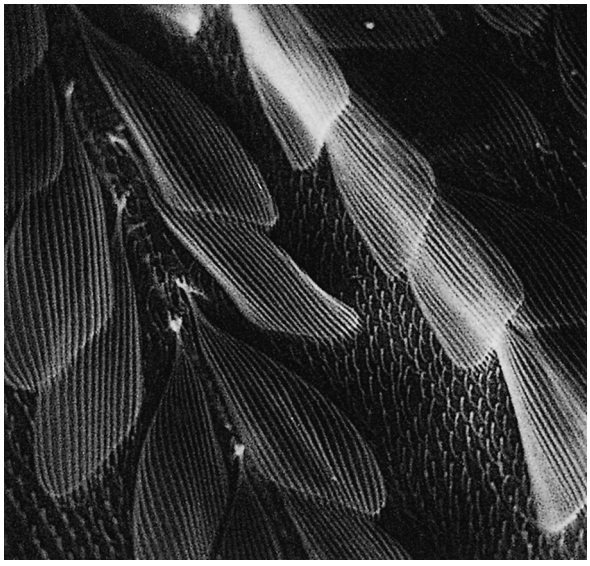


Fig. 1.285 Wing scales of *Mansonia*.
The adults of *Mansonia* are distinguished from other culicines by the typical, large wing scales. Compare with the wings of *Culex* in 1.286. (x 370.) (Courtesy, Professor H. Townson.)



Fig. 1.287 Aquatic stages of *Mansonia*.
Unlike *Anopheles* or *Culex* which are suspended by their siphons from the water–air interface, *Mansonia* larvae have siphons which attach to underwater roots, stems and leaves of aquatic plants. Note the saw-edged tips of the siphons, which are used to penetrate the plants. (x 60.)

Downloaded from Vet-eBooks.com



Fig. 1.288 *Mansonia* breeding sites, India.
An irrigation canal in Kerala, India, choked with water hyacinths, water lettuce and water lilies. These plants are commonly used as attachment sites by larvae and pupae of *Mansonia* species, which acquire oxygen from them. (Courtesy, Dr L. Nabarro.)



Fig. 1.289 Peridomestic culicine breeding site, India.
Septic pits and drains containing highly polluted, stagnant water are ideal breeding grounds for *Culex quinquefasciatus*, a peridomestic vector of bancroftian filariasis.



Fig. 1.290 Taro plants, breeding sites for vectors of the *Aedes (Stegomyia) scutellaris* group in the south-west Pacific.
Rainwater accumulating in leaf axils such as those of taro, banana and pineapple is readily colonized by many species of mosquitoes in forested areas.

Downloaded From Vet-eBooks.com

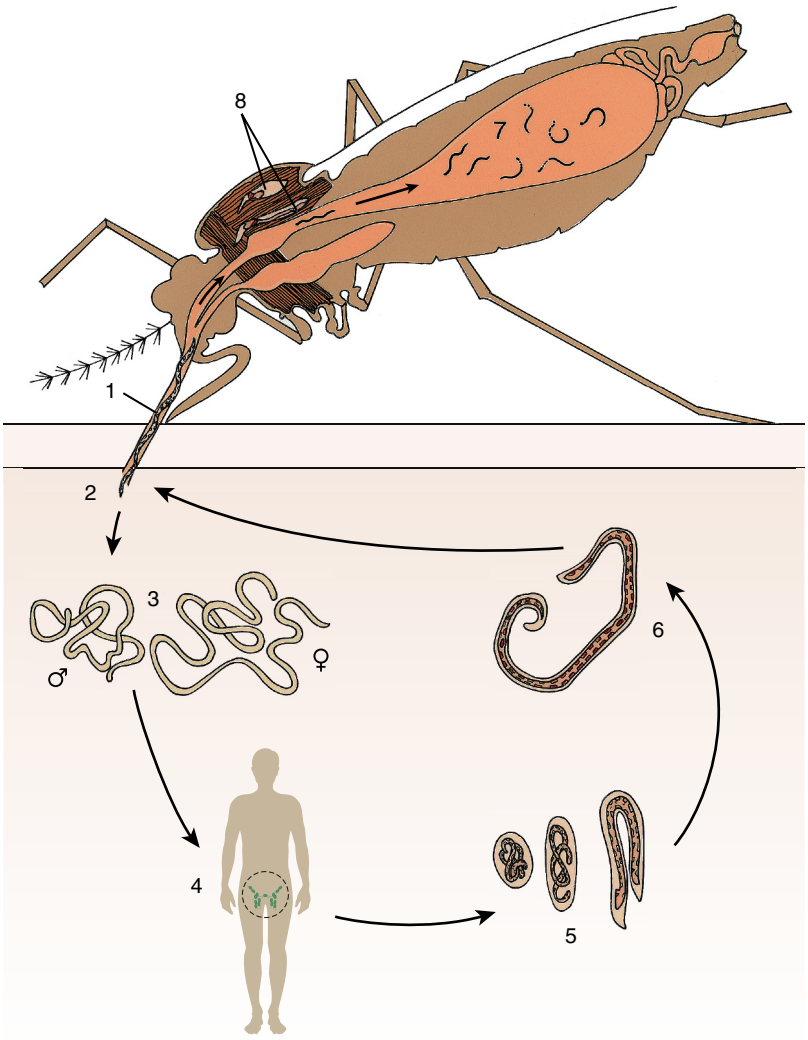


Fig. 1.291 Life cycle of *Wuchereria bancrofti* and *Brugia malayi*.
Third-stage infective larvae (1) from the mouthparts of the mosquito enter the skin through the proboscis when the mosquito feeds (2). The larvae pass to the lymphatics, where they mature to thread-like adults (3). Female worms are 8–10 cm x 0.3 mm, whilst males are smaller at 4 cm x 0.1 mm. After mating, they remain in the lymphatics, (4) where the females develop eggs (5) and larvae (6), which are released as microfilariae into the peripheral circulation. The microfilariae are ingested by another mosquito during a blood meal (7). The larvae penetrate the gut wall of the insect to enter the thoracic muscles (8), where they moult to produce sausage-shaped, second-stage larvae and then long, thin, infective third-stage larvae (1), which migrate to the proboscis.



Fig. 1.292 Larvae in mosquito thorax.
Ingested microfilariae exsheath, migrate from the midgut and penetrate the thoracic muscles, where they mature to sausage-shaped first-stage and second-stage larvae. (x170.)



Fig. 1.293 Head of *Culex quinquefasciatus* showing infective larvae emerging from the proboscis.
After about two weeks, the larvae develop into third-stage, filariform larvae, which enter the mosquito's proboscis. These infective larvae later penetrate the skin of a new host through the puncture wound made when the mosquito bites. (x 20.)

Downloaded From Vet-eBooks.com

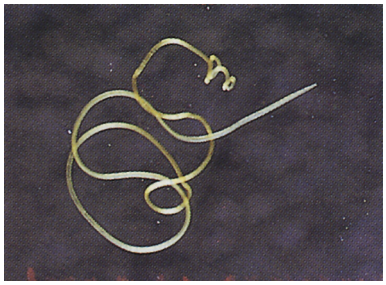


Fig. 1.294 Male *Wuchereria bancrofti* adult.
Adult filarial nematode worms localize to the lymphatics. Adult male *W. bancrofti* are about 4 cm long. (x 9.)

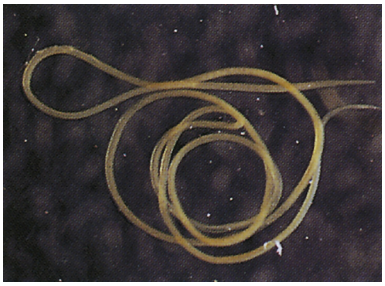


Fig. 1.295 Female *Wuchereria bancrofti* adult.
Female adult *W. bancrofti* are 8–10 cm long. (x 9.)

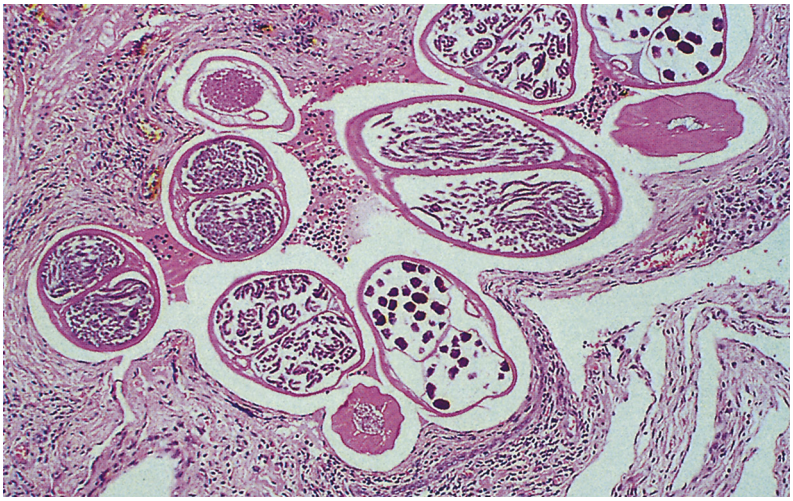


Fig. 1.296 *Wuchereria bancrofti* in an occluded lymphatic vessel.
Note the marked cellular reaction surrounding the microfilaria-containing female worms, seen here in cross section. (H&E x 20.) (Courtesy, R. Suswillo.)



Fig. 1.297 Acute lymphangitis.
Fever, painful lymphadenopathy and lymphangitis may occur early in disease. Recurrent episodes of lymphangitis damage the lymphatics leading to lymphoedema. (Photo Contributor - Liudvikas Jagminas MD. From Knoop, K. Atlas of Emergency Medicine, 2nd edition. New York: McGraw-Hill; 2002.)



Fig. 1.298 Early filarial lymphoedema.
This man has mild lymphoedema of the right leg secondary to filarial infection. The differential diagnosis for unilateral lymphoedema includes malignancy, tuberculosis and recurrent cellulitis. In certain high-altitude areas with volcanic soils, podoconiosis may also cause lymphoedema, although this is usually bilateral. (Courtesy, Dr J. T. Doherty.)

Downloaded From Vet-eBooks.com



Fig. 1.299 Cellulitis in a patient with lymphatic filariasis (LF).
Bacterial skin infections are common in people with LF. Frequent skin inspection and good foot care is essential to prevent recurrent cellulitis which may worsen lymphoedema. Some patients may require daily prophylactic penicillin V. (Courtesy, Dr R. Banerjee.)



Fig. 1.301 Hydrocoele in a Tanzanian man.
Hydrocoele is common in men with Bancroftian filariasis. Initial episodes of acute swelling may resolve completely, but recurrent episodes result in thickening of the tunica vaginalis and the hydrocoele slowly increases in size. It is usually painless unless complicated by superadded bacterial infection.



Fig. 1.300 Elephantiasis.
Note the severe lymphoedema, hyperkeratotic skin and hyper- and hypo-pigmented areas in this patient with severe filarial lymphoedema. This is commonly known as elephantiasis due to its resemblance to the foot of an elephant both in appearance and skin texture. (Courtesy, Dr N. Clayton.)

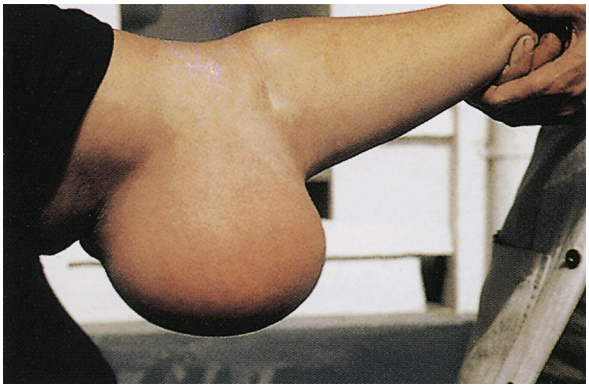


Fig. 1.302 Elephantiasis of right epitrochlear gland in a Fijian.
A feature of Bancroftian filariasis that is unusually frequent in the South Pacific is gross enlargement of the epitrochlear lymph node. (Courtesy, Dr J. F. Kassel.)

Downloaded from Vet-eBooks.com



Fig. 1.303 Chyluria.
Rarely, dilated abdominal lymphatics may rupture into the urinary tract resulting in chyluria. As chyle is rich in fat and protein together with lymphocytes, immunoglobulins and fat-soluble vitamins, prolonged chyluria may lead to severe malnutrition. (Courtesy, Dr J. F. Doherty.)



Fig. 1.304 Lymphogram in patient with chyluria.
This lymphogram shows obstruction of the cisterna chyli and its tributaries. (Courtesy, Professor D. Katamine.)

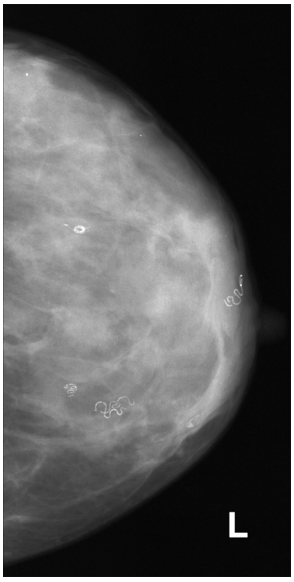


Fig. 1.305 Calcified adult filarial worms in a mammogram.
Occasionally, adult filarial nematodes may develop in the lymphatics of the breast. The adults seen here in the mammogram of a young Cameroonian woman have become calcified, forming palpable nodules appearing as serpiginous shadows that are readily distinguished from neoplastic changes. (Courtesy, Drs H. Alkadhi and E. Garzoli.)



Fig. 1.306 Early lymphoedema in a patient with *Brugia malayi*.
In Brugian filariasis, lymphoedema is less severe and rarely extends above the knee. Genital involvement is rare.

Downloaded from Vet-eBooks.com



Fig. 1.307 Abscesses in groin and thigh due to *Brugia timori*.
Abscess formation, usually along the line of the great saphenous vein in the upper thigh, is fairly common in the early stages of *B. timori* infection. (Courtesy, Dr J. H. Cross.)

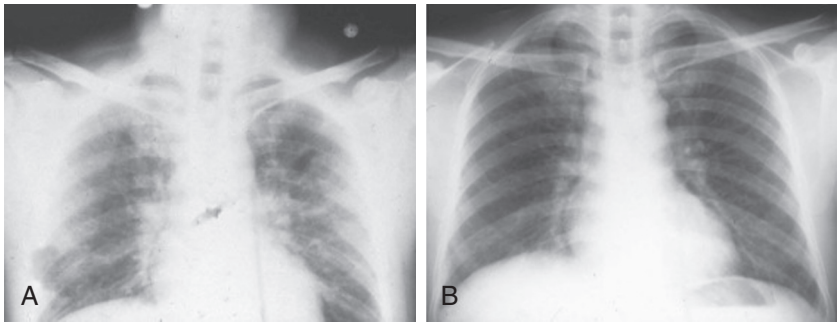


Fig. 1.308 Chest radiograph of tropical pulmonary eosinophilia (TPE) before and after treatment with diethylcarbamazine (DEC).
TPE is an uncommon condition caused by immune hyper-responsiveness to microfilariae in the lungs. The typical presentation is with paroxysmal, nocturnal cough with wheeze and eosinophilia. Note the subpleural opacities and bilateral perihilar interstitial thickening on the initial radiograph (A). Following treatment, the radiograph has normalized (B). (From Kim, K., Weiss, L., Tanowitz, H. Parasitic Infections. In Murray and Nadel's Textbook of Respiratory Medicine, 6th edition, Pages 682–698.e8, Fig. 39.2. Copyright © 2016, 2010, 2005 Saunders, an imprint of Elsevier Inc.)

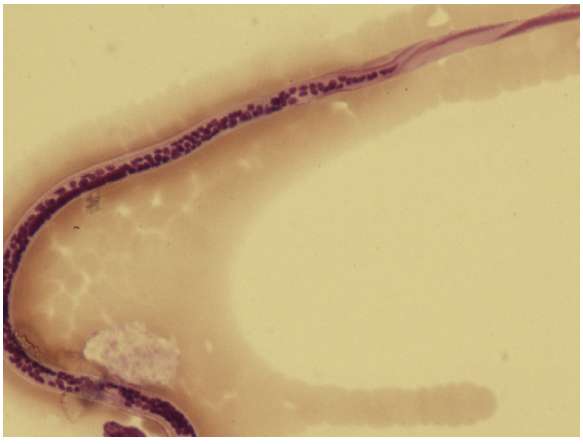


Fig. 1.309 *Microfilaria of Wuchereria bancrofti*.
A blood film stained with Giemsa or Wright and drawn between 10 pm and 2 am will allow identification of the infecting parasite and an estimate of parasite density per millilitre. Note the large elegant body curves and the presence of a sheath. The nuclei in the body are distinct and there are no nuclei at the tip of the tail which is pointed. The microfilariae measure 275–300 μm x 8–10 μm. (Courtesy, H. Edwards.)

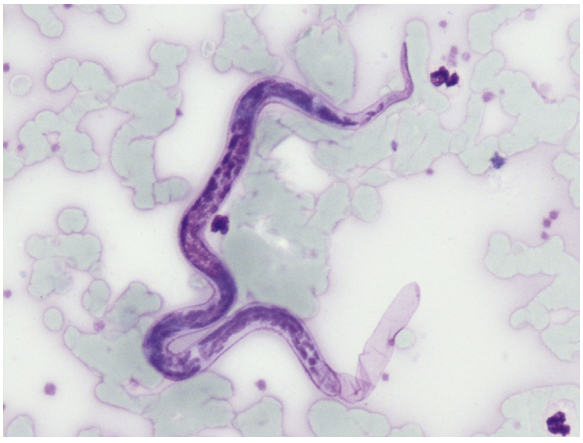


Fig. 1.310 *Microfilaria of Brugia malayi*.
B. malayi measures 200–275 μm x 5–6 μm. The body is coiled and kinked and the sheath stains darkly. The nuclei in the body are large and dense and difficult to distinguish from each other. The tail tapers irregularly and has two nuclei at its end, better seen in Fig. 1.311. (Courtesy, H. Edwards.)

Downloaded from Vet-eBooks.com



Fig. 1.311 *Microfilaria of Brugia malayi.*
Note the two nuclei at the tip of the tail.



Fig. 1.312 *Brugia timori.*
Like *B. malayi*, *B. timori* has two nuclei at the end of the tail. However, it can be distinguished from *B. malayi* by its greater length (290–325 μm x 5–6 μm), paler staining sheath and longer cephalic space. (From Simonsen, P. E., Fischer, P. U., Hoerauf, A., et al. The Filariases. Manson's Tropical Diseases. 23rd edition. Pages 737–765.e5, Fig. 54.5. Copyright © 2014, Elsevier Limited. All rights reserved.)

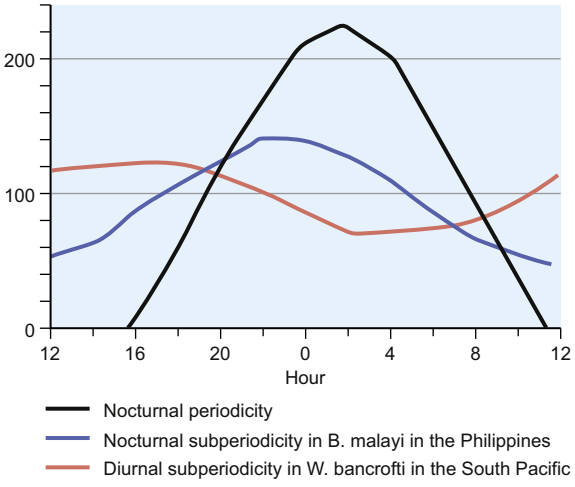


Fig. 1.313 Microfilarial periodicity.
Microfilarial counts in the blood vary during the day and are maximal at the time when the principal vector is biting. In general, both *Wuchereria* and *Brugia* species are nocturnally periodic and microfilariae peak in the blood between 10 pm and 2 am. Diagnostic blood films should be performed between these times to maximize the chance of identifying the parasite. However, in areas where the local vectors bite during the day or at dusk, microfilariae may display nocturnal subperiodicity or even diurnal periodicity. (Adapted from Simonsen, P. E., Fischer, P. U., Hoerauf, A. et al. The Filariases. In Manson's Tropical Diseases. 23rd edition. Pages 737–765.e5, Fig. 54.6. Copyright © 2014, Elsevier Limited. All rights reserved.)

Downloaded from Vet-eBooks.com

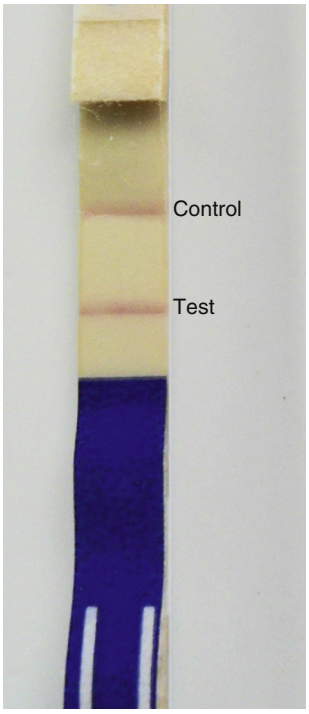


Fig. 1.314 Rapid serological diagnosis of *Wuchereria bancrofti*.
Rapid diagnostic tests have been developed which detect circulating filarial antigen (CFA) released by adult worms. CFA is present in the blood of both microfilaraemic and amicrofilaraemic individuals but is not found in people with past infection. Antigen levels are stable in the blood so the test can be performed at any time of day. This figure shows an Alere filariasis test strip which is recommended by the WHO for transmission assessment surveys in *W. bancrofti* endemic areas. The upper line is a control line, indicating that the test is working, the lower line is the test line, indicating a positive result. (From Weil GJ, Curtis KC, Fakoli L et al. Laboratory and Field Evaluation of a New Rapid Test for Detecting Wuchereria bancrofti Antigen in Human Blood. Am J Trop Med Hyg. 2013 Jul 10; 89(1): 11–15. doi: 10.4269/ajtmh.13-0089.)

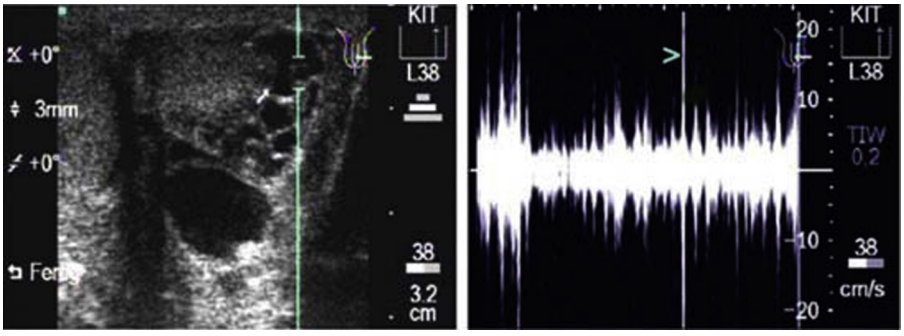


Fig. 1.315 Ultrasound of filaria in the lymphatics.
Ultrasound can be used to visualize individual adult worms 'dancing' in the lymphatics. The panel on the left shows an enlarged lymphatic vessel containing a worm nest. The panel on the right shows the ultrasound in pulse wave Doppler (PWD) mode where the movement of the worms are visualized as an undulating band with sharp irregular peaks. It is this constant irregular movement that distinguishes the dancing worms from the regularly pulsating blood vessels. (From Mand, S., Marfo-Debrekyei, Y., Dittrich, M., et al. Animated documentation of the filaria dance sign (FDS) in Bancroftian filariasis. Filaria Journal, 2003, Volume 2, page 3.)

Downloaded from Vet-e-Books.com

Loiasis

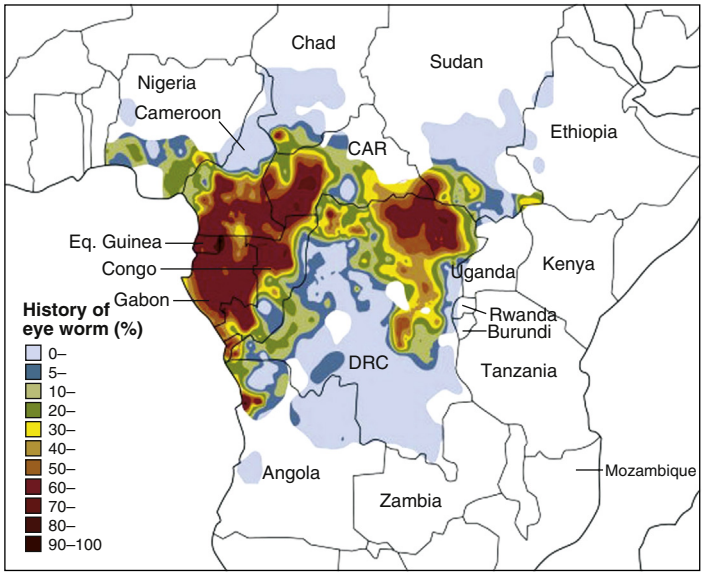


Fig. 1.316 Distribution of *Loa loa*.
Loa loa only occurs in West and Central Africa. An estimated 3–13 million people are infected in this area but many remain asymptomatic making it difficult to define accurately the epidemiology. This map documents the community prevalence of eye worm, as established by the Rapid Assessment Procedure for Loiasis (RAPLOA), and gives some idea of the extent of disease in endemic areas. (Adapted from Zouré, H. G., Wanji, S., Noma, M. et al. The geographic distribution of Loa loa in Africa: results of large-scale implementation of the Rapid Assessment Procedure for Loiasis (RAPLOA). PLoS Neglected Tropical Diseases, 2011, Volume 5, Page e1210.)

Downloaded from Vet-e-Books.com

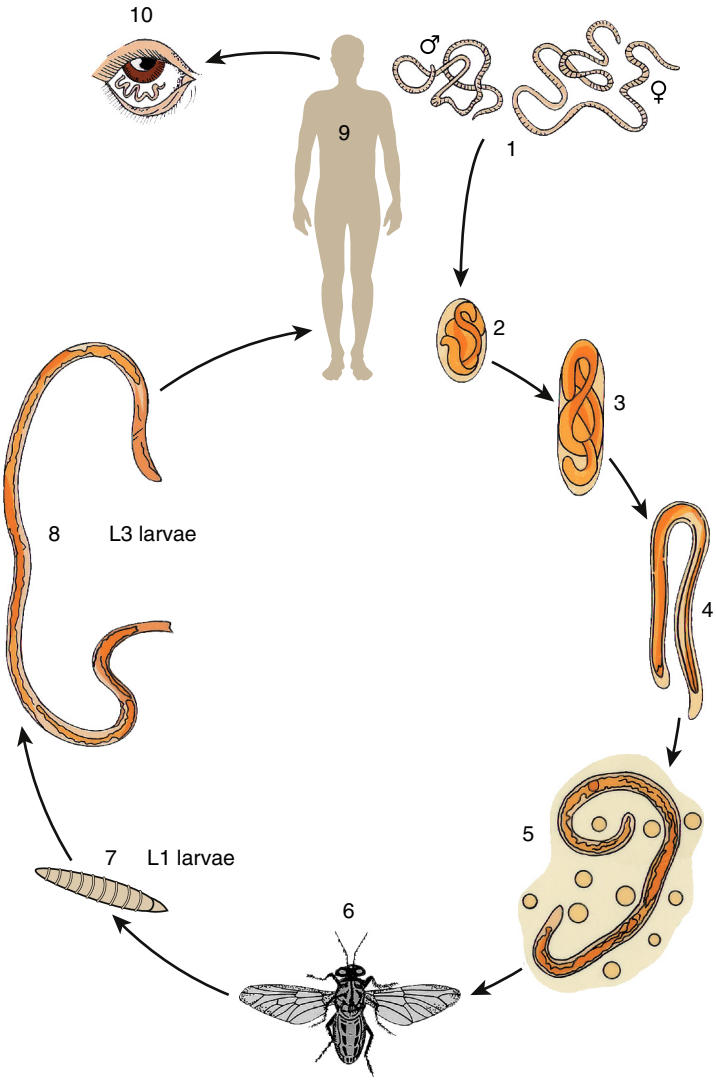


Fig. 1.317 Life cycle of *Loa loa*.
The adult worms (1) live in humans for 4–12 years. They migrate through subcutaneous tissues causing Calabar swellings and may cross the front of the eye under the conjunctiva (10). Adult females produce sheathed microfilariae (5) which develop from larvae (2–4) and circulate in the blood. The microfilaraemia peaks in the daytime, corresponding with the period when *Chrysops* vectors are biting (6). Once ingested, the microfilariae shed their sheaths, penetrate the midgut wall and enter the thoracic muscles. Here they mature, first to 'sausage-like' L1 larvae (7) and then to infective third-stage larvae over a period of 8–12 days (8). These larvae infect a new host (9) when the *Chrysops* takes another blood meal, and mature to adult worms within 6–12 months.

Downloaded From Vet-eBooks.com



Fig. 1.318 *Chrysops*.
Chrysops are medium-sized day-biting flies with iridescent eyes. At rest, the wings are held in an open scissor formation over the abdomen. They breed in the rainforest canopy, laying their eggs in jungle swamps. (Courtesy, S. McIntyre.)

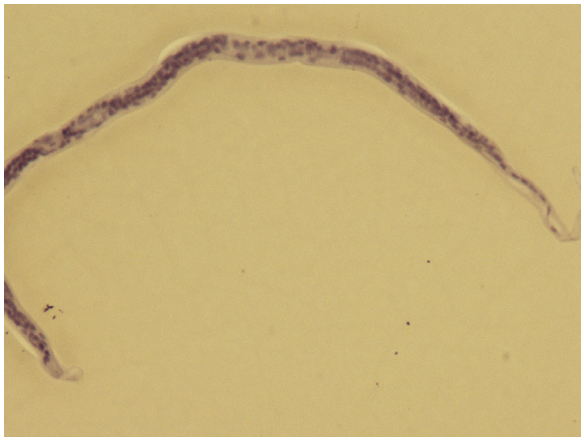


Fig. 1.319 Microfilaria of *Loa loa*.
Loa loa microfilariae are 250–300 μm x 8–10 μm. The dark, densely stained nuclei extend to the rounded tip of the tail. Although a sheath is present, it does not stain well and may be difficult to see. (Courtesy, H. Edwards.)

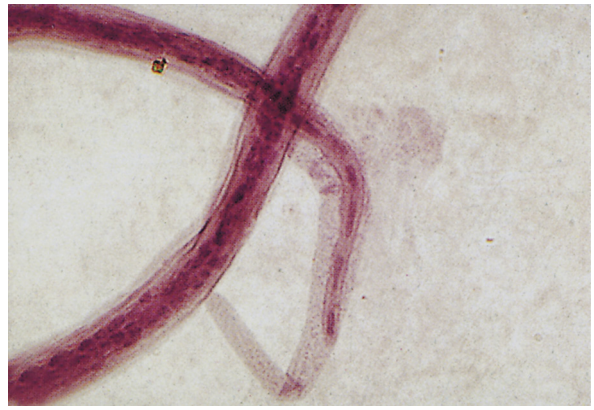


Fig. 1.320 Microfilaria of Loa loa.
Note the nuclei that extend to the rounded tip of the tail and the poorly staining ('ghost') sheath seen here. *Loa* microfilariae show diurnal periodicity and peak in the blood between 10 am and 2 pm.



Fig. 1.321 Calabar swelling.
The host immune response to migrating adult worms may result in Calabar swellings. These are painless swellings that appear, last for hours to days and then recur at irregular intervals. They typically occur on the hands or forearms as seen in this patient. (From Klion, A. D. Loiasis. In: Hunter's Tropical Medicine and Emerging Infectious Diseases. 9th edition. Pages 823–826, Fig. 111.3. Copyright © 2013, Elsevier Inc. All rights reserved. Courtesy, J. Kamgno.)

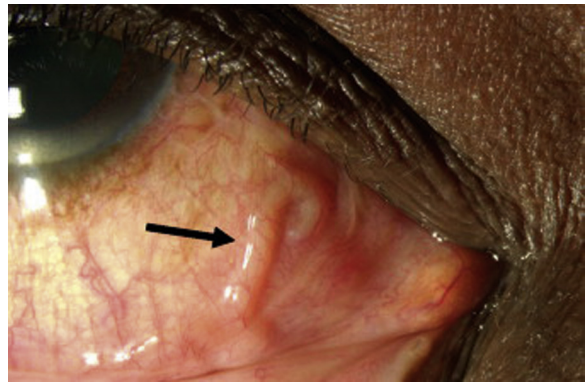


Fig. 1.322 Subconjunctival *Loa loa*.
Migrating adult worms (arrowed) may pass under the conjunctiva, giving rise to considerable irritation and congestion. (From Jain, R., Chen, J., Butcher, A. et al. Subconjunctival *Loa loa* worm. International Journal of Infectious Diseases, 2008-11-01, Volume 12, Issue 6, Pages e133–e135, Fig. 1. Copyright © 2008 International Society for Infectious Disease.)

Downloaded From Vet-eBooks.com

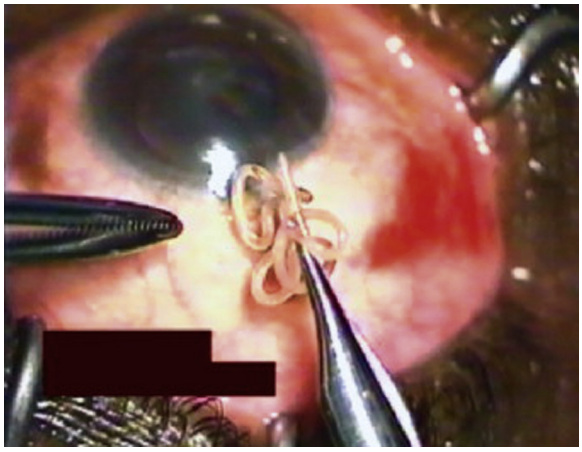


Fig. 1.323 Surgical extraction of a subconjunctival *Loa loa*.
The adult worm can be extracted with fine forceps after anaesthetizing the conjunctiva. (From Jain, R., Chen, J., Butcher, A. et al. Subconjunctival *Loa loa* worm. International Journal of Infectious Diseases, 2008-11-01, Volume 12, Issue 6, Pages e133–e135, Fig. 3. Copyright © 2008 International Society for Infectious Disease.)



Fig. 1.324 Tail of male *Loa loa*.
The spicules at the posterior end of the male adult worm are typical of this species. (x 90.)

Onchocerciasis

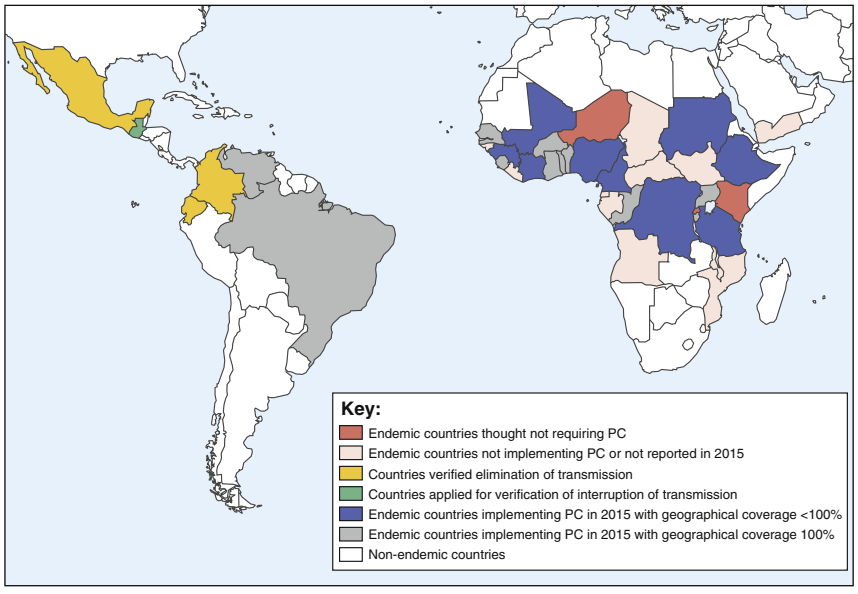


Fig. 1.325 Distribution of onchocerciasis.
Ninety-nine per cent of onchocerciasis, also known as river blindness, occurs in 31 countries in sub-Saharan Africa. In 2006, an estimated 37 million people were infected, with 120 million people at risk of infection. A handful of small foci of disease existed in South and Central America but bi-annual mass drug administration of ivermectin in endemic areas has largely eliminated this. Ongoing transmission now only occurs in a focal area of Brazil and Venezuela. PC - preventative chemotherapy. (Courtesy, WHO.)

Downloaded from Vet-eBooks.com

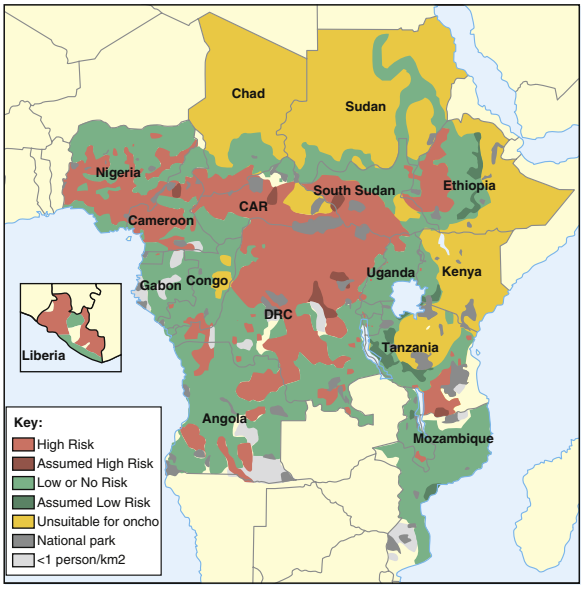


Fig. 1.326 High and low risk areas for onchocerciasis transmission in APOC (African Programme for Onchocerciasis Control) countries.
Within endemic countries, transmission only occurs in focal areas where environmental and social conditions are optimal for the *Simulium* black fly vector to bite and infect humans. This map shows the distribution of disease in 20 APOC countries; note the focal distribution of disease. (From Noma, M., Zouré, H., Tekle, A., et al. The geographic distribution of onchocerciasis in the 20 participating countries of the African Programme for Onchocerciasis Control: (1) priority areas for ivermectin treatment. Parasites and Vectors, 2014, Volume 7, Page 325, Figure 4.)

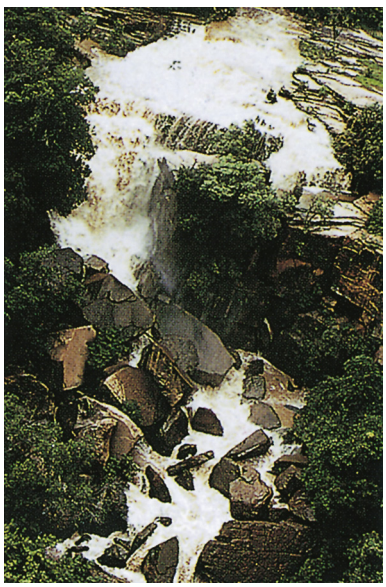


Fig. 1.328 Typical locality of *Simulium* in West Africa.
Fast-moving, highly oxygenated water in streams, rivers and waterfalls provide the essential ecological environment for *Simulium* to breed. Eggs are laid on partially submerged objects or dropped into the water during flight. (Courtesy, Dr D. A. T. Baldry.)



Fig. 1.327 Adult *Simulium damnosum*.
Simulium or blackfly are small-bodied biting flies which transmit *O. volvulus*. Note the hunched body shape, low-slung head and large wings which cover each other completely at rest. In sub-Saharan Africa, the principal vector of *O. volvulus* is *S. damnosum*. The thickened hind legs with a white band are characteristic of this species. (Courtesy, S. McIntyre.)



Fig. 1.329 Larvae of *Simulium* attached to a submerged plant.
Larvae attach to a fixed object such as a submerged plant by posterior hooks and a pad of silk. Note the cephalic fans that filter food from river water. In this manner they pass through six to nine larval instars.



Fig. 1.330 *Simulium* larvae and pupae on a crab.
In East Africa, larvae and pupae of the *S. neavei* complex attach to fresh-water crabs. Several of each stage of *S. nyasalandicum* can be seen on this preserved specimen of *Potamonautes pseudoperlatus*, which inhabits small hill streams in Tanzania.

Downloaded From Vet-eBooks.com



Fig. 1.331 Life cycle of *Onchocerca volvulus*.
Microfilariae in the subepidermis (1) are taken up with blood when the *Simulium* bites. From the blackfly midgut (2), the larvae pass into the haemocoele, then enter the thoracic muscles, where they grow and undergo two moults. In the process, they pass through an L2 'sausage' stage (3), then become long, thin, infective L3 larvae (4); the whole process takes from 6 to 12 days depending upon the ambient temperature. The infective larvae make their way to the proboscis, through which they enter the skin when the fly feeds. Infective larvae mature into adults as they migrate through the subcutaneous tissues, with males and females mating and becoming encapsulated by fibrous tissue in prominent subcutaneous nodules (5). Within the nodules, the females produce larvae and these microfilariae (6) migrate into the nearby subepidermal tissues. (Adapted from Geigy and Herbig, 1955.)

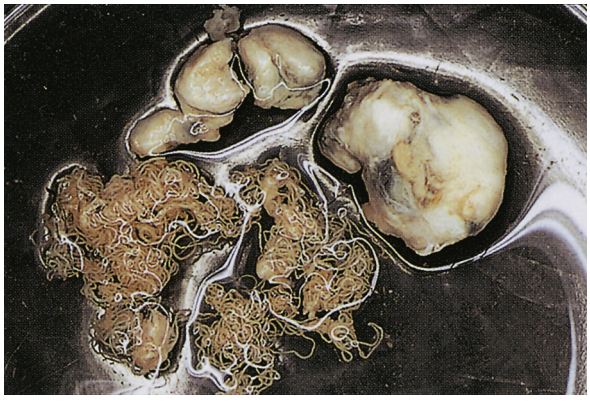


Fig. 1.332 Macroscopic section of an *Onchocerca* nodule.
In this cross section of a nodule, the adult worms can be seen entwined within a nodule. They lie in a matrix of inflammatory cells and fibrinoid material. Microfilariae are released by the female worms to migrate through the skin and eyes. (x 2.) (Courtesy, Dr B. Duke.)

Downloaded From Vet-eBooks.com

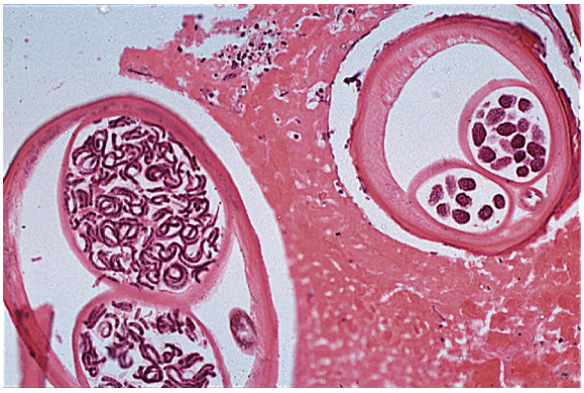


Fig. 1.333 Cross section through an adult female *Onchocerca volvulus*.
Note the microfilariae visible in the uterus of this adult female *O. volvulus*. (Courtesy, Professor S. Lucas.)



Fig. 1.334 Onchocerca nodules on the iliac crests.
The location of nodules is said to reflect the biting preferences of the local *Simulium* population. In Africa, most nodules occur in the pelvic region whilst in South and Central America, head and trunk nodules are more common. Although some find them unsightly, they are usually painless unless they compress local structures such as nerves. (Courtesy, Drs J. Anderson and H. Fuglsang.)

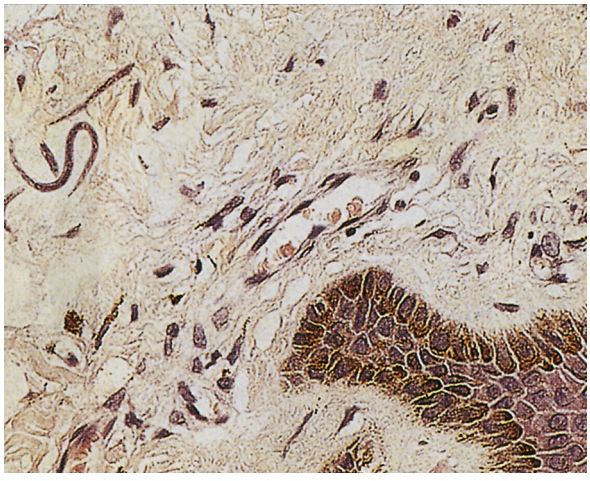


Fig. 1.335 Microfilaria in skin biopsy.
After discharge from the female uterus, the microfilariae migrate through the skin and eyes. Treatment even with a single dose of a microfilaricide such as diethylcarbamazine can trigger a severe allergic response, the 'Mazzotti reaction', due to rapid killing of the skin-dwelling microfilariae. (H&E x 350.) (Courtesy, Professor C. D. Mackenzie.)

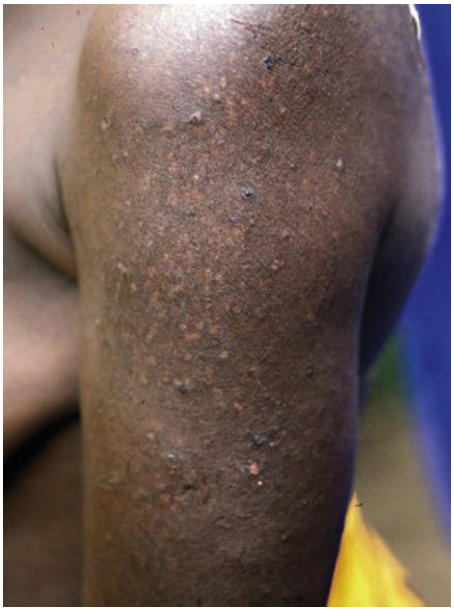


Fig. 1.336 Onchocercal dermatitis.
Dying microfilariae provoke an inflammatory reaction in the skin resulting in severe pruritus. Papules, vesicles or pustules may occur and the skin can become secondarily infected through itching. (From Simonsen, P. E., Fischer, P., Hoerauf, A., et al. The Filariases. In Manson's Tropical Diseases. Pages 737–765, Figure 54.18. Courtesy, D.W. Buttner.)

Downloaded From Vet-eBooks.com



Fig. 1.337 Leopard skin.
Recurrent episodes of acute inflammation and excoriation result in hypertrophic, lichenified skin with areas of hypo- and hyperpigmentation. Leopard skin, as seen here, principally occurs on the pretibial regions and consists of depigmentation with preserved pigment around hair follicles.

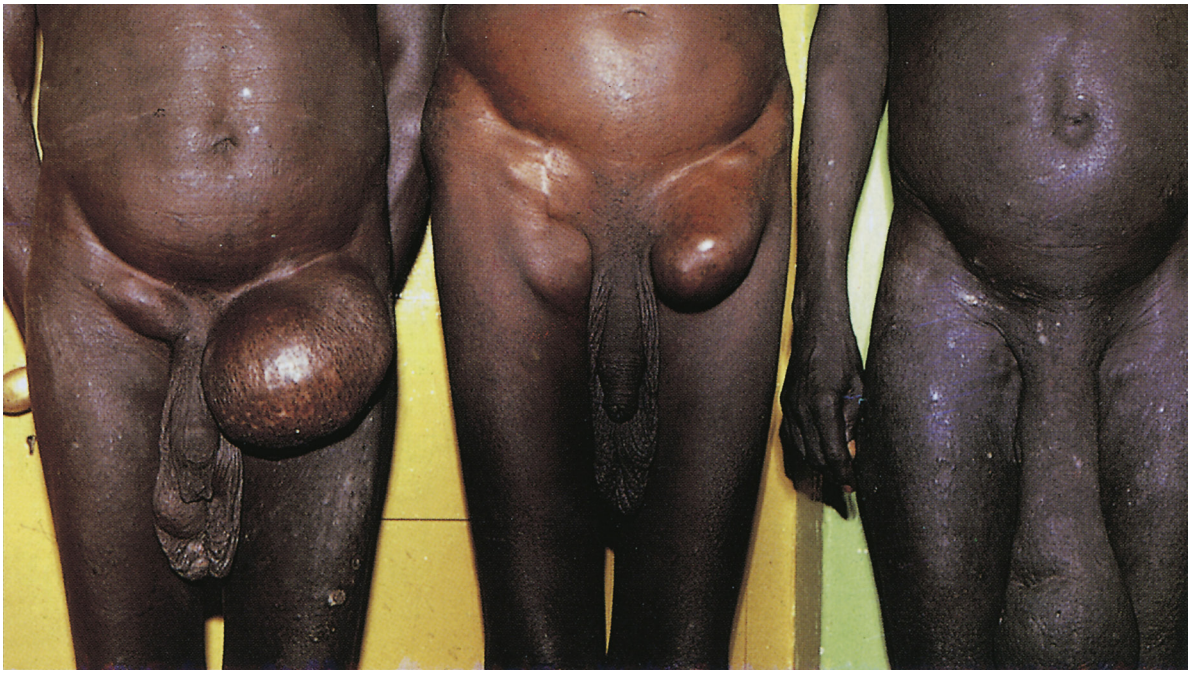


Fig. 1.338 'Hanging groin' and scrotal elephantiasis.
Skin atrophy around the groin may result in the inguinal lymph nodes 'hanging' in folds of loose skin. (Courtesy, Dr O. P. Arya.)

Downloaded from Vet-eBooks.com



Fig. 1.339 'Leonine facies'.
Severe skin atrophy on the face may give rise to leonine facies, as seen here in this Guatemalan man. Lepromatous leprosy can give a similar appearance. (Courtesy, Professor A. Woodruff.)

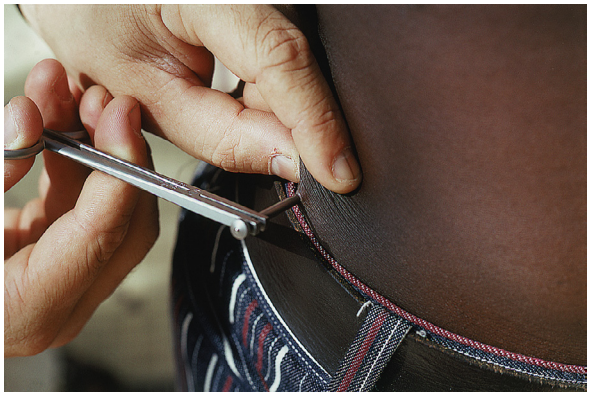


Fig. 1.340 Skin snip technique.
A tiny piece of skin, often from the back of the shoulders, iliac regions or calf, is snipped off and placed in a drop of saline on a microscope slide under a cover slip, where it is left for up to 30 minutes at room temperature. The use of a scleral puncture as seen here permits the removal of a standard-sized sample to be taken for quantitative assessment of the microfilarial load. A simpler method is to raise the skin with a needle tip, then remove a piece of skin with a scalpel blade. As with all procedures, an aseptic technique should be used.

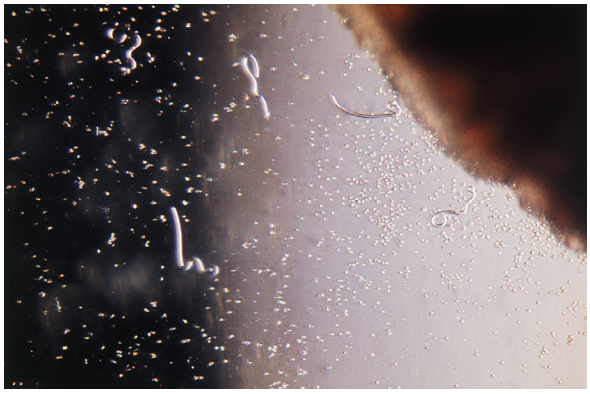


Fig. 1.341 Living microfilariae of *Onchocerca volvulus*.
After some time, actively moving microfilariae emerge from the skin into the surrounding saline where they can be counted. (x 350) (Courtesy, The Director, Armed forces Institute of Pathology, Washington, DC.)

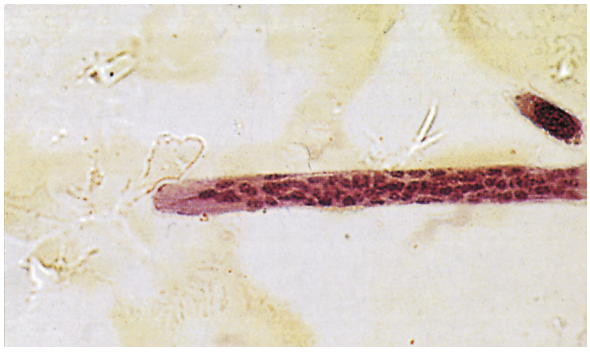


Fig. 1.342 Head of *Onchocerca volvulus* microfilaria in skin snip.
Microfilariae measure 240–360 μm x 5–9 μm. Note the absence of a sheath, the slightly enlarged head and anterior nuclei. (x 930)

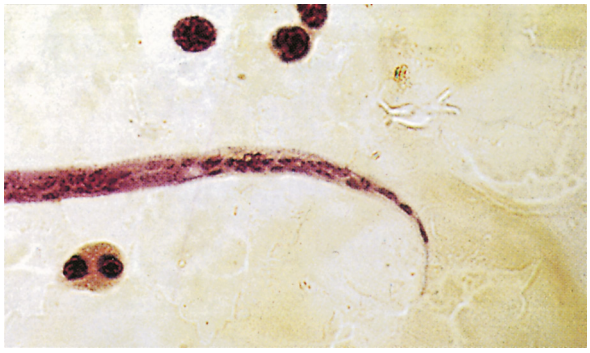


Fig. 1.343 Tail of *Onchocerca volvulus* microfilaria in skin snip.
Note the long pointed tail and the absence of nuclei at the tip of the tail. (x 930)

Downloaded From Vet-eBooks.com

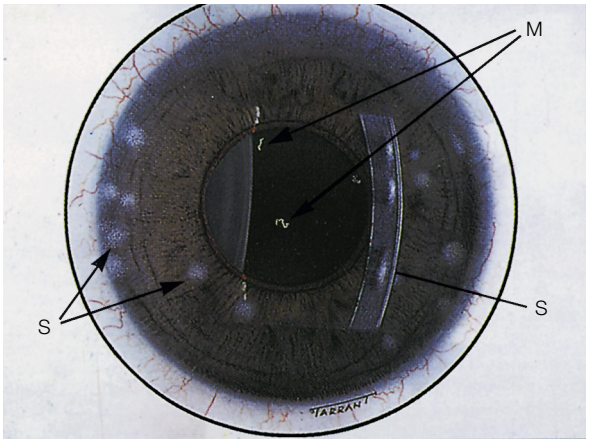


Fig. 1.344 Slit lamp examination of the eye.
Slit lamp examination often reveals numerous microfilariae (M) in the anterior chamber of the eye. They are best sought in the inferior medial quadrant. Note the 'snowflake-like opacities' (S) in the cornea. (Courtesy, Dr J. Walters.)

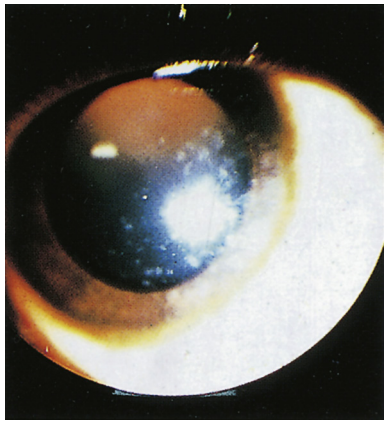


Fig. 1.345 Early corneal involvement.
The tissue reaction associated with dead microfilariae in the cornea gives rise to 'snowflake-like' opacities as seen in this figure. This punctate keratitis may clear with time. Heavy microfilarial infection can lead to the development of progressive, sclerosing keratitis that commonly produces blindness.



Fig. 1.346 Optic atrophy.
A variety of choroidoretinal lesions may follow damage by microfilariae to the anterior segment of the eye; optic atrophy may develop finally, as seen in this eye.



Fig. 1.347 *Onchocerca* head nodule.
Head nodules are associated with greater risk of ocular disease and blindness due to their proximity to ocular structures. They should be excised where possible. This blind man from Burkina Faso has a nodule just above his eye. (Courtesy, Dr D. A. T. Baldry.)



Fig. 1.348 The social cost of onchocerciasis.
Onchocerciasis is the second commonest infectious cause of blindness. In endemic areas, blindness may reduce life expectancy by 10 years and leave people completely dependent on their family and community. (Copyright © 2008 Science Photo Library.)

Downloaded from Vet-e-Books.com



Fig. 1.349 Nodding syndrome.
In meso and hyper-endemic onchocerciasis endemic regions with a sub-optimal onchocerciasis elimination programme, a high prevalence and incidence of onchocerciasis associated epilepsy (OAE) is observed. Nodding syndrome and Nakalanga features are phenotypic presentations of onchocerciasis associated epilepsy. This 21 year old male, living in an onchocerciasis endemic village in the DRC has "Nakalanga syndrome" with stunted growth, generalized tonic-clonic epilepsy since the age of 9 years, muscular atrophy and severe cognitive impairment. A recent prospective study in Cameroon showed a microfilaria load-dependent risk to developing epilepsy later in life following childhood infection with *Onchocerca volvulus*. However, it remains to be elucidated how the *O. volvulus*, directly or indirectly is causing OAE. New evidence in 2017 suggests that one mechanism may be through an autoimmune encephalitis triggered by development of antibodies to *O. volvulus* proteins which cross-react with leiomodin-1 receptors in the brain. (Courtesy, Professor R. Colebunders.)



Fig. 1.350 Helicopter spraying over a breeding site of *Simulium damnosum* on the River Milo, Republic of Guinea.
Between 1974 and 2002, the Onchocerciasis Control Programme used aerial spraying to control *Simulium* populations in endemic areas. (Courtesy, Professor D. H. Molyneux.)



Fig. 1.351 Ivermectin distributed through APOC.
Since 1995 the African Program for Onchocerciasis Control (APOC) has distributed ivermectin (Mectizan), donated free of cost by Merck, to 22 endemic countries in Africa. By the end of 2014, 112.4 million people were receiving regular doses with an estimated 73% reduction in prevalence compared with pre-APOC rates. (From Ōmura, S., Crump, A. Ivermectin: panacea for resource-poor communities? Trends in Parasitology, 2014-09-01, Volume 30, Issue 9, Pages 445–455, Figure 6. Photograph by Andy Crump.)

Other Filarial Infections

Mansonella.



Fig. 1.352 *Mansonella perstans* and *Loa loa* in a blood film.
M. perstans is a widely distributed filarial parasite that occurs in sub-Saharan Africa and in localized parts of Central and South America and the Caribbean. Adult worms live in serous cavities producing microfilariae that circulate in the blood. Many people are asymptomatic but some may experience Calabar swellings, fever, joint pain or pruritus. This film shows a mixed infection with the large microfilariae of *L. loa* (250–300 μm) and the smaller *M. perstans* (190–240 μm). *(Giemsa x 100)*

Downloaded from Vet-eBooks.com



Fig. 1.353 Adult female *Culicoides*.
Culicoides are small biting midges 1–2 mm in length. They have prominent eyes, short legs and an irritating bite. They are vectors for both *M. perstans* and *M. streptocerca*.



Fig. 1.354 Larva of *Culicoides*.
Culicoides larvae are 5–6 mm long with a small head and 12 body segments. They are found in damp environments rich in organic matter, such as the banks of small ponds, tree holes and leaf axils.



Fig. 1.355 Pupae of *Culicoides*.
Like mosquito pupae, the pupae of *Culicoides* obtain air by piercing the surface water film with their respiratory trumpets. (x10.)



Fig. 1.356 Breeding sites of *Culicoides* in an African village.
The leaf axils of bananas, such as in this Liberian rainforest village plantation, are excellent breeding sites for *Culicoides* species in tropical areas.

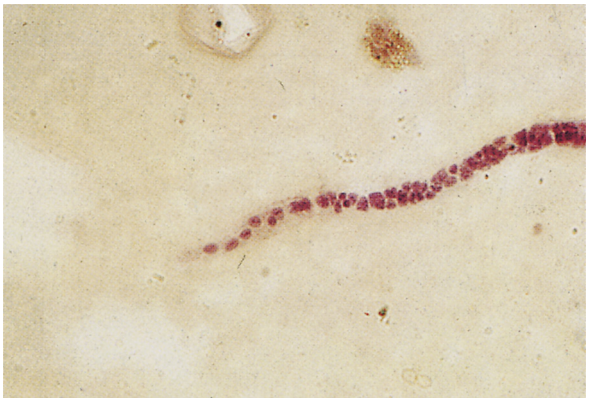


Fig. 1.357 Head of *Mansonella streptocerca* microfilaria.
M. streptocerca occurs in Central and West Africa. Both adult worms and microfilariae live in the skin around the chest and shoulders. Most infections are asymptomatic but dermatitis may occur resulting in a pruritic hypopigmented maculopapular rash. Microfilariae are small, 180–240 μm x 5 μm, and do not have a sheath. The anterior nuclei, seen here, stand in single file.

Downloaded from Vet-eBooks.com



Fig. 1.358 Tail of *Mansonella streptocerca* microfilaria.
Note the nuclei that extend to the tip of the rounded, hooked tail and the absence of a sheath.

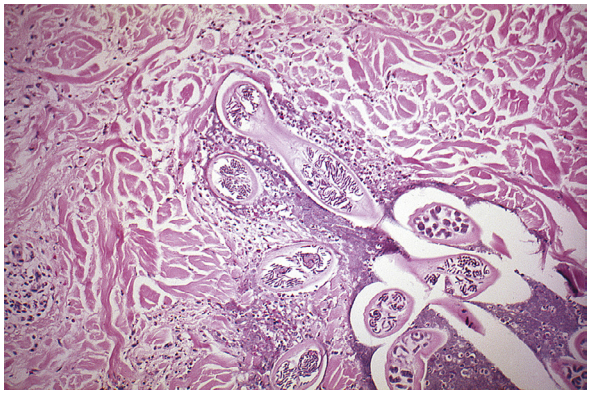


Fig. 1.359 *Mansonella streptocerca* adult females in section of human skin.
Female *M. streptocerca* measure approximately 27 mm x 0.08 mm and live tightly coiled in the subcutaneous tissues from where they release unsheathed microfilariae. Sections of these can be seen within the adult worms here. (H&E x 200.)

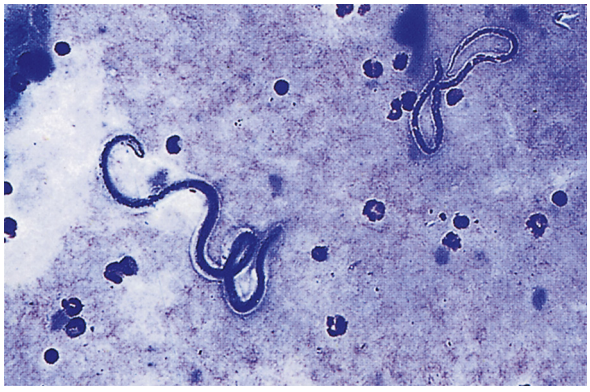


Fig. 1.360 Microfilaria of *Mansonella ozzardi* and *Wuchereria bancrofti*.
M. ozzardi (right) is found in the blood of people from parts of South America and the Caribbean. The microfilaria is readily distinguished from the larger and sheathed microfilaria of *W. bancrofti* (left) which also occurs in the same region. Vague symptoms of various types have been attributed to infection with the parasite, but causality has not been proven. (x 340.) (Courtesy, Professor Y. Gutierrez.)

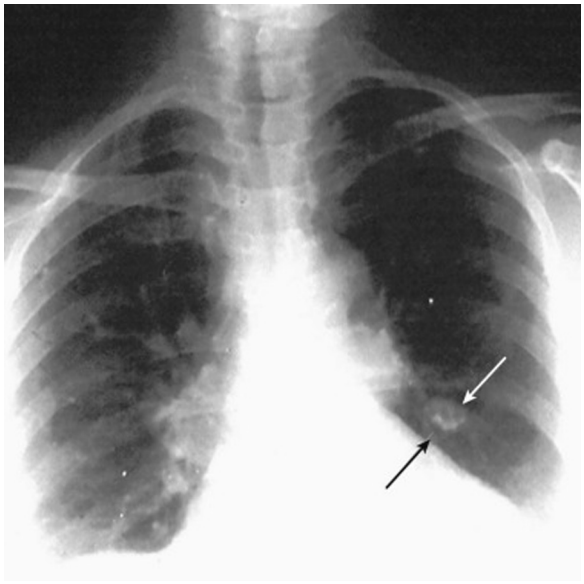


Fig. 1.361 Pulmonary dirofilariasis.
Dirofilaria immitis, or dog heartworm, is a canine filariasis, transmitted by mosquitoes. Humans may accidentally acquire infection but are dead-end hosts; the infecting L3 larvae are unable to mature to fertile adulthood to produce microfilariae. In humans, most cases are asymptomatic. Occasionally, as seen here, they become coin lesions in the lung, which require biopsy to exclude a malignant diagnosis. (From McCall, J.W., Genchi, C., Kramer, L.H., et al. Heartworm disease in animals and humans. Advances in Parasitology, 2008, Volume 66, Pages 193–285. Courtesy, F. Simón, University of Salamanca, Spain.)

Downloaded from Vet-eBooks.com

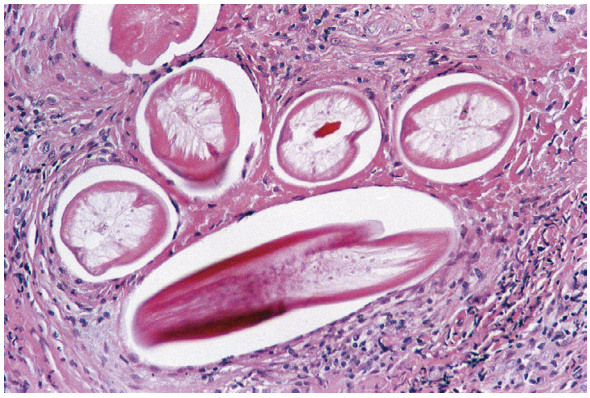


Fig. 1.362 Cross sections of *Dirofilaria repens* in a subcutaneous nodule.
Dirofilaria repens is a filarial parasite of dogs and cats that causes subcutaneous nodules with microfilariae in the blood of its natural hosts. Humans are occasionally infected, but L3 larvae are usually unable to mature to adulthood or produce microfilariae. Occasionally, these immature worms may cause subcutaneous nodules in humans, as is seen here in a patient from Northern Italy. The muscular layer, lateral nerve cord and uteri can be seen. (H&E x 10.) (Courtesy of Drs M. Lisci and G. Cera.)

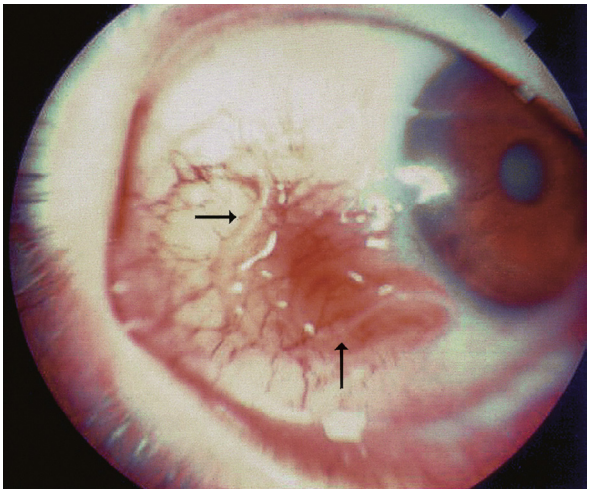


Fig. 1.363 Adult female *Dirofilaria repens* in a human eye.
The figure shows a mass situated under the bulbar conjunctiva of a 51-year-old Italian farmer. Excision and microscopic examination of the mass revealed *D. repens* measuring 95 mm in length with a diameter of 0.45 mm. (Courtesy, Professor A. E. Bianco, Dr A. Biglino and Dr A. Casabianca.)

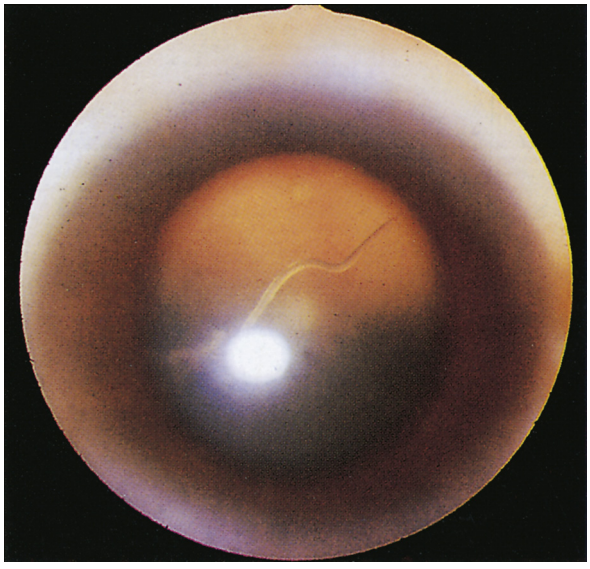


Fig. 1.364 *Thelazia callipaeda* in the human eye.
The adult worms of this nematode, which are 1–2 cm long, normally inhabit the lacrimal ducts and conjunctival sacs of dogs and rabbits. The females are viviparous and the L1 larvae in the lacrimal secretions may be picked up by eye-haunting flies such as *Musca* and *Fannia*. The flies may then transfer the larvae to fresh hosts, including humans, in whom the worms develop to adults within 3–6 weeks. The two species that have been found in humans are *T. callipaeda*, which is common in people living in poor socioeconomic conditions in many Asian countries, and *Thelazia californiensis*, which occurs in North America. An adult *T. callipaeda* is seen here in the eye of a Malaysian man. (Courtesy, Professor A. S. Dissanaike.)

Downloaded from Vet-eBooks.com

2. Infections Acquired Percutaneously

SOIL

There are estimated to be billions of microorganisms in a handful of soil, so it might be considered surprising that it does not serve as a source for more pathogens. Indeed, given that soil cannot be decontaminated globally, and thus soil-acquired infections like tetanus can never be eradicated, this is fortunate. 'Soil-transmitted helminths' (STHs) is the collective term (interchangeable with 'geohelminths') applied principally to three intestinal nematode infections for which egg-contaminated soil plays an important lifecycle role: roundworm (*Ascaris lumbricoides*), whipworm (*Trichuris trichiura*) and hookworms (*Ancylostoma duodenale* and *Necator americanus*). However, the term can be confusing, as the former two are acquired through ingestion of food or water contaminated by helminth eggs from the soil (and therefore described in Chapter 3), whereas hookworm larvae enter the human body through the skin by direct contact. Though *Strongyloides stercoralis* is acquired in a similar fashion to hookworm and is thus strictly speaking an STH, it is rarely considered as part of this group because of lower prevalence and lower associated morbidity. It is also not included in mass drug administration programmes for STH control.

Bacterial



Fig. 2.01 Neonatal tetanus.
Routine childhood vaccination has rendered tetanus a relatively rare diagnosis of adults except where vaccination coverage is poor, despite the ubiquitous presence in soil of spores of the causative organism *Clostridium tetani* (which renders eradication impossible). However, neonatal tetanus, in *C. tetani* exposed babies born to unvaccinated mothers, often through umbilical cord stump contamination, still causes around 50,000 newborn deaths each year. (Courtesy, Dr M.Y. Lam.)

Downloaded from Vet-eBooks.com

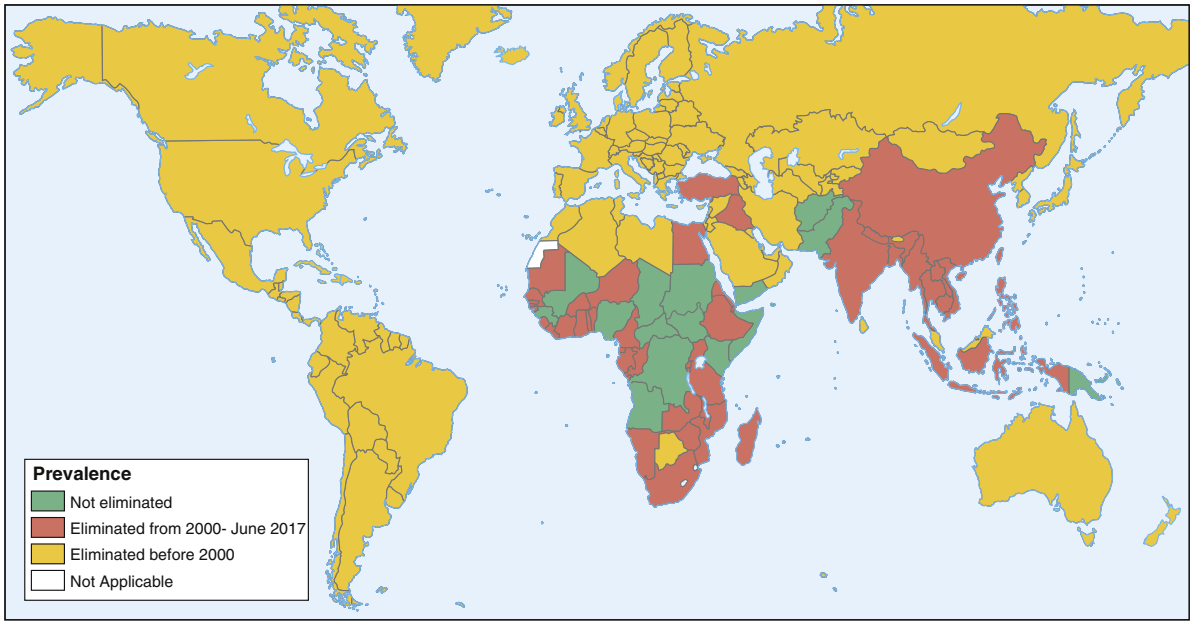


Fig. 2.02 Progress towards elimination of maternal and neonatal tetanus.
Elimination at country level is defined as <1 case per 1000 live births in every district. Since 2000 impressive progress towards elimination has been achieved through vaccination (as part of DTP or DT), with 41 of 59 remaining countries achieving elimination. Between 1990 and 2010 a 90% reduction in global neonatal tetanus mortality was achieved. As of October 2016 only 18 countries had not yet reached elimination: Afghanistan, Angola, Central African Republic, Chad, Congo DR, Ethiopia, Guinea, Haiti, Kenya, Mali, Nigeria, Pakistan, Papua New Guinea, Philippines, Somalia, Sudan, South Sudan and Yemen. (From WHO; http://www.who.int/immunization/diseases/tetanus/maternal_neonatal/Remaining_MNTE_June17cc.jpg?ua=1)



Fig. 2.03 Opisthotonos in tetanus.
The generalized muscle contraction leads to arching of the back and limb rigidity; in the conscious patient this is extremely painful and distressing. Urgent treatment with antitetanus immunoglobulin, appropriate muscle relaxants and, if indicated, supportive ventilation are essential. (Courtesy, Dr M.Y. Lam.)



Fig. 2.04 Risus sardonicus in adult tetanus.
Facial muscle spasm results in the characteristic facies with raised eyebrows. (Courtesy, Dr M.Y. Lam.)

Downloaded from Vet-eBooks.com



Fig. 2.05 *Burkholderia pseudomallei*, the cause of melioidosis.
This biosafety level III Gram-negative pathogen demonstrates colony variation with different morphology on Ashdown's agar from a single clonal type. Susceptibility to co-amoxiclav but intrinsic aminoglycoside resistance is the clue that the organism is not *Pseudomonas aeruginosa*, with which it may be otherwise confused on identification. Microscopy reveals a Gram-negative rod with bipolar staining giving the so-called 'safety-pin' appearance. Previously thought to be largely limited to South East Asia, it is increasingly recognised to be present in tropical environments worldwide. (From Cohen, J., Powderly, W., Opal, S. Infectious Diseases 3rd edition. Pages 1213–1217. Fig. 119.5B. Copyright © 2010 Mosby.rd)

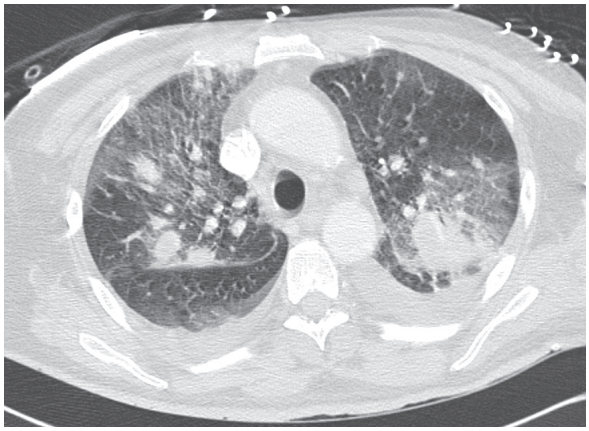


Fig. 2.06 Pneumonia due to melioidosis.
Manifestations of melioidosis range from an indolent suppurative condition, typically causing parotid abscesses, to a fulminant sepsis with aggressive necrotizing pneumonia and multifocal abscess formation. This 66-year-old man returned to London from Thailand with severe sepsis, multiple lung and prostatic abscesses and confusion. He was assumed to have acquired the infection through a large abrasion sustained to his leg in a fall outdoors. Diabetes is a strong predisposing factor. (Courtesy, Professor D. A. J. Moore.)



Fig. 2.07 Suppurating parotid abscess due to *Burkholderia pseudomallei*.
More indolent manifestations include localized septic foci which are most commonly seen in the parotid (as in this Thai boy), skin and soft tissues, liver, spleen and lymph nodes. At one time it was known in the United States as the 'Vietnam timebomb' in recognition of the large number of soldiers exposed to contaminated soil during many years of conflict; it appears that rarely the organism may establish a state of latency from which reactivation may occur many years later, including with fulminant disease. (Courtesy, D A Warrell.)

Downloaded from Vet-eBooks.com

Helminthic

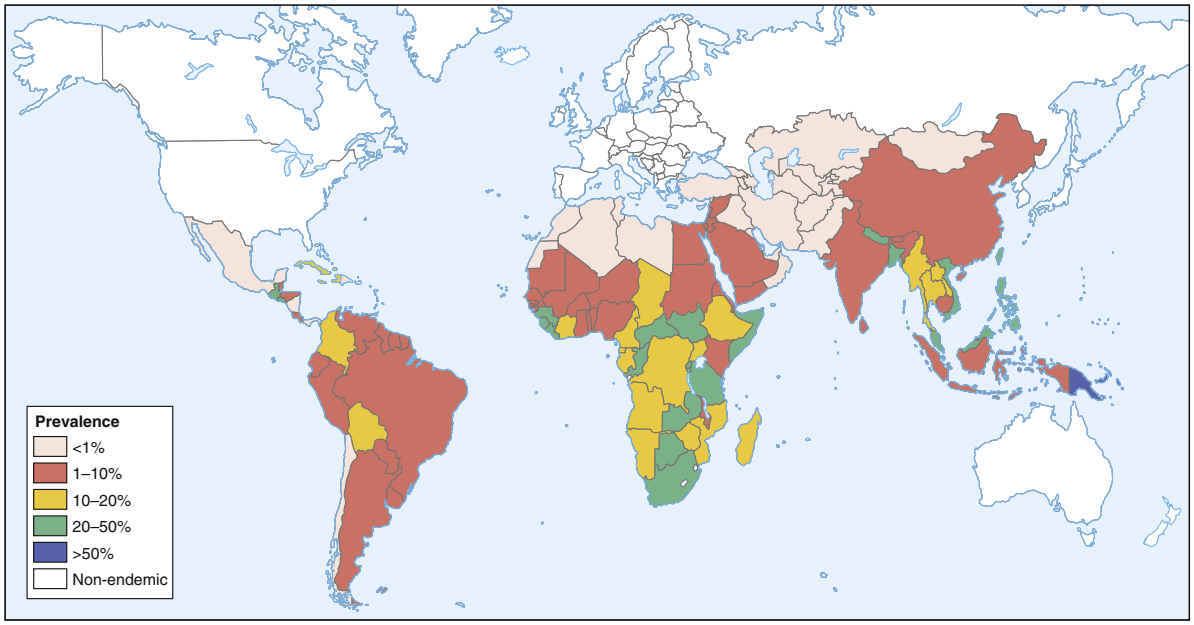


Fig. 2.08 Estimated global burden of hookworm.
Over 60% of the 5.2 million disability-adjusted life years lost to soil-transmitted helminths are attributable to hookworm, largely mediated through the effects of iron deficiency anaemia. Geographical reach is constrained by the ecological requirement of warm moist soil for larval development. (From Pullan, RL et al. Global numbers of infection and disease burden of soil transmitted helminth infections in 2010. © Pullan et al.; licensee BioMed Central Ltd. 2014. Figure 3a.)

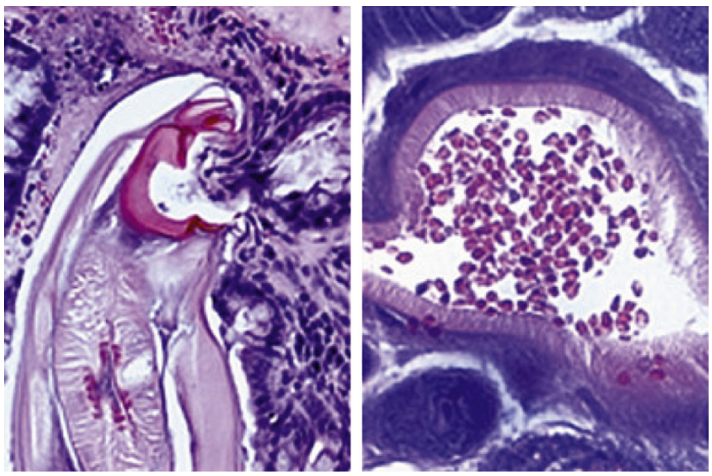


Fig. 2.09 Adult *Ancylostoma* attached to intestinal mucosa (left) with ingested red blood cells visible in the intestine of the worm in cross-sectional view (right).
Estimates suggest that a single *A. duodenale* can draw 0.2 ml daily and *N. americanus* 0.05 ml. Morbidity due to anaemia is thus determined by worm burden, and compounded by other causes such as malaria and malnutrition. The hookworm life cycle (Fig. 2.10 below) requires egg-hatching outside the human host, so worm burden is related to the intensity of exposure to infective larvae. (Courtesy, R. Bungiro. From Harris, J. R., Hotez, P. J. Intestinal nematodes. In: Principles and Practice of Paediatric Infectious Diseases. 4th edition. Fig. 276.3. Copyright © 2018 by Elsevier, Inc. All rights reserved.)

Downloaded from Vet-eBooks.com

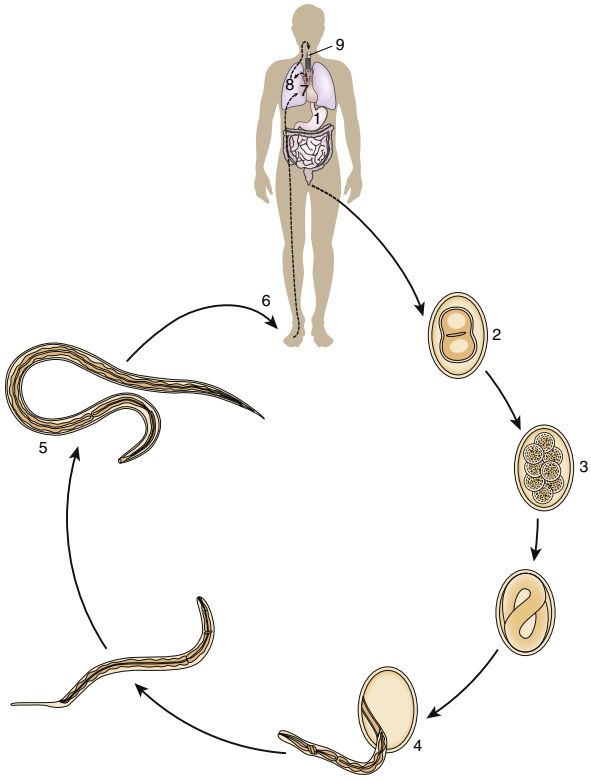


Fig. 2.10



Fig. 2.12



Fig. 2.13



Fig. 2.11



Fig. 2.14

Fig. 2.10–2.14 Life cycle of *Necator americanus* and *Ancylostoma duodenale*.
[1] Adults, characteristically curved and 1 cm long, are attached to the walls of the jejunum (Fig. 2.11) by the buccal capsule. [2] Females lay large numbers of eggs, which are passed out with the faeces. [3] The eggs mature through four-segment and eight-segment stages (Fig. 2.12) to larvae, which [4] hatch out in the soil. There they feed on bacteria and undergo two moults through rhabditiform larvae (L1 are 250 µm long with long buccal canal) (Fig. 2.13) to produce [5] infective, filariform larvae (500 µm long, pointed tail, striated sheath) (Fig. 2.14). [6] These penetrate the skin of a new host, usually on the feet. [7] They travel through subcutaneous venules and lymphatics, enter the right heart and pulmonary circulation landing in pulmonary capillary beds. [8] Here they grow before penetrating capillary walls to enter the alveoli. [9] They migrate up to the trachea, on into the pharynx where they are swallowed and passed into the small intestine, where they moult and mature into adult forms (Fig. 2.11). From skin penetration to establishment as an adult in the intestine takes from 5 to 9 weeks.

N. americanus appears only to enter the human body through skin penetration, whereas the infective larvae of *A. duodenale* are additionally capable of establishing infection through ingestion of contaminated food and soil. *A. duodenale* further differs from *N. americanus* in exhibiting the phenomenon of arrested development, in which it has the apparent ability to remain within the host at a larval stage for many months before finally reaching maturity. (Figs. 2.13 and 2.14- Courtesy, CDC; https://www.cdc.gov.)

Downloaded From Vet-eBooks.com



Fig. 2.15 Ecology of geohelminth infection.
In tropical and subtropical areas, wet soil (such as that found at the edges of rice fields, rubber plantations and the surroundings of villages in areas of high rainfall) supports the maturation of hookworm larvae from eggs deposited by indiscriminate defaecation; this limits their geographical distribution. In contrast, the well-protected eggs of nematodes with only a direct cycle of transmission (*Ascaris lumbricoides, Trichuris trichiura*) can survive in drier conditions even at freezing temperatures.



Fig. 2.16 Hookworm anaemia.
Severe anaemia is the classic feature of hookworm disease. This young Thai woman with a heavy load of *Necator americanus* had a haemoglobin of 22 g/l. (Courtesy, Professor A. M. Fallis.)



Fig. 2.17 Cutaneous larva migrans ('creeping eruption') due to larvae of animal *Ancylostoma* hookworms.
The infective filariform larvae of various species of animal hookworms (e.g. *Ancylostoma braziliense, A. caninum, A. ceylanicum)* are unable to penetrate the human dermis. After entering the skin they migrate through the epidermis leaving typical highly pruritic, serpiginous tracks known also as 'creeping eruption'. Contact with soil or (typically amongst travellers) beach sand contaminated with dog or cat faeces facilitates entry at the point of contact; feet are thus the most commonly affected part of the body. Treatment with ivermectin is usually curative. (From Checkley, A. M., Chiodini, P. L. Eosinophilia in returning travellers and migrants from the tropics: UK recommendations for investigation and initial management. J Infection 2010, Volume 60, Issue 1, Pages 1–20, Fig. 2. Copyright, Dr. R Behrens)

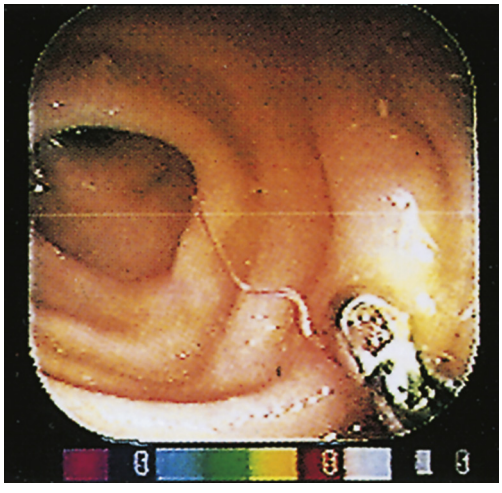


Fig. 2.18 Adult *Ancylostoma caninum* in human ileum.
In the humid north of Queensland, Australia, the larvae of this dog hookworm cause eosinophilic enteritis —a form of visceral larva migrans. The infection is probably acquired by the deep penetration of infective larvae from contaminated grass through the skin of the feet. Severe inflammatory lesions in the small intestine are associated with recurrent abdominal colic and sometimes diarrhoea, which is characterized by eosinophilia and is relieved by anthelminthic treatment. Resection of the severely inflamed segment of bowel shows oedema and eosinophilic inflammation of the wall. In the case seen here, the worm was situated in a nodule in the terminal ileum, from where it could be removed under visual control through a fibreoptic endoscope. (Courtesy, Dr J. Croese and Dr P. Prociv.)

Downloaded from Vet-eBooks.com

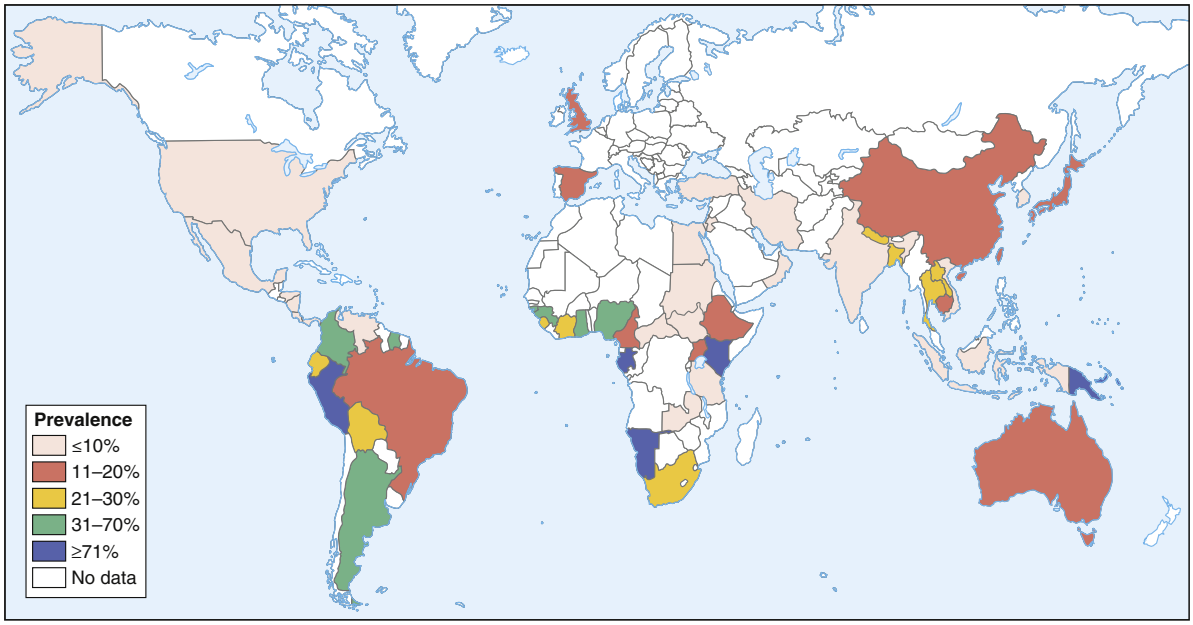


Fig. 2.19 Distribution of strongyloidiasis.
While mainly distributed in humid tropical and subtropical areas where its larvae can survive in the soil, *Strongyloides stercoralis* is also transmitted in some cooler areas (e.g. in warm and humid deep mines). It has also been reported to be spread on occasion from human to human by contamination with faeces containing infective rhabditiform larvae (e.g. in psychiatric institutions and prisons and through sexual contact). The map illustrates areas of high prevalence, as reported in country-based community studies. These studies do not include immigrants from high-risk countries but nor are they necessarily population-representative. The UK data, for example, derive from a study of World War II veterans who acquired infection some 60 years earlier during deployment in southeast Asia, highlighting the potential longevity of infection which results from the auto-infection cycle (see Fig 2.20). The association between strongyloidiasis and human T-cell leukaemia virus (HTLV-1) infection is particularly well recognized in the Caribbean, Peru and Japan (see also Fig. 2.119). (From Schar F., Trostdorf U., Giardina F. et al. Strongyloides stercoralis: global distribution and risk factors. PLoS Negl Trop Dis 2013, Volume 7, Issue 7, e2288, Fig. 4.)

Downloaded from Vet-eBooks.com

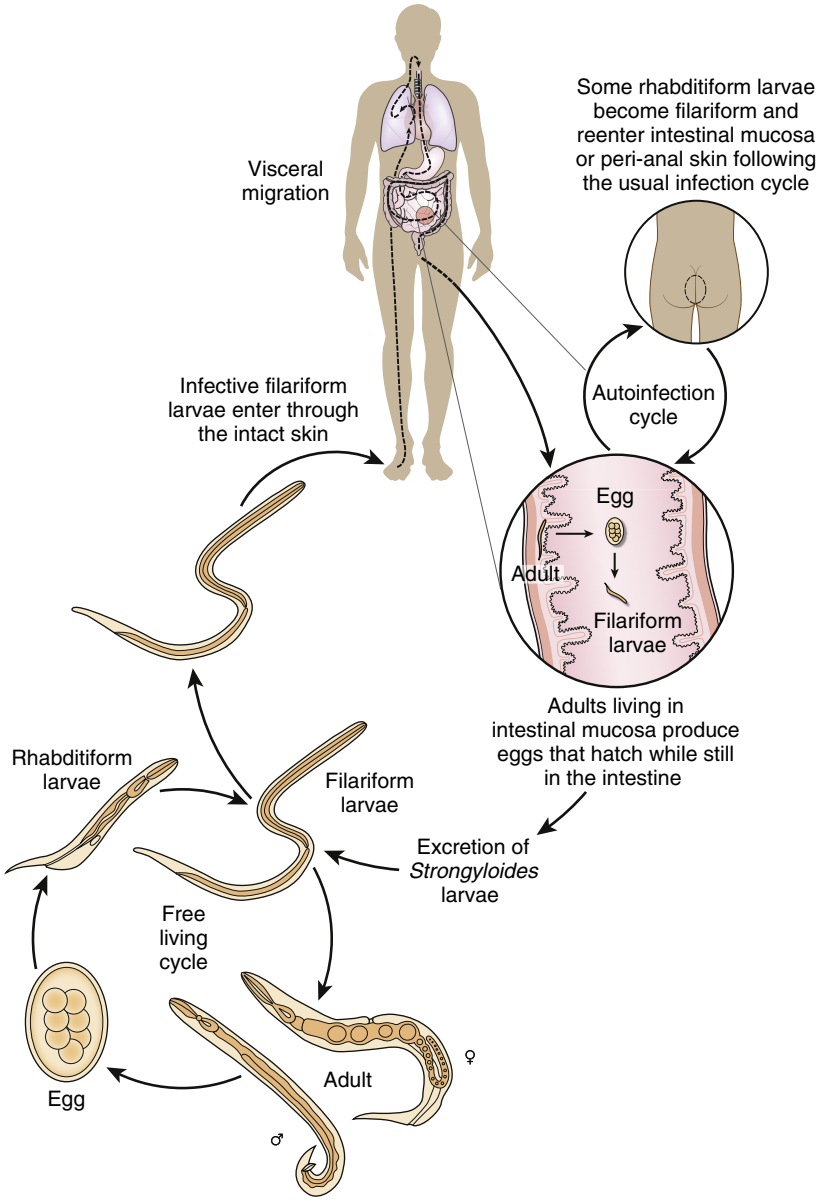


Fig. 2.20 Life cycle of *Strongyloides stercoralis*.
For most helminths worm burden in the host is proportional to the number of exposures to either larval skin penetration or egg ingestion. *Strongyloides* is an unusual nematode in that, in addition to an extrinsic life cycle in soil, it is also capable of completing a life cycle and proliferating within the human host. This has important implications in the situation in which host anti-helminth immunity is compromised, which is most clearly seen in HTLV-1 co-infection (see Fig. 2.119), resulting in higher prevalence of intestinal infection (due to poor natural clearance, though treatment efficacy is also diminished) and increased risk of (invasive) hyperinfection syndrome. (Adapted from Requena-Mendez, A., Buonfrate, D., Bisoffi, Z., Muñoz Gutiérrez, J. Advances in the diagnosis of human strongyloidiasis. Current Tropical Medicine Reports, 2014, Volume 1, Issue 4, Pages 207–215.)

Downloaded From Vet-eBooks.com



Fig. 2.21 Rhabditiform larva of *Strongyloides stercoralis* in faeces.
The figure shows a rhabditiform larva, which is usually the only stage seen in faeces. Eggs, which are rarely seen, resemble those of hookworm but contain maturing larvae. Larvae of *Strongyloides stercoralis* can readily be distinguished, by their active, snake-like movements, from larvae of hookworms (which sometimes hatch in faecal specimens that have been left standing for some time). (From Dent, A. E., Kazura, J. W. Strongyloidiasis. In: Nelson Textbook of Paediatrics 20th edition. Pages 1738–1739.e1, Fig. 295.1. Copyright © 2016 by Elsevier, Inc.)

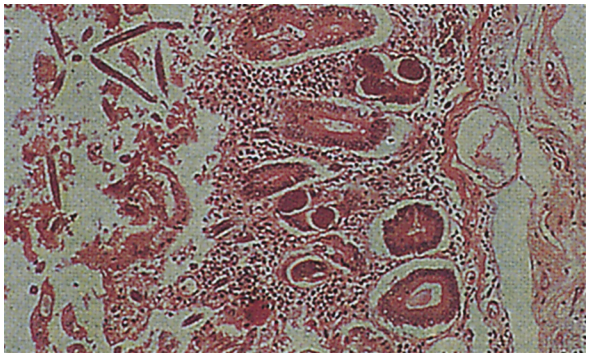


Fig. 2.22 Sections of parasitic female and eggs embedded in jejunal mucosa.
The parasitic females lying in the intestinal mucosa may reproduce parthenogenetically, with the eggs filtering through to the intestinal lumen or first hatching in the mucosa. Free-living females in the soil (about 1 mm long) are smaller than the forms found in the intestine (up to 2.2 mm). Males are normally found only in the soil and are about 0.7 mm long.



Fig. 2.23 Migrating larvae of *Strongyloides stercoralis* in skin—larva currens.
Autoinfection can lead to severe 'creeping eruption' which usually occurs on the trunk, buttocks or thighs. This characteristically evanescent rash, known as larva currens, may occur many years (30 or more) after initial infection. (Courtesy, Dr J. Walters.)



Fig. 2.24 Haemorrhagic pneumonia in disseminated *Strongyloides stercoralis* infection.
The chest radiograph shows bilateral, confluent, interstitial and alveolar infiltration. Sputum microscopy would likely have demonstrated large numbers of larvae. (Courtesy, Dr P. Caramello.)

Downloaded From Vet-eBooks.com

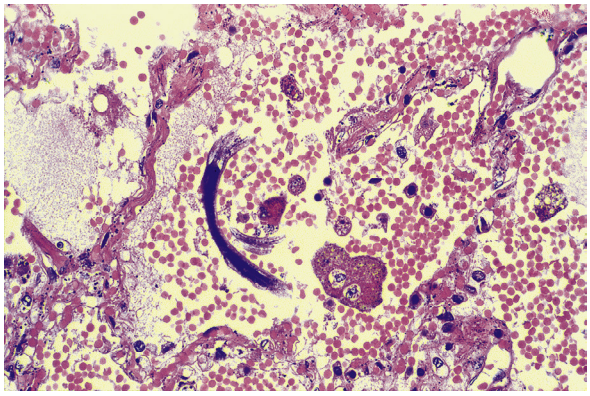


Fig. 2.25 Section of lung from a patient with disseminated *Strongyloides stercoralis*.
At post-mortem the lungs of the patient whose chest X-ray is shown in Fig. 2.24 show haemorrhagic pneumonia with thickening of the alveolar walls, inflammatory infiltration with erythrocytes and eosinophils and sections of filariform larvae within an alveolus. In some cases eosinophils may be absent in this condition, which is fatal in 50% to 75% of all cases, even with intensive anthelminthic therapy. (Courtesy, Dr P. Caramello.)

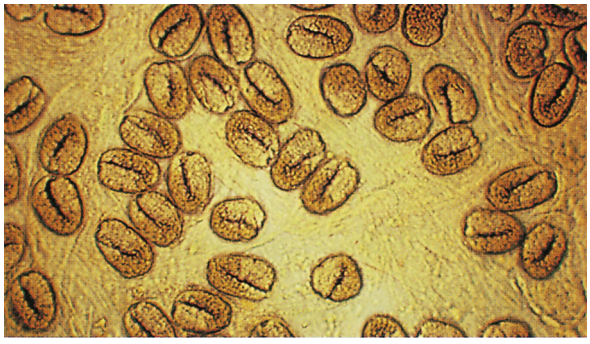


Fig. 2.26 Eggs of *Strongyloides fülleborni* in faeces.
S. fülleborni, a common intestinal nematode in African and Asian primates, is found in humans in a number of countries, including Zambia, where 10% of human *Strongyloides* infections may be caused by this species. Massive infections with a subspecies of this nematode, *S. fülleborni kellyi*, cause an often fatal illness in infants in the southern and central parts of Papua New Guinea, a country from which monkeys are absent. This condition, known as 'swollen belly sickness', is characterized by respiratory distress, abdominal distension and generalized oedema. Very heavy egg loads, as seen here, occur in such cases. The custom of mothers carrying babies in a woven bag known as a 'billum', which is often lined with soggy material, encourages autoinfection and may account for the very heavy worm loads found in their infants. (Courtesy, Dr R. W. Ashford.)

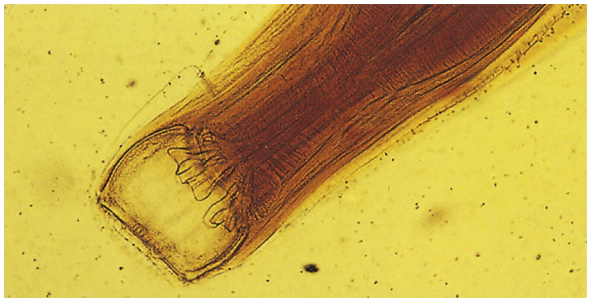


Fig. 2.27 Head capsule of adult *Ternidens deminutus*.
In some areas such as East Africa and Zimbabwe, infection commonly occurs with a hookworm-like parasite of monkeys, *Ternidens deminutus*, which also infects monkeys in Asia. The adult worm, which is about 1 cm long, is found at any level in the small and large intestine. Normally, infection is asymptomatic.

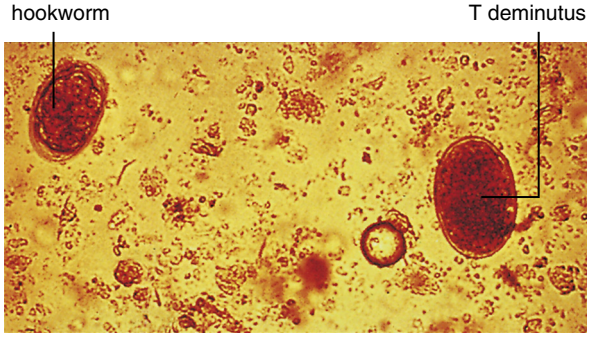


Fig. 2.28 Eggs of *Ternidens deminutus* and hookworm compared.
The eggs of *T. deminutus* (right) are usually mistaken for those of hookworm, but the adults passed incidentally during hookworm therapy are distinctive. (Courtesy, Dr J. M. Goldsmid.)



Fig. 2.29 Adult male *Trichostrongylus*.
Various species of *Trichostrongylus* inhabit the digestive tract of herbivores, burrowing into the mucosa (like hookworms) to obtain their nutrition. They have been encountered infrequently in humans in many different countries, although in one Iranian town they were said to be present in 70% of the population. They are readily distinguished from human hookworms by their smaller size and more slender shape. The male bursa is different in form from that of *A. duodenale*. (Courtesy, Professor D. Greenwood.)

Downloaded From Vet-eBooks.com

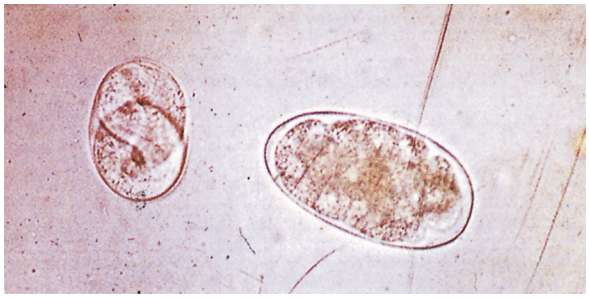


Fig. 2.30 Eggs of Trichostrongylus and *Strongyloides stercoralis* in faeces.
The hookworm-like egg of Trichostrongylus (right) is much larger (about 60 x 40 μm) than that of *S. stercoralis*, which contains an embryonic larva ready to hatch. (Courtesy, World Health Organization.)



Fig. 2.31 *Oesophagostomum bifurcum* in the human colon.
Human infections with this nematode occur in localized areas of West and East Africa. The eggs, which resemble those of hookworms, mature in the soil and produce infective third-stage larvae, which are morphologically distinct from those of the common hookworms that frequently coexist. When swallowed, the larvae develop into adults in the mucosa and submucosa of the large intestine, where they produce small abscesses. After maturation, the adults leave the abscesses to attach to the colonic mucosa. The figure, which shows part of the wall of the colon resected from a patient in northern Ghana, is characteristic of the multinodular form of the infection, which can give rise to intestinal obstruction necessitating surgery. The numerous, pea-sized nodules each contain a juvenile worm. (Courtesy, Professor E. van Marck)



Fig. 2.32 'Dapaong tumour' in a Togolese boy.
Infection with *Oesophagostomum bifurcum* is common in the north of Togo and Ghana, with a prevalence rate as high as 50% in some villages. In some individuals the worms cause large abdominal masses in the epigastric or periumbilical region, a condition known locally as 'Dapaong tumour'. These abdominal masses may be large, inflamed and painful, as in the child seen here, but are often smaller and less prominent. They characteristically contain a single juvenile worm about 10–12 mm long. (Courtesy, Professor A M Polderman)

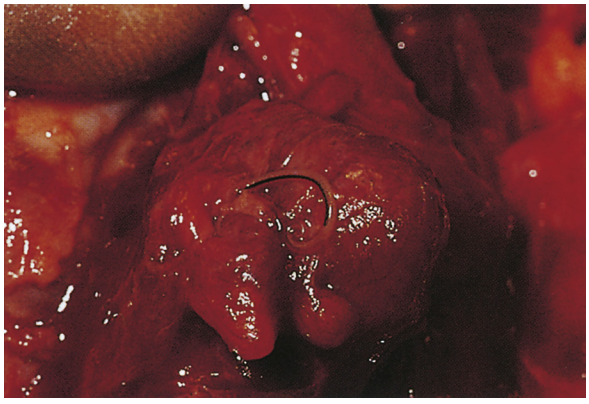


Fig. 2.33 *Oesophagostomum* in a human appendix.
The specimen seen here was found at operation for appendicitis in a Ugandan patient. (Courtesy, Professor P. Anthony.)

Downloaded From Vet-eBooks.com

WATER

Humans have a daily need for water for multiple purposes. In addition to the danger posed by ingestion of unsafe water (Chapter 3), cutaneous and mucocutaneous contact with contaminated water can also expose individuals to a significant number of infectious pathogens.

Bacterial

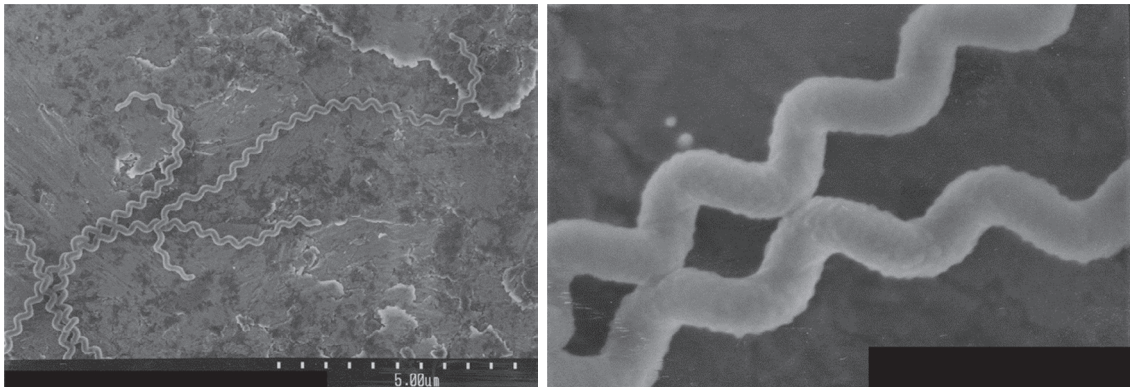


Fig. 2.34 High-resolution scanning electron microscopy of leptospires.
Leptospirosis is a zoonotic infection with a global distribution and is seen most frequently in the tropics. Infection is acquired through exposure to infected animals or, more commonly, water contaminated with the urine of infected animals. When present, spirochaetes are readily identified in silver-stained preparations. (Courtesy, Professor J Vinetz.)



Fig. 2.35 Environment characterized by hyperendemic leptospirosis.
The inhabitants of the Belen district of the city of Iquitos in the Peruvian Amazon are exposed on a daily basis to leptospira-contaminated water. Leptospirosis is a frequent cause of undifferentiated fever in such a setting, though the vast majority of infections are asymptomatic and severe disease is rare. (Courtesy, Professor J Vinetz.)

Downloaded from Vet-eBooks.com

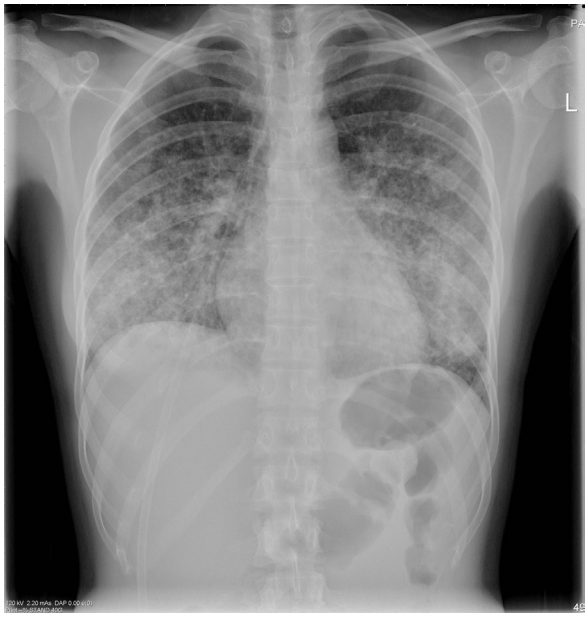


Fig. 2.36 Pulmonary involvement in leptospirosis.
The clinical manifestations of symptomatic leptospirosis are often described as 'protean', meaning almost any symptom is possible. Pulmonary involvement is increasingly recognized as an important cause of morbidity and mortality, as in this patient who returned to the UK from an adventure holiday in South East Asia and developed increasing dyspnoea and worsening hypoxia on day 4 of an abrupt febrile illness with headache, myalgia, conjunctival suffusion and abdominal pain. Acute leptospirosis serology was strongly positive and she made a full recovery. (Courtesy, Professor D. A. J. Moore.)

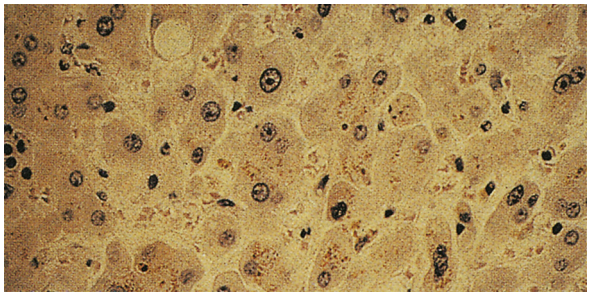


Fig. 2.37 Hepatic changes in leptospirosis.
In severe cases—even where hepatic dysfunction and jaundice are present—hepatocellular necrosis is unusual, but large amounts of bilirubin can be seen in the hepatocytes.

Protozoal

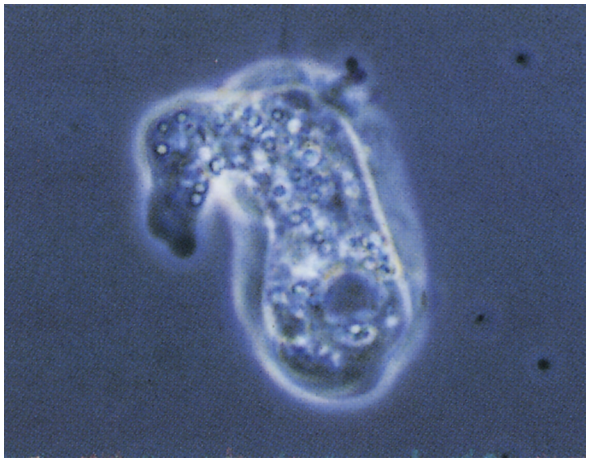


Fig. 2.38 Trophozoite of *Naegleria fowleri*.
This free-living amoeba is the caustive agent of the rare condition of primary amoebic meningoencephalitis. Infection is believed to be acquired through exposure to contaminated warm water (e.g. in thermal baths) and with pathogen entry achieved by penetration of the cribriform plate of the nasal cavity following immersion. Outbreaks in Pakistan have been associated with ritual ablutions (nasal cleansing before prayer) using *N. fowleri*-contaminated mosque water. Case-fatality is high. (Courtesy, Professor D. C. Warhurst.)

Downloaded from Vet-eBooks.com



Fig. 2.39 Warning sign indicating risk of primary amoebic meningoencephalitis associated with bathing.
Some water sources such as this pool along the course of the Avon River in York, Western Australia, are known to be particularly high-risk environments for *Naegleria* exposure. Cyst susceptibility to dessication probably explains why wider dispersal is not seen. (Courtesy, Professor J Ackers)

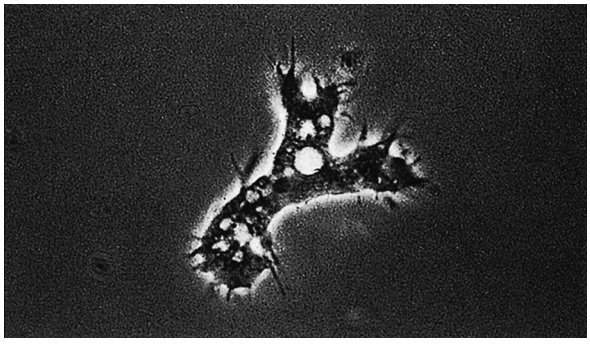


Fig. 2.40 Trophozoite of *Acanthamoeba* sp.
Free-living *Acanthamoeba* species are responsible for two disease manifestations, granulomatous amoebic encephalitis and chronic amoebic keratitis. The prickly surface membrane from which the name is derived is clearly seen here.

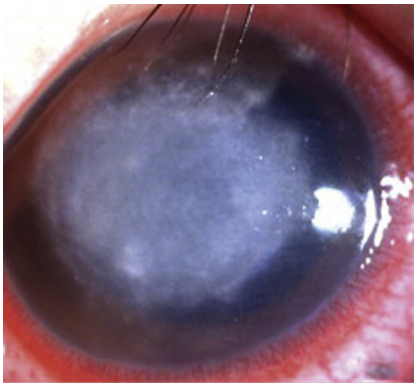


Fig. 2.41 *Acanthamoeba* keratitis.
This condition is mostly seen in users of soft contact lenses. (From Chao, J., Xuguang, S. Acanthamoeba keratitis: clinical characteristics and management. The Ocular Surface 2015, Volume 13, Issue 2, Pages 164–168, Fig. 3A. Copyright © 2015 Elsevier Inc.)



Fig. 2.42 *Balamuthia* causing an extensive plaque on the face of a Peruvian boy.
This free-living amoeba is found in soil and fresh water and infection is thought to occur through exposure of broken skin or possibly inhalation of contaminated dust. A granulomatous pathology can result in painless violaceaous plaques on the face. More importantly, it is a rare cause of granulomatous amoebic encephalitis (which has a case fatality of 90%). (Courtesy, Dr F Bravo. From Kollipara, R. et al. Emerging infectious diseases with cutaneous manifestations. Journal of the American Academy of Dermatology 2016, Volume 75, Issue 1, Pages 19–30, Fig. 9. Copyright © 2016 American Academy of Dermatology, Inc.)

Downloaded From Vet-eBooks.com

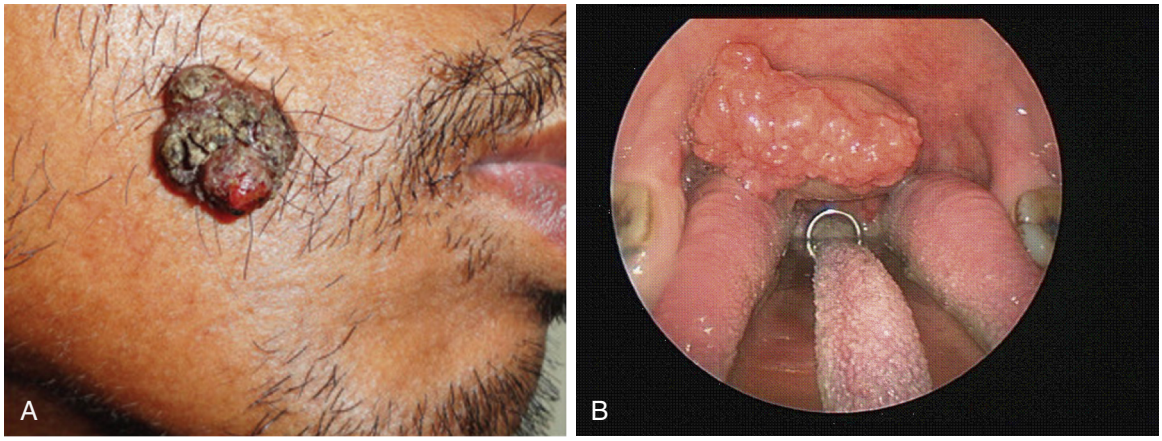


Fig. 2.43 Rhinosporidiosis (A) on a 25 year-old Indian man and (B) in a 35 year-old Sri Lankan man.
This chronic granulomatous infection of the skin and mucous membranes, caused by *Rhinosporidium seeberi* – an aquatic mesomycetozoan parasite of amphibians and fish – is most commonly recognized in India, Sri Lanka and Latin America. It is believed to be acquired via inoculation of traumatized epithelium typically affecting the nasal mucosa, conjuctivae and genitals. The painless, non-tethered swelling on the face (A) and three others on the abdomen, chest and arm, had been present for 6 months at the time of presentation. Presentation with nasal obstruction and rhinorrhoea with epistaxis (B) led to attempts at surgical resection and 'polypectomy', however cure was only achieved following the introduction of adjunctive dapsone. ((A) From Ghosh, S. K., Agarwal, M., Rudra, O. Polymorphic keratotic nodules in an immunocompetent man. Lancet Infectious Diseases, 2016, Volume 16, Issue 10, Pages 1202–1202, Figure A. Copyright © 2016 Elsevier Ltd. (B) Courtesy, Mr. S. Richards.)

Helminthic

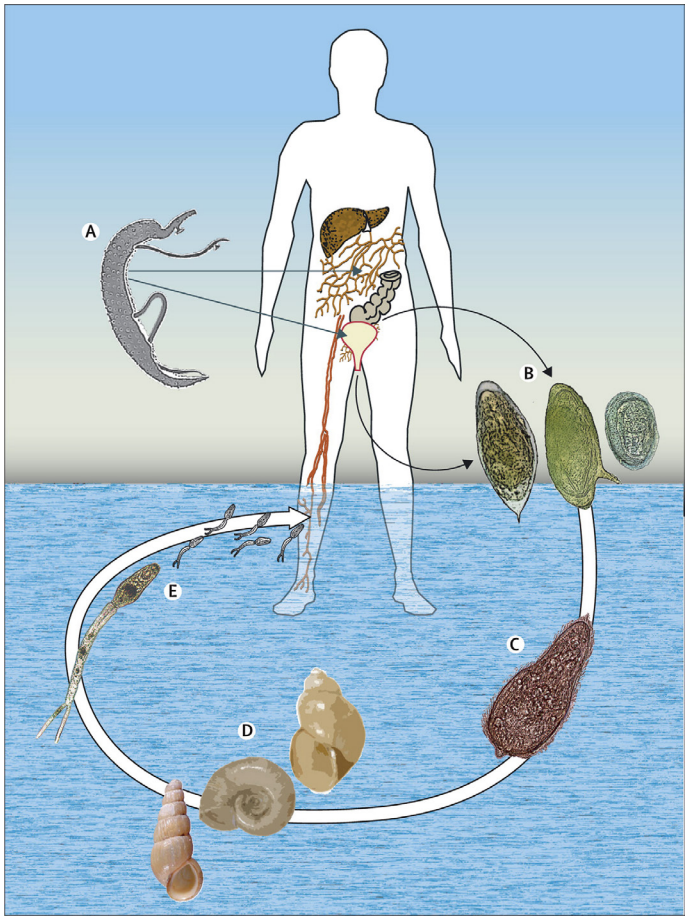


Fig. 2.44 Life cycle of schistosomes.
Paired adult worms (A) live in the veins of the mesenteric or vesical plexus or portal tract depending upon species, from where egg-laying takes place. Pathology of schistosomiasis is driven by granulomatous inflammation due to trapped eggs, either in the liver via the portal venous system or in the genitourinary or gastrointestinal tracts. Successfully extruded eggs (B, from left to right *S. haematobium, S. mansoni, S. japonicum*) reaching either the bladder or gut lumen, again depending upon species, are excreted into water to continue the cycle. Ciliated miracidia (C) hatch from the eggs and penetrate the appropriate snail host (D), subsequently emerging as infectious cercariae into the water, from where they penetrate human skin (E). Migration through tissues leads eventually to the venous system where males and females meet. (From Colley D.G., Bustinduy A.L., Secor W.E., King C.H. Human schistosomiasis. Lancet 2014, Volume 383, Number 9936, 2253-2264, Fig. 1)

Downloaded From Vet-eBooks.com



Fig. 2.45 Male and female *Schistosoma mansoni* adult worms. The slender female lies enveloped within the gynaecophoral groove of the larger male. (Courtesy, D. Establet. Beltran S., Boissier, J. Schistosome monogamy: who, how and why? In Trends in Parasitology, 24(9), 386-391. Fig. 1. 2008, Elsevier.)

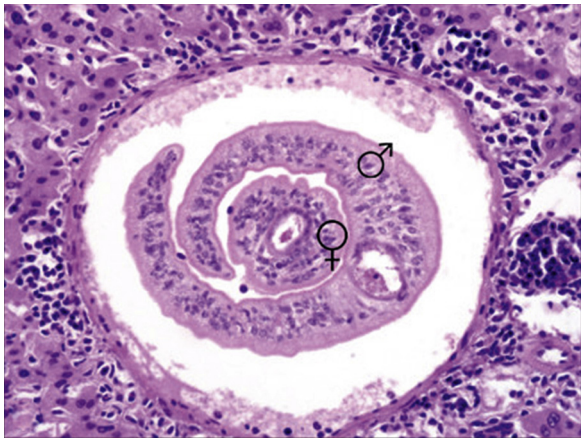


Fig. 2.46 Adult *Schistosoma mansoni* worm pair in portal tract. Cross-sectional view of adult worm pair in a state of permanent copulation in a branch of the portal vein. (Courtesy B.A.Mathison, from Zaki S.R., Alves V.A.F., Hale G.L. Non-hepatotropic viral, bacterial and parasitic infections of the liver. In: MacSween's Pathology of the Liver, Ch 7, 416-490. Figure 7.73B. e7. 2018. Elsevier.)

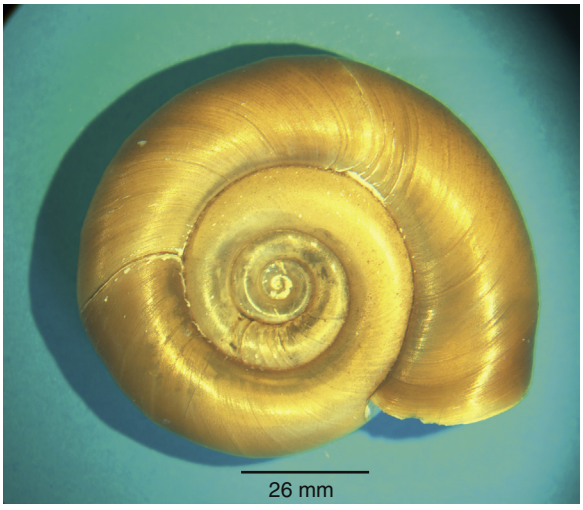


Fig. 2.47 Biomphalaria sp. The snail intermediate host of *Schistosoma mansoni*. (Courtesy, C. Whitehorn)

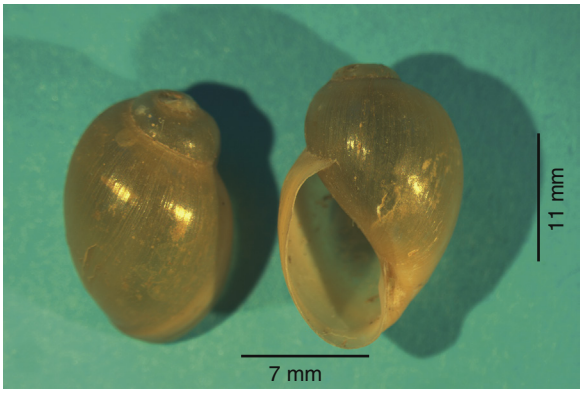


Fig. 2.48 Bulinus sp. The snail intermediate host of *Schistosoma haematobium*. (Courtesy, C. Whitehorn.)

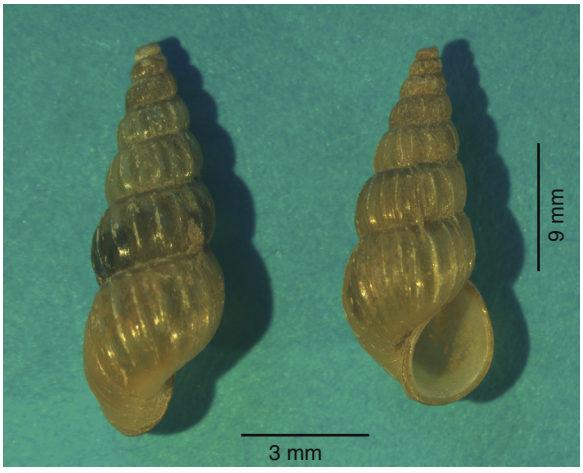


Fig. 2.49 Oncomelania sp. The snail intermediate host of *Schistosoma japonicum*. (Courtesy, C. Whitehorn.)

Downloaded From Vet-eBooks.com

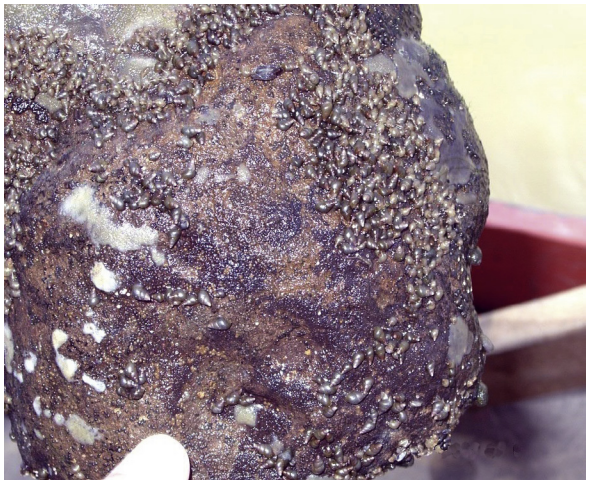


Fig. 2.50 *Neotricula aperta.*
The tiny snail intermediate host of *Schistosoma mekongi.* (From Attwood S. W., Upatham E. S. A population growth trend analysis for Neotricula aperta, the snail intermediate host of Schistosoma mekongi, after construction of the Pak-Mun Dam. PLoS Neglected Tropical Diseases, 2013, Volume 7, Issue 11, Page e2539, Fig. S1.)



Fig. 2.51 A snail shedding bifurcate cercaria of *Schistosoma mansoni.*
Shedding during daylight hours may last as long as 200 days, shedding up to 1500–2000 cercaria each day.

Downloaded From Vet-eBooks.com

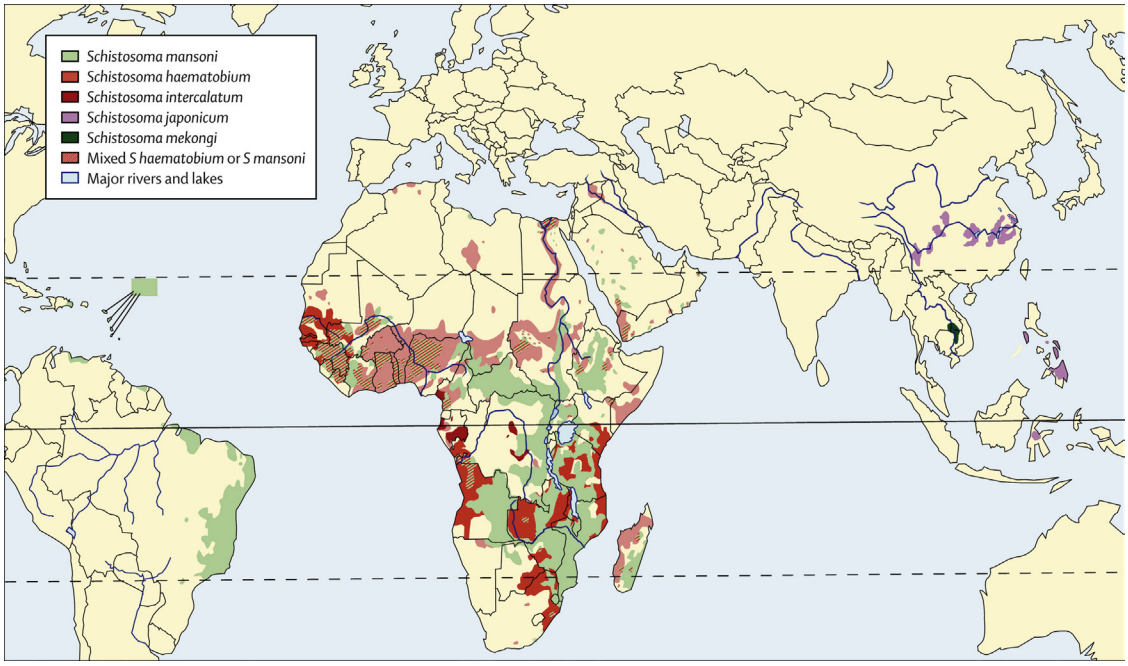


Fig. 2.52 Global distribution of countries where human schistosomiasis is transmitted.
Schistosome species have specific snail hosts whose habitat range defines the distribution of human disease. Thus only *Schistosoma mansoni* is found in the Americas and *Schistosoma japonicum* is only found in Asia, predominantly China and the Philippines. *Schistosoma haematobium* and *Schistosoma mansoni* are found throughout Africa and the Middle East. *Schistosoma mekongi* (Mekong River basin) and *Schistosoma intercalatum* (Central and West Africa) account for a minor portion of disease and have geographically more restricted distributions. (From Colley D.G., Bustinduy A.L., Secor W.E., King C.H. Human schistosomiasis. Lancet 2014, Volume 383, Number 9936, 2253–2264, Fig. 2. (adapted from Gryseels and colleagues). www.thelancet.com)



Fig. 2.53 Ecology of *Schistosoma mansoni*.
Exposure to the aquatic environment favoured by *Biomphalaria* snails in a schistosomiasis transmission area is likely to lead to infection. (Courtesy, Dr A Bustinduy.)

Downloaded From Vet-eBooks.com

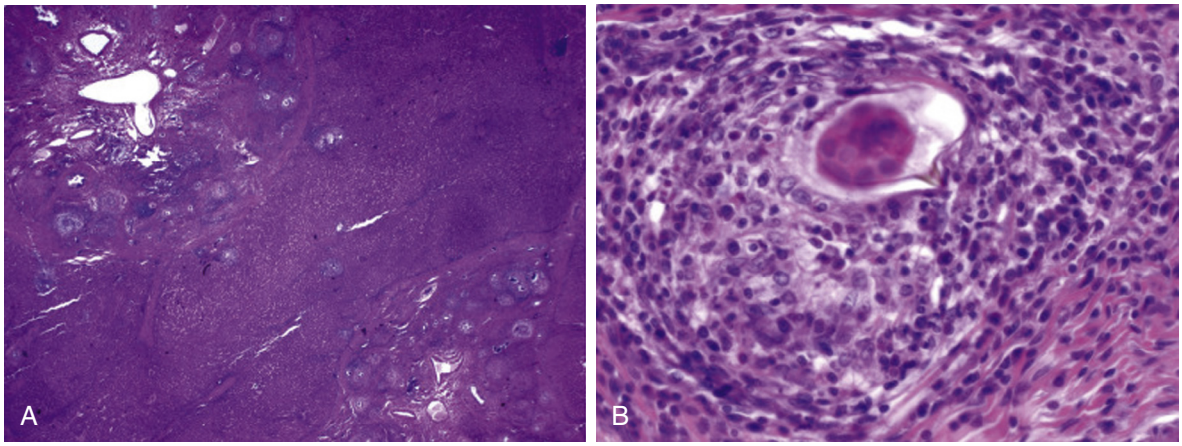


Fig. 2.54 Egg granuloma of *Schistosoma mansoni* in the liver.
Chronic granulomatous inflammation precedes the development of liver fibrosis and portal hypertension. Here the liver shows marked expansion of two portal areas with fibrosis and numerous granulomas, consistent with Symmer's pipestem fibrosis (A). There is no evidence of cirrhosis in the remaining liver. Under high-power a granuloma surrounding a schistosome ovum with the characteristic lateral spine is clearly seen (B). (From Masia, R., Misdraji, J. Liver and bile duct infections. In: Diagnostic Pathology of Infectious Disease. 2nd edition. Pages 272–322, Fig. 11.35. Copyright © 2018 by Elsevier, Inc. All rights reserved.)



Fig. 2.55 Periportal 'pipestem' fibrosis.
This is the characteristic pathological lesion of hepatic schistosomiasis. Pipestem refers to the similarity of the appearance to old clay tobacco pipes. (Courtesy, Professor S Lucas)



Fig. 2.56 Hepatosplenomegaly due to *Schistosoma mansoni*.
An enlarged liver with splenomegaly in this young Ugandan boy would progress, if untreated, to development of ascites and collateral venous circulation reflecting portal hypertension in late-stage schistosomiasis. Gastrointestinal haemorrhage from oesophageal varices carries a slightly better prognosis than if the underlying cause is alcoholic liver disease, because the latter is further complicated by poor synthetic function and coagulopathy, which is not a feature of schistosomiasis. (Courtesy, Dr A Bustinduy.)

Downloaded From Vet-eBooks.com



Fig. 2.57 Gastrointestinal disease due to *Schistosoma mansoni*. Adult worm pairs migrate to the mesenteric plexus. Egg-laying provokes granulomatous inflammation resulting in polyp formation and diarrhoea, which is sometimes bloody. (Courtesy, Dr H. Hoogstraal.)



Fig. 2.58 Ecology of *Schistosoma haematobium*.
Activities of daily living, such as washing clothes or utensils, utilizing water sources near the home which contain *Bulinus* intermediate host snails result in significant exposure to schistosomal infection. (From Schistosomiasis, In Manson's Tropical Diseases. Bustinduy, Amaya L. King, Charles H, January 1, 2014. Pages 698-725.e6. Figure 52.12. From WHO/TDR/Crump.)

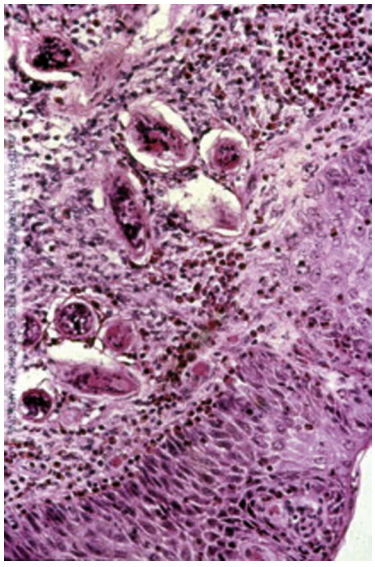


Fig. 2.59 Granulomatous inflammation around a *Schistosoma haematobium* egg in the bladder wall.
Bladder biopsy reveals the cause of haematuria to be *Schistosoma haematobium*. Eggs laid by the adult worms in the vesical plexus get caught in the urogenital tract, causing inflammation. Depending upon the location, this can result in bleeding, manifest as painless haematuria, and obstructive uropathy. Infertility is an increasingly recognized associated problem. (Courtesy, E Vandenenden From Gryseels, B. Schistosomiasis. Infectious Disease Clinics of North America, 2012. Volume 26, Issue 2, Pages 383–397.)

Downloaded From Vet-eBooks.com



Fig. 2.60 Spinal schistosomiasis.
Though reported with all the major species, spinal involvement due to metastatic egg entrapment in spinal vessels is most frequently associated with *Schistosoma japonicum*. In this coronal T1-weighted image cyst-like lesions are seen in the conus medullaris as well as patches of enhancement on the lower thoracic cord (arrowed). (From Yu-Gang, J., Ming-Ming, Z., Jun, X. Spinal cord schistosomiasis japonica: a report of 4 cases. Surgical Neurology, 2008, Volume 69, Issue 4, Pages 392–397, Fig. 3. Copyright © 2008 Elsevier Inc.)

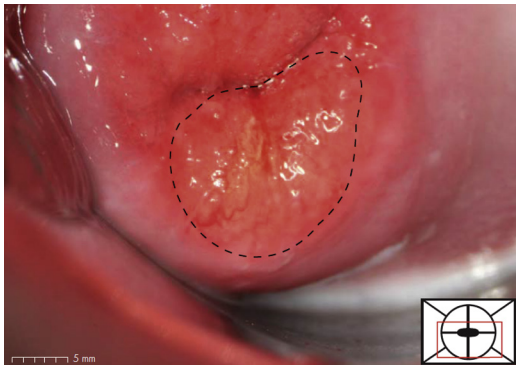


Fig. 2.61 Sandy patch on cervix visualized on speculum examination.
The association of *Schistosoma haematobium* infection in men with lumpy consistency of semen is well known. Only in recent years has there been a growing recognition of the significant burden and importance of female genital schistosomiasis. To disseminate information a WHO booklet 'Female genital schistosomiasis—a pocket atlas for clinical healthcare professionals' was created, from which this image has been taken. (From WHO Female Genital Schistosomiasis—a pocket atlas for clinical healthcare professionals)



Fig. 2.62 Early chronic schistosomiasis morbidity.
(A) A child under 5 years of age with intestinal schistosomiasis, and (B) a pre-school child collecting water in cercariae-infested fresh water. Pre-school children were previously, and erroneously, not thought to be at risk of significant pathology prior to reaching the age of entry into education and inclusion in school-based control programmes. Increasing attention is finally being directed at this group. (Courtesy, Dr A Bustinduy.)

Downloaded from Vet-eBooks.com



Fig. 2.63 Ecology of *Schistosoma japonicum*.
This zoonotic infection can be detected in cattle and domestic animals. Human infection occurs during exposure to contaminated water, for example when planting rice in paddy fields. (Courtesy, Dr. K. Woods.)



Fig. 2.64 Ecology of *Schistosoma mekongi*.
Removal of the intermediate snail host, *Neotricula aperta*, of this most recently identified human schistosome is challenging, so mass drug administration of affected populations has been the mainstay of human disease control. The tiny snails are found on the submerged underside of rocks just like those upon which these children are sitting (see also Fig. 2.50). (Courtesy, Dr A Stich.)

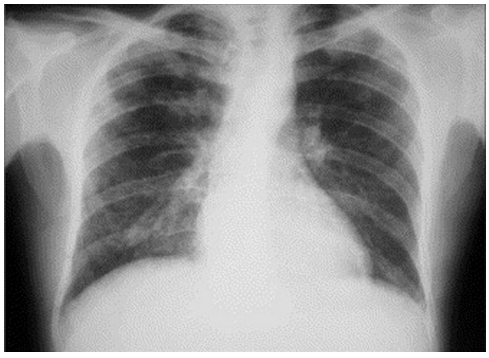


Fig. 2.65 Katayama fever.
Helminthic migration is often associated with eosinophilia, and during the initial acute phase of schistosomal infection, as egg laying commences, this may rarely be accompanied by fever and marked urticaria, known as Katayama fever. This is said to be most common in *Schistosoma japonicum*, less common with *Schistosoma mansoni* and least common with *Schistosoma haematobium*. A non-productive cough with pulmonary infiltrates on chest radiograph may be observed, as in this patient. (From Ross, A. G., Vickers, D. Katayama syndrome. The Lancet Infectious Diseases, 2007, Volume 7, Issue 2, Pages 218–224, Fig. 2. Reprinted with permission from the Prince Leopold Institute of Tropical Medicine.)



Fig. 2.66 Liver cirrhosis with *Schistosoma japonicum*.
The classic 'turtle shell' appearance of severe liver fibrosis with calcification seen with *Schistosoma japonicum* is visualized by CT or ultrasound scan. This Filipino woman spent her childhood getting reprimanded for playing in the rice terraces of Leyte province. (Courtesy, Professor D. A. J. Moore.)

Downloaded from Vet-eBooks.com



Fig. 2.67 Cercarial dermatitis 3 days after exposure.
Though 'swimmer's itch' usually describes the cercarial dermatitis caused by human pathogenic schistosomes, as here, cercarial dermatitis can occur in countries non-endemic for human schistosomiasis, following exposure to avian schistosomes. (From Pavlin, B. I., Kozarsky, P., Cetron, M. S. Acute pulmonary schistosomiasis in travelers: Case report and review of the literature. Travel Medicine and Infectious Disease, Volume 10, Issues 5–6, Pages 209–219, Fig. 2. Copyright © 2012 Elsevier Ltd.)



Fig. 2.68

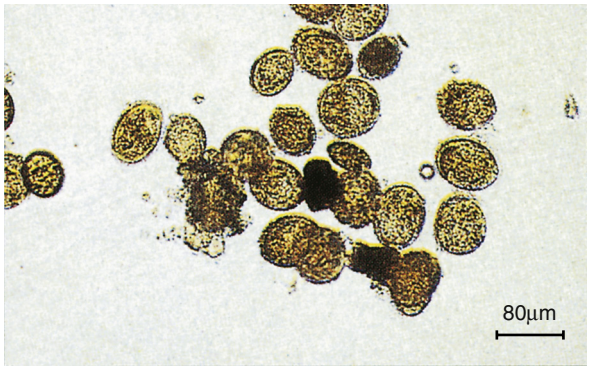


Fig. 2.69

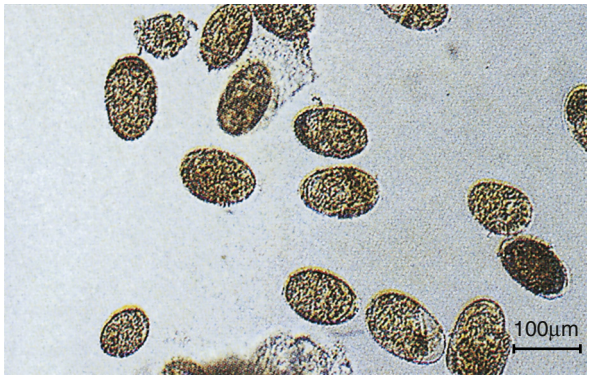


Fig. 2.70

Fig. 2.68–2.70 Eggs of unusual schistosomes seen in humans.
Eggs of *Schistosoma intercalatum* (Fig. 2.68) are morphologically similar to those of *Schistosoma haematobium*, but are only found in faeces. *Schistosoma mekongi* (Fig. 2.69) is similar in appearance to *Schistosoma japonicum* (Fig. 2.70). (Courtesy, Dr R. Muller.)

Downloaded From Vet-eBooks.com

SEX

Sexual contact is an efficient mode of transmission for a number of infections that result in genital pathology, the classic sexually transmitted infections, but is also increasingly recognized as an important secondary route for some non-genital infections such as Ebola (Figs. 2.123–2.128) and Zika viruses (Figs. 1.34–1.37).

Viral



Fig. 2.71 *Herpes simplex* virus type 2 (HSV-2).
The overwhelming majority of sexually acquired genital HSV infections are caused by HSV-2 (HSV-1 is the more common cause of stomatitis and cold sores). HSV is the commonest cause of genital ulcer disease. (From White, G. M., Cox, N. H. Diseases of the skin. 2nd edition. Copyright © 2006, Mosby.)



Fig. 2.72 HSV-2 infection in a patient with HIV.
In the presence of HIV co-infection the extent and duration of HSV ulceration are significantly increased. HSV infection is associated with an increased risk of both HIV transmission and acquisition. (Courtesy, Professor P Mayaud.)



Fig. 2.73 Hepatoma due to chronic hepatitis B virus (HBV) infection.
This Gambian wrestler complained of abdominal pain and weight loss for 2 months. This vaccine-preventable malignancy kills 300,000 people each year, accounting for one-third of hepatoma deaths (hepatitis C accounts for another third). Aflatoxin, a carcinogenic metabolite found in *Aspergillus*-contaminated maize and nuts, has a synergistic effect in further increasing the risk of hepatitis B-induced hepatocellular carcinoma, and is estimated to account for between 25,000 and 150,000 cases worldwide each year, one-quarter occurring in HBV-uninfected individuals. (Courtesy, Professor D. Mabey.)

Downloaded from Vet-eBooks.com

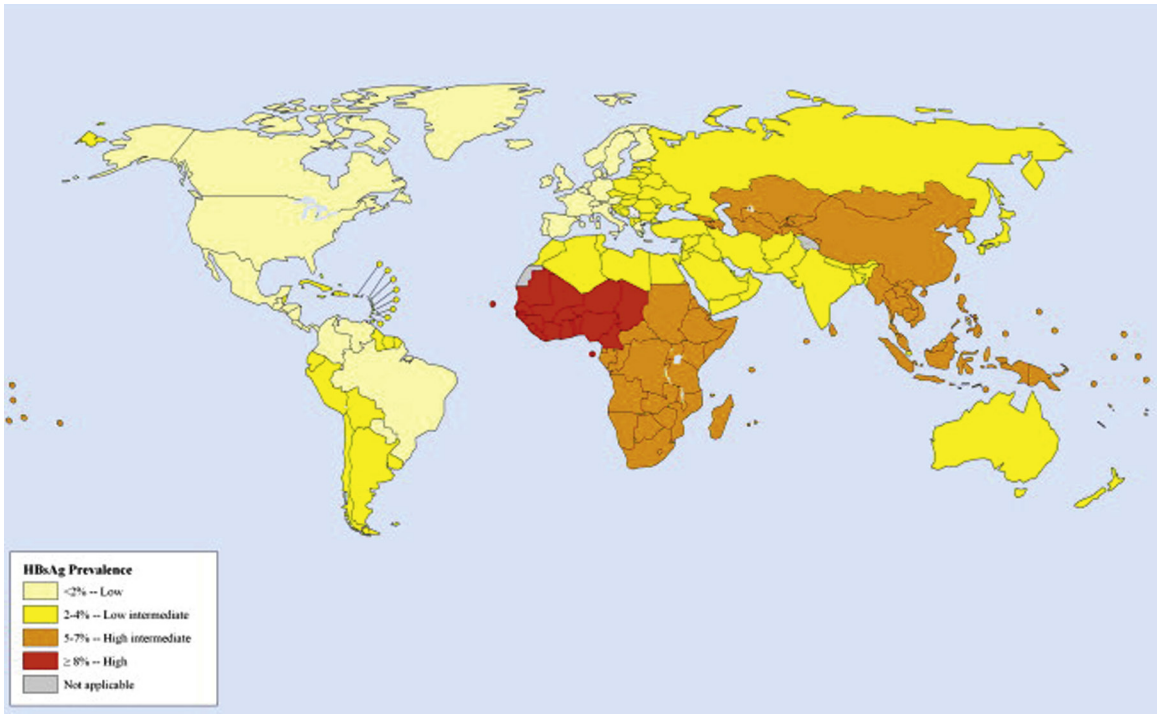


Fig. 2.74 Global epidemiology of hepatitis B virus (HBV) infection — prevalence in 2005 amongst adults aged 19–49 years.
Sub-Saharan Africa and South East Asia bear a disproportionate share of the global HBV burden, for which vertical infection remains a major preventable route of transmission. (From Ott, J. J. et al. Global epidemiology of hepatitis B virus infection: New estimates of age-specific HBsAg seroprevalence and endemicity. Vaccine, 2012-03-09, Volume 30, Issue 12, Pages 2212–2219. Copyright © 2012 Elsevier Ltd.)



Fig. 2.75 Genital warts due to human papilloma virus (HPV) infection.
HPV is the cause of genital warts, condylomata acuminata; appearances differ from those of condylomata lata of secondary syphilis (see Fig. 2.86). (From Habif, T. P. Sexually transmitted viral infections. Clinical Dermatology. 6th edition. Pages 418–447, Fig. 11.5. Copyright © 2015 Elsevier)

Downloaded from Vet-eBooks.com

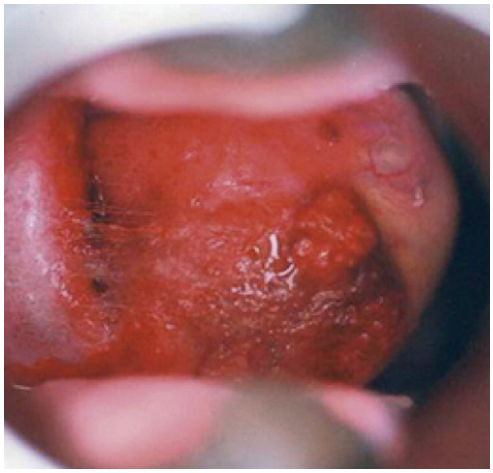


Fig. 2.76 Cervical cancer due to vaccine-preventable human papilloma virus (HPV) infection.
A limited number of serotypes account for the oncogenic potential of HPV infection. Roll-out of HPV vaccination has the potential to drastically reduce the incidence of cervical cancer, but delivery to resource-constrained settings is currently limited by cost.

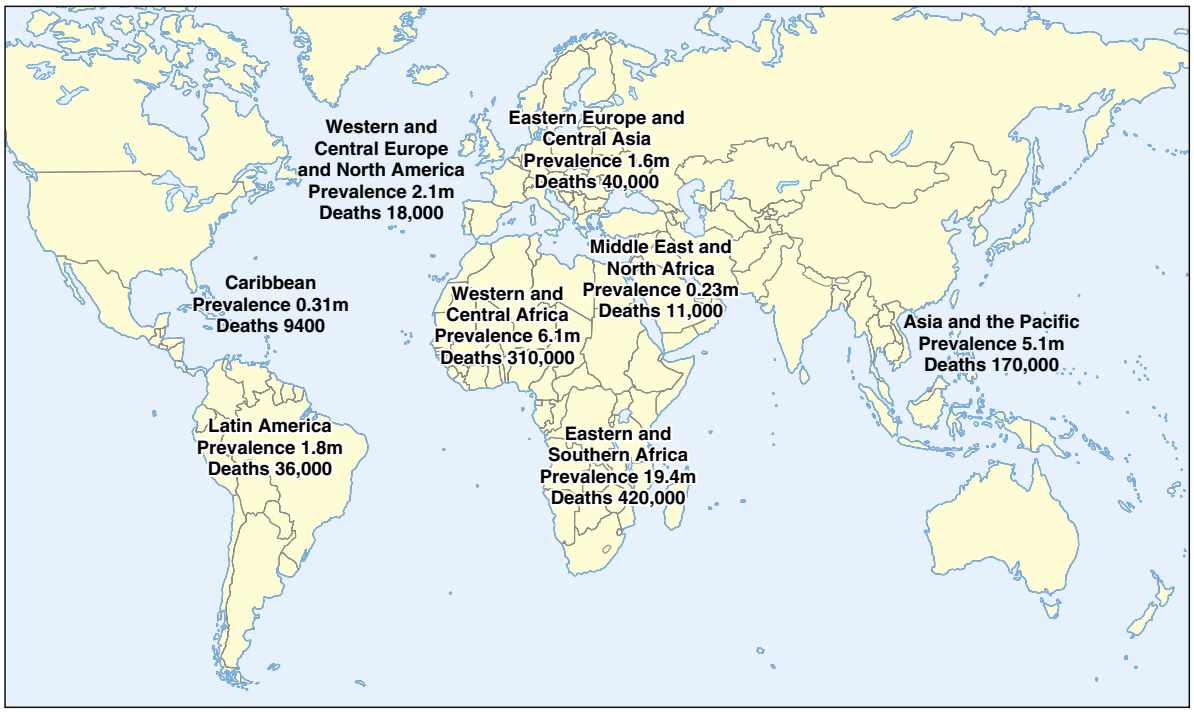


Fig. 2.77 Global epidemiology of HIV infection.
Since the first descriptions of an acquired immunodeficiency in the early 1980s the global pandemic of HIV has taken tens of millions of lives, orphaned tens of millions of children, and left no nation unaffected. Sexual contact is the principal mode of transmission. Mother-to-child transmission can be almost completely prevented through the use of timely antenatal anti-retroviral therapy. Globally, previously rising incidence has slowed down. The effectiveness and astonishing scale of combination antiretroviral therapy rollout has dramatically altered the life expectancy of HIV-infected individuals. As survival improves substantially in the face of largely unaltered incidence, global prevalence of HIV infection continues to rise.

Downloaded from Vet-eBooks.com

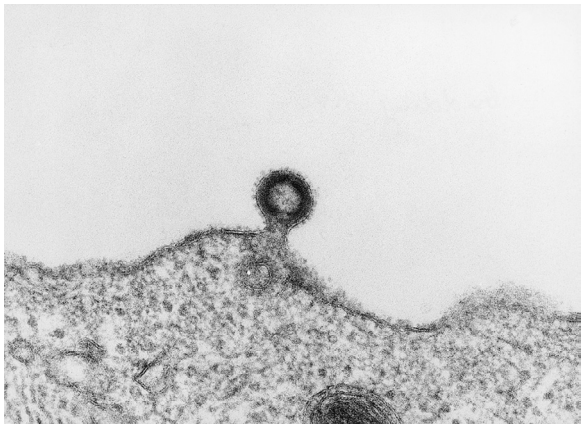


Fig. 2.78 Human immunodeficiency virus (HIV).
The virus infects numerous cell types but many of the major consequences of HIV infection arise as a result of the predilection for the immunologically pivotal T helper (CD4) lymphocytes. (Courtesy, Dr C. Grewe.)



Fig. 2.79 Acute HIV-1 infection.
Acute infection with HIV may be associated with a classic glandular-fever like illness with fever, rash, sore throat and lymphadenitis, clinically indistinguishable from other causes of infectious mononucleosis. (From Dhanireddy, S., Harrington, R. Human immunodeficiency virus infection and the acquired immunodeficiency syndrome: diagnosis and management. In: Atlas of Sexually Transmitted Diseases and AIDS. 4th edition. Pages 256–286, Fig. 15.1. Copyright © 2010, Elsevier Limited. All rights reserved.)

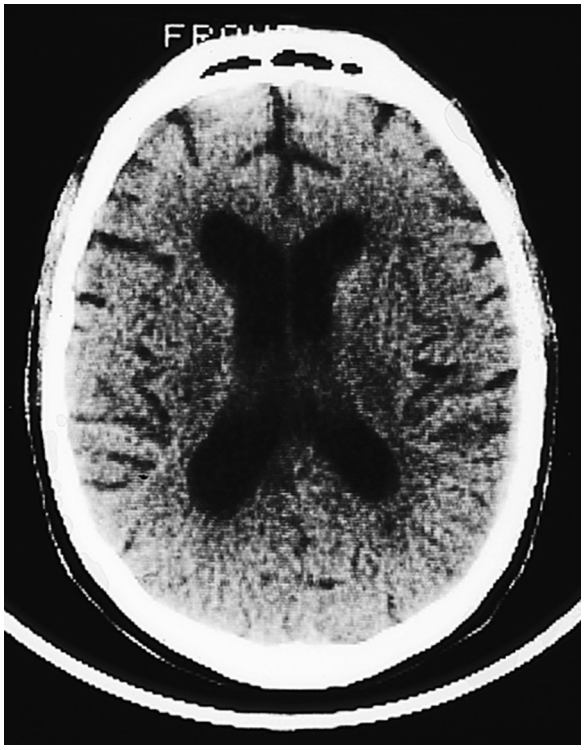


Fig. 2.80 Cerebral atrophy in HIV-1 infection.
Whilst opportunistic infections and malignancies are responsible for the majority of 'brain syndromes' in people living with HIV, the virus itself can directly affect brain function. An acute aseptic meningitis and/or encephalitis occasionally complicates primary infection. Long-standing infection may be associated with cerebral atrophy, as in the case shown here, for which no other aetiology could be demonstrated.

Downloaded From Vet-eBooks.com

Table 2.1 HIV-associated opportunistic infections and neoplastic disorders

Category	Agent	Clinical syndrome	Distribution	Atlas reference
Viral infections	CMV	Retinitis, colitis, oesophagitis	Global	2.103, 2.104
	HSV	Mucocutaneous ulceration of increased severity	Global	2.72
	VZV	Increased risk of varicella zoster reactivation ('shingles') and dissemination	Global	4.16, 4.17
	JC virus	Progressive multifocal leucoencephalopathy	Global	3.12
	Molluscum contagiosum virus	Molluscum contagiosum (more extensive and persistent in HIV)	Global	2.105
	EBV	Oral hairy leukoplakia, lymphoma	Global	2.102
Bacterial infections	*Mycobacterium tuberculosis*	Pulmonary and extrapulmonary TB	Global	4.34-4.70
	Mycobacterium avium intracellulare	Fever, reticulo-endothelial system involvement	Global	-
	Streptococcus pneumoniae	Pneumonia and sepsis	Global	4.18-4.20
	Non-typhoidal salmonellae	Sepsis syndrome	Global	1.137
	Mycobacterium leprae	Modified disease manifestations	Leprosy-endemic regions	4.71-4.93
	Bartonella henselae	Bacillary angiomatosis	Global	2.135
Fungal infections	*Cryptococcus sp.*	Meningitis, sepsis	Global	4.111-4.113
	Pneumocystis jirovecii	Pneumonia	Global	4.94, 4.95
	Candida sp.	Oral and oesophageal candidiasis	Global	2.160, 2.161
	Talaromyces (formerly *Penicillium*) *marneffei*	Sepsis syndrome, rash	South-east Asia	4.97-4.99
	Histoplasma capsulatum	Rash, pneumonia, bone-marrow involvement	Global	4.100-4.102
	Paracoccidioidomycosis	Cutaneous, mucosal, pulmonary, reticulo-endothelial system involvement	Central and South America	2.175, 4.103-4.107
Protozoal infections	*Plasmodium sp.*	Malaria	Malaria endemic regions	1.102-1.166
	Toxoplasma gondii	Cerebral abscess	Global	3.53, 3.57
	Trypanosoma cruzi	Meningoencephalitis, myocarditis	Central and South America	1.197-1.220
	Leishmania sp.	Visceral leishmaniasis[1]	Leishmania endemic regions	1.221-1.282
	Cryptosporidium sp.	Diarrhoea	Global	3.38, 3.52

Downloaded From Vet-eBooks.com

Table 2.1 HIV-associated opportunistic infections and neoplastic disorders—cont'd

Category	Agent	Clinical syndrome	Distribution	Atlas reference
	Isospora sp.	Diarrhoea	Global	3.38, 3.51
	Microsporidia (*Encephalitozoon hellem, Enterocytozoon bineusi*)	Diarrhoea	Global	3.59
Malignancies	Kaposi sarcoma	Cutaneous, pulmonary and gastrointestinal involvement	Global – aetiological agent is KSHV (HHV-8)	8.5
	Non-Hodgkins lymphoma	Visceral and lymph node lymphoma	Global – associated with EBV infection	-
	Primary cerebral lymphoma	Cerebral space-occupying lesion	Global – associated with EBV infection	-
	Cervical carcinoma	Cervix mass lesion	Global – associated with HPV infection	2.76
	Anal squamous cell carcinoma	Anal mass lesion	Global – associated with HPV infection	-
	Multicentric Castleman's disease	Lymph node enlargement	Global – associated with HHV-8 infection	-

[1]Lack of evidence of increased risk of cutaneous leishmaniasis in HIV.CMV, cytomegalovirus; EBV, ebola virus; HHV, human herpes virus; HPV, human papilloma virus; HSV, herpes simplex virus; JC virus, John Cunningham virus; KSHV, Kaposi sarcoma-associated herpes virus; TB, tuberculosis; VZV, varicella zoster virus.
[1]Lack of evidence of increased risk of cutaneous leishmaniasis in HIV.

Bacterial

In settings lacking appropriate laboratory capacity, syndromic management of genital ulcer disease delivers empiric antibacterial therapy to cover the treatable (non-HSV) causes of genital ulcers. Similarly, management of urethral discharge takes advantage of the limited number of causative bacterial pathogens, facilitating treatment of the syndrome without precise microbiological diagnosis.



Fig. 2.81 Painful genital ulcers of chancroid.
Haemophilus ducreyi is a common cause of genital ulcers in tropical regions. Associated painful inguinal lymphadenopathy is often seen (see also Fig. 2.159 cutaneous chancroid). (Courtesy, Professor D Mabey.)

Downloaded from Vet-e-Books.com



Fig. 2.82 Donovanosis (Granuloma inguinale).
The beefy red genital ulcers caused by *Klebsiella* (formerly *Calymmatobacterium*) *granulomatis* are usually painless. Inguinal ulcers or buboes may also occur. Donovanosis incidence has fallen in many parts of the world but remains an important cause of genital ulcer disease in India, Papua New Guinea, southern Africa, Brazil and the Caribbean. (Courtesy, Professor D. Mabey.)

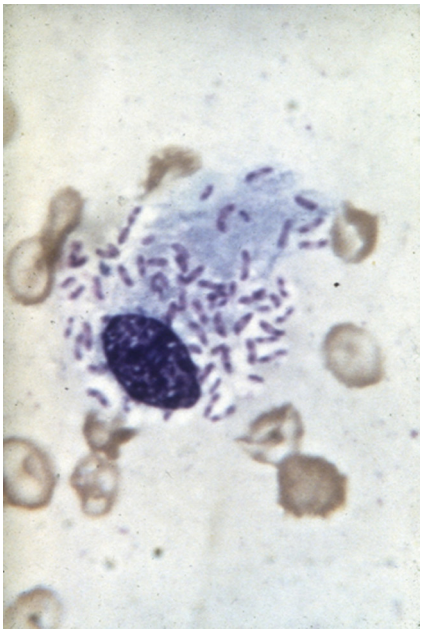


Fig. 2.83 Donovan bodies in exudate.
A Giemsa-stained smear of ulcer exudate demonstrates the closed safety-pin appearance of *Klebsiella granulomatis* inside the macrophage. (Courtesy, Professor D. Mabey.)



Fig. 2.84 Primary chancre of syphilis.
The genital ulcer of primary syphilis is painless and in the absence of treatment will self-heal in a few weeks without scarring. Dark field microscopy of exudate fluid from the ulcer will reveal large numbers of *Treponema pallidum* spirochaetes. (Courtesy, Professor D. Mabey.)

Downloaded from Vet-eBooks.com

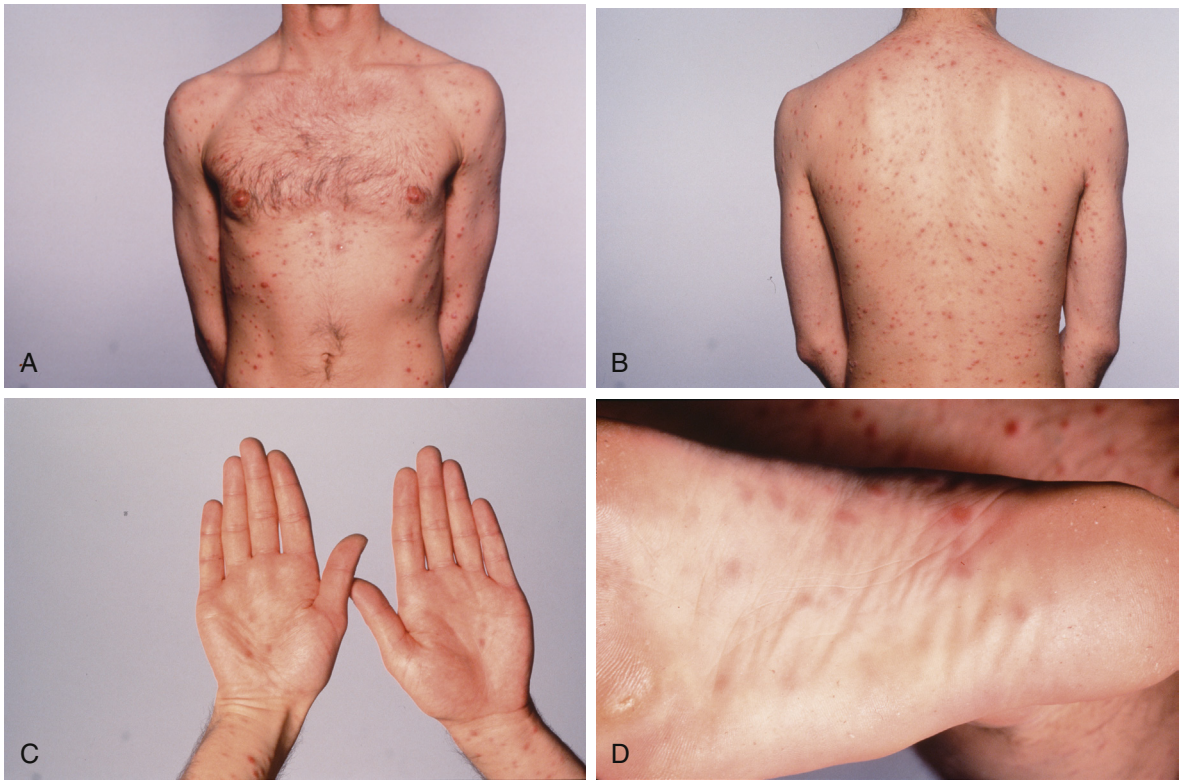


Fig. 2.85 Extensive rash of secondary syphilis.
Characteristically this widespread maculopapular rash involves the palms and soles of the feet. (Courtesy, Dr W Newsholme.)



Fig. 2.86 Condylomata lata of secondary syphilis.
These genital lesions may be distinguished from condylomata acuminata (genital warts caused by human papilloma virus) by their smooth, moist surface and flattened appearance. They are teeming with spirochaetes. (Courtesy, Professor D. Mabey.)



Fig. 2.87 Corona veneris of secondary syphilis.
Discoid lesions on the face and scalp may appear in secondary syphilis. (Courtesy, Professor A. Bryceson.)

Downloaded from Vet-e-Books.com



Fig. 2.88 Congenital syphilis in a neonate.
In 2012 undiagnosed antenatal syphilis in an estimated 930,000 women was calculated to have been responsible for 350,000 adverse pregnancy outcomes including 143,000 early fetal deaths and stillbirths, 62,000 neonatal deaths, 44,000 preterm or low-weight births, and 102,000 infected infants worldwide. (Courtesy, Professor D. Mabey.)



Fig. 2.89 Congenital syphilis rash.
The characteristic skin rash is seen here on hands (Fig. 2.88) and feet (Fig. 2.89). (Courtesy, Professor D. Mabey.)





Fig. 2.90 Congenital syphilis in a young child.
This miserable baby has nasal snuffles, hepatosplenomegaly and long-bone osteitis. (Courtesy, Professor D. Mabey.)

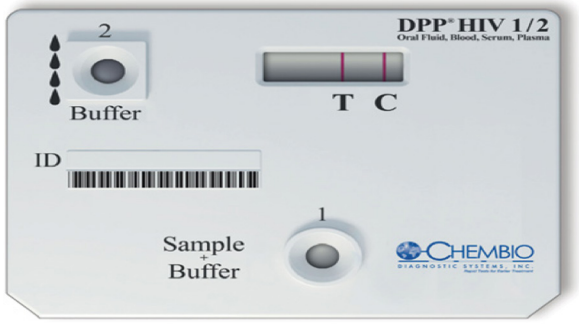


Fig. 2.91 Point of care (POC) lateral flow assay for syphilis and HIV.
Congenital syphilis is preventable with a single injection of benzathine penicillin during pregancy, but case identification has previously been hampered by lack of access to reliable diagnostic testing. New POC rapid diagnostics remove this barrier and can transform the epidemiology of this condition. (Courtesy, Professor R. Peeling.)

Fig. 2.92 Urethral discharge in gonorrhoea.
Neisseria gonorrhoea is the commonest cause of urethral discharge in men. Complications of the infection-driven inflammation include urethral stricture. (Courtesy, Professor D. Mabey.)

Downloaded from Vet-eBooks.com

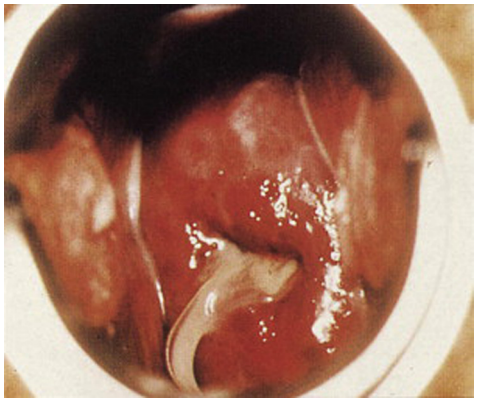


Fig. 2.93 Cervical discharge in gonorrhoea.
In women gonorrhoea causes urethritis and cervicitis. Ascending infection may result in pelvic inflammatory disease with resulting risk of infertility and ectopic pregnancy. (From Ison, C.A., Lewis, D.A. Gonorrhea. In: Atlas of Sexually Transmitted Diseases and AIDS. 2010, Pages 24–39, Fig. 2.11. Copyright © 2010, Elsevier Limited. All rights reserved.)



Fig. 2.94 Ophthalmia neonatorum.
Congenital infection with *Neisseria gonorrhoea* acquired during vaginal delivery. This potentially blinding condition can be prevented through the topical application of antibiotic or silver nitrate eyedrops at birth. Only chloramphenicol and silver nitrate protect against chlamydia as well. (Courtesy, Professor D. Mabey.)

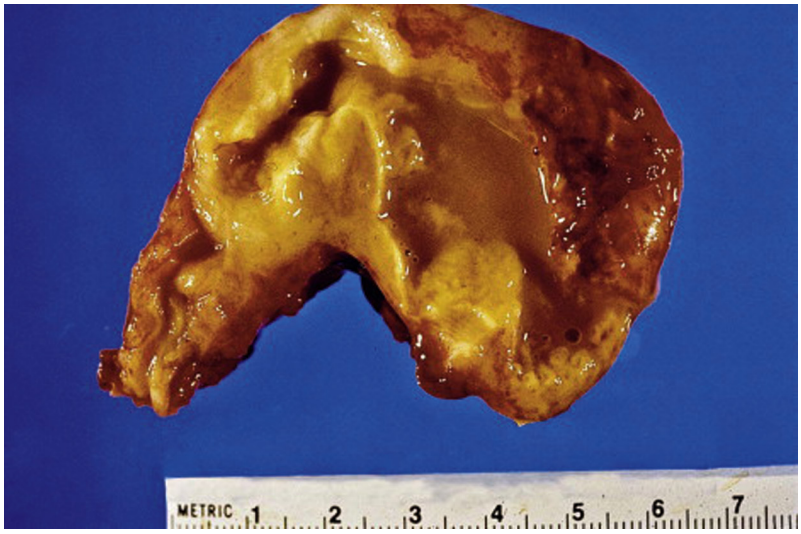


Fig. 2.95 Pelvic inflammatory disease with thickened fallopian tube wall due to *Chlamydia trachomatis*.
This is a common cause of the triad of lower abdominal pain, vaginal discharge and cervical motion tenderness, in regions with high prevalence of sexually transmitted infections. Though frequently polymicrobial, *Chlamydia trachomatis* (serovars D–K) is the predominant cause. Complications include tubo-ovarian abscess, ectopic pregnancy and infertility. (From Wiesenfeld, H., Paavonen, J. Pelvic inflammatory disease. In: Atlas of Sexually Transmitted Diseases and AIDS. 4th edition. Pages 94–110, Fig. 6.17. Copyright © 2010, Elsevier Limited. All rights reserved.th)

Downloaded from Vet-eBooks.com



Fig. 2.96 Lymphogranuloma venereum (LGV).
This condition, caused by *Chlamydia trachomatis* serovars L1, L2 and L3, may cause urethritis or (through anal sex) proctitis, but most frequently is marked by inguinal lymphadenitis, characteristically 'sausage-shaped' with shiny, purplish overlying skin. (Courtesy, J.S. Bingham. From Goering, R. V., Dockrell, H. M. Sexually transmitted infections. In: Mims' Medical Microbiology, 5th edition. 2012, Pages 245–267. Fig. 21.10. Copyright © 2013 by Saunders, an imprint of Elsevier Ltd.)

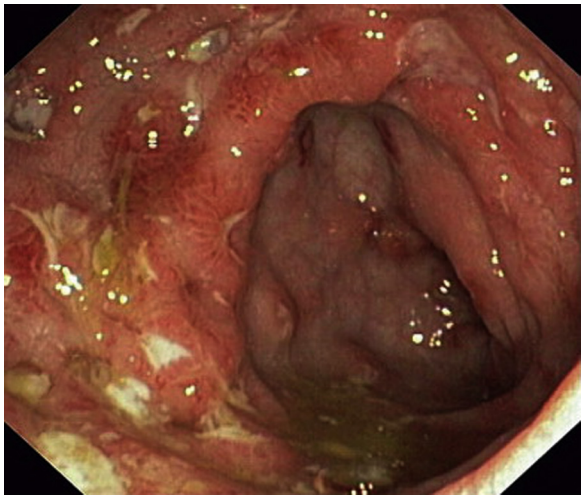


Fig. 2.97 Lymphogranuloma venereum (LGV) proctitis.
Recent receptive anal intercourse is a risk factor for LGV proctitis/proctocolitis, for which a 21-day course of doxycycline is effective treatment. (From Felt-Bersma, R. J. F., Bartelsman, J. F. Haemorrhoids, rectal prolapse, anal fissure, peri-anal fistulae and sexually transmitted diseases. Best Practice and Research: Clinical Gastroenterology, Volume 23, Issue 4, Pages 575–592, Fig. 4. Copyright © 2009 Elsevier Ltd.)

Protozoal

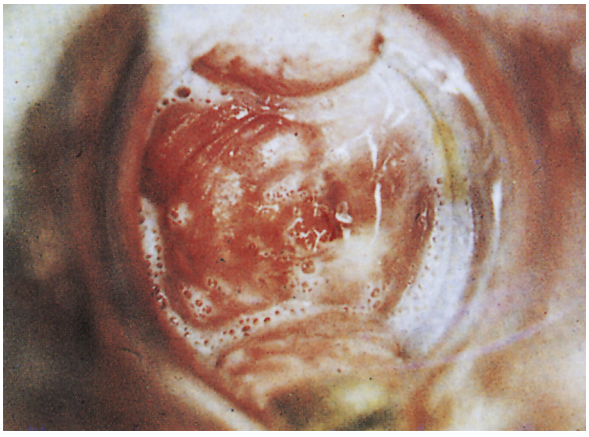


Fig. 2.98 Trichomoniasis.
Infection with *Trichomonas vaginalis* in women causes a vaginitis resulting in frothy vaginal discharge. (Courtesy, Dr A. Wisdom.)

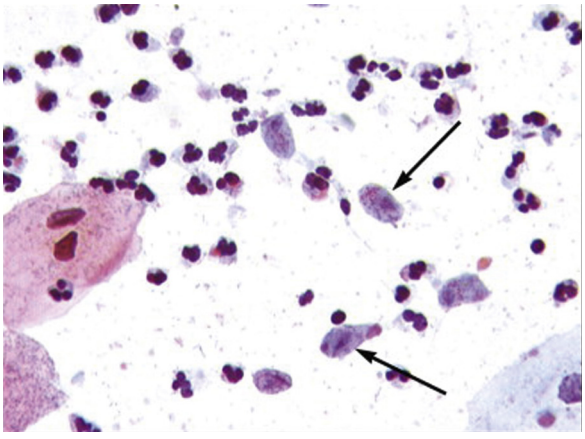


Fig. 2.99 *Trichomonas vaginalis* in vaginal discharge.
The diagnosis of trichomoniasis is usually clinical, though the organisms are readily identified as small blue bodies (arrowed) with elongated nuclei in vaginal discharge viewed under the microscope. (From Bean, S., Prat, J., Robboy, S. J. Vagina. Pathology of the Female Reproductive Tract. 3rd edition. Pages 132–159, Fig. 7.20. Copyright © 2014, Elsevier Limited. All rights reserved.)

Downloaded from Vet-eBooks.com

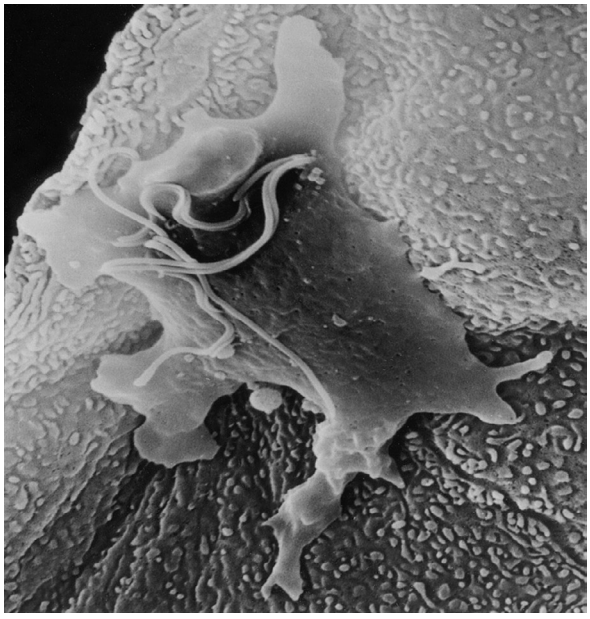


Fig. 2.100 Cytoadherent amoeboid form of *Trichomonas vaginalis* on vaginal epithelial cells.
Within minutes of contact the organism transforms into this form with thin lamellopodia forming multiple contact points with the cells. The flagella and undulating membrane can still be distinguished.

OTHER CUTANEOUS OR MUCOUS MEMBRANE CONTACT

Viral



Fig. 2.101 Acute HSV-1 ulcerative gingivostomatitis.
Primary infection with HSV-1 can cause severe oral ulceration with gingivitis. (Courtesy, Professor R. Hendrickse.)



Fig. 2.102 Oral hairy leukoplakia (OHL).
Notwithstanding the perils of making a purely clinical diagnosis, OHL is one of very few clinical signs that are considered virtually diagnostic of underlying HIV infection. Vertical streaks of white keratin on the lateral border of the tongue that cannot be scraped off are the hallmark of this otherwise benign Epstein–Barr virus-associated condition. (From Neville, B. W., Damm, D. D. Viral infections. In: Oral and Maxillofacial Pathology. Pages 218–258, Fig. 7-34. Copyright © 2016 by Elsevier, Inc. All rights reserved.)

Downloaded From Vet-eBooks.com

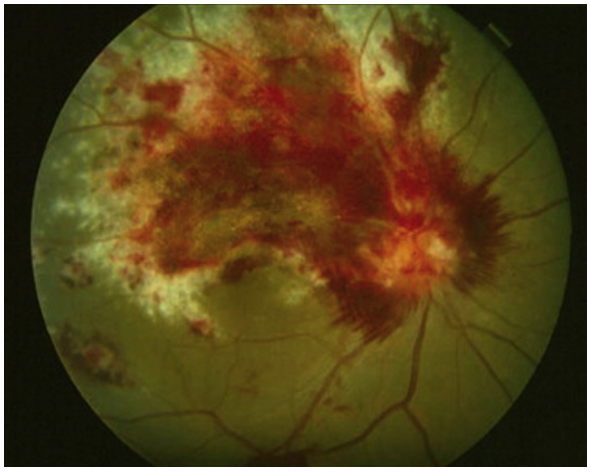


Fig. 2.103 Cytomegalovirus (CMV) retinitis.
CMV infection in the immunocompetent often passes unnoticed or may rarely cause a glandular fever-like infectious mononucleosis. In the immunocompromised HIV patient CMV can disseminate widely with principal end-organ inflammation seen in the gastrointestinal tract, lungs, brain and eyes. (From Jabs, D. A. Cytomegalovirus Retinitis and the Acquired Immunodeficiency Syndrome—Bench to Bedside: LXVII Edward Jackson Memorial Lecture. American Journal of Ophthalmology, Volume 151, Issue 2, Pages 198–216.e1, Fig. 1. Copyright © 2011 Elsevier Inc.)

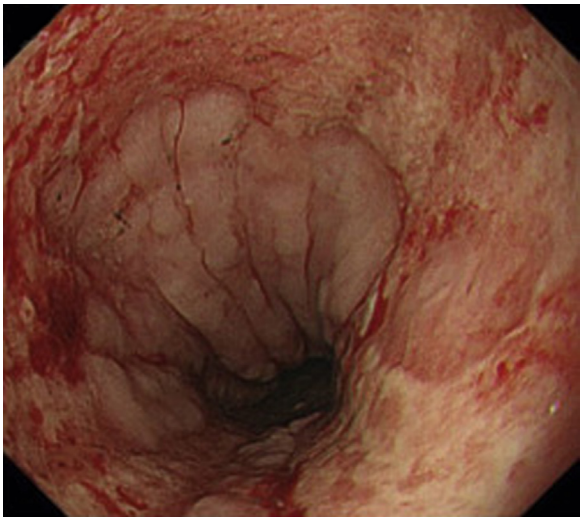


Fig. 2.104 Cytomegalovirus (CMV) oesophagitis.
Severe dysphagia and odynophagia result from extensive oesophageal ulceration in this manifestation most commonly seen in association with advanced HIV infection. CMV colitis has a similarly ulcerative pathology. (From Rintaro, H., Akimichi, C. Esophagitis caused by cytomegalovirus infection in an immune-competent patient. Gastroenterology and Hepatology, 2016, Volume 14, Issue 12, Pages e143–e144.)

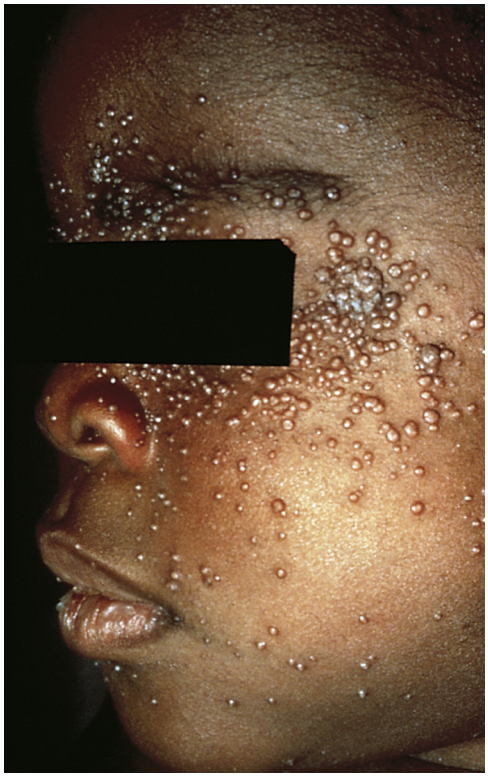


Fig. 2.105 Molluscum contagiosum in HIV.
Numerous umbilicated papules characterize this infection, most commonly on the face. The virus is transmitted person-to-person by direct contact, so is frequently seen in otherwise healthy young children. However, extensive molluscum, as seen here, is a feature of HIV infection. (Courtesy, G.B. Scott, MD, and M.T. Mastrucci, MD, Miami, Fla. From Michaels, M. G., Nowalk, A. J. Infectious disease. In: Atlas of Pediatric Physical Diagnosis. 2012, Pages 469–529, Fig. 12.73.)

Downloaded From Vet-eBooks.com

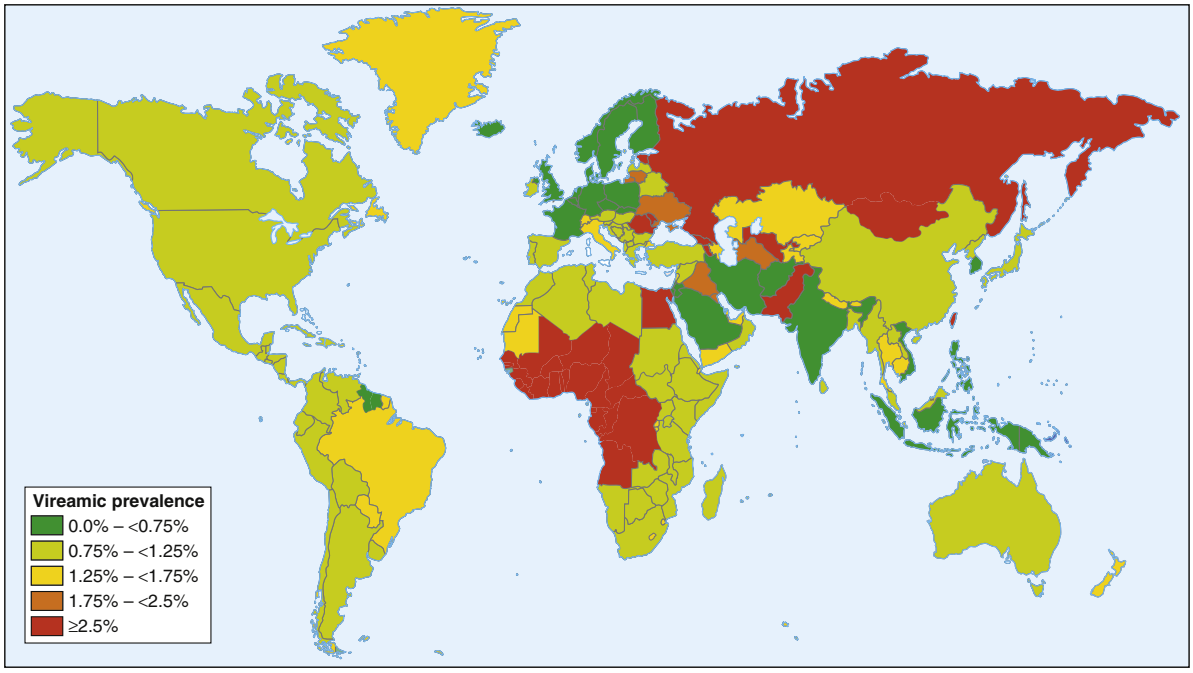


Fig. 2.106 Global epidemiology of hepatitis C virus (HCV) infection — viraemic prevalence.
The sharing of contaminated equipment during injecting drug use, iatrogenic inoculation during the use of contaminated equipment for medical or dental procedures and the transfusion of unscreened blood are believed to be the major modes of transmission of HCV. (From Gower, E., Estes, C. Global epidemiology and genotype distribution of the hepatitis C virus infection. Journal of Hepatology, 2014, Volume 61, Issue 1, Pages S45–S57.)



Fig. 2.107 Vasculitis in hepatitis C virus infection.
Cryoglobulinaemia precipitating vasculitis may be the presenting clinical manifestation of HCV infection.



Fig. 2.108 Centrifugal development of smallpox rash.
Within a decade the successful eradication campaign initiated by the World Health Organization in 1967 had removed this terrible scourge due to *Variola major*, which was still endemic in many tropical countries 50 years ago. (Courtesy Centers for Disease Control, Atlanta, GA.)

Downloaded from Vet-eBooks.com

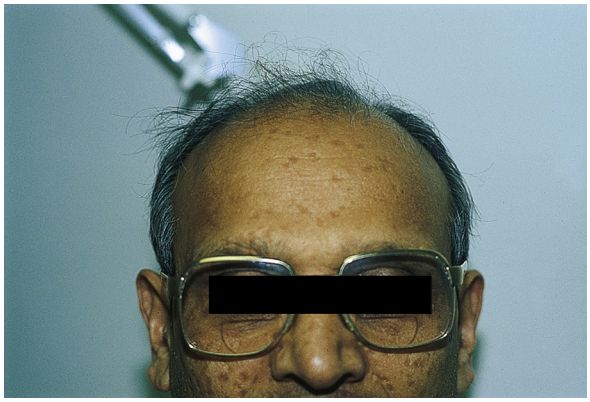


Fig. 2.109 Residual scars ('pockmarks') of smallpox.
Residual scarring is an unmistakable sign of past smallpox infection, as shown in this Indian man. The lesions, unlike those of chickenpox, were peripheral and appeared as a single crop.



Fig. 2.110 Advanced haemorrhagic smallpox in an Indian patient.
The mortality in such serious cases as this was very high; survivors were left with extensive residual pockmarking. (Courtesy Wellcome Photo Library N0022812 and Professor H. Lambert.)

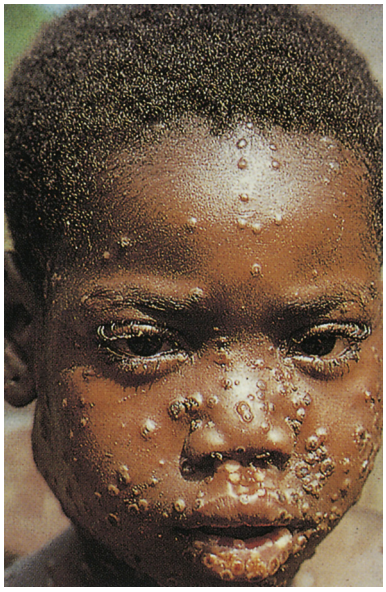


Fig. 2.111 Papulo-pustular rash of monkeypox involving eyelids and lips.
Despite the name it is believed that wild rodents such as rope squirrels are the main reservoir of this virus, which is closely related to smallpox. Monkeys and humans are secondary, spillover hosts. (Courtesy, Dr M. V. Steniowski.)



Fig. 2.112 Inguinal and femoral lymphadenopathy of monkeypox.
Clinically milder than smallpox and distinguishable owing to the presence of marked cervical and inguinal lymphadenopathy, sporadic cases and periodic outbreaks continue to occur in Central African Republic, Democratic Republic of Congo, Nigeria and Cameroon, but human-to-human transmission is limited. (From Munoz, F. M. Viral exanthems. In: Manson's Tropical Diseases, 23rd edition. Pages 225–241 e1, Fig. 20.6. Copyright © 2014, Elsevier Limited. All rights reserved.rd)

Downloaded From Vet-eBooks.com



Fig. 2.113 Clinical rabies.
Though preventable by pre- and post-exposure vaccination, once clinical rabies is established, the disease is almost universally fatal. Hydrophobia and aerophobia provoke distressing spasms. (Courtesy, Professor D. A. Warrell.)

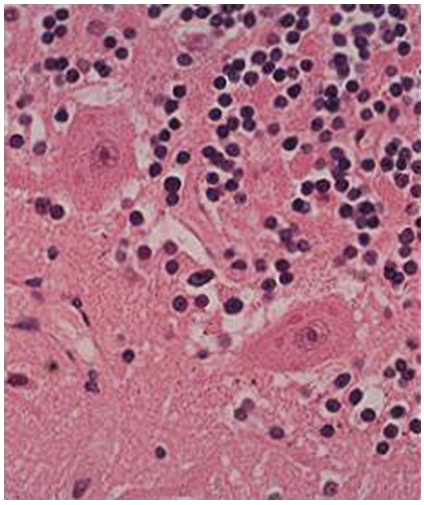


Fig. 2.114 Negri bodies in rabies.
The pathognomonic hallmark of rabies in the brain is intracytoplasmic inclusion bodies (Negri bodies). (Courtesy, Professor S Lucas)

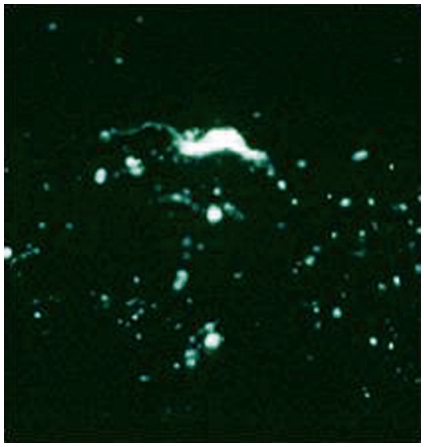


Fig. 2.115 Demonstration of rabies virus by immunohistochemistry.
Ante-mortem diagnosis is usually clinical. However, clinical samples that can be tested include saliva (virus isolation or polymerase chain reaction), serum, cerebrospinal fluid (antibody) and skin biopsies of hair follicles at the nape of the neck (where rabies antigen may be detectable in the cutaneous nerves at the base of hair follicles). (Courtesy, Professor S Lucas)



Fig. 2.116 Mass vaccination of dogs.
Rabies is a zoonotic disease. In the urban environment dogs are responsible for most transmission. In a 2015 demonstration of the feasibility of mass vaccination in Malawi, 35,000 dogs were vaccinated in 20 days. (Courtesy, Dr R Mellanby.)

Downloaded from Vet-eBooks.com



Fig. 2.117 Vampire bat bites on a cow.
In some rural areas, including the Peruvian Amazon, vampire bats, *Desmodus rotundus*, are responsible for most human infections. Bloodmeals are usually taken from cattle, but occasional human bites lead to transmission. (From Warrell, D. A. Animals hazardous to humans. In: Hunter's Tropical Medicine and Emerging Infectious Diseases. 9th edition. Pages 938–965, Fig. 134.6.9. Copyright © 2013, Elsevier Inc. All rights reserved. © Dr I Vargas Meneses.)



Fig. 2.118 Aerophobia in rabies (in response to a fan being turned on).
Aerophobia is less well known than hydrophobia as a cardinal symptom of rabies. Hypersalivation and profuse sweating due to autonomic dysfunction may also predominate. Paralytic rabies accounts for 20% of rabies cases but is probably often misdiagnosed as snakebite, Guillain-Barré or myelitis. Transmission of rabies to healthcare workers from an infected patient has never been reported, though vaccination is usually recommended for those in close contact due to the theoretical infectious risk of mucous membrane droplet splash. (From Spicer, W. John. Acute encephalitis and poliomyelitis, Clinical Microbiology and Infectious Diseases, 2008, Pages 96–97, Fig. 1.)

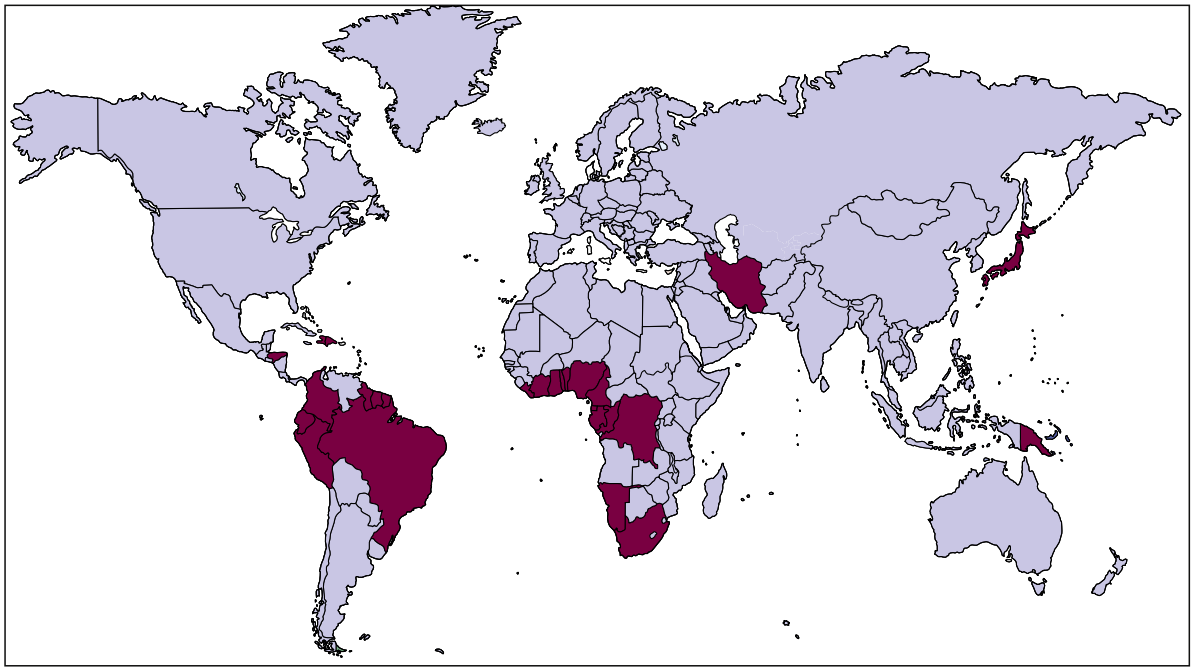


Fig. 2.119 Global distribution of HTLV-1 infection.
The greatest burden of this infection is in Latin America and the Caribbean, sub-Saharan Africa and the Pacific rim, particularly Japan. Prevalence in the general population exceeds 2% in shaded regions. HTLV-1 infection is a risk factor for disseminated disease in strongyloidiasis (Fig. 2.24). (From Tadashi, Y., Jaffe, E. S. Adult T-Cell Leukemia/Lymphoma, Hematopathology. 2017, Pages 619–629.e4,Fig. 33.1.)

Downloaded From Vet-eBooks.com



Fig. 2.120 MRI of cervical and upper thoracic cord showing HTLV-1 associated myelopathy (HAM).
Signal changes can be seen in this T2-weighted MRI of a 39-year-old woman with a 2-year history of gait difficulty and urinary dysfunction. Also referred to as Tropical Spastic Paraparesis (TSP), this manifestation results in spastic paraparesis, bladder and bowel dysfunction, indistinguishable from other causes of paraparesis. (From Unsong, O., Jacobson, S. Treatment of HTLV-I-Associated Myelopathy/Tropical Spastic Paraparesis: Toward Rational Targeted Therapy. Neurologic Clinics, 2008, Volume 26, Issue 2, Pages 781–797, Fig. 1.)



Fig. 2.121 HTLV-1 associated uveitis.
Often under-recognised as a cause of uveitis, this Spanish woman presented with intermediate uveitis which preceded development of lower limb weakness by several months. (From Millán-Rodríguez, A.C., Fernández-Cid, C. Intermediate uveitis due to human T-cell lymphotropic virus type 1. Archives of the Spanish Society for Ophthalmology, 2012, Volume 87, Issue 2, Pages 44–46, Fig. 1. Copyright © 2010 Sociedad Española de Oftalmología.)

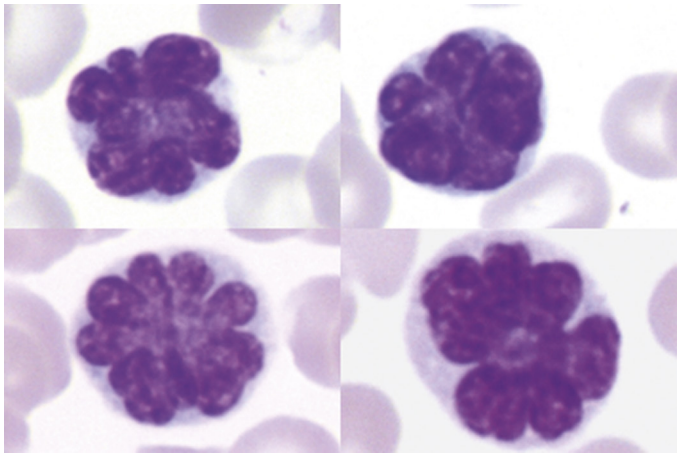


Fig. 2.122 HTLV-1 associated T cell lymphoma.
This is an important complication of long-term HTLV-1 infection. Circulating neoplastic T cells may have a characteristic 'flower like' form. (From O'Connor, O. A., Marchi, E. T-Cell Lymphomas, Hematology: Basic Principles and Practice. 7th edition. 2012, Pages 1267–1302.e8, Fig. 84-6.)

Downloaded From Vet-eBooks.com



Fig. 2.123 Yambuku, former Zaire, from the air.
The village of Yambuku, and ultimately the hospital itself, was the epicentre of the first documented outbreak of Ebola virus disease. (Courtesy, Professor B. P. Piot.)

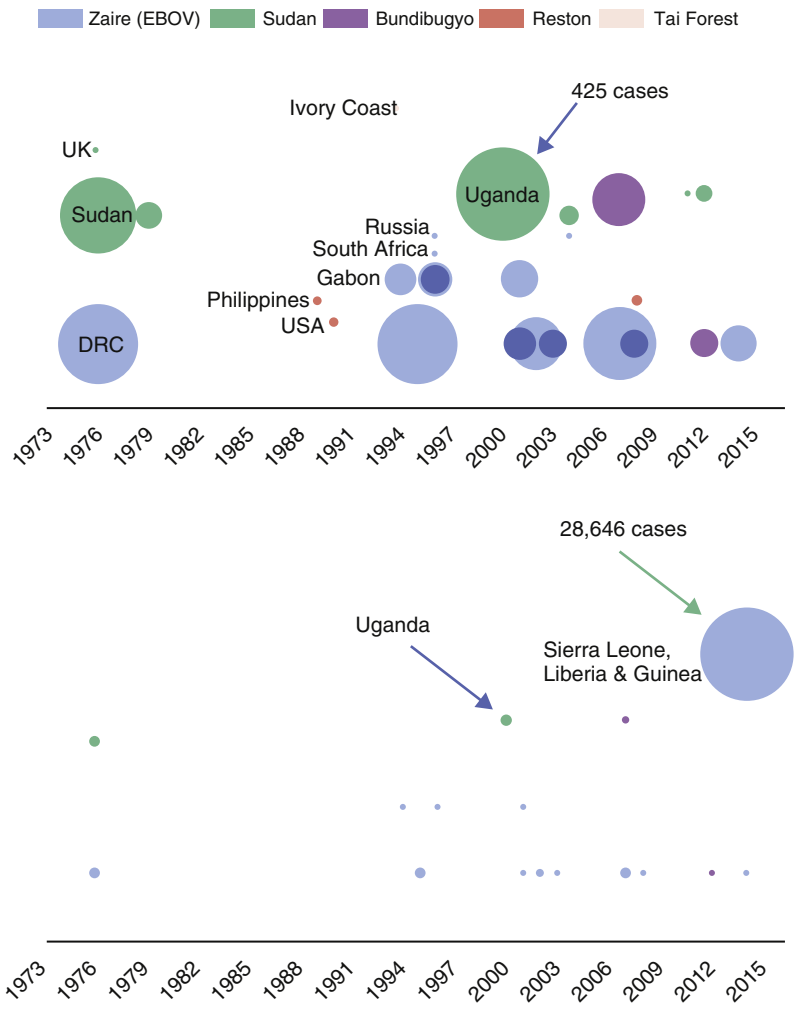


Fig. 2.124 Global chronology and scale of Ebola outbreaks, scaled prior to and following 2014.
The comparative scale of the 2014/15 west Africa ebola epidemic is shown by the outbreak chronogram without (above) and then with (below) its inclusion. Prior to 2014, outbreaks of haemorrhagic fever due to Ebola virus were confined to remote rural regions, quickly terminated, and total reported cases numbered 2361. Over 28,000 cases were reported from West Africa from 2014 to 2016. (Courtesy, Dr C Brown.)

Downloaded from Vet-eBooks.com



Fig. 2.125 A holding centre in west Africa.
During the explosive 2014/15 outbreak of Ebola virus disease (EVD) in West Africa the establishment of holding centres for diagnostic triage was essential to reduce transmission in the community whilst awaiting the results of diagnostic tests. Though some nosocomial transmission is likely to have occurred in these centres, the opportunity for amplification within the community was blocked. Here the screening area is seen to the left and shelter for patients to the right. (Courtesy, Dr C. Brown.)



Fig. 2.126 An Ebola treatment centre, Sierra Leone 2014.
After diagnosis patients with confirmed EVD were managed in strict isolation facilities. Delivery of nursing and medical care was hugely challenging due to soaring temperatures, bulky personal protective clothing and profoundly sick patients requiring intensive management. (Courtesy, Dr C. Brown.)



Fig. 2.127 Ebola survivors.
Serosurveys suggest that the EVD clinical attack rate is close to 100%. Pauci-symptomatic or asymptomatic infections appear to occur very rarely, if at all. Survivors have been seen in much larger numbers in West Africa than in previous outbreaks. (Courtesy, Dr C Brown.)

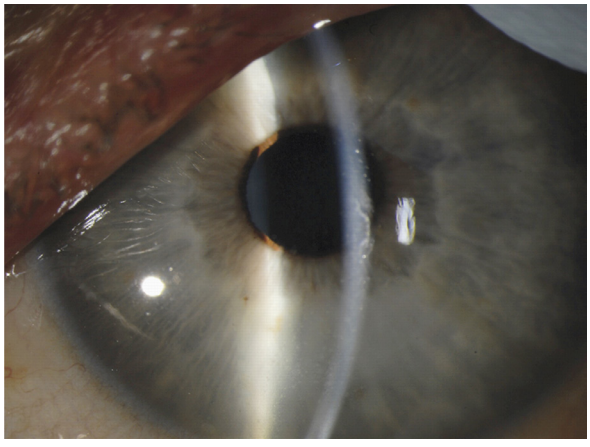


Fig. 2.128 Ophthalmological complication (anterior uveitis) of Ebola virus disease (EVD).
The much smaller scale of previous epidemics had not yielded sufficient survivors for a clear understanding of longer-term complications. It is clear from the West Africa epidemic that a constellation of symptoms continue to affect those who survive the severe infection. These include ophthalmological and audiological deficit, musculoskeletal pain and fatigue. In some areas survivor guilt is further compounded by ostracism by communities, leading to significant psychological distress. (Courtesy, Dr I. Crozier.)

Downloaded from Vet-eBooks.com

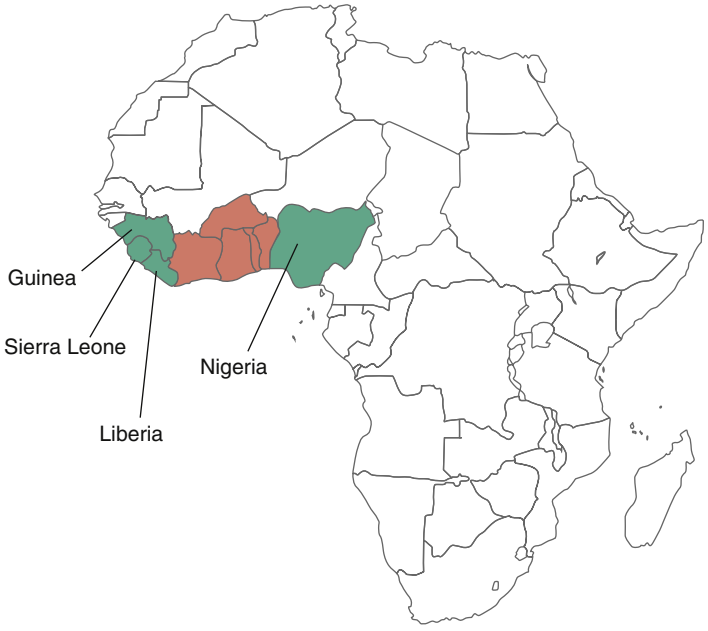


Fig. 2.129 Distribution of Lassa fever.
Lassa fever is a viral haemorrhagic fever primarily of West Africa where it is estimated that about one-quarter of a million people are infected each year. Most confirmed disease occurs in Guinea, Sierra Leone, Liberia (the three countries affected by the 2014/15 EVD epidemic) and Nigeria.

Serosurveys and sporadic cases also indicate infections occur in Mali, Ghana, Togo, Benin, Côte D'Ivoire, Burkina Faso and Senegal, as well as occasionally in Central African Republic and Democratic Republic of Congo.



Fig. 2.130 *Mastomys natalensis*, the rodent reservoir of Lassa fever.
The multimammate rat may be the most common rodent in Africa and is found in a high proportion of rural dwellings. Exposure to rat urine is the major risk for infection.



Fig. 2.131 Facial swelling and subconjunctival haemmorhage in a boy with Lassa fever in Sierra Leone.
In comparison to Ebola virus disease (EVD), the clinical attack rate is lower for Lassa fever, with only 20% of those infected developing clinically apparent disease. From 1 to 3 weeks after infection severe pharyngitis, respiratory distress, unprovoked bleeding and facial oedema develop with shock and marked chest, abdominal and back pain. Case fatality is usually 5–20% amongst hospitalized adults but only about 1% for all infections overall. As with EVD, infection during pregnancy is associated with very poor maternal and foetal outcomes. Deafness is a common long-term sequela. (From Bausch, D. G. Viral Hemorrhagic Fevers, Goldman-Cecil Medicine. Pages 2247–2256.e2, Fig.381.1. Copyright © 2016 Saunders, an imprint of Elsevier Inc.)

Downloaded from Vet-eBooks.com

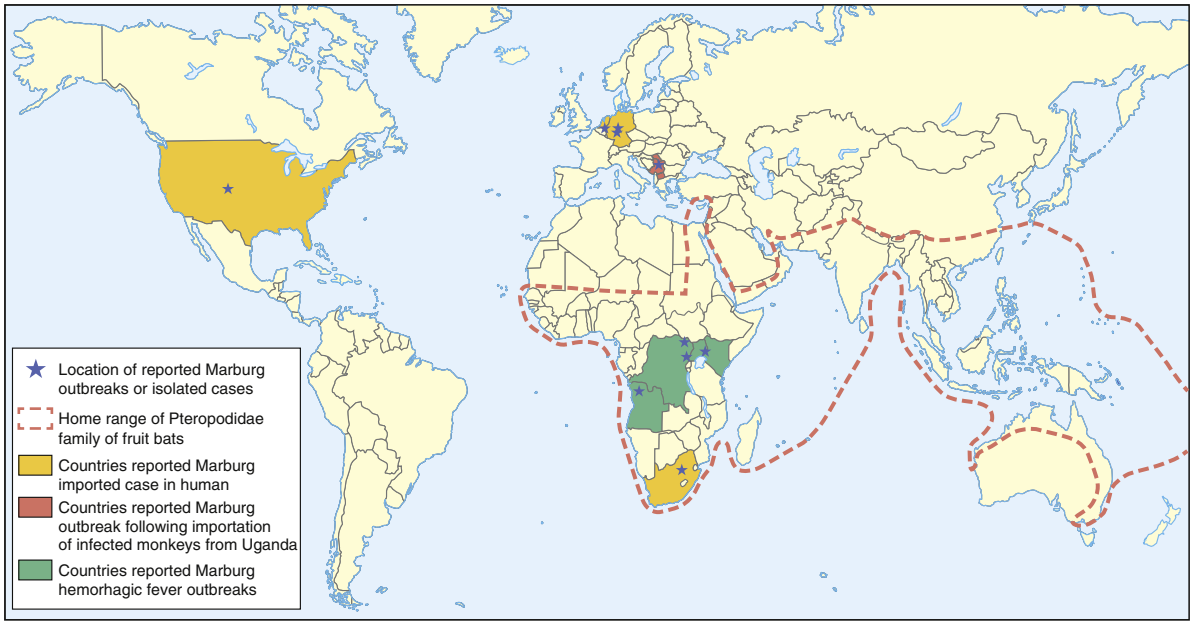


Fig. 2.132 Marburg map.
Although only a handful of countries have reported endemic transmission of Marburg virus—Kenya, Uganda, Democratic Republic of Congo, Angola (and possibly Zimbabwe in 1975)—the geographic range of the fruit bats believed to be important reservoirs is very large. (From WHO; http://www.who.int)

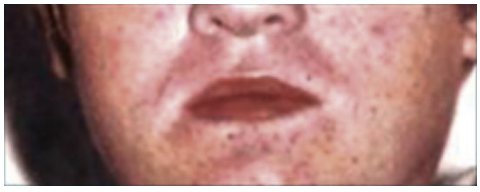


Fig. 2.133 Marburg rash.
This blanching maculopaular rash appears during the first week of Marburg virus disease. Illness develops abruptly with severe headache and malaise. Severe haemorrhagic complications occur between days 5 and 7, and case fatality is high in Africa, often over 80%. Human infection originates from contact with infected animals, particularly monkeys or fruit bats, and person-to-person contact through infectious blood and body fluids. (From McFee, R. B. Viral hemorrhagic fever viruses. Disease-a-Month, 2012, Volume 59, Issue 12, Pages 410–425, Fig. 2. Copyright © 2013 Mosby, Inc.)

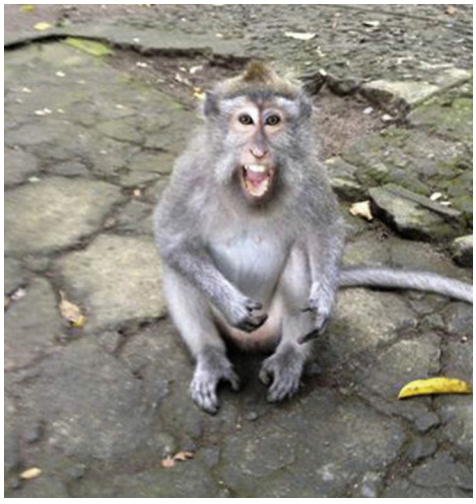


Fig. 2.134 Rhesus macaque, a frequent carrier of herpes B virus.
Whilst over 75% of adult rhesus macaques are believed to carry herpes B virus, infection is essentially asymptomatic. In contrast, inadvertent human infection, largely in macaque handlers or those with close contact with macaque bodily fluids, causes a severe encephalitis with a high case-fatality. (From Johnston, W. F., Yeh, J. Exposure to macaque monkey bite. Journal of Emergency Medicine, 2015, Volume 49, Issue 5, Pages 634–637, Fig. 2. Copyright © 2015 Elsevier Inc.)

Downloaded From Vet-eBooks.com

Bacterial



Fig. 2.135 Bacillary angiomatosis in HIV.
Bartonella henselae, the cause of cat scratch disease, can cause this angioproliferative condition, particularly in patients with concurrent HIV infection (From Motswaledi, M. H. The spectrum of HIV-associated infective and inflammatory dermatoses in pigmented skin. Dermatologic Clinics, 2014, Volume 32, Issue 2, Pages 211–225, Fig. 4.)



Fig. 2.136 Buruli ulcer with undermined edges.
Mycobacterium ulcerans is the causative agent of Buruli ulcer, a condition that can result in life-changing disfigurement. The classic appearance of a large ulcer with undermined edges and a cotton-wool like appearance in the base is shown here. (Courtesy, Dr R. Phillips.)



Fig. 2.137 Contractures resulting from previous healing of a large Buruli ulcer.
Lack of active management of healing ulcers can result in disabling contractures. (Courtesy, Dr R. Phillips.)



Fig. 2.138 Early Buruli ulcer plaque.
A firm, painless, elevated, well-demarcated lesion more than 2 cm in diameter with irregular edges. The skin over the lesion is often reddened or otherwise discoloured. (Courtesy, Dr R. Phillips.)

Downloaded From Vet-eBooks.com



Fig. 2.139 A typical environment where *Mycobacterium ulcerans* inoculation is believed to take place.
Contact with water seems to be an important risk factor for development of Buruli ulcer, although attempts to demonstrate *M. ulcerans* in the environment have been unrewarding to date. (Courtesy, Dr R. Phillips.)



Fig. 2.140 *Mycobacterium marinum*.
Cosmopolitan in fresh and saltwater, *M. marinum* infection (known as fishtank granuloma when occuring on the hand) can spread proximally along the lymphatics mimicking sporotrichosis, so-called sporotrichoid spread (see 2.173). (Courtesy, Dr L Nabarro.)



Fig. 2.141 Inoculation mycobacteriosis at the site of insulin injection.
Use of contaminated insulin or insulin needles led to the development of multiple injection site infections and severe mycobacterial infection of the abdominal wall. (Courtesy, Professor G. Varghese.)

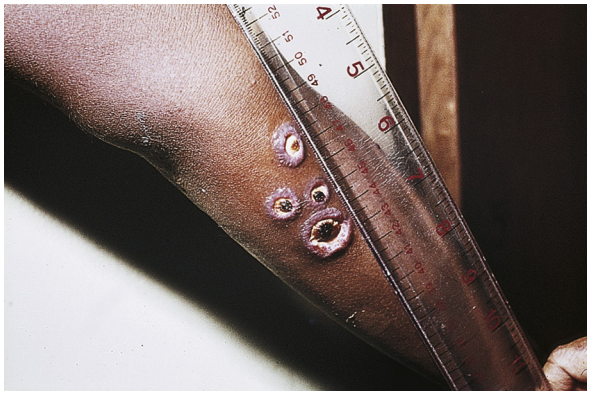


Fig. 2.142 Cutaneous anthrax.
Four discrete lesions on the arm of an African patient infected with *Bacillus anthracis*. The black eschars are associated with direct inoculation through a break in the skin after contact with infected animal material. The lesion is painless without pus but is often surrounded by an arc of oedema and ultimately heals, leaving a scar.

Downloaded From Vet-eBooks.com

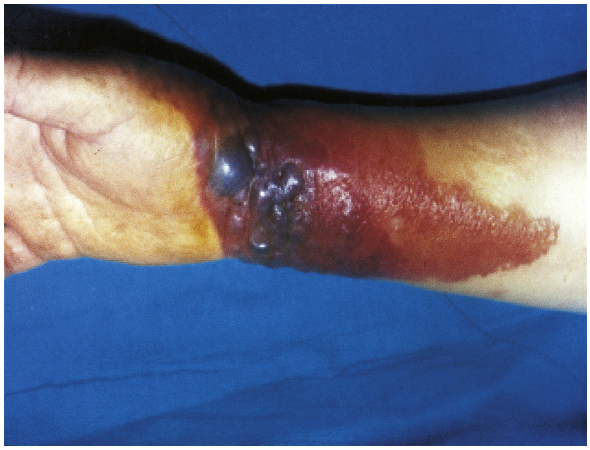


Fig. 2.143 Extensive erythema and haemorrhagic bullae in cutaneous anthrax.
This condition may be seen 2–4 days after the initial infection. People who work with potentially contaminated animals or animal skins are especially liable to this type of infection by anthrax spores. Although about 95% of all human anthrax lesions are located in the skin, infection acquired by the ingestion of contaminated meat or game or inhalation of spores may cause life-threatening disease of the internal organs.



Fig. 2.144 Rat bite fever.
Infection with *Spirillum minus* in this young Brazilian woman following a rat bite resulted in a local ulcerative lesion associated with high fever and cervical lymphadenopathy. The spirochaete-like organisms were detected by dark field examination of material from the ulcer. This patient's infection responded to antibiotic therapy, but, untreated, death may occur in 10% of cases. *Streptobacillus moniliformis* is another rare infection associated with rat bites or accidental contamination with rat excreta.



Fig. 2.145 Tropical pyomyositis.
The right thigh is swollen with infection by *Staphylococcus aureus*. Such infections are common in tropical Africa but uncommon in temperate climates. It is not understood why the organism selects muscle rather than any other tissue in which to multiply. This suppurative muscle infection may occur in as many as 1 per 1000 individuals in tropical countries.



Fig. 2.146 Cancrum oris (noma).
This gangrenous polymicrobial condition of the facial region commences with necrotizing stomatitis, which can evolve very rapidly (within 24–48 hours). Soft and hard tissues of the cheek can be destroyed, leading to gross disfigurement, as well as death in a significant proportion of patients in spite of intensive antibiotic and local treatment. An association with measles has been commonly noted. Gross disfigurement usually results. (Courtesy, Professor Y. Larsson.)

Downloaded from Vet-eBooks.com

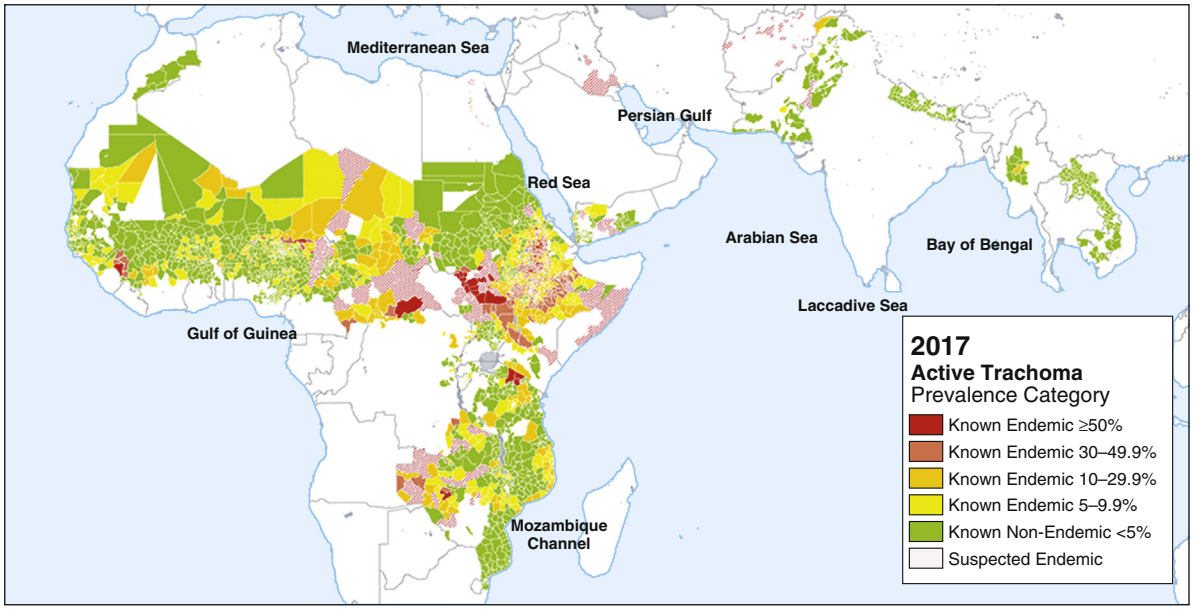


Fig. 2.147 The Global Trachoma Mapping Project (GTMP).
Trachoma is the leading infectious cause of blindness worldwide. It is caused by infection with *Chlamydia trachomatis* and is spread from person to person through contact with contaminated faeces, fingers, clothing and eye-seeking flies. Trachoma is a disease of poverty and is prevalent in communities with limited access to water and sanitation. In 2017, 232 million people lived in trachoma-endemic regions. Of the 51 trachoma-endemic countries, 14 in sub-Saharan Africa represent 80% of the disease burden. Trachoma is treatable and blindness preventable using the multifaceted **SAFE** strategy. Recommended by the World Health Organization, **SAFE** is a comprehensive public health approach combining treatment (**S**urgery and **A**ntibiotics) with prevention (**F**acial-cleanliness and **E**nvironmental improvement). In the largest infectious diseases survey ever undertaken, the GTMP collected data on 2.6 million people in 29 countries in only 3 years (2013–2015). The Trachoma Atlas consolidates this data to produce maps of trachoma prevalence and **SAFE** implementation through an open-access platform. (From Trachoma Atlas © 2018 Global Atlas of Trachoma; http://www.trachomaatlas.org/global-trachoma-atlas)

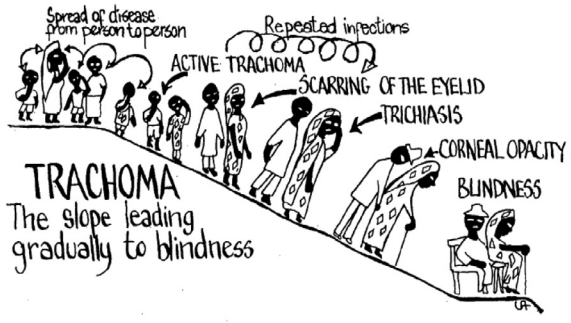


Fig. 2.148 The gradual slope towards blindness in trachoma.
The stepwise progression to eventual blindness after many years of disease. Active trachoma is caused by infection with *C. trachomatis*. Chronic conjunctival inflammation from repeated infection leads to conjunctival scarring, trichiasis and blindness. (From 'Trachoma Control: a guide for programme managers' (WHO 2006, Geneva).)

Downloaded from Vet-eBooks.com



Fig. 2.149 A normal conjunctiva.
The conjunctiva is easily visualized by everting the upper eyelid. A normal conjunctiva has clearly visible blood vessels. (Courtesy, Dr A Last.)

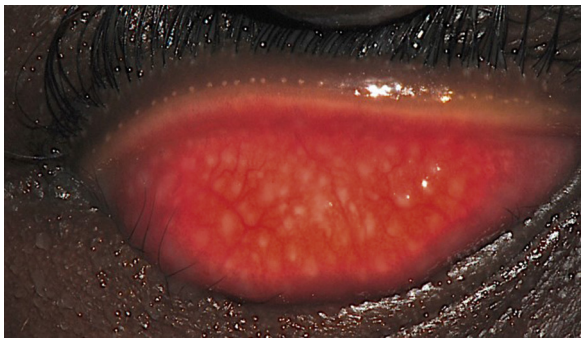


Fig. 2.150 Active trachoma: inflammatory trachoma – follicular (TF).
In TF, multiple lymphoid follicles are seen in the central zone of the everted eyelid. (Courtesy, Dr A Last.)



Fig. 2.151 Active trachoma: inflammatory trachoma – intense (TI).
The thickened, oedematous conjunctival surface is inflamed. The deep tarsal vessels are not seen. There is often a high burden of *Chlamydia trachomatis* with TI. (Courtesy, Dr A Last.)

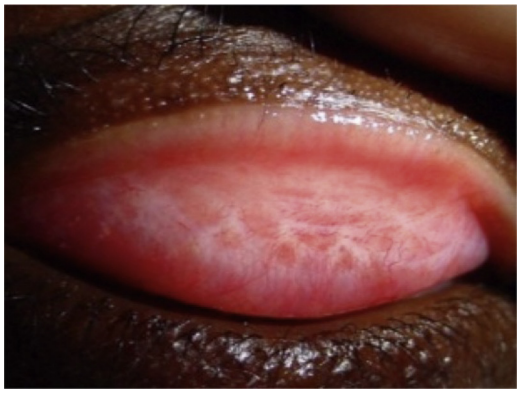


Fig. 2.152 Trachomatous scarring (TS).
The conjunctiva is thickened and scarred and difficult to evert. The lacy white pattern in the central zone is typical of TS. TS is the sequela following repeated episodes of infection and inflammation. *C. trachomatis* is not usually found. (Courtesy, Dr A Last.)

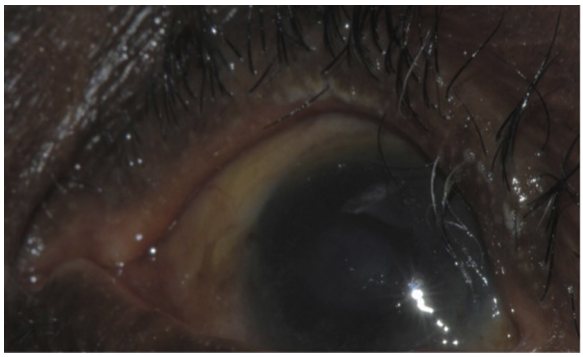


Fig. 2.153 Trachomatous trichiasis (TT).
Trachoma scarring deforms the surface of the eyelid, leading to inversion of the lid margin (entropion) causing the eyelashes to scratch the cornea. This is extremely painful and provokes corneal inflammation. Surgical intervention is required to prevent chronic corneal damage and blindness. (Courtesy, Dr A Last.)

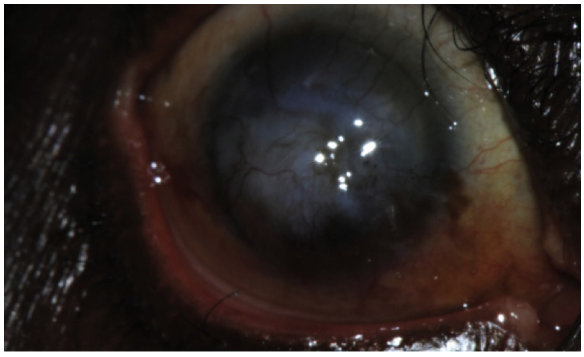


Fig. 2.154 Corneal opacity (CO).
In severe TT, multiple lashes scratch the cornea. Chronic corneal inflammation leads to scarring. A central corneal opacity obscures the pupil and leads to irreversible blindness. (Courtesy, Dr A Last.)

Downloaded from Vet-eBooks.com



Fig. 2.155 Primary yaws lesions of skin and mucous membranes.
The commonest of the non-venereal treponematoses has once again been targeted for eradication, facilitated by the demonstrated treatment efficacy of single-dose azithromycin. These infections, diagnosed in Western Province of the Solomon Islands, have presumably been acquired by direct person-to-person contact. In the absence of treatment, the painless lesions self-heal in 3–6 months. (Courtesy, Dr M Marks.)



Fig. 2.156 Yaws bony lesions.
Untreated cutaneous yaws can progress to secondary bony involvement. These osteoperiostitis lesions are painful but will resolve with treatment. (Courtesy, Dr M. Marks.)



Fig. 2.157 Bejel.
There are few photographs of this rare non-venereal treponematosis. Gummatous destruction of nasal cartilage, bone and skin can ensue if left untreated, as in this individual from the Middle East. (Courtesy, Liverpool School of Tropical Medicine.)

Downloaded from Vet-eBooks.com



Fig. 2.158 Pinta.
Treponema carateum, the causative agent of this non-venereal treponemal skin disease of Latin America (also known as carate), is morphologically indistinguishable from *T. pallidum*. Plaques that develop from papules become depigmented in the later stages, as seen here. This condition is now very rarely diagnosed. (From James, W. D., Berger, T. G., Elston, D. M. Syphilis, yaws, bejel, and pinta. In: Andrews' Diseases of the Skin. Pages 343–358.e2, Fig. 18.11. Copyright © 2016 by Elsevier, Inc. All rights reserved.)



Fig. 2.159 Cutaneous chancroid.
Often previously mistaken for yaws, the use of improved diagnostic testing has led to the growing recognition of *Haemophilus ducreyi* as a cause of cutaneous ulcers in children, presumably spread by person-to-person contact. (Courtesy, Dr M. Marks.)

Fungal



Fig. 2.160 White plaques of oral candidiasis.
In HIV infection oral candida may be extensive and refractory to topical treatment. (From Goh, B. T. Sexually transmitted infections. In: Hutchison's Clinical Methods: An Integrated Approach to Clinical Practice. 2012, Pages 439–451, Fig. 21.7.)

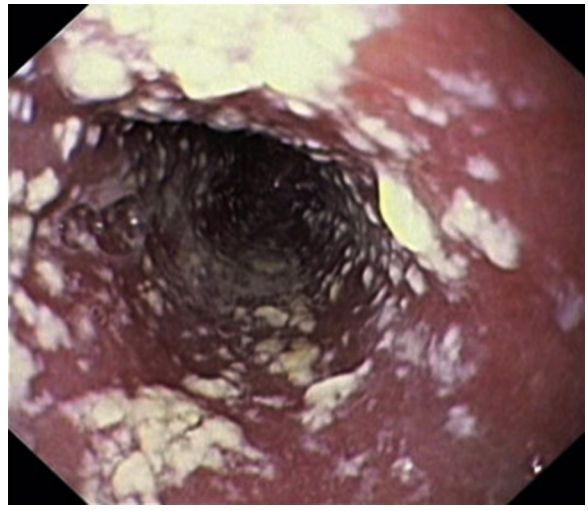


Fig. 2.161 Candidal oesophagitis.
Oesophageal candidiasis indicates underlying immune suppression and in patients with HIV infection is indicative of advanced disease. (From Forgacs, I., Raja, O. Diabetes and the gastrointestinal tract. Medicine. 2015, Volume 43, Issue 6, Pages 347–351, Fig. 2. Copyright © 2015 Elsevier Ltd.)

Downloaded From Vet-eBooks.com



Fig. 2.162 Tinea imbricata.
Tinea imbricata is a chronic, superficial mycoses caused by *Trichophyton concentricum* found in the Pacific, South East Asia and Central America. Treatment is with prolonged courses of grieosfulvin or oral terbinafine, although cure rates are poor. (Courtesy, Dr M Marks.)



Fig. 2.163 Tinea imbricata in Western Province of the Solomon Islands.
The characteristic flaking edge with lesions in parallel lines and concentric circles are clearly seen on the arms of this young boy. (Courtesy, Dr M. Marks.)



Fig. 2.164 Tinea cruris.
Common in young men in hot, humid regions, this superficial dermatophyte infection of the groin and adjacent skin is most frequently caused by *Trichophyton rubrum* or *Epidermophyton floccosum*. Note the well-demarcated, active border and characteristic sparing of the penis and scrotum. (Courtesy Kenneth E. Greer. From Marchetti, M. A.,Wilson, B. Dermatologic conditions, In: DeLee & Drez's Orthopaedic Sports Medicine, Pages 285–297, Fig. 26-8. Copyright 2015 by Saunders, an imprint of Elsevier Inc.)



Fig. 2.165 Pityriasis versicolor.
Superficial infection with yeasts of the *Malassezia* genus is a common cause of otherwise asymptomatic depigmentation of dark skins in tropical regions. Yellow-green fluorescence is seen under Wood's light, in contrast to other causes of depigmentation. Repigmentation of treated skin is usual. (From Rogers, M., Phillips, R., Wong, Li-Chuen. Skin disorders. Practical Paediatrics. 2012, Pages 756–778, Fig. 21.1.17. © 2012 Elsevier Ltd. All rights reserved.)

Downloaded from Vet-eBooks.com

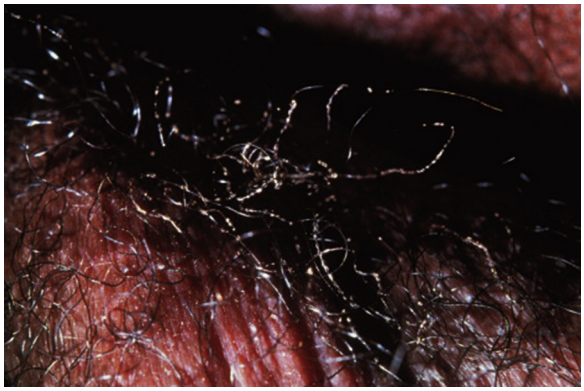


Fig. 2.166 Black piedra.
This superficial fungal infection of the hair due to *Piedraia hortae* is common in warm, humid environments, notably in South America and South East Asia. Largely asymptomatic aside from dark nodules on hair shafts on the scalp and axillae, the hair can become brittle in heavy infections. (Courtesy, Dr. C. Kalter. From Grayson, W. Infectious diseases of the skin. In: McKee's Pathology of the Skin. Pages 760-895, Fig. 18.269. Copyright © 2012 Elsevier Ltd.)



Fig. 2.167 White piedra.
More commonly affecting pubic and facial hair, white piedra is caused by *Trichosporon sp.* and has a more cosmopolitan distribution, although it is also frequent in Latin America and Asia. (From James, W. D., Berger, T. G., Elston, D. M. Diseases resulting from fungi and yeasts. In: Andrews' Diseases of the Skin. Pages 285–318.e4, Fig. 15.17. Copyright © 2012, Elsevier Ltd.)



Fig. 2.168 Chromoblastomycosis.
This chronic fungal infection had been indolently expanding up the leg of this man from the Caribbean for many years. (Courtesy, Professor D. A. J. Moore)

Downloaded From Vet-eBooks.com



Fig. 2.169 Chromoblastomycosis of the hand.
This inoculation infection can also affect the hand, as in this man from north-east Brazil.



Fig. 2.170 Lobo's disease.
Lobomycosis, presenting with shiny, keloid-like lesions as seen here, is similar to chromoblastomycosis and is also seen in north-east Brazil. It is caused by *Loboa lobo*.



Fig. 2.171 Mycetoma, 'Madura foot'.
Mycetoma may be caused by fungi (eumycetoma) or *Actinomycetes* bacteria, which enter by accidental inoculation. It may be found in Africa, Asia and Latin America. This patient was seen in India. (Courtesy, Dr A Manesh.)

Downloaded From Vet-eBooks.com

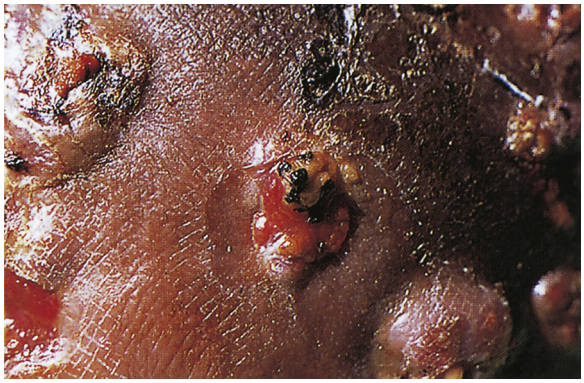


Fig. 2.172 Fungal grains discharging.
Bacterial and fungal species that cause mycetoma each lead to the discharge of granules of characteristic colours—red, yellow/white or black.



Fig. 2.173 Sporotrichosis.
The primary lesion on the thumb with lymphatic spread up the forearm are characteristic of this fungal infection, seen here in a woman from Saõ Paulo.



Fig. 2.174 Early lesions of sporotrichosis.
The lower leg of this patient from Mauritius shows the early nodular lesions of *Sporothrix schenckii* infection.



Fig. 2.175 Mucocutaneous lesions in paracoccidioidomycosis.
Paracoccidioidomycosis is an endemic mycosis of tropical South and Central America caused by the dimorphic fungus *Paracoccidioides brasiliensis*. Though most infections are subclinical, two clinical forms exist. In adults a chronic pulmonary, mucocutaneous and lymph node disease is seen, whereas in children a more acute, systemic illness with fever, lymphadenitis and sinus formation occurs.

Severe granulomatous destruction of mucocutaneous tissues can arise following inoculation of this fungus, as can occur when sticks from the forest are used as toothpicks (See Figs. 4.103–4.107.)

Downloaded From Vet-eBooks.com

3. Infections Acquired Through the Gastrointestinal Tract

Many of the important pathogens that gain entry through the gastrointestinal tract are cosmopolitan in their distribution. They include viruses, bacteria, protozoa, helminths and endoparasitic arthropods. The first three of these can be directly infectious for humans when they are passed in the faeces but, in the case of helminths, the eggs may become infectious only after maturation in the soil (e.g. Ascaris lumbricoides) or after passing through an intermediate host (e.g. Taenia saginata). Helminthiases acquired from the soil and those requiring a snail intermediate host are considered in Chapter 2. Some pathogens pass from the intestinal tract to cause systemic infection and may localize in other organs (e.g. poliomyelitis, acute viral hepatitis, trichinosis). Localized infection of the gastrointestinal tract itself with pathogenic viruses or bacteria accounts for a high proportion of deaths in infants and young children in low- and middle-income countries.

The most important pattern of transmission is the passage of infective material from human faeces into the mouth of a new host, which is known as 'faeco–oral' transmission. This occurs mostly through inapparent faecal contamination of food, water and hands—the three main points of contact with the mouth.

VIRAL INFECTIONS

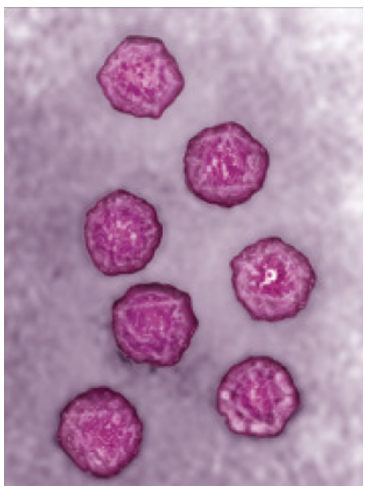


Fig. 3.1 Poliomyelitis virus.
Spherical virus particles 25 nm in diameter. Transmission is by the faeco–oral route. Virus can be detected, either by isolation in culture or by polymerase chain reaction in faeces (and during surveillance also in sewage), occasionally from the throat and rarely from cerebrospinal fluid. (From Parker, E. P. K., Grassly, N. C. Unravelling mucosal immunity to poliovirus. Lancet Infectious Diseases, 2016, Volume 16, Issue 12, Pages 1310–1311.)

Downloaded From Vet-eBooks.com



Fig. 3.2 The shrinking global map of polio.
Polio was eliminated from the Americas in 1991, 6 years after the Pan American Health Organization (PAHO) declared the target. Mass national vaccination days were a strength in many countries. Although theoretically possible as there is no non-human reservoir of infection, the polio global eradication 'end-game' remains a major challenge due to the complexities of the remaining regions with ongoing transmission. By early 2017, Afghanistan, Pakistan and Nigeria were the only countries still reporting wild poliovirus transmission. Well-established surveillance for acute flaccid paralysis helps to flag potential new outbreaks where rapid vaccination responses can be deployed. It may also facilitate identification of novel aetiological pathogens, such as cycloviruses, which have been linked to unexplained sudden onset paraplegia in Malawi and encephalitis in Vietnam.



Fig. 3.3 Administration of bivalent oral polio vaccine in Jalalabad, Afghanistan.
In 1988 the World Health Assembly declared the goal of polio eradication by 2000. Mass vaccination campaigns with three oral doses reduced endemic countries from 125 to 6 by 2003. The title of the article originally accompanying this photograph in 2010 was 'polio eradication within 5 years now a real possibility'. The justifiable optimism was subsequently dented by detection of cases in Somalia, Syria, Cameroon, Ethiopia and Kenya in addition to the known hard-to-reach populations in Nigeria, Pakistan and Afghanistan. Civil unrest and lack of public trust and confidence, as well as consequent security risks for vaccination teams (including tragic instances of vaccinators being murdered), are important threats to vaccine programmes. (From Senior, K. Polio eradication within 5 years now a real possibility. The Lancet Infectious Diseases, 2010, Volume 10, Issue 3, Pages 148–149. Copyright © 2010 Cornelia Walther/UNICEF.)

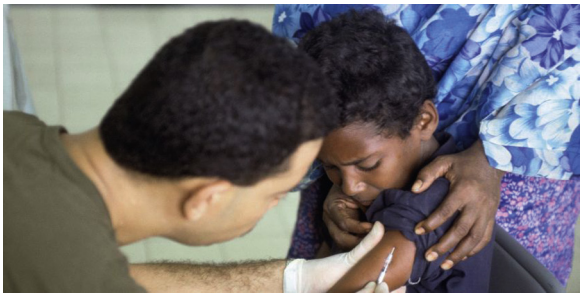


Fig. 3.4 Adminstration of inactivated polio vaccine (IPV).
In the decade leading up to 2015, 10 billion doses of live attenuated oral polio vaccine given to 2.5 billion children had prevented more than 10 million estimated cases of polio. Nevertheless, countries approaching elimination switch to use of IPV to avert the 1-per-million-dose risk of vaccine associated paralytic polio (VAPP). In 2015, virus identified as vaccine-derived polio virus was detected in 23 cases of acute flaccid paralysis in Ukraine, Madagascar, Guinea, Laos and Myanmar, countries with no wild virus poliomyelitis. Globally there were 66 cases of wild virus polio in the same year, all from Pakistan and Afghanistan.

Downloaded from Vet-eBooks.com



Fig. 3.5 Flaccid paralysis due to polio.
Disability with lifelong limb weakness is a direct indictment of the failure of the health system to vaccinate all children.



Fig. 3.6 Enterovirus 71.
Enterovirus 71, for which there is currently no available vaccine, is a common cause of hand, foot and mouth disease in East Asia, notably Vietnam, China and Taiwan. It is also rarely associated with neurological disease including encephalitis and a polio-like flaccid paralysis. Infection is passed from person to person by direct contact with nose and throat discharges, saliva, blister fluid or the faeces of infected persons (enterovirus describes the location of pathogen carriage not pathology). (From Mong How, O., See Chang, W. Clinical features, diagnosis, and management of enterovirus 71. The Lancet Neurology, 2010, Volume 9, Issue 11, Pages 1097–1105, Figure 1.)

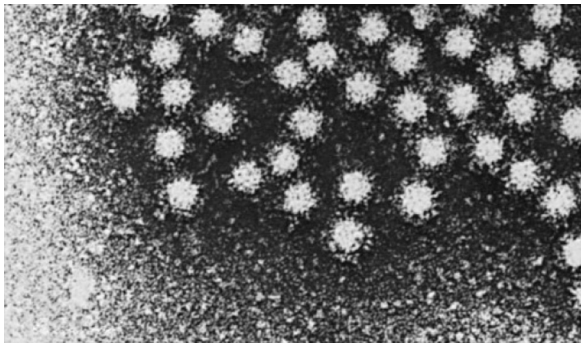


Fig. 3.7 Hepatitis A virus.
This RNA virus is transmitted by the faeco–oral route and therefore either through ingestion of contaminated water or food (typically shellfish, but imported soft fruits washed in contaminated water have also caused outbreaks) or more directly from person to person (close contact amongst children, ano–oral sexual contact). Aside from their commonly used names and a tendency to cause liver inflammation, the hepatitis viruses A to E have little in common; moreover, yellow fever virus, Ebstein–Barr virus (EBV) and cytomegalovirus (CMV) amongst other viruses may also be considered hepatotropic and no less closely related. Hepatitis B (Figs 2.73, 2.74) and hepatitis C viruses (Figs 2.106, 2.107), which account for significant morbidity and mortality due to the consequences of chronic infection, are considered in Chapter 2. (Courtesy, Dr J. Dienstag. From Leung, D. H., Chen, L. L. Hepatitis. In: Feigin and Cherry's Textbook of Pediatric Infectious Diseases, 7th edn. © 2014 Elsevier Inc. All rights reserved. Pages 648-658.e4, Figure 47-1.)

Downloaded From Vet-eBooks.com

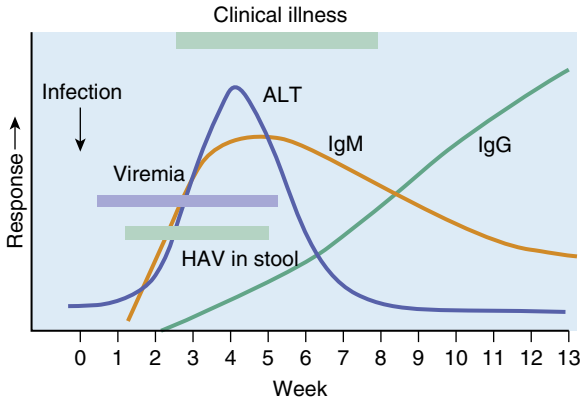


Fig. 3.8 Course of acute hepatitis A infection.
After an incubation period of 14–28 days, infection with hepatitis A virus may cause an unremarkable, self-limiting diarrhoeal illness with fever and anorexia, with or without jaundice. Many infections pass unnoticed in children, although symptoms are more commonly seen in adults. Seroprevalence (IgG) amongst adults in tropical settings such as Bangladesh can exceed 90%. Immunity is lifelong after natural infection (and probably after immunization with modern vaccines). There is no chronic form of the disease, and severe fulminating hepatitis with liver failure, which is almost exclusively confined to adults, is extremely rare. (From Williams, R. E., Sharapov, U. M. Hepatitis A virus. In: Principles and Practice of Pediatric Infectious Diseases. 2012. © Elsevier, Pages 1180–1185.e3, Figure 237-4.)

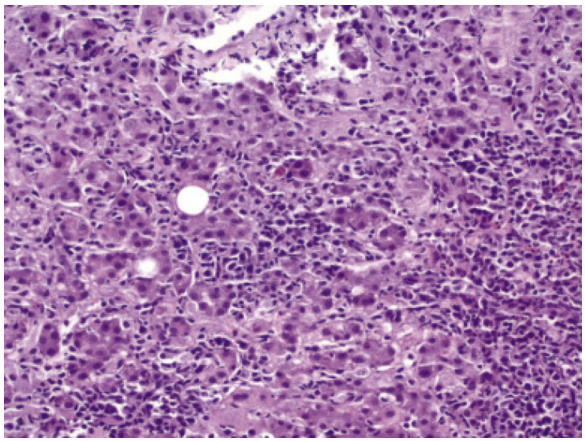


Fig. 3.9 Panlobular inflammation and lobular disarray due to hepatitis A.
Liver biopsy is rarely needed in hepatitis A, which is generally a self-limiting febrile illness readily diagnosed by serological testing (anti-HAV IgM). (From Misdraji, J. Liver and bile duct infections. In: Diagnostic Pathology of Infectious Disease. 2010, Pages 255–295, Figure 10-1.)

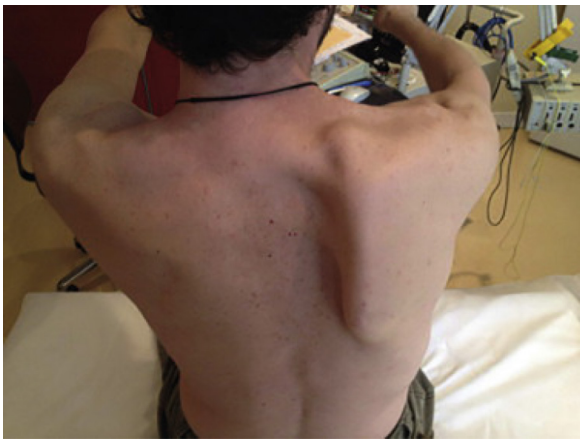


Fig. 3.10 Brachial neuritis and unilateral scapula winging in hepatitis E.
As with hepatitis A virus, transmission is via the faeco–oral route. Similarly, a significant proportion of infections are asymptomatic. However, hepatitis E differs in a number of important ways. It has a particularly dangerous course in pregnant women, amongst whom the risk of fulminating liver failure is greatly increased, and who account for the vast majority of the rare mortality associated with this infection. Neurological extra-hepatic manifestations including Guillain–Barré syndrome are increasingly recognized, as are cryoglobulinaemia and renal involvement. Amongst immunosuppressed subjects chronic carriage has (very rarely) been described. Epidemiology shows a global distribution with ingestion of undercooked pork products a clear risk factor, particularly in low endemicity countries, reflecting the reservoir in pigs in some populations. (From Deroux, A., Brion, J.P. Association between hepatitis E and neurological disorders: Two case studies and literature review. Journal of Clinical Virology, 2014, Volume 60, Issue 1, Pages 60–62, Figure 1.)

Downloaded from Vet-e-Books.com

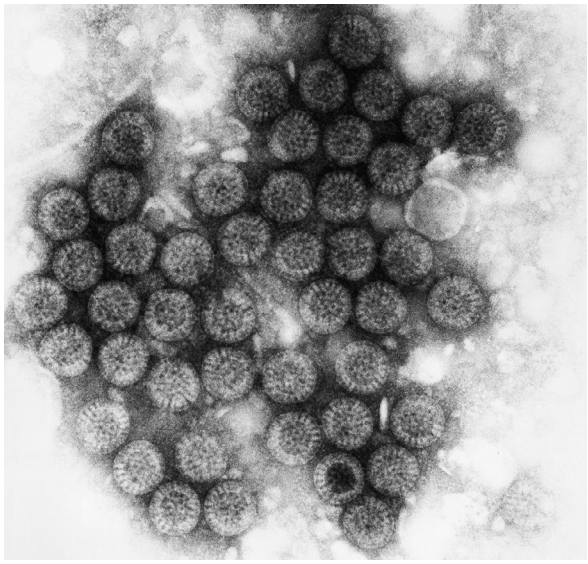


Fig. 3.11 Rotavirus.
Diarrhoea is responsible for 10% of the 5.9 million deaths of children under 5 years of age occurring in the world each year. The Global Enteric Multicenter Study (GEMS) demonstrated that rotavirus, for which effective oral vaccines are available, is the commonest cause of moderate to severe diarrhoea amongst infants in low-income countries, accounting for one-fifth of episodes. In addition to causing explosive outbreaks, there is increasing recognition that endemic norovirus is also a common cause of childhood diarrhoea. (Courtesy, Dr I. L. Chrystie.)

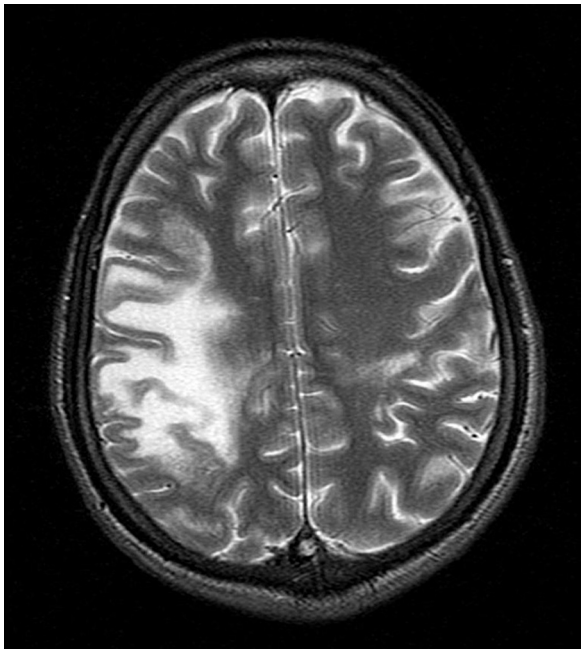


Fig. 3.12 Progressive multifocal leucoencephalopathy (PML).
This opportunistic infection was rarely seen in profoundly immunosuppressed individuals prior to the advent of the HIV pandemic. JC virus (named after John Cunningham, a patient from whom the agent was first identified in 1965) is a (probably) faceo-orally transmitted polyoma virus, also excreted in the urine. It causes a debilitating neurological disease which progresses over weeks or months, usually to death.

BACTERIAL INFECTIONS

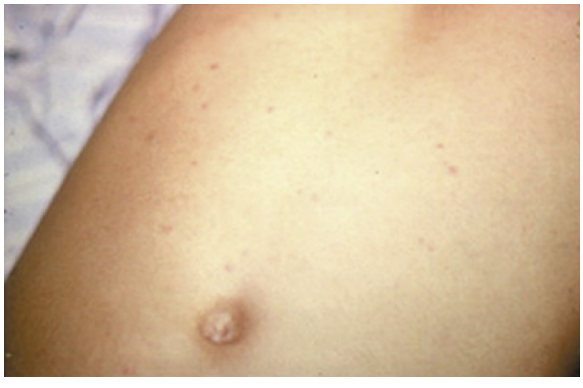


Fig. 3.13 Rose spots in enteric fever.
On dark skin these blanching maculopapular lesions, 1–4 mm in diameter and characteristically found on the trunk in enteric fever, are difficult to see. (Courtesy, C. M. Parry. From Dolecek, C. Typhoid fever and other enteric fevers. In: Infectious Diseases. 2010, Pages 1143–1147, Figure 109.3)

Downloaded From Vet-eBooks.com





Fig. 3.14 Unsafe domestic water supply, the source of an outbreak of multidrug-resistant enteric fever in Kinshasa.
Infection is acquired through ingestion of contaminated water (or food) and in endemic regions often reflects lack of access to a safe water supply. The widespread presence of *Salmonella typhi* and *Salmonella paratyphi* resistant to first-generation quinolones is a major concern in Asia, though not yet in Africa. Nevertheless, the use of traditional agents chloramphenicol, trimethoprim-sulfamethoxazole and ampicillin has become problematic with the spread of multidrug-resistant (MDR) strains carrying a single plasmid conferring resistance to all three agents. In the MDR outbreak associated with the water sources shown here, ineffective first-line therapy prolonged the illness and led to an epidemic of peritonitis, a classic 'week 3 complication'. (From Muyembe-Tamfum, J.J., Veyi, J. An outbreak of peritonitis caused by multidrug-resistant Salmonella Typhi in Kinshasa, Democratic Republic of Congo. Travel Medicine and Infectious Disease, 2009, Volume 7, Issue 1, Pages 40–43, Figure 2.)

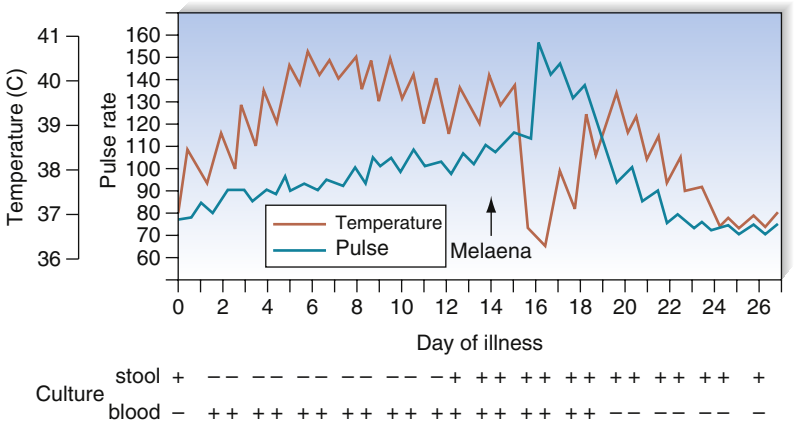


Fig. 3.15 Temperature chart in typhoid.
The fever, which often rises in a stepwise fashion, is high and accompanied by confusion and severe prostration ('typhoid state'), sometimes with a vague tickly cough. There may be a dissociation between pulse and temperature (Faget's sign, a relative bradycardia), though this is neither sensitive nor specific for the diagnosis. White cell differential count often indicates a leucopenia, and keen observers report the eosinophil count is (almost) invariably zero. Defervescence lags behind subjective clinical improvement after effective therapy is initiated, such that fever persisting for several days into treatment should not be regarded as indicative of treatment failure.

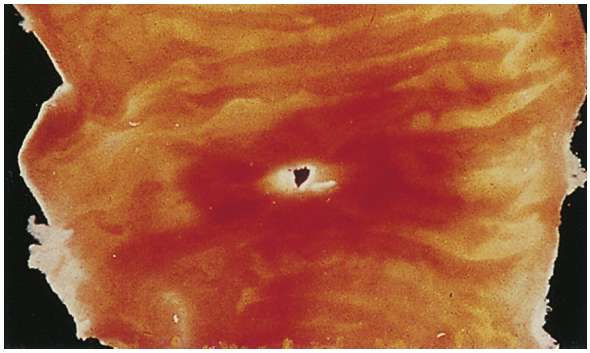


Fig. 3.16 Ulceration of Peyer's patches.
The life-threatening complications of enteric fever, gastrointestinal haemorrhage and perforation, typically arise during the third week of the illness and are due to ulceration of Peyer's patches. (Courtesy, Professor A. Bryceson.)

Downloaded from Vet-eBooks.com

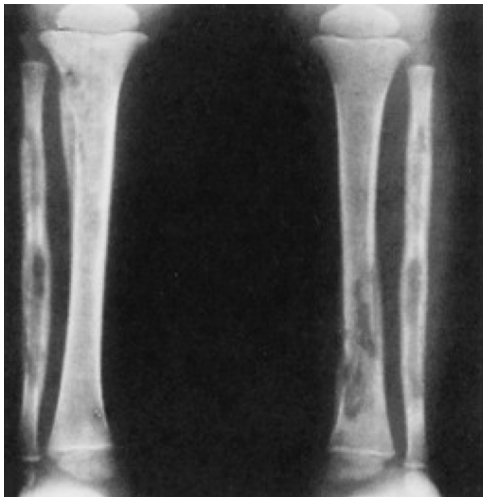


Fig. 3.17 *Salmonella* osteomyelitis of both tibias and fibulas in sickle cell anaemia.
Though *Salmonella* gastroenteritis is usually a self-limiting diarrhoeal illness (albeit unpleasant), bacteraemia with non-typhoidal salmonellae can lead to osteomyelitis, particularly in individuals with sickle cell disease. (Courtesy, Dr J. Dorst. From Old, J. Hemoglobinopathies and Thalassemias. In: Emery and Rimoin's Principles and Practice of Medical Genetics. © 2013 Elsevier. Pages 1–44. Figure 71-7.)

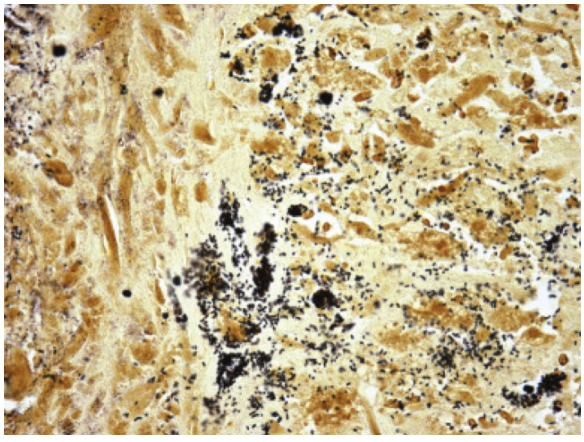


Fig. 3.18 *Salmonella* mycotic aneurysm.
Patients with HIV infection and children with severe malaria are at particular risk of secondary non-typhoidal salmonella sepsis. This is also a feature of Oroya fever (Fig. 1.77). Endovascular infection with *Salmonella* species is a rare but serious further complication. *Salmonella typhimurium* is stained black by the silver stain in this aortic anuerysmal wall. (From Aretz, H. T., Kradin, R. L. Cardiac infections. In: Diagnostic Pathology of Infectious Disease. 2010, Pages 189–213, Figure 8-23.)

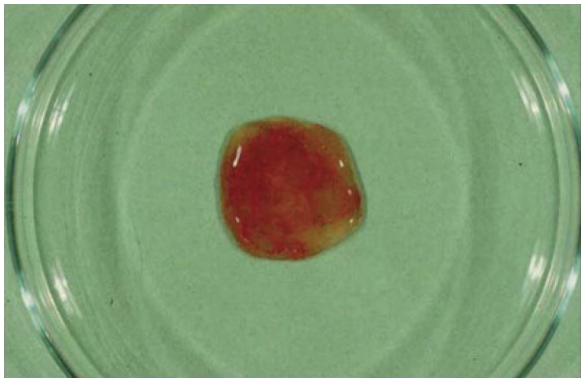


Fig. 3.19 Bloody, mucoid diarrhoea from a patient with shigellosis.
Bacillary dysentery due to shigellosis is characterized by fever, cramping abdominal pain, tenesmus and the frequent passage of small volume, bloody, mucoid stool with relatively little faecal matter. The four *Shigella* species responsible for most human infection—*Shigella dysenteriae, S. flexneri, S. sonnei* and *S. boydii*—are transmitted by the faeco–oral route and thus most frequently occur where sanitation is deficient. (From Löscher, T., Alberer, M. Clinical presentation and management of travelers' diarrhea. In: Travel Medicine. 2013, Pages 197–206, Figure 20.2.)



Fig. 3.20 Toxic megacolon due to *Shigella dysenteriae*.
The dilated loops of bowel can be clearly seen in this severely ill Bangladeshi child. In the Global Enteric Multicenter Study (GEMS) *Shigella sp.* accounted for 52% of diarrhoea in 1-year-olds and 68% in 2–5-year- olds in Bangladesh, significantly more than in any other sites. (From Keusch, G. T., Salam, M. A., Kopecko, D. J. et al. Shigellosis. In: Tropical Infectious Diseases: Principles, Pathogens and Practice. 2011, Pages 137–144, Figure 18.8.)

Downloaded From Vet-eBooks.com

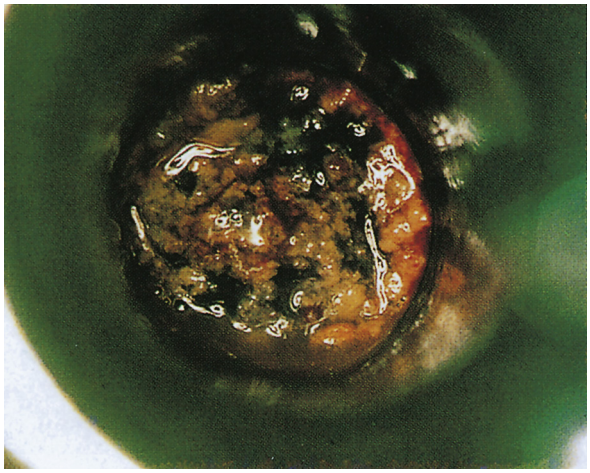


Fig. 3.21 Shigellosis affecting the sigmoid colon.
Shigella species produce an enterotoxin. The organisms affect initially the distal small intestine, causing painful cramps, fever and bloody diarrhoea. Once in the colon they multiply in the lamina propria and destroy the overlying mucosa, as seen in this sigmoidoscopic view of colonic mucosa from a fatal case of *Shigella dysenteriae* infection. (Courtesy, Professor W. E. Farrar.)

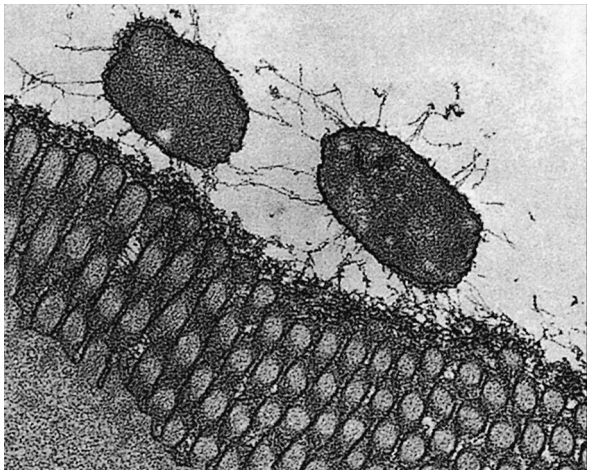


Fig. 3.22 Enterotoxigenic *Escherichia coli* adhering to the brush border of the (intact) human intestinal mucosa.
Enterotoxigenic *Escherichia coli* accounted for between 5% and 10% of moderate to severe diarrhoea in all age groups at all sites in the Global Enteric Multicenter Study (GEMS). (Courtesy, Dr S. Knutton.)



Fig. 3.23 The perils of formula milk feeding (or why 'breast is best').
Amongst the myriad advantages of breast feeding, the sterile storage, instant availability and lack of a need for immediate access to clean water for milk formula reconstitution are amongst the most important. Ill-prepared bottled formula milk, particularly if water sterility is uncertain, can present an important hazard, potentially delivering enteropathogens directly into the vulnerable gastrointestinal tract of the infant. (Courtesy, Professor R. Hendrickse.)

Downloaded from Vet-eBooks.com

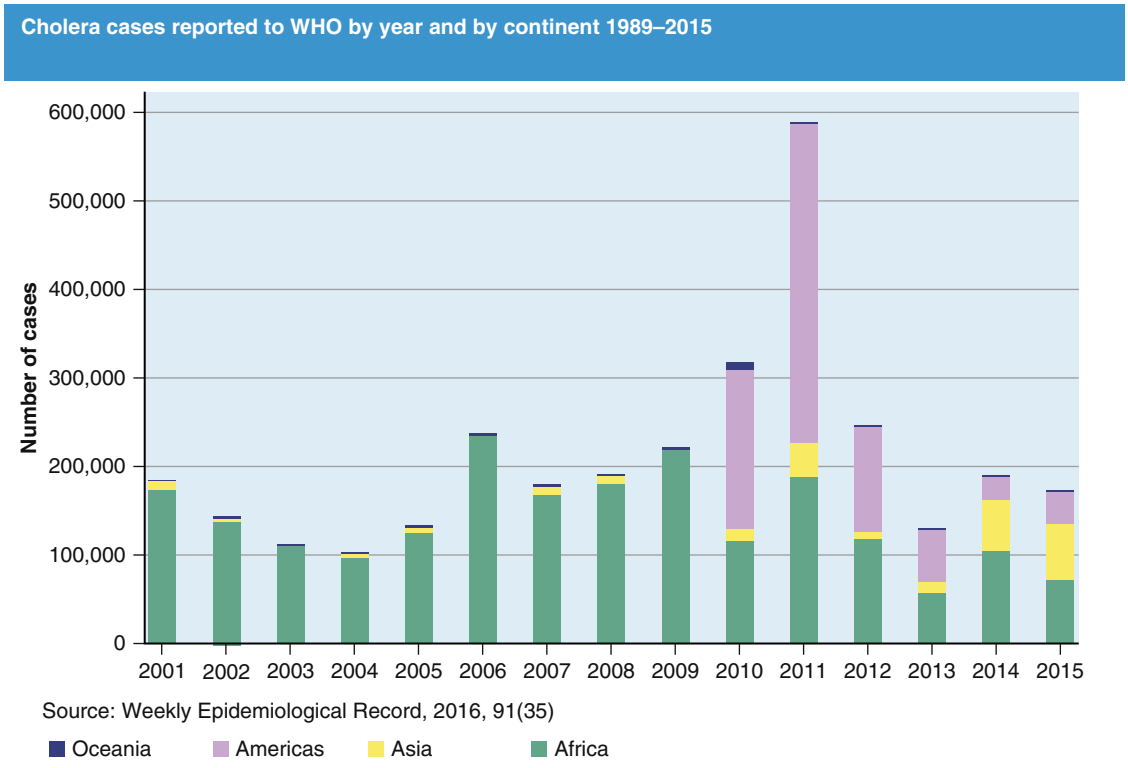


Fig. 3.24 Cholera in the 21st century.
In 2015, 172,454 cases and 1304 deaths from cholera were reported to WHO worldwide. Overall, 41% of cases were reported from Africa, 37% from Asia and 21% from the Americas. A similar number were reported from Haiti alone during the first year of the outbreak that followed in the aftermath of a devastating earthquake in 2010. (Courtesy, WHO.)



Fig. 3.25 An ancient epicentre of cholera.
Mass assemblies of pilgrims for religious activities such as that seen here on the river Ganges are an important source of epidemic cholera, as well as other waterborne infections. Symptomless carriers, who may represent 75% of those infected with the El Tor serovar, are very important in the epidemiology of this disease, as they may transport the organisms over long distances and from country to country. (Courtesy, P. Montague.)

Downloaded from Vet-eBooks.com

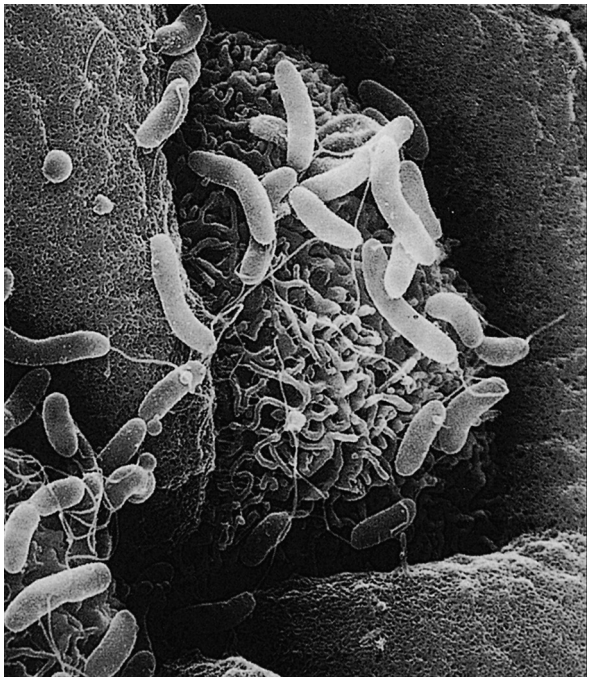


Fig. 3.26 Cholera vibrios.
Vibrios are very sensitive to an acid environment and relatively few survive in individuals with normal gastric acidity. Stored, cooked rice, milk and milk products with a high pH that become contaminated make excellent media for the multiplication of the organisms. Those vibrios that pass the stomach enter the small intestine and adhere to its luminal cells, as seen in this scanning electron micrograph. (Courtesy, Dr T. Yamamoto.)



Fig. 3.27 Choleraic facies.
Profound dehydration is being corrected initially with intravenous fluids in this patient treated for cholera by MSF at Maw Ker Refugee Camp in Thailand (1999). Typically patients with cholera have abrupt-onset torrential diarrhoea with little or no associated pain, and fever is unusual. Though only 20% of infections are symptomatic (the asymptomatic 80% have transiently detectable *Vibrio cholerae* in stool for a few days), patients with severe cholera (5% of all infections) can easily lose 20 litres in 24 hours. (Courtesy, Dr P. Du Cros.)

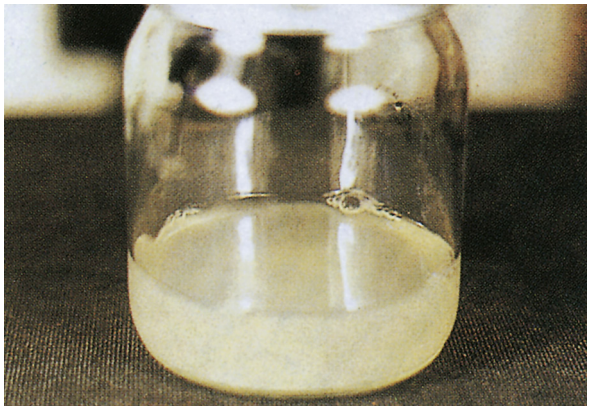


Fig. 3.28 'Rice-water' stool of cholera.
The stool has the appearance of the water left over after cooking rice and has a relatively inoffensive odour. The cholera toxin binds to the intestinal mucosa, activates adenylate cyclase and triggers a dramatic secretory diarrhoea.



Fig. 3.29 Cholera bed in a treatment ward.
A hole in the cholera bed facilitates drainage of the liquid stool into a bucket underneath. Patient comfort is improved and case management is aided as fluid losses can be more accurately monitored. (From Shirley, D-A. T., Laurens, M. B. Cholera. In: Feigin and Cherry's Textbook of Pediatric Infectious Diseases, 7th edition. Pages 1548–1555.e2, Figure 117.2. Copyright © 2014 Saunders, an imprint of Elsevier Inc.)

Downloaded From Vet-eBooks.com



Fig. 3.30 Access to clean water is fundamental in controlling a cholera outbreak.
Since faecally contaminated water is the source of almost all infections that are not spread person-to-person, the provision of safe, clean water is critical to interrupting the transmission cycle. This water, laboriously collected in Port-au-Prince, Haiti, needs to be stored carefully to avoid contamination during usage, ideally with a tap for dispensing and a lid to prevent contaminated cups being dipped into it. The use of oral cholera vaccine either pre-emptively in humanitarian emergencies or reactively early in cholera outbreaks has rapidly become part of the cholera control armamentarium, despite the logistically challenging schedule of two doses 1 week apart. (From Pure Water for the World at Peer Water Exchange. https://peerwater.org.)



Fig. 3.31 Seafood as a source of cholera infection.
Raw or improperly cooked seafood (e.g. shellfish and crabs) has been incriminated as a source of infection with El Tor cholera. Infections arose in the USA in 1991 in individuals who ate crabs such as these that were imported by travellers from Ecuador, while ceviche was implicated in the 1991 Peru outbreak. These, as well as various molluscs such as oysters, may form part of the natural cycle of some strains of *V. cholerae*, which could account in part for the transcontinental spread of the vibrios, probably in ships' ballast tanks. Other species of vibrio that may be acquired by eating raw, contaminated seafood are *Vibrio vulnificus* and especially *V. parahaemolyticus*.

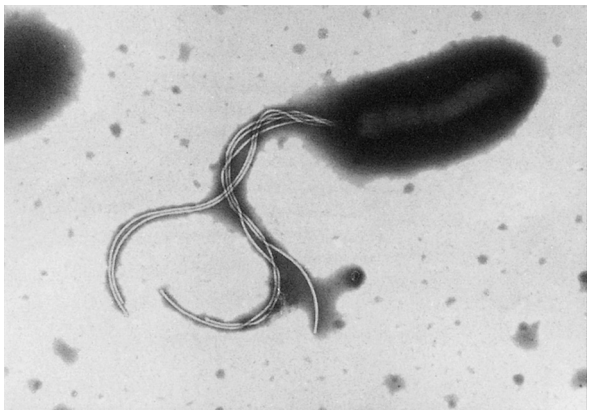


Fig. 3.32 *Helicobacter pylori*.
This microaerophilic, Gram-negative bacterium with a complex terminal flagellum is found on the mucosa of the stomach and duodenum of up to 80% of adults living in low-income countries, where the incidence increases with decreasing socioeconomic status and worsening sanitation. The prevalence is much lower in the industrialized world. *H. pylori* is associated with chronic gastritis, peptic ulceration, gastric adenocarcinoma and MALT lymphoma. (Courtesy, Dr T. B. Nutman.)

Downloaded from Vet-eBooks.com



Fig. 3.33 Enteritis necrotica (also known as clostridial necrotizing enteritis, CNE) seen at operation.
This condition, colloquially known as pigbel, is caused by toxins of *Clostridium perfringens* type C which are found abundantly in pigs intestines. Inadequate butchering, cold storage and cooking allow a large toxin load to be ingested, for example during a ceremonial pig feast. Under normal circumstances the toxin is readily neutralized by gut trypsin. However, in settings such as Papua New Guinea, trypsin activity is compromised by dietary sweet potato, which is high in anti-trypsin, and infection with *Ascaris* worms which utilize anti-trypsin for self-defence. Thus unopposed clostridial toxin activity is able to cause patchy necrosis of the small intestine. (Courtesy, Dr I. Maddocks and the Medical Learning Resources Unit, University of Papua New Guinea.)

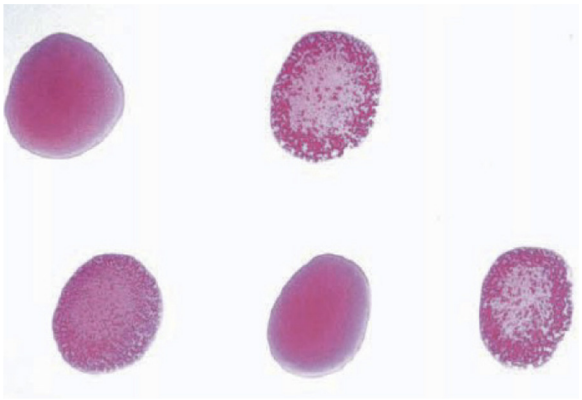


Fig. 3.34 Rose Bengal test for brucellosis.
This screening agglutination test utilizes Rose Bengal-stained *Brucella abortus* to detect antibody to *Brucella sp.* lipopolysaccharide (LPS). Brucellosis may present subacutely with an enigmatic, undifferentiated fever for several weeks or with a focal infection, most commonly of the bone. Neurological involvement, though rare, may result in a variety of clinical syndromes including acute meningoencephalitis, demyelination or spastic paraplegia.

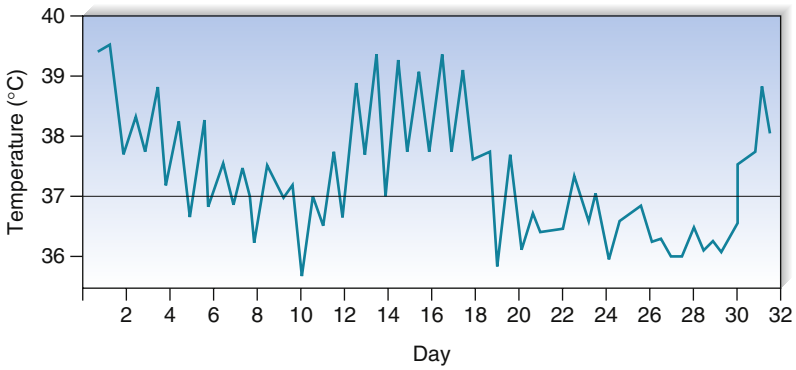


Fig. 3.35 Temperature chart in brucellosis.
The sometimes undulant nature of the fever, which gives brucellosis one of its other names (undulant fever), is evident here. This infection is acquired from the animal reservoirs—goats, sheep, cows, pigs, camels—either through ingestion of unpasteurized milk or milk products or through direct occupational contact, e.g. abbatoir workers or veterinarians. *Brucella abortus* is of lower pathogenicity than *B. melitensis*, so the disease is milder and 9 out of 10 infections are subclinical, many of which are occupationally acquired. In contrast, subclinical infection is uncommon with *B. melitensis;* acquisition by oral ingestion means that outbreaks can occur and disease can be severe. Another name previously used was Malta fever, reflecting the place of discovery of the causative agent by David Bruce and Joseph Caruana Scicluna in 1887, probably imported from the Crimea. Malta is now brucellosis-free.

Downloaded from Vet-eBooks.com



Fig. 3.36 *Brucella* spondylitis.
This sagittal T1 weighted MRI demonstrates *Brucella melitensis* spondylitis (with a confluent abscess that extended into the psoas) in a 71-year-old woman who presented with 2 months of back pain, intermittent fever and weight loss. She enjoyed drinking fresh, unpasteurized milk from a favoured farm during visits to Mexico. (From Vinetz, J. Brucella spondylitis. Journal of Clinical Microbiology, 2012, Volume 50, Issue 3, Pages 922–926, Figure 1b.)



Fig. 3.37 Subcutaneous haemorrhage due to *Streptococcus suis* sepsis.
Streptococcus suis is a part of the normal flora of the pig nasopharynx, although it is also capable of causing illness in pigs and it is an emerging human pathogen in East Asia. Purulent meningitis is the most frequently reported clinical manifestation, followed by sepsis syndrome. The custom of drinking pig's blood—*tiet canh*—in Vietnam is likely to be a relevant epidemiological exposure in this population. (Reproduced from Yu H, Jing H, Chen Z, et al: Human . Emerg Infect Dis 2006; 12: pp. 914-920, with the permission of Centers for Disease Control and Prevention.)

Downloaded from Vet-eBooks.com

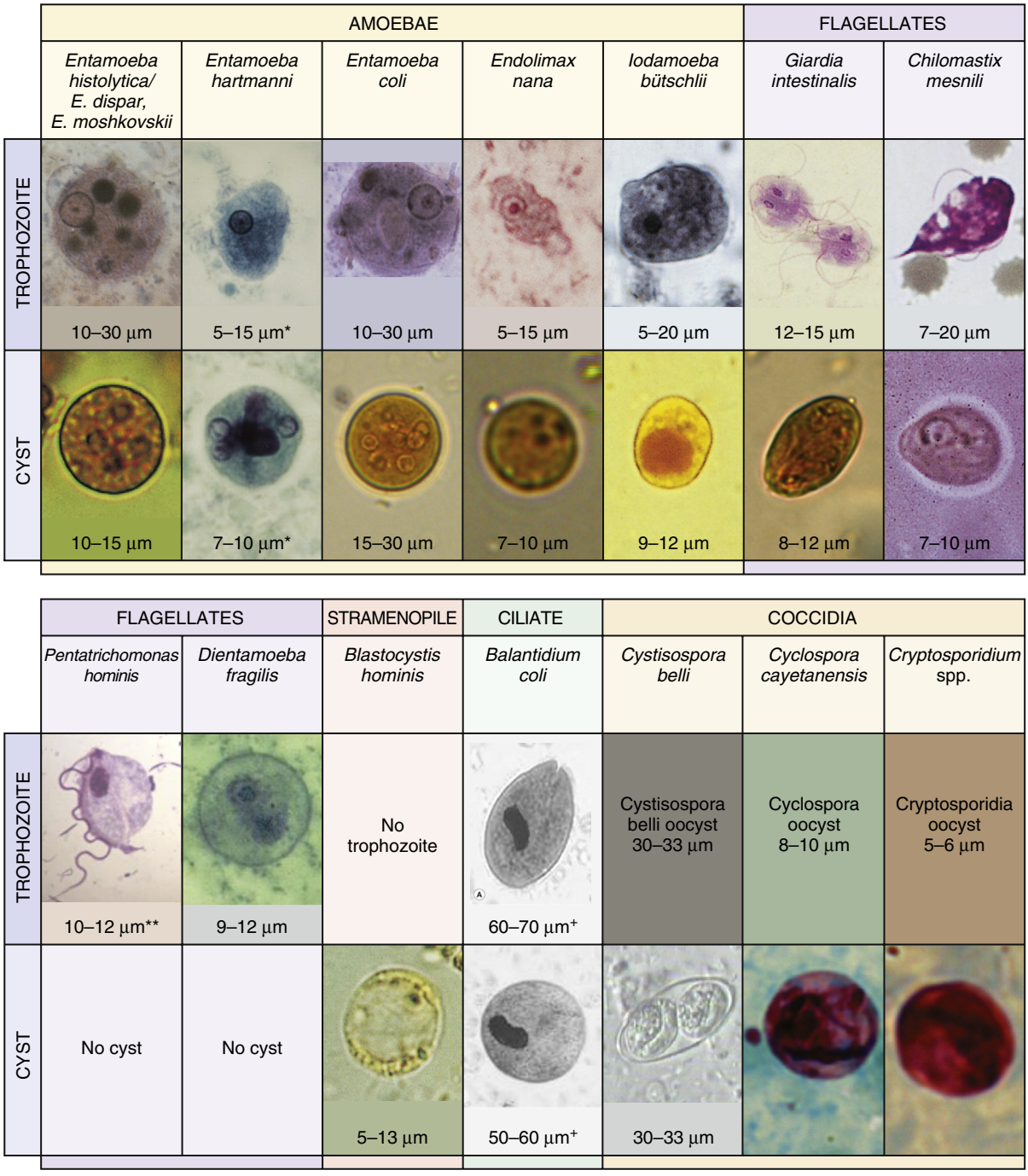


Fig. 3.38 Trophozoites and cysts of intestinal protozoa (after Ackers).

These protozoan cysts and trophozoite forms are distinguishable both by morphology and size. *Entamoeba histolytica, Giardia intestinalis, Balantidium coli, Isospora belli, Cyclospora cayetanensis, Cryptosporidium* spp. are pathogenic. It remains controversial whether *Dientamoeba* and *Blastocytis* are causative or bystander in patients with gastrointestinal disturbance. (From *Garcia, L. S. Protozoa: intestinal and urogenital amebae, flagellates and ciliates. In: Infectious Diseases. 2010, Pages 1868–1875, Figure 180.2. **Pentatrichomonas hominis: prevalence and molecular characteristization in humans, dogs and monkeys in northern China. Li WC, Ying M Gong PT et al. Parasitology Research 2016; 115 (2): 569-74. Figure 1d. +Garcia, L. S. Miscellaneous intestinal protozoa. In: Hunter's Tropical Medicine and Emerging Infectious Diseases. Pages 685–690, Figure 94-2. ++Atambay, M., Bayraktar, M.R. A rare diarrheic parasite in a liver transplant patient: Isospora belli. Transplantation Proceedings, 2007, Volume 39, Issue 5, Pages 1693–1695. Figure 2.)

Downloaded From Vet-eBooks.com

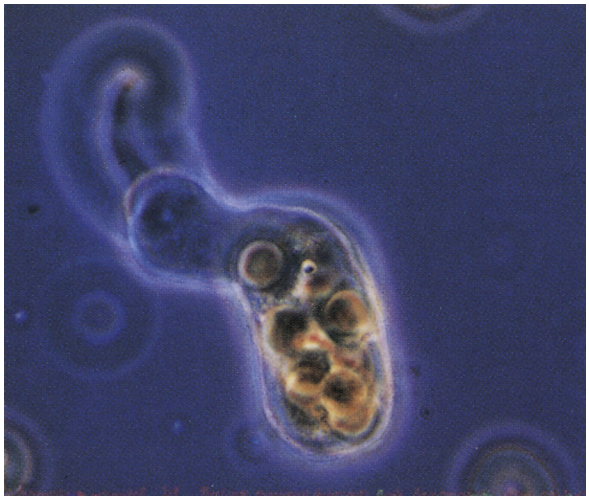


Fig. 3.39 Live *Entamoeba histolytica*.
The cysts of non-pathogenic *Entamoeba dispar* are morphologically indistinguishable from those of pathogenic *E. histolytica*, so cyst identification in a symptomatic individual may not be helpful in establishing a diagnosis. In contrast, microscopic examination of a 'hot stool' from a patient with amoebic dysentery may yield the diagnostic finding of amoebic trophozoites containing ingested erythrocytes (which does not occur with *E. dispar*). (Courtesy, Professor D. C. Warhurst.)

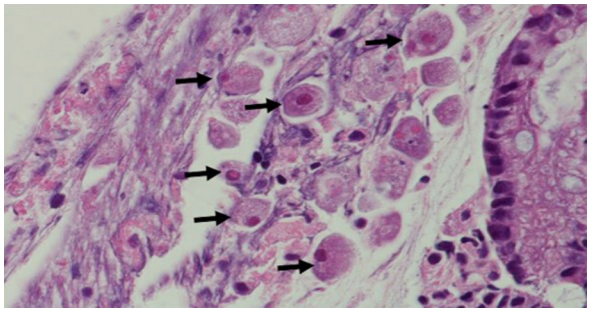


Fig. 3.40 *Entamoeba histolytica* proctocolitis.
Entamoeba histolytica can cause locally invasive disease of the large bowel (ingested erythrocytes are arrowed in the amoebic trophozoites within the wall of the rectum) resulting in amoebic dysentery (bloody diarrhoea, abdominal pain, fever). (Courtesy, Professor D. A. J. Moore.)



Fig. 3.41 Amoebic perforation and surgical resection.
Early recognition and antimicrobial treatment of amoebic dysentery results in excellent outcomes. However, delayed diagnosis can lead to local and systemic complications. This patient returned from India and developed an acute abdomen due to perforation (arrows) after an acute diarrhoeal illness. A more indolent form of chronic colitis may occasionally be misdiagnosed as inflammatory bowel disease if the possibility of amoebic disease is overlooked. Steroid therapy can be catastrophic, with subsequent disease exacerbation leading to unnecessary and avoidable bowel resection.

Downloaded From Vet-eBooks.com



Fig. 3.42 Amoebic liver abscess.
Invasion and metastatic abscess formation is the other serious complication of amoebic disease. Haematogenous ascent through the portal vein facilitates establishment of an amoebic liver abscess (ALA), more commonly in the right lobe of the liver, which is usually solitary. Though intestinal amoebic disease is equally frequent amongst men and women, the incidence of ALA is tenfold higher in men than in women. The increasing availability of ultrasound in secondary care facilities in low- and middle-income countries is helpful both diagnostically and therapeutically. Spread to lungs and (very rarely) brain may also occur. (Courtesy, Professor D. A. J. Moore.)



Fig. 3.43 Right upper-quadrant tenderness in a patient with an amoebic liver abscess.
Right hypochondrial tenderness is evident in this patient but is not always so marked.

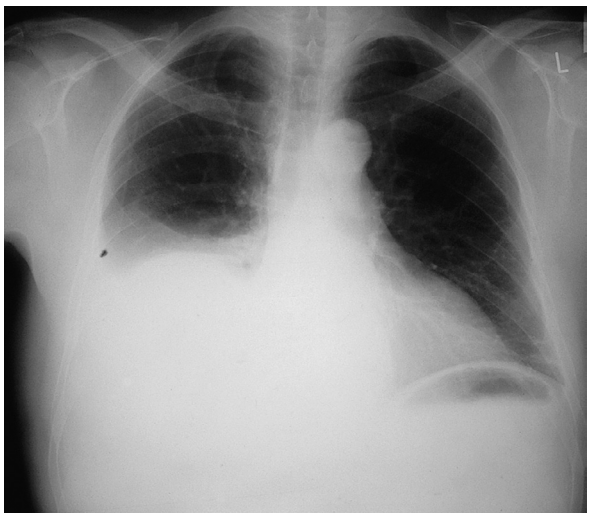


Fig. 3.44 Chest radiograph in a patient with an amoebic liver abscess.
Characteristically the right hemi-diaphragm will be elevated, sometimes with adjacent collapse. Abscess rupture with perforation through the diaphragm into the pleura or pericardium is a risk for large lesions lying close to the superior liver capsule.

Downloaded from Vet-e-Books.com



Fig. 3.45 Aspiration of amoebic liver abscess.
Medical treatment with metronidazole is highly effective for most amoebic liver abscesses (ideally followed by a luminal amoebicide such as diloxanide or paromoycin to clear intestinal cyst carriage). However, it is occasionally necessary to aspirate abscesses due to diagnostic uncertainty or because of risk of imminent rupture. The aspirated pus is described as like an 'anchovy sauce' in its grey-brown-pink appearance and, in important contrast to a pyogenic abscess, is odourless.



Fig. 3.46 Amoebiasis of the skin.
Infection of the skin might arise by direct spread or from a primary abscess. Occasionally it may complicate a sinus tract if a drain is left too long in an amoebic abscess (though a drain is rarely needed unless there has been an internal rupture). This patient was operated on erroneously for a perforated duodenal ulcer.

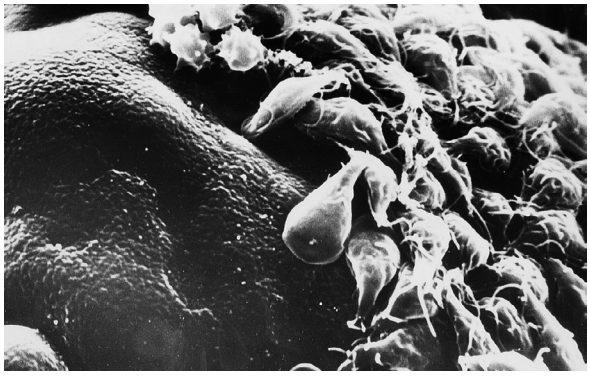


Fig. 3.47 *Giardia intestinalis* in jejunal biopsy.
Giardia intestinalis (formerly *G. lamblia*) adheres to the jejunal epithelium. It is the most frequent human intestinal protozoan parasite identified globally and may cause acute or chronic diarrhoea, the latter sometimes accompanied by significant systemic symptoms of fatigue and malaise, or indeed carriage may be asymptomatic. (Courtesy, Professor T. Harinasuta.)

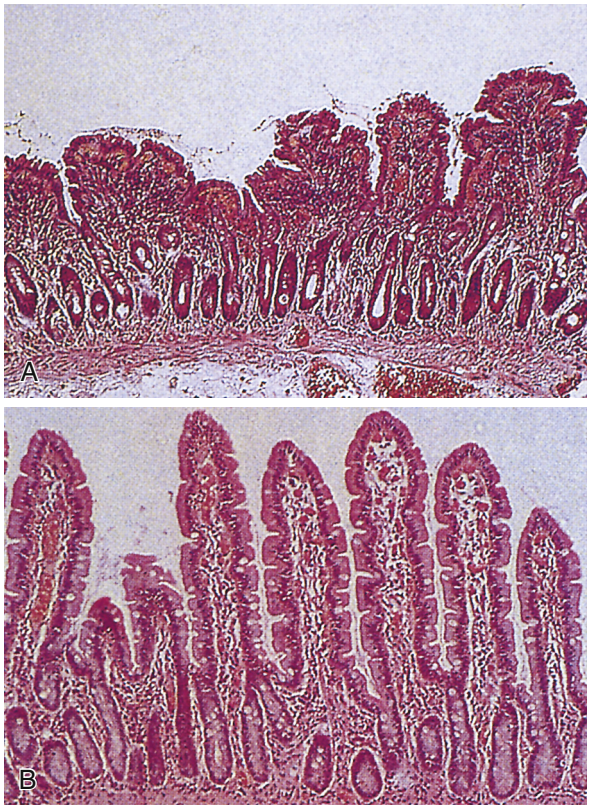


Fig. 3.48 *Giardia*-mediated partial villous atrophy.
Diarrhoea with malabsorption is characterized by bulky stools that are hard to flush away (where flush toilets are available) due to high fat content; this reflects the histopathological finding of partial villous atrophy seen in (A) as compared with normal epithelium in (B). Diagnosis by stool microscopy can be challenging due to low numbers of organisms, and so duodenal aspiration or the string test can be used to retrieve upper gastrointestinal secretions to search for *Giardia* trophozoites. In practice, empirical tinidazole or metronidazole therapy is often used as a therapeutic trial. (Courtesy, Professor S. Lucas.)

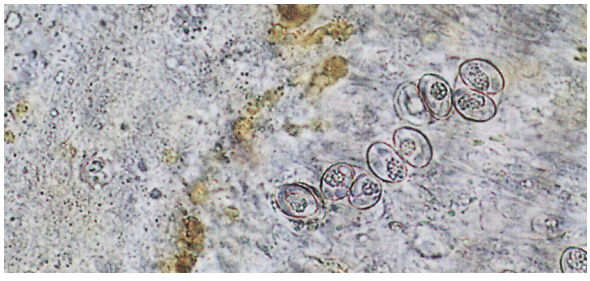


Fig. 3.49 *Sarcocystis* oocysts in intestinal epithelium.
This coccidian parasite is acquired from consumption of inadequately cooked beef. (Courtesy, Dr R. W. Ashford.)

Downloaded from Vet-eBooks.com

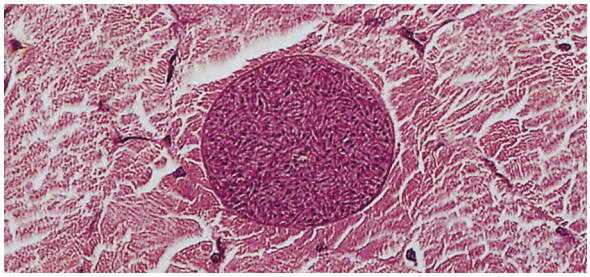


Fig. 3.50 Section of sarcocyst in human muscle.
Outbreaks of a febrile myositis syndrome amongst European travellers to a Malaysian island were reported in 2011, 2012 and 2014, although symptomatic infection is otherwise very uncommon.



Fig. 3.51 HIV-associated *Cystisospora belli* in mucosal cell of the ileum.
Coccidial infections cause significant problems for the immunocompromised patient, and HIV co-infection demonstrates this particularly well. *Cystisospora* shown here within an ileal cell in oocyst form with three sporozoites seen in section, causes chronic diarrhoea in patients with advanced HIV disease. (Courtesy, Dr P. Sarathchandra.)

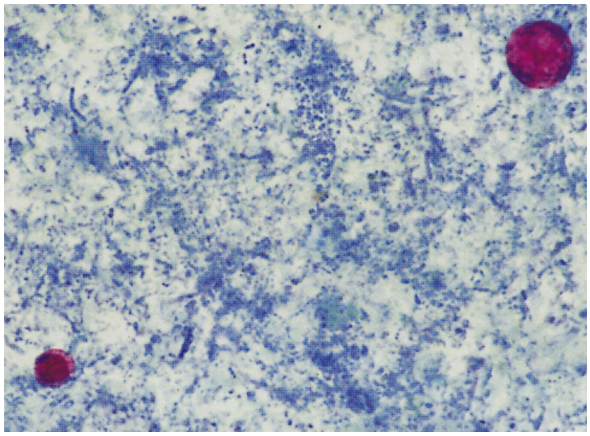


Fig. 3.52 Oocysts of *Cryptosporidium hominis* and *Cyclospora cayetanensis* compared.
Detection of these two opportunistic coccidian parasites is facilitated by Ziehl-Neelsen stain of faecal concentrates. Differentiation depends upon knowledge of cyst size range (see Fig. 3.38); *Cyclospora* is larger. *Cryptosporidium hominis*, which survives normal chlorination and filtration, is occasionally responsible for outbreaks of diarrhoeal disease due to contaminated water supplies. Illness is self-limiting in the immunocompetent but can be chronic and cause catastrophic weight loss in the immunocompromised individual. *Cyclospora*, first described at Cayetano Heredia University in Peru, causes diarrhoea and has been associated in non-endemic countries with consumption of imported soft fruits, presumably previously washed with contaminated water.

Downloaded from Vet-eBooks.com

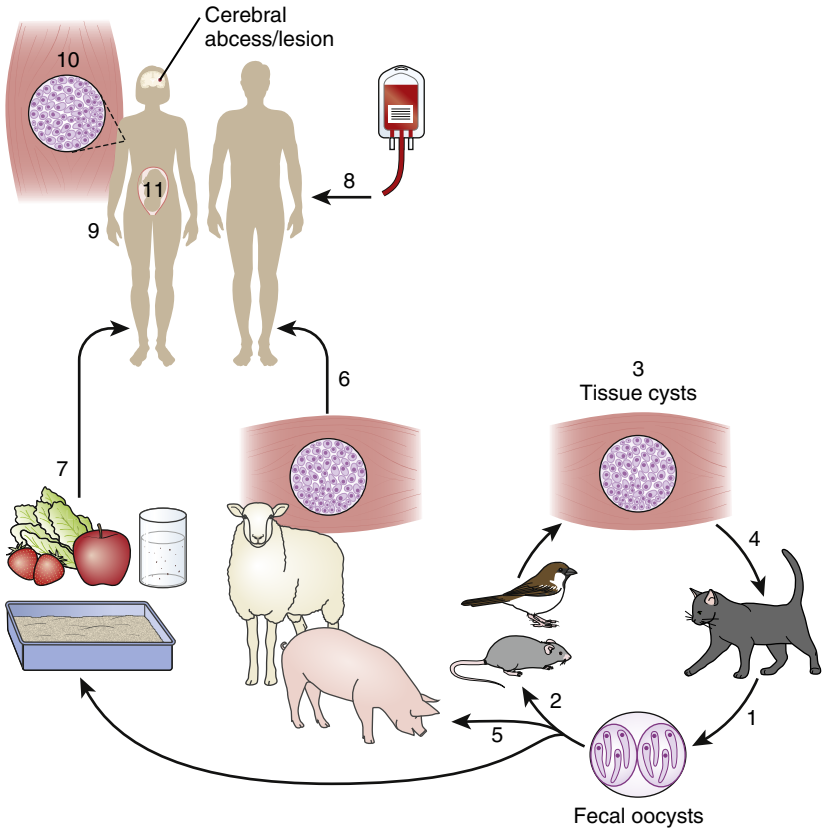


Fig. 3.53 *Toxoplasma gondii* life cycle.
Cats are the only known definitive hosts for *Toxoplasma gondii*, so for human infection, domestic cats shedding oocysts in faeces are important. After a couple of weeks of heavy faecal shedding, unsporulated oocysts take 1–5 days to sporulate in the environment and become infective. Birds and rodents ingest contaminated soil, water or plant material from which ingested oocysts quickly transform into tachyzoites. These localize in brain and muscle tissue, developing into tissue cyst bradyzoites. Cats become infected after consuming rodents and other intermediate hosts with tissue cysts. They, and food livestock animals, can also become infected through direct ingestion of sporulated oocysts from the environment. Human infection occurs through eating of undercooked meat containing cysts, consumption of food or water contaminated by cat faeces, or contact (e.g. changing a cat litter tray) with contaminated environment and inadvertent transfer from hand to mouth of cysts. In the human host the parasites form tissue cysts, most commonly in skeletal muscle, myocardium, brain and eyes; these cysts may remain throughout the life of the host. Reactivation of toxoplasmosis during immunosuppression is of particular importance in advanced HIV disease, where cerebral toxoplasma abscess formation is the most common presentation. (From CDC; https://www.cdc.gov/parasites/toxoplasmosis/biology.html)



Fig. 3.54 Hydrocephalus in congenital toxoplasmosis.
Vertical transmission may occcur and acquisition of infection during early pregnancy is associated with the congenital toxoplasmosis syndrome which can result in major neurological impairment in survivors. (Courtesy, Dr M. Dynski-Klein.)

Downloaded from Vet-eBooks.com

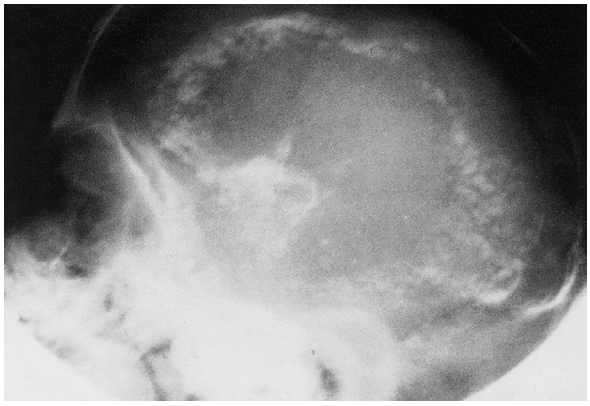


Fig. 3.55 Skull radiograph in congenital toxoplasmosis.
Subependymal and ventricular calcification are seen. (Courtesy, Dr J. Walters.)



Fig. 3.56 Fundal changes in congenital toxoplasmosis.
Congenital toxoplasmosis may produce choroidoretinitis. A necrotizing macular lesion is seen here with ectopic choroidal pigmentation. (Courtesy, Professor C. D. Forbes and Dr W. F. Jackson.)

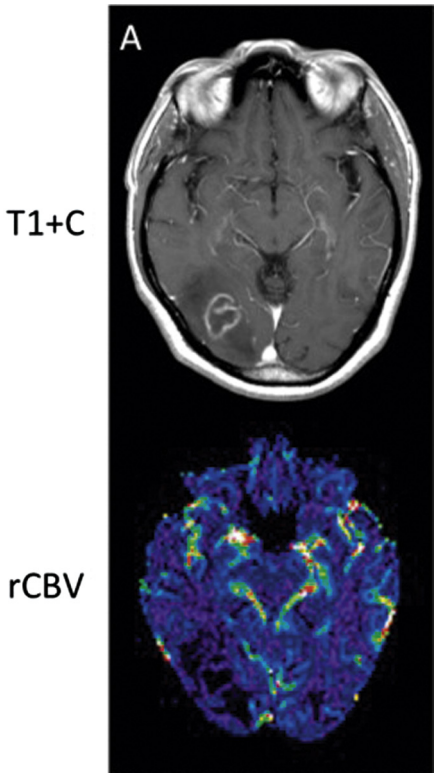


Fig. 3.57 Cerebral toxoplasmosis in HIV infection.
The typical image of a ring-enhancing cerebral toxoplasmosis lesion with surrounding oedema is seen here in the posterior temporal lobe. Though not diagnostic, toxoplasmosis is one of the few conditions in the differential diagnosis (which includes tuberculosis and lymphoma) which should respond quite quickly to empiric therapy. The imaging appearances are not always typical however. (From Dibble, E. H., Boxerman, J. L. Toxoplasmosis versus lymphoma: Cerebral lesion characterization using DSC-MRI revisited. Clinical Neurology and Neurosurgery, 2017, Volume 152, Pages 84–89, Figure 1(A).)

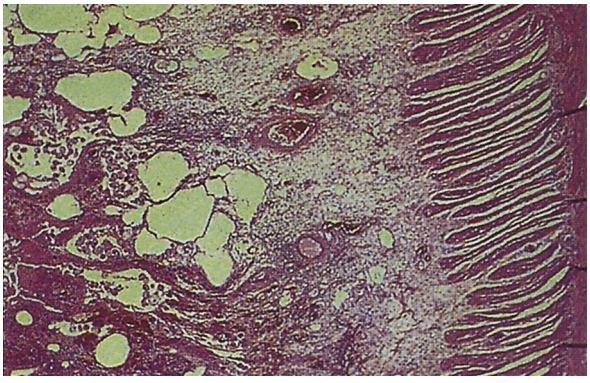


Fig. 3.58 Balantidial ileitis.
Balantidium coli is a common commensal of the large intestine of wild and domestic pigs but can (very rarely) be the cause of severe diarrrhoea in humans. In this section numerous trophozoites are invading the submucosa of the ileum.

Downloaded From Vet-eBooks.com

FUNGI

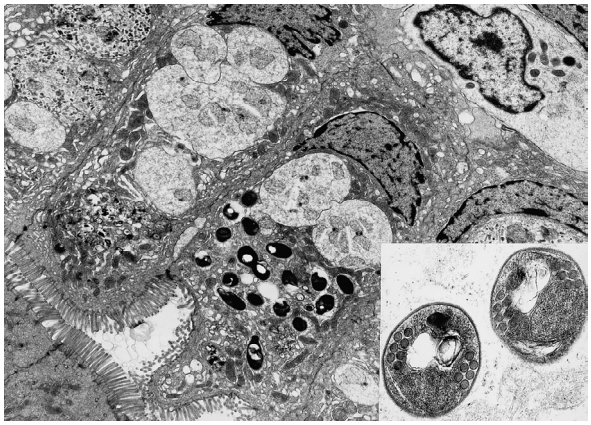


Fig. 3.59 Mature spores of *Enterocytozoon bieneusi* in human jejunal enterocyte.
Previously treated as protozoal organisms, microsporidia are now regarded as obligate intracellular parasitic fungi. Microsporidiosis in humans is largely a chronic diarrhoeal disease of individuals with advanced HIV immunosuppression, caused by *Enterocytozoon bieneusi*, *Encephalitozoon intestinalis* or *Encephalitozoon hellem*. It has also been implicated as a potential aetiology of sclerosing cholangitis in this group of patients. Diagnosis is largely clinical and specific treatment options are severely limited. Antiretroviral therapy with restoration of immune function is the most effective management approach. (Courtesy, G. Tovey.)

HELMINTH INFECTIONS

Nematodes

Enterobiasis



Fig. 3.60 *Enterobius vermicularis* visible at colonoscopy.
Adult worms (also called threadworms or pinworms) are small and threadlike. Males measure 2.5 mm in length whilst females measure 10 mm. They live in the colon, emerging onto the perianal region to lay eggs and then die. (From Ackroyd, R. Endoscopic image of a threadworm. In: Diseases of the gastrointestinal system. Medicine & Surgery. An integrated text book. Chapter 4, Pages 229–297, Figure 4.18.)



Fig. 3.61 Ovum of *Enterobius vermicularis*.
Eggs measure 60 µm by 30 µm and are oval in shape with one slightly flattened side. They are deposited perianally where they cause intense pruritis. Eggs are directly infectious to humans on ingestion; autoinfection is common, particularly in children with poor hygiene. (Courtesy, H. Edwards.)

Downloaded from Vet-eBooks.com

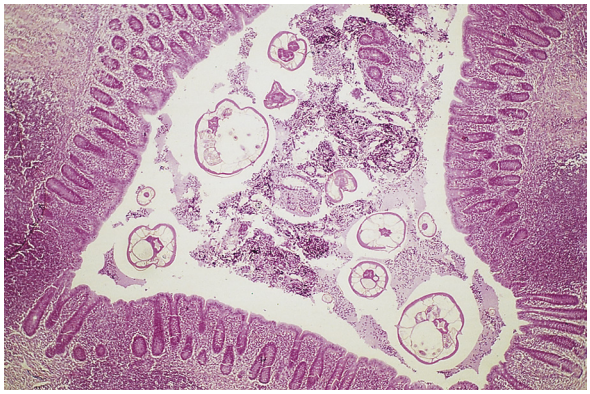


Fig. 3.62 Adult pinworms in appendix.
Worms are occasionally found in the appendix but their role as a cause of acute appendicitis is uncertain. Sections of several adult worms are seen here. (H&E x 13.)

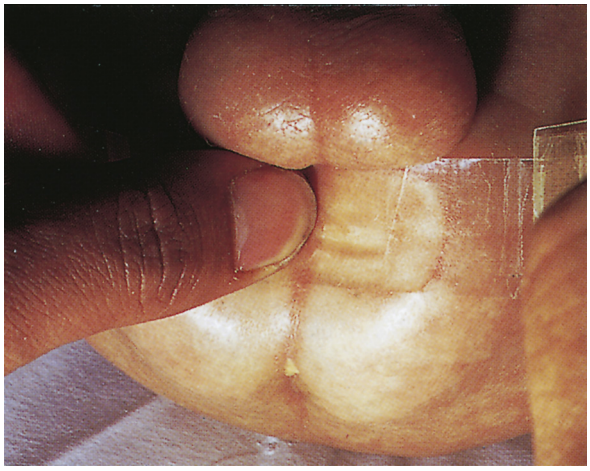


Fig. 3.63 Sellotape test to demonstrate perianal eggs.
The sellotape test is still a common way to diagnose infection. Sellotape is placed on the perianal skin first thing in the morning. Gloves should be worn, as eggs are infectious. (Courtesy, Dr B. Heyworth.)



Fig. 3.64 Sellotape test to demonstrate perianal eggs.
The tape is then removed and stuck to a glass slide which is examined for eggs of *E. vermicularis*. Gloves should be worn to avoid risk of infection acquisition.

Downloaded from Vet-eBooks.com

Ascariasis

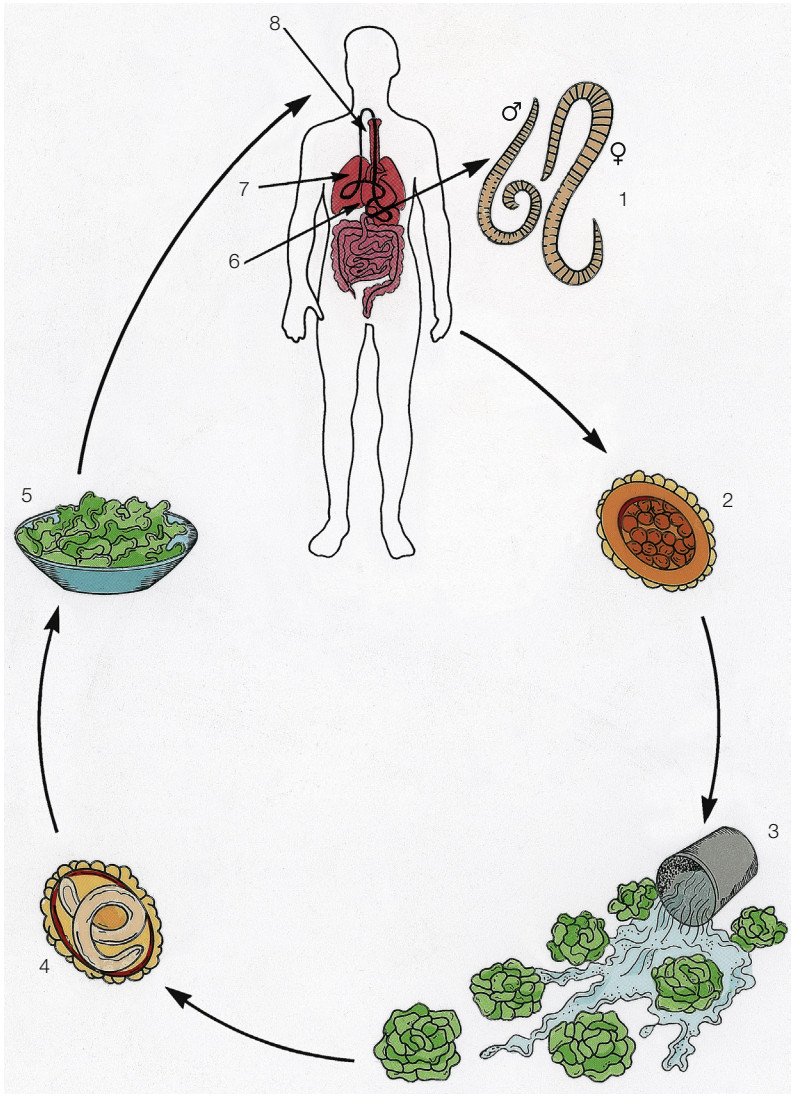


Fig. 3.65 Life cycle of *Ascaris lumbricoides*, the roundworm.
Adult worms (1) live in the small intestine where they lay large numbers of eggs (2). Unfertilized eggs are passed in the stool and can readily contaminate vegetables, for example, when night soil (3) is used as fertilizer. Depending on environmental conditions, eggs require at least 18 days in the soil to embryonate and become infective (4). When swallowed (5), the larvae hatch in the duodenum and penetrate the mucosa (6). They are carried through the circulation to the lungs (7) where they grow, moulting twice before escaping from the capillaries into the alveoli. Larvae migrate up the bronchial tree, are swallowed (8), and pass to the small intestine where they grow to adulthood.



Fig. 3.66 Adult *Ascaris lumbricoides*.
Adult males are 15–30 cm long and may have a curled tail. Females are 20–35 cm long with a straight tail.

Downloaded From Vet-eBooks.com

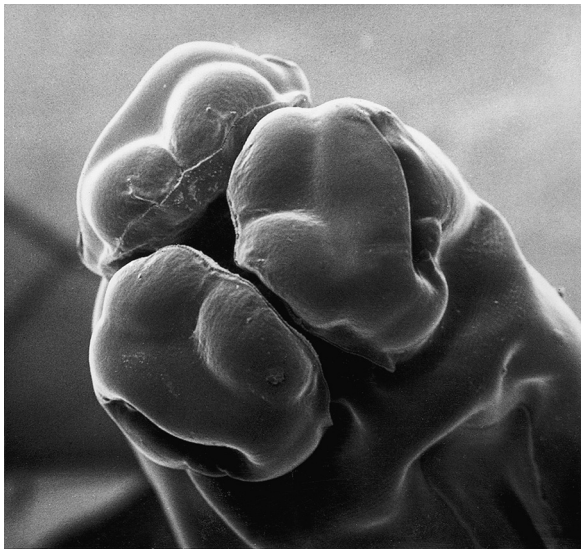


Fig. 3.67 Head of adult.
Note the three lips typical of *Ascaris* visible on this electron micrograph. (x 110.) (Courtesy, Dr B. E. Matthews.)

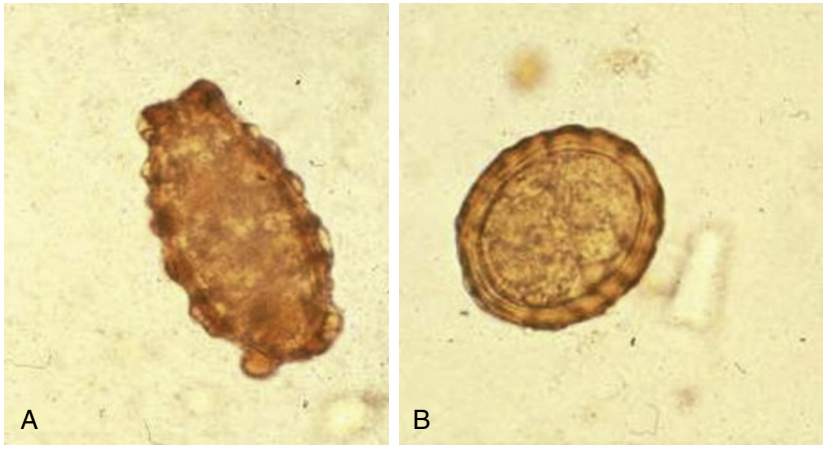


Fig. 3.68 Unfertilized and fertilized egg of *Ascaris lumbricoides*.
The unfertilized ovum (A) measures up to 90 μm in length and is an elongated oval shape containing multiple refractile granules. The shell is thin with an external layer, which varies from smooth to quite knobbly (mammillated). The fertilized ovum (B) is round or oval measuring up to 75 μm in length with a thick shell and external mammillated layer. It contains a visible embryo or developing larva. (Courtesy, H. Edwards.)



Fig. 3.69 Ecology of infection with *Ascaris* and *Trichuris*.
The use of fresh nightsoil (human faeces) to fertilize green-leaf vegetables, which are then eaten without adequate washing, is a sure way to maintain the transmission cycle of these roundworms. Their prevalence in a community is a good indicator of standards of personal hygiene and sanitation. Since their eggs can survive even in a cold climate, distribution is global.

Downloaded from Vet-eBooks.com



Fig. 3.70 Second-stage larva of *Ascaris lumbricoides* hatching in gut.
The first-stage larva undergoes one moult within the egg and hatches when the egg reaches the jejunum. (x 380.)

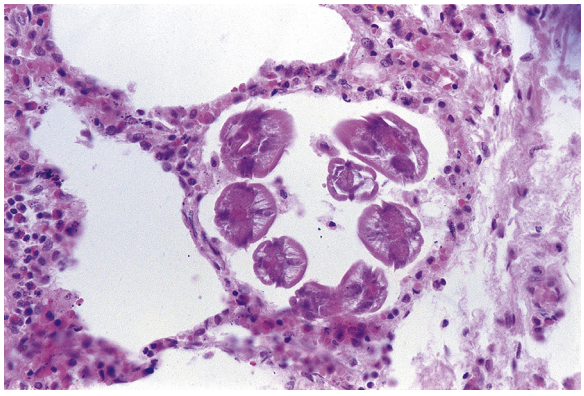


Fig. 3.71 Transverse sections of *Ascaris lumbricoides* larvae in the pulmonary alveoli.
This post-mortem specimen shows transverse sections of larvae migrating through the lungs with eosinophilic infiltration of the alveolar walls. (H&E x 300.) (Courtesy, Dr A. M. de Oliviera Ramos.)



Fig. 3.72 Loeffler's syndrome.
Passage of larvae through the lungs may result in dry cough, dyspnoea and haemoptysis, also known as Loeffler's syndrome. This may occur in any nematode infection where larvae pass through the lungs including hookworm and *Strongyloides*. Characteristically, the radiographic appearances are of patchy transient infiltrates that clear spontaneously within a month. (From Müller, N. L., Fraser, R. S., Colman, N. C., et al. Radiologic Diagnosis of Diseases of the Chest. Philadelphia, WB Saunders, 2001.)



Fig. 3.73 A bolus of *Ascaris* expelled from a child with heavy infection following anthelminthic treatment.
Although most infections are asymptomatic, some people experience abdominal pain, diarrhoea and other gastrointestinal symptoms. Rarely, heavy infection may be complicated by intestinal obstruction. (Courtesy, Professor B. Ochoa.)

Downloaded From Vet-eBooks.com



Fig. 3.74 Adult roundworms migrating in liver.
The adult worms have a marked tendency to penetrate any available hole in their vicinity and may escape through abdominal fistulae during operation. Occasionally they emerge from the mouth or nose or obstruct the biliary or pancreatic ducts. (Courtesy, Professor B. Ochoa.)

Trichuriasis

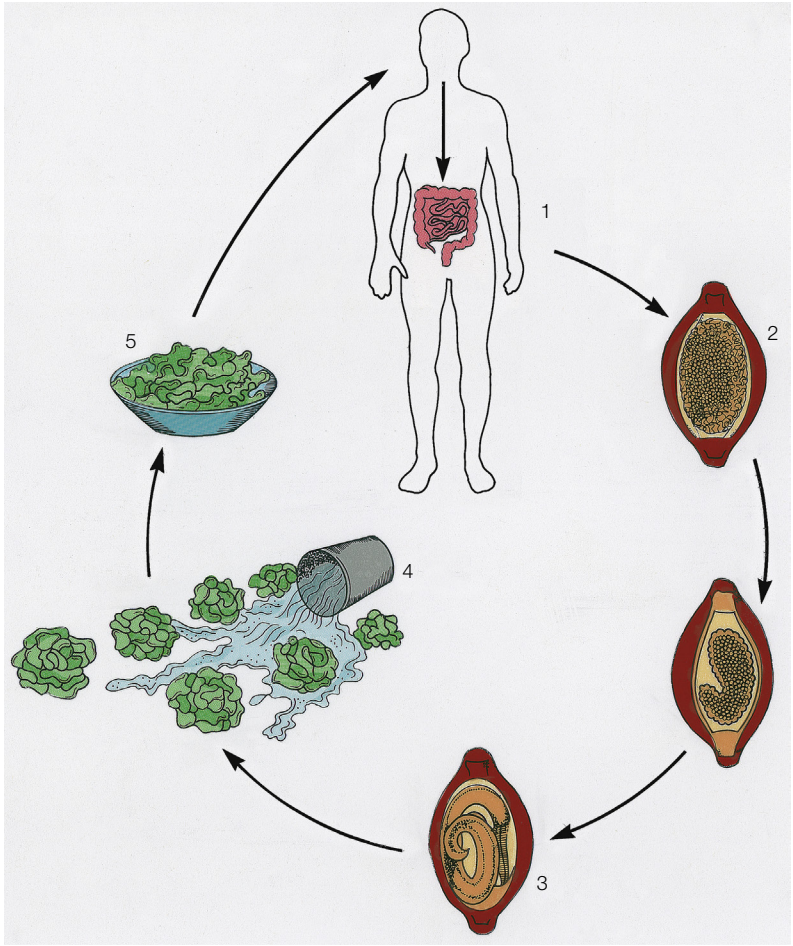


Fig. 3.75 Life cycle of *Trichuris trichiura* (whipworm).
Adults inhabit the caecum (1) and ascending colon where they are attached to the mucosa. Unembryonated eggs are passed in stool (2) and mature in the soil to larvae over 15–30 days (3). Eggs can readily contaminate vegetables (4) and are then swallowed in unwashed food (5). The eggs hatch in the small intestine and the developing larvae pass directly to their attachment sites. Females commence egg-laying after 3 months and each adult lives around 1 year.

Downloaded from Vet-eBooks.com



Fig. 3.76 Adult morphology of *Trichuris trichiura*.
Adult worms are 3–5 cm long with the females being slightly larger. Here, a male worm is seen in the centre, identified by his coiled posterior end. He is surrounded by female worms with straight posterior ends. The whip-like anterior portion becomes entwined in the mucosa and anchors the worm in place. (x 2.) (Courtesy, The Director, Armed Forces Institute of Pathology, Washington.)

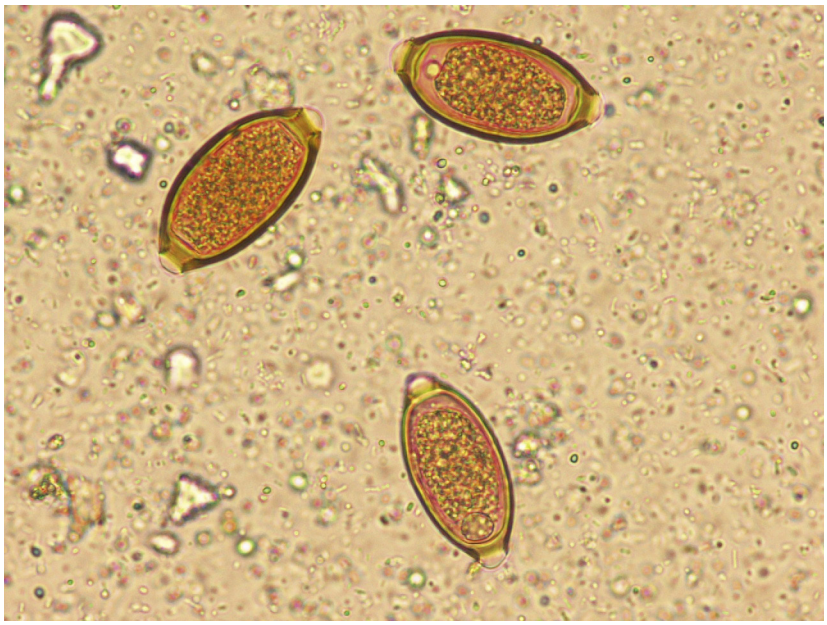


Fig. 3.77 Ova of *Trichuris trichiura*.
Ova measure around 55 μm x 20 μm and have a thick shell. They are barrel shaped with a distinctive pair of polar plugs at each end. (Courtesy, H. Edwards.)

Downloaded From Vet-eBooks.com

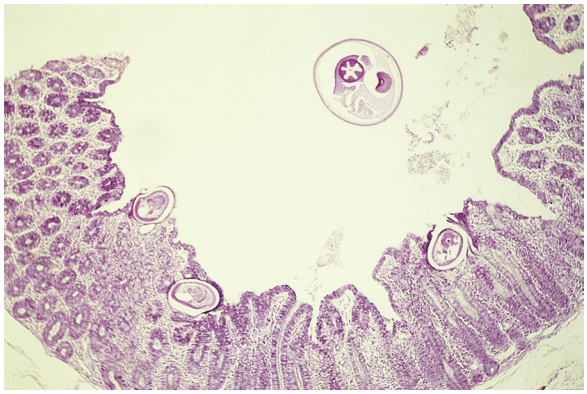


Fig. 3.78 Cross-section of *Trichuris trichiura* associated with caecal tissue.
Note the slender anterior ends of *T. trichiura* embedded in the mucosa and the cross section of an adult worm hanging in the lumen of the caecum.



Fig. 3.79 Rectal prolapse in a child with *Trichuris trichiura*.
Although most infections are asymptomatic, heavy infection may result in rectal prolapse in children. (Courtesy, Dr F. Beltran.)

Anisakiasis

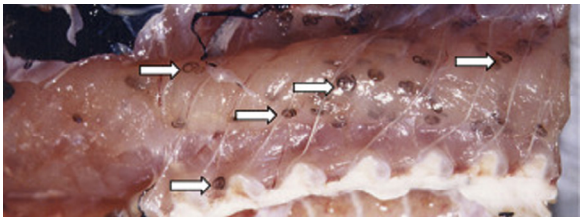


Fig. 3.80 Third larval stage of *Anisakis simplex* in a hake fillet.
Anisakiasis is the marine mammal equivalent of Ascariasis. Adult worms live embedded in the stomach mucosa of large marine mammals such as seals and dolphins. Eggs are passed in the stool which become first- then second-stage larvae. When ingested by crustaceans, the second-stage larvae migrate to muscle tissue. When these are eaten by fish, third-stage larvae develop in the muscles, as seen here (arrows). These are infectious to marine mammals but also to humans if raw fish is consumed. (From Audicana, M. T., Kennedy, M. W. *Anisakis simplex*: from obscure infectious worm to inducer of immune hypersensitivity. Clinical Microbiology Reviews 2008, Volume 21, Pages 360–379, Figure 2. Reprinted with permission.)

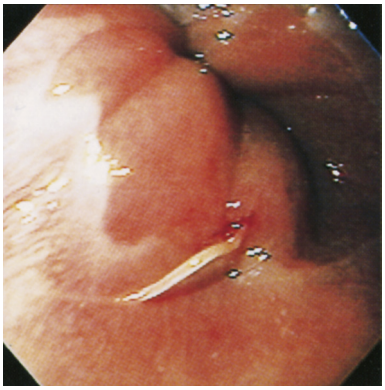


Fig. 3.81 Third-stage larva of *Anisakis simplex*.
Anisakiasis is particularly common in Japan due to consumption of raw fish as sushi or sashimi. Raw fish is rendered non-infectious by freezing to -20°C for 72 hours. Gastric anisakiasis occurs when the larva attaches to the stomach as seen on endoscopy in this Japanese woman. Abdominal pain and vomiting occur around 6 hours after ingestion of larvae. Removal of the worm endoscopically may give symptomatic relief. (Courtesy, Dr I. Sato.)

Downloaded from Vet-eBooks.com

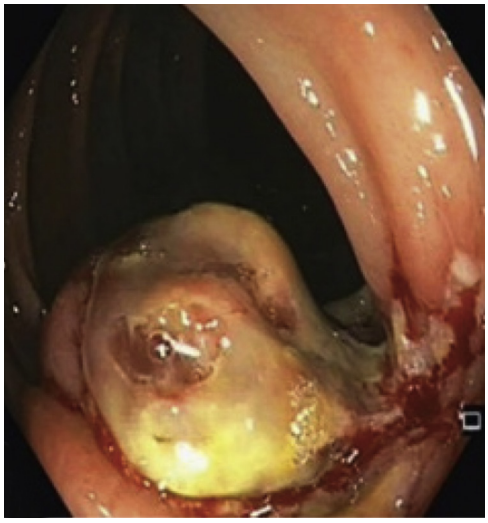


Fig. 3.82 Colonic anisakiasis.
Intestinal and colonic anisakiasis occur one or more weeks after larval ingestion and cause symptoms of abdominal pain and distension. This patient presented with an intussusception and was found to have a 5 cm polypoid lesion in the ascending colon surrounding an *Anisakis simplex* larva. (From Andrisani, G., Spada, C., Petruzziello, L. et al. An unusual colonic tumour. Digestive and Liver Disease, Volume 46, Issue 5, Pages 477–478, Figure 1, Panel A.)



Fig. 3.83 Morphology of third-stage larva of *Anisakis* species.
Anisakis larva have three bilobed lips and a boring tooth, seen here, which allow the larva to burrow into the host mucosa. (From Murata, R., Suzuki, J., Sadamasu, K., et al. Morphological and molecular characterization of Anisakis larva. Parasitology International, Volume 60, Issue 2, Pages 193–198, Figure 1, panel 1a.)

Capillariasis



Fig. 3.84 Koi pla, raw fish salad eaten in Laos PDR and Thailand.
The definitive host of *Capillaria philippinensis* are fish eating birds. Fish, the intermediate hosts, ingest eggs in fresh water, and larvae migrate to muscle tissues. Most human infection are seen in South East Asia where outbreaks may occur following ingestion of raw or undercooked fish, such as in this dish koi pla. In this region, undercooked fish may also lead to infection with the oriental liver fluke, *Opisthorchis viverrini*. (From Grundy-Warr, C., Andrews, R., Sithithaworn, P., et al. Raw attitudes, wetland cultures, lifecycles: Socio-cultural dynamics relating to *Opisthorchis viverrini* in the Mekong Basin. Parasitology International, 2012-03-01, Volume 61, Issue 1, Pages 65–70, Figure 2.)

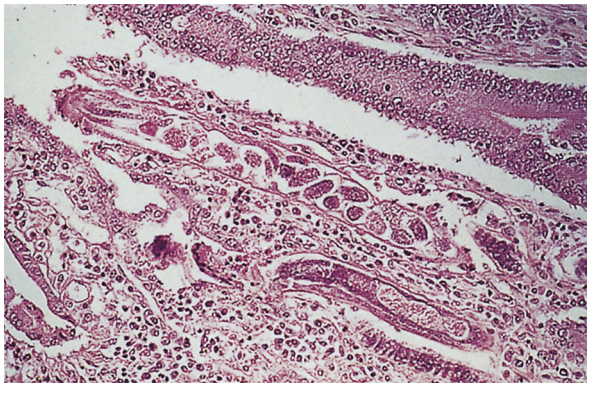


Fig. 3.85 *Capillaria philippinensis* invading the small intestine.
Like *Strongyloides*, *C. philippinensis* can autoinfect its human host, resulting in very high parasite loads. Symptoms include severe watery diarrhoea, abdominal pain and eosinophilia. Malabsorption may occur resulting in cachexia and even death. (H&E x 150.) (Courtesy, Dr J. C. Crook.)

Downloaded From Vet-e-Books.com



Fig. 3.86 Female *Capillaria philippinensis* from human faeces. Eggs and larvae may be found in the stool of infected people. Note the typical eggs seen in the vulval region of this female adult worm. (x 300.)

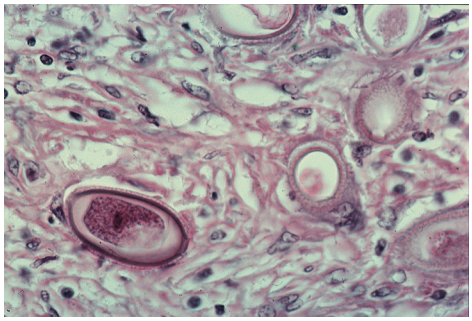


Fig. 3.87 *Capillaria hepatica* in a liver section. *Capillaria hepatica* principally affects rodents, dogs and other mammals, but human infection occasionally occurs. Eggs are ingested in contaminated food or water and larvae released in the small bowel. They migrate to the liver, mature into adults and deposit eggs in the liver parenchyma. Although the immune system destroys the adult worms, the eggs remain viable. In the animal host, these eggs remain in the liver until the animal dies when the eggs are released into the environment or ingested by a predator. In humans the eggs may provoke an inflammatory reaction resulting in hepatomegaly, hepatitis and eosinophilia. Note the egg visible in this section from liver biopsy. It measures 60 x 30 μm with a striated shell and shallow polar prominences. (Courtesy, Professor S. Lucas.)

Downloaded from Vet-eBooks.com

Trichinellosis

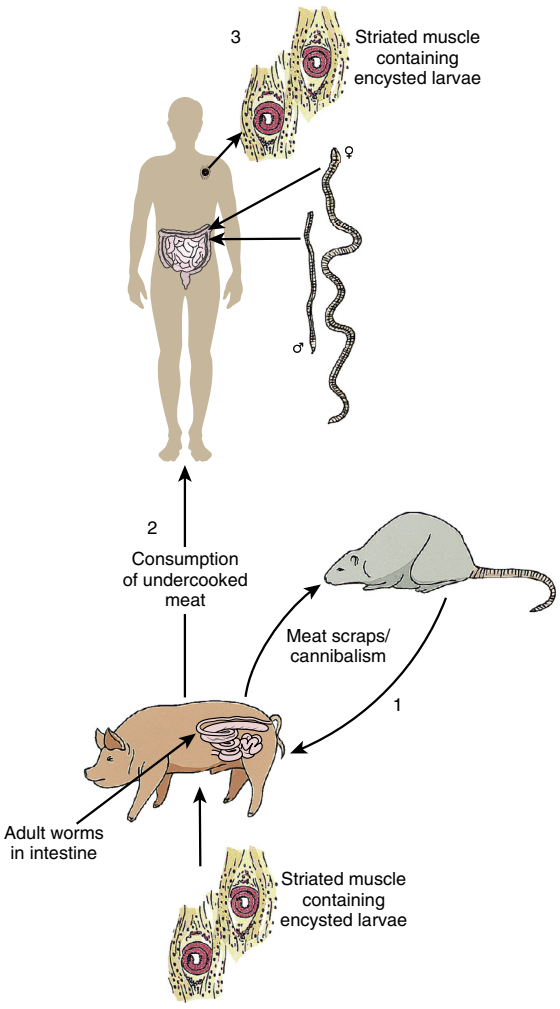


Fig. 3.88 Life cycle of *Trichinella spiralis*.
There are nine species of *Trichinella* occuring in various ecosystems worldwide. The commonest, *T. spiralis*, is found in a variety of omnivores and carnivores, including rats and pigs. Unusually, the vertebrate host acts as both a definitive and intermediate host; the adult worms live within the intestine whilst the larvae encyst in striated muscle (1). However, larvae cannot develop into adults within a single host, requiring a second host to reach maturity. Humans become infected by eating undercooked pork containing encysted larvae (2). Larvae are released in the small intestine and develop into adult worms in the mucosa of the small bowel. These survive for around 1 month. Females produce larvae which migrate to, and encyst in, striated muscle, eventually becoming calcified (3).



Fig. 3.89 Wild reservoir of trichinellosis.
A common reservoir of infection is the wild pig, such as the African bush pig seen here.



Fig. 3.90 Adult female *Trichinella spiralis*.
The adult female worm is 2–3 mm long and 90 μm in diameter; the male 1–2 mm by 60 μm. Adult worms survive in the small bowel for around 1 month. Females produce larvae after 1 week. (x 45.)

Downloaded From Vet-eBooks.com

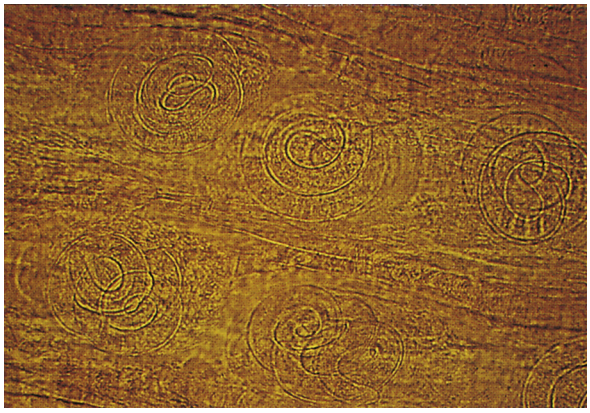


Fig. 3.91 *Trichinella spiralis* larvae in crush preparation.
Here, larvae are seen in a muscle biopsy compressed between two glass slides. The sensitivity of biopsy is highest if taken from symptomatic muscles near a tendinous insertion. (x 175.)

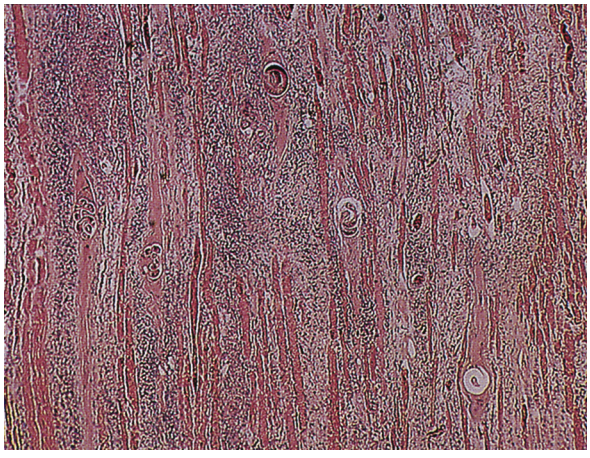


Fig. 3.92 Larvae in muscle from a fatal human case.
Although many infections are asymptomatic or mild, heavy infections may lead to fatal myocarditis or encephalitis. Encysted larvae are found in the muscles at biopsy (or post-mortem). Calcification of the encysted larvae occurs at around 18 months and may be detected by radiograph, but the encysted larvae remain alive for years. (H&E x16.)





Fig. 3.93 Patient with acute trichinellosis.
In the first week of infection, patients may develop nausea, diarrhoea and abdominal pain as the larvae excyst and enter the intestinal mucosa. The cardinal clinical signs of trichinellosis — myalgia, periorbital oedema and eosinophilia—occur as the larvae invade muscle. This patient has marked periorbital odema with conjunctival haemorrhages. (From Shandro, J. R., Jauregui, J. M. Wilderness-Acquired Zoonoses. Auerbach's Wilderness Medicine. 7th edition. 2017, Pages 692-728. Figure 34-44. Copyright © 2017 Elsevier, Inc. All rights reserved. From Centers for Disease Control and Prevention Public Health Image Library. Courtesy Dr. Thomas Sellers, Emory University.)



Fig. 3.94 Splinter haemorrhages.
Nail bed haemorrhages may be visible in acute trichinellosis. (Courtesy, Professor W. E. Farrar.)

Fig. 3.95 Polar bear, host of *Trichinella nativa*.
Although *T. spiralis* is the commonest cause of trichinellosis worldwide, a number of other species exist in particular habitats. *T. nativa* infects bears, foxes and walruses in arctic areas. Outbreaks occur where native communities ingest undercooked polar bear meat. Consumption of polar bear liver may also lead to vitamin A toxicity. (From Freer, L. Bear behaviour and attacks. Auerbach's Wilderness Medicine. 7th edition. 2017, Pages 674–686, Figure 32.2. Copyright © 2017 Elsevier, Inc. All rights reserved. Courtesy, S.D. Evans.)

Downloaded From Vet-eBooks.com

Toxocariasis

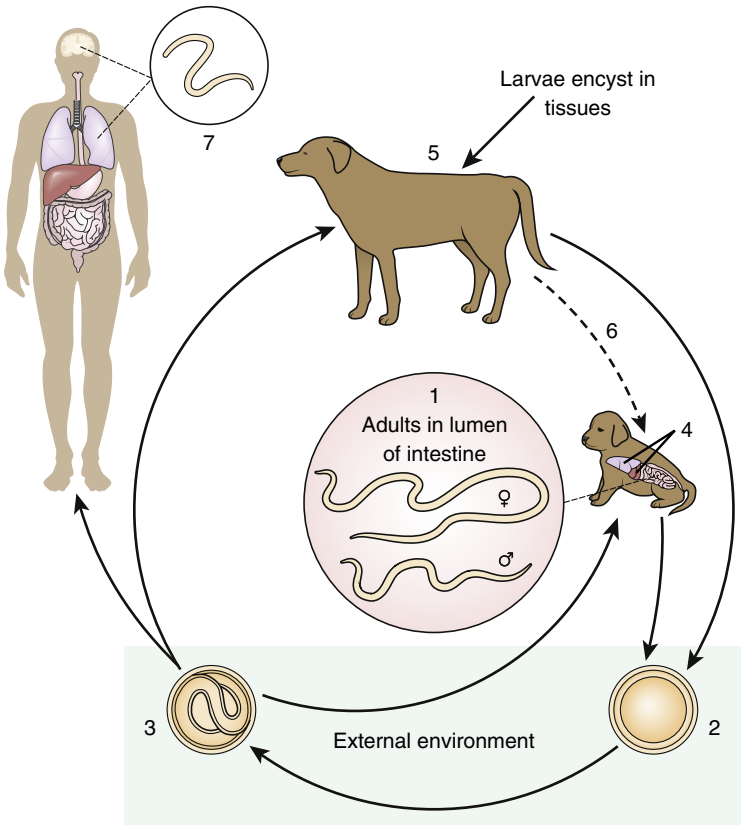


Fig. 3.96 Life cycle of *Toxocara canis*.
Adult worms live in the small intestines of young dogs (1). Eggs are passed in the stool (2) and embryonate in the environment (3). When ingested by a young dog, eggs hatch in the intestine, releasing larvae which migrate through the gut wall, to the liver and then lungs (4). They move up the bronchial tree, are swallowed, and adult worms develop in the small intestine (1). In older dogs, larvae encyst in tissues (5), but are reactivated in pregnancy and pass through the placenta and breast milk to puppies (6). Puppies develop infection with adult worms in their small intestine (1) and are the main source of environmental contamination. When humans accidentally ingest eggs, larvae migrate through tissue causing a visceral or ocular larva migrans but are unable to develop to maturity (7). (Adapted from CDC.)



Fig. 3.97 Embryonated *Toxocara* ovum.
Note the larva visible in this embryonating *Toxocara* ovum. (Courtesy, H. Edwards.)



Fig. 3.98 Adult worm of *Toxocara*.
Female worms measure 6–10 cm in length whilst male worms are slightly smaller at 4–6 cm. They have three lips at the anterior end of the worm and large arrow-shaped striated alae. (From Despommier, D. D., Hotez, P. J. Tissue nematodes. Principles and Practice of Pediatric Infectious Diseases, Volume 277, Pages 1334–1341.e2, Figure 277-1.)

Downloaded From Vet-eBooks.com

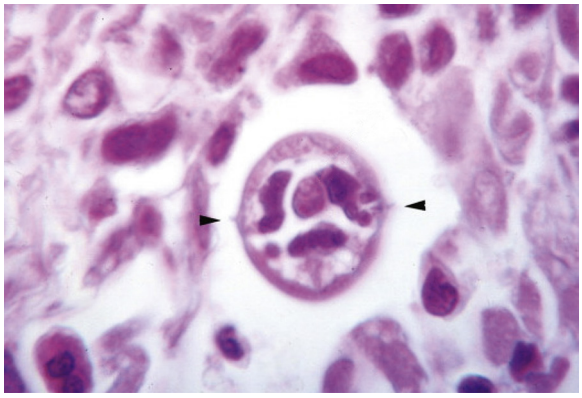


Fig. 3.99 *Toxocara canis* migrating through the lung.
Note the characteristic lateral alae (arrowheads) visible in this *T. canis* larva migrating through the lung. (From Procop, G., Neafie, R. C. Human parasitic pulmonary infections. Pulmonary Pathology, Pages 287–314, Figure 14-7.)

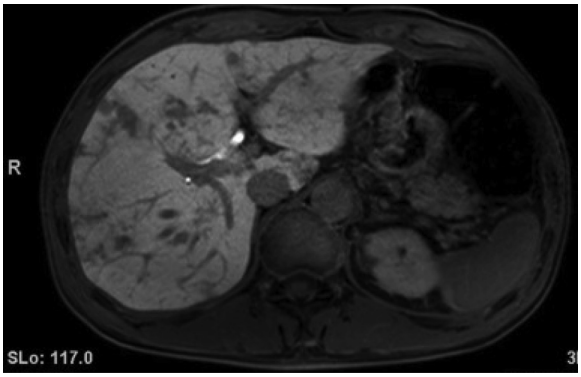


Fig. 3.100 Visceral larva migrans.
Migrating larvae may result in symptoms of fever, malaise, wheeze and urticarial skin lesions. Hepatomegaly is a common clinical sign; multiple irregular low attenuating nodules are seen in this patient with visceral larva migrans secondary to *Toxocara canis* infection. (From Morii, K., Oda, T., Satoh, H. et al. *Toxocara canis* – associated visceral larva migrans of the liver. International Journal of Infectious Diseases, 2015-01-01, Volume 30, Pages 148–149, Figure 2.)



Fig. 3.101 Urticarial skin lesions in a patient with toxocariasis.
Cutaneous manifestations may occur in toxocariasis (From Gavignet, B., Piarroux R., Aubin, F., et al. Cutaneous manifestations of human toxocariasis. *Journal of the American Academy of Dermatology*. 2008-12-01, Volume 59, Issue 6, Pages 1031–1042, Figure 2.)

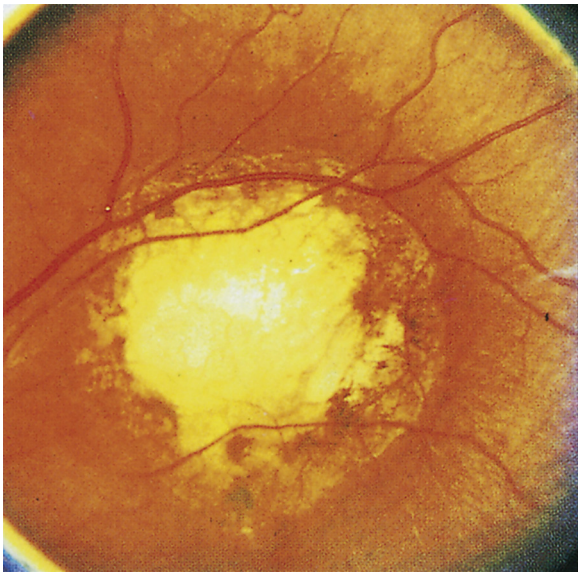


Fig. 3.102 Ocular larva migrans.
The penetrating larva has become encysted, leading to the formation of a large granuloma seen here at the posterior pole of the fundus. The granuloma resembles a retinoblastoma and may lead to blindness. (Courtesy, Dr P. Dobson.)

Downloaded from Vet-eBooks.com

Angiostrongyliasis

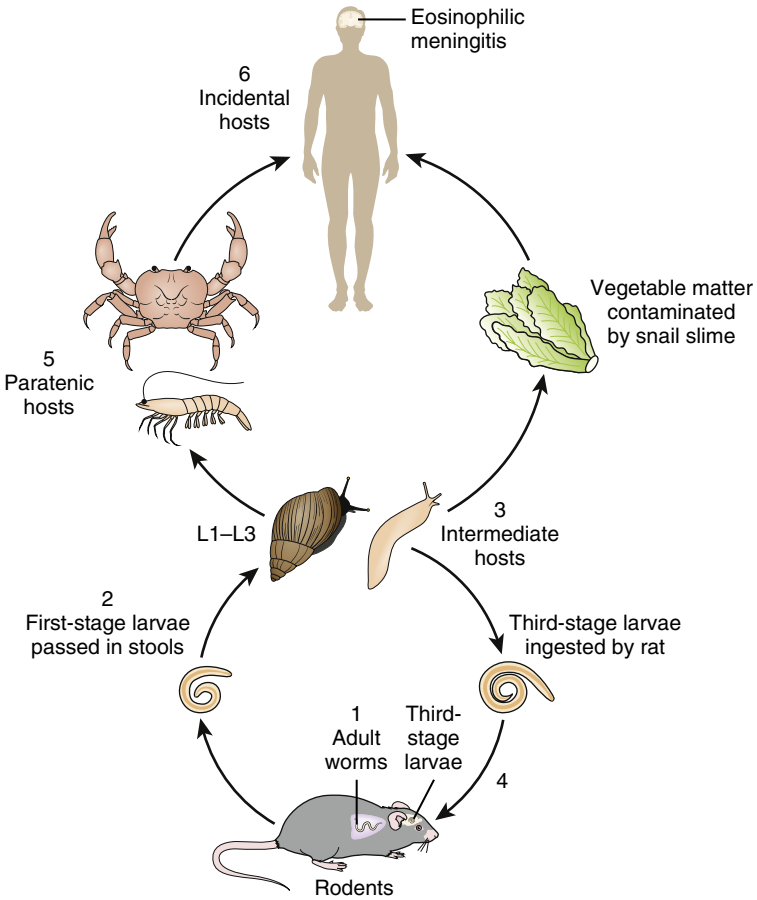


Fig. 3.103 Life cycle of *Angiostrongylus cantonensis*.
Adult worms live in the pulmonary arteries of rats, producing eggs (1). The eggs become first-stage larvae in the lungs, before migrating to the pharynx where they are swallowed and passed in stools (2). L1 larvae are ingested by molluscs where they mature to L3 larvae, which may be passed in snail slime (3). When ingested by a rat, L3 larvae migrate to the meninges where they mature to adult worms before returning to the pulmonary arteries (4). Shrimp and crabs may serve as paratenic hosts (5). Humans may become infected by ingestion of raw or undercooked molluscs or paratenic hosts, or by contamination of vegetable matter by snail slime (6). Larvae may migrate to the brain, causing an eosinophilic meningitis, but are unable to develop into adult worms within the human host.

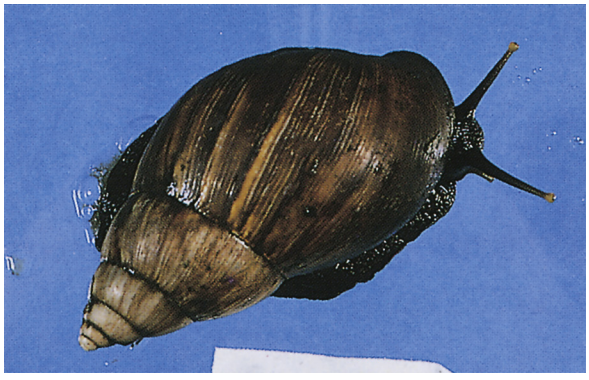


Fig. 3.104 *Achatina fulica*, the giant African land snail.
The giant African land snail is an intermediate host in which first-stage larvae mature to third-stage larvae. Although native to East Africa, it reproduces rapidly and has invaded much of Asia and the Americas, displacing local snail populations and damaging crops. It is sometimes kept as a pet or for educational purposes in schools. It is important to ensure that such molluscs are locally bred and not imported from countries where *A. cantonensis* is enzootic. (Half life-size) (Courtesy, Professor S-N. Chen.)

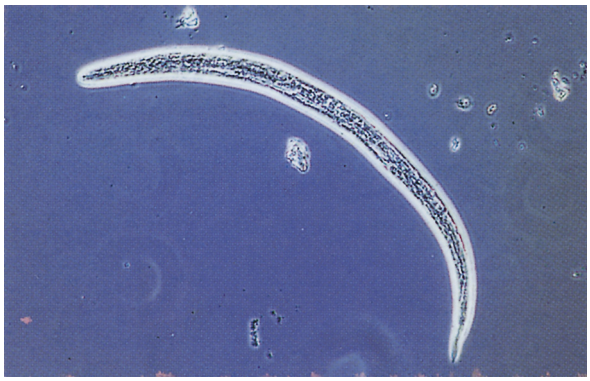


Fig. 3.105 Third-stage larvae of *Angiostrongylus cantonensis*.
Rats become infested when they eat snails containing third-stage larvae. (x 100.)

Downloaded from Vet-eBooks.com

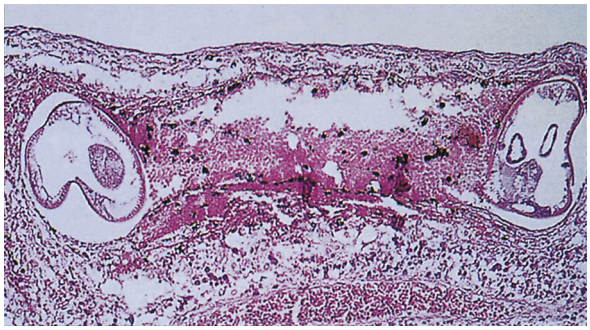


Fig. 3.106 Section of *Angiostrongylus cantonensis* larvae in meninges of human brain.
Ingestion of raw or undercooked molluscs may result in human infection (such as has been reported in an Australian who swallowed a slug for a dare). The larvae migrate to the brain, where they cause an eosinophilic meningitis or meningoencephalitis. Disease severity is dependent on the larval burden. Most infections resolve spontaneously with a mortality rate of less than 1%. (x 60.) (Courtesy, Dr J. C. Crook.)

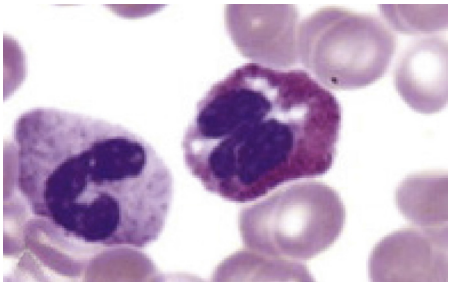


Fig. 3.107 Eosinophil and neutrophil.
Note the neutrophil on the left and the eosinophil on the right of this figure. The eosinophil has a bilobed nucleus with large acidophilic granules with a purple-red hue. The neutrophil has a multilobed nucleus with smaller, paler staining granules. (From Kremyanskaya, M. Eosinophilia, eosinophil-associated diseases, chronic eosinophil leukemia, and the hypereosinophilic syndromes. In: Hematology: Basic Principles and Practice. Chapter 70, Pages 1077–1094, Figure 70.1, Panel A.)

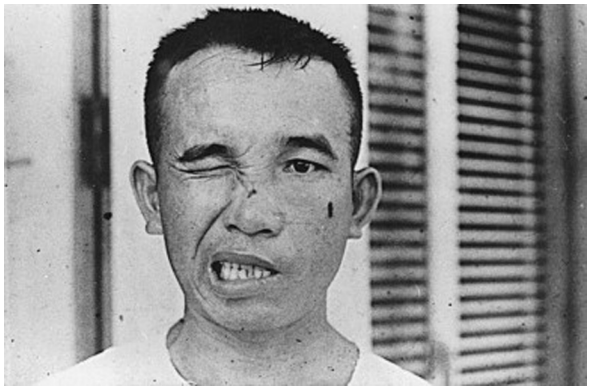


Fig. 3.108 Unilateral facial nerve palsy in *Angiostrongylus* meningitis.
Facial nerve palsy develops in around 5% of patients with eosinophilic meningitis. (From Wattanagoon, Y., Cross, J.H. Eosinophilic meningitis. In: Hunter's Tropical Medicine and Emerging Infectious Diseases. Chapter 118. Pages 856-858. Figure 118.1. Courtesy, Professor T. Bunnag, Thailand.)

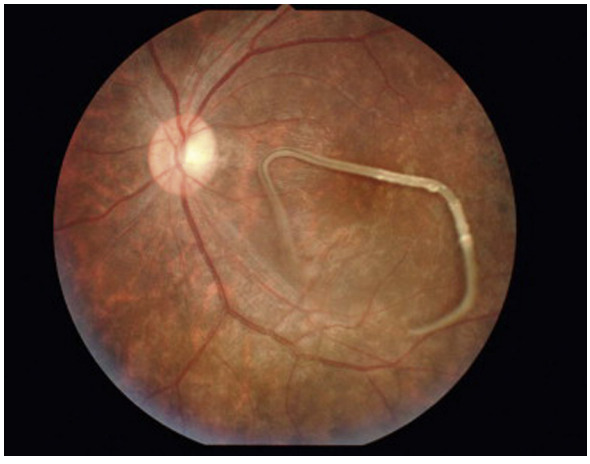


Fig. 3.109 Ocular Angiostrongyliasis.
Rarely larvae enter the eye causing unilateral blurred vision with or without meningitis. (From Wattanagoon, Y., Cross, J.H. Eosinophilic meningitis. In: Hunter's Tropical Medicine and Emerging Infectious Diseases. Chapter 118. Pages 856-858. Figure 118.2. Courtesy, Dr S. Sinawat, Thailand.)

Downloaded from Vet-eBooks.com



Fig. 3.110 *Angiostrongylus costaricensis.*
A. costaricensis is also a parasite of rats with molluscs as intermediate hosts. In rats, the adult worms live in mesenteric arteries, releasing eggs and larvae through the bowel wall where they are passed in the stool. Humans are occasionally infected through ingestion of undercooked molluscs typically in Central or South America. L3 larvae mature to adult worms which inhabit the mesenteric arteries. The adult worms and eggs provoke an inflammatory reaction resulting in endothelial damage with arteritis and thrombosis. Patients may present acutely with abdominal pain and diarrhoea, mimicking appendicitis, or chronically with a mass which may be misdiagnosed as a tumour. Here, an adult *A. costaricensis* (arrowed) is seen within the lumen of an artery. (From Martins, F.P., Lacombe, F.O., Ganc, R.L. et al. Colon mass secondary to angiostrongyliasis. Gastrointestinal Endoscopy, 2009-06-01, Volume 69, Issue 7, Pages e69–e71, Figure.3.)

Baylisascariasis

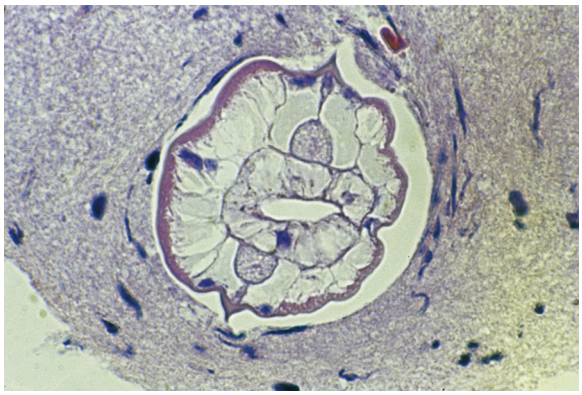


Fig. 3.111 Cross section of a larva of *Baylisascaris procyonis* from a child with neural larva migrans.
This parasite was discovered in a brain biopsy from a teenage boy with a history of pica living in California. The adult nematode lives in the intestine of peridomestic raccoons in the United States. Human infection is acquired following accidental ingestion of eggs from contaminated soil (raccoon 'latrines'). The larvae, measuring 1.5 mm to 2 mm in length, hatch in the stomach and migrate through the tissues causing visceral or ocular larva migrans. Because they are larger than *Toxocara* larvae, they cause more severe tissue damage. They also have a propensity to invade the CNS resulting in an eosinophilic meningitis. (H&E x 800.) (Courtesy, Professor L. R. Ash.)

Gnathostomiasis



Fig. 3.112 Adult *Gnathostoma spinigerum.*
Adult worms reside in nodules in the stomach wall of definitive carnivorous hosts. These include cats, dogs and tigers. Male worms have a red tail whilst female worms are larger with a curly tail. Unembryonated eggs are passed in faeces and develop into first-stage larvae in water. (x 1.3.) (Courtesy, Professor I. Miyazaki.)

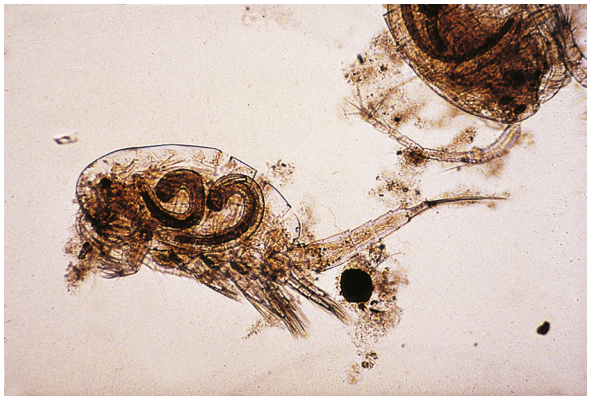


Fig. 3.113 First-stage larvae of *Gnathostoma nipponicum* in *Eucyclops serrulatus.*
First-stage larvae develop into second-stage larvae within small crustaceans. (x 75.) (Courtesy, Dr J. Horton and Professor P. Kraivichian.)

Downloaded From Vet-eBooks.com



Fig. 3.114 Third-stage larva of *Gnathostoma spinigerum* encysted in fish muscle.
When the crustacean is eaten by a fish or reptile, second-stage larvae migrate to muscle where they encyst to form third-stage larvae. If then ingested by a definitive host, third-stage larvae will penetrate the stomach wall and mature to adulthood, forming a nodule and passing eggs in the stool. If ingested by a further paratenic host, including herons, pigs or humans, larvae cannot mature to adulthood but instead wander through subcutanous tissues causing cutaneous or visceral larva migrans. (Courtesy, Dr J. Horton and Professor P. Kraivichian.)

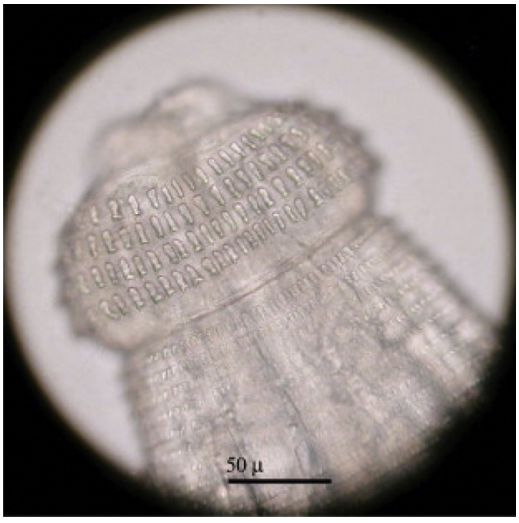


Fig. 3.115 Head of adult *Gnathostoma spinigerum*.
Humans become infected by eating raw or undercooked fish, typically in South East Asia. Note the bulbous head and rows of cuticular spines which cause significant damage and inflammation as the worm migrates through cutaneous or visceral tissue. (From Vonghachack, Y., Dekumyoy, P., Yoonuan, T., et al. Sero-epidemiological survey of gnathostomiasis in Lao PDR. Parasitology International, Volume 59, Issue 4, Pages 599–605, Figure 3, Panel B.)



Fig. 3.116 Periorbital larva migrans.
Wandering *Gnathostoma spinigerum* cause migratory subcutaneous swellings associated with boring pain and eosinophilia. Third-stage larvae may be visualized with ultrasound and recovered surgically from swellings in suitable locations. (Courtesy, Dr J. Horton and Professor P. Kraivichian.)

Downloaded from Vet-eBooks.com

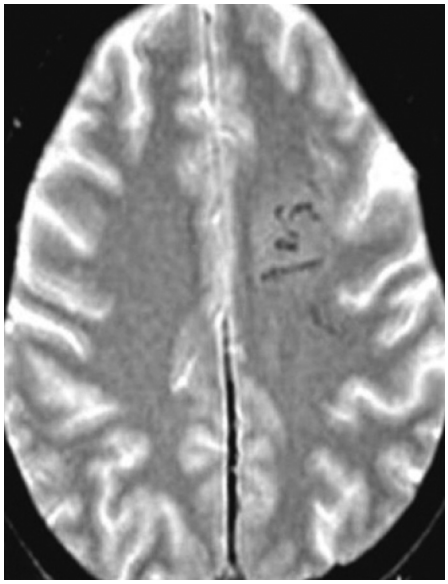


Fig. 3.117 Larval track from intracerebral Gnathostomiasis.
When *Gnathostoma spinigerum* migrates to the central nervous system, it may cause eosinophilic meningoencephalitis, subarachnoid haemorrhage or focal neurological signs. Larval tracks can clearly be seen in the MRI of this patient with intracerebral gnathostomiasis. (From Heckmann, J. M., Bhigjee A.I. Tropical neurology. In: Manson's Tropical Diseases. Chapter 71, Pages 1047–1060, Figure 71.5 A.)

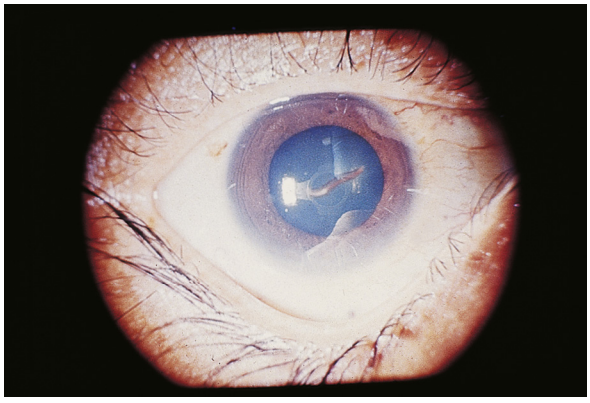


Fig. 3.118 Late third-stage larva of *Gnathostoma spinigerum* in the eye.
Note the migrating third-stage larva of *G. spinigerum* in the anterior chamber of the eye in this Thai patient. (Courtesy, Dr J. Horton and Professor P. Kraivichian.)

Downloaded from Vet-eBooks.com

Dracunculiasis (Guinea Worm)



Fig. 3.119 Life cycle of *Dracunculus medinensis* (Guinea worm).
The mature gravid female worm settles in the subcutaneous tissues of the human host causing a blister (1). When the skin is immersed in fresh water, the blister bursts, releasing large numbers of active rhabditiform larvae from the female's uterus (2). Larvae are swallowed by copepods such as water fleas in water and then penetrate the gut wall and enter the new host's body cavity. They grow and undergo two moults (3). When infected copepods are swallowed by humans in untreated drinking water (4) the larvae are released and penetrate the wall of the duodenum. They migrate through the body and, after undergoing two further moults, males and females mate in the subcutaneous tissues. The males subsequently die whilst the fertilized females migrate along muscle planes to the subcutaneous tissue, usually of the lower limbs. Females are ready to oviposit about 1 year after entering the human host. Dogs may also become infected (5).

Downloaded from Vet-eBooks.com

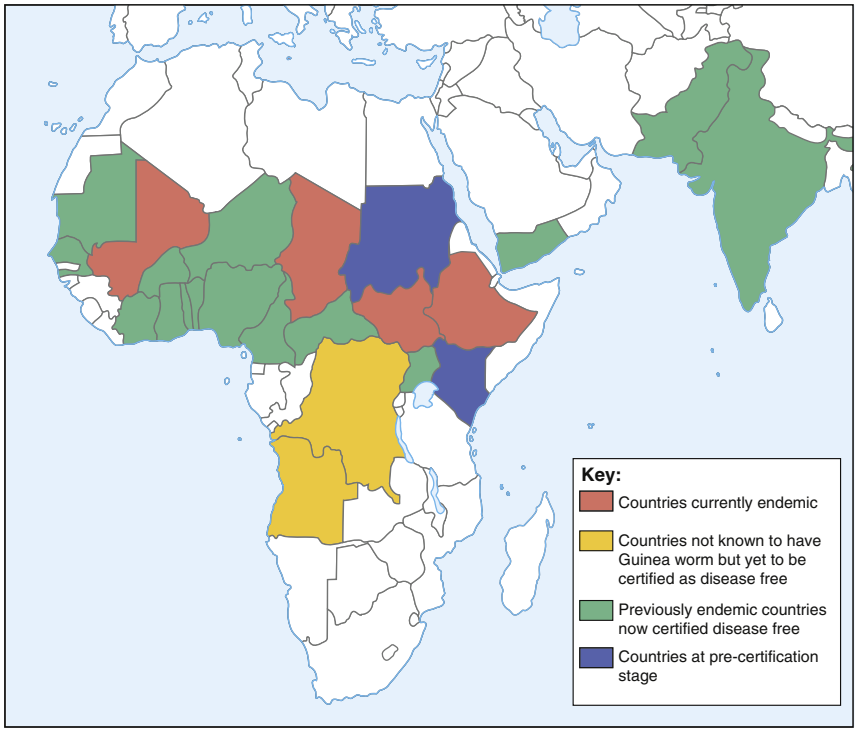


Fig. 3.120 Global distribution of *Dracunculus medinensis*, updated to 2017.
In 1986, there were an estimated 3.5 million cases of *D. medinensis* occuring in 21 endemic countries in Africa and Asia. In 2015, there were just 22 cases worldwide, nine of which occurred in Chad. Public health strategies including improvements in water supply, routine filtration of drinking water, vector control using larvicidal agents and health education has brought *D. medinensis* to the verge of eradication.

Downloaded from Vet-eBooks.com

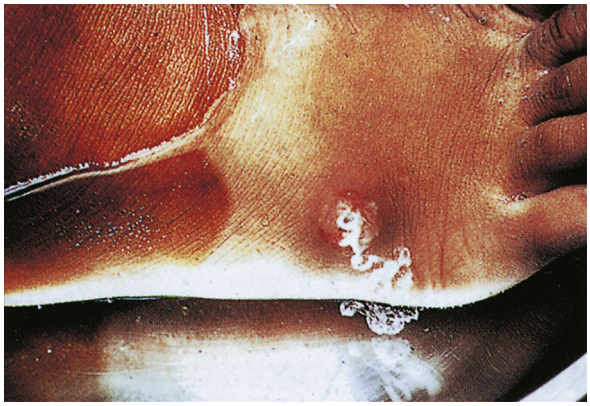


Fig. 3.121 Contamination of surface water.
A papule forms where the adult female worm reaches the skin surface; it ulcerates when the skin is immersed in water. A loop of the worm's uterus prolapses and ruptures, releasing large numbers of rhabditiform larvae into the water. (Courtesy, Wellcome Museum of Medical Science and Dr A. J. Duggan.)



Fig. 3.122 An adult female worm emerging from the skin.
Adult females can be extracted by progressively winding them round a matchstick as they emerge from the subcutaneous tissues. (Courtesy, Dr C. Bodimeade.)

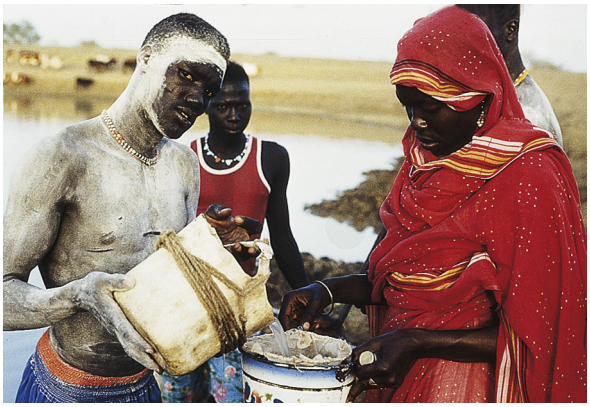


Fig. 3.123 Filtering water for drinking through a nylon gauze sieve.
Water filtration, through a plastic mesh filter as seen here, removes copepods from drinking water, preventing transmission. Temephos, an organophosphate larvicide, can also be applied to drinking water supplies. In low concentrations it is toxic to copepods but safe for human ingestion. (Courtesy, Dr A.Tayeh.)



Fig. 3.124 Guinea worm in dogs.
In Chad, there are increasing reports of *Dracunculus medinensis* infection in dogs, with more than 1000 cases reported in 2016. Dogs tend to scare away copepods as they lap water and are thus unlikely to be infected through drinking water alone. Instead, it is hypothesized that they become infected by eating the entrails of copepod-ingesting fish in fishing villages. They can then reintroduce larvae back into drinking water presumed to be safe for human consumption. (Courtesy, Ligue Pour la Protection des Animaux.)

Downloaded from Vet-eBooks.com

Cestodes

Cestodes of medical importance.

Table 3.1

Order	Genus and species	Definitive (D) Intermediate (I) Paratenic host (P)	Clinical syndrome
Pseudophyllidae	*Diphyllobothrium latum*	D - humans, mammals I – crustacean, small fish P – larger fish	Intestinal tapeworm B12 deficiency
	Spirometra spp.	D – cats, dogs I – crustaceans P - fish, amphibians, reptiles, humans	Cutaneous or visceral larva migrans
Cyclophyllidae	*Hymenolepis nana*	D – rodents, humans I - arthropods including fleas and beetles	Intestinal tapeworm Autoinfection
	Hymenolepis diminuta	D – rodents, humans I - arthropods including grain beetles	Intestinal tapeworm
	Dipylidium caninum	D - cats, dogs, humans I - fleas	Intestinal tapeworm
	Taenia solium	D – humans I – pigs, humans	Intestinal tapeworm Cysticercosis
	Taenia saginata	D - humans I - cattle	Intestinal tapeworm
	Echinococcus granulosus	D – dogs I - sheep, humans	Cystic echinococcosis
	Echinococcus multilocularis	D – foxes I - small rodents, humans	Alveolar echinococcosis

Downloaded From Vet-eBooks.com

Diphyllobothriasis (The Fish Tapeworm)

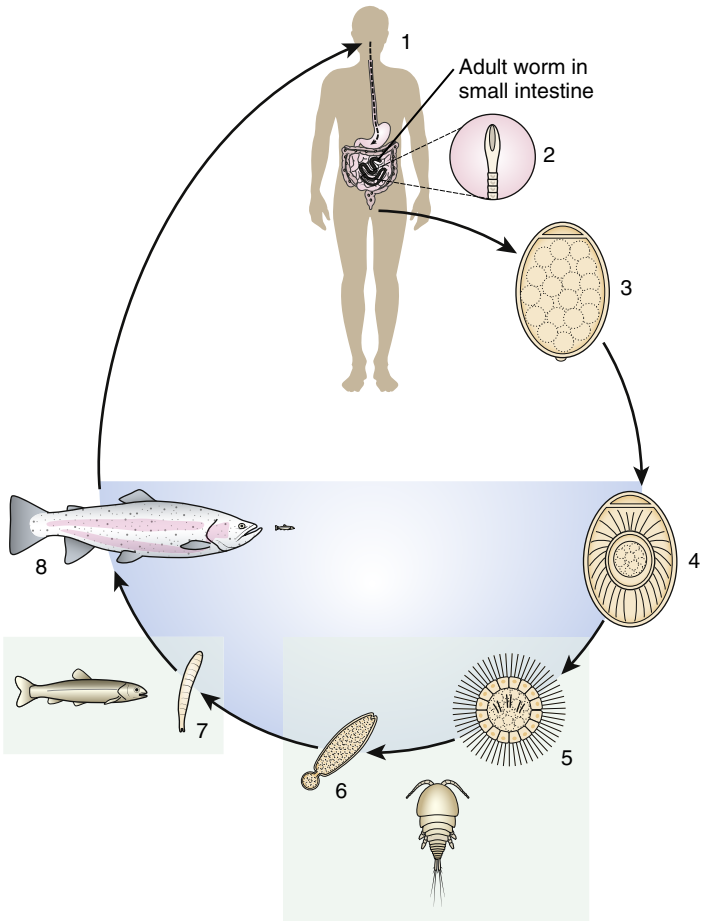


Fig. 3.125 Life cycle of *Diphyllobothrium latum*. Humans are the definitive hosts of *D. latum*, although other mammals may also be infected (1). The adult tapeworm lives in the small intestine (2), passing unembryonated eggs in the stool (3). These embryonate in water (4), hatching to release coracidia which are ingested by small copepods (5). Coracidia mature to procercoid larvae within the body cavity of the copepod (6). When eaten by small freshwater fish such as minnows, procercoid larvae migrate to the flesh and mature to plerocercoid larvae (7). This is repeated if small fish are ingested by predator fish which act as paratenic hosts (8). When humans eat raw infected fish, the plerocercoid develops into an adult tapeworm in the small intestine (1). (Adapted from CDC; https:// www.cdc.gov.)

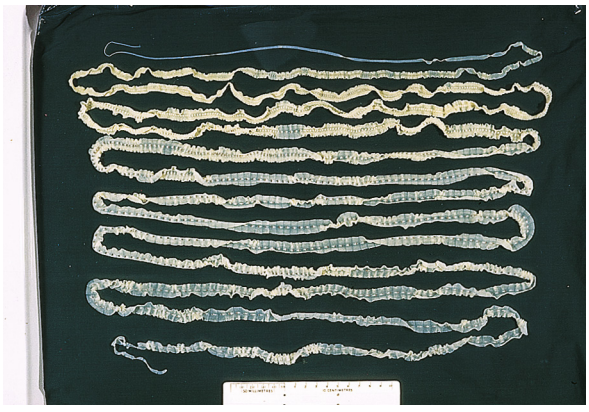


Fig. 3.126 Intact adult *Diphyllobothrium latum*. *D. latum* is the largest human tapeworm, measuring up to 25 m and 4000 segments in length. Infection is commonest in northern Europe, the former USSR and Japan, particularly in areas where raw or undercooked fish is consumed.

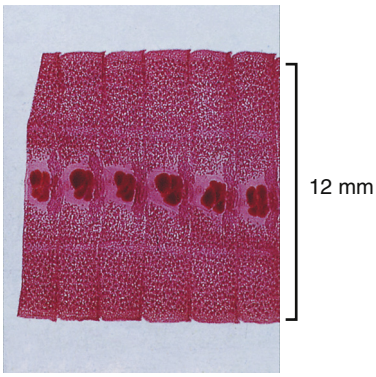


Fig. 3.127 Segments of adult *Diphyllobothrium latum*. Segments are rarely seen in the stool but are readily distinguished from those of *Taenia* species as they are wider than they are long (4 mm long by 12 mm wide). Note the central rosette-shaped uterus from which millions of eggs are released through the uterine pore.

Downloaded from Vet-e-Books.com



Fig. 3.128 Ovum of *Diphyllobothrium latum*.
D. latum eggs are found in the stool of infected people. They are oval, measuring 60 µm x 40 µm, with an operculum at one end and an abopercular knob at the other, both of which may be difficult to identify. Eggs embryonate in water developing into coracidia. (Courtesy, H. Edwards.)



Fig. 3.129 Copepod containing procercoid larvae of *Diphyllobothrium latum*.
Coracidia are ingested by copepods, such as *Cyclops*, where they develop into procercoid larva.

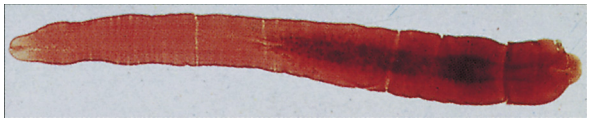


Fig. 3.130 Plerocercoid larva.
When the copepod is ingested by a small fish, such as a minnow, the procercoid larva migrates to fish muscle and develops into a plerocercoid larva. If the small fish is ingested by a larger fish (further intermediate host), this will become infected with the plerocercoid larva. If either the secondary or further intermediate hosts are ingested uncooked by a human, an adult tape worm will form.

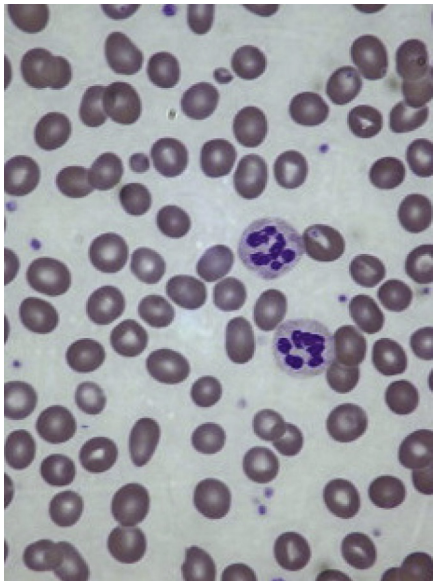


Fig. 3.131 Peripheral blood film of a patient with megaloblastic anaemia.
Most people with *D. latum* infection are asymptomatic or have mild gastrointestinal symptoms. However, unlike other cestodes, *D. latum* competes with its host for vitamin B12. Forty per cent of those infested are B12 deficient, but only 2% develop megaloblastic anaemia, as humans usually store enough B12 to last for several years. Note the macrocytosis and hypersegmented neutrophils seen here which are typical of megaloblastic anaemia. (From Howard, M. R., Hamilton, P. J., Megaloblastic anaemia. In: Haematology: An illustrated colour text. Chapter 13, Pages 26–27, Figure 13.3.)

Sparganosis



Fig. 3.132 Edible frog and seafood on a Thai market stall.
Spirometra are pseudophyllidae tapeworms of cats and dogs. Humans become infected with plerocercoid larvae by drinking water containing the intermediate host, procercoid-infected invertebrates or by ingestion of a paratenic host, such as undercooked frogs or snakes. In some parts of East Asia, freshly killed frogs or snakes are applied as a poultice to wounds, and infection can also be transmitted through this practice.

Downloaded From Vet-eBooks.com



Fig. 3.133 Sparganosis of a human breast.
Although the tapeworm cannot reach maturity in humans, the plerocercoid larva, also known as a sparganum, is mobile and up to 50 cm in length. It moves through subcutaneous tissue causing swellings which may be migratory. Occasionally larvae enter the central nervous system with severe consequences. This patient presented with a breast lump and sensation of movement within her breast. She had a history of eating undercooked frogs and snakes in childhood. Excision revealed a sparganum. (From Moon, H. -G., Jung, E-J., Park, S-T. Breast sparganosis presenting as a breast mass with vague migrating pain. Journal of the American College of Surgeons, 2008-08-01, Volume 207, Issue 2, Pages 292–292, Figure D.)

Hymenolepiasis

Hymenolepis nana (The Dwarf Tapeworm)

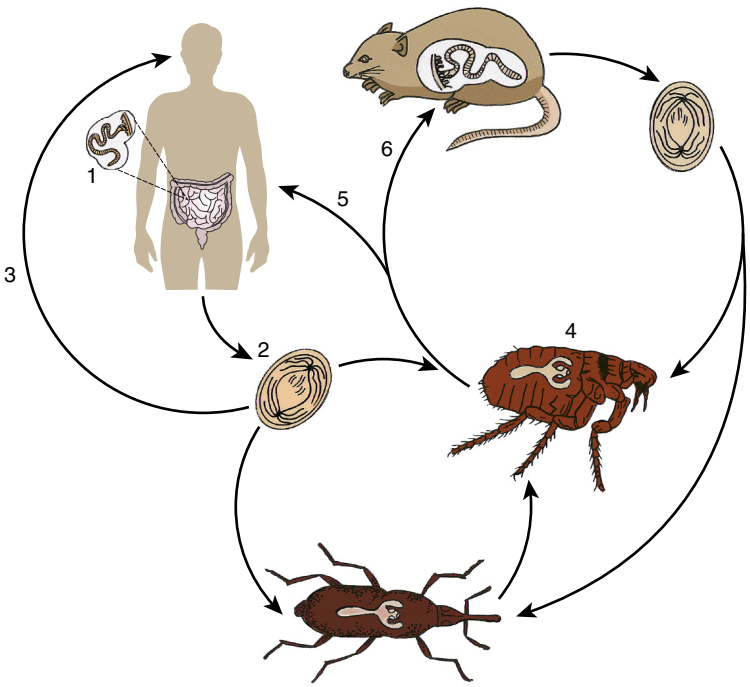


Fig. 3.134 Life cycle of *Hymenolepis nana*.
Humans are the definitive host of *H. nana*. Adult worms live in the ileum (1). Eggs are released from gravid proglottids through the genital atrium and passed in stool (2). If ingested by a human, they are immediately infectious (3). The egg hatches, releasing a motile six-hooked hexacanth larva (an onchosphere) which burrows into a villus. Here it develops into a tailless cysticercoid larva (a cercocyst) causing the villus to rupture, releasing the cysticercoid into the gut lumen. The scolex evaginates, attaches to the ileal mucosa, and the larva develops into an adult.

Less commonly, arthropods may act as an intermediate host (4). Eggs ingested by fleas or beetles hatch and develop into cysticercoids within the body cavity of the arthropod. These are infectious to humans (5) and to rodents (6) if the arthropod is accidentally ingested. The more common parasite of rodents is *H. nana* var *fraterna*; this is morphologically identical to *H. nana* with a rodent definitive host and an arthropod intermediate host.

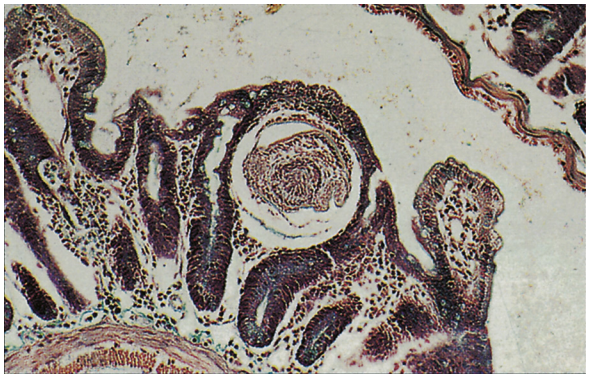
Downloaded from Vet-eBooks.com



Fig. 3.135 *Adult Hymenolepis nana.*
Adult worms measure 3 cm to 4 cm in length. Although they only survive for 6 weeks, their ability to autoinfect allows chronic infection to be established particularly in children and institutionalized adults. (From Bailey, G., Garcia, H.H. Other cestode infections: intestinal cestodes, cysticercosis, other larval cestode infections. In: Manson's Tropical Diseases. Chapter 57, Pages 820–832, Figure 57.13. Courtesy of Tropical Resources Unit, Wellcome Trust.)



Fig. 3.136 Scolex of *Hymenolepis nana.*
The *H. nana* scolex has four suckers and a single circle of up to 30 hooks. Morphologically it is similar to *Taenia saginata* but can be distinguished by the absence of hooks in the latter. (From the collection of Herman Zaiman, 'A Presentation of Pictorial Parasite'.)



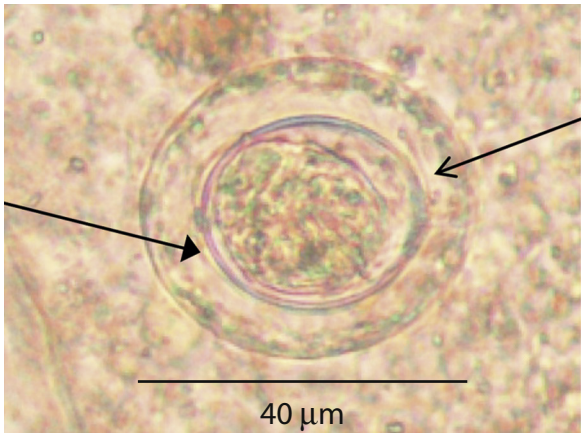


Fig. 3.137 *Hymenolepis nana* ovum.
Eggs of *H. nana* are found in the stool. They are oval and measure 30–50 µm in length. The inner membrane has four to eight filaments at each pole (see arrow). The oncosphere has six hooks but usually only some of these are visible. (Courtesy, H. Edwards.)



Fig. 3.138 Mature proglottid of *Hymenolepis nana.*
Proglottids of *H. nana* are rarely found in stool. They are wider than they are long, measuring 0.2 mm by 0.8 mm, and usually overlap neighbouring proglottids. They are filled with eggs with no visible uterus. The adult worm measures up to 4 cm in length. (From Fritsche, T. R., Pritt, B.S. Medical parasitology. In: Henry's Clinical Diagnosis and Management by Laboratory Methods. Pages 1231–1283. e3, Figure 63.20, Panel C.)

Fig. 3.139 Cercocyst in intestinal villi.
In humans, the six hooked hexacanth larva (oncosphere) burrows into a villus where it matures into the cercocyst seen here. The villus subsequently ruptures, releasing the larva which attaches to the ileal mucosa and develops into an adult. (x 140.)

Downloaded From Vet-eBooks.com

Hymenolepis diminuta (The Rat Tapeworm)

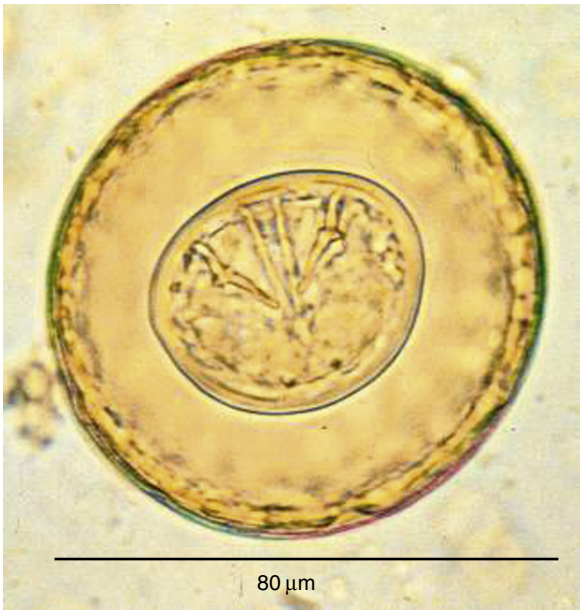


Fig. 3.140 *Hymenolepis diminuta* egg.
H. diminuta is a tapeworm of rats with arthropods, including fleas and beetles, as intermediate hosts. Humans are accidental hosts, occasionally infected following ingestion of infected arthropods, when the tapeworm may develop to maturity. The life cycle is similar to *H. nana* but the adult worms are larger measuring up to 60 cm in length. The eggs are also larger, measuring up to 85 µm, and lack polar filaments. (Courtesy, H. Edwards.)



Fig. 3.141 Cysticercoid of *Hymenolepis diminuta* in an arthropod.
The cysticercoid develops in the intermediate arthropod host and is infectious to rats and humans. (x 90.) (Courtesy, Dr E. H. Pike.)



Fig. 3.142 *Tribolium confusum*, the confused flour beetle.
T. confusum is a common grain pest worldwide and is an intermediate host of *Hymenolepis diminuta*. *T. confusum* feeds on broken pieces of grain and contaminates supplies with faeces and bodily secretions which have an extremely pungent smell. This spoils the grain for both human and animal consumption.

Downloaded from Vet-eBooks.com

Dipylidiasis (The Dog Tapeworm)

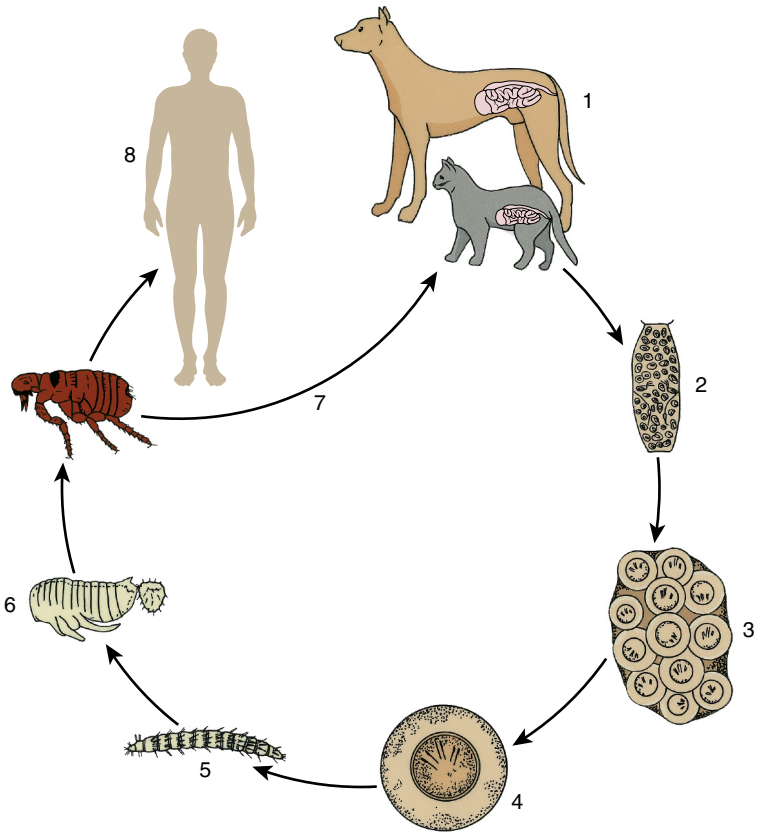


Fig. 3.143 Life cycle of *Dipylidium caninum*.
The adult worm inhabits the small intestine of cats and dogs (1). Proglottids are passed in the stool (2) and rupture to release egg clusters (3) or individual eggs (4) to the environment. Eggs are ingested by an intermediate host, such as *Ctenocephalides* larva, releasing oncospheres in the flea's intestine (5). Larvae enter the arthropod body cavity where they mature into a cysticercoids (6). When the infected flea reaches maturity, it feeds on a cat or dog which may accidentally ingest the flea during grooming (7). The cysticercoids develop into adult tapeworms in the small intestine, reaching 60 cm in length (1). Humans, particularly children, may be infected through accidental ingestion of a flea. The tapeworm reaches maturity and may result in mild gastrointestinal symptoms (8).



Fig. 3.144 Scolex of *Dipylidium caninum*.
The scolex has four suckers and a retractable conical rostellum carrying up to 150 hooks in one to seven rows. (From the collection of Herman Zaiman, `A Presentation of Pictorial Parasite'.)

Downloaded from Vet-eBooks.com

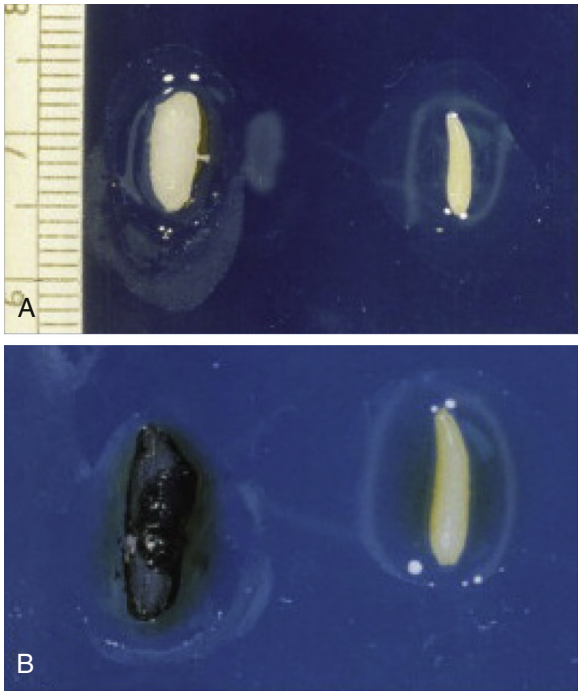


Fig. 3.145 Proglottid of *Dipyliduim caninum* passed in stool.
Proglottids passed in stool may look like grains of rice but are often motile. Here, a rice grain is seen on the left, next to a segment of *D. caninum (A)*. The rice stains dark blue with iodine but the proglottid remains unstained (B). (From Richards, F. O., Montgomery, S.P. Diphyllobothrium, Dipylidium, and Hymenolepis species. In: Principles and Practice of Pediatric Infectious Diseases. Chapter 279, Pages 1347–1350.e1, Figure 279-1. Courtesy, J. E. Mortensen, and S. S. Long, Philadelphia, PA.)

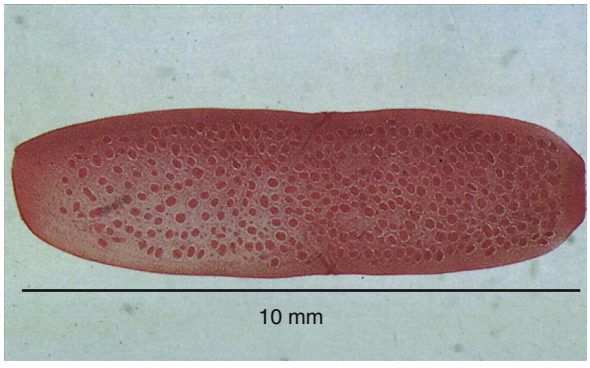


Fig. 3.146 Mature proglottid of *Dipylidium caninum*.
Proglottids measure 10 mm x 3 mm and are tapered at each end. They do not have a visible uterus, but instead contain multiple egg-filled capsules. The genus is named for the presence of a genital pore on either side of the proglottid; *Dipylidium* means two pores. (x 9.)



Fig. 3.147 Egg capsule.
As the mature segments disintegrate, encapsulated clusters of eggs are passed in the stool. Larval hooks may be seen within these. (x 240.)



Fig. 3.148 *Ctenocephalides felis*, the cat flea.
C. felis is a common intermediate host of *D. caninum*. Note the oval body shape and mesopleural rod. The presence of a genal and pronotal comb distinguishes *Ctenocephalides* from *Pulex irritans* and *Xenopsylla*. (Courtesy, C. Whitehorn.)

Downloaded from Vet-eBooks.com

Taeniasis

Taenia solium (The Pork Tapeworm)

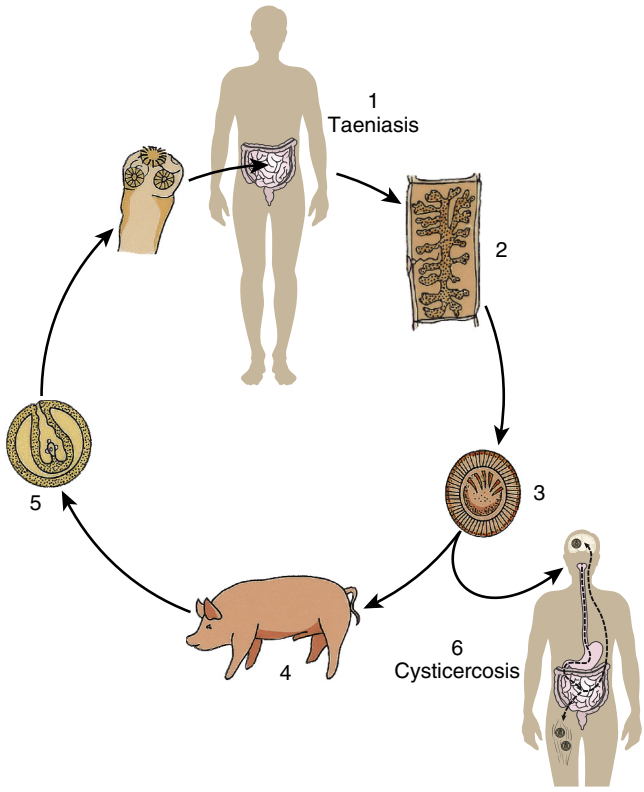


Fig. 3.149 Life cycle of *Taenia solium*.
Humans are the definitive host of *T. solium* with pigs as the intermediate hosts (1). Adults live in the small intestine, releasing motile, gravid segments in the stool (2). Large numbers of eggs (3) are released into the environment where they are ingested by pigs (4). The eggs hatch, releasing an oncosphere, which migrates through the intestinal wall, into blood vessels, finally reaching striated muscles. Here it encysts to forming a cysticercus (5). When inadequately cooked meat containing cysts is eaten by humans, the oncosphere excysts and develops into an adult tapeworm in the small intestine (1). If humans ingest *T. solium* eggs, they become intermediate hosts. The oncosphere migrates through the intestinal wall, forming cysts in muscle or brain, resulting in cysticercosis (6).

Humans are also the definitive host of *T. saginata* with cattle as intermediate hosts. However, unlike *T. solium*, humans cannot become intermediate hosts of *T. saginata* and do not develop cystic disease.



Fig. 3.150 Adult *Taenia solium*.
Adults range from 2 m to 8 m in length with 1000 proglottids. Each proglottid may produce 50,000 eggs. Multiple infections can occur.



Fig. 3.151 Scolex of *Taenia solium*.
The head of *T. solium* has four suckers and two rows of hooks. There is a small rostellum at the top of the scolex. By contrast, the scolex of *T. saginata* has neither hooks or rostellum (see Fig. 3.164). (x 40.)

Downloaded From Vet-eBooks.com

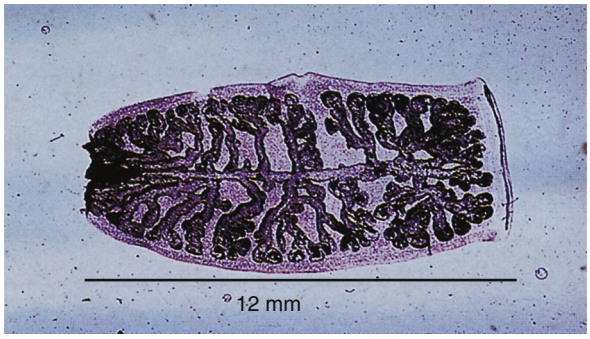


Fig. 3.152 Mature proglottid of *Taenia solium*.
The gravid segments of *T. solium* measure 12 mm x 5 mm. The central uterine trunk has between 7 and 13 lateral branches. By contrast, *T. saginata* is larger and has more than 15 lateral uterine branches (see Fig. 3.165). The eggs of both species are identical and should be treated with caution, as ingestion of *T. solium* eggs may result in cysticercosis. (Courtesy, Professor D. Greenwood. (x 6.))



Fig. 3.153 Cysticercosis in pork.
The larval cysticercoid stage occurs in the pig, giving rise to 'measly pork'. Humans acquire the tapeworm by ingesting inadequately cooked meat. (Courtesy, Professor C. D. Mackenzie.)

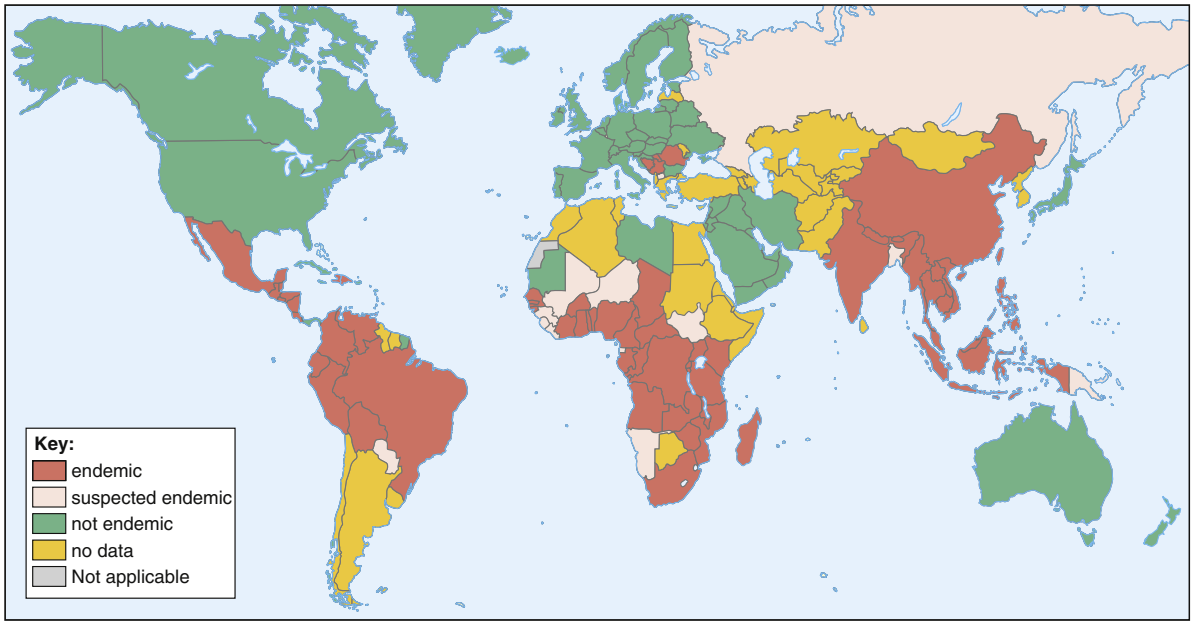


Fig. 3.154 Worldwide distribution of *Taenia solium*.
Cysticercosis is endemic throughout South America, sub-Saharan Africa and Asia, and is thought to affect 50 million people worldwide. It is the commonest cause of epilepsy in much of the developing world. Prevalence is highest in rural areas with inadequate sanitation where pigs are raised in close proximity to people. Cysticercosis is not acquired through eating infected pork meat, but by ingestion of *T. solium* eggs contaminating soil or unwashed vegetables. (Adapted from WHO; http://www.who.int.)

Downloaded from Vet-eBooks.com



Fig. 3.155 Subcutaneous lumps in cysticercosis.
This patient, who had travelled extensively in Central America, was initially seen and diagnosed with a ganglion of the wrist. Patients with cysticercosis may present with subcutaneous lumps in any part of the body and may develop epilepsy if there is cerebral involvement.



Fig. 3.156 Radiograph of cysticercosis of soft tissues.
As cysticerci age, calcification may occur. Calcified cysticerci may be seen as cigar-shaped opacities on radiograph of soft tissues. In heavy infection, acute myopathy can occur.

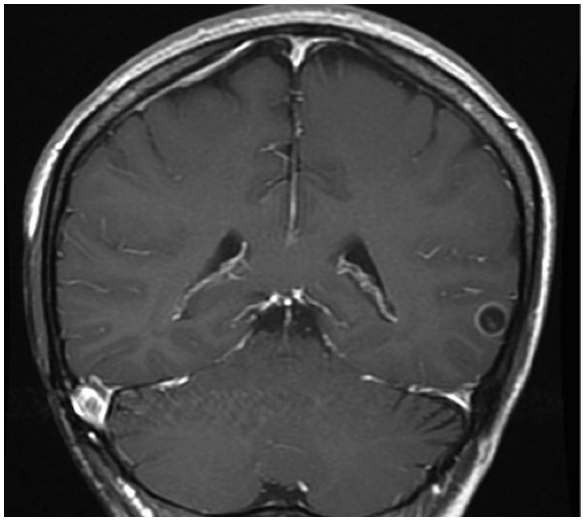


Fig. 3.157 Vesicular parenchymal cyst.
Sixty per cent of people with neurocysticercosis have a parenchymal brain lesion. Vesicular cysts are viable parasites with intact membranes and no surrounding host reaction. Note the scolex visible as a dot within the cyst and the lack of surrounding oedema. (Courtesy, Professor R. Jager.)

Downloaded from Vet-eBooks.com

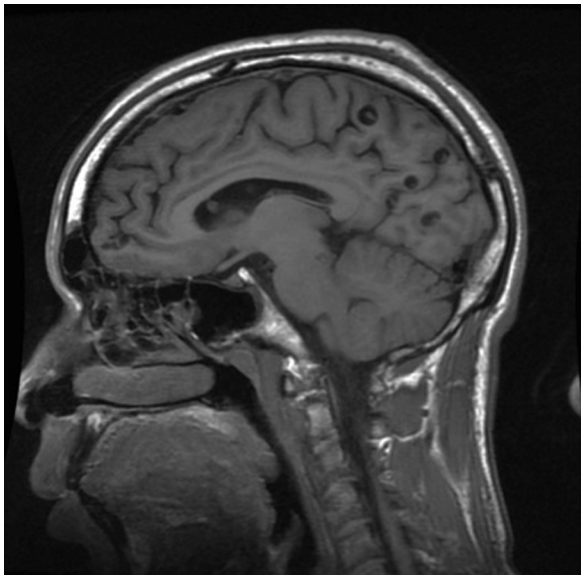


Fig. 3.158 Multiple vesicular lesions in a patient with neurocysticercosis.
In neurocysticercosis, neurological symptoms and signs depend on the number of cysts, their location and associated inflammation. Patients with a single cyst are often asymptomatic and may have negative serology. Patients with multiple cysts are more likely to have symptoms and positive serology. (Courtesy, Professor R. Jager.)

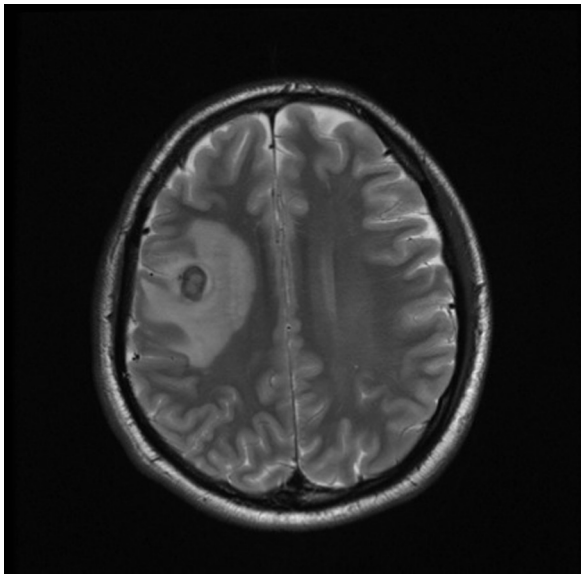


Fig. 3.159 Granular nodular cyst.
As the parasite dies, the membrane becomes leaky, provoking a host inflammatory response which may result in neurological symptoms including seizures. Here a ring enhancing lesion with surrounding oedema is seen on MRI. This may mimic a tuberculoma. (Courtesy, Professor R. Jager.)



Fig. 3.160 Obstructive hydrocephalus.
Cysticerci within the ventricles may result in obstructive hydrocephalus if the cyst blocks the ventricular outflow tract This patient has a cyst floating in the fourth ventricle (arrowed). (From Camelo-Piragua, S., Hedley-Whyte, E. T. Infections of the nervous system. In: Diagnostic Pathology of Infectious Disease, 2nd edition. Pages 507–541. Copyright © 2018 by Elsevier, Inc. All rights reserved.)

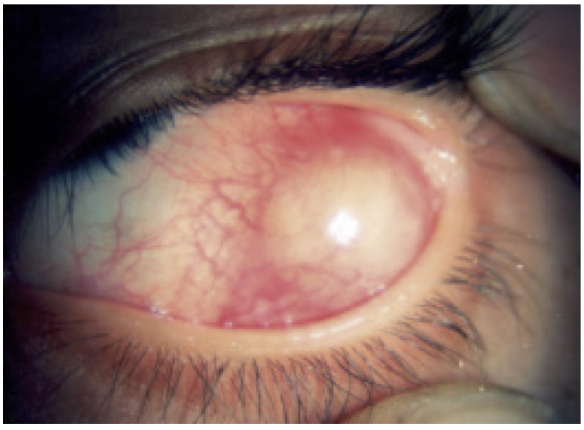


Fig. 3.161 Subconjunctival cysticercosis.
This patient has a subconjunctival cysticercus which is impeding eye movement. Ocular cysticercosis may affect any part of the eye. Inflammation from dying cysticerci may result in chorioretinitis, vasculitis or retinal detachment. (From Agrawal, S., Agrawal, J., Agrawal, T.P. Cysticercosis. *In:* Roy and Fraunfelder's Current Ocular Therapy. Pages 104–108, Figure 58.1, Panel E.)

Downloaded from Vet-eBooks.com

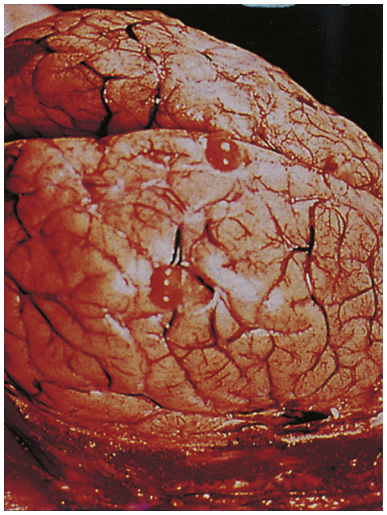


Fig. 3.162 Fatal cerebral cysticercosis.
Multiple cysts can be seen in the brain of this patient who died of neurocysticercosis. (Courtesy, Dr J. M. Goldsmid.)

Taenia saginata (The Beef Tapeworm)



Fig. 3.163 Adult *Taenia saginata*.
Humans are the definitive host of *T. saginata* with cattle as intermediate hosts. The adult measures 2–5 m in length, occasionally up to 25 m, with around 2000 proglottids. (Courtesy, Dr R. Owen.)

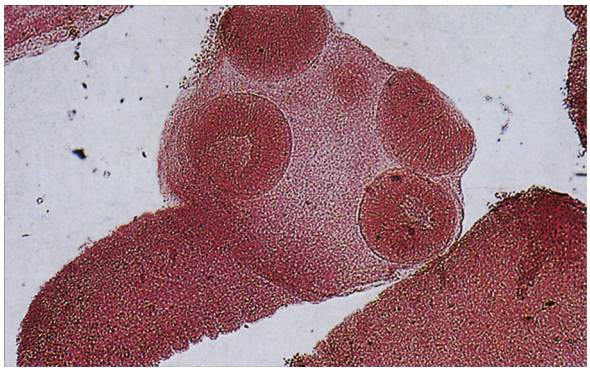


Fig. 3.164 Scolex of *Taenia saginata*.
The scolex of *T. saginata* has four suckers but has no hooks (unarmed). There is no rostellum. Compare this with the scolex of *T. solium* in Fig. 3.151. (x 40.)

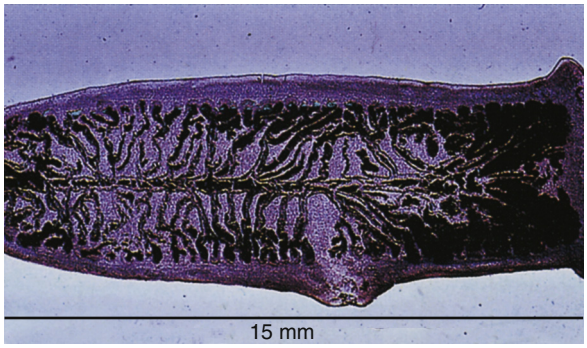


Fig. 3.165 Mature proglottid of *Taenia saginata*.
Proglottids of *T. saginata* measure 15–20 mm by 5–7 mm and are commonly seen in stool. They are motile and may be felt as they emerge from the anus and seen wriggling in the stool. The uterus has a central stem with more than 15 lateral branches in contrast to *T. solium* which has up to only 13 lateral branches (see Fig. 3.152). (x 6.) (Courtesy, Professor D. Greenwood.)

Downloaded From Vet-eBooks.com



Fig. 3.166 *Taenia sp.* ovum.
Eggs of *T. saginata* and *T. solium* are morphologically indistinguishable. They are spherical and measure 35 µm in diameter. The thick radially striated shell contains a six-hooked oncosphere. (Courtesy. H. Edwards.)

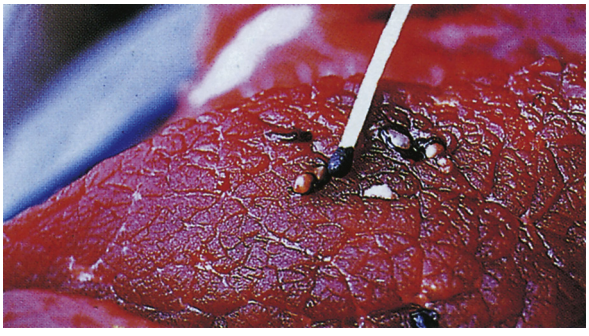


Fig. 3.167 Cysticercus in beef.
The cysticercal stage of *T. saginata* occurs in cattle and has not been documented in humans. The fluid-filled translucent cysts are 5–10 mm in diameter.



Fig. 3.168 Kitfo, an Ethiopian delicacy of raw beef.
Humans become infected with adult tapeworm if they ingest raw or partially cooked beef. In Ethiopia, kitfo, spiced and minced raw beef, is a traditional delicacy and *T. saginata* infection is common.



Fig. 3.169 Meat inspection: certificate of health.
Taeniasis is prevented by strict abattoir supervision, including adequate inspection of carcasses and condemnation of 'measly' meat.

Downloaded from Vet-eBooks.com

Echinococcosis

Echinococcus granulosus (Cystic Echinococcosis)

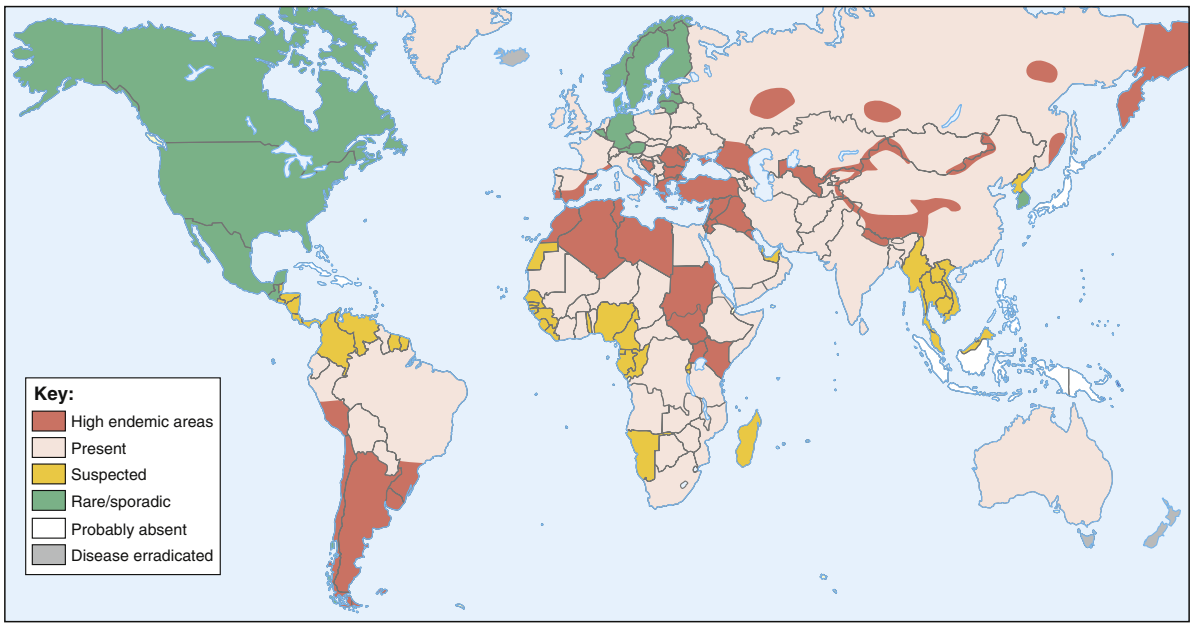


Fig. 3.170 The global distribution of cystic echinococcosis (CE).
CE has a worldwide distribution. The highest prevalence is found in pastoral communities, particularly in China and central Asia, where reported prevalence reaches 9%. (From Control of Neglected Tropical Diseases. © World Health Organization, 2011. Available at: http://gamapserver.who.int/mapLibrary/Files/Maps/Global_echinococcosis_2009.png)

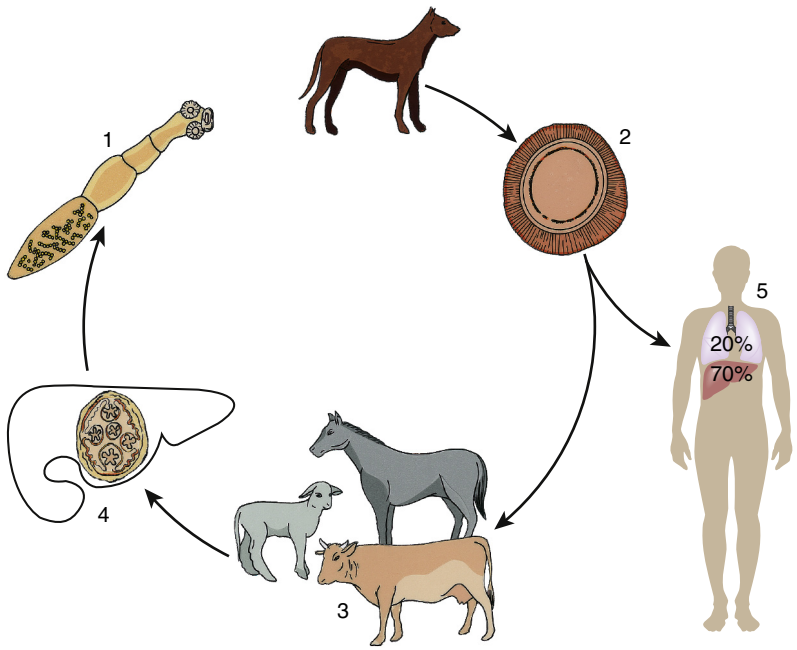


Fig. 3.171 Life cycle of *Echinococcus granulosus*.
The adult tapeworm, *E. granulosus* (1), inhabits the small intestine of dogs. Typical taeniid eggs are passed in the faeces (2) which contaminate pasture land. Eggs are ingested by herbivores, typically sheep but also cows and horses (3). The egg hatches in the duodenum, releasing an oncosphere which invades the intestinal wall. It is carried by the portal vein to the liver where a cyst forms. Less commonly, oncospheres are carried to the lung or other organs where cysts can be established (4). Dogs become infected when they eat offal containing cysts from infected herbivores. Humans (5) are infected if they accidentally ingest eggs from the stool of infected dogs, typically through ingestion of unwashed vegetables, and are dead-end hosts. In humans, 70% of cysts are found in the liver, 20% in the lung and 10% elsewhere.

Downloaded From Vet-eBooks.com

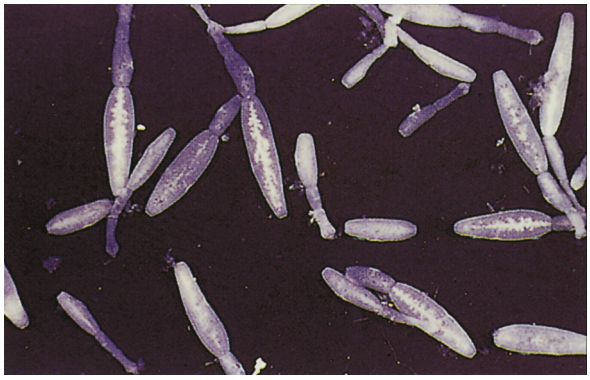
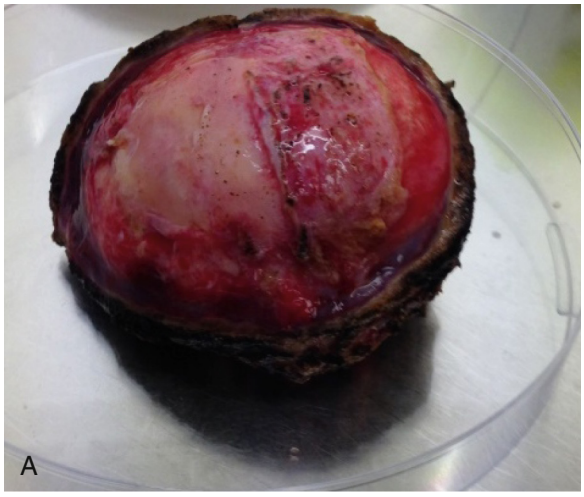


Fig. 3.172 Adult *Echinococcus granulosus*.
The adult tapeworm is 3–8 mm long. Large numbers may be found in the small intestines of dogs that are infected by eating the offal of sheep, cattle or other animals containing hydatid cysts. (Courtesy, Dr H. Zaiman.)



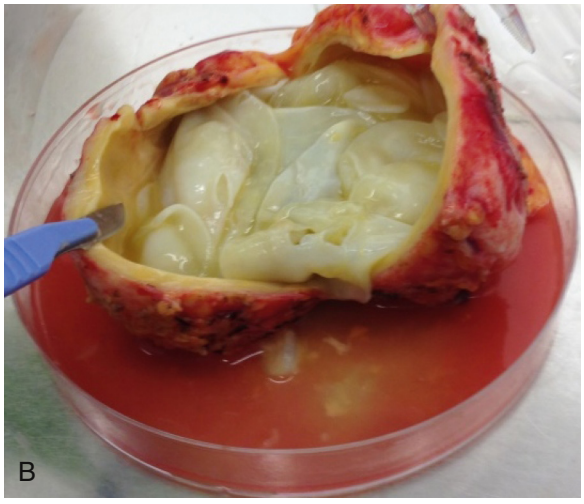


Fig. 3.173 Resected hepatic cyst.
This intact *E. granulosus* cyst was removed from the liver of a patient (A). Note the thick wall of the mother cyst and visible daughter cysts in the dissected specimen (B). (Courtesy, Professor P. L. Chiodini.)

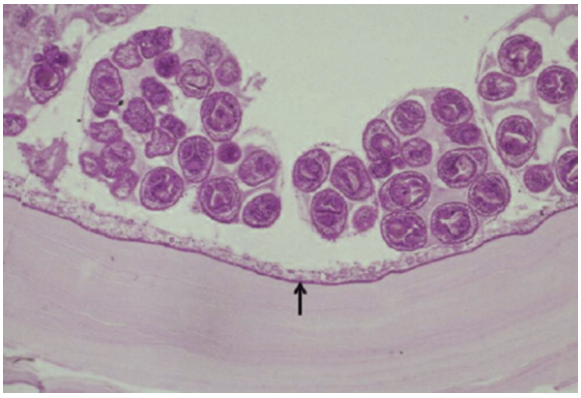


Fig. 3.174 Histology section showing the cyst structure.
The cyst has a thick outer acellular membrane, known as the laminated membrane. Within this is a fertile, cellular germinal membrane (arrowed) which produces brood capsules containing the infectious protoscolices. Within the mother cyst, brood capsules, protoscolices and hooklets float, collectively forming 'hydatid sand', which on ultrasound can be visualized as shifting shadows. In the absence of visible daughter cysts or membranes, this is a useful maker to distinguish cystic echinococcosis cysts from simple cysts. (From Lewin-Smith, M. R., Neafie, R. C. Helminth infections. In: Pathology of Infectious Diseases. Chapter 27, Pages 575–609, Figure 27.7.)

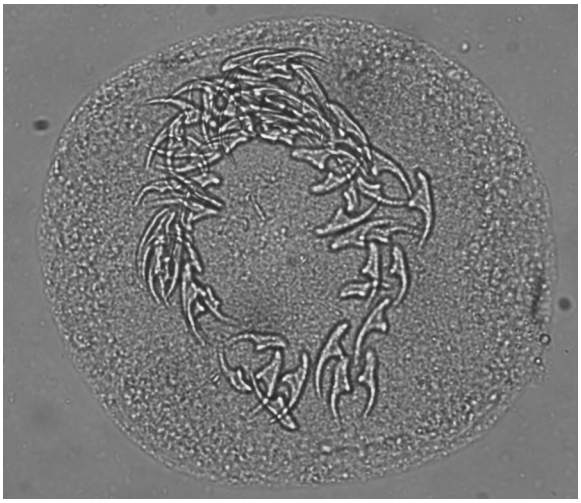


Fig. 3.175 Unstained *Echinococcus granulosus* protoscolex.
Protoscolices containing visible hooks may float freely within the cyst or be contained within brood capsules. Even when protoscolices have degenerated, the pathognomonic hooklets may still be readily recognized. (Courtesy, Professor P. L. Chiodini.)

Downloaded From Vet-eBooks.com



Fig. 3.176 Transmission cycle of *Echinococcus granulosus*.
The offal from this slaughtered sheep will be eaten by waiting dogs. If the offal contains cysts of *E. granulosus*, the dogs will become infected and develop adult tape worms. (From Craig, P. S., McManus D. P., Lightowlers M. W. et al. Prevention and control of cystic echinococcosis. Lancet Infectious Diseases, 2007-06-01, Volume 7, Issue 6, Pages 385–394, Figure 4 B.)

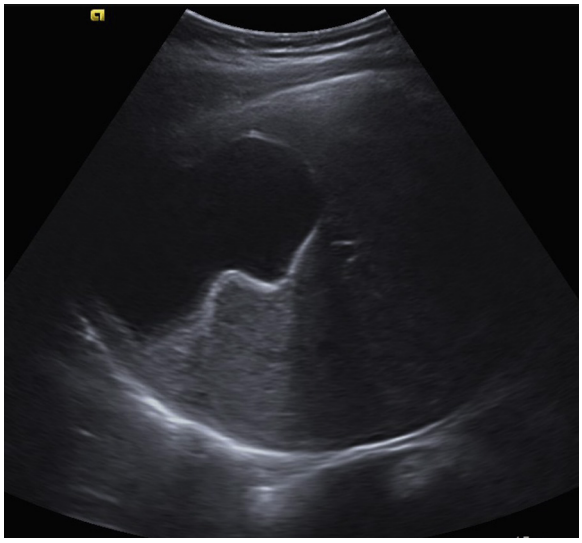


Fig. 3.178 WHO stage 1 hepatic cyst.
Early CE cysts are unilocular and may be misidentified as simple cysts. The WHO staging system for CE identifies these as CE1 cysts. Small cysts may be treated with albendazole alone. Cysts over 5 cm need percutaneous aspiration, injection then reaspiration of a protoscolicidal agent such as hypertonic saline (PAIR procedure) with albendazole cover. (Courtesy, Professor P. L. Chiodini.)



Fig. 3.177 Massive cystic echinococcosis (CE) cyst in a Kenyan child.
CE is very common in the Turkana region of northern Kenya, where there is a close association between dogs and humans. This young boy has an enormous hepatic hydatid cyst. His abdomen bears the scars of local treatment aimed at alleviating pain over the grossly enlarged liver.

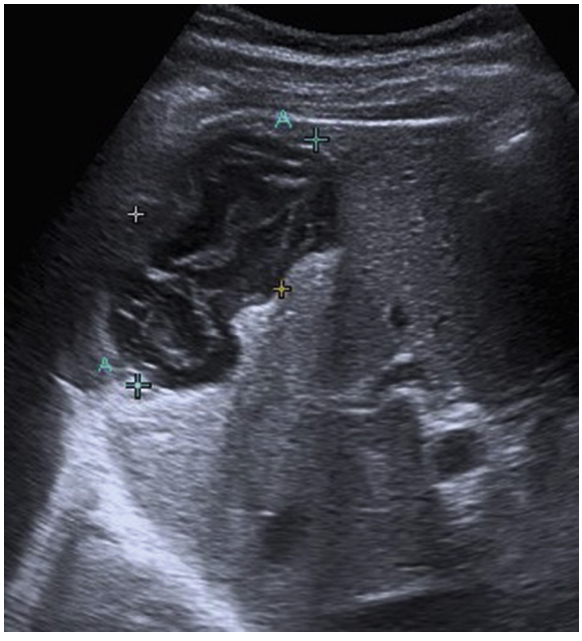


Fig. 3.179 Collapse of a CE 1 cyst following a PAIR procedure.
The cyst in Fig. 3.178 underwent a puncture-aspiration-injection-reaspiration (PAIR) procedure. One month after the procedure it was predominantly solid with little cystic content. Note the visible collapsed membranes. (Courtesy, Professor P. L. Chiodini.)

Downloaded From Vet-eBooks.com

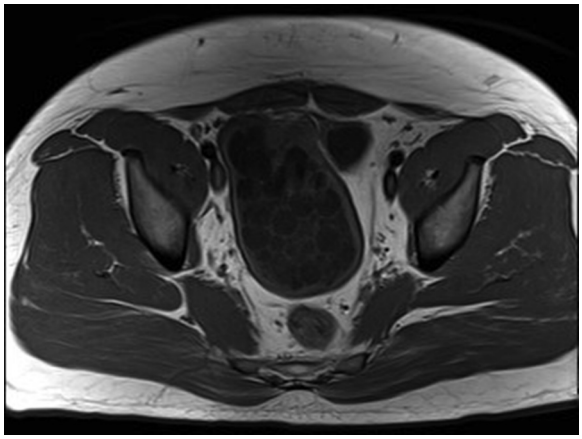


Fig. 3.180 CE 2 cyst adjacent to the bladder.
Although most CE cysts are found in the liver or lung, they may be present in any organ. This patient had a cyst adjacent to the bladder wall. As the cyst grows, it may develop daughter cysts which float within the mother cyst in a rosette or honeycomb pattern. These are known as CE2 cysts and contain viable, infectious material. These cysts do not respond to drug treatment alone but require resection with albendazole cover. (Courtesy, Professor P. L. Chiodini.)

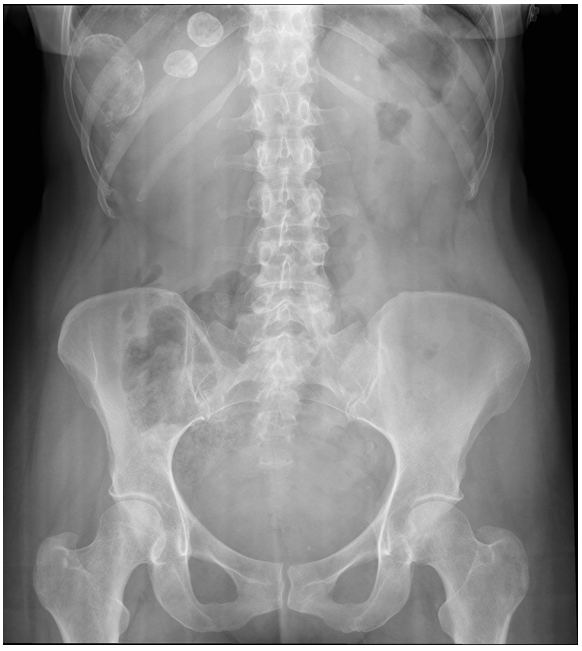


Fig. 3.182 Non-viable CE 5 cyst.
These calcified hepatic hydatid cysts are non-viable and do not need treatment. (Courtesy, Professor P. L. Chiodini.)

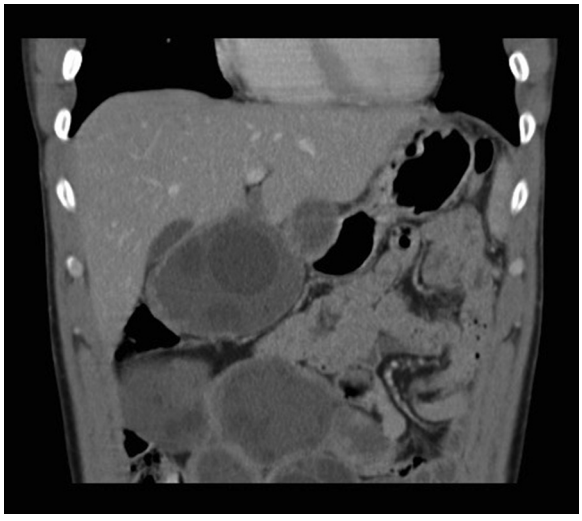


Fig. 3.181 CE 3B transitional cyst.
This hepatic cyst is transitioning from a viable CE 2 cyst to a non-viable cyst. The mother and daughter cysts solidify, resulting in a complex cyst with both solid and cystic components. These cysts should be treated with surgery and albendazole treatment. (Courtesy, Professor P. L. Chiodini.)



Fig. 3.183 Hepatic and pulmonary cyst.
This patient's hepatic cyst eroded through the diaphragm and into the lung. It subsequently ruptured and the patient expectorated daughter cysts (Fig. 3.184). (Courtesy, Professor P. L. Chiodini.)

Downloaded from Vet-eBooks.com



Fig. 3.184 Expectorated cysts following rupture of a pulmonary cyst.
If a cyst ruptures into the bronchial tree, the patient may cough up cyst material and fluid, with a characteristically salty taste. (Courtesy, Professor P. L. Chiodini.)



Fig. 3.185 Intracerebral cyst.
CE cysts may occur in any organ. This post-mortem specimen shows multiple CE cysts within the brain parenchyma and ventricles. (Courtesy, Professor S. Lucas.)

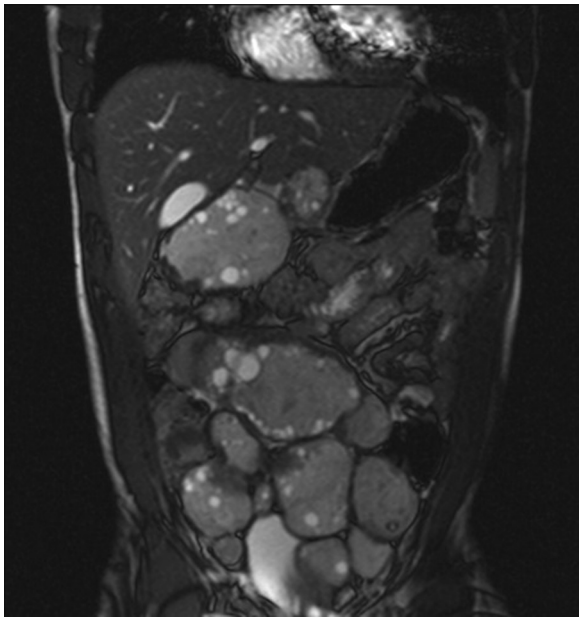


Fig. 3.186 Disseminated intra-abdominal cystic echinococcosis.
Rupture of a CE cyst may result in dissemination of disease. This patient was admitted to hospital with abdominal pain and underwent an appendicectomy which revealed a normal appendix. Many years later she presented with slowly increasing abdominal distension and was found to have disseminated intra-abdominal CE. The initial abdominal pain was probably caused by the rupture of a CE cyst. Untreated, this led to dissemination of disease. (Courtesy, Professor P. L. Chiodini.)

Downloaded from Vet-eBooks.com

Echinococcus multilocularis (Alveolar Echinococcosis)

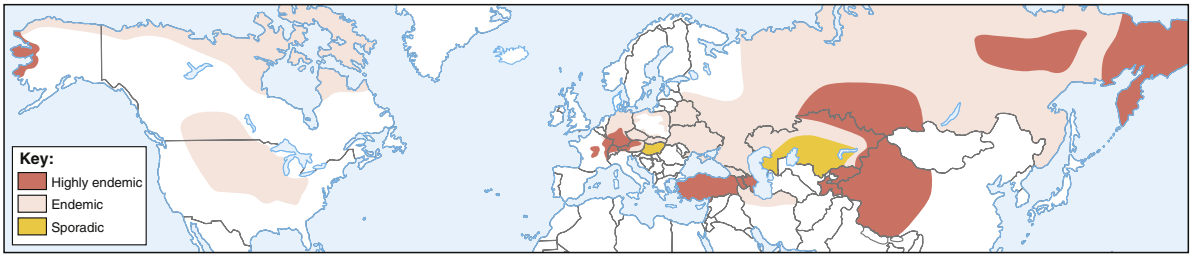


Fig. 3.187 Global distribution of alveolar echinococcosis (*Echinococcus multilocularis*).
Alveolar echinococcosis (AE) is caused by infection with the larval stage of *E. multilocularis*. Adult tapeworms live in the small intestine of wild canines, especially foxes, whilst the usual larval hosts are rodents. An estimated 18,000 cases occur worldwide each year, of which 91% occur in China and the rest are distributed through northern Europe, Russia and Central Asia. Human infection is especially common in areas where domestic dogs consume rodents and are in close contact with wild canines. (Data from Torgerson PR, Keller K, Magnotta M, Ragland N: The global burden of alveolar echinococcosis, PLoS Negl Trop Dis 4:e722, 2010.)

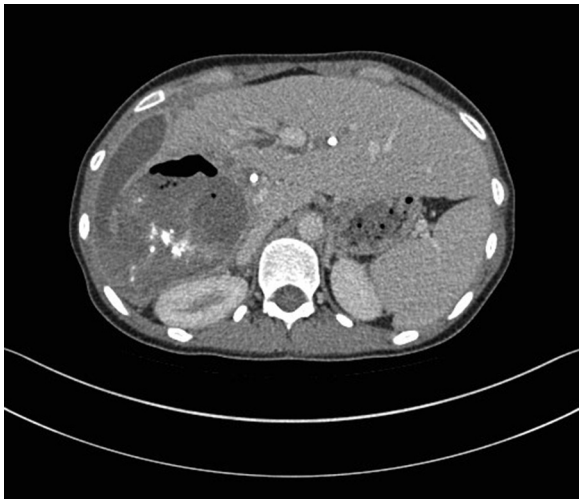


Fig. 3.188 Hepatic alveolar echinococcosis (AE).
Primary infection occurs in the liver. Patients often remain asymptomatic until the mass is large and compressing structures such as bile ducts or invading other organs. This MRI shows a space occupying lesion in the liver with central necrosis and infiltrative growth at the margins. Note the calcification which is found scattered through the lesion rather than confined to the wall, as is seen in cystic echinococcosis. (Courtesy, Professor P. L. Chiodini.)

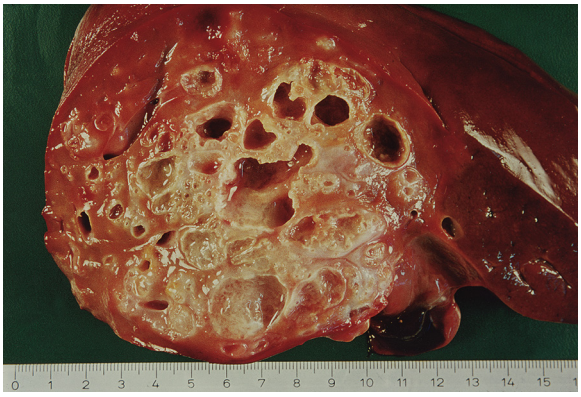


Fig. 3.189 Alveolar echinococcosis (AE) in a human liver.
Note the conglomerate small cystic lesions infiltrating the liver in this post-mortem section from a patient with AE. Often these are misdiagnosed as malignant lesions.



Fig. 3.190 Histological section of alveolar echinococcosis (AE) cyst.
Cysts consist of an outer acellular laminated membrane surrounding an inner proliferative germinal membrane. Although rodent hosts develop brood capsules and protoscoleces within the cyst, these are rarely seen in humans. Polymerase chain reaction can be used to confirm the diagnosis. (x 40.) (Courtesy, Professor S. Lucas.)

Downloaded From Vet-eBooks.com



Fig. 3.191 Metastatic lesions of alveolar echinococcosis (AE) in the brain.
Hepatic disease may metastasize to the lung, brain or elsewhere via the vasculature. Note the multilocular cystic lesion seen in this patient's brain. (From Thurnher, M. Other infections of the brain. In: Imaging of the Brain. Chapter 42, Pages 889–908, Figure 42-18, Panel E.)

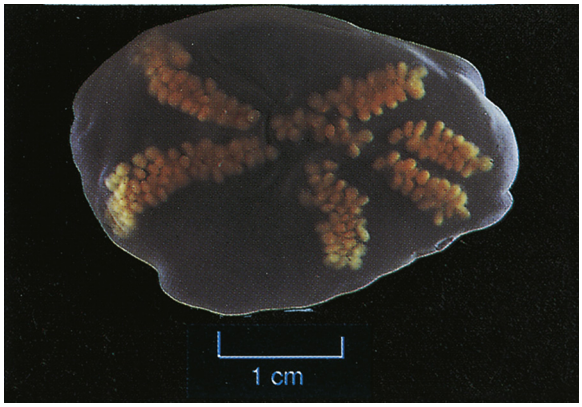


Fig. 3.193 *Coenurus cerebralis* of sheep.
The definitive host of *Taenia multiceps* is the dog whilst sheep are intermediate hosts. Cystic lesions develop in the hindbrain of sheep leading to 'staggers'. Humans are occasionally infected, developing symptoms suggestive of an intracranial mass. Cysts grow to 2 cm or more and can be distinguished histologically from *T. solium* and *E. granulosus* by the ridged cuticle and the presence of multiple protoscolices. (Courtesy, Professor R. E. Howells.)

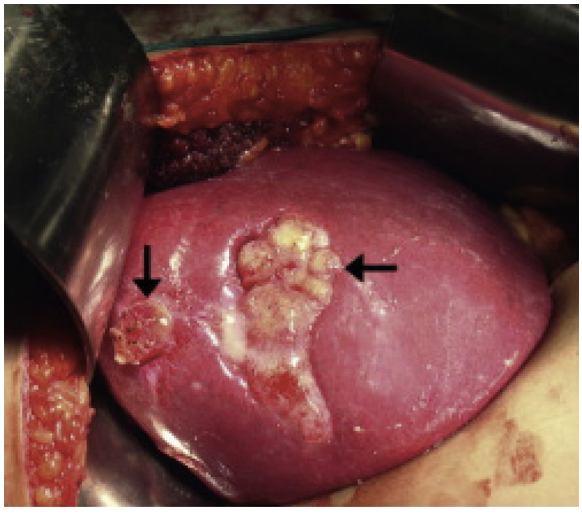


Fig. 3.192 Polycystic echinococcosis caused by *Echinococcus vogeli*.
Larvae of *E. vogeli* cause polycystic echinococcosis in South and Central America. The definitive hosts are canines, with pacas and rodents as intermediate hosts. Humans are accidentally infected, developing multivesicular cysts usually in the liver. Cysts bud exogenously to form new cysts. (From de Almeida, F. B., Corrêa, C. L., de Siqueira, N. G. et al. Histopathological findings of an uncommon co-infection: *Echinococcus vogeli*, HIV, hepatitis C virus, and hepatitis B virus. *International Journal of Infectious Diseases*, 2013-10-01, Volume 17, Issue 10, Pages e925–e927, Figure 1, panel B.)



Fig. 3.194 *Taenia crassiceps* in a human eye.
T. crassiceps, a tapeworm of carnivores with rodents as the intermediate host, rarely causes human infection. Note the multiple cystic lesions seen here in the eye of an immunocompetent person. Cysticercerci in the brain and subcutaneous tissue are occasionally reported in immunocompromised humans, particularly patients with AIDS. (From Witner, M., White, A. C., Tanowitz, H. B. *Taenia* and other tapeworm infections. In: Tropical Infectious Diseases: Principles, Pathogens and Practice. Pages 839–847, Figure 121.9. Courtesy of Drs G. J. Weil, R. S. Chuck, and R. J. Olk, Washington University School of Medicine, St Louis, MO.)

Downloaded from Vet-eBooks.com

Trematodes

Intestinal Flukes

Fasciolopsiasis

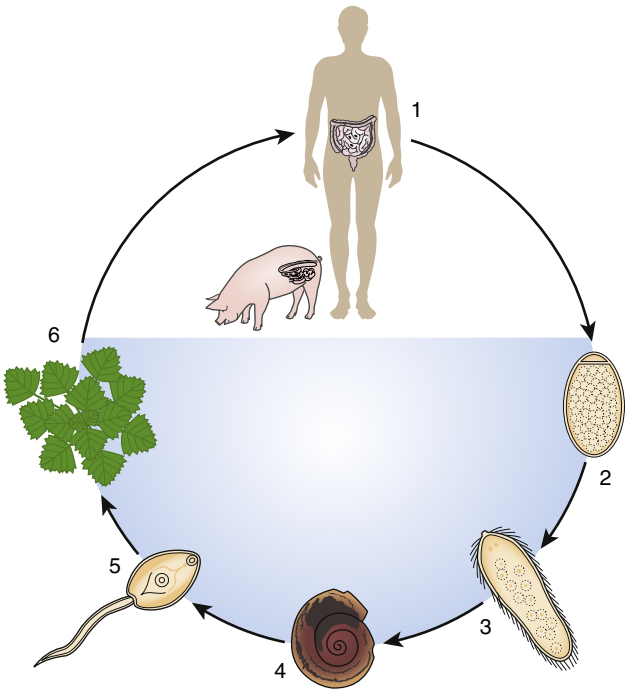


Fig. 3.195 Life cycle of *Fasciolopsis buski*. Adult flukes inhabit the intestine of humans and pigs (1). Unembryonated eggs are passed in stool (2) and embryonate in water, releasing miracidia (3). These penetrate a snail intermediate host (4) and develop from miracidia to sporocysts, rediae and finally cercariae which leave the snail (5). They encyst on aquatic plants as metacercariae (6) and are ingested by humans, pigs or other mammals. After excysting in the duodenum, they attach to the intestinal wall where they mature to adulthood over 3 months. Adults produce up to 25,000 eggs per day and survive around 1 year. (Adapted from CDC; https://www.cdc.gov/dpdx/fasciolopsiasis/index.html)



Fig. 3.196 *Segmentina hemisphaerula*. This snail and a number of species of *Hippeutis* are the first intermediate hosts of *F. buski*. (Courtesy, Professor S-N. Chen. *(x 2.7)*)



Fig. 3.197 The water caltrop. *F. buski* is found in focal areas of China, India and South East Asia and is most common in children. Most infection occurs in wet lowland areas where people regularly consume raw aquatic vegetables and sanitation may be poor. The water caltrop is an aquatic plant which bears a nut-like fruit surrounded by a hard shell. Metacercariae encyst on the hard shell. Although the shell is not eaten, people commonly peel them with their teeth, thereby ingesting metacercariae attached to the shell. (Courtesy, Professor B. G. Maegraith.)

Downloaded from Vet-eBooks.com



Fig. 3.198 Adult *Fasciolopsis buski*.
The adult *F. buski* is the largest parasitic trematode of humans and may reach 7.5 cm in length. Like all flukes, it has both an oral and a ventral sucker. It attaches to the intestinal mucosa resulting in mechanical injury, eosinophilic infiltration and inflammation. Although many infections are asymptomatic, heavy infection may result in severe ulceration with abscess formation, malabsorption and occasionally obstruction.

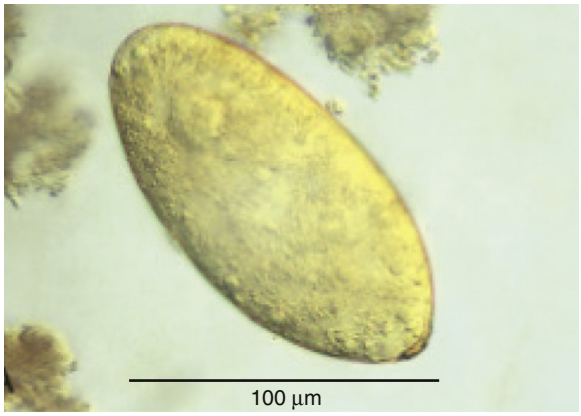


Fig. 3.199 Ovum of *Fasciolopsis buski*.
Eggs of *F. buski* are difficult to distinguish from those of *Fasciola hepatica* (see Fig. 3.225). They measure 140 µm x 80 µm and are ellipsoid in shape. The shell is thin with an indistinct operculum which is often difficult to see. (From Fritsche, T., Pritt, B. S. Medical parasitology. In: Henry's Clinical Diagnosis and Management by Laboratory Methods. Pages 1231–1283.e3, Figure 63-22, Panel A.)

Other Intestinal Flukes



Fig. 3.200 Adult *Metagonimus yokogawai*: an example of a small intestinal fluke.
Many species of small intestinal flukes can infect humans. In general, these measure less than 2.5 mm in length and rarely cause symptoms except in very heavy infection. The best described are *M. yokogawai* in East Asia and *Heterophyes heterophyes* in the Middle East and North Africa. Adults inhabit the small intestine, producing less than 50 eggs per day. Stool examination for ova is insensitive and the diagnosis is often only made after the host receives a dose of praziquantel and adult flukes are passed in the stool. Note the anterior oral sucker, two posterior testes and multiple eggs seen in this adult *M. yokogawai. (x 45.)* (Courtesy, Professor I. Miyazaki.)

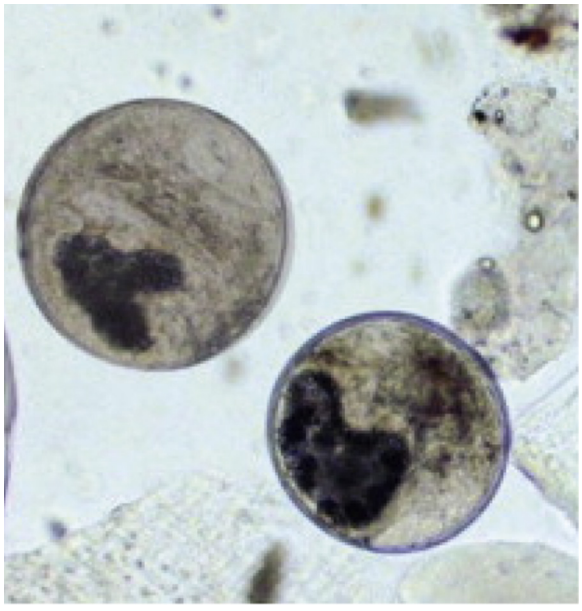


Fig. 3.201 *Metagonimus yokogawai* metacercariae removed from sweetfish.
The life cycles of the *M. yokogawai* and *Heterophyes heterophyes* are similar to that of *Fasciolopsis buski*. However, rather than encysting on aquatic plants, cercariae penetrate the skin of freshwater fish and encyst in their tissue. Humans are infected by ingestion of raw or undercooked fish. These metacercariae were found in the flesh of sweetfish, *Plecoglossus altivelis*, a common delicacy in Korea and Japan. (From Tsubokawa, D., Sugiyama, H., Mikami, F. et al. Collection methods of trematode eggs using experimental animal models. Parasitology International, 2016-10-01, Volume 65, Issue 5, Pages 584–587, Figure 3, Panel A.)

Downloaded From Vet-eBooks.com

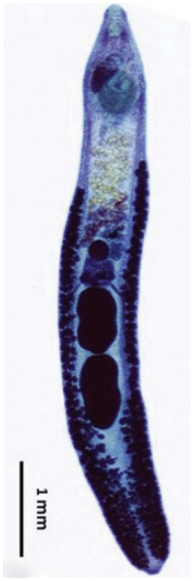


Fig. 3.202 *Echinostoma ilocanum*.
The definitive hosts of *Echinostoma* species are birds and mammals. Humans are accidentally infected by eating raw snails, fish or molluscs in which cercariae encyst. Infection predominatly occurs in South East Asia and most people are asymptomatic except in heavy infections. The differing species vary in size but most measure 3–10 mm in length. (From Sithithaworn, P., Sripa, B., Kaewkes, S., et al. Food-borne trematodes. In: Manson's Tropical Diseases. Chapter 53, Pages 726–736.e2, Figure 53.7, Image A.)

Liver Flukes

Clonorchiasis and opisthorchiasis

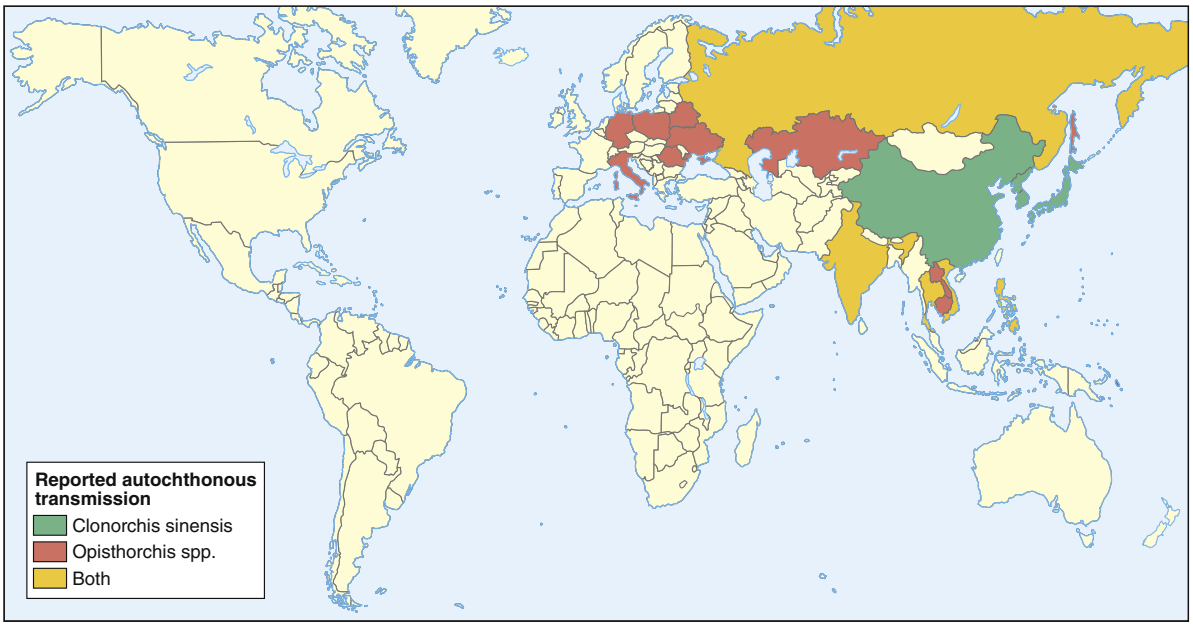


Fig. 3.203 Global distribution of *Clonorchis sinensis*, *Opisthorchis viverrini* and *Opisthorchis felineus*.
This map demonstrates countries reporting autochthonous transmission of various species of liver flukes. *Fasciola* species are not included as they are found worldwide. *C. sinensis* is the commonest liver fluke with an estimated 35 million people infected worldwide, 15 million of whom live in China. *O. viverrini* is predominantly found in South East Asia and India; in Thailand prevalence reaches 15% in some communities. *O. felineus* has a broad distribution stretching from Europe to the Far East with particularly high prevalence in rural fish-eating communities in Siberia. *Metorchis* species have been reported to infect humans in Russia, Greenland and North America but its distribution is currently unclear. (Adapted from Fürst, T., Duthaler, U., Sripa, B., et al. Opisthorchiasis and Clonorchiasis: the oriental liver flukes. Trematode Infections; liver and lung flukes. Infectious Disease Clinics of North America 2012, Volume 26, Pages 399–419.)

Downloaded from Vet-eBooks.com

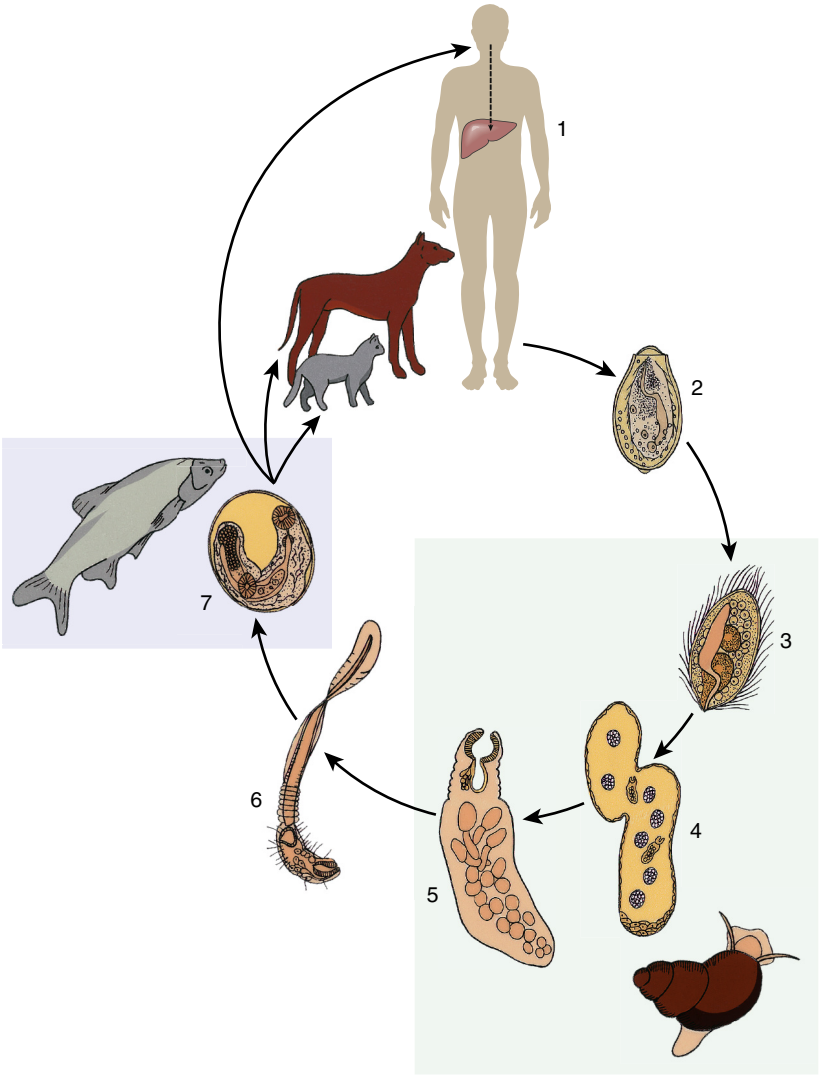


Fig. 3.204 Life cycle of the *Clonorchis sinensis*, *Opisthorchis viverrini* and *Opisthorchis felineus*.
The definitive hosts of *Clonorchis* and *Opisthorchis* species include humans, dogs, cats and other fish-eating mammals. All three flukes have a similar life cycle and pathogenesis. Adult flukes live in small peripheral intrahepatic bile ducts (1), producing embryonated eggs which are passed in faeces (2). When ingested by a snail host, the eggs hatch releasing miracidia (3). Within the snail, these develop into sporocysts (4) then rediae (5) which multiply and become cercariae (6). These leave the snail and penetrate the skin of freshwater fish, encysting within the flesh to form metacercariae (7). When consumed raw by a carnivore, the immature flukes emerge, migrating through the ampulla of Vater, up the bile ducts and eventually settling to mature in the small peripheral branches of the biliary tree (1).

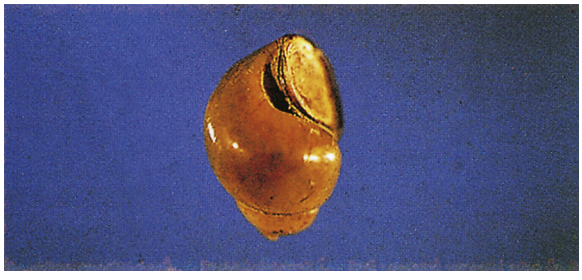


Fig. 3.205 Intermediate host of *Clonorchis sinensis* and *Opisthorchis spp.*
Bithynia funiculata is an intermediate host of *C. sinensis*, *Opisthorchis spp.* and *Echinostoma* species. (x 3.2.) (Courtesy, Dr S. Vajasthira.)

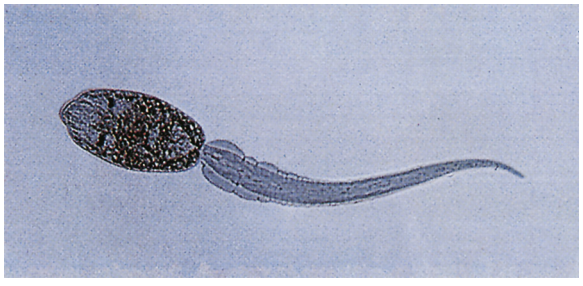


Fig. 3.206 Cercaria of *Clonorchis sinensis*.
Cercariae leave the snail to encyst under the scales of various species of freshwater cyprinoid fish. (x 62.) (Courtesy, Professor M. Suzuki.)

Downloaded from Vet-eBooks.com

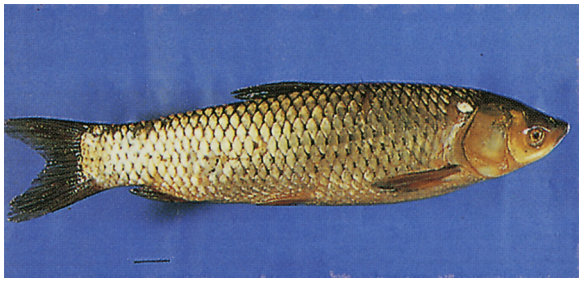


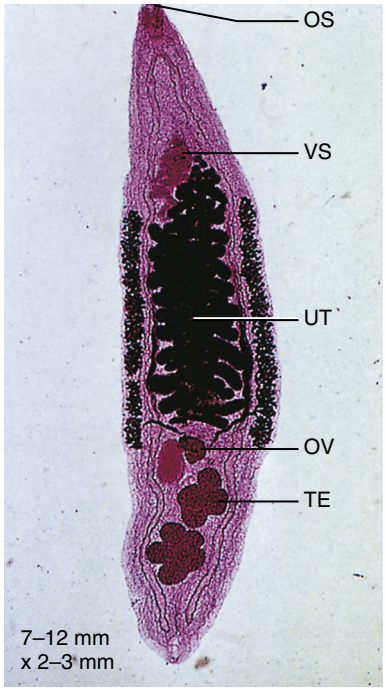
Fig. 3.207 *Ctenopharyngodon idella.*
Ctenopharyngodon idella, the grass carp, is a regular host for metcercariae of *C. sinensis* and is a common food product, particularly in China. More than five million tonnes of this fish are produced through aquaculture each year, making it the most commonly farmed fish species worldwide. (Courtesy, Professor S-N. Chen.)

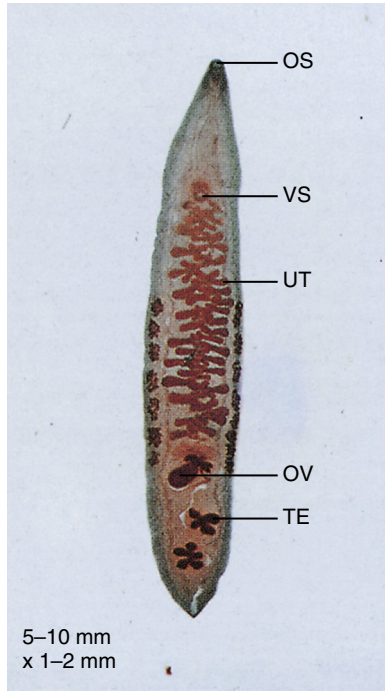


Fig. 3.208 Metacercaria in fish flesh.
Humans are infested by eating raw or undercooked fish containing metacercariae. These excyst in the duodenum. (x 160.) (Courtesy, Professor M. Suzuki.)



Fig. 3.209 Living adult *Clonorchis sinensis.*
The immature flukes migrate up the common bile duct to the small peripheral intrahepatic bile ducts. When mature, they reach 2.5 cm in length and may live for many years. (x 2.5.) (Courtesy, Professor I. Miyazaki.)





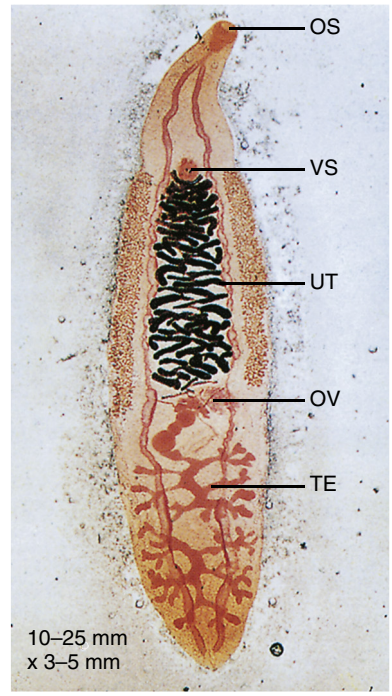


Fig. 3.210–212 Adult flukes of *Opisthorchis felineus* (left, 3.194), *Opisthorchis viverrini* (centre, 3.195), and *Clonorchis sinensis* (right 3.196).
All three flukes have a similar life cycle, pathogenesis and egg morphology. However, adult flukes of each species can be distinguished morphologically. Both genera have a ventral sucker that is smaller than the oral sucker. The species differ in their overall size together with the shape of their testes (marked).
Key: OS – oral sucker, VS – ventral sucker, UT – uterus, OV – ovary, TE – testes.

Downloaded from Vet-eBooks.com



Fig. 3.213 Ovum of *Clonorchis sinensis*.
Ova measure 30 µm x 15 µm and are oval in shape. There is an operculum and a small abopercular knob. (From Fritsche, T. R., Pritt, B. S. Medical parasitology. In: Henry's Clinical Diagnosis and Management by Laboratory Methods. Chapter 63, Pages 1231–1283.e3, Figure 63–22, Panel D.)



Fig. 3.214 Section of *Clonorchis sinensis* in the bile duct.
Direct mechanical damage, chemical irritation from excreted fluke products and immune-mediated inflammation result in fibrotic changes in the bile duct. (x 25.) (Courtesy, Professor S. Lucas.)

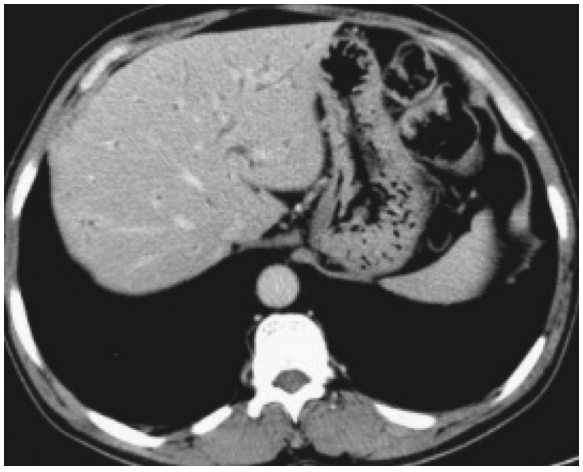


Fig. 3.215 CT changes in *Clonorchis sinensis* infection.
Many infected people remain asymptomatic, although some may develop right upper quadrant pain with biliary tract symptoms. Non-malignant complications include gallstones, cholecystitis, cholangitis and obstructive jaundice. Imaging typically shows dilatation of the peripheral intrahepatic bile ducts, which is diffuse and uniform and spares the extrahepatic ducts, which remain of normal calibre. (From Lim, J. H., Kim, K. W., Choi, D-i. Biliary tract and gallbladder. In: CT and MRI of the Whole Body. Chapter 42, Pages 1192–1267, Figure 42-43, Panel A.)



Fig. 3.216 Endoscopic retrograde cholangiography (ERCP) in a patient with *Clonorchis sinensis* infection.
ERCP, or magnetic resonance cholangiography, may reveal small leaflike filling defects measuring 2 mm to 10 mm in the intrahepatic bile ducts, indicated here by arrowheads. (From Lim, J. H., Kim, K. W., Choi, D-i. Biliary tract and gallbladder. CT and MRI of the Whole Body. Chapter 42, Pages 1192–1267, Figure 42-44, Panel A.)

Downloaded From Vet-eBooks.com

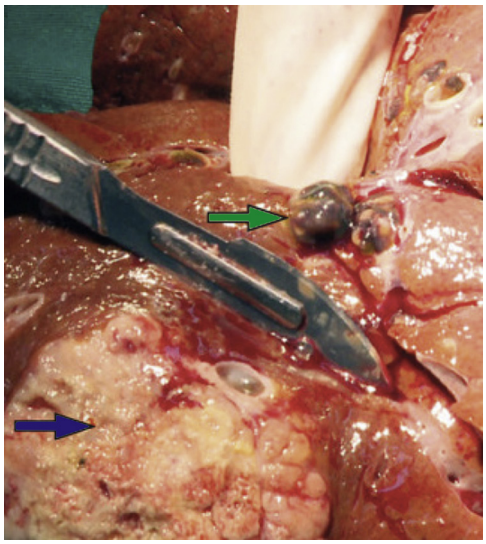


Fig. 3.217 Liver infected with *Clonorchis sinensis* causing cholangiocarcinoma.
C. sinensis and *Opisthorchis viverrini* are associated with a 5 to 15 times increased risk of cholangiocarcinoma. This is a major public health issue in some areas such as north-east Thailand where cholangiocarcinoma is one of the leading causes of death. There is increasing evidence for the association between *Opisthorchis felineus* and cholangiocarcionma. Note the cholangiocarcinoma in the lower left corner (blue arrow) and a *C. sinensis* fluke in the upper right corner (green arrow). (From Qian, M.-B., Utzinger, J., Keiser, J., et al. Clonorchiasis. The Lancet, 2016-02-20, Volume 387, Issue 10020, Pages 800–810, Figure 2, Panel A.)

Fascioliasis

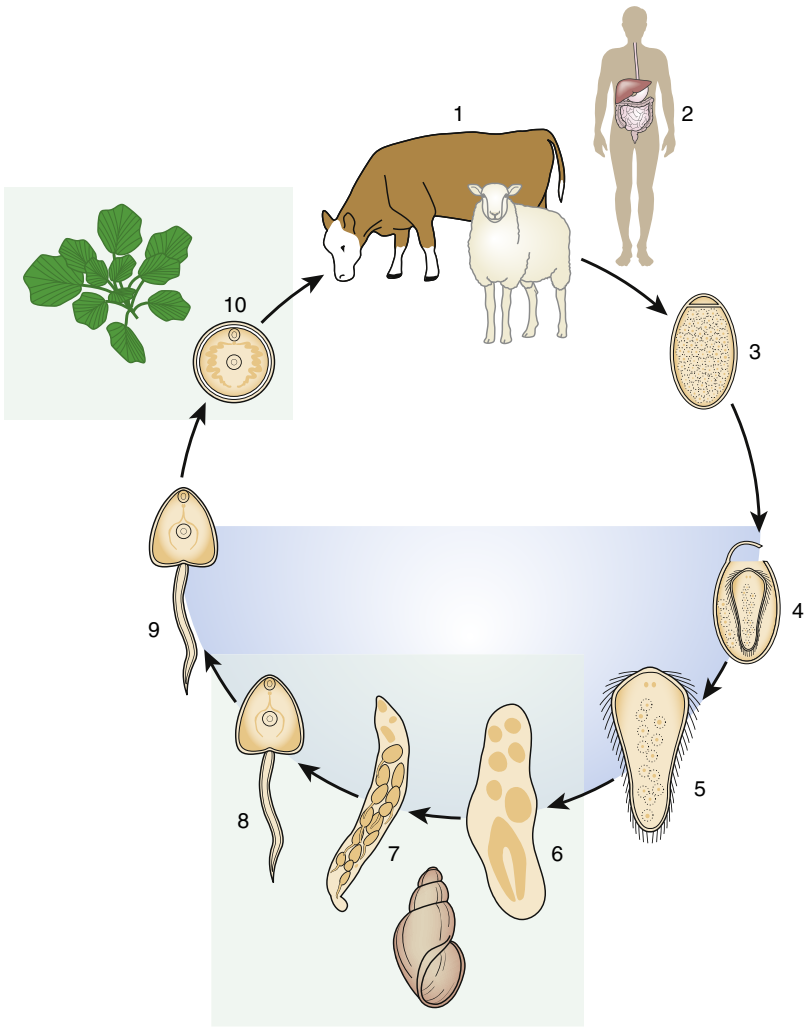


Fig. 3.218 Life cycle of *Fasciola* species.
Sheep and cattle are the definitive hosts of *Fasciola hepatica* and *Fasciola gigantica* (1). Humans are accidentally infected but can also act as definitive hosts (2). The adult fluke lives in the large bile ducts, releasing unembryonated eggs in the stool (3). These embryonate in water (4), releasing miracidia (5) which penetrate the snail intermediate host. Within the snail, miracidia develop into sporocysts (6), then rediae (7), then cercariae (8). Cercariae leave the snail intermediate host (9), encysting as metacercariae on aquatic plants such as watercress (10). When ingested by the mammalian host, the metacercariae excyst in the duodenum. The immature fluke migrates through the duodenal wall and, via the peritoneum, into the liver where it finally rests in the large bile ducts, causing considerable parenchymal damage along the way. (Adapted from CDC; https://www.cdc.gov/dpdx/fascioliasis/)

Downloaded from Vet-eBooks.com

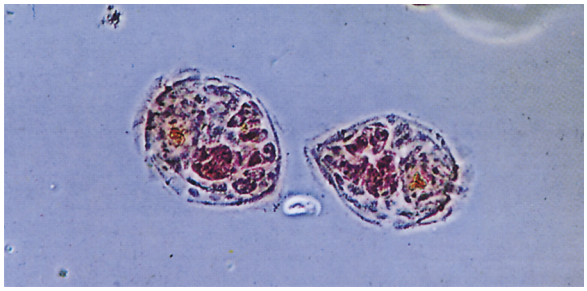


Fig. 3.219 Miracidia of *Fasciola hepatica*.
Motile miracidia hatch from eggs passed in faeces and infect snails of the genus *Galba*. *(x 225.)*



Fig. 3.220 *Galba truncatula* (formally *Lymnaea truncatula*).
This snail is a common intermediate host of *F. hepatica*. The broad geographical and climate range of the family Lymnaeidae is in part responsible for the global distribution of fascioliasis. (x 5.) (Courtesy, Dr J. M. Jewsbury.)



Fig. 3.221 Redia from intermediate host.
In the snail host, redia develop from a sporocyst to become a cercaria. (x 30.)

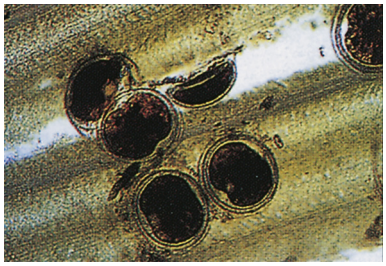


Fig. 3.222 Metacercariae on grass.
Cercariae encyst on aquatic plants as metacercariae where they can be ingested by herbivores or humans. (x 75.) (Courtesy, Dr M. Murray.)



Fig. 3.223 Watercress: a common source of *Fasciola* infection.
Herbivores are infected by grazing wet pasture where the intermediate hosts are found. Humans are most often infected by eating wild watercress which grows commonly in swampy pasture by small streams and is a rich source of vitamin K, C and A.



Fig. 3.224 Adult *Fasciola hepatica*.
Adult flukes of *F. hepatica* measure up to 30 mm in length in contrast to *F. gigantica* which can measure 75 mm. Note the cone-shaped anterior end which gives the parasite a leaf-like shape. (From Fürst, T., Duthaler, U., Sripa, B., et al. Trematode infections. Infectious Disease Clinics of North America, 2012-06-01, Volume 26, Issue 2, Pages 399–419, Figure 3, Panel C.)

Downloaded From Vet-eBooks.com

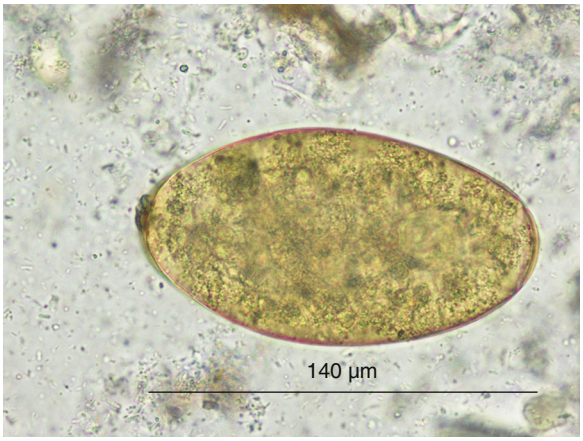


Fig. 3.225 Ovum of *Fasciola hepatica.*
Eggs of *F. hepatica* are difficult to distinguish from those of *Fasciolopsis buski* (see Fig. 3.199). They measure 140 µm x 75 µm and are ellipsoid in shape with a thin shell. An operculum is present but this may be difficult to see. The abopercular end is sometimes irregular and roughened, a feature not seen in *F. buski*. (Courtesy, H. Edwards.)



Fig. 3.226 Migrating immature flukes in sheep liver.
After ingestion, the metacercariae pass through the intestinal wall and the peritoneum before penetrating the liver capsule to enter the liver parenchyma. The fluke's transit track is often characterized by a prominent inflammatory response. (H&E x 20.)

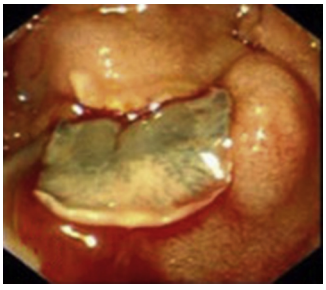


Fig. 3.227 Adult Fasciola hepatica in duodenum.
This adult *Fasciola hepatica* was seen on endoscopy. (Soga K., Handa O., Yamada M., et al. In vivo imaging of intestinal helminths by capsule endoscopy. Parasitology International 2014. 63 (1) Pages 221-228. Figure 1B.)

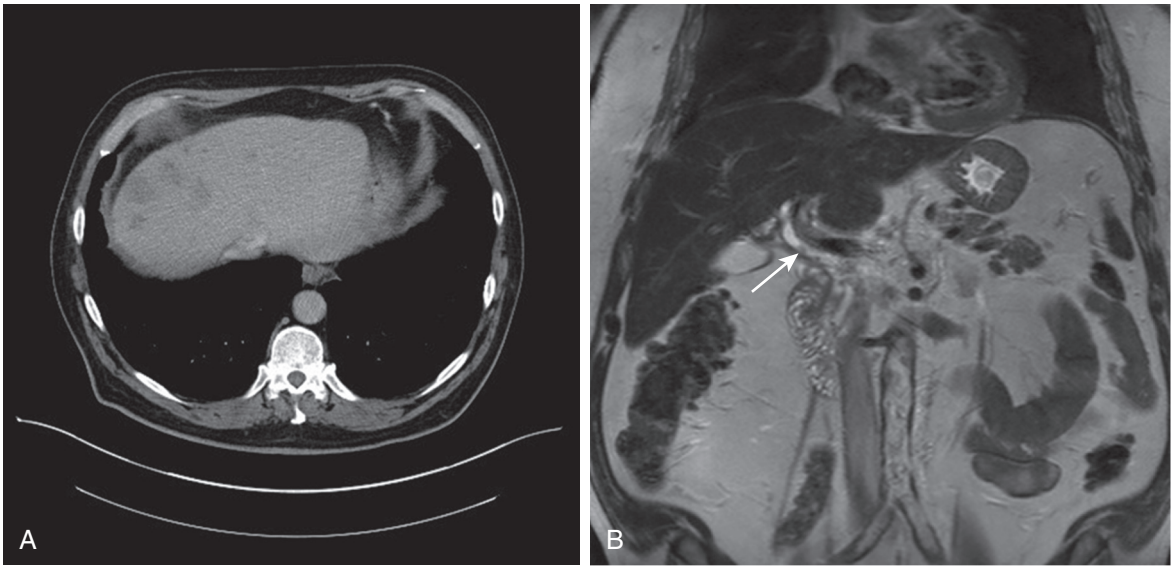


Fig. 3.228 (A, B) Acute *Fasciola hepatica* infection.
This patient presented with right upper quadrant pain, an eosinophilia and deranged liver function tests. CT imaging revealed patchy nodular abnormalities in both hepatic lobes which was initially thought to represent metastatic malignancy (A). Biopsy showed an eosinophilic infiltrate and eggs of *Fasciola spp.* were subsequently identified in the stool. Note the filling defect in the common bile duct (B). (Courtesy, P. L. Chiodini.)

Downloaded from Vet-eBooks.com



Fig. 3.229 Ectopic cutaneous *Fasciola gigantica*.
Immature flukes occasionally cause cutaneous or visceral larva migrans by migrating to an ectopic destination. The haemorrhagic migration tract of this ectopic *F. gigantica* is clearly shown in the subcutaneous tissue of this patient. (From Wattanagoon, Y., Bunnag, D. Liver fluke infections. In: Hunter's Tropical Medicine and Emerging Infectious Diseases. Pages 887–891, Figure 124.6. Copyright © 2013, Elsevier, Inc. All rights reserved.)

Dicrocoeliasis

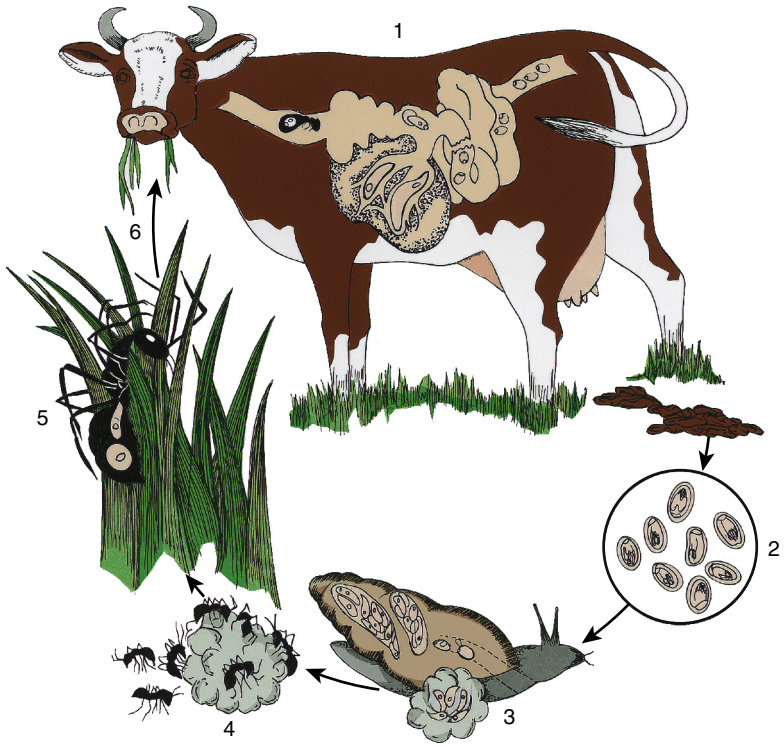


Fig. 3.230 Life cycle of *Dicrocoelium dendriticum*.
The definitive hosts of *D. dendriticum* are ruminants (1) and snails are the first intermediate host. However, it is unusual in having a second intermediate host—an arthropod—in which it induces behavioural change that increases transmission of the parasite. Embryonated eggs are passed in stool (2) and ingested by the snail intermediate host. Within the snail, miracidia hatch to become sporocysts and then cercariae (3). Cercariae are ejected from the snail in slime balls, each containing several hundred cercariae. These are eaten by ants where cercariae encyst into metacercariae within the body cavity (4). Their presence causes a remarkable change in the behaviour of the ants inducing them to climb to the tips of vegetation where they remain overnight (5). This makes them significantly more likely to be ingested by grazing animals in the cooler hours, thus facilitating parasite transmission (6). Once ingested by the herbivore, the parasites excyst in the duodenum and migrate to the smaller bile ducts.

Downloaded from Vet-eBooks.com

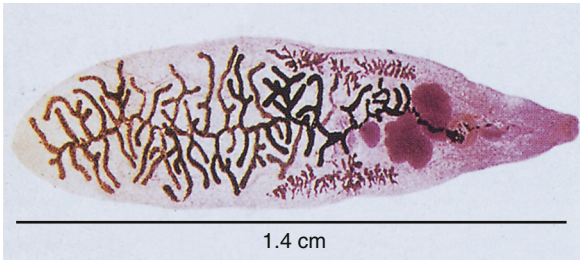


Fig. 3.231 Adult *Dicrocoelium dendriticum*.
Adults of *D. dendriticum* measure up to 1.5 cm in length and inhabit the small bile ducts. Human infection is rare and usually asymptomatic. Heavy infection may occasionally result in cholecystitis or liver abscess.

Lung Flukes

Paragonimiasis

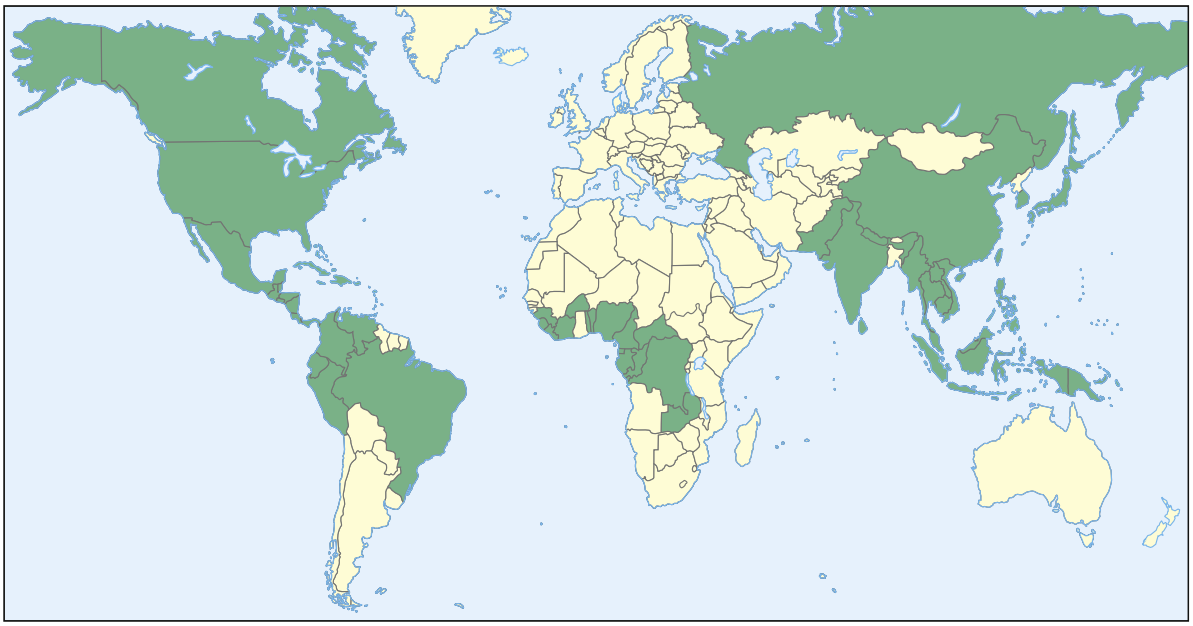


Fig. 3.232 The global distribution of paragonimiasis.
This map demonstrates countries reporting autochthonous transmission of *Paragonimus* species. An estimated 20 million people are infected worldwide, 10 million of whom live in China. Species vary geographically. *P. westermani* accounts for most infections and occurs in China, Japan and Korea. *P. heterotremus* is found in South East Asia and *P. uterobilateralis* in Nigeria. (From Fürst, T., Duthaler, U., Sripa, B., et al. Trematode infections. Infectious Disease Clinics of North America, 2012-06-01, Volume 26, Issue 2, Pages 399–419, Figure 1, panel E.)

Downloaded From Vet-eBooks.com

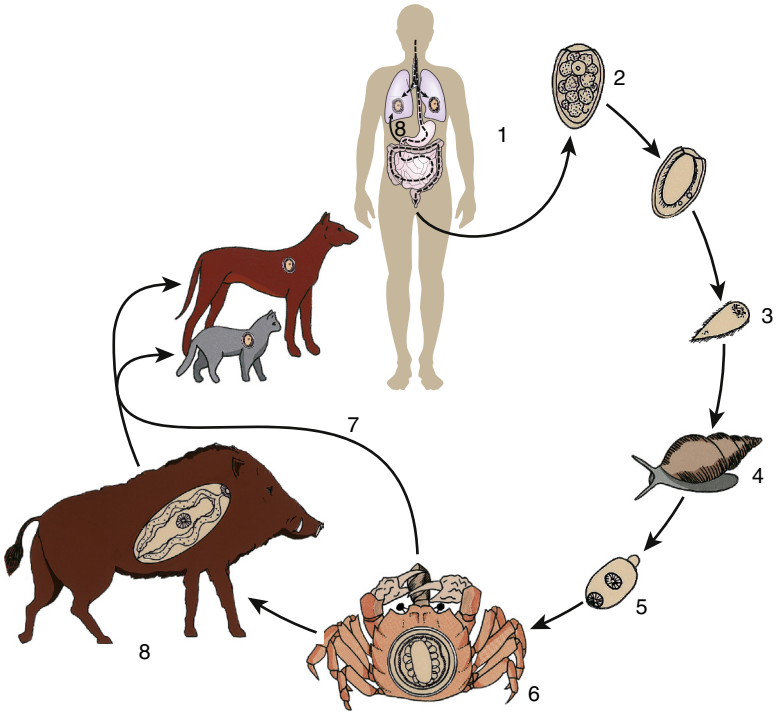


Fig. 3.233 Life cycle of *Paragonimus* species.
Adult flukes live partly encapsulated in the lung parenchyma of infected carnivores, most commonly canines, felines and humans (1). Unembryonated eggs pass into the alveoli and are then coughed up in sputum or swallowed and passed in the stool (2). Eggs embryonate in water and hatch to release miracidia (3). These penetrate the first intermediate host, the snail, multiplying into rediae and then cercariae (4). The cercariae leave the snail (5) and encyst as metacercariae on the gills or in the flesh of crustaceans, the second intermediate host (6). Carnivores become infected by eating the raw flesh of crustaceans containing metacercariae (7). These hatch in the duodenum, producing young flukes which migrate through the gut wall, the mesentery and diaphragm to reach the pleural cavity and finally the lung parenchyma. Here they mature, become partially encapsulated and produce eggs (1). Wild boar serve as paratenic hosts for *P. pulmonalis* and humans may become infected by eating their uncooked flesh (8).



Fig. 3.234 The African civet, *Civettictis civetta*.
This carnivore is a primary reservoir host for both *Paragonimus africanus* and *P. uterobilateralis* in West Africa. (Courtesy, Dr N. Cumberlidge.)



Fig. 3.235 *Ranguna smithiana*: a host of lung fluke.
This species is a host of *Paragonimus heterotremus* in Thailand. Crabs are commonly eaten raw or in the form of an uncooked paste, with which the metacercariae are ingested. (Courtesy, Professor I. Miyazaki.)

Downloaded From Vet-eBooks.com

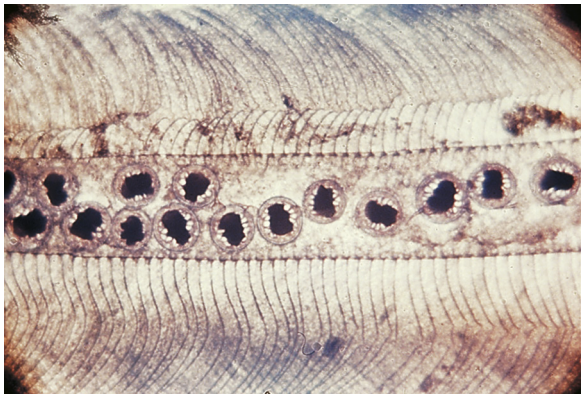


Fig. 3.236 Metacercariae of *Paragonimus pulmonalis*.
Here they are located along a gill bar of the crab *Eriocheir japonicas*. (Courtesy, Professor I. Miyazaki.)

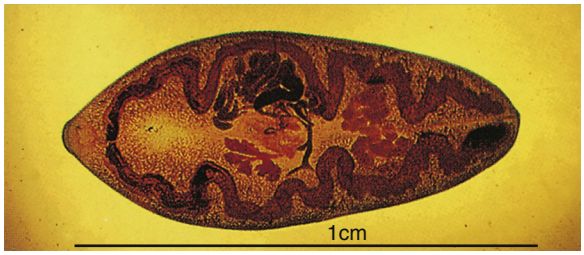


Fig. 3.237 Adult *Paragonimus westermani*.
Adult flukes measure 1 cm x 0.5 cm and are ovoid in shape. The lobed ovary is located anterior to two branching testes. (Courtesy, Dr S. Vajasthira.)



Fig. 3.238 Living adult *Paragonimus westermani*.
Living adult *P. westermani* are lemon shaped. Compare this with the specimen above which has been flattened and distorted during preparation. (x 4.3.) (Courtesy, Professor Y. Yoshida.)



Fig. 3.239 Lung histology in paragonimiasis.
Encapsulated within an inflammatory and fibrotic host tissue reaction, two adult *Paragonimus westermani* flukes are seen in this lung section. (H&E x 20.)

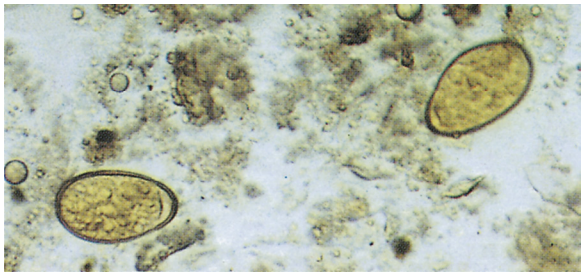


Fig. 3.240 Eggs in human sputum.
Eggs measure 85 μm x 50 μm and are ovoid in shape. They are often asymmetrical; the opercular end is flatter whilst the abopercular end has a slightly thickened shell. (x 150.) (Courtesy, Professor D. A. Warrell.)

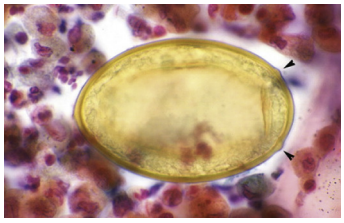


Fig. 3.241 *Paragonimus kellicotti*.
P. kellicotti occasionally causes infection following consumption of raw crayfish in the USA. The eggs differ slightly to *P. westermani;* note the opercular shoulders (arrowheads) and the absence of abopercular thickening. (From Procop, G. W., Neafie, R. C. Human parasitic pulmonary infections. Pulmonary Pathology, Chapter 14, Pages 287–314, Figure 14-16)

Downloaded from Vet-eBooks.com

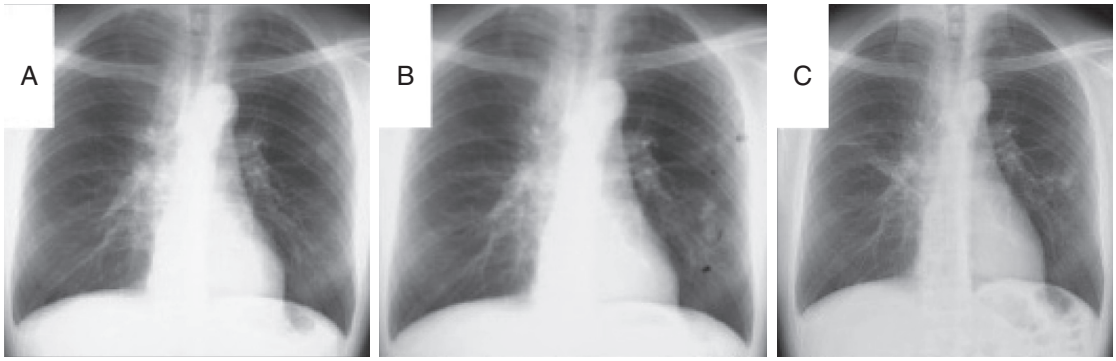


Fig. 3.242 Chest radiographs showing wandering lung nodules.
This Japanese man developed an eosinophilic pneumonia after eating raw crab and later developed chronic haemoptysis. These chest radiographs are taken at 1 year intervals; note the wandering pulmonary nodules. (From Yatera, K., Hanaka, M., Hanaka, T. A rare case of paragonimiasis miyazakii with lung involvement diagnosed 7 years after infection: A case report and literature review. Parasitology International, Volume 64, Issue 5, Pages 274–280. Fig. 1A-C.)

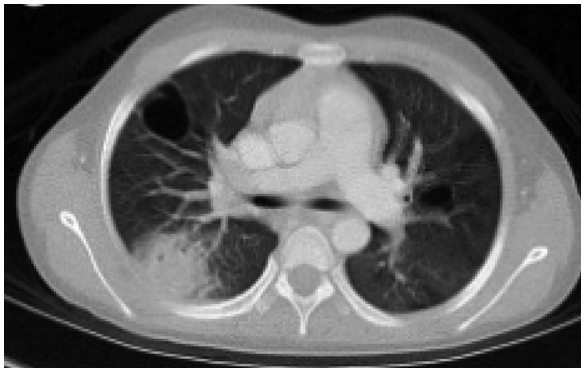


Fig. 3.243 Chronic pulmonary paragonimiasis.
Paragonimiasis is frequently misdiagnosed as tuberculosis (TB), although, in the former, lesions characterictically occur in the mid or lower zones and are peripherally located. This child had been diagnosed with pulmonary TB on the basis of multiple cavitatory pulmonary lesions. She subsequently developed seizures and was initially thought to have developed TB meningitis (see Fig. 3.244). Lung biopsy revealed a pulmonary eosinophilia and stool sample was positive for ova of *P. westermani*. (From Kohli, S., Farooq, O., Jani, R. B. et al. Cerebral paragonimiasis: an unusual manifestation of a rare parasitic infection. Pediatric Neurology, 2015-03-01, Volume 52, Issue 3, Pages 366–369, Figure 1, panel B.)

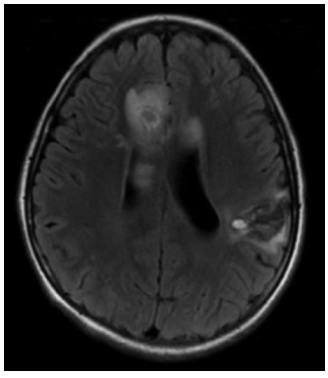


Fig. 3.244 Cerebral paragonimiasis.
Cerebral paragonimiasis, due to ectopic fluke migration, is rare but may have severe consequences. Note the ring-enhancing lesion in the frontal lobe with surrounding oedema and the second lesion in the parietal lobe. Cerebral lesions may mimic tuberculosis, cerebral abscess or neurocysticercosis on imaging. (From Kohli, S., Farooq, O., Jani, R.B. et al. Cerebral paragonimiasis: an unusual manifestation of a rare parasitic infection. Pediatric Neurology, 2015-03-01, Volume 52, Issue 3, Pages 366–369, Figure 2, panel A.)

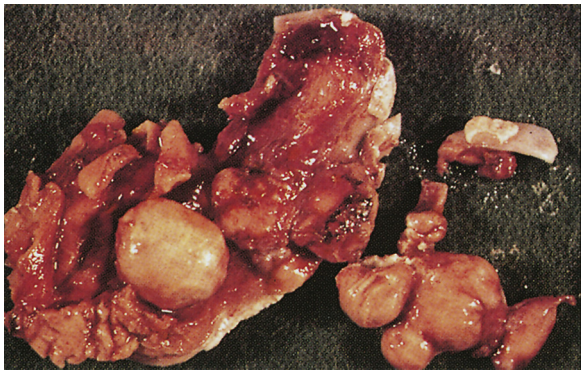


Fig. 3.245 *Paragonimus* cyst extracted from brain at autopsy.
A cyst of *P. westermani* found at autopsy of a 21-year-old Japanese girl. (Courtesy, Professor A. Ishii and Dr N. Suzuki.)

Downloaded From Vet-eBooks.com

PARASITIC CRUSTACEANS

Pentastomiasis



Fig. 3.246 *Adult Linguatula serrata* from a dog.
Pentastomids are a group of parasitic maxillopod crustaceans which occasionally cause human infection. Adult *L. serrata* live in the upper respiratory tract of carnivores, and eggs are shed in saliva, nasal secretions and stool. (Courtesy, H. Rowe.)



Fig. 3.247 Adult *Linguatula serrata*.
Ova ingested by herbivores or humans become larvae in the gut, migrating through the gut wall to encyst within tissues, most commonly the liver. This figure shows the cephalic third of the adult worm which can reach 10 cm in length. Note the oral opening and four hooks which give this subclass its name, *Pentastomida*, meaning five openings. (x 3.)



Fig. 3.248 Halzoun syndrome in a Lebanese woman.
In countries such as Lebanon, Iran and Sudan, where people consume dishes containing raw goat or sheep liver, a clinical syndrome known as halzoun or marrara occasionally occurs. Patients present with sneezing, cough, nasal congestion and facial oedema following ingestion of raw liver. *L. serrata* larvae may subsequently be retrieved from their nasopharynx. Both *Fasciola hepatica* and *Dicrocoelium dendriticum* have been reported to cause a similar clinical syndrome. (Courtesy, Dr G. Khalil and Professor J. F. Schacher.)



Fig. 3.249 Adult *Porocephalus crotali* in rattlesnake lung.
Adult worms of *P. crotali* and *Armillifer armillatus* live in the airways of large snakes. Eggs are shed into the environment in airway secretions and faeces. When ingested by mammalian hosts such as rodents and monkeys, the eggs hatch and larvae encyst in viscera. The life cycle is completed when the small mammal is ingested by a snake. Note the multiple adult worms in the lungs of this rattlesnake. (Courtesy, Professor J. T. Self.)

Downloaded from Vet-eBooks.com



Fig. 3.250 Adult male and female *Armillifer armillatus*.
Humans are occasionally infected with larvae following ingestion of contaminated food. Most remain asymptomatic; occasionally patients may present with abdominal pain, chronic cough, intestinal obstruction or enterocolitis depending on the site and burden of infection. (x 0.7.) (Courtesy, The Director, Armed Forces Institute of Pathology, Washington, DC.)

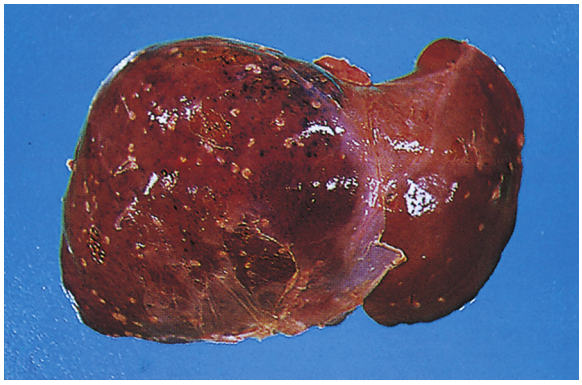


Fig. 3.251 Larvae of *Armillifer armillatus* in a human liver.
Third-stage larvae are seen under the capsule of the liver of a Nigerian at post-mortem. (Courtesy, Dr J. A. Smith and Ibadan University.)

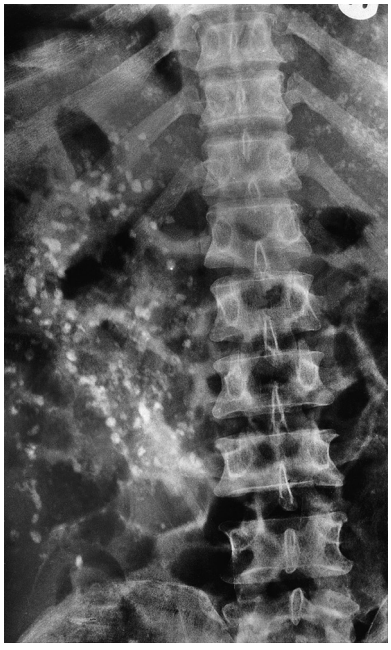


Fig. 3.252 Radiograph of calcified nymphal cysts of *Armillifer armillatus*.
The C-shaped, encysted nymphs of *A. armillatus* are occasionally seen in diagnostic radiographs taken for unrelated symptoms. The burden of infection seen here is remarkable.

Downloaded from Vet-eBooks.com

4. Infections Acquired by Airborne Transmission

Pneumonia continues to exert a terrible toll on health, especially in childhood, where it is the leading infectious cause of death in under-fives. Airborne infections, whether viral, bacterial or fungal, are principally acquired by inhalation of pathogenic organisms, either directly from the environment as spores or attached to dust particles, or within aerosolized droplets and droplet nuclei generated by the respiratory tract mucosa. Some respiratory tract viral infections may also be transmitted by contaminated hands and fomites.

For most of the respiratory viruses the reservoir is human, and there is little demonstration of a capacity to cross species barriers effectively. However, the past 2 decades have witnessed several examples of the potentially devastating effects of cross-species viral transmission: in late 2002 a newly identified animal coronavirus causing a severe acute respiratory syndrome (SARS) gave rise to a major epidemic that disseminated globally through international air travel with alarming rapidity. A decade later another animal virus causing severe respiratory illness was identified in Saudi Arabia—Middle East Respiratory Syndrome coronavirus (MERS-CoV).

These two infections dramatically illustrate the unpredictable epidemic potential of zoonotic viruses that are able to transmit across species barriers and cause human respiratory infection. Indeed, perhaps the most alarming global health threat remains that of a novel transmissible and pathogenic avian influenza strain—for which there are a number of historical pandemic precedents. An array of measures have been developed to limit the pandemic potential of highly pathogenic avian influenza. These include continual sentinel site surveillance, prompt quarantine, flock vaccination and mass culling of domestic poultry when necessary. However, it is clear that humans will continue to be exposed to both old and new zoonotic viral infections for as long as we maintain close exposure to animals.

By contrast, few bacterial pneumonias are zoonotic in origin, the usual reservoir being the respiratory tract of human carriers. Thus, mass population gatherings, whether through displacement caused by strife and famine or voluntary pilgramages such as the Hajj, provide opportunities for transmission and may even play a role in promoting pathogen evolution. Vaccines directed against the virulent bacterial serotypes of *Streptococcus pneumoniae* have been introduced into mass childhood immunization campaigns, along with vaccines against *Haemophilus influenzae* serotype B, diphtheria toxin and whooping cough (*Bordetella pertussis*), and these have impacted significantly on the incidence of severe childhood pneumonia. Understandably, much attention is now focused on the evolution of serotype replacement and switching.

Tuberculosis (TB) is currently the leading infectious cause of death worldwide, with over 10 million estimated new cases in 2016, accounting for 1.4 million deaths. Primarily a disease of lower-income populations, its epidemiological map overlaps with that of HIV infection, particularly in sub-Saharan Africa, and TB causes one-third of HIV deaths. Concerted public health drives have reduced both TB incidence and mortality over the past 2 decades, but enormous challenges remain. Affordable diagnostics are insensitive, treatment courses prolonged, and one-quarter of the world's population is latently

Downloaded From Vet-eBooks.com

infected and remains at persistent risk of reactivation; most worryingly, the prevalence of multi-drug resistance, with its associated difficulties and costs of treatment, is increasing.

The universal distribution of environmental fungi means that inhalation of spores is an unavoidable occurrence. Subsequent development of systemic and potentially life-threatening disease, however, is dependent upon the burden of exposure, the integrity of host immunity and the pathogenic potential of the particular fungal species inhaled—the epidemiology of which will reflect local climatic and geographical conditions.

VIRAL INFECTIONS

Coronaviruses

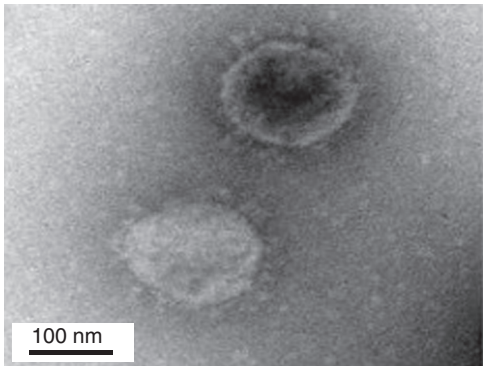


Fig. 4.1 Electron micrograph of severe acute respiratory syndrome-coronavirus (SARS-CoV).
The morphology of an enveloped virus with protruding spikes is characteristic of coronaviruses. SARS-CoV was identified as the causative agent of a novel 'severe acute respiratory syndrome' (SARS). Originating in Guangdong Province, China in 2002, the outbreak continued for 8 months before it was contained; the economic cost of the epidemic was estimated at US$40 million. (From Sridhar, S., To, K.K.W., Chan, J.F.W., et al. A systematic approach to novel virus discovery in emerging infectious disease outbreaks. Journal of Molecular Diagnostics, 2015, Volume 17 (3), Pages 230–241 Figure 2. Copyright © 2015 American Society for Investigative Pathology and the Association for Molecular Pathology.)

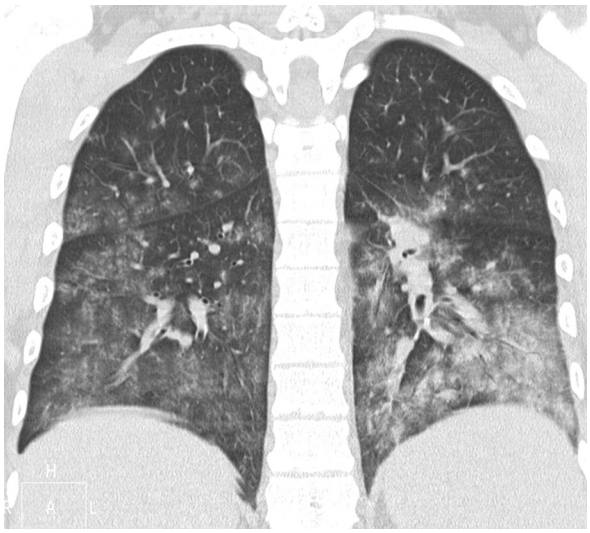


Fig. 4.2 Lung changes in severe acute respiratory syndrome (SARS).
SARS in a previously healthy 43-year-old woman with dyspnoea and fever. Coronal CT shows bilateral ground-glass pneumonitis in lower lung zones. By the end of the SARS epidemic over 8000 cases had occurred across 37 countries, spread by global travel and person-to-person transmission. The novel infection carried a case mortality rate of over 9.5% (From Franquet, T. The normal chest. In: Grainger & Allison's Diagnostic Radiology, 6th edition. Pages 246–266, Figure 12.30. Copyright © 2014 Elsevier Ltd.)



Fig. 4.3 The masked palm civet, *Panguma larvata*, a possible reservoir of the SARS-CoV.
This animal, a popular local culinary delicacy, was farmed in large numbers in Guangdong Province in 2002 at the time of the SARS outbreak. Although it was implicated as the likeliest original source of the epidemic after isolation of the virus from market animals, the civet probably represented an intermediate conduit from other animal species, including several species of *Rhinolophus* horseshoe bat, which probably comprise the natural reservoir. As with other zoonotic infections, SARS-CoV is unlikely to be eradicated globally and could still represent a recurrent threat to human health. (Courtesy, China Daily and H. Xiao.)

Downloaded from Vet-eBooks.com



Fig. 4.4 Camels—a possible reservoir of Middle East respiratory syndrome coronavirus (MERS-CoV).
As with SARS, MERS-CoV is another zoonotic respiratory viral illness where bats have been implicated as the original reservoir, and camels have been proposed as the main zoonotic species providing human exposure. The mechanism of transmission is not yet elucidated, nor whether other animal reservoirs exist, but there are some temporal associations suggestive of a link with weaning of camel foals. Human-to-human transmission of MERS-CoV has occurred primarily in healthcare settings, with a mortality rate exceeding 35% in those with impaired immunity. (Courtesy, L. Freer. From Phillips, L.L. and Semple, J. In Auerbach's Wilderness Medicine. Pages 617–645, Figure 30–35. Copyright © 2017 Elsevier Inc. All rights reserved.)

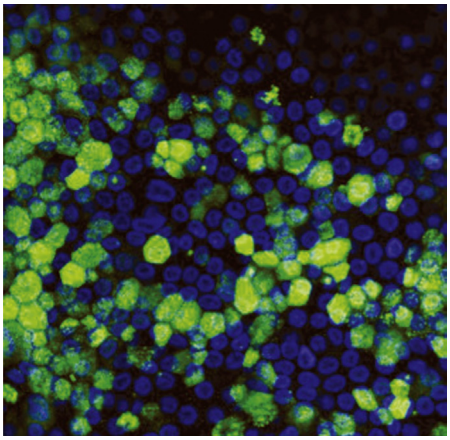


Fig. 4.5 Middle East respiratory syndrome-coronavirus (MERS-CoV) in a bronchoalveolar lavage specimen.
MERS-CoV antigen detection using an indirect immunofluorescent antibody stain showing virally infected human airway cells (green staining are MERS-CoV-positive cells, blue staining are uninfected respiratory epithelium). The emergence of a novel pathogen brings special challenges: the development of both an accurate clinical case definition and new diagnostic assays. (From Zumla, A., Hui, D.S., and Perlman, S. Middle East respiratory syndrome. Lancet Volume 386, Pages 995–1007, Figure 2. Copyright © 2015 Elsevier Ltd.)

Influenza Viruses



Fig. 4.6 Domestic ducks in an Asian wet market.
Migratory waterfowl are the natural reservoir for avian influenza viruses that can spread into domestic poultry causing up to 100% flock mortality within 48 hours. Intensive close-contact poultry farming encourages opportunities for viral recombination, mutational events and cross-species transmission; the virulent H5N1 strain caused deaths in 1997 and again in 2004 and 2005 in China and Vietnam, and necessitated destruction of millions of chicken and ducks. (©FAO/Hoang Dinh Nam.)



Fig. 4.7 Raw poultry in a Shanghai market.
The handling of contaminated, uncooked poultry as seen on this market stall, as well as contact with live birds, represents a potential risk for the spread of avian influenza viruses to humans. Infected humans, too, can harbour the virus widely throughout body tissues and fluids, including faeces, indicating a potential for human-to-human spread by fomites in crowded environments.

Downloaded from Vet-eBooks.com

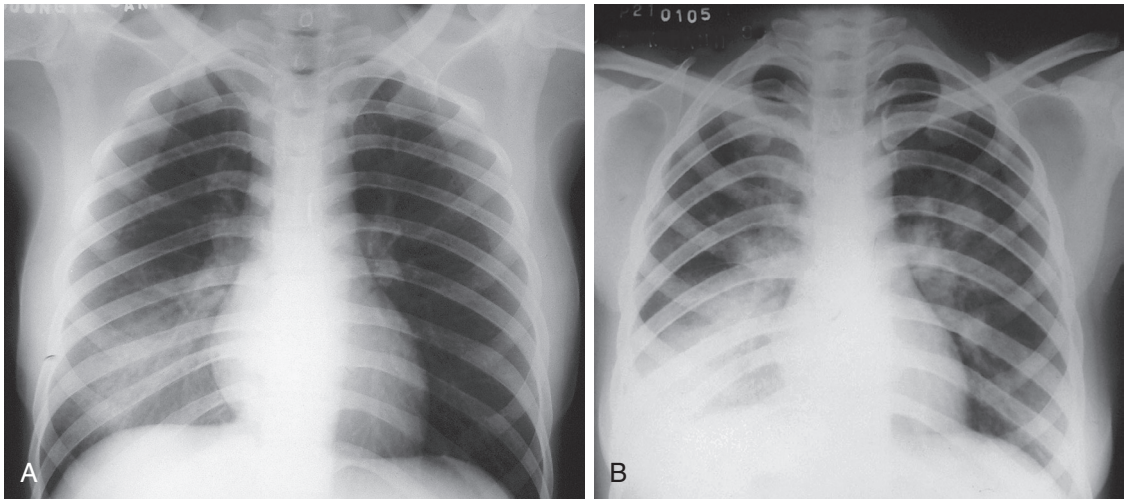


Fig. 4.8 Chest radiographs of a child with H5N1 avian influenza.
These chest radiographs demonstrate progressive right lower zone consolidation from Day 5 (A) to Day 8 (B) with extension into the left lung fields. (Courtesy, Dr T. H. Tran and Dr J Farrar.)

Henipaviruses



Fig. 4.9 *Pteropus* fruit bat (flying fox), reservoir of Nipah virus.
Nipah virus infection was first recognized in Malaysia in 1998, causing an acute form of encephalitis with a mortality rate of about 50%. Occurring especially among pig farmers in a wide geographical area extending from from west Bengal and Bangladesh through to Malaysia and Singapore, the reservoir is the fruit bat. The bats, which appear to be asymptomatically infected, excrete viable virus in their urine and saliva. Pigs are believed to acquire infection by eating contaminated fruit dropped by scavenging bats; in Malaysia it is thought that humans acquired Nipah virus infection through close contact with the pigs, and transmission from farm to farm was primarily by the transport of infected pigs. Control was rapidly effected by using appropriate protective equipment and by a cull of over 1 million pigs. In Bangladesh it is unclear whether humans are infected directly by contact with contaminated foodstuffs or by aerosol of bat urine. An outbreak in Kerala in 2018 highlighted the ongoing potential for emergence of Nipah in new environments within the home range of the *Pteropus* bats. (Copyright © 2013 Joe Mcdonald, Visuals Unlimited/Science Photo Library.)

Downloaded from Vet-eBooks.com

Hantaviruses



Fig. 4.10 The deer mouse, *Peromyscus maniculatus*, reservoir for the North American hantavirus Sin Nombre virus.
Over a dozen different Hantavirus species may cause human disease. Each is associated with a single wild rodent species reservoir. Two forms of acute febrile disease exist: Old World haemorrhagic fever with renal syndrome (HFRS) and New World hantavirus pulmonary sydrome (HPS). Present in the excreta of infected rodents, human transmission is believed to occur primarily through aerosol inhalation. Hantaviruses show tropism for vascular endothelial cells of the heart, lungs, kidneys and reticuloendothelial system causing intense local capillary leak. Organ function support may be required, but no specific antiviral treatment currently exists. (From Shandro, J. R. et al. Wilderness-Acquired Zoonoses. In: Auerbach's Wilderness Medicine 7th edition. Pages 692–728, Figure 34–30. Copyright © 2017 Elsevier Inc. All rights reserved. From Centers for Disease Control and Prevention Public Health Image Library. Courtesy, J. Gathany.)

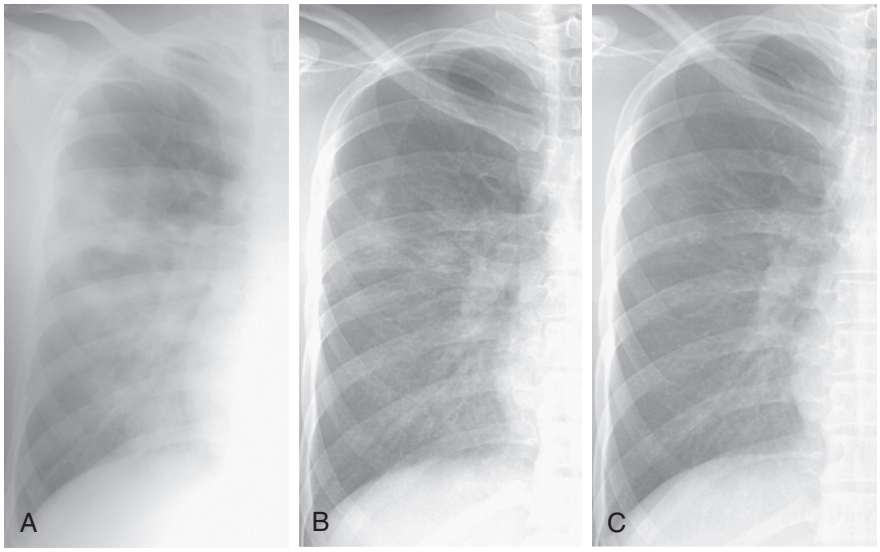


Fig. 4.11 Acute pulmonary oedema in Hantavirus haemorrhagic fever with renal syndrome (HFRS).
Three chest radiographs of a 21-year-old man who presented with fever, shortness of breath and oliguria. Progressive resolution of the interstitial pulmonary oedema in response to haemodialysis is apparent, over a 10-day period. Day 0 (A), Day 7 (B), Day 10 (C). (From Müller, N. L. and Silva, C. I. S. Imaging of the Chest 1st edition. Pages 391–407, Figure 18.7. Copyright © 2008 Elsevier. Courtesy, Dr. K. S. Lee, Samsung Medical Center, Seoul, Korea.)

Downloaded from Vet-eBooks.com

Measles

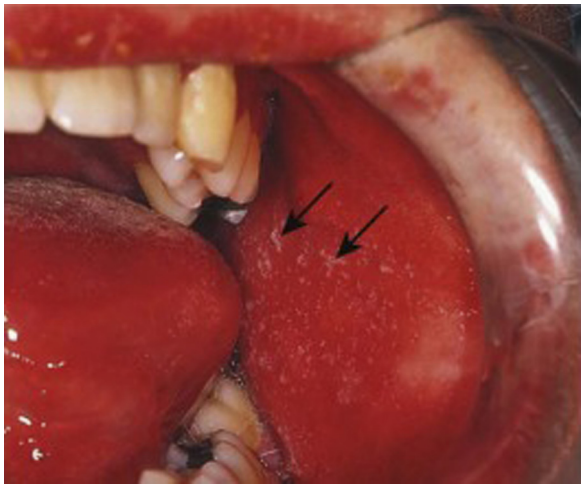


Fig. 4.12 Koplik's spots.
Koplik's spots are pathognomonic of measles. They are found on mucous membranes during the prodromal stage and although they may occur anywhere in the mouth, they are most easily detected on the mucosa of the cheeks opposite the molar teeth. They resemble course grains of salt on the surface of the inflamed membrane (arrows). Histologically, the spots consist of small necrotic patches in the basal layers of the mucosa, with exudation of serum and infiltration by mononuclear cells. (From Dockrell, D. H., Sundar, S., Angus, B. J. and Hobson, R. P. et al. Davidson's Principles and Practice of Medicine. Pages 293–386, Figure 13.7B. Copyright © 2014 Elsevier.)



Fig. 4.13 Typical exanthem of measles.
As the morbilliform rash spreads cephalocaudally from face to trunk and then to the extremities, increasingly irregular macules in the proximal areas become more confluent to leave 'islands' of unaffected skin, most easily seen on light skin. (From Dockrell, D. H., Sundar, S., Angus, B. J. and Hobson, R. P. Davidson's Principles and Practice of Medicine. Pages 293–386, Figure 13.7A. Copyright © 2014 Elsevier.)



Fig. 4.14 Measles in twins.
Measles is one of the most important causes of childhood mortality in the tropics, even though a safe and highly cost-effective vaccine exists. It is estimated that in 1980 measles caused 2.6 million childhood deaths globally, with local epidemics sometimes recording 50% mortality rates; in 2014 the mortality figure had dropped to below 115,000. However given the extreme infectiousness of measles virus, reducing mortality further will depend on ensuring that vaccine coverage includes the 15% of infants who have not even received one vaccine dose by their first birthday. Severe disease tends to occur in malnourished children, and not infrequently precipitates kwashiorkor. The twin on the left shows typical post-measles desquamation but is otherwise recovering. The other twin has post-measles encephalitis. (Courtesy, Professor R. Hendrickse.)

Downloaded from Vet-eBooks.com



Fig. 4.15 Measles in an African child.
The desquamating skin rash of measles was accompanied by herpes simplex stomatitis and rhinitis in this child, who died from respiratory complications. Streptococcal infections (both *S. pneumoniae* and *S. pyogenes*) are associated with post-measles complications. (Courtesy, Professor W. E. Farrar.)

Varicella zoster virus



Fig. 4.16 Disseminated varicella zoster in the context of immune compromise.
Humans are the only known host for varicella zoster virus (VZV) infection. Airborne transmission of the neurotropic virus is highly efficient, with an attack rate of nearly 90% in susceptible household contacts. After the primary manifestation of chickenpox, latent viral infection persists in dorsal root ganglia, but may reactivate presenting as the painful vesicular monodermatomal eruption of shingles. Rarely, multi-dermatomal dissemination occurs, and is strongly associated with compromised cell-mediated immunity, the commonest cause of which globally is HIV-1 infection. Secondary bacterial infection is a common complication, as in this case with peri-oral impetigo. (From Dias, F. M., Marcel, F., Oliveira, J. et al. Exuberant varicella-zoster exanthema and pneumonia as clinical clue for HIV infection. Journal of Pediatrics, Volume 166, Issue 1, Page 199, Figure 1.)

Downloaded from Vet-eBooks.com



Fig. 4.17 Varicella zoster (VZV) pneumonitis.
Both primary and reactivating VZV infection may include neurological, ophthalmological and visceral complications. VZV pneumonitis, typically occurring within one week after the onset of skin lesions, carries a high mortality rate of up to 40%, and is characterized by a dry cough and increasing dyspnoea. This chest radiograph of the same patient as Fig. 4.16 shows typical multifocal nodular shadowing. (From Dias, F. M., Marcel, F., Oliveira, J. et al. Exuberant varicella-zoster exanthema and pneumonia as clinical clue for HIV infection. Journal of Pediatrics, Volume 166, Issue 1, Page 199, Figure 2.)

BACTERIAL INFECTIONS

Pneumococcal Infection

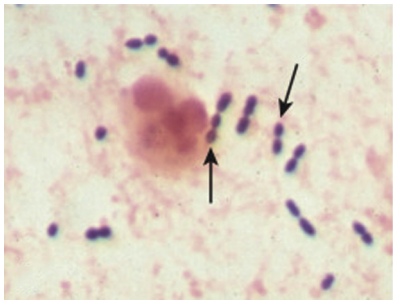


Fig. 4.18 *Streptococcus pneumoniae* in sputum.
Microscopy of a Gram-stained sputum sample from a patient with pneumonia, demonstrating the characteristic morphology of *Streptococcus pneumoniae* bacteria as elongated Gram-positive cocci, usually grouped in pairs and short chains (arrowed). A neutrophil is also visible. (Courtesy, Dr. K. van Horn. From Kumar, V. et al. General Pathology of Infectious Diseases. In: Robbins Basic Pathology, Tenth Edition. Copyright © 2018 by Elsevier Inc. All rights reserved. Figure 9.3.)



Fig. 4.19 Lobar pneumonia.
Chest radiograph demonstrating right upper lobe consolidation with air bronchograms in a 43-year-old woman with lobar pneumonia. Globally, two-thirds of children with bacterial pneumonia fail to access effective low-cost antibiotics, and public health measures have focussed on early breast-feeding, nutritional supplementation, household ventilation improvements and, more recently, immunisation. (From Muller, N. L. High Yield Imaging: Chest. Pages 130–131, Figure 1. Copyright © 2009, Elsevier.)

Downloaded From Vet-eBooks.com

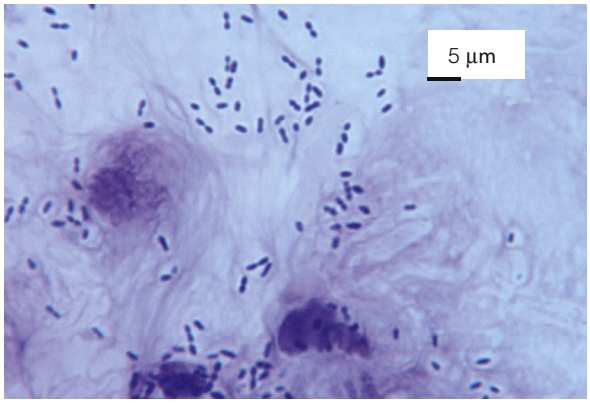


Fig. 4.20 Pneumococcal meningitis.
Directly stained cerebrospinal fluid from a young infant brought to hospital unconscious after a seizure. Numerous lanceolate (lancet-blade shaped) pneumococci are clearly visible, mostly in pairs and with many displaying the characteristic circumferential 'halo' caused by a thick capsule. Neutrophil polymorphs show ingested bacteria.
The incidence of invasive pneumococcal disease is substantially increased in the context of immunosuppression such as uncontrolled HIV infection. Recent introduction of childhood conjugate pneumococcal immunisation schemes directed against the most pathogenic serotypes has profoundly reduced the incidence of invasive disease in both children and adults. The sustained benefit of such vaccine strategies depends on the lesser pathogenicity of the replacement serotypes which become more prevalent through vaccine-induced selective pressure. (Courtesy, Dr. S. Morris-Jones)

Meningococcal Infection

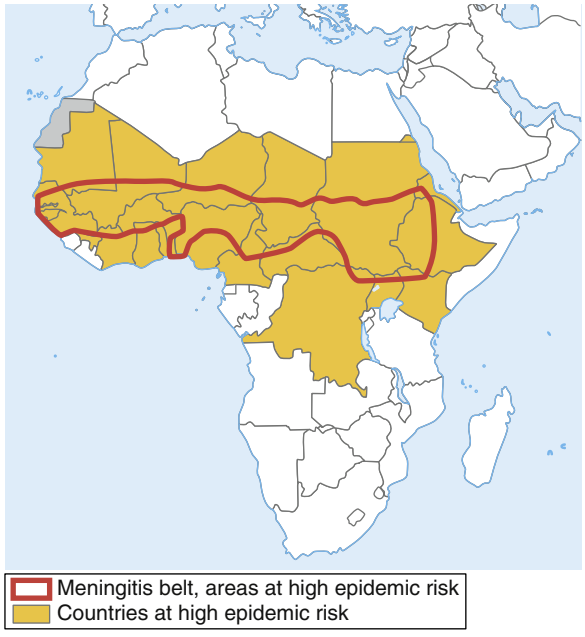


Fig. 4.21 Distribution of the 'meningococcal meningitis belt' in Africa.
Until recent immunization initiatives, meningococcal meningitis occured in 2–10 yearly epidemic cycles in the so-called 'meningitis belt' of tropical Africa, the zone lying between approximately 5° and 15° north of the equator, which is characterized by an annual rainfall of between 300 mm and 1100 mm. Infection was historically primarily with *N. meningitidis* serogroup A in this zone, but introduction of the MenAfriVac has dramatically reduced disease incidence due to serogroup A wherever it has been used. In order for the efficacy of vaccination strategies to be sustained, monitoring and vigilance of serogroup switching will be needed. Effective vaccines are currently available against serogroups A, B, C, W135 and Y and can be deployed according to local epidemiology. (From Memish, Z. A., Goubeaud, A., Bröker, M., et al. Invasive meningococcal disease and travel. Journal of Infection and Public Health, 2010, Volume 3, Issue 4, Pages 143–151, Figure 1. Source: WHO, Geneva. http://www.who.int/ith/en/; 2009 [accessed 15.06.10].)



Fig. 4.22 Rash of acute meningococcaemia.
The rash typically consists of irregular, scattered, non-blanching petechiae, which tend to be peripherally distributed. The lesions, variable in size, may be macular, papular or clearly purpuric. (Courtesy, Professor W. E. Farrar.)



Fig. 4.23 Meningococcal septicaemia.
Non-blanching and necrotic lesions on the hand of an African patient with meningococcal septicaemia.

Downloaded from Vet-e-Books.com



Fig. 4.24 Subconjunctival petechial haemorrhages.
As early petechial lesions may be masked on pigmented skin, conjunctival examination is frequently rewarding, as in this case where numerous subconjunctival petechiae were visible in a Nigerian boy with meningococcal meningitis and meningococcaemia. (Courtesy, Professor D. A. Warrell.)

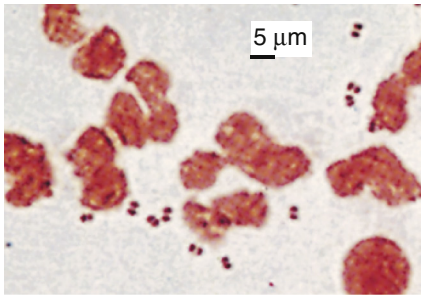


Fig. 4.25 Direct microscopy with Gram stain of cerebrospinal fluid.
Neisseria meningitidis is a Gram-negative, bean-shaped diplococcal organism.

Other Bacterial Infections



Fig. 4.26 Child with subconjunctival haemorrhage due to whooping cough.
Whooping cough is caused by the Gram-negative bacillus *Bordetella pertussis*, and severe disease occurs mostly in young children and infants. The catarrhal phase is commonly characterized by paroxysms of coughing and apnoea, but frank pneumonia is a relatively frequent complication. Subconjunctival haemorrhages are a common accompaniment of the severe coughing spasms, but the haemorrhages resolve rapidly with recovery. Pertussis has been successfully incorporated into a combined diphtheria and tetanus toxoid vaccine (DTP) as part of the WHO Expanded Programme on Immunization since 1974. (From Sadoh, A. E., Oladokun, R. E. Re-emergence of diphtheria and pertussis: implications for Nigeria. Vaccine, © 2012 Elsevier Ltd, Volume 30, Issue 50, Pages 7221–7228, Figure 1.)

Downloaded From Vet-eBooks.com

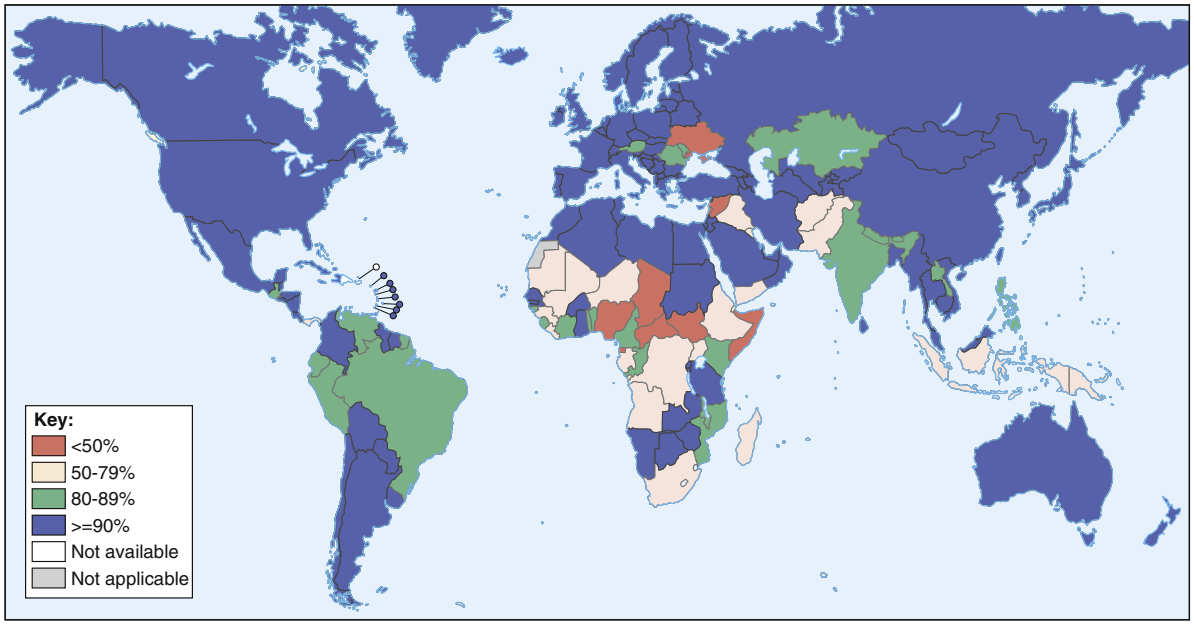


Fig. 4.27 Map showing global diphtheria, tetanus and pertussis (DTP) immunization coverage rates in infants, 2016.
The recommended three-dose primary immunization schedule for DTP has achieved an estimated 86% global coverage. 2017/18 outbreaks of diphtheria in humanitarian crises in war-affected Yemen and Rohingya refugees fleeing Myanmar for camps in Bangladesh reflect inadequate vaccination coverage and ideal conditions for transmission with overcrowding and undernutrition. (Courtesy, World Health Organization; http://www.who.int)



Fig. 4.28 Pseudomembrane in a patient with respiratory diphtheria.
Diphtheria is caused by a potent phage-encoded toxin released from the bacterium *Corynebacterium diphtheriae*. Infection results in a sore throat with a characteristic leathery grey membrane and typically swollen cervical adenopathy. Occasionally airway obstruction may occur, and systemic effects of the toxin may be life-threatening with cardiac arrhythmias and nerve paralysis. Treatment is with antitoxin and clearance of carriage using a macrolide or penicillin. (From: Guerrant, R. L. Walker, D. H., Weller, P. F. Tropical Infectious Diseases: Principles, Pathogens and Practice. Pages 223–227, Figure 34.3. Copyright © 2011 Elsevier.)

Downloaded from Vet-eBooks.com



Fig. 4.29 Healing cutaneous diphtheria.
Although usually causing respiratory disease, diphtheria may also be acquired by contact from droplets or contaminated surfaces. Ulcers have characteristic appearance with a rolled crater edge, as in this healing case in a Congolese woman. Her strain was toxigenic but did not produce sufficient toxin to cause systemic disease. (Courtesy, Dr. S. Morris-Jones.)

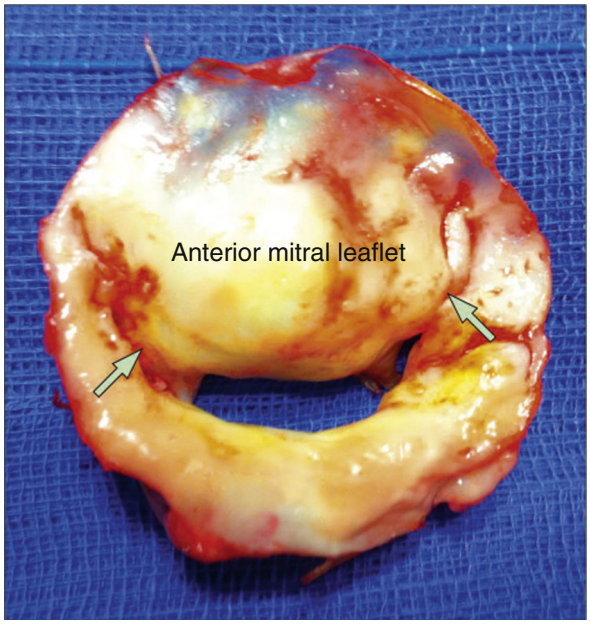


Fig. 4.30 Rheumatic heart disease of the mitral valve.
Streptococcus pyogenes (Group A Streptococcus) causes bacterial pharyngitis, but may produce the non-suppurative complications of acute rheumatic fever and glomerulonephritis. Rheumatic fever is believed to occur as a result of molecular mimicry: antibodies and T cells raised in response to streptococcal antigens cross-react with human cardiac tissue proteins. The precise role of bacterial and host susceptibility factors remains unclear. Rheumatic heart disease is the leading cause of cardiovascular death during the first five decades of life in low- and middle-income countries. Typical features of chronic rheumatic valvular disease are shown with commissural fusion (arrows) and retraction of the anterior valve leaflet. (From Marijon, E., Mirabel, M., Celermajer, D. S., Jouven, X. Rheumatic heart disease. Lancet, 2012 Volume 379, Issue 9819, Pages 953–964, Figure 2.)

Downloaded From Vet-eBooks.com

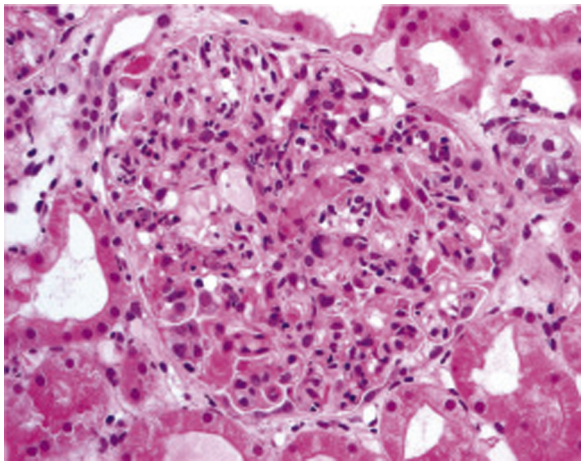


Fig. 4.31 Acute post-streptococcl glomerulonephritis.
Deposition of streptococcal antigens on the glomerular basement membrane lead to antibody-mediated immune complexes and glomerulonephritis. Cutaneous streptococcal strains appear more commonly nephritogenic than pharyngeal strains, although identification of responsible antigens remains elusive. Glomerular microscopy exhibits diffuse endocapillary proliferation and neutrophil infiltration. (After Marsh FP. Postgraduate Nephrology. Oxford: Butterworth Heinemann; 1985.)

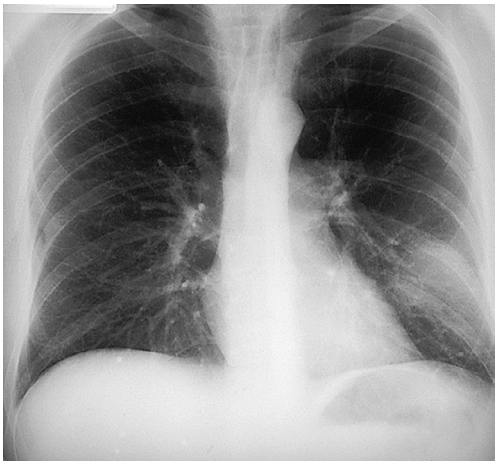


Fig. 4.32 Chest radiograph of a patient with Q fever pneumonia.
Coxiella burnetii is an extremely hardy bacterium that causes abortion in ruminant mammals. It is shed into the environment via faeces, urine, milk and placental tissue in which the bacterial burden is particularly high. Bacteria may remain viable for months in soil. Humans become infected by inhalation of infected aerosols, sometimes carried in dust by the wind, and present acutely with pneumonia, often with headache and transaminitis.

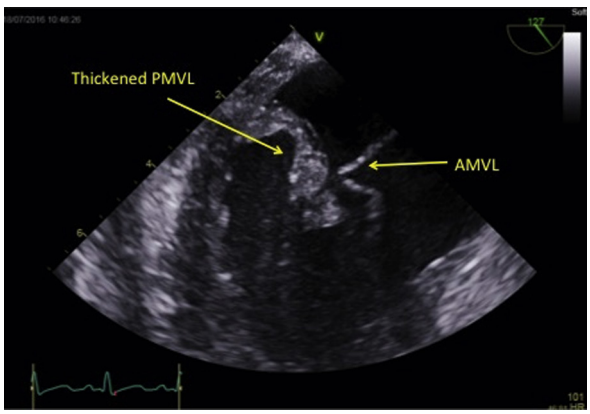


Fig. 4.33 Echocardiogram of Q fever endocarditis.
Individuals with underlying valve disease may develop chronic Q fever endocarditis. Onset may be insidious with worsening heart failure. This archaeologist with mitral valve prolapse had probably been infected during professional digs in the Middle East. Note the thickened posterior mitral valve leavlet (PMVL) compared with the anterior MVL. (Courtesy, Dr. S. Morris-Jones.)

Tuberculosis

The overlap between tuberculosis (TB) and HIV in some, but not all, regions of the world is demonstrated in Fig. 4.34 and Fig 4.35. Integrated control programmes are essential to tackle the bi-directional interaction between these two infections. Incidence rates (cases per 100,000 people per year) as shown in Fig. 4.34 indicate the concentration of disease within countries, but population size will also dictate the absolute number of cases that health systems have to address. China and India account for half of all TB cases globally. Fig. 4.36 highlights the emerging issue of multi-drug resistant TB, the diagnosis and management of which poses additional problems. The countries most affected are frequently those with the least resourced healthcare facilities (Fig. 4.37).

Downloaded from Vet-eBooks.com

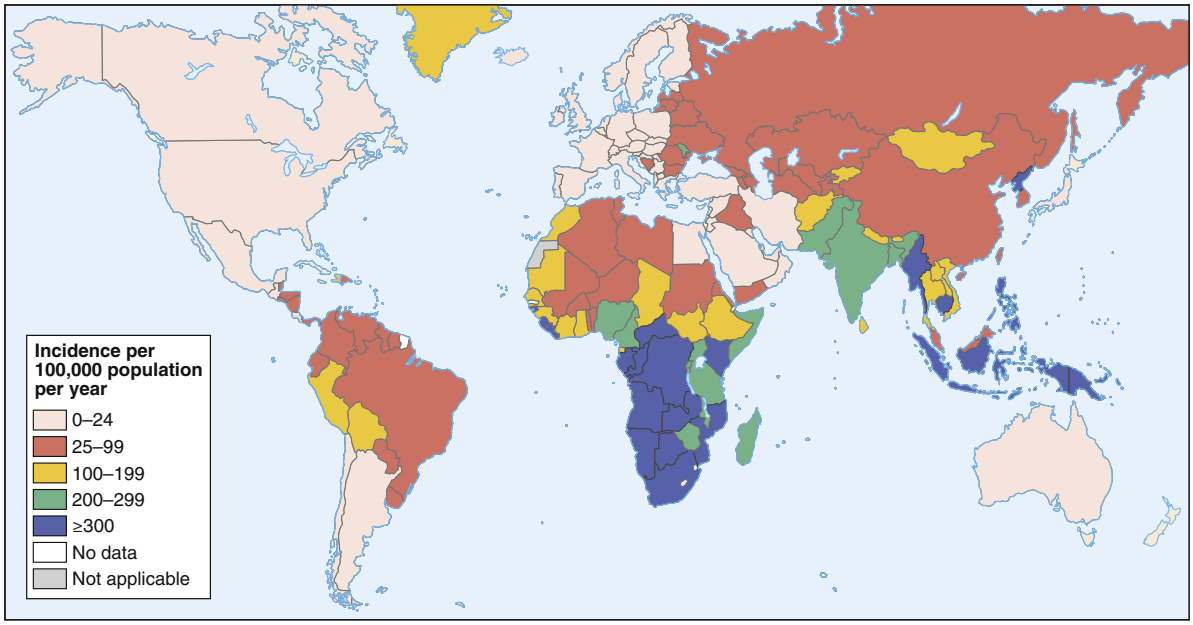


Fig. 4.34 Estimated global tuberculosis incidence rates for of all forms of tuberculosis, 2016. (From Global Tuberculosis Report, 2017. World Health Organization, Page 31, Figure 3.4. http://www.who.int/tb/publications/global_report/en/)

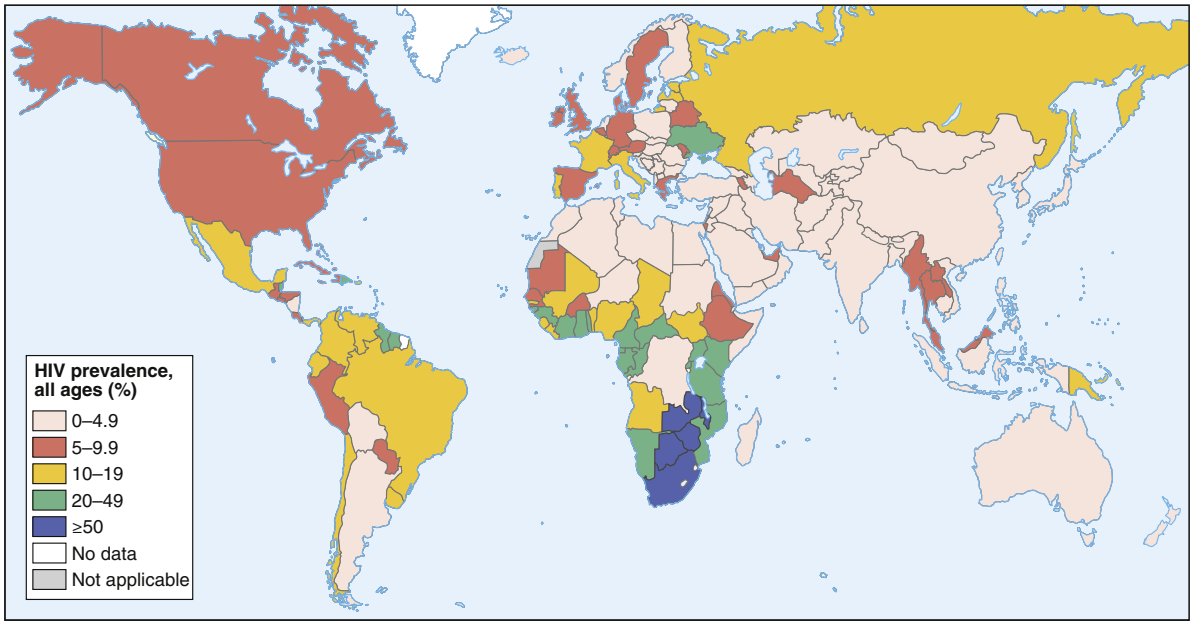


Fig. 4.35 Estimated global rates of HIV prevalence in active tuberculosis cases, 2016. (From Global Tuberculosis Report, 2017. World Health Organization, Page 32, Figure 3.5 http://www.who.int/tb/publications/global_report/en/)

Downloaded From Vet-eBooks.com

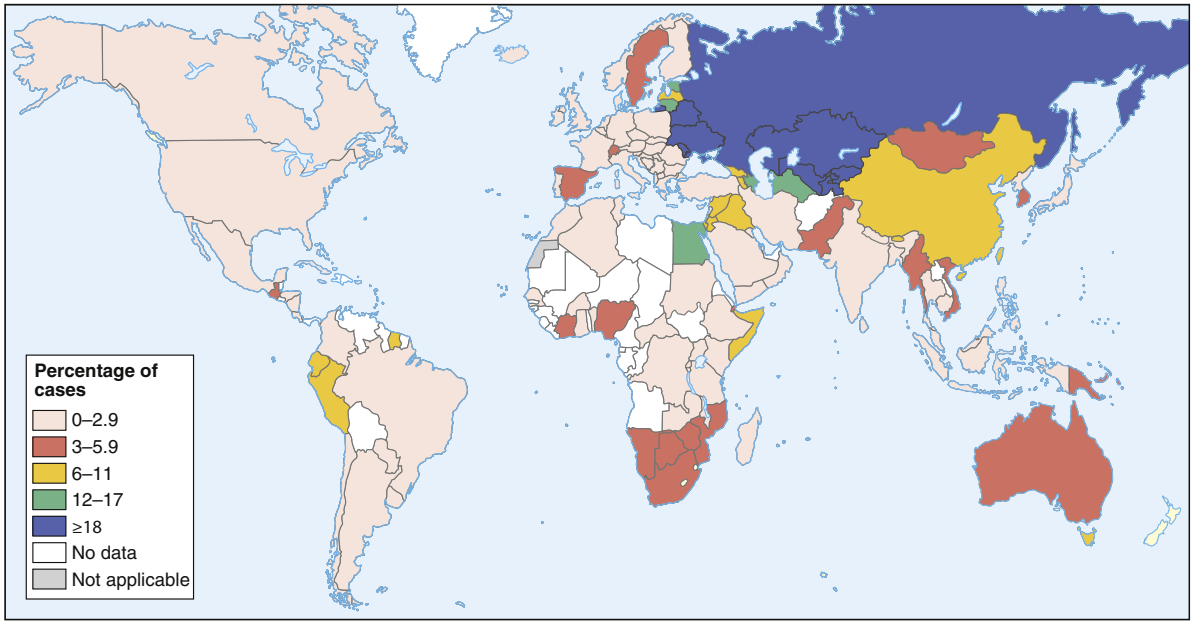


Fig. 4.36 Percentage of new tuberculosis cases with Rifampicin resistant or multi-drug resistant tuberculosis, 2016. (From Global Tuberculosis Report, 2017. World Health Organization, Page 46, Figure 3.20. http://www.who.int/tb/publications/global_report/en/)

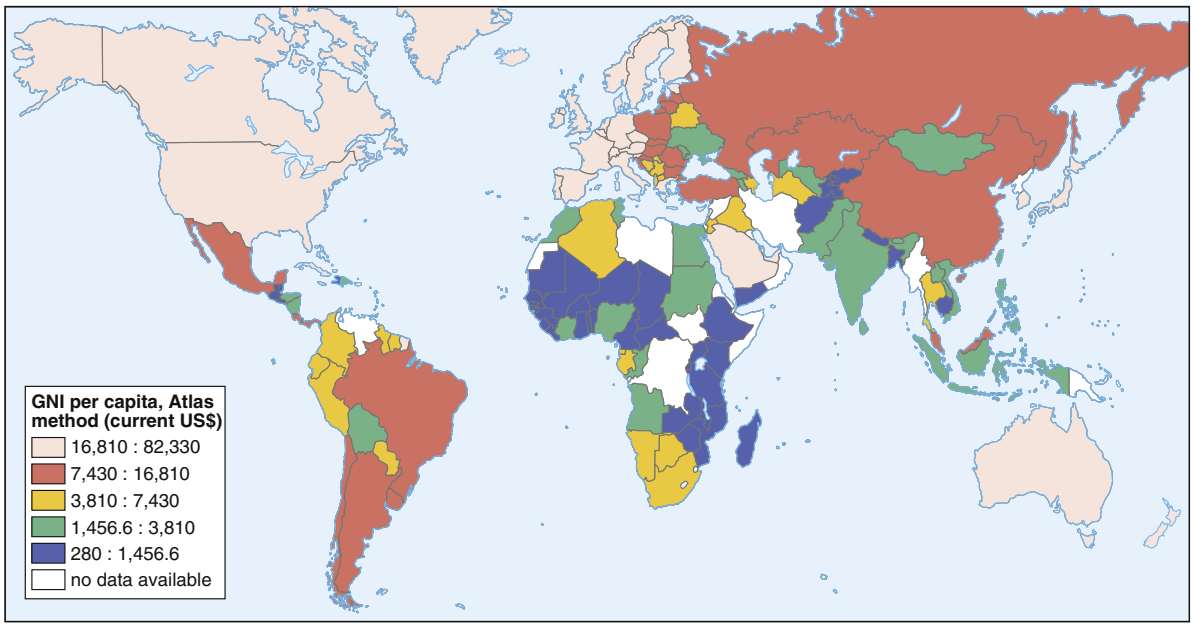


Fig. 4.37 Global distribution of Gross National Income per capita (in US Dollars), 2017. (From The World Bank https://data.worldbank.org/products/wdi-maps)

Downloaded From Vet-eBooks.com

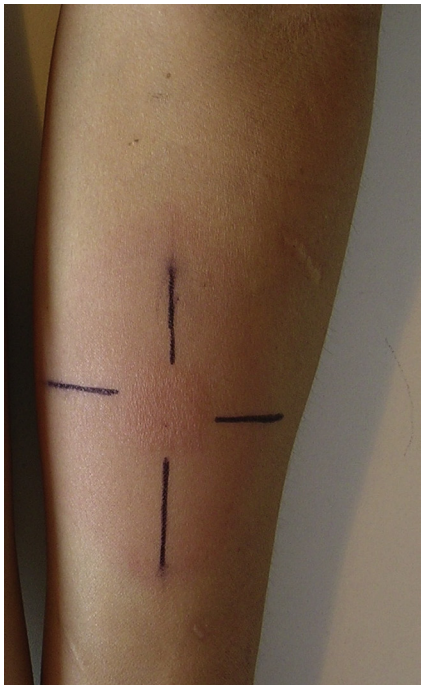


Fig. 4.38 Positive tuberculin skin test (TST).
Other diagnostic tests provide alternatives to the direct visualization or culture of the *M. tuberculosis* organism. The tuberculin skin test, usually performed as a Mantoux test and previously as a Heaf (or tine) test, measures the delayed-type hypersensitivity response to an intradermal injection of purified protein derivative (PPD) of *M. tuberculosis*, and is an indicator of prior exposure to this organism. TST is conventionally injected into the volar surface of the forearm and the site examined 48–72 hours later for induration; this figure shows a positive reaction in a patient with active tuberculosis. In higher-income settings, interferon-gamma release assays (IGRAs) may be preferred to the TST, as they involve a single blood sample and have superior specificity over the TST. Sensitivities of both TST and IGRAs tests are compromised in active infection or immunosuppression. (Courtesy, J. Coronel.)

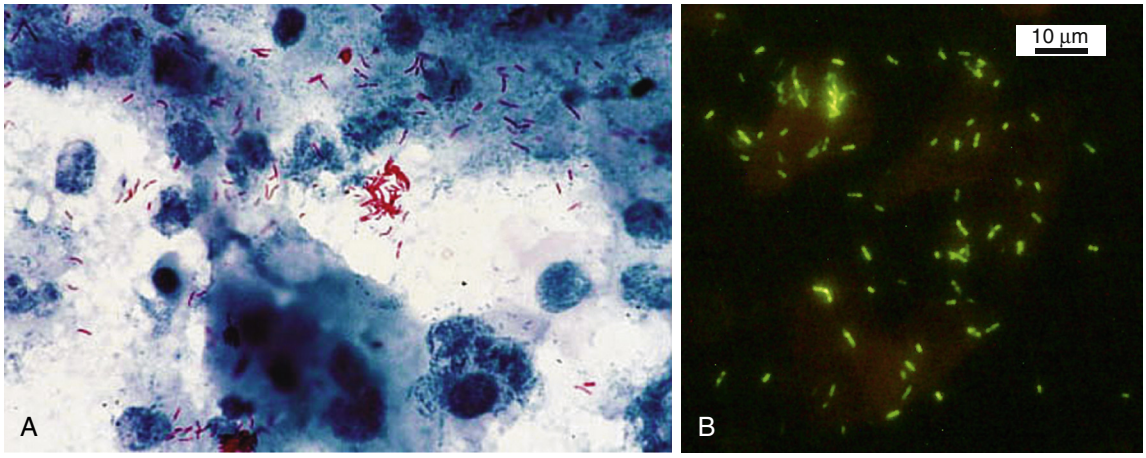


Fig. 4.39 *Mycobacterium tuberculosis* in sputum.
Mycobacterium tuberculosis is a remarkable bacterium that may infect any organ of the body; the lungs and associated lymph nodes are most commonly affected, reflecting the initial acquisition route. Diagnosis may be confirmed by the microscopic demonstration of acid-fast bacilli, as seen in this sputum specimen. Microscopy does not provide information on the drug susceptibility of the organism. Images using (A) Ziehl–Neelsen stain, (B) Auramine dye. Auramine staining improves sensitivity when bacillary burden is low, but requires a fluorescent microscope. (B, Courtesy, Dr. S. Morris-Jones.)

Downloaded from Vet-eBooks.com



Fig. 4.40 *Mycobacterium tuberculosis* growing on solid medium.
Isolation of dry, beige, crumbly colonies of *M. tuberculosis* grown from a sputum sample on Lowenstein-Jensen medium. The incubation period for *M. tuberculosis* on solid media typically takes 10–11 days longer than with liquid culture, but may have lower contamination rates. (Courtesy, S. Froman and A. Gaytan. From Pfyffer, G. E., Inderlied, C., B. (2010). Mycobacteria. In J. Cohen, S. M. Opal, W. G. Powderly (Eds.), Infectious Diseases, Pages 1777-1800, Figure 174.12. Elsevier Ltd.)

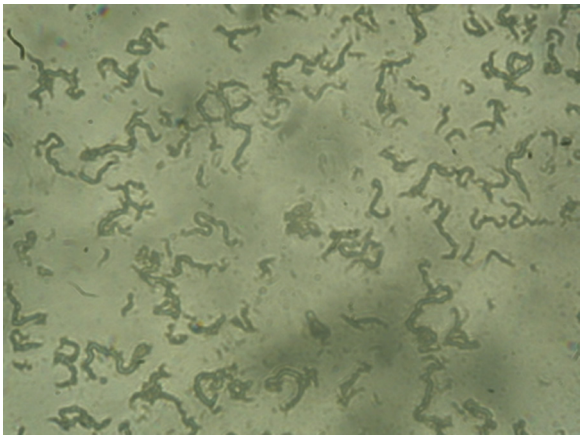


Fig. 4.41 Characteristic cording of colonies of *Mycobacterium tuberculosis* growing in liquid medium in the Microscopic Observation of Drug Susceptibility (MODS) assay.
Colonies of *M. tuberculosis* are visible in the culture liquid within 7 days of incubation at 37°C. Resistance to first-line anti-tuberculous agents has become an important management issue in some regions (Fig. 4.36), and availability of rapid susceptibility testing is an urgent requirement. The WHO-endorsed non-commercial MODS assay offers low-cost, liquid culture TB detection and rapid drug-susceptibility testing direct from sputum, without the need for a primary isolation and secondary culture. Alternative commercial phenotypic and genotypic methodologies have also been rolled out at scale, yet the delivery of universal drug susceptibility testing remains a distant prospect due to budgetary and infrastructure constraints. (Courtesy, Professor D. A. J. Moore.)

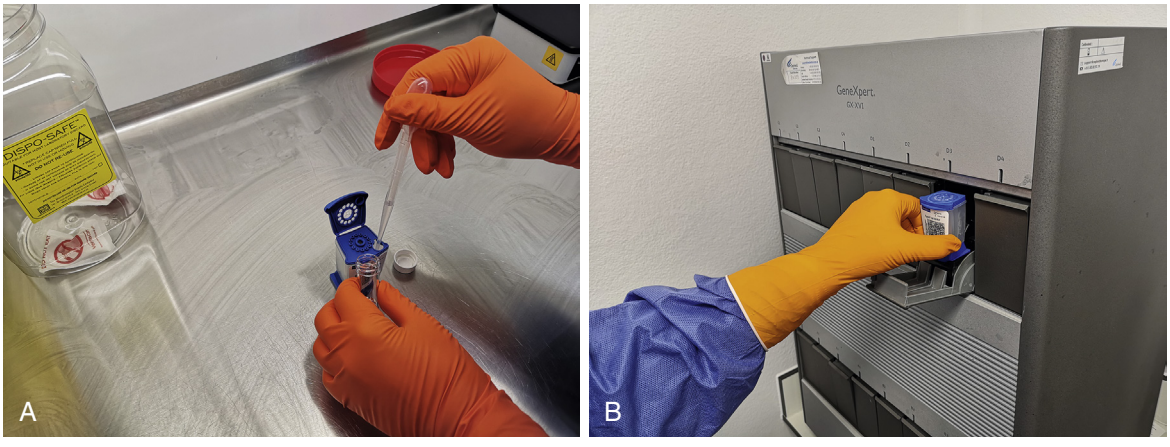


Fig. 4.42 Rapid molecular testing for *Mycobacterium tuberculosis*.
Development and marketing of a commercial polymerase chain reaction test to detect *M. tuberculosis* and the principal mutations conferring rifampicin resistance directly from unprocessed sputum samples within 2–3 hours (A) may represent a huge technological advance, but for many low-income settings its impact is limited by the requirement for electricity, capital and recurring costs of equipment and single-use cartridges, and the struggle to link diagnosis to initiation of effective TB treatment. (B). (A, B: Courtesy, Dr. S. Morris-Jones.)

Downloaded from Vet-eBooks.com

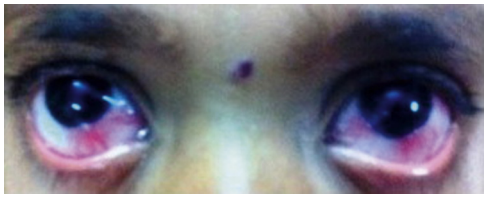


Fig. 4.43 Phlyctenular conjunctivitis.
This rare nodular disorder of the conjunctiva is found in children and young adults and is an allergic response to a sensitizing antigen. A broad range of infectious triggers are recognized, including bacterial, fungal and parasitic helminthic agents. In this 6-year-old girl examination revealed axillary and supraclavicular lymphadenopathy. Acid–fast bacilli were seen on a node aspirate along with granulomata. The ocular abnormalities had completely resolved within 5 weeks of the start of antituberculous therapy. (From Sharma, K., Kalakoti, P., Juneja, R. et al. Re-emphasizing Thygeson's warning: conjunctival phlyctenulosis as presenting sign of impending clinical tuberculosis. Canadian Journal of Ophthalmology, 2014, Volume 49, Issue 6, Pages e135–e137, Figure 1.)

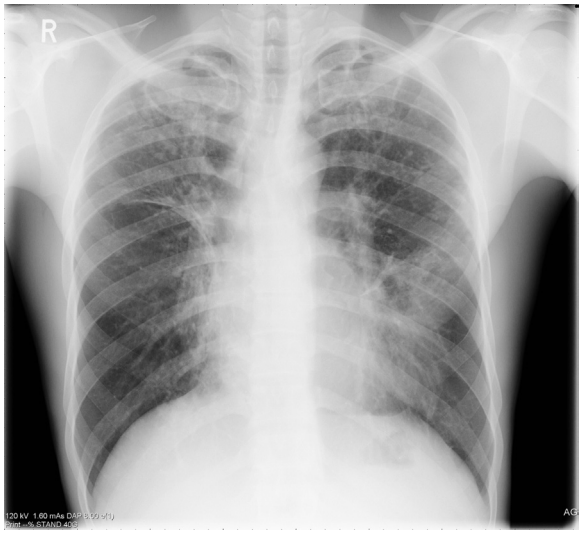


Fig. 4.44 Pulmonary tuberculosis with cavitation.
Prevention of pulmonary tuberculosis is essential for tuberculosis control, as this is the form of disease responsible for onward transmission of the infection. Infectiousness is dependent on the bacillary burden and the ability to aerosolize infectious droplets. Patients with cavitatory disease on the chest radiograph, as shown here in the right upper lobe, are more likely to be smear-positive on sputum microscopy and to pose a greater infectious risk to their contacts. (Courtesy, UCL Hospitals Radiology)

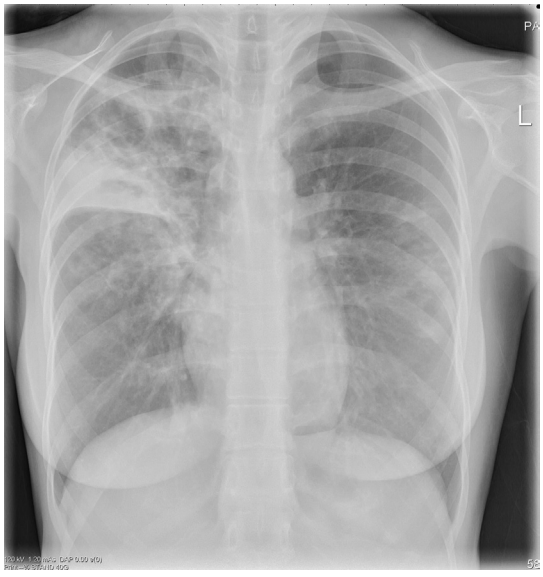


Fig. 4.45 Chest radiograph of drug-resistant pulmonary tuberculosis.
Resistance of *Mycobacterium tuberculosis* to rifampicin and isoniazid defines multi-drug-resistant (MDR) tuberculosis. Additional resistance to a fluoroquinolone and one of the class of second-line injectable agents defines extensively drug-resistant disease (XDR-TB), as in the case of this young woman from Mumbai. (Courtesy, UCL Hospitals Radiology.)

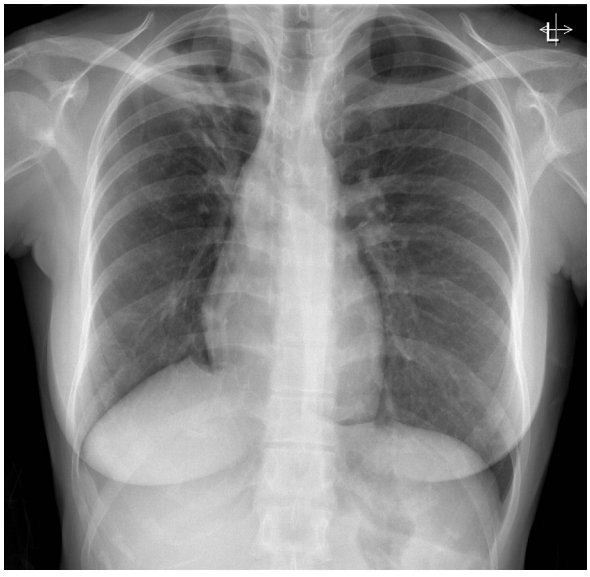


Fig. 4.46 Chest radiograph showing response to treatment.
Chest radiograph of the same patient as Fig. 4.45 after 9 months of treatment. The lung fields have cleared with residual right apical fibrosis and loss of lung volume. Thick-walled cavities may provide barriers to effective drug penetration and surgery is sometimes required. (Courtesy, UCL Hospitals Radiology.)

Downloaded from Vet-eBooks.com

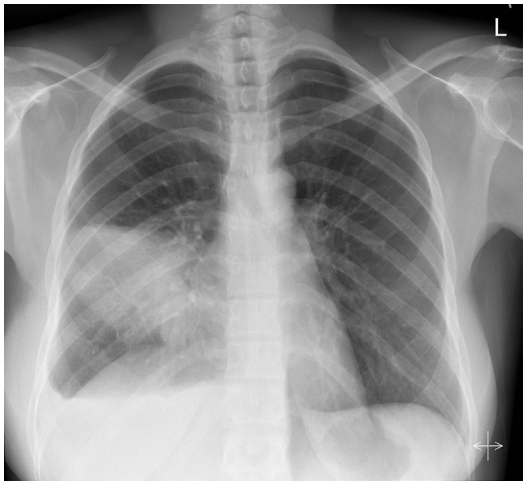


Fig. 4.47 Chest radiograph showing right lower zone consolidation and unilateral pleural effusion.
This young woman presented with a month of weight loss and increasing breathlessness. Her unilateral pleural effusion was heavily lymphocytic and, along with pleural tissue and blood, yielded cultures that were positive for *Mycobacterium tuberculosis*. An HIV test was positive. The strongest risk factor for tuberculosis is infection with HIV (see Figs 4.34 and 4.35), though diabetes mellitus confers a threefold increase in risk and global prevalence is tenfold greater than HIV and continuing to rise. (Courtesy, UCL Hospitals Radiology.)



Fig. 4.48 Tuberculous cervical lymphadenitis.
The commonest form of extrapulmonary tuberculosis involves the lymph nodes, most often the cervical and supraclavicular nodes. Usually relatively painless, caseating 'cold abscesses' may discharge necrotic pus. Lymphoma is one of the most important differential diagnoses. (Courtesy, Dr. W. Newsholme.)



Fig. 4.49 Aspiration of tuberculous supraclavicular abscess.
Aspiration may be performed for immediate symptom relief and, when possible, should be used to confirm the diagnosis and obtain the isolate susceptibility profile. (Courtesy, Dr. W. Newsholme.)

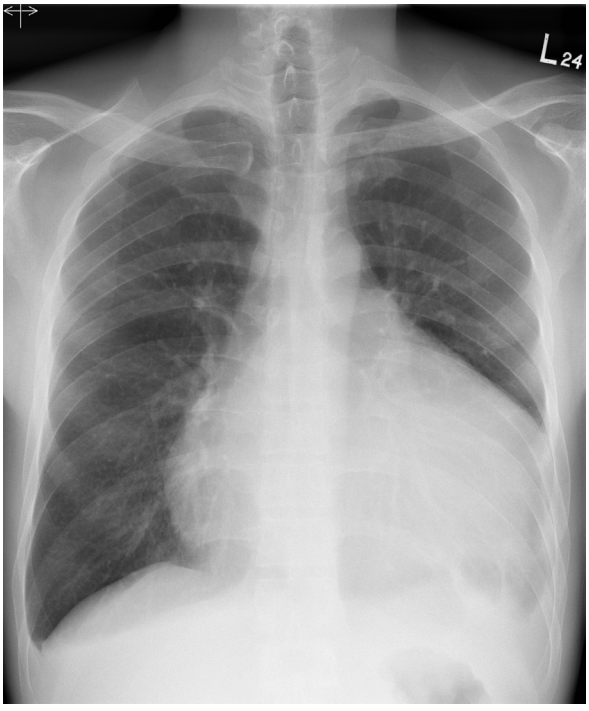


Fig. 4.50 Tuberculous pericarditis.
Tuberculous pericardial involvement often produces a large pericardial effusion in the early stages; subsequent constriction may reduce the heart shadow. This HIV-positive patient presented with fevers, night sweats and shortness of breath. His chest radiograph shows a massively enlarged cardiac shadow and a left pleural effusion; fully drug-susceptible *M. tuberculosis* was cultured from pericardial fluid and lymph node tissue. (Courtesy, UCL Hospitals Radiology.)

Downloaded from Vet-eBooks.com

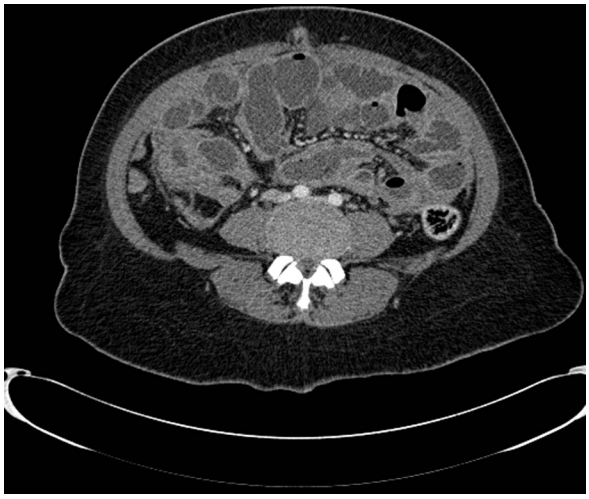


Fig. 4.51 Peritoneal and omental tuberculosis.
This Afro-Caribbean woman presented with signs of small bowel obstruction on a background of a 12-month history of weight loss and altered bowel habit. Appearances at laparotomy were interpreted as disseminated intra-abdominal malignancy. Peritoneal biospies demonstrated necrotizing granulomata, and fully drug-susceptible *Mycobacterium tuberculosis* was isolated in culture. She made a full recovery on anti-tuberculous therapy. A preoperative CT scan of her pelvis demonstrates a thickened and nodular peritoneum and widespread thickened small intestinal mucosa. (Courtesy, UCL Hospitals Radiology.)



Fig. 4.52 Tuberculosis of the breast.
A lactating mother was thought to have developed a large right breast galactocoele, but CT imaging demonstrated contiguity with a loculated right pleural effusion; culture of the aspirate confirmed the diagnosis of tuberculosis. (Courtesy, UCL Hospitals Radiology.)

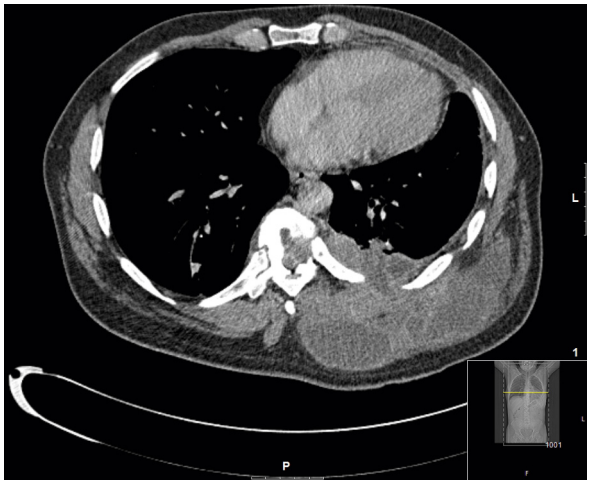


Fig. 4.53 Extensive pleuro-vertebral tuberculous disease.
A man with psychiatric illness presented with a large lump over the left side of his back. The CT scan demonstrates the remarkable ability of tuberculosis to track through tissue planes. Although encroaching on the spinal canal, no neurological deficit ensued as the tuberculous abscess tracked from the eroded T8/9 vertebral bodies to pass between the rib spaces and create a large chest wall collection (see Fig. 4.54). (Courtesy, UCL Hospitals Radiology.)

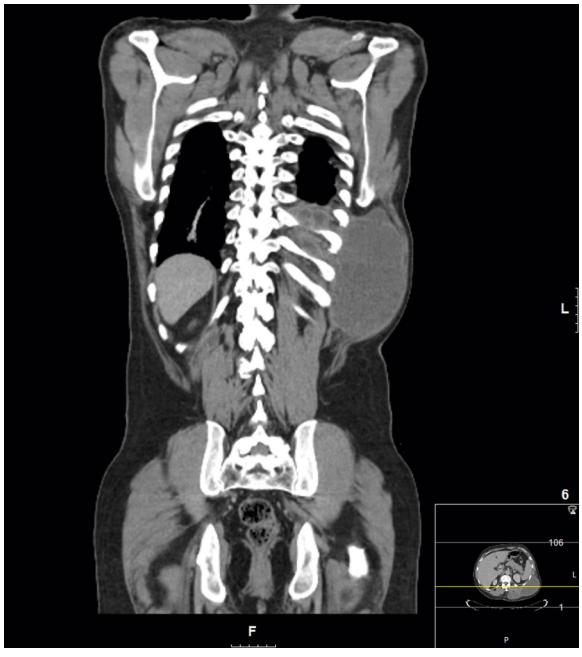


Fig. 4.54 Tuberculous chest wall collection.
Aspiration of several litres of purulent necrotic material yielded a positive culture of *Mycobacterium tuberculosis*. (Courtesy, UCL Hospitals Radiology.)

Downloaded From Vet-eBooks.com



Fig. 4.55 Tuberculous psoas abscess.
Abdominal swelling initially mistaken as a fibroid was subsequently found to be an anterior extension of a huge abscess in the left psoas muscle. In most cases of psoas abscess there is also involvement of the lower lumbar spine, since the psoas muscle originates from anterior and lower surfaces of the transverse processes of all lumbar vertebrae. It is unusual for psoas abscesses to present with such prominence anteriorly.



Fig. 4.56 Bilateral psoas abscesses.
Plain lumbar radiograph shows marked reduction in the size of the L3/4 disc space and prominent bulging psoas shadows. (Courtesy, UCL Hospitals Radiology.)



Fig. 4.57 Spondylodiscitis and psoas abscesses.
Magnetic resonance imaging of same patient as Fig. 4.56 shows the spondylodiscitis and huge bilateral psoas abscesses due to tuberculosis. (Courtesy, UCL Hospitals Radiology.)

Downloaded from Vet-eBooks.com

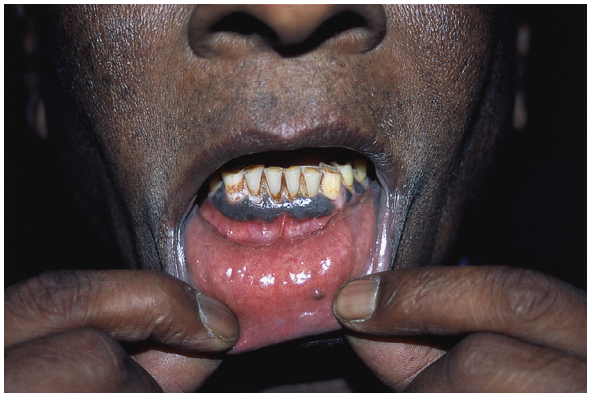


Fig. 4.58 Gum hyperpigmentation in Addison's disease due to tuberculous adrenal involvement.
This patient presented with fever and collapse and was found to be grossly hypoadrenal. Tuberculosis is probably still the commonest cause of hypoadrenalism worldwide; this may often be induced by the initiation of rifampicin therapy, which induces liver enzymes to metabolize glucocorticosteroids more rapidly. The CT scan of this patient's abdomen showed a large adrenal on the right and calcification on the left.

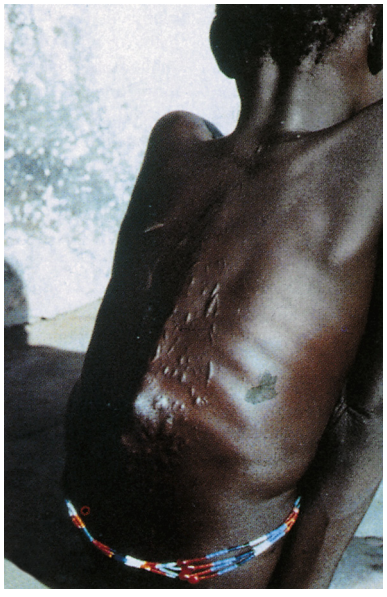


Fig. 4.59 Tuberculosis of the spine (Pott's disease).
The spinal column is a common bony site for involvement by tuberculosis. Vertebral involvement may cause severe deformity as seen in this young African patient. (Courtesy, Professor J. Cohen. From Friedland, J. S. Tuberculosis. In: Cohen, J., Powderly, W., eds. Infectious Diseases. 2nd edition. Edinburgh: Mosby, 2004, Pages 401–418.)



Fig. 4.60 Thoracic spine of patient with Pott's disease.
Computerized tomographic imaging shows that the kyphosis associated with Pott's disease is caused by the destruction of the intervertebral disc with consequent loss of disc space and the anterior wedge-shaped erosion of the adjacent vertebral bodies causing angulation (gibbus). (Courtesy, UCL Hospitals Radiology.)



Fig. 4.61 Vertebral body destruction in tuberculosis.
This sagittal view shows collapse of the anterior T6 vertebral body, a T7 intraosseous abscess and a prevertebral inflammatory abscess stripping the longitudinal ligament. The most dangerous consequence of vertebral tuberculosis is involvement of the spinal cord. (Courtesy, UCL Hospitals Radiology.)

Downloaded From Vet-eBooks.com

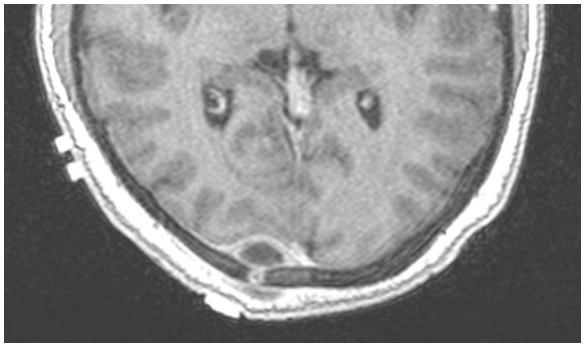


Fig. 4.62 Skull MRI cranial tuberculosis.
A taxi driver reported hitting the back of his head and subsequently developing a slowly enlarging non-painful scalp mass. Imaging studies illustrated a mass that had destroyed the occipital bone and was compressing the cerebral cortex. *M. tuberculosis* was isolated from aspirated necrotic granulomatous tissue. (Courtesy, UCL Hospitals Radiology.)

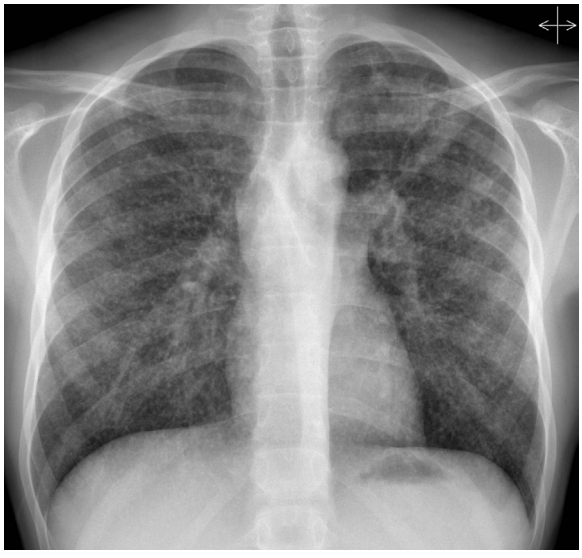


Fig. 4.63 Chest radiograph in miliary tuberculosis.
Miliary tuberculosis occurs when there is haematogenous spread of mycobacteria. Pulmonary involvement is demonstrated radiographically by bilateral reticulonodular parenchymal shadowing. In the case of this 15-year-old Sudanese boy, there was also a spinal focus as shown in Fig. 4.61. (Courtesy, UCL Hospitals Radiology.)

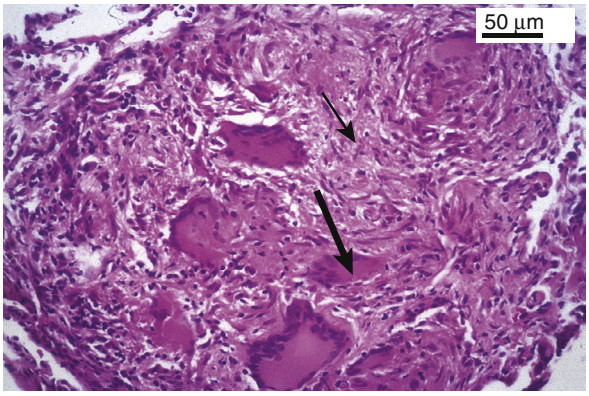


Fig. 4.64 Pathology of miliary tuberculosis.
Langhans giant cells (larger arrow) are derived from the fusion of epithelioid cells and have multiple nuclei arranged in a characteristic horseshoe shape. Lymphocytes and plasma cells are also present in granulomas, and together surround areas of indistinct caseating necrosis (smaller arrow). (Haematoxylin and eosin stain.)



Fig. 4.65 Tuberculous meningitis.
In infants, miliary tuberculosis and meningitis have a high mortality. This 3-month-old Nepalese infant with tuberculous meningitis and demonstrating pronounced head retraction died despite intensive anti-tuberculous chemotherapy. Tuberculous meningitis in infants results in permanent neurological sequelae in at least 50% of cases. (Courtesy, Brig. Gen. G. O. Cowan.)

Downloaded from Vet-eBooks.com

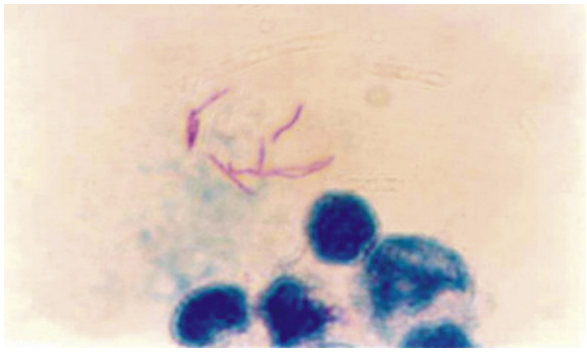


Fig. 4.66 Cerebrospinal fluid (CSF) of patient with tuberculous meningitis.
Bacilli of *Mycobacterium tuberculosis* can be seen as acid fast bodies in this Ziehl-Neelsen stain of a CSF preparation. (From Thwaites, G. (2014). Tuberculosis In J. Farrar, J. P. Hotez, T. Junghanss, G. Kang, D. Lalloo, N. J. White (Eds.), Manson's Tropical Diseases, Pages 468-505, Figure 40-11C. Elsevier Ltd.)

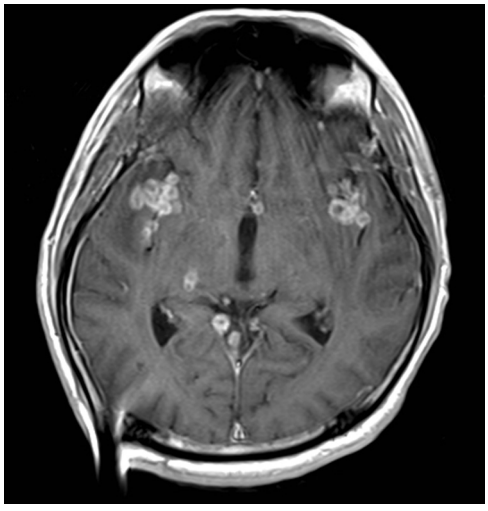


Fig. 4.67 Tuberculomata and tuberculous meningitis.
Multiple sub-arachnoid tuberculomata developed along the meninges in a patient who had been treated for drug-resistant tuberculous meningitis that required ventriculo-peritoneal shunt insertion. The size of individual tuberculomata may vary over time, and may reflect intracranial paradoxical reactions. (Courtesy, UCL Hospitals Radiology.)

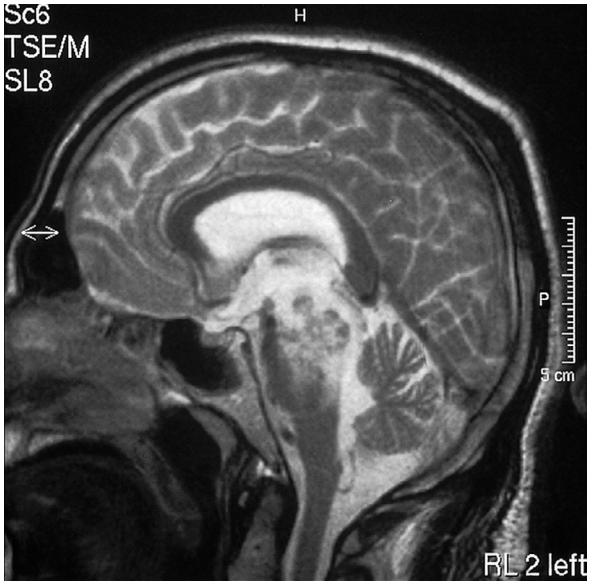


Fig. 4.68 Tuberculous involvement of the brain stem.
Cerebral tuberculosis may mimic neoplasia, as in this patient where stereotactic biopsy confirmed *Mycobacterium tuberculosis* infection.

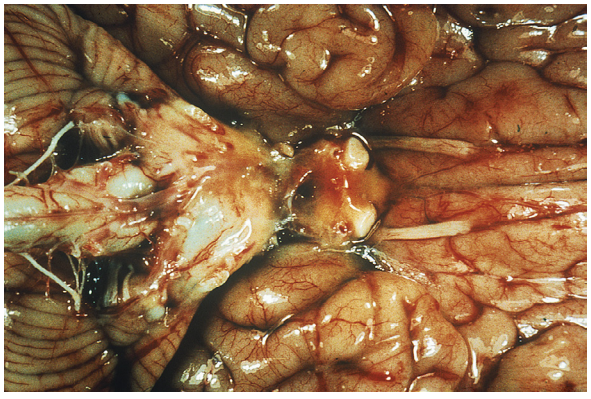


Fig. 4.69 Post-mortem appearance of tuberculosis of the base of the brain.
This post-mortem specimen shows the gelatinous and fibrinous material that collects particularly at the base of the brain in tuberculous meninigitis.

Downloaded From Vet-eBooks.com

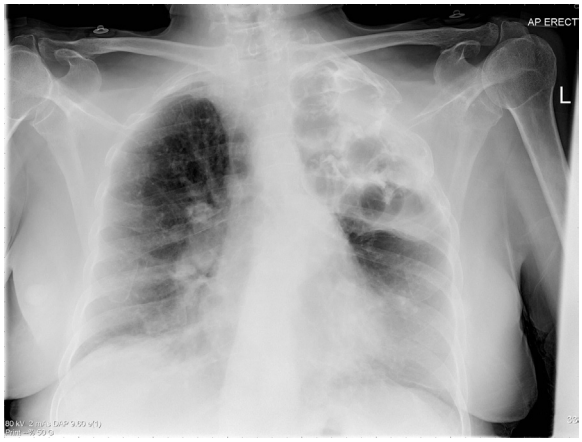


Fig. 4.70 Chest radiograph with left upper zone plombage.
In Europe and the United States during the era before antituberculous therapy, surgery was sometimes an effective treatment for cavitatory disease. Plombage involved deflation of the infected lung by the extrapleural insertion of acrylic spheres as shown in this radiograph of an elderly English woman. (Courtesy, UCL Hospitals Radiology.)

Leprosy

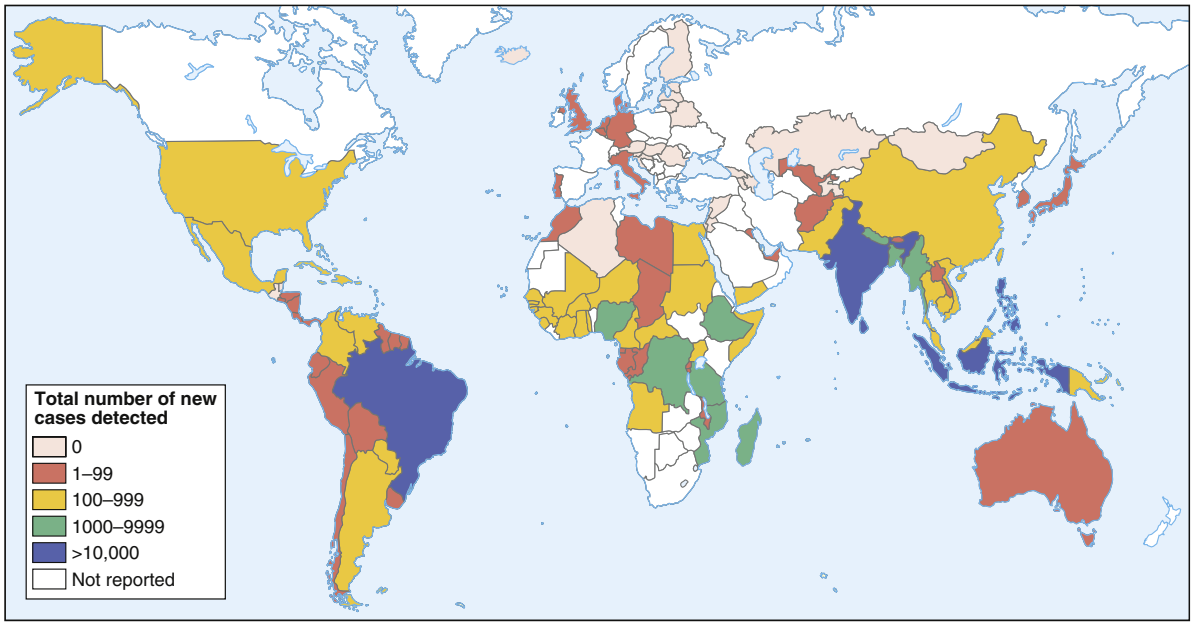


Fig. 4.71 Global distribution of new leprosy case detection, 2016.
Leprosy is caused by a very slow-growing mycobacterium, *Mycobacterium leprae*, and is presumed to be transmitted through droplets during close contact. The infection primarily affects the skin, the peripheral nerves, and the eyes, and untreated will cause permanent damage to these organs. Since 1981 multi-drug therapy (MDT) of dapsone, rifampicin and clofazamine has been recommended, and resistance has not been documented to the drugs when used in combination. MDT has been made available free of charge since 1995, and over the subsequent 20 years prevalence rates have dropped by over 99%. The current global strategy is to reduce new acquisiton cases, especially in children, thereby reducing disability. Disease prevalence is disproportionately distributed across the world, with 14 countries responsible for reporting 94% of the global burden and three (India, Brazil and Indonesia) accounting for over 80%. In some small-population countries, transmission appears to remain intense. (From Weekly Epidemiolgical Record, World Health Organization, 2016, Volume 92, Issue 35, Pages 501–520, Map 1.)

Downloaded from Vet-eBooks.com

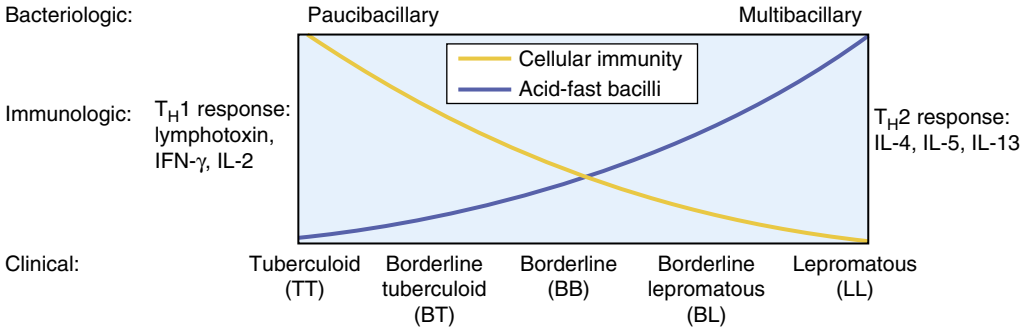


Fig. 4.72 The spectrum of immunological reponse to leprosy.
Both the bacteriological and clinical features of infection are determined by the type of immunological response. In tuberculoid leprosy (TT) the cell-mediated immunity T_H1-type response is robust and few or no *Mycobacterium leprae* bacilli are detectable (paucibacillary disease). At the other immunological extreme lies lepromatous leprosy (LL), characterized by a T_H2 immune response type, where bacterial clearance is ineffective and lesions are multibacillary. Leprosy bacilli may disseminate widely throughout the body. Whereas the immune response is stable at both of these extremes, most leprosy cases present with features of the immunologically less stable borderline disease (BT, BB or BL), and type 1 leprosy reactions are an important feature. (From Goldman, L., Schafer, A. I. Goldman-Cecil Medicine. Pages 2042–2046, Figure 326-1. Copyright © 2016 Elsevier.)

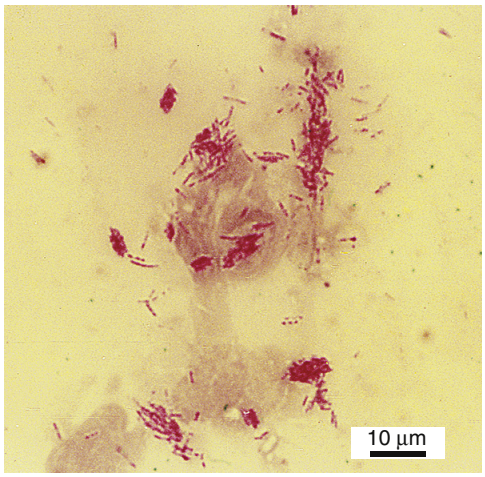


Fig. 4.73 *Mycobacterium leprae* bacilli.
Acid–fast bacteria in a slit-skin smear preparation using Ziehl–Neelsen stain. The organism cannot be cultured *in vitro*; slit-skin smear microscopy and, if available, histology of skin biopsy will supplement clinical diagnosis and aid disease classification. Numerous bacilli are visible in this smear from a patient with lepromatous leprosy.



Fig. 4.74 Rapid progression of lepromatous leprosy in the era before chemotherapy.
Across societies and throughout history including the present day, leprosy has been associated with profound social stigma, arising from its ability to inflict gross disfigurement and inexorable disability. These photographs from the early 1930s show the dramatic changes in appearance of a 13-year-old Hawaiian over a 2-year period. (From Cruz, A. T. (2019). Leprosy and Buruli ulcer: the major cutaneous mycobacterioses. In J. D. Cherry, G. J. Harrison, S. L. Kaplan, W. J. Steinbach, P. J. Hotez Feigin and Cherry's Textbook of Pediatric Infectious Diseases, Pages 1392–1418, Figure 98-11. Elsevier, Inc.)

Downloaded from Vet-eBooks.com

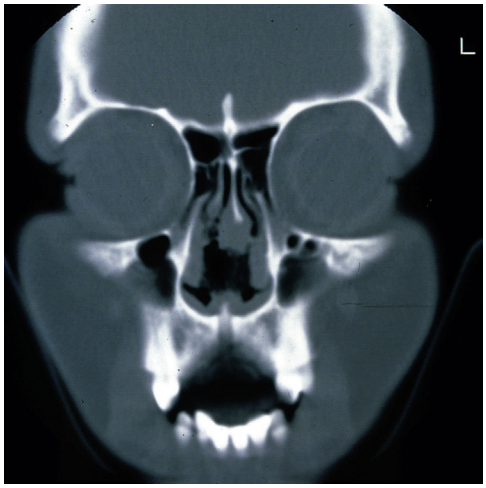


Fig. 4.75 Mucosal infiltration and septal destruction in lepromatous leprosy (LL).
Local-level epidemiology demonstrates case clustering within households and families. This suggests that transmission requires close and prolonged exposure and is believed to be via inhalation of infected aerosols. The facial CT scan from this Trinidadian woman with LL showed early destruction of the septal cartilage and pronounced mucosal thickening due to bacillary infiltration. Such patients may shed over 10 million bacilli from nasal secretions each day. Host genetics may also play a role in susceptibility to the development of disease following exposure. (Courtesy, UCL Hospitals Radiology.)



Fig. 4.76 Cutaneous manifestations of lepromatous leprosy (LL).
Numerous ill-defined nodules and poorly demarcated indurated plaques on the arms of a patient with LL. Leprosy patients often first present to healthcare facilities with long-standing skin complaints. (From Fragola, Jr L. A. et al. Dermatology Essentials. Pages 591–602, Figure 62.3B. Copyright © 2012 Elsevier. Courtesy, L. A. Fragola, Jr.)



Fig. 4.77 Facial lepromatous leprosy (LL).
The 'leonine' facies of LL caused by extensive bacillary infiltration of the facial dermis; the face of this Ethiopian man demonstrates many characteristic features including skin corrugation from chronic oedema, nodular thickening of the ears, madarosis (loss of eyelashes and eyebrows) and a collapsed nasal septum.

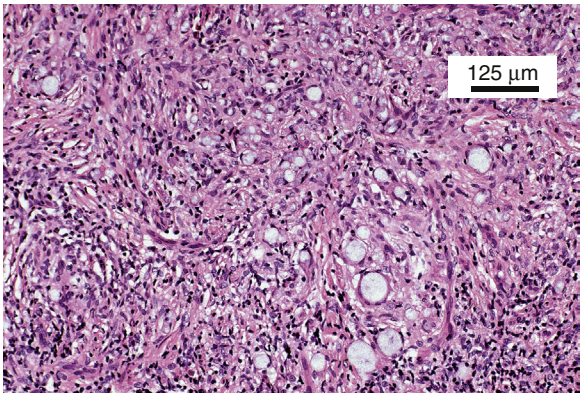


Fig. 4.78 Histology of a skin nodule in lepromatous leprosy.
This high-power section shows many 'foamy' histiocytes. No organisms are visible on staining with haematoxylin and eosin.

Downloaded from Vet-eBooks.com

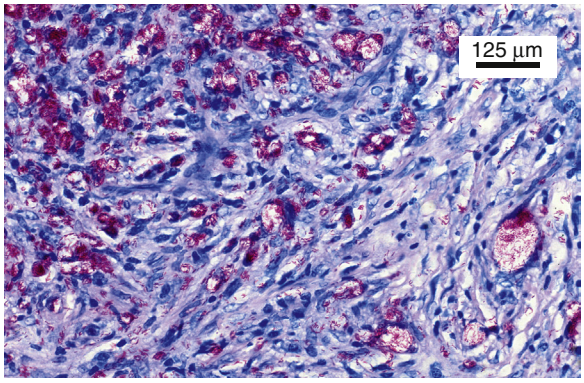


Fig. 4.79 Ziehl–Neelsen staining of a lepromatous leprosy skin nodule.
Appropriate Ziehl–Neelsen staining demonstrates huge numbers of (pink) acid–fast bacilli, many of them packed inside vacuolated macrophages.



Fig. 4.80 Neuropathic pathology in lepromatous leprosy.
Subclinical peripheral neuropathy occurs earlier in lepromatous than tuberculoid leprosy, with loss of temperature perception one of the modalities first affected. Progressive nerve damage results in a vicious cycle of trauma-related ulcers, infection, followed by bone and tissue loss. (Courtesy, Professor S. Lucas.)

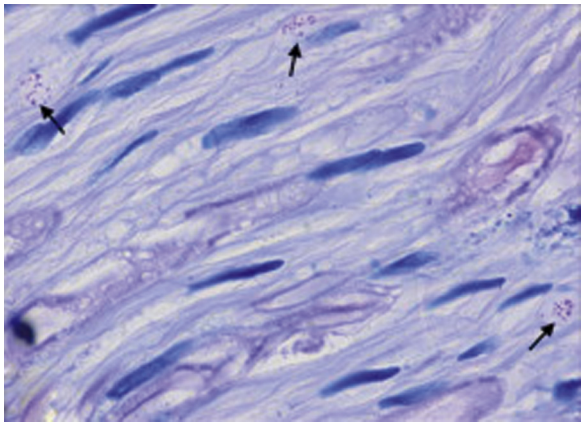


Fig. 4.81 Histology of nerve bundles in lepromatous leprosy.
Neuropathy in lepromatous leprosy is by direct bacillary invasion of the Schwann cells leading to demyelination. Acid–fast bacilli of *Mycobacterium leprae* are visible in globi (arrowed) within the nerve fibres. (High power x1000, modified Ziehl–Neelsen stain.) (From Kumar, N. et al. Comprehensive electrophysiology in leprous neuropathy – is there a clinico-electrophysiological dissociation?, Clinical Neurophysiology, 2016, Volume 127, Pages 2747–2755, Figure 2F.)



Fig. 4.82 Gynaecomastia in leprosy.
This condition, which is relatively common in adult males with long-standing lepromatous leprosy, follows testicular bacillary infiltration and subsequent atrophy.

Downloaded from Vet-eBooks.com

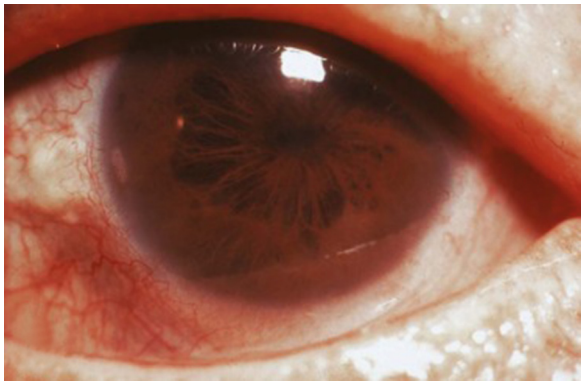


Fig. 4.83 Ocular involvement in leprosy.
Leprosy is a common cause of blindness globally, with 40% of leprosy patients suffering ocular disability. Involvement of the nerves providing muscular innervation leads to miosis, while sensory impairment can lead to corneal ulceration. Conglomerations of dead bacilli may lodge in the anterior chamber and produce pathognomonic 'iris pearls'; a single such pearl is visible here, accompanied by iris atrophy. (From Salmon, J., Bowling, B. Uveitis. In Kanski's Clinical Ophthalmology, 8th Edition. Pages 395–465, Figure 11.74C. Copyright © 2016 Elsevier Limited. All rights reserved.)

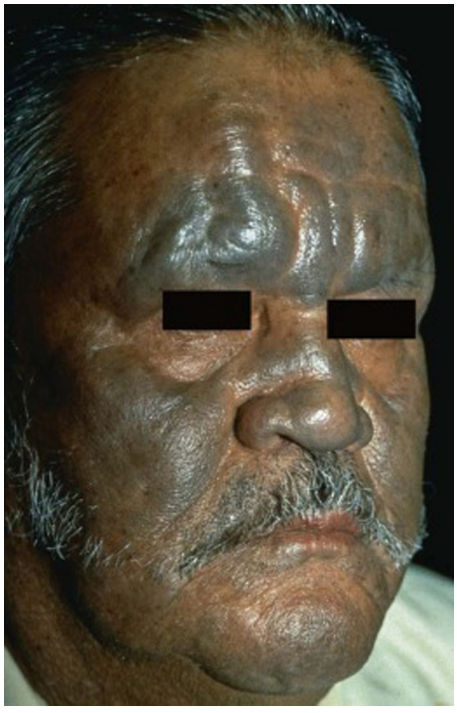


Fig. 4.84 Clofazimine-induced discolouration in leprosy.
Clofazimine, used as part of multi-drug treatment for lepromatous leprosy, is an iminophenazine dye that discolours the skin purple-grey, as shown in this man's face. (From James, W. D., Berger, T., Elston, D. Hansen's Disease. In: Andrews' Diseases of the Skin, 12th edn. Pages 331–342, Figure 17.12. Copyright © 2016 by Elsevier, Inc. All rights reserved.)



Fig. 4.85 Lesion of tuberculoid leprosy on the buttock.
A typical lesion of tuberculoid (TT) leprosy in a Nigerian man. The lesion is very well demarcated with an inflamed reddish border surrounding an area of hypopigmentation and loss of sensation. Sweating may also be diminished in the centre of such lesions, which are therefore often slightly drier than the surrounding skin. A slit-skin smear had been performed and was microscopy negative (paucibacillary leprosy). (Courtesy, Dr S. Morris-Jones.)



Fig. 4.86 Ulnar nerve involvement.
Damage to peripheral nerves in tuberculoid leprosy leads to weakness and wasting. As in this case, the paralysis and atrophy of the hand muscles innervated by the ulnar nerve result in the characteristic picture of the 'main de prédicateur'.

Downloaded from Vet-eBooks.com



Fig. 4.87 Loss of extremities in late tuberculoid leprosy.
Neurotrophic atrophy eventually leads to the loss of phalanges, especially following trauma resulting from the anaesthesia. The hands, as seen in this Liberian man, or feet may be affected with devastating implications for function. (Courtesy, Dr S. G. Browne.)



Fig. 4.88 Nerve thickening in tuberculoid leprosy.
The presence of thickened peripheral nerves is a common feature of tuberculoid leprosy. In this Congolese boy, the great auricular nerve is prominent whereas the associated macule overlying the mandible is barely visible. (From Guerrant, R., Walker, D., Weller, P. Tropical Infectious Diseases: Principles, Pathogens and Practice, 3rd Edition. Figure 37.6. Copyright © 2011 Elsevier.)

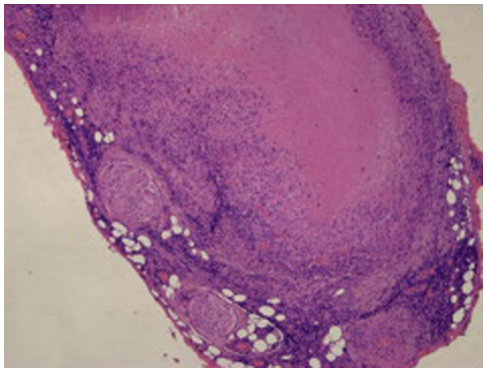


Fig. 4.89 Nerve bundle in tuberculoid leprosy.
Enlarged nerve fibres in tuberculoid leprosy demonstrating well-formed granulomas, intense cellular infiltration and frank necrosis. (Low power x50, haematoxylin and eosin.) (From Kumar, N. Malhotra, H. S., Garg, R. K., et al. Comprehensive electrophysiology in leprous neuropathy – is there a clinico-electrophysiological dissociation?, Clinical Neurophysiology, 2016, Volume 127, Pages 2747–2755, Figure 2A.)



Fig. 4.90 Borderline tuberculoid (BT) leprosy.
In borderline leprosy more skin lesions are found than in the TT form, but they may still be well demarcated, as on this man's back. Many patients with leprosy first present with skin complaints that may be misdiagnosed as fungal dermatophyte or treponemal infections.

Downloaded From Vet-eBooks.com



Fig. 4.91 Type 1 reversal reaction.
Reversal reactions may occur before, during or after treatment and are commoner in immunologically unstable borderline leprosy. Type 1 reversal reactions are believed to be due to increased cell-mediated recognition, accounting for the sudden and painful increased inflammation in pre-existing skin lesions. There is intense erythema and oedema on this woman's facial plaque. (From Bolognia, J. L., Schaffer, J., Duncan, K., Ko, C. Dermatology Essentials. Pages 591–602, Figure 62.8A. Copyright © 2014 Elsevier.)



Fig. 4.92 Type 2 reversal reaction, erythema nodosum leprosum (ENL).
ENL is believed to be the result of an immune complex-mediated vasculitis. It is characterized by the appearance of an erythematous papulo-nodular rash, usually accompanied by marked systemic upset with fever and arthralgia. (From Fragola, Jr L. A. et al., Dermatology, 3rd edn. Pages 1221–1242, Figure 75.9B. Copyright © 2012 Elsevier. Courtesy, L. A Fragola, Jr.)



Fig. 4.93 Lucio's phenomenon.
This rare manifestation of lepromatous leprosy is largely confined to Central America. A necrotizing cutaneous vasculitis, it is characterized by crops of bullous and ulcerating nodules. (From James, W. D., Berger, T., Elston, D. Andrews' Diseases of the Skin, 12th Edition. Pages 331–342, Figure 17.11. Copyright © 2016 Elsevier.)

Downloaded From Vet-eBooks.com

FUNGAL INFECTIONS

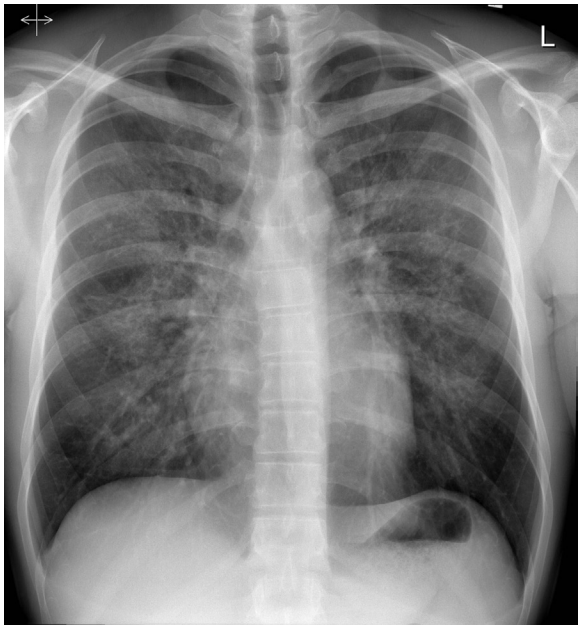


Fig. 4.94 *Pneumocystis* pneumonia (PCP).
Pneumocystis jirovecii is a major cause of life-threatening pneumonia in patients with reduced cell-mediated immunity, such as those with advanced HIV infection. Chest radiography typically shows bilateral interstitial opacification ('ground glass') in the perihilar region with sparing of the peripheral lung fields. Acquisition is inhalational, although the main risks remain unclear. Most of the population have been exposed by late childhood and asymptomatic low-burden lung colonization is common. (Courtesy, UCL Hospitals Radiology.)

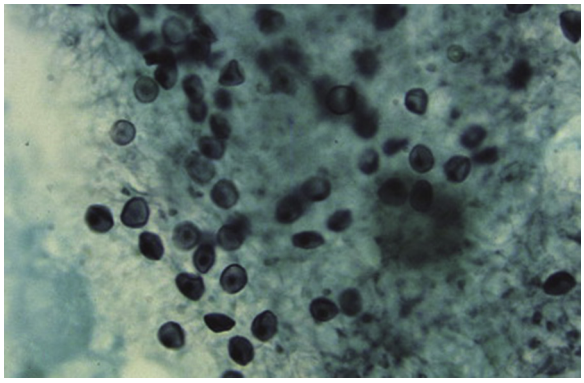


Fig. 4.95 *Pneumocystis* cysts in a bronchoalveolar lavage (Gomori silver stain).
As *Pneumocystis jirovecii* cannot be cultured, definitive diagnosis is by demonstration of characteristic fungal cysts by methenamine silver stains on deep respiratory tract specimens. Molecular detection methods are in development. (From Fristche, T. Human Immunodeficiency Virus Infection and the Acquired Immunodeficiency Syndrome: Diagnosis and Management. In: Atlas of Sexually Transmitted Diseases and AIDS, 4th edn. © 2010, Elsevier Limited. All rights reserved. Pages 256–286, Figure 15–28. Courtesy, T. Fritsche, Division of Laboratory Medicine, Marshfield Clinic Health System, Marshfield, WI.)

Downloaded From Vet-eBooks.com

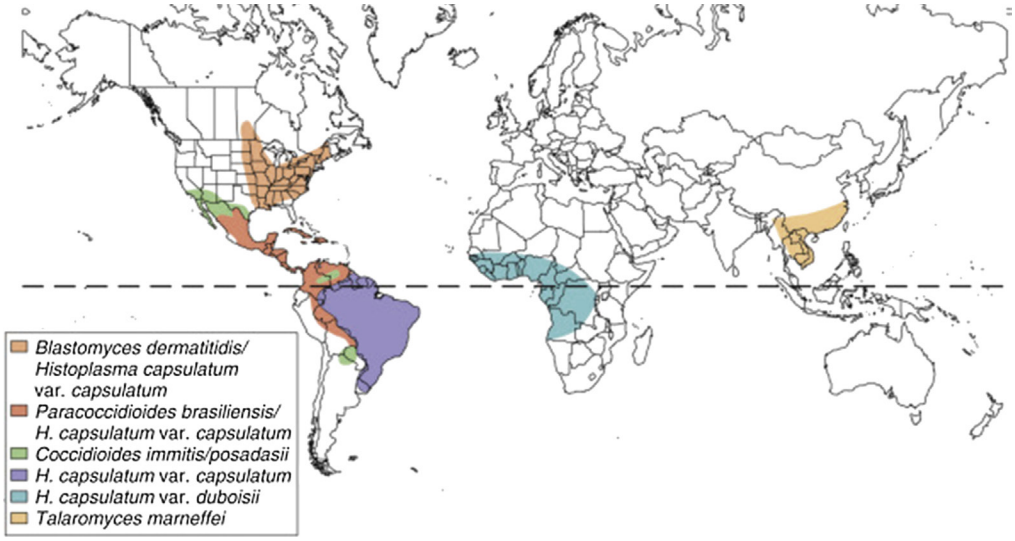


Fig. 4.96 Geographic distribution of the endemic mycoses.
There are two variety forms of *Histoplasma capsulatum* (var. *capsulatum* and var. *duboisii*); they have different geographical distributions and clinical presentations. (From Murray, P.R., Rosenthal, K.S., Pfaller, M.A. (2016). Systemic mycoses caused by dimorphic fungi. In Medical Microbiology, Pages 627-642.Figure 64.2. Elsevier Inc.)

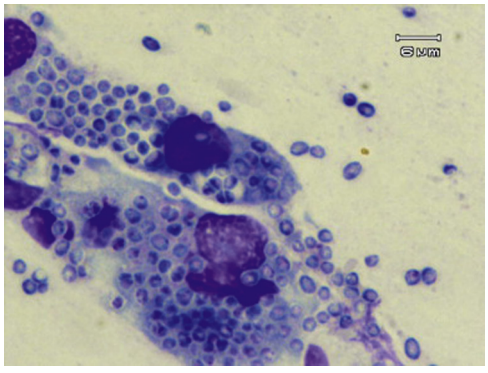


Fig. 4.97 Talaromycosis (penicilliosis) in HIV infection.
The Chinese bamboo rat is the only known non-human host for the dimorphic fungus *Talaromyces* (formerly *Penicillium*) *marneffei*, explaining the restricted geographical distribution of infection. Acquisition is believed to occur when contaminated soil or water is aerosolized and inhaled during heavy rainstorms. Infections in the immunocompromised typically present with respiratory, cutaneous or reticuloendothelial manifestations. Numerous intracellular sepate yeasts are visible in this respiratory specimen. (Wright's stain.) (From Magill, A. J., Ryan, E. T., Soloman, T., Hill, D. R. Hunter's Tropical Medicine and Emerging Infectious Diseases. Pages 644–646, Figure 85.4. Copyright © 2012 Elsevier.)



Fig. 4.98 Cutaneous talaromycosis.
Dissemination of talaromycosis (as here), histoplasmosis and cryptococcosis may each produce umbilicated cutaneous lesions that resemble molluscum contagiosum. (From Guerrant, R., Walker, D., Weller, P. Tropical Infectious Diseases: Principles, Pathogens and Practice. Pages 586–588, Figure 87.2. Copyright © 2011 Elsevier.)

Downloaded from Vet-eBooks.com

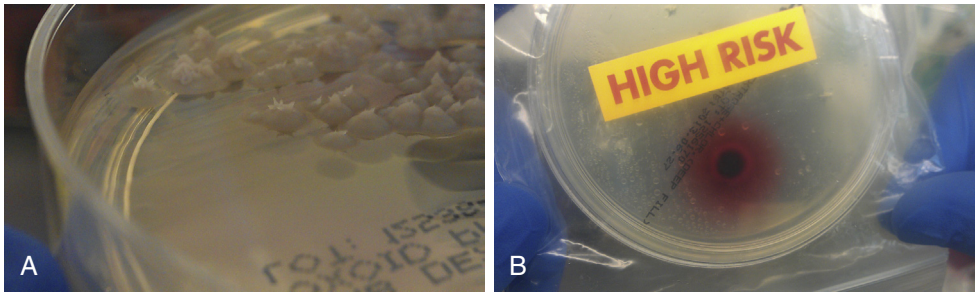


Fig. 4.99 *Talaromyces marneffei* in culture on Sabouraud agar.
Talaromyces marneffei is a dimorphic fungus that exists as a septate yeast at 37°C (A), but as a mould at 25°C producing a distinctive red pigment (B). (A, B Courtesy, Dr S. Morris-Jones.)

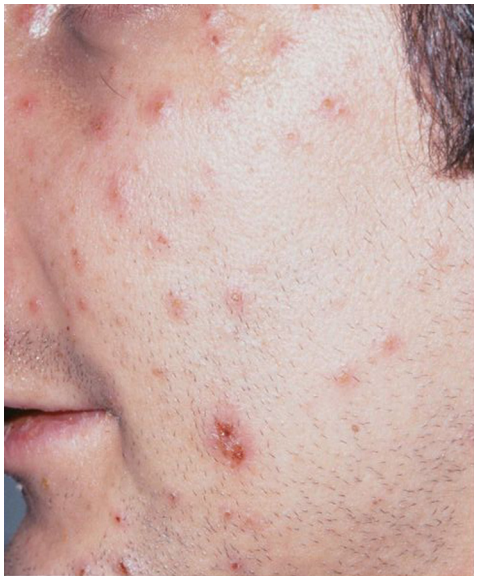


Fig. 4.100 Cutaneous histoplasmosis.
Histoplasma capsulatum has a worldwide, primarily temperate distribution and is found in particular abundance in soil contaminated with bat or bird droppings. Presentation is usually with respiratory illness, but may develop into reticuloendothelial system dissemination in the context of immune compromise. (Courtesy, Dr S. Morris-Jones.)

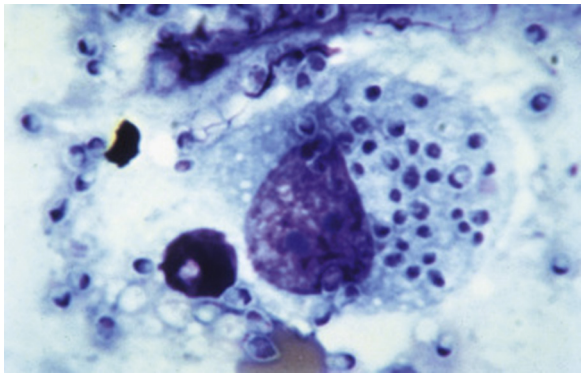


Fig. 4.101 Intracellular *Histoplasma capsulatum* var. *capsulatum*.
Histoplasmosis caused by *Histoplasma capsulatum* var. *capsulatum*, distributed through North, Central and South America, typically causes a pulmonary syndrome after spore inhalation. Dissemination within the reticuloendothelial system occurs in those with impaired cellular immunity. Yeast forms are clearly visible in this tissue macrophage (Giemsa stain). (From Murray P. R., Rosenthal, K. S., Pfaller, M. A. (2016). Systemic mycoses caused by dimorphic fungi. In *Medical Microbiology*. Pages 627-642, Figure 64.10. Elsevier Inc.)

Downloaded from Vet-eBooks.com

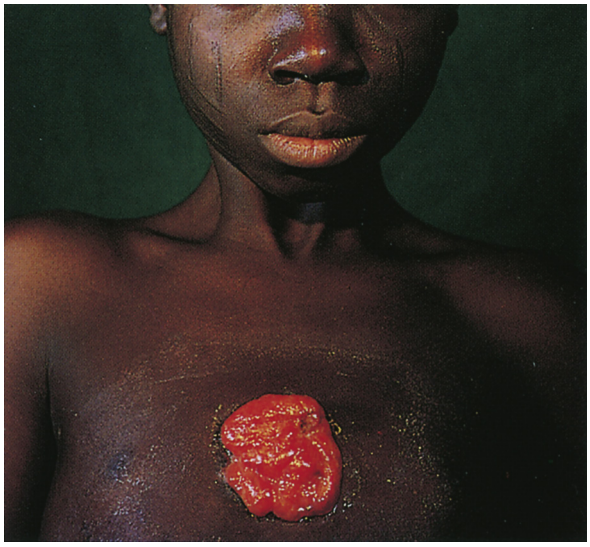


Fig. 4.102 African histoplasmosis.
African histoplasmosis, caused by *H. capsulatum* var. *duboisii*, produces mostly cutaneous or bony disease with large, destructive lesions.



Fig. 4.104 Nasal lesions in paracoccidioidomycosis.
Mucosal lesions can affect the nasopharynx with granulomatous infiltration and crusted ulceration. (From Marques, S. A. Paracoccidioidomycosis. Clinics in Dermatology, 2012, Volume 30, Issue 6, Pages 610–615, Fig. 4. Copyright © 2012 Elsevier Inc.)

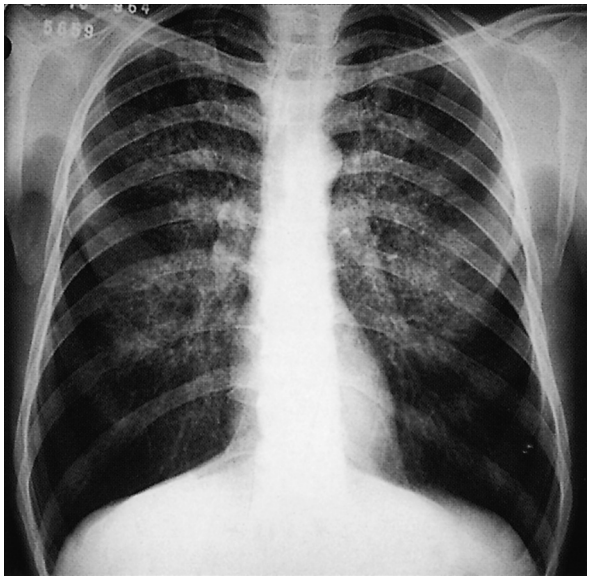


Fig. 4.103 Radiograph of pulmonary paracoccidioidomycosis.
Chronic pulmonary *Paracoccidioides brasiliensis* infection may result in fibrosis and eventual death from respiratory insufficiency.

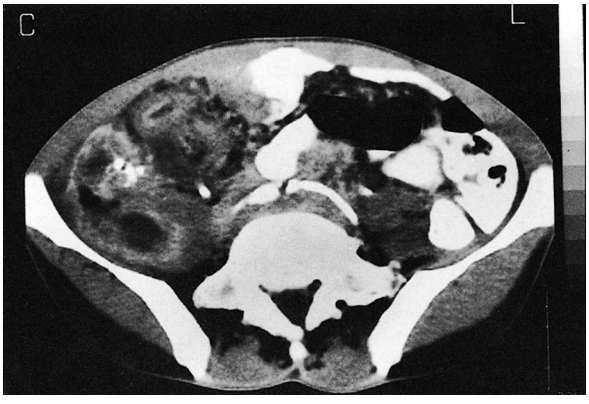


Fig. 4.105 Pseudotumoural form of paracoccidioidomycosis.
Fifteen years after an oropharyngeal infection, a 57-year-old Brazilian man presented with lumbar pain and massive weight loss. Initial examination suggested a colonic carcinoma, but CT imaging revealed a psoas abscess as well as calcification in the thickened ileocaecal region. Material removed during radical surgery confirmed *Paracoccidioides brasiliensis* infection. (Courtesy, Dr R. Chojniak and Revista da Sociedade Brasiliera de Medicina Tropical.)

Downloaded from Vet-eBooks.com

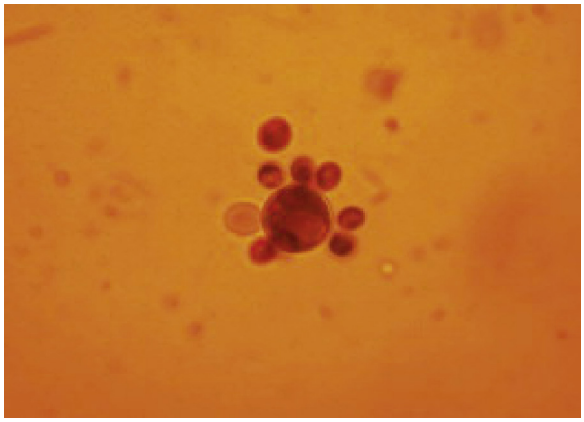


Fig. 4.106 Classic 'Pilot wheel' appearance of *Paracoccidioides brasiliensis*.
Said to be reminiscent of a ship's steering wheel, the peripheral buds of the yeast form provide a diagnostic appearance when identified in clinical samples. (From Negroni, R., Anstead, G. M., Graybill, J. R. Paracoccidioidomycosis. In: Tropical Infectious Diseases: Principles, Pathogens and Practice. 3rd edition. Pages 582–585, Fig. 86.1. Copyright © 2011, Elsevier Inc. All rights reserved.)

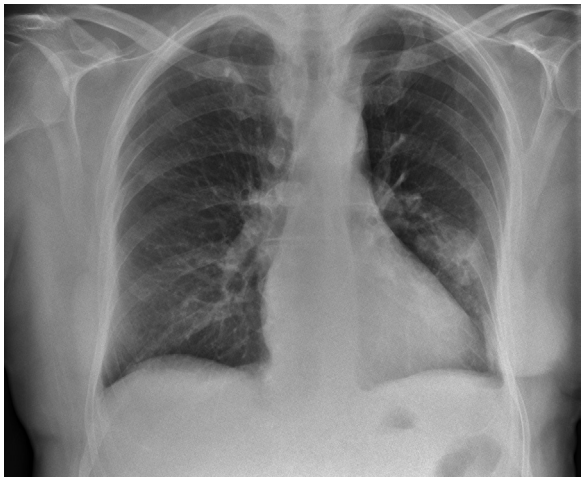


Fig. 4.108 Radiograph of coccidioidomycosis.
Persistent left-sided parenchymal infiltration on the radiograph of this 74 year old man with a history of prostatic carcinoma and asbestos exposure. He had also recently visited relatives in Arizona. (Courtesy, UCL Hospitals Radiology.)



Fig. 4.107 Paracoccidioidomycosis in a Brazilian hild.
In children, *Paracoccidioides brasiliensis* infection is an infection of the reticuloendothelial system and induces an acquired immunodeficiency. Although rare before adolescence, this $4\frac{1}{2}$-year-old boy demonstrated hepatosplenomegaly, ulcerating lymphadenopathy and generalized emaciation. (Courtesy, Dr G. L. Barbosa.)

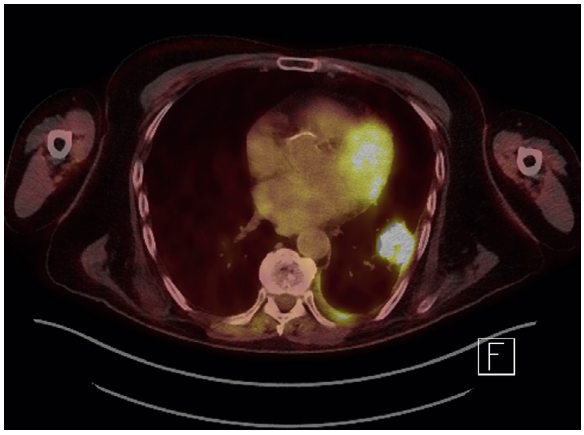


Fig. 4.109 Positron emission tomography of pulmonary coccidioidomycosis.
Imaging using a radionuclide glucose analogue provides information of physiological activity. Intense activity is seen in the left lower lobe mass of the same patient as in the previous Fig. 4.108. (Courtesy, UCL Hospitals Radiology.)

Downloaded from Vet-eBooks.com

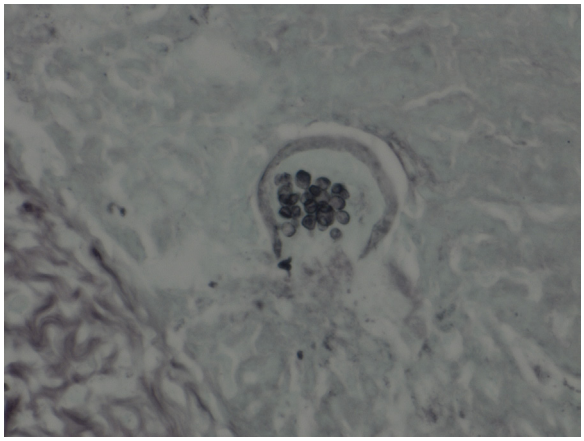


Fig. 4.110 Histopathological appearance of *Coccidioides immitis* in tissue.
The characteristic appearance of a spherical, thick-walled spherule containing small uninucleate endospores is seen on this silver Grocott stain of a biopsy from the pulmonary lesion seen in the previous Fig. 4.109. (Courtesy, Dr. U. Mahadeva, Dr. D. Arul.)

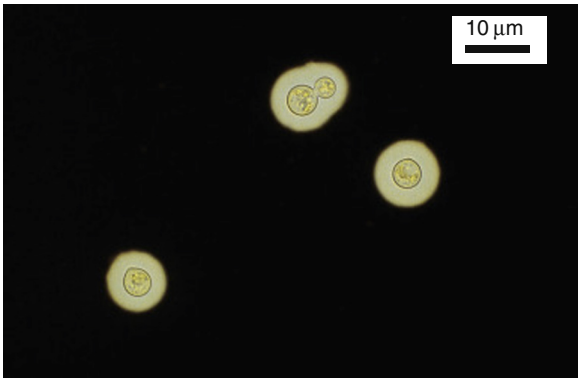


Fig. 4.112 *Cryptococcus neoformans* in cerebrospinal fluid.
Cryptococcus neoformans and *C. gattii* are both encapsulated yeasts that are easily visualized in Indian ink preparations of cerebrospinal fluid (CSF). The organisms may also be cultured from CSF and blood or, more rarely, urine. Cryptococcal antigen agglutination assays performed on serum or CSF have been the mainstay of diagnosis, but the recent development of high-quality near-patient lateral flow assays has provided opportunities for screening and earlier case detection for initiation of prompt antifungal therapy. (From Mandell, G., Bennett, J., Doin, R. Mandell, Douglas and Bennett's Principles and Practice of Infectious Diseases. Pages 2934–2948, Figure 264-6. Copyright © 2011 Elsevier.)

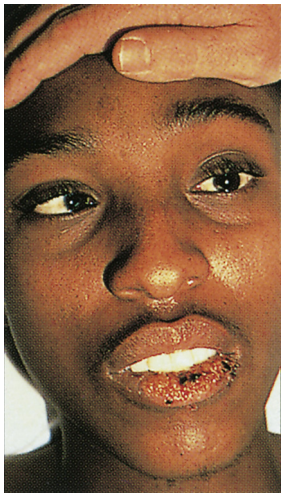


Fig. 4.111 Cryptococcal meningo-encephalitis in advanced HIV infection.
Cryptococcus neoformans is a leading infectious cause of both morbidity and mortality in HIV-infected patients. This HIV-positive Zimbabwean man with cryptococcal meningitis has a left sixth cranial nerve paralysis. (Courtesy, Professor D. A. Warrell.)



Fig. 4.113 Chronic cryptococcal meningoencephalitis.
Infection with *Cryptococcus neoformans* or *C. gattii*, is most often manifested as a chronic meningitis as in this Papuan man. Infection, however, may localize in the lungs or disseminate to other organs such as the prostate, especially in immunocompromised individuals. In disseminated disease, cutaneous and lytic bone lesions are common. (Courtesy, Professor D. A. Warrell.)

Downloaded from Vet-eBooks.com

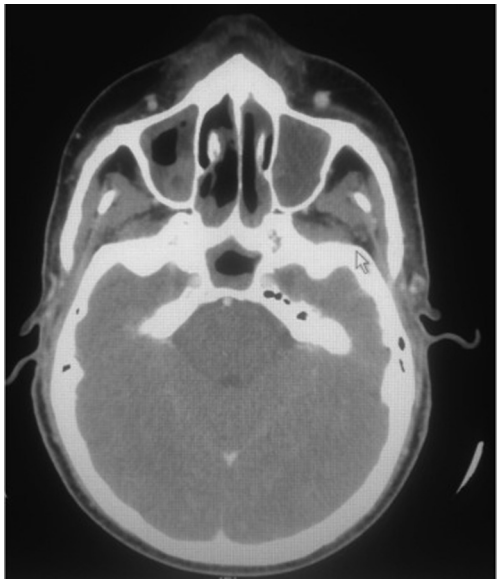


Fig. 4.114 Invasive rhinocerebral mucormycosis.
Mucor is an environmental mould that may cause devastating opportunistic disease in those with compromised immunity, particularly diabetes mellitus. This diabetic lady presented with fever and facial pain which progressed rapidly to develop multiple cranial nerve palsies (II, III, IV and V). CT imaging confirmed an extensive sinusitis with orbital bone erosion and cavernous sinus invasion. Radical surgical debridement combined with prolonged antifungal therapy achieved resolution. (Courtesy, UCL Hospitals Radiology.)

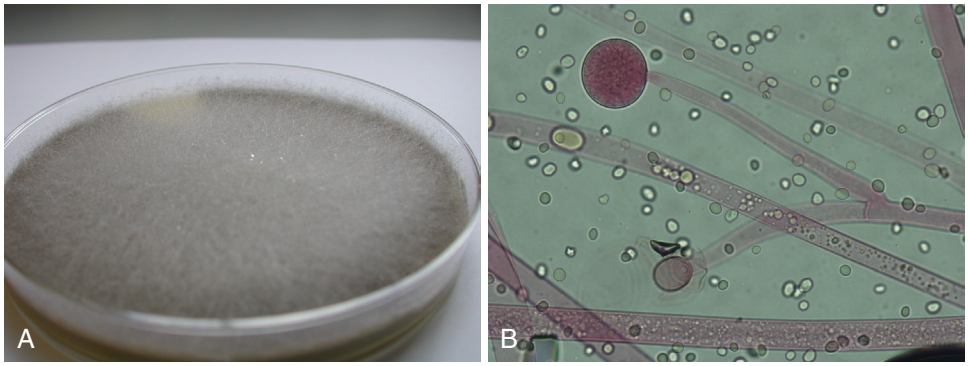


Fig. 4.115 Typical appearance of *Mucor*.
Mucor colonies grow extremely fast, covering a Sabouraud plate within 72 hours (A); globular spore-bearing bodies (sporangia) and the virtual absence of hyphal septae are characteristic (B, Congo Red stain). (Courtesy, Dr S. Morris-Jones.)



Fig. 4.116 Surgical wound infection with *Mucor*.
This Indian patient required surgical debridement after a road traffic accident. Airborne *Mucor* contaminated the wound, leading to rapid tissue necrosis that required prompt limb amputation and prolonged antifungal therapy. (Courtesy, Dr L. Nabarro.)

Downloaded From Vet-eBooks.com

5. Ectoparasites

Some arthropods are of medical importance predominantly because of the direct effect of infestation and these are considered in this chapter. Arthropods that cause illness through envenomation (mainly arachnids) are discussed in the following chapter along with other noxious exposures (bites, stings, venoms, toxins). Others, considered elsewhere (Chapter 1), are responsible for disease primarily because they are vectors of viral, bacterial or parasitic pathogens. The few that are both vectors and direct causes of pathology are included in sections describing the vector-borne disease.

Among the ectoparasitic arthropods, the cosmopolitan scabies mites, lice and bedbugs are particularly prevalent. Other cosmopolitan species of mite (Table 5.1) that commonly cause local and/or systemic pathological changes are especially likely to be encountered in a tropical environment and are therefore considered here. Tungiasis is a significant problem in many tropical areas, where it can be a major cause of disability and afflict more than 50% of the indigenous population. However no global estimates of prevalence are available. Although the myiases are rare and can be very serious or even lethal, the larvae of one species of fly are returning to favour as cleansers of contaminated wounds.

Table 5.1 Mites of medical importance

Genus and species	Notes
Thryeophagus entomophagus	Causes 'pancake syndrome'
Dermanyssus gallinae	Poultry red mite, infests humans
Ornithonyssus bacoti	Tropical rat mite
Ornithonyssus sylviarum	Northern fowl mite
Ornithonyssus bursa	Tropical fowl mite
Dermatophagoides pteronyssinus	Main house dust allergen
Dermatophagoides farinae	Common house dust allergen
Euroglyphus maynei	Common house dust mite
Sarcoptes scabiei	Scabies, Norwegian scabies
Pyemotes ventricosus	Grain, straw mite, causes dermatitis
Cheyletiella parasitovorax	In dog fur, causes dermatitis
Cheyletiella blakey	Mainly in dog fur
Cheyletiella yasguri	In dog, cat, rabbit fur
Demodex folliculorum	In human hair follicles
Demodex brevis	In sebaceous glands
Neotrombicula autumnalis	'Harvest mite'
Leptotrombidium akamushi	Vector of *Orientia tsutsugamushi* (scrub typhus) in Japan
Leptotrombidium deliense	Vector of *Orientia tsutsugamushi* (scrub typhus) in rest of South East Asia

Downloaded from Vet-e-Books.com

MITES *(see Table 5.1)*

Aside from trombiculid mites of the genus *Leptotrombidium*, the larval forms of which are the vectors of scrub typhus in South East Asia, mites only cause pathology as a consequence of direct host contact. Some have a cosmopolitan distribution whilst others have more restricted niches. Globally, the faeces of the house dust mite triggers several allergic conditions and profoundly itchy scabies infestation can occur either sporadically or in outbreaks. Several species, such as the poultry red mite, provoke intense cutaneous irritation in defined epidemiological niches.

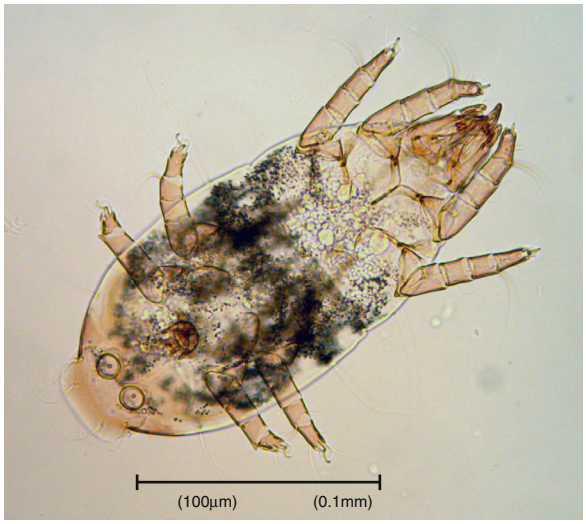


Fig. 5.1 Male *Thyreophagus entomophagus*.
Pancake syndrome results from an anaphylactic reaction to the ingestion of foods made with mite-contaminated wheat flour. Numerous *Thyreophagus entomophagus* mites were found in the culprit flour after a young man presented to the emergency department with anaphylaxis after consumption. Pancake syndrome has been reported from Venezuela, Brazil, United States, Japan and Taiwan. (Courtesy, C. Whitehorn)

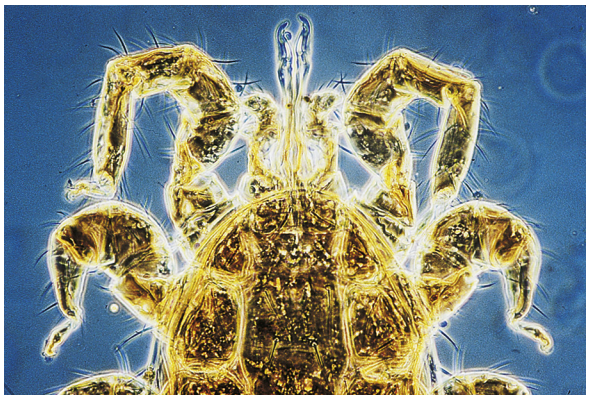


Fig. 5.2 *Ornithonyssus bacoti*, the tropical rat mite.
Gamasid mites of the family Dermanyssidae are ectoparasites of birds and small mammals. Humans are an accidental host but the bites of a number of gamasid species cause severe cutaneous reactions. *O. bacoti* is a cosmopolitan species found commonly in seaports. It frequently bites humans and produces large, irritating, papular lesions. Most species feed nocturnally and all those that affect humans tend to produce a similar response consisting firstly of itching, the onset of which may be delayed by some hours, followed by a rash. This varies in character from simple macules, papules or wheals to a varicelliform reaction. The history of exposure, which may be related to the individual's occupation, gives a clue to the diagnosis of the condition. The mites are relatively large (many about 1 mm long) compared with sarcoptid mites (see Fig. 5.7) (the cause of scabies) and trombiculid mites (see Fig 1.72) (the vector of scrub typhus).

Downloaded From Vet-eBooks.com



Fig. 5.3 *Ornithonyssus bursa*, the tropical fowl mite.
This mite lives in birdnests and breeds on birds but may migrate into the household to find alternative food sources after birds leave the nest. Vesiculo-papular spots appear at the site of mite bites. (Courtesy, L. Knott.)



Fig. 5.4 Varicelliform reaction to bites of *Dermanyssus gallinae*, the red poultry mite.
Note the scratch marks due to the intense irritation on the skin of this man, who was bitten by the red poultry mite, another of the gamasid mites, while plucking turkeys. (Courtesy, Dr M. Young.)



Fig. 5.5 Skin test for hypersensitivity to house dust mite.
Dermatophagoides pteronyssinus and *Dermatophagoides farinae* are commonly found in house dust and have been associated in recent years with the common 'stuffy nose' syndrome that afflicts many people at night. They feed mainly on dead epithelial scales and other organic matter in house dust. The presence of protein from dead mites, which is probably responsible for allergic reactions to these mites, can also precipitate paroxysms of asthma in sensitized individuals and may cause atopic skin eruptions, including eczema, in others. Over 100 mites/g of dust have been recovered from the house dust of some asthmatic individuals, whose condition may improve if they can be moved to a mite-free environment. (Courtesy, Dr. J. Lukawska.)

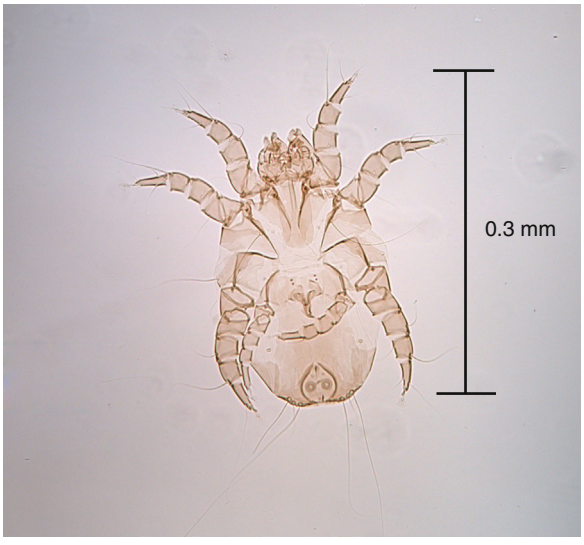


Fig. 5.6 *Dermatophagoides* male.
Proteases in the 20–30 faecal pellets produced each day by the house dust mite trigger allergic conditions including asthma, eczema and allergic rhinitis. (Courtesy, C. Whitehorn)

Downloaded from Vet-eBooks.com

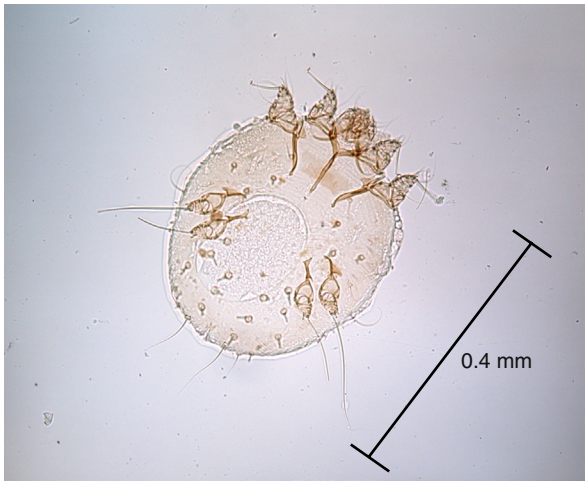


Fig. 5.7 Female scabies mite.
The gravid female *Sarcoptes scabiei*, with short, stumpy legs and suckers on its forelegs, burrows into the epidermis, lays its eggs and dies at the end of the tunnel. It is cosmopolitan in distribution. (Courtesy, C. Whitehorn.)



Fig. 5.8 Scabies burrows, papules and vesicopustules on the foot of an infant.
The foot is the second commonest site of early infection in infants, with the axillae and neck also being invaded in some cases. (From Burkhart, C.N., Burkhart, C.G., Morrell, D.S. Infestations. In: Dermatology. Pages 1423–1434, Figure 84.3B. Copyright © 2012 Elsevier.)



Fig. 5.9 Scabies lesions.
Lesions are commonly found in interdigital spaces of the hand, flexor surfaces of wrists and elbows, axillae, groins, natal cleft, umbilicus and genitalia. In young children head and neck involvement and early formation of pustules are more commonly seen. (From Dirk M. Elston, Ectoparasites (Lice and Scabies), pages 1294-1298.e1, Figure 257.6. In: Principles and Practice of Pediatric Infectious Diseases 5th Edition. Copyright © 2018 by Elsevier, Inc.)

Downloaded From Vet-eBooks.com



Fig. 5.10 Secondary erythema in scabies.
Secondary infection is common, and erythema may be associated with bacterial invasion of the sarcoptic tracks. In some populations, best described in Australian indigenous communities, there is a clear association between secondary bacterial infection of endemic scabies and outbreaks of acute post-streptococcal glomerulonephritis and rheumatic fever. (Courtesy, Professor H. Morgan.)



Fig. 5.12 Hyperkeratotic ('Norwegian') scabies in a patient who had suffered a 70% burn injury.
This condition is often associated with immunosuppression, including that due to HIV infection. Here the underlying cause was severe burns from which the hands were spared, but then subsequently severely affected by scabies. (Courtesy, Dr J. O'D. Alexander.)



Fig. 5.11 Chronic eczematous scabies in a Gambian woman.
The backs of the hands and arms are heavily infested in this woman. Constant scratching due to the intense itching may result in lichenification of the dry skin. The condition would need to be differentiated from onchocerciasis in settings where both conditions are present. (Courtesy, Dr S. Lindsay.)



Fig. 5.13 'Norwegian' scabies in an elderly man.
This 91-year-old man had suffered pruritus with crusty skin lesions, some over 1 cm thick, for 6 months prior to admission to hospital. In addition to the discovery of a heavy scabies infection he was found to have carcinoma of the bladder. The skin condition improved rapidly following anti-mite treatment.

Downloaded from Vet-eBooks.com

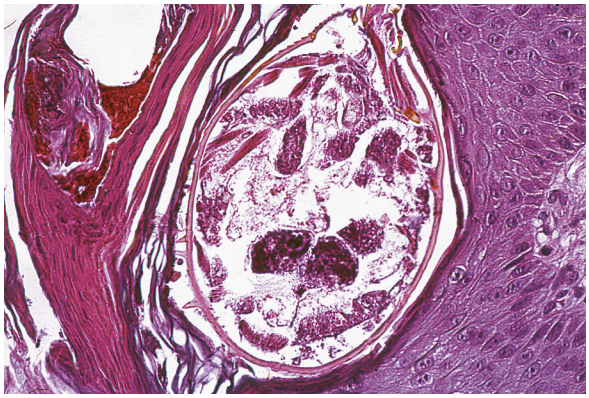


Fig. 5.14 Section of biopsy from patient with 'Norwegian' scabies. This skin section shows some of the cuticular spines and internal organs of a female mite which lies within a subepidermal pocket under a thick layer of dead epidermis. In such patients the mites can be present in vast numbers.



Fig. 5.15 Rash caused by *Cheyletiella parasitivorax*. The lesions developed in a woman who had recently acquired a puppy and consisted of small, erythematous papules with haemorrhagic, vesicular centres, which were intensely irritating. They may become pustular and be excoriated by scratching. Management of cases should include the use of acaricides to rid pet animals and their bedding of the mites. (Courtesy, Dr J. O'D. Alexander.)

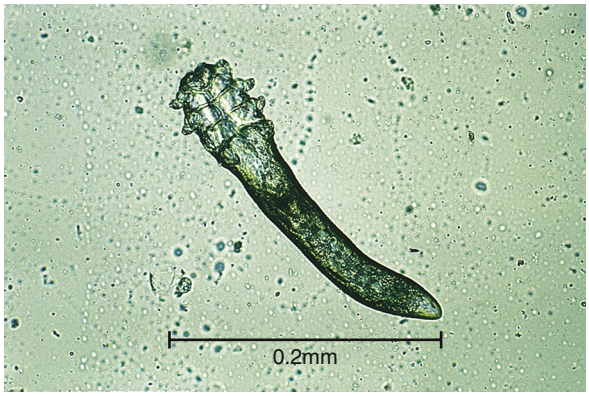


Fig. 5.16 Ventral view of *Demodex folliculorum*. This species inhabits human hair follicles, especially on the head and ears. It is believed that the mites can be found if carefully looked for in most healthy adults, in whom they cause no pathological changes. The mites are especially common in sebaceous skins and have been associated with folliculitis, rosacea, inflammatory blepharitis and pityriasis folliculorum. In recent years a second species has been identified in human sebaceous glands, *Demodex brevis*. (Courtesy, Professor E. M. Grosshans.)



Fig. 5.17 Videodermatoscopic observation of a skin-attached and feeding larval *Neotrombicula autumnalis mite*. (Magnification ×150.)
These 'harvest mites' are common in grassland in temperate climates. The larvae, the only parasitic form of the life cycle, normally feed on small mammals and birds, but may also attack humans, causing intense irritation. Related trombiculid mites are responsible for transmission of scrub typhus (caused by *Orientia tsutsugamushi*) in South East Asia. (Courtesy, Centers for Disease Control and Prevention, Atlanta, GA. From Nasca, M. R., Lacarrubba, F., Micali, G. Diagnosis of trombiculosis by videodermatoscopy. Emergency Infectious Diseases 2014, Volume 20, Pages 1059–1060.)

Downloaded From Vet-eBooks.com

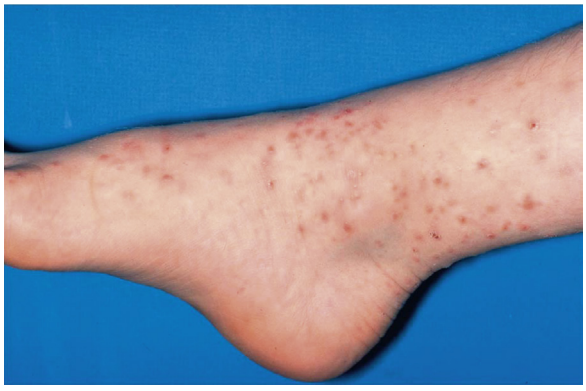


Fig. 5.18 Chigger bites to the ankles.
The trombiculid mite larvae do not bite to ingest blood. Instead they inject digestive enzymes into the skin through a 'stylostome' and feed on dissolved host tissue. These salivary secretions are responsible for the intense itching, papules and wheals that may develop. (From James, W. D., Berger, T. G., Elston, D. M. Parasitic infestations, stings, and bites. In: Andrews' Diseases of the Skin. Pages 418–450. Copyright © 2016 Elsevier.)

LICE

Trench fever (due to *Bartonella quintana*) and epidemic typhus (due to *Rickettsia prowazekii*) are transmitted by the human body louse *Pediculus humanus corporis* (see Fig. 1.60). Direct effects of louse infestation are severe irritation and dermatitis.



Fig. 5.19 *Pediculus humanus capitis* infestation.
The head louse, *P. h. capitis*, is very common, and heavy infestations can cause severe irritation. The eggs ('nits') are attached to the hairs and appear as masses of white dots (A). Unlike *P. h. corporis*, *P. h. capitis* is not known to be a disease vector. (B) 'Nits' attached to hairs. (C) Adult *Pediculus humanus capitis*. [(A) Courtesy, Professor S. P. Deshpande; (B, C) Courtesy, C. Whitehorn.]

Downloaded from Vet-eBooks.com



Fig. 5.20 (A) Severe pediculosis corporis caused by *Pediculus humanus corporis*. (B) *Pediculus humanus corporis*.
Heavy infestation is common where people live in unhygienic conditions. Body lice spread rapidly wherever suitable ecological conditions prevail and are common in soldiers during wartime, in displaced populations and refugees, and in prisons. Severe dermatitis due to a heavy louse infestation and the scratching that the bites stimulate, especially at night, is often accompanied by pigmentation of the affected areas, formerly known as 'vagabond's disease', restlessness causing loss of sleep and, in chronic cases, lichenification and eczema. As in this patient, thousands of lice may be present on the patient's body and in his clothes. [(A) Courtesy, Dr A. C. Chu; (B) Courtesy, C. Whitehorn.]



Fig. 5.21 Adult *Pthirus pubis*.
The pubic louse is readily spread through sexual contact. The compact and rounded body is 'crab-like' and the louse has large claws on mid and hind legs. It is not a vector of other infections. (Courtesy, C. Whitehorn.)



Fig. 5.22 (A) Egg of *Pthirus pubis*, (B) here attached to the bases of the eyelashes.
Eggs with characteristic raised operculum are attached to pubic and facial hair only. (Courtesy, C. Whitehorn.)

Downloaded from Vet-eBooks.com

BED BUGS

The medical importance of bed bugs remains confined to the dermatological consequences of bites, usually acquired at night. Apparently increasing global prevalence, particularly in regions where bed bugs had previously become uncommon, has raised interest in potential vector competence; for now this remains unproven though researchers have proposed that further investigation into possible transmission of arboviruses, drug-resistant bacteria and parasites, amongst many other candidates, is warranted.

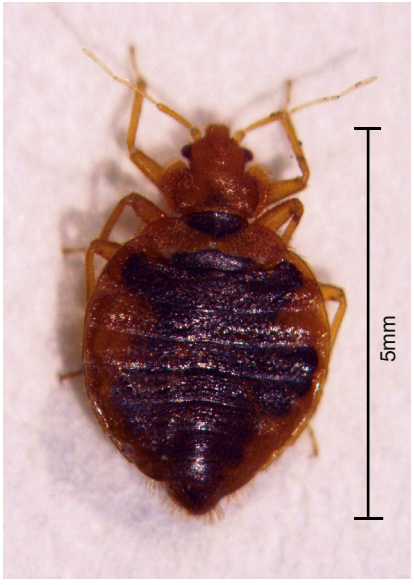


Fig. 5.23 *Cimex lectularius*.
This species and the tropical bed bug, *Cimex hemipterus*, frequent houses, where they feed on the blood of the inhabitants at night. Bites are commonly multiple and may be due to interrupted feeding by a single bug (so-called 'breakfast-lunch-dinner' line of lesions). Blood is actively sucked up by pumping action of the hypopharynx once the stylets have pierced a small blood vessel, taking 10–20 minutes for the bug to become fully engorged. The bite itself is not painful but erythema and itching develop later. (Courtesy, C. Whitehorn.)

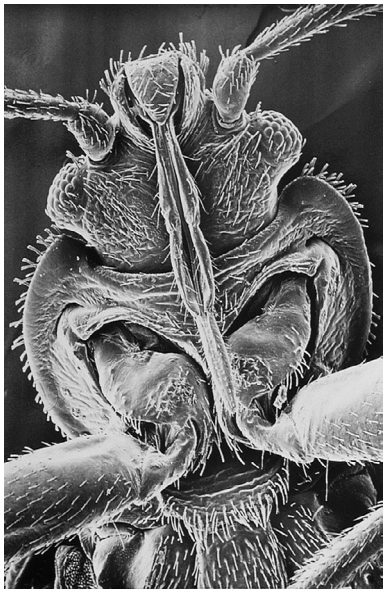


Fig. 5.24 Ventral surface of head of *Cimex hemipterus* showing proboscis.
Scanning electron micrograph showing the biting mouth parts of the tropical bed bug. They are contained in the proboscis, which is held under the body when not in use. (Courtesy, Professor V. Zaman.)

FLEAS

Some fleas are vectors of important bacterial diseases in humans (e.g. *Xenopsylla cheopis* carrying *Yersinia pestis*, the cause of plague, and *Rickettsia typhi*, the cause of murine typhus) (Chapter 1). Those considered here are primarily causes of dermatological irritation either directly due to sensitivity to a bite or through egg-laying inside a burrow containing a gravid female (tungiasis).

Downloaded from Vet-eBooks.com

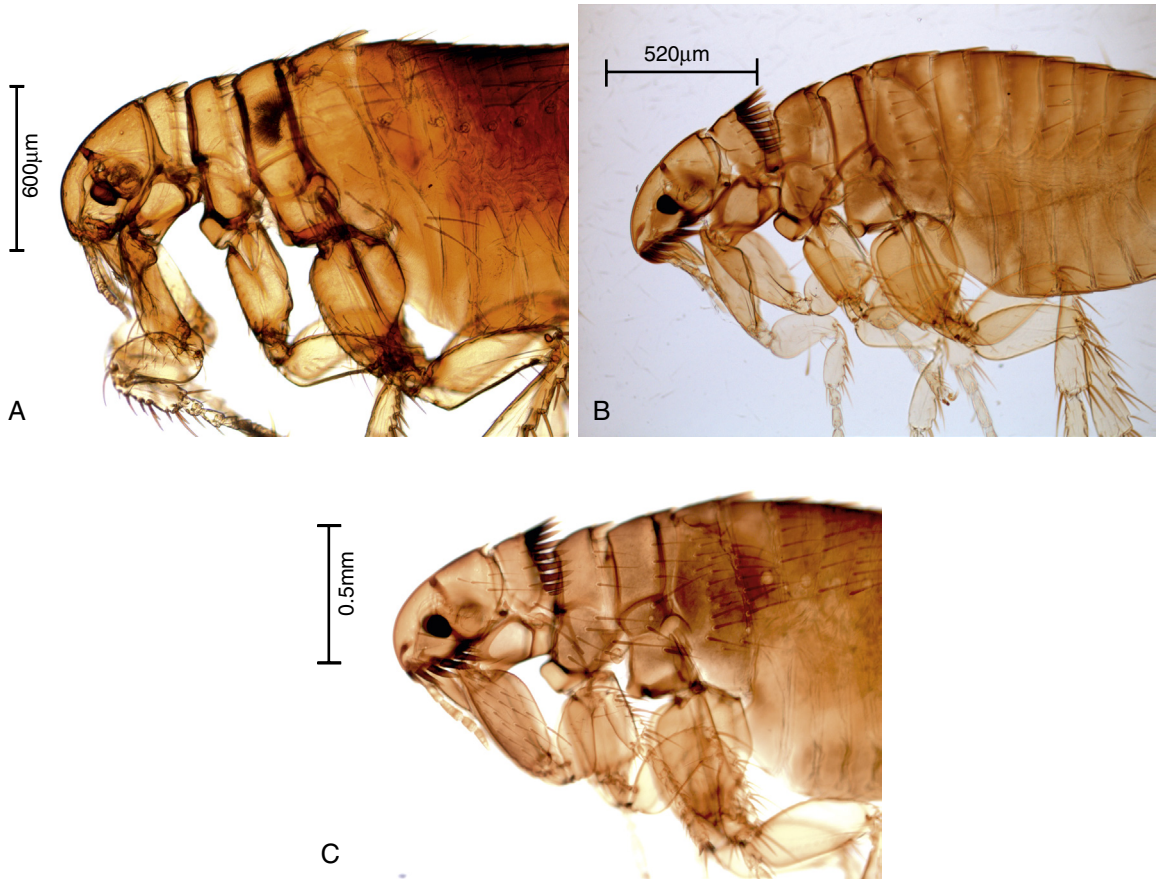


Fig. 5.25 (A) *Pulex irritans*, (B) *Ctenocephalides felis* and (C) *Ctenocephalides canis*.
The 'human flea' (A) is a cosmopolitan species that is becoming uncommon in houses in many temperate countries. Under especially favourable climatic and environmental conditions, fleas may appear in almost epidemic proportions. Humans are most commonly bitten by cat (B) and dog (C) fleas of the genus *Ctenocephalides*. (Courtesy, C. Whitehorn.)



Fig. 5.26 Extensive papular urticaria caused by massive flea infestation.
The intense irritation in the lumbar region caused this man to scratch incessantly, producing marked excoriation of lesions that were accessible. (Courtesy, Dr J. O'D. Alexander.)

Downloaded from Vet-eBooks.com

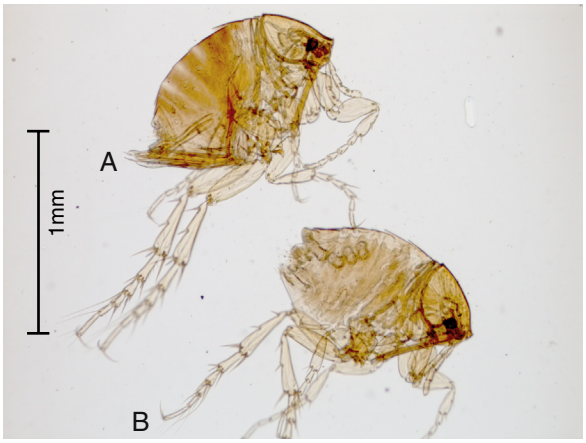


Fig. 5.27 (A and B) Male and female *Tunga penetrans*.
Not to be confused with the chigger which is a mite (see Fig. 5.18 above), the 'jigger' or 'chigoe' flea, which is common in tropical areas of South America and Africa, is only 1 mm long and is the smallest flea known. The male (A), which has a characteristically angular head, is free-living; however it is the female (B), that causes pathology in humans, burrowing into skin in contact with soil in order to lay eggs. (Courtesy, C. Whitehorn.)



Fig. 5.28 Female jigger flea penetrating the skin of a toe.
The gravid female (arrow) burrows into the epidermis, where it settles with its posterior end facing the entrance hole. The periungual region is a favoured site of entry. Here there is inflammation and desquamation of the adjacent skin. Secondary infection is common when pathogenic microorganisms enter through the entry hole.



Fig. 5.29 Section of female *Tunga penetrans* in the skin.
Having buried itself in the skin, often under the toenails, the female swells up to the size of a small pea within 8–10 days as its eggs mature. (Courtesy, Dr H. Lieske.)



Fig. 5.30 Female *Tunga penetrans* laying eggs.
Some 150–200 eggs per day are actively ejected through the entry hole as seen in this photograph showing a line of recently projected eggs. Oviposition continues over a period of about 5 weeks, after which the flea dies. (Courtesy, Dr S. Morris-Jones.)



Fig. 5.31 Living egg of *Tunga penetrans*.
The oval egg, which is readily seen macroscopically as a tiny pearly object (see Fig. 5.30), is about 0.5 mm long and 0.3 mm in diameter.

Downloaded from Vet-eBooks.com



Fig. 5.32 Heavy infection with *Tunga penetrans* in the fingers of a Brazilian patient.
Although the feet are most commonly infected, other parts of the body may also be implicated in tungiasis, such as in this patient with two severely damaged fingernails. Of 1184 Brazilian 'favela' residents surveyed, 33.6% had tungiasis. Lesions affected the hands in 6% and were also noted on the elbows, thighs and gluteal areas.



Fig. 5.33 Massive infection with *Tunga penetrans*.
This patient in Cayenne had about 1000 female *T. penetrans* embedded in his hands, feet, buttocks, elbows and knees. He made an uneventful recovery after removal of the insects with forceps following the local application of salicylated petroleum jelly. Tetanus vaccination is essential and antibiotic cover may be worthwhile in such patients.



Fig. 5.34 *Tunga trimamillata* gravid female.
A second species of jigger flea, *T. trimamillata*, has been described in patients with tungiasis in Ecuador where it was first observed in pigs, goats and cattle. This species co-exists with *T. penetrans* in some localities. Here the gravid female has been extracted from a site at the corner of the patient's left big toe. Although only 10 species of Tunga have been recognized to date it seems quite likely that others remain unidentified up to now.

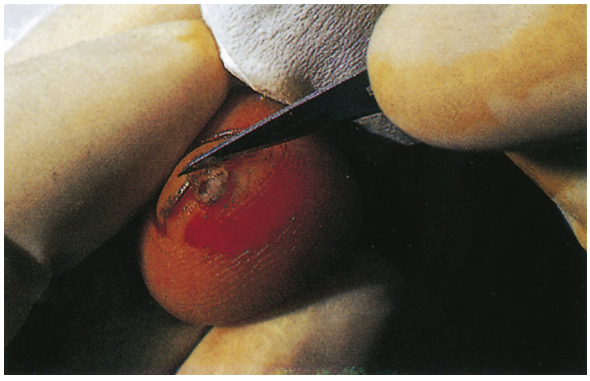


Fig. 5.35 Jigger flea being removed from toe.
Habitual sufferers shell the gravid females out of the skin with a pin or sliver of bamboo, usually scattering eggs in the process. Tetanus is a potential sequel to this type of self-treatment. In heavy infections the application of salicylated petroleum jelly leads to the death of the embedded fleas with minimal trauma to the host. (Courtesy, Professor A. Bryceson.)

Downloaded from Vet-eBooks.com

Table 5.2 Myiasis-producing diptera of medical importance

Family/subfamily	Genus and species	Other names	Notes
Calliphoridae/Calliphorinae			
'Metallic group'	*Chrysomya bezziana*	Old world screw worm	Feed on living tissue in wounds
	Cochliomyia hominivorax	New world screw worm	
	Lucilia spp.	Greenbottles	Feed on dead tissue in wounds
	Calliphora spp.	Bluebottles, blow flies	
	Phormia regina	'Black blow fly'	Can cause dermal, enteric myiasis
	Cynomopsis cadaverina		Invades wounds
'Nonmetallic group'	*Auchmeromyia senegalensis*	Congo floor maggot	Sucks blood from skin
	Cordylobia anthropophaga	Tumbu, mango fly	Causes subcutaneous boils
Calliphoridae/Sarcophaginae			
	Wohlfahrtia spp.	Flesh flies	Invade wounds or normal tissue, especially on head
	Wohlfahrtia magnifica		Commonest species in humans
	Sarcophaga haemorrhoidalis		May occur in gut
Cuterebridae			
	Dermatobia hominis	Human bot fly	Causes subcutaneous boils
	Cuterebra spp.	North American bot flies	Skin and eye lesions
Hypodermatidae			
	Hypoderma spp.	Warble flies	Cause dermal, eye or nasopharyngeal lesions
	Hypoderma tarandi	Reindeer warble	Ophthalmomyiasis
Oestridae			
	Oestrus ovis	Sheep nasal bot fly	Invades nasopharynx and eye

Modified from Zumpt, F. Myiasis in man and animals in the old world. Butterworths, London, 1965 and Lane, R. P., Crosskey, R. W. (eds) Medical insecta and arachnids. Chapman & Hall, London, 1993.

MYIASIS

This is the description given to the infection of human tissue by a fly larva (colloquially known as a maggot). In endemic regions extensive infestations may be seen and infection of animals can have significant economic consequences. Travellers to tropical areas of South America and Africa are also at risk, particularly of *Dermatobia hominis* and *Cordylobia anthropophaga* (Table 5.2).

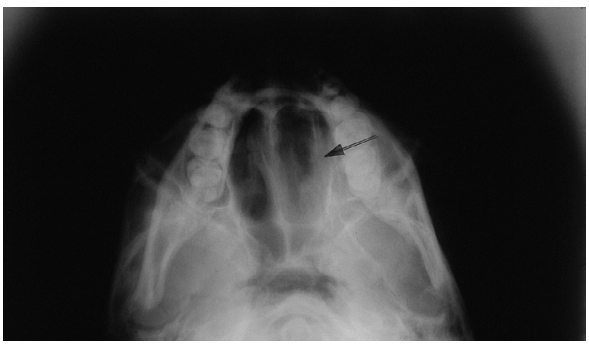


Fig. 5.36 Radiograph of nasal sinuses invaded by larvae of *Chrysomya bezziana*.
The Old World screw worm is an obligate parasite, requiring a mammal host for egg-laying by the metallic green adult female fly. Hatched larvae feed on healthy (not necrotic) tissue, as in this 14-year-old girl from the eastern province of Saudi Arabia who complained of recurrent nose bleeding and pain of 5 days' duration. Radiography showed that the lateral wall of her left nasal cavity (indicated by the arrow) had been destroyed. More than 80 larvae were removed surgically from the sinuses and the patient recovered. (Courtesy, Dr M. A. Ansari.)

Downloaded from Vet-eBooks.com

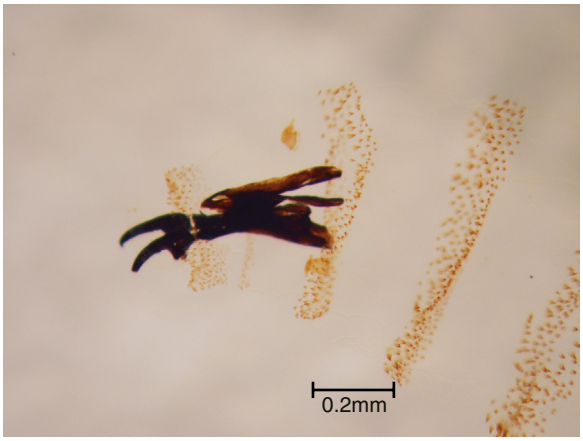


Fig. 5.37 *Chrysomya bezziana* larva - head segments.
The epidemiological range extends through tropical Africa, the Indian subcontinent, South East Asia, China, the Philippines and Papua New Guinea – this larva was removed from the cheek of an 18-year-old male from Laos. The primary tracheal trunks, not visible in the image of the larval head shown here, are only pigmented for the last part of the 12th segment, distinguishing this larva from that of *Cochliomia hominivorax* which are pigmented from the 12th to the 10th segment (see Fig. 5.41). (Courtesy, C. Whitehorn.)

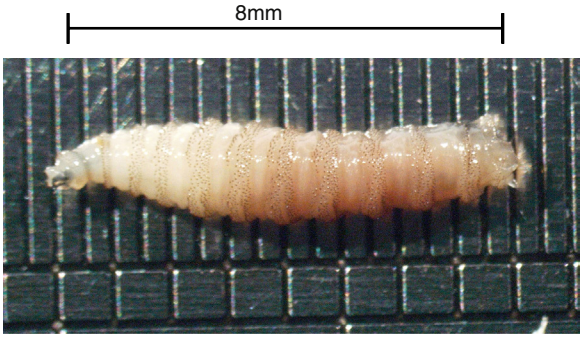


Fig. 5.38 New world screw worm – *Cochliomyia hominivorax* larva.
The New World screw worm is a notorious parasite of domestic livestock and its depravations in the 1950s and 1960s caused huge economic losses in North, Central and South America amounting to over US$100 million. Humans may become infected. (From Centers for Disease Control and Prevention [CDC], Atlanta, GA. CDC Public Health Image Library, image 1427, 16-mm long third-stage (instar).)



Fig. 5.39 Adult male *Cochliomyia hominivorax* fly.
Fortunately the female only mates once and this has made a control campaign possible using mass-reared, irradiation-sterilized males that has pushed the frontier southwards from the United States towards Mexico. The fly was discovered for the first time in Africa in Libya in the 1980s (probably having been imported with cattle from South America), where it infected over 2000 cattle and 200 people before its presence was exposed. A mass international campaign using sterilized males was successful in eradicating it. (Courtesy, US Department of Agriculture.)

Downloaded From Vet-eBooks.com



Fig. 5.40 Massive screw worm infection of the leg.
A large mass of larvae of *Cochliomyia hominivorax* can be seen in a gaping wound in the right leg of this 72-year-old man in Cayenne. The local application of a solution of 10% ivermectin in propylene glycol rapidly paralysed the larvae so that, within 24 hours, over 150 dead larvae could be removed easily. A heavy infection with *C. hominivorax* can kill a large animal such as a cow in 10 days. (Courtesy, Professor R. Pradinaud.)



Fig. 5.41 Unwelcome *Cochliomyia hominivorax* souvenir from holiday to Jamaica.
On return to the UK from a 2-week holiday in Jamaica a 24-year-old female patient complained of severe scalp tenderness. Thirty larvae, demonstrating the characteristic dark tracheal trunks (extending down to the 10th segment) of *C. hominivorax*, were removed from a lump on the scalp. (Courtesy, C. Whitehorn.)

Downloaded from Vet-eBooks.com



Fig. 5.42 Adult female *Lucilia sericata*.
The larvae of these 'greenbottles' are opportunistic feeders on carrion and other dead organic matter, and will sometimes invade wounds but feed only on dead tissue.

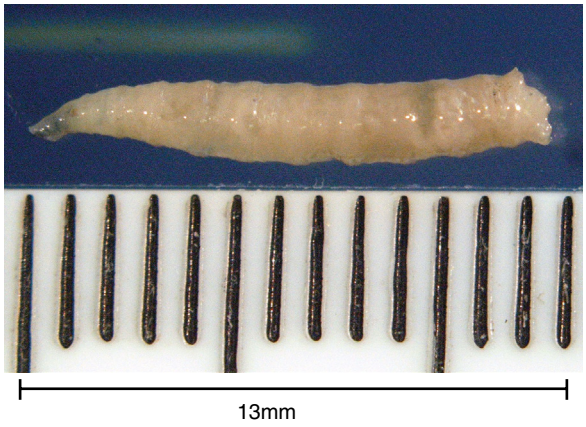


Fig. 5.43 Third instar larva of *Lucilia sericata*.
Note the fleshy posterior appendages known as 'anal lobes'. This is one of seven third instar larvae, each 12 mm long, removed from the infected toe of a 73-year-old male recently returned to the UK from Tenerife. Because they do not invade healthy tissue, the larvae of this calliphorid fly have been used to help in the debridement of infected wounds, for example under occlusive plaster of Paris splints in patients with osteomyelitis. The US FDA approved the use of this species as medical maggots for wound debridement in 2004. (Courtesy, C. Whitehorn.)



Fig. 5.44 Tumbu fly lesions.
Multiple infections with larvae of *Cordylobia anthropophaga* (known variously as tumbu, mango, putzi fly) caused painful boils on the body and arm of this 53-year-old man who had acquired the infestation in Zimbabwe about 2 weeks earlier. The fly lays its eggs on damp clothing left to dry from which larvae hatch and proceed to penetrate the warm skin of the human host. Larvae mature in boil-like lesions over 8–15 days. Probably one of the commonest myiasis species seen in man. Ironing of clothes abrogates the risk.

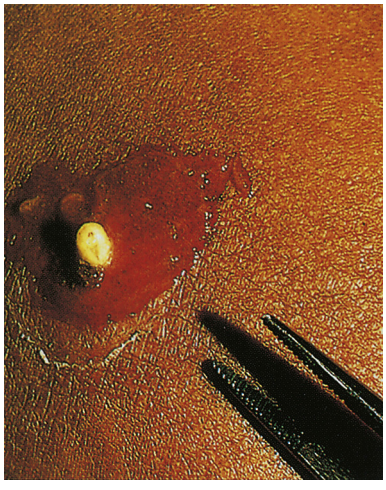


Fig. 5.45 Extracting a larva.
The larva leaves the skin if it is covered in oil or petroleum jelly, which blocks the spiracles. It can then usually be readily removed with forceps. (Courtesy, Professor A. Bryceson.)

Downloaded from Vet-eBooks.com



Fig. 5.46 Larva of *Cordylobia anthropophaga*.
The figure shows the numerous small black spines in rows. (From Choontanom, R. et al. A souvenir from Ghana. The Journal of Pediatrics, 2008, Volume 153, Issue 2, Pages 297–297. Copyright © 2008 Mosby, Inc.)

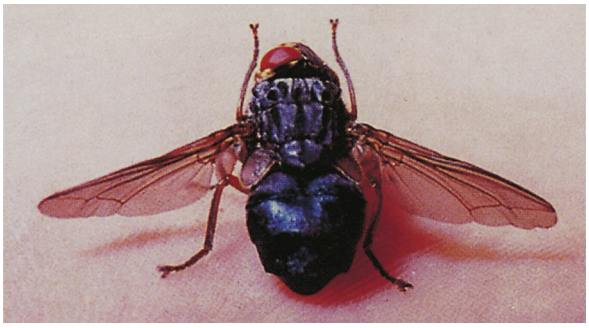


Fig. 5.47 Adult *Dermatobia hominis*.
The larvae of this fly are a cause of serious cutaneous myiasis in Brazil and other tropical areas of the New World. (Courtesy, Dr A. J. Shelley.)



Fig. 5.48 Larva of *Dermatobia hominis* visible on the upper cheek.
The spiracles of this larva, probably in the second instar, can just be discerned in the centre of the lesion in a patient who was infected in Guyana. (Courtesy, Dr W. A. D. Griffiths.)



Fig. 5.49 Second instar larva of *Dermatobia hominis*.
The immature stages have characteristic rows of dark spines. The larvae often have to be removed surgically as the application of such material as petroleum gel frequently fails to kill them. This larva was extracted from the skin of an entomologist! (Courtesy, Dr R. Lane.)

Downloaded from Vet-e-Books.com

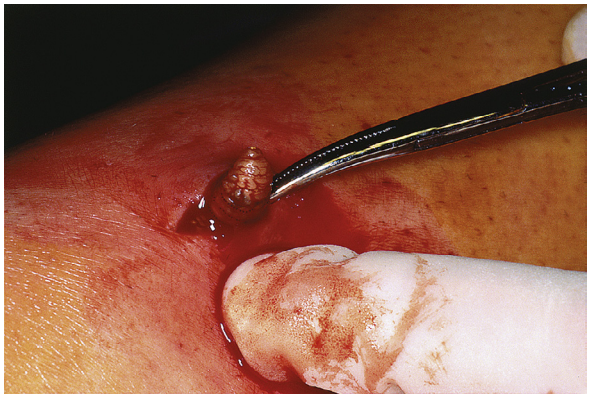


Fig. 5.50 Third instar larva of *Dermatobia hominis*.
In addition to the larger size of this larva, the multiple rows of finer spines can be seen. In contrast to *Cordylobia anthropophaga* (Figs 5.44, 5.45, 5.46), which can usually be grabbed with tweezers as it emerges from petroleum jelly suffocation, the larger size and exuberant spines mean a surgical, often cruciate, incision may be required for removal.

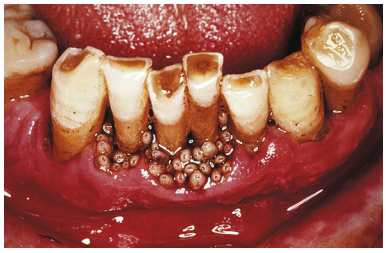


Fig. 5.51 Mouth of an elderly man infected with larvae of an unidentified *Wohlfahrtia* species.
The larvae of this genus of 'flesh flies' of the subfamily Sarcophaginae are essentially scavengers in decaying flesh, faeces and rotting food, but are occasionally found in wounds and sores. The females are larviparous, producing batches of 20–40 first instar larvae, which develop rapidly, the third instars burrowing in soil to pupate. This man was infected while asleep under a tree in a Middle East country. The spiracles of the numerous larvae are very obvious in this view. Normally they are not easily seen, since they are situated within a larval pit. (Courtesy, Drs Y. Schlein and R. Seltser.)



Fig. 5.52 Larvae of *Sarcophaga* in the nose of a man with a nasal tumour.
The spiracles, concealed in the spiracular pits, are not visible in this figure. Like *Wohlfahrtia*, the larvae of flies in this closely related genus are normally found in decaying organic matter but may be laid in malodorous wounds or tumours, as in this case. (Courtesy, Dr K. Y. Mumcuoglu.)

Downloaded From Vet-eBooks.com

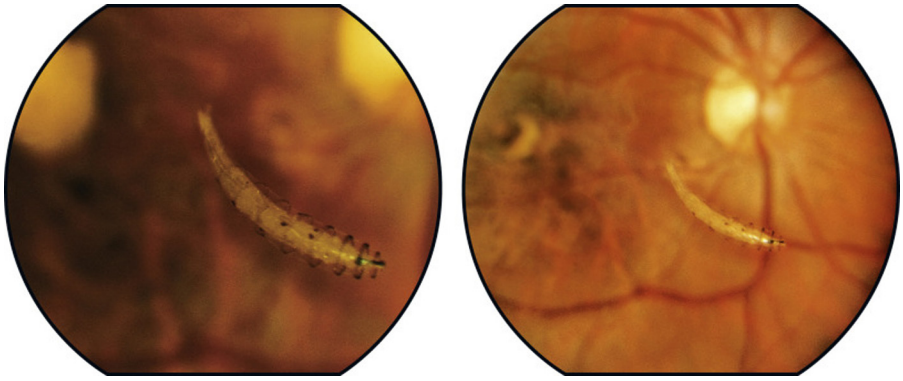


Fig. 5.53 Ophthalmomyiasis.
Migrating larvae in humans usually remain in the subdermal tissues but can make their way to various organs, including the eye. Here the *Diptera* larvae are clearly seen in the vitreous. (From Yannuzi, L. A. Infection. In: The Retinal Atlas. Pages 305–380. Copyright © 2010, Elsevier Limited. All rights reserved.)

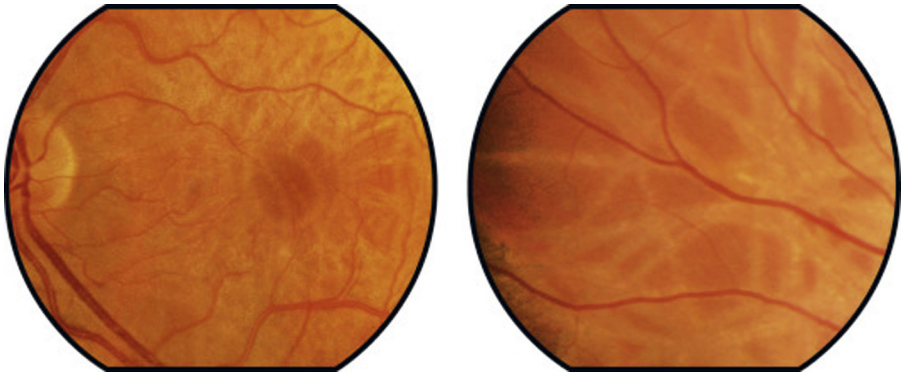


Fig. 5.54 Effect of ophthalmomyiasis in the subretinal space.
The criss-crossing lines of atrophic tracts seen in the retinal pigment epithelium here are caused by random migration of the larva in the subretinal space and are regarded as pathognomonic of ophthalmomyiasis. (From Yannuzi, L. A. Infection. In: The Retinal Atlas. Pages 305–380. Copyright © 2010 Elsevier Limited. All rights reserved.)

Downloaded From Vet-eBooks.com

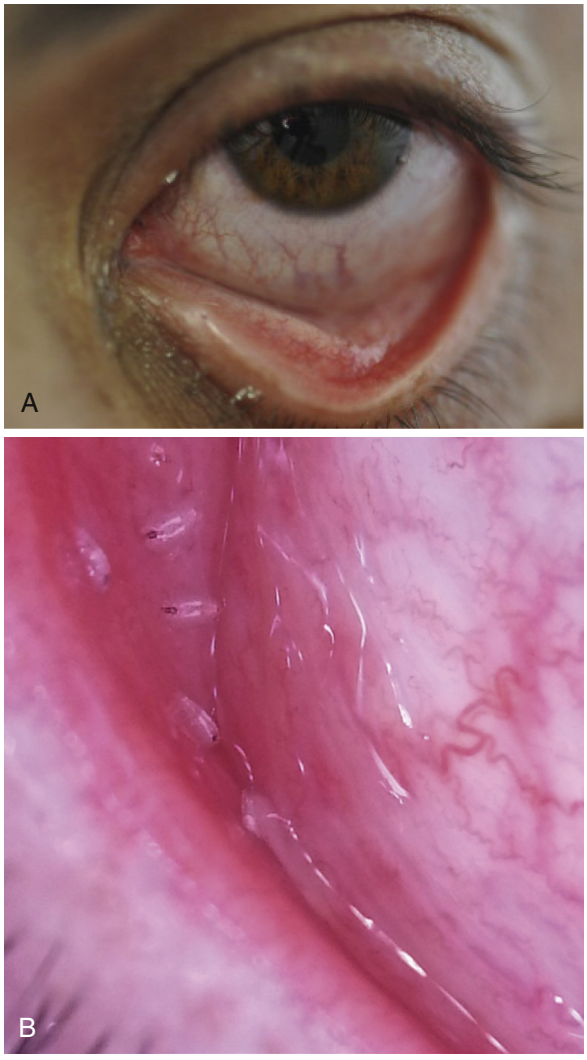


Fig. 5.55 (A and B) Conjunctivitis and watery eye in ophthalmomyiasis due to first instar larvae of *Oestrus ovis*.
This 27-year-old Israeli man reported intense pain and uncontrollable flow of tears from the affected eye. The sheep nasal bot fly, which is a parasite of the nasal cavities and sinuses, is now found wherever sheep are raised on a large scale. The females, which are viviparous, swarm round the heads of their victims and deposit first instar larvae (not eggs) in the nostrils, or sometimes in the orbit, of sheep. Ophthalmomyiasis externa is not uncommon among shepherds and others working closely with sheep. The larvae do not grow beyond the first instar but cause a painful inflammation within the conjunctival sac for several days. This may be difficult to see without magnification, as illustrated in the figure. Aided by a slit lamp an ophthalmologist subsequently removed 14 live larvae. Patients often report having been hit or stung in the eye by an insect, as in this case and also in a cluster of cases reported following a large gathering of sheep at a festival in southern France in 2013. (From Naimer, S. A. Man with pain in left eye. Annals of Emergency Medicine, Volume 65, Issue 6, Pages e7–e8. Copyright © 2015 American College of Emergency Physicians.)

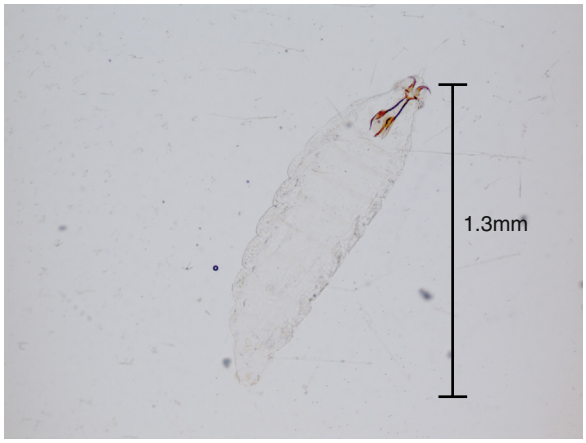


Fig. 5.56 First instar larva of *Oestrus ovis* (sheep nasal bot fly).
Occasionally the larvae are deposited in the ears, nose or mouth, and they can invade the nasal sinuses. (Courtesy, C. Whitehorn.)

Downloaded from Vet-e-Books.com

6. Bites, stings, venoms, toxins

Venomous invertebrate and vertebrate animals are to be found anywhere in the world but are especially common in the tropics and subtropics, where they may be particularly hazardous. The following figures illustrate a few examples, including marine and terrestrial invertebrates and vertebrates. Although bites and stings are usually individual hazards and recognition depends upon understanding of the local epidemiology, the problem can take on public health significance, as can envenomation by the consumption of poisonous invertebrates or other animals.

MARINE INVERTEBRATES

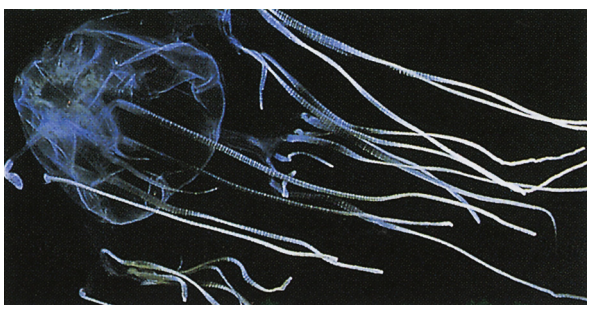


Fig. 6.1 The 'sea wasp', *Chironex fleckeri*.
Some species of so-called 'box' jellyfish, such as *Chironex fleckeri*, produce a potent venom. The box-shaped bell is around 10 cm tall and the tentacles may be up to a metre long; some other venomous species may have tentacles as long as 30 m. (Courtesy, Dr B. W. Halstead.)



Fig. 6.2 Effects of an encounter with *Chironex fleckeri*.
Most *Chironex fleckeri* stings, which are sustained when the stinging nematocysts on the tentacles come into contact with and discharge venom into bare skin, cause severe, immediate pain and linear welts. Much less commonly systemic envenomation occurs with rapid onset (within 5 minutes) of panic, hypotension, autonomic dysfunction and profound myalgia occasionally leading to death. Topical application of vinegar inhibits further discharge of any remaining nematocysts. (Courtesy, Professor D. A. J. Moore.)

Downloaded from Vet-eBooks.com



Fig. 6.3 Geographic distribution of *Chironex fleckeri*.
True jellyfish stings tend to be a particular problem in the Indopacific region. This jellyfish can be found along most of the coast of northern and eastern tropical Australia and in Papua New Guinea, Vietnam and the Philippines.

Downloaded From Vet-eBooks.com

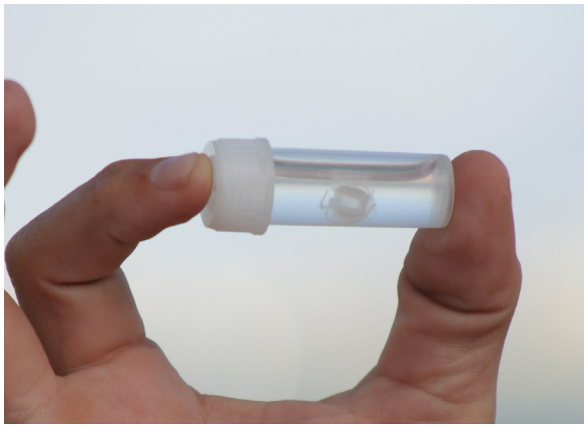


Fig. 6.4 *Carukia barnesii*.
Irukandji syndrome describes the clinical presentation following the sting of one of several (currently seven) small box jellyfish species found around the tropical waters of northern and eastern Australia; these include *Carukia barnesii*, shown here, which was the first to be identified by Jack Barnes in the region inhabited by the inidigenous Irukandji people. It is characterized by a delay in symptom onset of around 30 minutes after contact, a relatively modest local reaction but a profound systemic upset with marked autonomic dysfunction and sweating, severe generalized pain and most notably a sense of impending doom. (Courtesy, Dr L-a. Gershwin.)



Fig. 6.5 *Physalia physalis*.
This cosmopolitan organism is moved around the oceans of the world by tides, winds and currents and so may be found in most tropical coastlines. Also known as the bluebottle or the Portuguese man o' war, it is actually a siphonophore, not a jellyfish; a collection of several inter-dependent organisms, rather than a single multicellular organism. Stings are painful and may resemble whip marks; fatalities are extrememly rare. Application of hot water (45°C) helps to inactivate the toxin and relieves symptoms better than application of iced water. Vinegar should not be used, as doing so may worsen symptoms. (From Haddad, V., Sardenberg, T. Management of venomous injuries. In: Green's Operative Hand Surgery. Pages 1788–1796. Fig. 52.7A. Copyright © Elsevier 2017. Courtesy, A. Mósca, Rio de Janeiro, Brazil.)



Fig. 6.6 *Conus purpurascens*, a venomous cone shell.
Cone shells are common along coasts of the Indo-Pacific area and are widely sought after by collectors. These molluscs catch small fish and other prey by injecting them with a cocktail of venoms, which is discharged through the barbed radular tooth that passes through the proboscis. This tooth is replaced from a reserve, as it is lost after use. The venom contains a large complex of conotoxins, which block a variety of ion channels in cell membranes or, in some cases, neurotransmitters. In addition to their value as research tools for the investigation of nerve function, a number of conotoxins in clinical trials show promise for the relief of severe neuropathic pain. (Courtesy, Dr J-P. Bingham.)



Fig. 6.7 A selection of poisonous cone shells.
Around 30 cone shell envenomation fatalities have been reported following shell mishandling. Envenomation is not usually painful.

Left: *Conus marmoreus* (3–15 cm) ranges from Indian Ocean to the western Pacific. Centre: *Conus geographus* grows to about 15 cm and is probably the most dangerous species of cone shells for humans. It is widespread in reefs of the Indo-Pacific region and the Red Sea. Right: *Conus textile*. This species, which grows up to about 10 cm, has caused a number of fatalities and is widely distributed from the Red Sea to Polynesia. (Courtesy, Dr J-P. Bingham)

Downloaded from Vet-eBooks.com



Fig. 6.8 *Hapalochlaena lunulata*.
Octopus envenomations are only reported for the greater blue-ringed (*Hapalochlaena lunulata*) and southern blue-ringed (*Hapalochlaena fasciata*) species. Both of these small animals (<20 cm in fully extended diameter) are found in coastal waters and tidal rock pools in Australia and the western Pacific. Saliva contains the potent neuromuscular tetrodotoxin (also found in puffer fish), so following a bite (which is rare), envenomation can occasionally lead to collapse with flaccid paralysis on the beach, in which case ventilatory support can be life-saving. (Courtesy, Professor D. A. Warrell.)



Fig. 6.9 *Saxidomus gigantea*, the butter clam.
Paralytic shellfish poisoning results from ingestion of saxitoxin which has been concentrated in filter-feeding molluscs that have fed on toxic algal blooms. The water-insoluble, heat-stable toxin is not inactivated by cooking, and ingestion can lead to nausea and abdominal pain, diarrhoea and vomiting, paraesthesia and burning of the mouth, head, neck and limbs, dyspnoea, slurred speech and loss of co-ordination. Many bivalves – mussels, oysters, scallops – will only store the toxin for a few weeks, but the butter clam has been known to retain saxitoxin for 2 years. Xanthid crabs harvested for local consumption from Pacific coral reefs can also occasionally result in saxitoxin poisoning.



Fig. 6.10 'Mussels'.
Amnesic shellfish poisoning is an extremely rare but well-recognized toxic ingestion syndrome due to consumption of mussels or razor clams in which domoic acid has accumulated through feeding on the microscopic marine diatom *Pseudonitzchia pungens*. Following gastrointestinal upset within 24 hours of ingestion subjects go on to develop dizziness, headache, disorientation and, through direct hippocampal toxicity, permanent short-term memory loss. Rarely, seizures, paralysis or even death may occur. Occasionally die-off of whales or sea lions may presage high levels of domoic acid in the food chain. (Photographs by Laura Coutts, courtesy of E.C. From Carrington, E. Along the silk road, spiders make way for mussels. Trends in Biotechnology, 2008, Volume 26, Issue 2, Pages 55–57. Copyright © Elsevier 2007.)

Downloaded From Vet-eBooks.com

MARINE VERTEBRATES

Poisonous Fish

Three toxic ingestion syndromes associated with fish consumption are well recognized: ciguatera poisoning, puffer fish poisoning and scombroid.

In some tropical regions the consumption of reef fish, notably barracuda, grouper, snapper or moray eel, is associated with the risk of ciguatera poisoning. The single-celled dinoflagellate *Gambierdiscus toxicus* lives on coral reefs and synthesizes ciguatoxin. This is non-toxic to the small fish that feed on it or the predatory fish higher up the food chain that consume the herbivorous fish, but causes significant morbidity in humans. Within 6–12 hours of ingestion nausea, vomiting, abdominal pain and diarrhoea occur, followed by a constellation of neurological symptoms that may include perioral parasethesia, painful parasethesia of extremities or, classically, paradoxical temperature sensation reversal (cold feels hot and vice versa). Ciguatoxin is heat stable and so is not destroyed by cooking. Hotspots include the Caribbean and Polynesia (estimated lifetime prevalence of 70%), though undoubtedly the global distribution of fish catches will lead to unsuspected and probably unidentified sporadic cases in non-tropical regions.

Puffer fish poisoning, most commonly reported from Japan, is caused by tetrodotoxin (see also Fig. 6.8 blue ringed octopus above) and results from incorrect preparation of the delicacy; the toxin is particularly concentrated in the liver of the fish. Following the rapid development of tongue and lip numbness soon after eating, paraesthesia and weakness progressively spread to involve the limbs, culminating in marked autonomic disturbance and respiratory failure with death within 6 hours.

Scombroid toxin poisoning also results from incorrect fish preparation, in this instance from a failure to adequately refrigerate after catching. Contact with air allows the gut enterobacteriaceae of fish species with a high histidine content in muscle, such as mackerel, tuna and bluefish, to break down the dead muscle generating histamine, ingestion of which, in a bolus form, causes flushing, sweating, tachycardia and an urticaria-like rash. A characteristic clue is a peppery taste in the mouth during ingestion.

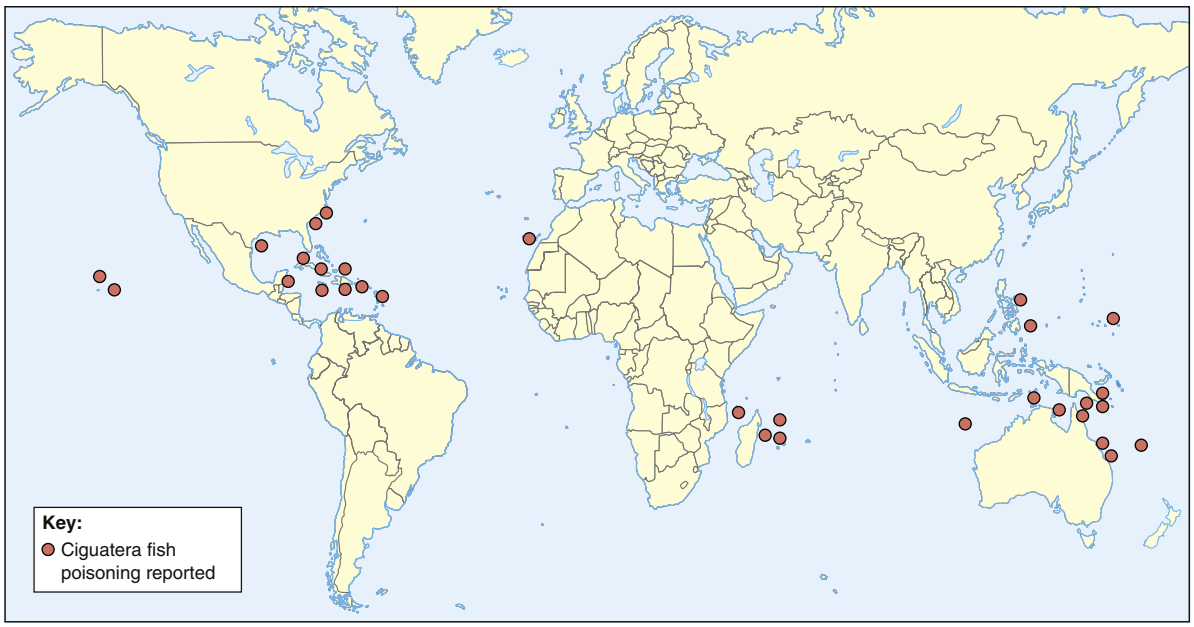


Fig. 6.11 Ciguatera poisoning – distribution map. (Courtesy of the National Office for Harmful Algal Blooms © Woods Hole Oceanographic Institution.)

Downloaded From Vet-eBooks.com



Fig. 6.12 Puffer fish.
Restaurant preparation and serving of the Japanese delicacy fugu is tightly controlled to minimize the very real risk of tetrodotoxin poisoning. (From Warrell D.A. In: Venomous Bites, Stings and Poisoning. Infectious Disease Clinics of North America. 2012; 26 (2). Fig 8. Pages 207–223.)

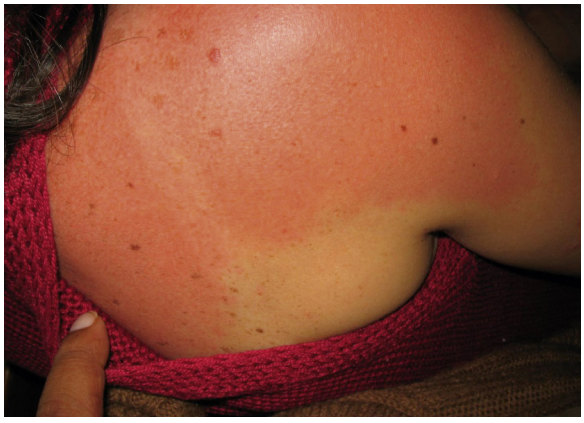


Fig. 6.13 Scombroid toxin poisoning.
This rash appeared soon after eating ceviche in Peru. (Courtesy, Dr D. Blazes.)

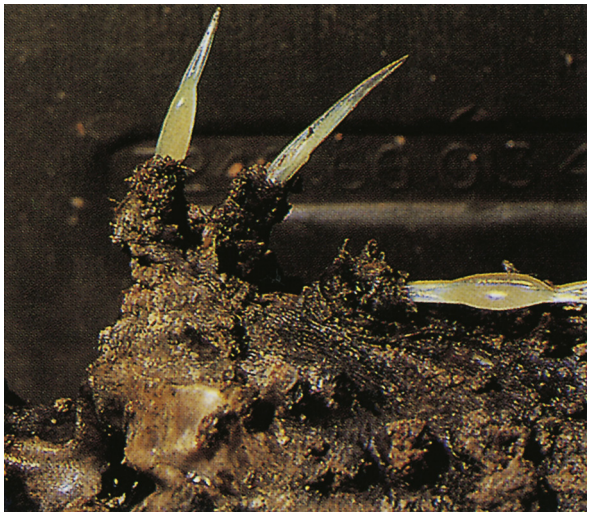


Fig. 6.14 Venomous spines of the stone fish *Synanceia horrida*.
Many species of fish, including weever fish and stone fish, have venomous spines. The stone fish lies well concealed in the sand of marine shores, or in the case of *S. horrida* in estuarine waters. Venom produced in glands that emerge at the tips of the dorsal spines causes intense pain if they enter the skin, and severe stings can be fatal. The pain that follows envenomation may be sufficient to cause delirium and can persist for days. This coastal stone fish, one of the most dangerous, occurs around Indo-Pacific coasts as far south as southern Australia. Many other stone fish species are found in the eastern Pacific and Atlantic coastal waters, as well as the Indo-Pacific region. As the venom is rapidly denatured by heat, placing the injured part in water as hot as can be tolerated safely may speed the rate of recovery. (Courtesy, Dr B. W. Halstead.)



Fig. 6.15 Foot of woman stung by the stone fish *Synanceia verrucosa*.
Concentric, necrotizing cellulitis spreading from two points of entry by stone fish spines is seen on the medial side of the forefoot of this patient, who was stung by a 'reef stone fish' in Tahiti. Secondary bacterial infection and slow healing are common. (Courtesy, Professor E. Caumes.)

Downloaded From Vet-eBooks.com

TERRESTRIAL INVERTEBRATES

Scorpions and spiders account for significant morbidity within geographically restricted ranges. Non-trivial cutaneous injury from wasp, bee and ant stings can also be accompanied by systemic complications, as can contact with the irritant mediators of venomous caterpillars (erucism), moths (lepidopterism) and beetles.

Scorpions

Distributed across the Americas, North Africa, the Middle East and southern Asia, scorpion stings are primarily a risk to children and the elderly, potentially causing pain, swelling, hyperaesthesia and autonomic disturbance (including priapism).



Fig. 6.16 A buthid scorpion: *Androctonus australis*.
The majority of scorpions are of little danger to humans, but of the 20 or so species that are, a number cause many deaths each year. This 'fat-tailed scorpion', which occurs throughout the Mediterranean littoral and northern and north-west Africa, is one of the most dangerous species. It was responsible for nearly 400 deaths among 20,000 people stung in Algeria between 1942 and 1958. The venom, which stimulates first the parasympathetic nervous system and then the sympathetic, can cause respiratory paralysis and death. Antivenoms are available against some species.



Fig. 6.17 *Tityus serrulatus, the Brazilian* yellow scorpion.
This is probably the most dangerous species of this New World, largely South American, genus. It is a common house-frequenting scorpion and is responsible for a large number of serious cases of scorpionism in Brazil, where an antivenom has been produced. Spraying houses with residual insecticides such as DDT has been beneficial in reducing its numbers.



Fig. 6.18 Male *Hemiscorpius lepturus*.
This species found in Iran, Iraq, Pakistan and Yemen has exceptionally long, thin, postabdominal segments and a very small spine on the sting. In spite of this, it is very dangerous and accounts for 10–15% of all stings in Iran in the summer and most stings in the winter months. (Courtesy, Dr M. Radmanesh.)

Downloaded from Vet-eBooks.com



Fig. 6.19 Facial oedema due to cardiac dysfunction following the sting of *Hemiscorpius lepturus*.
If a sufficiently high concentration of the venom of this scorpion reaches the circulation, it can exert serious changes in the central nervous and cardiovascular systems, as well as causing acute haemolysis, which may necessitate blood transfusion, and lymphopenia. This Iranian boy is one of 54 who showed systemic effects among 2534 patients stung by *H. lepturus*. (Courtesy, Dr M. Radmanesh.)

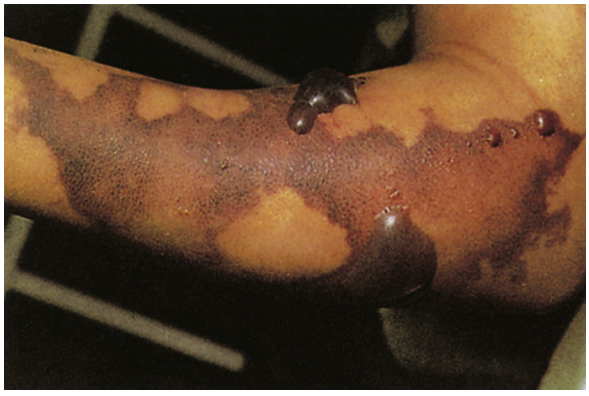


Fig. 6.20 Lesions following sting of *Hemiscorpius lepturus*.
In contrast to the neurotoxicity of other scorpions, the principal effect of the *H. lepturus* sting is cytotoxic, which can result in localized blistering and necrosis, as in this child's arm. (Courtesy, Dr M. Radmanesh.)



Fig. 6.21 Extensive sloughing of skin and epidermis of arm.
The figure shows complete sloughing of the skin of the arm in the child seen in Fig. 6.20, necessitating extensive skin grafting. (Courtesy, Dr M. Radmanesh.)

Spiders

Four genera of spiders are associated with significant morbidity in humans: *Atrax* (Australian funnel web), *Loxoceles* (recluse spiders), *Latrodectus* (widow spiders and Australian redback) and *Phoneutria* (also known as Brazilian wandering spiders or banana spiders).



Fig. 6.22 Female *Atrax robustus*.
This 'Sydney funnel web spider' (female body length up to 4 cm) is a large, nocturnal spider the bite of which is very painful, leaving visible puncture marks and local bleeding. Systemic envenomation (almost always due to bites from males) occurs when neurotoxic atracotoxin enters the bite site. Symptoms develop within 10–30 minutes with piloerection, sweating, perioral parasesthesia with tachycardia and hypertension. Progression to nausea and vomiting, dyspnoea, agitation and confusion may occasionally lead to death (for which children are at higher risk), though this is now very rare due to the availability of specific antivenom.

Downloaded From Vet-eBooks.com



Fig. 6.23 *Loxosceles reclusa*.
Though *Loxosceles* spiders are widely distributed throughout much of the world, virtually all reports of envenomation come from the Americas and concern only four of the more than 60 species, namely *Loxosceles laeta*, *L. reclusa*, *L. gaucho* and *L. rufescens*. Also known as 'brown spiders' (for obvious reasons) or 'violin spiders' (for reasons that only become clear when one gets a very close look at the thoracic markings), the venom of these spiders can result in markedly cytotoxic and/or haemolytic effects. They are mainly nocturnal and, since they seek dark places to shelter, are commonly attracted to human habitations. (From Elston, D. M. Arthropods and leeches. In: Goldman-Cecil Medicine. Pages 2171–2177.e2, Figure 359-4. Copyright © 2016, Saunders, an imprint of Elsevier Inc.)



Fig. 6.24 Girl bitten by *Loxosceles laeta*.
Loxoscelism presents in two forms, the first limited to the skin and subcutaneous tissues and the second systemic due to the haemolytic effects of the venom when absorbed. This Chilean child shows the effects of severe intravascular haemolysis, as well as the beginning of blistering and necrosis of the skin. The massive facial oedema is evident and she is comatose. This type of response to envenomation occurs in 10–15% of the victims of *L. laeta* bites. Up to one-third of such cases die with haematuria, anuria and other evidence of haemolysis unless treated urgently with antivenom and general supportive therapy. (Courtesy, Professor H. Schenone.)



Fig. 6.25 Sloughing of skin following spider bite.
This Chilean child was bitten by *Loxosceles laeta*. Necrosis and sloughing followed severe blistering at the site of the bite and generalized facial oedema. (Courtesy, Professor H. Schenone.)

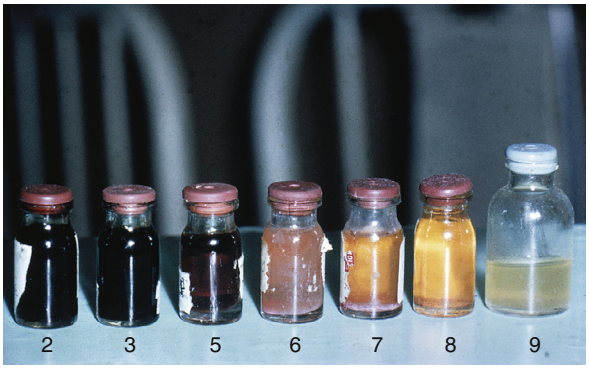


Fig. 6.26 Urinary changes following a bite by *Loxosceles laeta*.
These urine samples, indicating transient haemolysis, were taken 2, 3, 5, 6, 7, 8 and 9 days following a bite that was treated by the administration of antivenom in a Chilean patient. (Increasing days from left to right or from right to left). (Courtesy, Professor H. Schenone.)

Downloaded from Vet-eBooks.com



Fig. 6.27 (A-F) Evolution of a recluse spider bite in a young Peruvian woman.
This 19-year-old student woke at 01:00 in her adobe house in a Lima shantytown with sharp pain in her right arm. She settled back to sleep but woke 6 hours later with pain and swelling in the arm, fever and rigors. From the initial violaceous discolouration discernable 8 hours after the bite an extensive area of dermal necrosis developed over the subsequent 2 weeks (images from days 0, 3, 8, 10, 14, and 16) requiring subsequent skin grafting. She also experienced transient haemolysis which resolved by day 4 following administration of anti-loxosceles antivenom. (Courtesy, Dr R. D. Vasquez Becerra.)



Fig. 6.28 Severe necrosis following the bite of *Loxosceles reclusa* in the western USA.
Significant skin loss typically requires skin grafting after initial recovery.



Fig. 6.29 The black widow spider, *Latrodectus mactans* – the reddish markings on the abdomen are a common feature of most female widow spiders.
Despite their notoriety, bites from *Latrodectus* species (including the widow spiders and the Australian Redback *L. hasselti*) are very rarely fatal. Latrodectism describes the clinical syndrome resulting from envenomation with latrotoxin, which stimulates massive release of acetylcholine, norepinephrine and GABA. Symptoms include pain at the bite site (may lack discernible puncture marks), which becomes more generalized with muscle rigidity, profuse sweating (which may be oddly localized) and piloerection and vomiting. Symptoms may take several days to subside. (From Juckett, G. Arthropod bites. American Family Physician, Volume 88, Issue 12, Pages 841–847. Copyright © 2013 American Family Physician.)

Downloaded from Vet-eBooks.com



Fig. 6.30 *Phoneutria* in defensive posture.
Brazilian wandering spiders, named for their nocturnal behaviour wandering the jungle floor, are also known as banana spiders due to occasional discovery within shipments of bananas. Aside from such accidental travellers, these species are only found in Central and South America, largely in forested areas. *Phoneutria* species have a reputation for aggression, though the stance shown here is a response to disturbance. Bites are painful, but only a minority are believed to lead to envenomation with the potent neurotoxin which can cause loss of muscle control and respiratory distress. In contrast to a billing as the world's most venomous spider, barely a dozen verified fatalities have ever been recorded. (Courtesy of Centers for Disease Control and Prevention's Public Health Image Library, Atlanta, Ga.)



Fig. 6.31 Female *Chiracanthium lawrencei*.
The 'sac spiders' are cosmopolitan and some frequent houses. It has been suggested that this species is the most common cause of spider bites worldwide, but there is a lack of consensus about whether envenomation, which certainly causes severe pain, is associated with dermatonecrosis. This aggressive species, which has widely separated fangs, is responsible for about 75% of all poisonous spider bites in the more humid parts of South Africa. (Courtesy, Dr G. Newlands.)

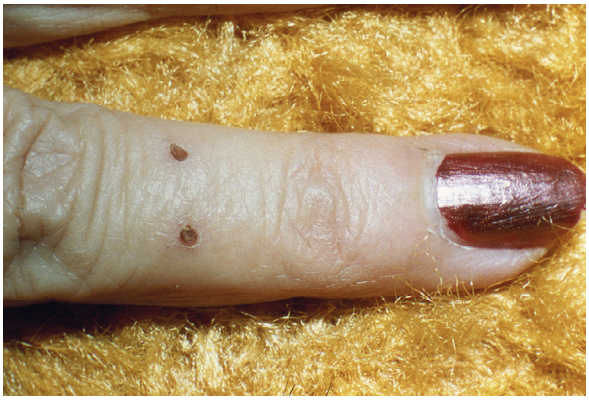


Fig. 6.32 Bite marks caused by *Chiracanthium lawrencei*.
The fang marks are distinctive and sometimes have a greenish tinge. This woman was bitten 1 week prior to being photographed. (Courtesy, Dr G. Newlands.)

Centipedes, Millipedes and Insects

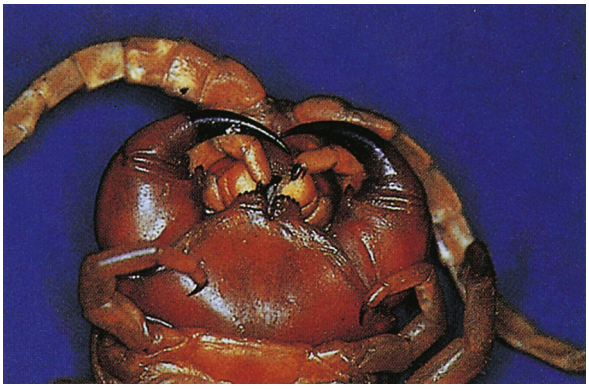


Fig. 6.33 Head of a venomous centipede.
A few of the large species of tropical centipedes are capable of inflicting an intensely painful but probably nonlethal sting. The venom is passed through the piercing forcipules seen on the ventral surface of the head of this large *Scolopendra* species from Singapore.

Downloaded from Vet-eBooks.com



Fig. 6.34 *Epibolus pulchripes* (Spirobolida).
These giant millipedes from East Africa are harmless unless provoked, preferring to hide in moist earth where they feed on vegetable matter. The glossy male is readily distinguished from the female, which has a comparatively matte surface. The pairs of orange legs on each segment and the bright orange, jointed antennae of the male are well illustrated here. Some tropical species, such as the African *Graphidostreptus gigas*, can exceed 28 cm in length.



Fig. 6.35 'Burn' caused by contact with *Epibolus pulchripes*.
The victim unwittingly slept on the millipede, which had entered his bed. Within an hour of contact with the exuded toxic secretions he noted itching and discomfort, and the following morning the site was erythematous. It subsequently turned purple. Five days later the hardened skin cracked and peeled, leaving a raw patch that eventually healed, leaving no residual pigmentation. A similarly toxic liquid squirted into the eyes by the giant *Polyconoceras alokistus* millipede in Papua New Guinea has reportedly caused temporary blinding in children.

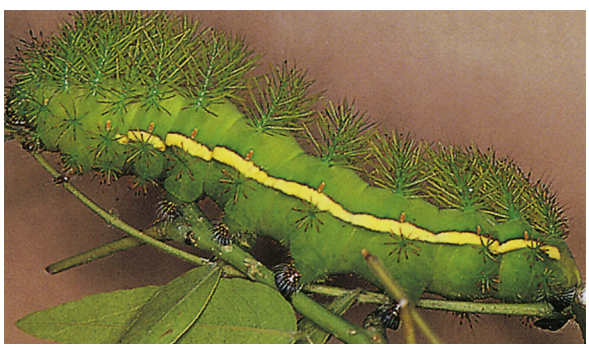


Fig. 6.36 Poisonous spines on a caterpillar.
The larvae of many species of moths are protected with venomous spines. The toxin of many species, including the saturniid species, *Automeris liberia*, from Cayenne, seen here, contains histamine.



Fig. 6.37 Female *Hylesia metabus*.
The abdomens of adult moths of this genus are covered with strongly barbed, urticating hairs (fléchettes) that are readily shed if the insects are damaged. Females may approach light sources and release clouds of bristles that can then penetrate and irritate human skin, so-called 'yellowtail dermatitis'. The presence of large numbers of these moths has caused epidemics of 'lepidopterism' or 'erucism' of sufficient gravity that a number of tropical tourist centres have had to be temporarily abandoned.



Fig. 6.38 Lepidopterism in the Peruvian Amazon
At an oil and gas prospecting installation deep in the Peruvian Amazon 64 of 230 site workers reported this intensely pruritic rash affecting the head and neck and upper limbs, often after coming off a night shift. Large numbers of *Hylesia* moths were attracted to the nocturnal light sources. (Courtesy, Dr R. D. Vasquez Becerra.)

Downloaded from Vet-eBooks.com



Fig. 6.39 Caterpillar of *Lonomia achelous*.
This hemileucine species, which occurs in the Amazon region of Brazil, has poison spines that deliver a potent fibrinolytic toxin. Similar toxic responses to saturniid caterpillars have been reported from Venezuela. Local inflammation at the point of contact is accompanied by ecchymoses indicating bleeding diathesis.



Fig. 6.40 Brazilian adult with severe haemorrhagic syndrome after being stung by a larva of *Lonomia achelous*.
Following contact with the insect there is a localized burning sensation, then headache and generalized discomfort. Extensive ecchymoses appear after 8–72 hours in the affected area and then over other parts of the body. There may be profuse gastrointestinal haemmorhage. (Courtesy, Dr H. Fraiha Neto.)



Fig. 6.41 Larva of *Premolis semirufa*.
The long barbed hairs at both ends of the insect are prominent in this picture, as are the brown dorsal tufts. The latter carry short, venomous hairs that cause a severe inflammatory reaction at the sites of the skin that are penetrated. (Courtesy, Dr H. Fraiha Neto.)



Fig. 6.42 Pararama – deformity of the hand in a Brazilian rubber tapper.
Premolis semirufa feeds on the leaves of the rubber tree and is commonly encountered by plantation workers. The stings cause deep inflammation around the joints with susbequent periarticular fibrosis and ankylosis that may leave the victim permanently disabled. (Courtesy, Professor R. Lainson)

Downloaded from Vet-eBooks.com



Fig. 6.43 Fire ant workers (*Solenopsis sp.*). Two sizes of worker of this unidentified species of 'fire ant' from Cayenne are seen feeding on a piece of meat. They have gained their name because of the extremely painful stings they inflict. The venom is unusual in being composed of oily alkaloids, mainly various 2,6-dialkylpiperidines, the exact compounds being species-dependent. They are haemolytic and cytolytic. Some proteinaceous material and a small quantity of phospholipase A and hyaluronidase are also present. (Courtesy, Dr C. Marty.)



Fig. 6.44 Acute renal failure following multiple stings by *Vespa affinis*.
Hornets in this genus occur worldwide and are generally large, very aggressive insects. They often attack in large numbers and are responsible for many deaths. A flurry of deaths in China in 2013 following attacks by *Vespa mandarinia* were blamed on climate-change–attributable expansion of numbers. *Vespa orientalis* occurs from North and East Africa through the Middle East and central Asia to South East Asia. This Thai soldier, who was stung by over 100 hornets, developed intravascular haemolysis associated with frank haemoglobinuria and acute tubular necrosis leading to renal failure. Rhabdomyolysis associated with myoglobinuria and renal failure has also been reported. (Courtesy, Professor S. Sucharit.)



Fig. 6.45 Fatal, multiple bee stings by *Apis mellifera scutellata*, the African 'killer bee'.
This highly aggressive bee, a hybridization of African and European bees, was introduced into Brazil in 1956 because of its good honey productivity. It has competed with the local subspecies of *Apis mellifera* and is now colonizing other countries of both South and North America, where the aggressive behaviour of its swarms has caused many casualties and deaths. As distinct from the stings of wasps, those of bees are barbed and cannot be removed from the site of the attack in skin. Unlike the venom of wasps, that of the Apidae is rich in phospholipases, hyaluronidase, a mast cell discharging peptide and histamine, the latter of which produces the acute pain following bee stings. The 13-year-old Brazilian boy shown here was attacked 48 hours earlier by a swarm of *Apis mellifera scutellata* in São Paulo State, Brazil, suffering more than 1500 stings. Initial development of extensive oedema and bruising was followed by oliguria and diminished consciousness. Progressive multi-organ failure ensued with bronchospasm, hypotension, intravascular haemolysis with haemoglobinuria, myoglobinuria and spontaneous bleeding from the mouth culminating in death on day 3. (Courtesy, Professor D. A. Warrell.)

Downloaded From Vet-eBooks.com

TERRESTRIAL VERTEBRTATES



Fig. 6.46 *Paederus fusca*.
These very small, colourful rove beetles produce vesicular lesions if crushed on the skin due to the release from their bodies of pederin, an extremely toxic alkaloid. They do not bite or sting and so should be blown or brushed carefully off the skin. *P. fusca* is common in rice fields in Thailand and other countries of South East Asia and causes blisters in rice pickers during the harvest season.



Fig. 6.47 'Nairobi eye' caused by *Paederus sabaeus*.
The 'Nairobi fly' is actually the red-and-black *Paederus sabaeus* beetle that is found in East Africa. As with *P. fusca* skin lesions develop within 12–36 hours of contact with pederin. Here severe periorbital swelling is seen, associated with a linear vesication of the upper eyelid and adjacent bridge of the nose, as well as a purulent conjunctivitis. Once on the skin, pederin can be spread elsewhere, including to the eye if rubbed. In this instance the patient was affected by a beetle that flew into his eye 39 hours earlier. *Paederus* species are cosmopolitan throughout the tropics. (Courtesy, Dr A. W. R. McCrae.)

Amphibians



Fig. 6.48 *Dendrobates tinctorius*, a tropical poison dart frog.
The skin of many species of frog and toad contains pharmacologically active compounds called batrachotoxins, some of which are extremely poisonous, even more so than curare and strychnine. They contain toxic alkaloids that have selective effects on ion permeability, leading to irreversible depolarization of nerve and muscle. This small frog, which grows up to about 6 cm in length, lives in the rain forests of Guyana, Surinam, Cayenne and parts of Brazil. The skin secretions were employed by Indian hunters to coat the tips of their arrows.

Snakes

Snakebite envenoming is a neglected global health problem, principally affecting the rural poor of Asia, Africa, Latin America and Oceania (Table 6.1). Data are sparse, but globally there are estimated to be at least 420,000 envenomings and 20,000 deaths annually, though the upper limit estimates reach figures of 1.8 million envenomings and 94,000 deaths. Vipers (including rattlesnakes) and elapids (including cobras, mambas, kraits and taipans) are responsible for most envenomings. Severe viper envenomation characteristically causes local swelling and necrosis, coagulopathy with bleeding and shock. In contrast, elapid envenomation (except for some cobras) is usually predominated by neurotoxicity with minimal local effects. The remaining minority of serious envenomations are caused by seasnakes (rhabdomyolysis, paralysis) and the arboreal boomslang of sub-Saharan Africa (consumptive coagulopathy). Pythons are non-venomous constrictors and have only very occasionally been responsible for the death of young children.

Downloaded from Vet-e-Books.com

Table 6.1 Principal venomous snakes organised by family, genus and species responsible for morbidity and mortality

	Common name	Distribution
Elapidae		
Naja nigricollis	Black-necked spitting cobra	Africa
Naja haje	Egyptian cobra†	Africa
Naja naja	Indian cobra*	South East Asia, Far East
Naja kaouthia	Asian cobra	South East Asia
Dendroaspis polylepis	Black mamba†	Africa
Dendroaspis angusticeps	Eastern green mamba	East Africa
Dendroaspis viridans	Western green mamba	West Africa
Bungarus caeruleus	Common krait*	South East Asia
Acanthophis spp.	Death adder	Australasia
Oxyuranus scutellatus	Common taipan	Australasia
Pseudechis australis	Mulga, king brown snake	Australasia
Pseudonaja textilis	Eastern brown snake	Australasia
Notechis scutatus	Eastern tiger snake	Australasia
Hydrophiidae		
Enhydrina schistosa	Beaked sea snake	South East Asia
Viperidae		
Crotalus adamanteus	Eastern diamondback rattlesnake	North America
Crotalus atrox	Western diamondback rattlesnake	North America
Crotalus viridis	Western rattlesnake	North America
Crotalus durissus durissus	Central American rattlesnake	Central America
Crotalus durissus terrificus	South American rattlesnake	South America
Bothrops atrox	Common lancehead‡	Central and South America
Bothrops asper	Fer-de-lance‡	Central and South America
Bothrops jararaca	Jararaca‡	South America
Calloselasma rhodostoma	Malayan pit viper	South East Asia
Trimeresurus spp.	Green pit vipers	South East Asia
Trimeresurus flavoviridis	Habu	Far East
Trimeresurus mucrosquamatus	Chinese habu	Far East
Vipera berus	Viper, adder	Europe
Vipera ammodytes	Long-nosed viper	Europe
Vipera palaestinae	Palestine viper	Asia, Middle East
Macrovipera lebetina	Levantine viper	Asia, Middle East, North Africa
Daboia russelii	Russell's viper*	Indian sub-continent, South East Asia
Echis carinatus	Saw-scaled viper*	Indian sub-continent, Middle East, central Asia
Echis ocellatus	West African carpet viper†	North-west Africa
Bitis arietans	Puff adder†	Africa
Colubridae		
Dispholidus typus	Boomslang†	Africa
Atractaspididae		
Atractaspis spp.	Burrowing asps, stiletto snakes	Africa, Middle East

*Most important public health threats in Asia.
†Most important public health threats in Africa.
‡Most important public health threats in Americas.

Downloaded From Vet-eBooks.com

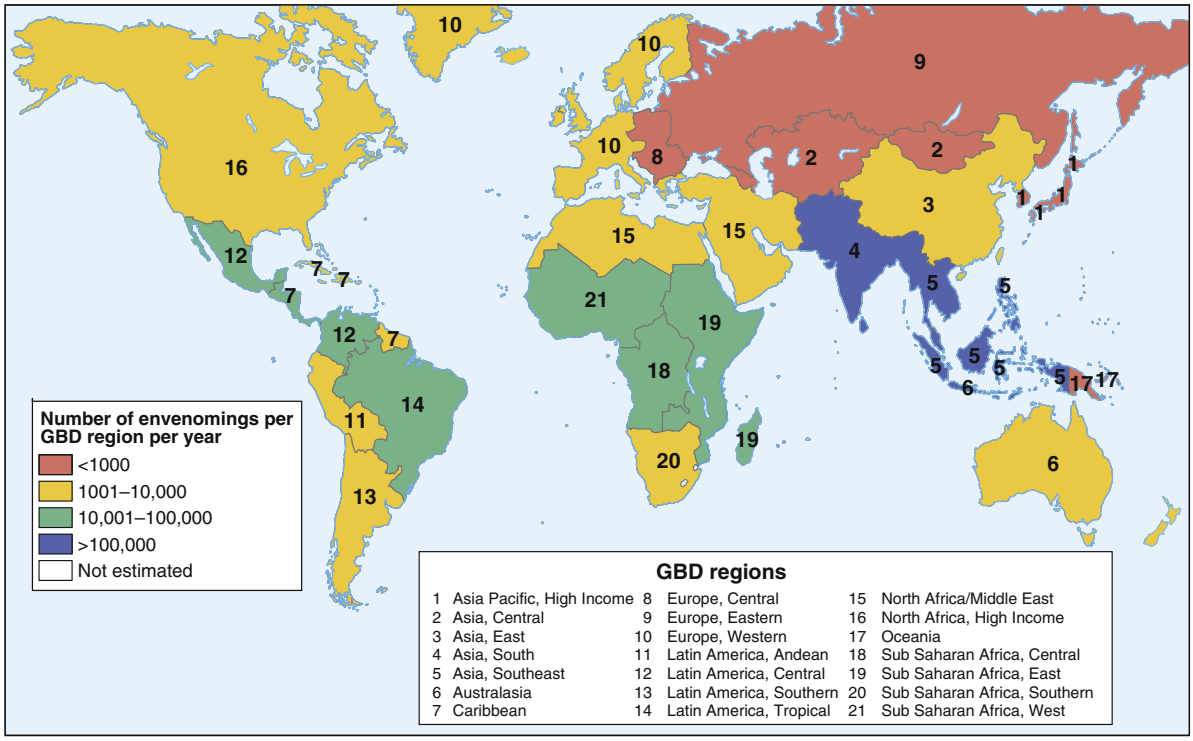


Fig. 6.49 Regional estimates of envenoming due to snakebite (low estimate).
From Kasturiratne A. et al PLoS MED 2008; http://journals.plos.org

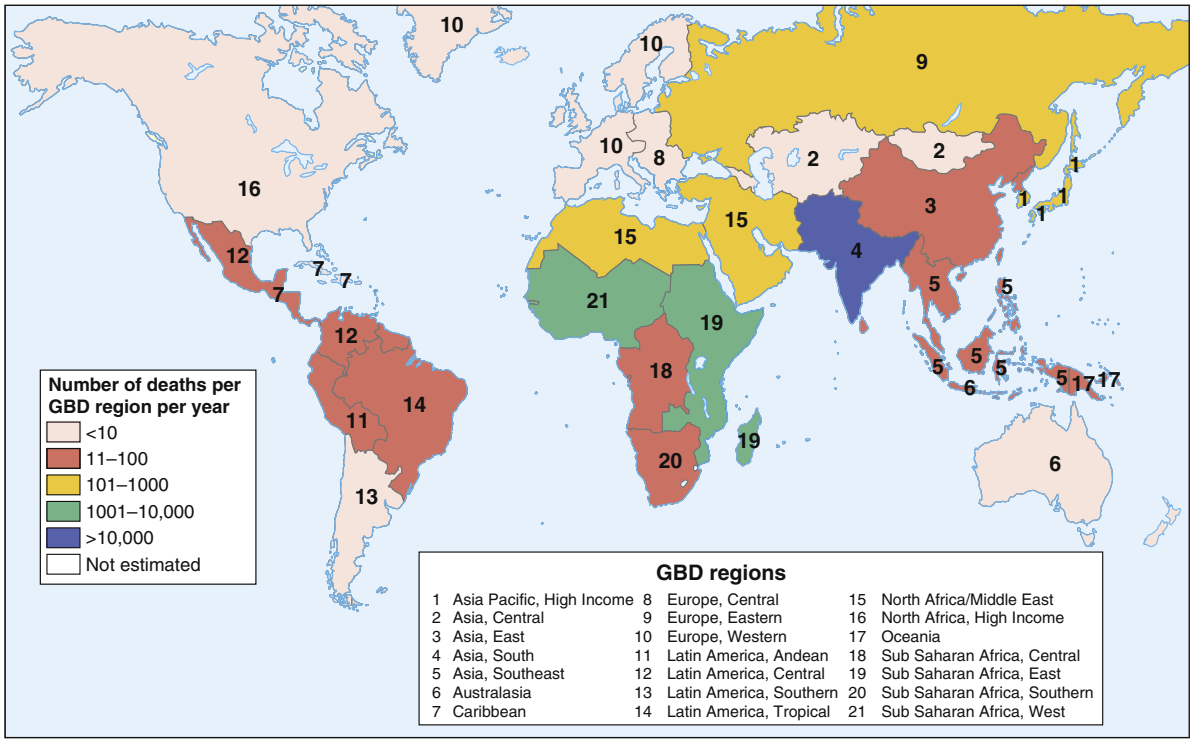


Fig. 6.50 Regional estimates of deaths due to snakebite (low estimate).
From Kasturiratne A. et al PLoS MED 2008; http://journals.plos.org

Downloaded from Vet-eBooks.com



Fig. 6.51 Viperidae – *Calloselasma rhodostoma*, the Malayan pit viper.
Pit vipers comprise a large group of snakes including rattlesnakes and the *Bothrops* snakes of South America. Their venoms, seen here being squeezed from the tip of the Malayan pit viper fang by gentle pressure over the venom glands, contain a variety of toxins causing variously thrombocytopenia, hypotension, local tissue necrosis and neurological compromise. (Courtesy, Dr H. A. Reid.)



Fig. 6.52 Severe tissue damage caused by a viper bite.
This Malaysian man, who was bitten on the hand by a Malayan pit viper (*Calloselasma rhodostoma*), developed massive oedema, spreading on to the trunk, extensive bruising, blistering and bleeding. (Courtesy, Dr H. A. Reid.)



Fig. 6.53 Spontaneous systemic bleeding after viper bite.
This Nigerian man had been bitten 2.5 hours previously by a West African carpet viper (*Echis ocellatus*). Bleeding from the gums and into the floor of the mouth indicates the effects of circulating venom haemorrhagins (metalloproteinases that damage vascular endothelium), which were also responsible for an intracranial haemorrhage from which he died 3 hours later. (Courtesy, Professor D. A. Warrell.)



Fig. 6.54 Elapid – *Naja kaouthia*, the Asian cobra.
The venom of these elapids contains postsynaptic neurotoxins that paralyse and cytotoxins that cause local tissue necrosis at the bite site. (Courtesy, Professor D. A. Warrell.)

Downloaded From Vet-eBooks.com



Fig. 6.55 Local necrosis after a cobra bite on the foot.
This Thai patient had been bitten 4 days earlier by an Asian cobra. There is a darkened, anaesthetic area surrounded by blisters, smelling of putrefaction, an early sign of tissue necrosis.



Fig. 6.56 Cobra bite on the foot.
This is the same patient as seen in Fig. 6.55, 10 days later, after spontaneous sloughing of the necrotic skin and subcutaneous tissue, exposing the tendons. (Courtesy, Professor D. A. Warrell.)



Fig. 6.57 Myoglobinuria following rattlesnake bite.
This patient was bitten by a tropical rattlesnake (*Crotalus durissus terrificus*) in Brazil. Eighteen hours after the bite she had 'myasthenic facies' resulting from paralysis of muscles innervated by the cranial nerves and was passing myoglobin in the urine. Both features are the result of venom phospholipases A2, which damage nerve endings and skeletal muscle. (Courtesy, Professor D. A. Warrell.)



Fig. 6.58 Ptosis due to elapid bite.
This boy had been bitten by a Papuan taipan (*Oxyuranus scutellatus canni*) 4.5 hours previously. Elapid venom results in neuromuscular block, initially of muscles innervated by the cranial nerves, progressing to bulbar respiratory and finally generalized paralysis. This patient shows bilateral ptosis (inability to open the eyes despite contraction of the temporalis muscle puckering the brow), external ophthalmoplegia (divergent squint), paralysis of facial muscles and inability to open the mouth and protrude the tongue. (Courtesy, Professor D. A. Warrell.)

Downloaded from Vet-eBooks.com



Fig. 6.59 20-minute whole-blood clotting test.
This is an invaluable bedside test to detect incoagulable blood resulting from consumption coagulopathy due to envenomation. Blood taken by venepuncture from the patient shown in Fig. 6.58 was left undisturbed in a new, clean, dry, glass vessel for 20 minutes. It remained liquid, indicating systemic envenoming. Where specific antivenom is available, this test can sometimes be used to titrate dosing. (Courtesy, Professor D. A. Warrell.)

PLANTS



Fig. 6.60 *Argemone mexicana* flower (Mexican prickly poppy), the cause of epidemic dropsy.
Epidemic dropsy, characterized by peripheral oedema, has been most frequently reported from India, where the largest outbreak (New Delhi 1998) affected more than 3000 people of whom 60 died. Contamination of mustard oil used for cooking with argemone oil (which can grow in the same fields) is the cause of this poisoning. Mustard oil is also used in Mauritius, Fiji, Nepal and Mozambique where outbreaks have also occurred.

Downloaded from Vet-eBooks.com

7. Nutrition

Food security remains a major challenge for communities that are dependent on climate-vulnerable subsistence farming and in settings of major humanitarian crisis including natural disaster, war, and massive population displacement. According to the World Food Programme, in 2015 one in nine people on the planet went to bed hungry each night. The management of severe acute malnutrition (SAM) in children has been revolutionized by a technological step forward (ready-to-use therapeutic food, RUTF) and the migration of the vast majority of care from hospital to the community that RUTF has facilitated (community-based management of acute malnutrition, CMAM). Inadequate nutrition due to poverty doesn't only mean undernutrition. The global epidemic of obesity and associated ill health that is spreading from wealthy countries to emerging economies creates the absurd paradox of concurrent hunger and gross excess within the borders of a single nation. Specific micronutrient deficiencies continue to contribute importantly to morbidity and mortality. In this context international scale-up of vitamin A supplementation for individuals under 5 years of age, sometimes delivered through the expanded programme of immunization (EPI), has been a significant public health success story.

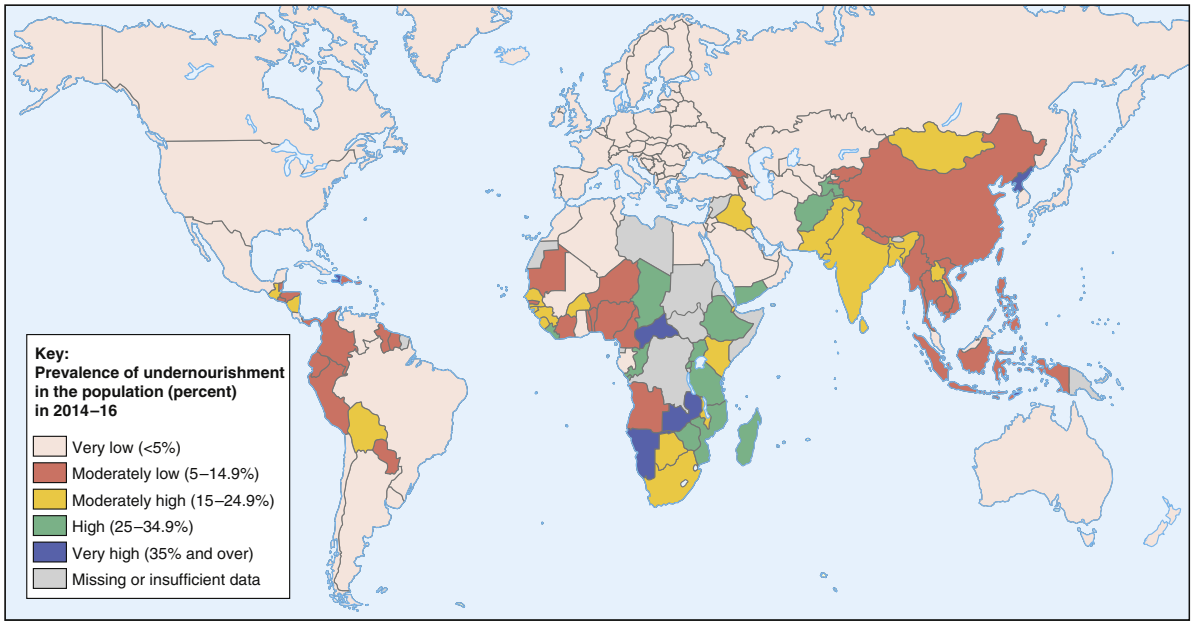


Fig. 7.1 The hunger map.
According to the World Food Programme, 795 million people went to bed hungry each night in 2015. (From World Food Programme http://www1.wfp.org)

Downloaded From Vet-eBooks.com

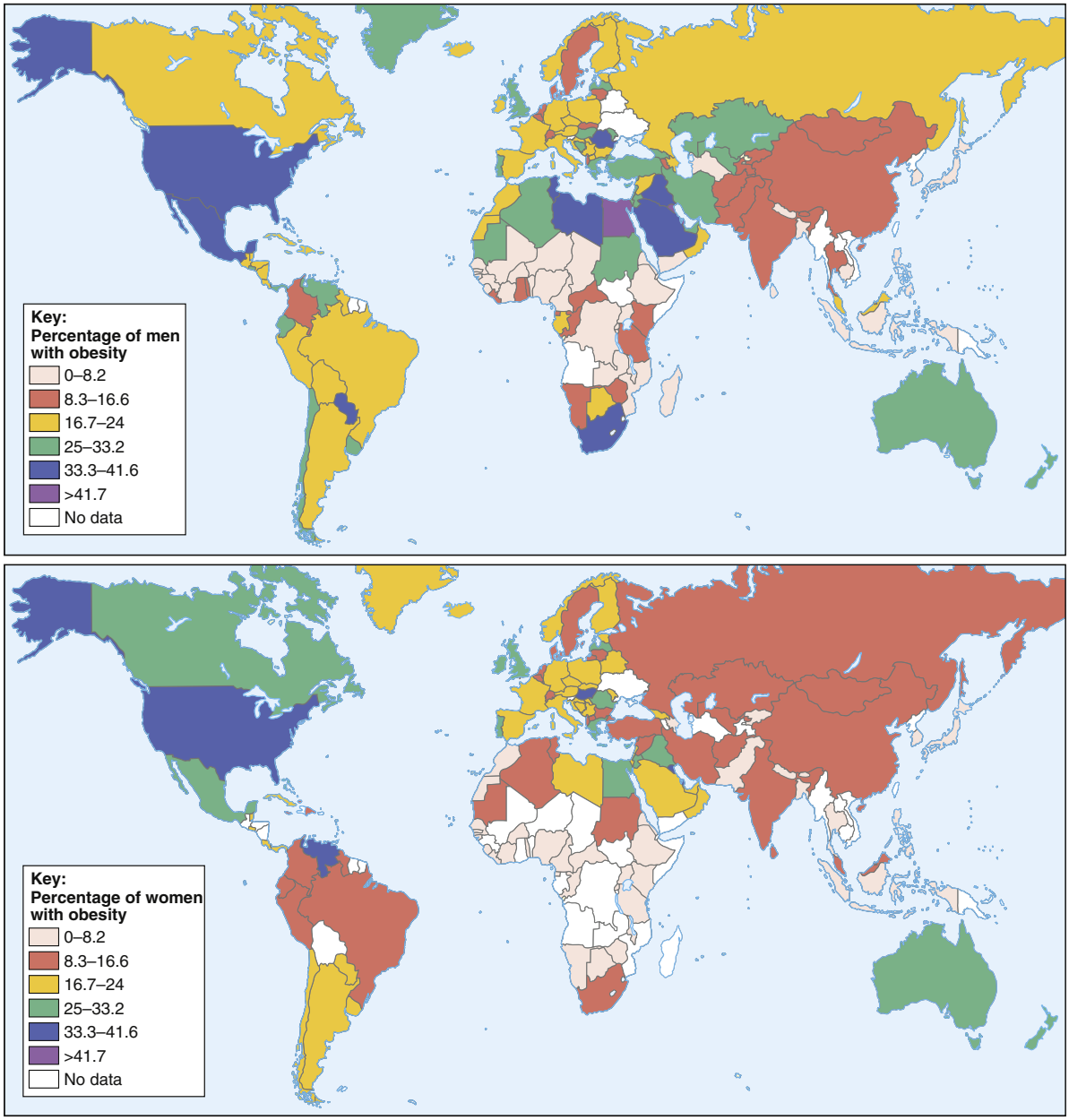


Fig. 7.2 The obesity map.
The global prevalence of obesity doubled between 1980 and 2014. (From http://www.worldobesity.org)

Downloaded From Vet-eBooks.com

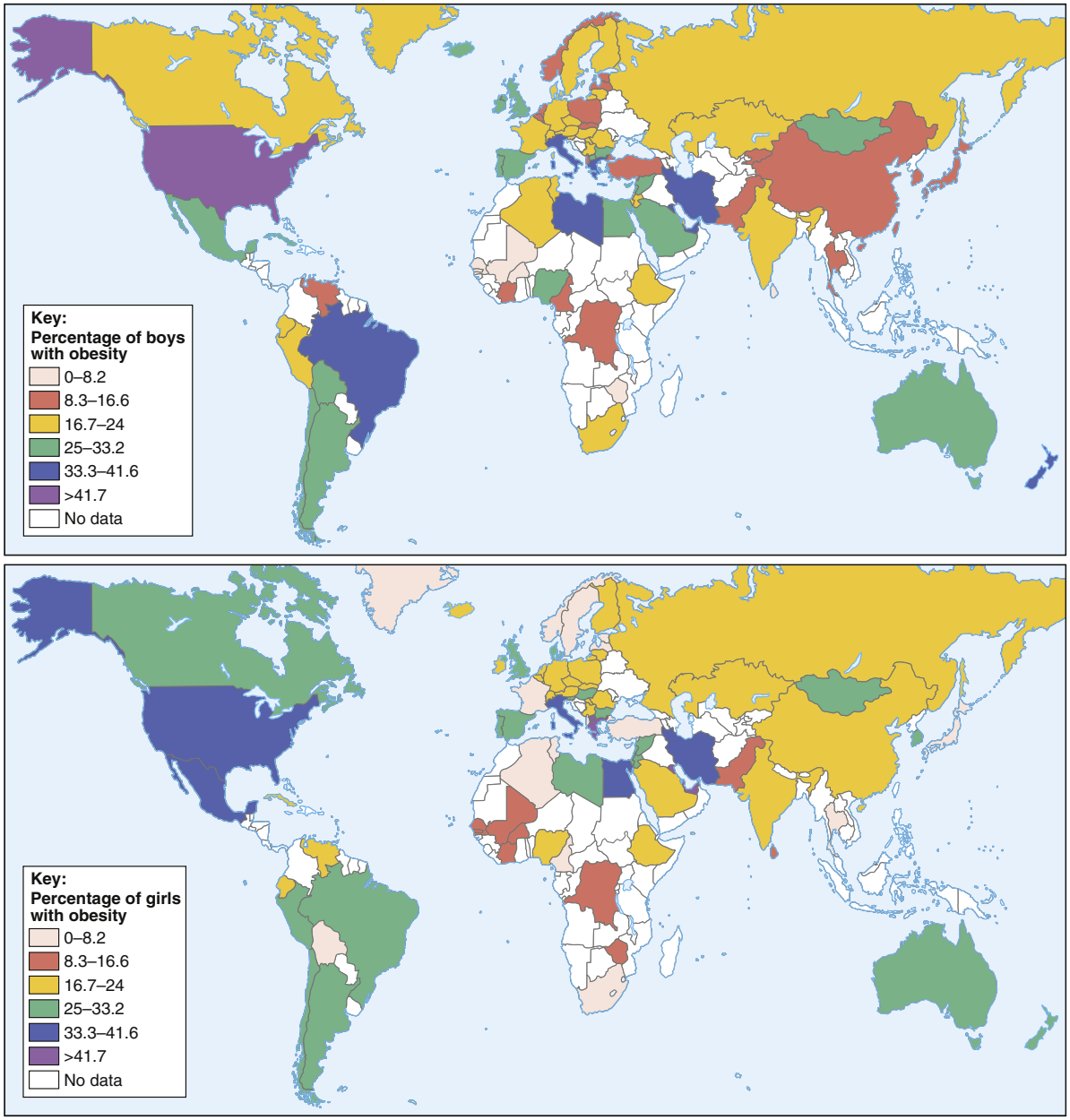


Fig. 7.2 cont'd

Downloaded From Vet-eBooks.com

MALNUTRITION

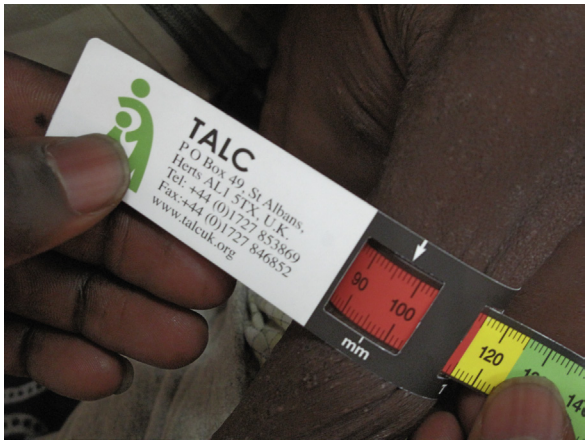


Fig. 7.3 Measuring mid-upper arm circumference (MUAC).
MUAC is a good marker of malnutrition-associated mortality risk and thus is widely used as an independent admission criterion for feeding programmes. This child's MUAC is in the 'red' zone (<115 mm), indicating severe acute malnutrition and eligibility for therapeutic feeding. The yellow zone (115 mm to <125) defines moderate acute malnutrition and eligibility for supplementary feeding; green (>= 125 mm) is in the 'normal' range for a child aged 6 to 59 months. (Courtesy, Dr M. Kerac.)



Fig. 7.4 Kwashiorkor and marasmus in brothers.
Though the traditional classification of protein energy malnutrition (PEM) into marasmus and kwashiokor is much less frequently used now, nevertheless the phenotypes are still often distinguishable. Compare the miserable distressed expression, pale hair, generalized oedema and skin changes in the child on the left, who has kwashiorkor, with the marasmic wasting of his less agitated, more listless older brother. Kwashiorkor frequently follows acute infection and/or diarrhoea in a child during the weaning period.



Fig. 7.5 Skin changes in kwashiorkor in a child in Sierra Leone.
Skin changes including erythema, 'black enamel' and then 'peeling paint' skin, as seen here, may terminate in extensive desquamation with widespread supericial ulceration. (Courtesy, Dr V. Sawicki.)



Fig. 7.6 Home-made ready-to-use therapeutic food being made in Sierra Leone.
The development of 'Plumpynut' and other ready-to-use therapeutic foods has transformed outpatient management of malnutrition. Locally produced ready-to-use therapeutic food (RUTF) can address an important need, create an income-generating opportunity, provide a market for local produce and subvert supply chain vulnerability. Approved recipes that are used deliver the appropriate nutritional balance using locally available resources. (Courtesy, Professor D. A. J. Moore.)

Downloaded from Vet-eBooks.com



Fig. 7.7 Cancrum oris (noma).
This necrotizing ulcerative stomatitis is often (though not invariably) associated with chronic malnutrition. It is a rapidly progressive, polymicrobial gangrene of the face with a high mortality and devastating and disabling sequelae in survivors. (Courtesy, Professor Y. Larsson.)

VITAMIN AND MINERAL DEFICIENCIES

Vitamin A Deficiency

The leading cause of preventable blindness in children, it is estimated by WHO that 250 million preschool children are vitamin A deficient, leading to half a million becoming blind each year. Half of those going blind die within 12 months.

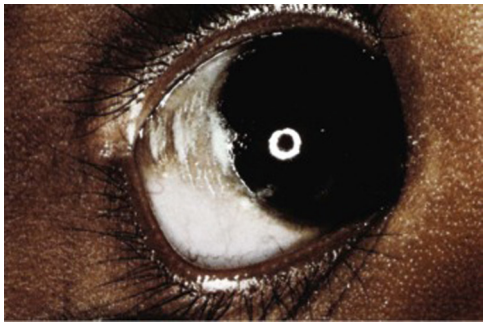


Fig. 7.8 Xerophthalmia.
Vitamin A deficiency is a common cause of blindness among preschool children in the tropics, especially in Asia. This 10-month-old Indonesian boy has xerophthalmia with Bitot's spots and hyperpigmentation. (From Oomen HAPC: Vitamin A deficiency, xerophthalmia and blindness, Nutr Rev 6:161–166, 1974.)



Fig. 7.9 Bitot's spots.
These are silver-grey, foamy spots, situated on the conjunctiva usually external to the cornea and often bilateral. These accumulations of keratin, which can be wiped off, are pathognomonic of vitamin A deficiency and usually disappear when vitamin A status improves. (Courtesy, N. Rogers. From Bowling, B. Cornea. In: Kanski's Clinical Ophthalmology. Pages 167–237, Figure 6.40A. Copyright © 2016, Elsevier Limited. All rights reserved.)

Downloaded From Vet-eBooks.com

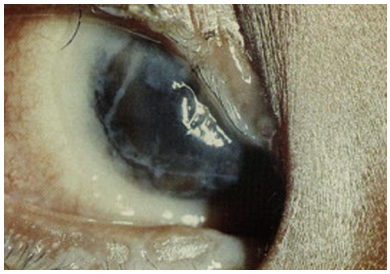


Fig. 7.10 Measles-associated blinding keratomalacia in a child with vitamin A deficiency. The cornea has completely melted away and only a thin sheet of fibrin covers the iris. A softening and thinning of the cornea occurs in chronic, severe vitamin A deficiency. The atrophic mucosal surface becomes covered with a keratinized stratified squamous epithelium which is opaque. (From Sandford-Smith, J. Eye Diseases in Hot Climates, 2nd ed. Oxford: Wright Publishers, Butterworth Heinemann; 1990: plate 12d.)

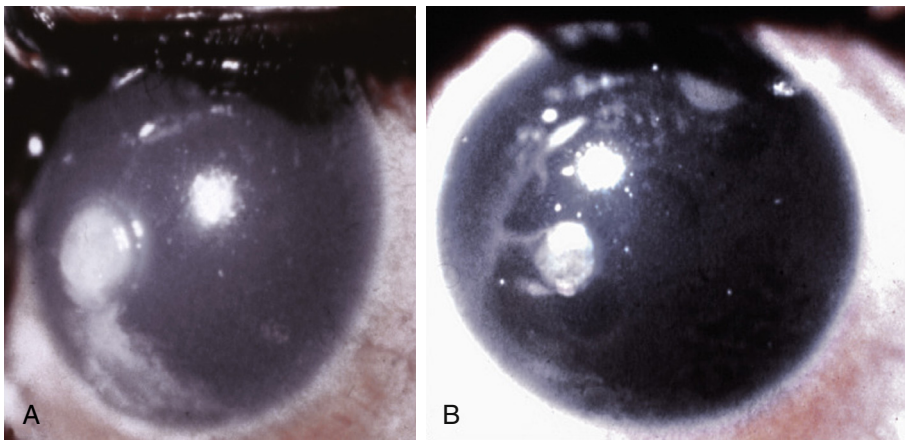


Fig. 7.11 Corneal ulceration.
Here corneal xerosis has progressed to a small ulcer (A). Ulcers may heal, with resultant corneal scarring impairing future visual acuity if the visual axis is involved. Prompt treatment can restore useful vision and protect the contralateral eye. Within 5 days there is marked improvement (B) following three doses of 200 000 IU vitamin A. (Courtesy, Dr A. Foster. From Mannis, T., Mannis, M. J., Paranjpe, D. R., et al. Nutritional disorders. In: Cornea. Pages 676-687. Fig 60.5. Copyright © 2017 Elsevier. All rights reserved.)

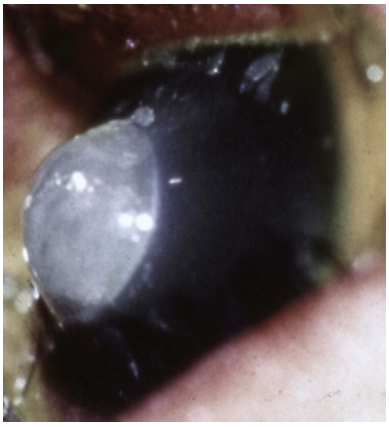


Fig. 7.12 Keratomalacia progressing to descemetocoele formation. The cornea has perforated and only Descemet's membrane is retaining the contents of the globe. Rupture of this fragile structure would lead to blindness. (Courtesy, Dr A. Foster. From Mannis, T., Mannis, M. J., Paranjpe, D. R., et al. Nutritional disorders. In: Cornea. Pages 676-687. Fig 60.7. Copyright © 2017 Elsevier. All rights reserved.)



Fig. 7.13 Phrynoderma due to vitamin A deficiency.
This papular, follicular hyperkeratosis has been associated with vitamin A deficiency. The name derives from a Greek term meaning toad-skin. (From Noguera-Morel, L., McLeish Schaefer, S., Hivnor, C. M. Dermatology, Volume 51, Pages 793–809. Fig. 51.7. e4. Copyright © 2018, Elsevier Ltd. All rights reserved.)

Downloaded From Vet-eBooks.com

Vitamin B1 (Thiamine) Deficiency

Conventionally characterized into 'wet' and 'dry' forms, affecting cardiac and neurological systems, respectively, more usually the disease phenotype is a mixture with one system predominating. Infantile beri beri, occurring in children breast-fed by thiamine-deficient mothers, can lead to heart failure and convulsions.

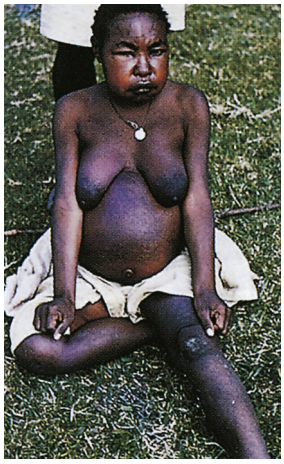


Fig. 7.14 'Wet' beri beri.
Oedema without proteinuria and high output, predominantly right-sided, cardiac failure.

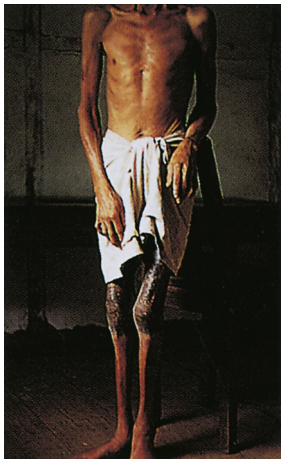


Fig. 7.15 'Dry' beri beri.
A mixed motor and sensory neuropathy can occur with wrist drop and wasting of the lower extremities; proprioceptive loss can give rise to a sensory ataxia.

Vitamin B2 (Riboflavin) Deficiency

Ariboflavinosis is commonly associated with protein energy malnutrition or pellagra and mainly causes oral and peri-oral lesions.



Fig. 7.16 Angular stomatitis.
Grey-white fissures at both angles of the mouth are seen in this African boy.



Fig. 7.17 Cheilosis and perleche.
Sore, red lips (cheilosis) and increased vertical fissuring (perleche) are clearly demonstrated in this 4-year-old Bangladeshi boy with riboflavin deficiency. (Courtesy, Dr A. Cambanis.)

Vitamin B3 (Niacin) Deficiency

Pellagra may result from dietary insufficiency of niacin, commonly in maize-dependent diets, or of its precursor tryptophan; less commonly deficiency can arise through a variety of conditions which reduce absorption or increase consumption. The deficiency leads to the classical triad of 'dermatitis, diarrhoea and dementia'.

Downloaded from Vet-eBooks.com



Fig. 7.18 Pellagra.
The scaly, desquamating, keratotic rash of pellagra is symmetrical, sharply demarcated and distributed in sun-exposed parts of the body; the classic appearance of 'Casal's necklace' is shown here. (Courtesy, Professor K. F. Schaller.)

Vitamin C Deficiency

Scarcity of fresh fruit and vegetables sufficient to cause scurvy is uncommon in the tropics, perhaps with the exception of desert regions.

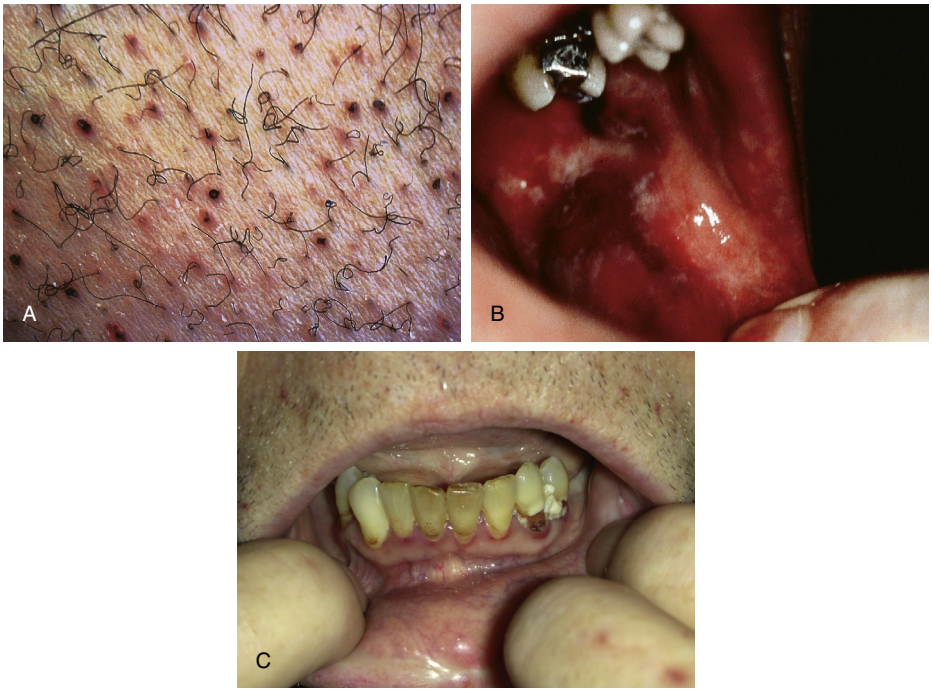


Fig. 7.19 Scurvy.
(A) Corkscrew hairs and perifollicular haemorrhage on the lower extremities. (B) Haemorrhage beneath the buccal mucosa. (C) Gingival hypertrophy and infection, with loosened teeth. (Courtesy, Dr J. Callen. From Bolognia L., Schaffer, J. V., Duncan, K. O., Ko, C.J. Nutritional disorders. In: Dermatology Essentials. Pages 359–373, Fig. 43.6. e1. Copyright © 2014, Elsevier Limited. All rights reserved.)

Downloaded From Vet-eBooks.com

Vitamin D Deficiency

Rickets in children and osteomalacia in adults are the clinical consequences of vitamin D deficiency. Few foods naturally contain vitamin D, so sun exposure is the most important source.



Fig. 7.20 Infantile rickets – 'rickety rosary'.
Breastmilk contains very little vitamin D, so infants with reduced sunlight exposure either due to local climate, air pollution, residence at high latitudes (where UVB is largely filtered by passage through the atmosphere) or cultural preference to protect infants from sunshine are at significant risk of rickets. Vitamin D3 synthesis is reduced in pigmented skin, further increasing risk of deficiency. Rounded swellings that appear over the costochondral junctions near the sternum give rise to the term 'rickety rosary'.

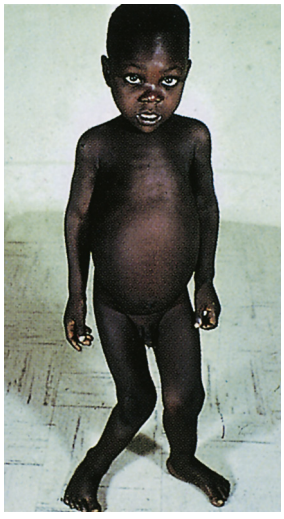


Fig. 7.21 Child with rickets.
The consequnces of infantile rickets may continue into childhood even after vitamin D deficiency has been corrected, with skeletal deformities such as knock knees, bow legs and the pigeon chest seen in this boy.



Fig. 7.22 Osteomalacia.
The increased demands of pregnancy may result in gross deformity of the pelvis. This occurs, for example, in mothers kept in purdah.

Iodine Deficiency

Low dietary iodine results in a range of iodine deficiency disorders (IDD) including foetal loss, stillbirth, congenital malformations, developmental delay and impaired mental development, and abnormal thyroid morphology and function.

Downloaded from Vet-e-Books.com

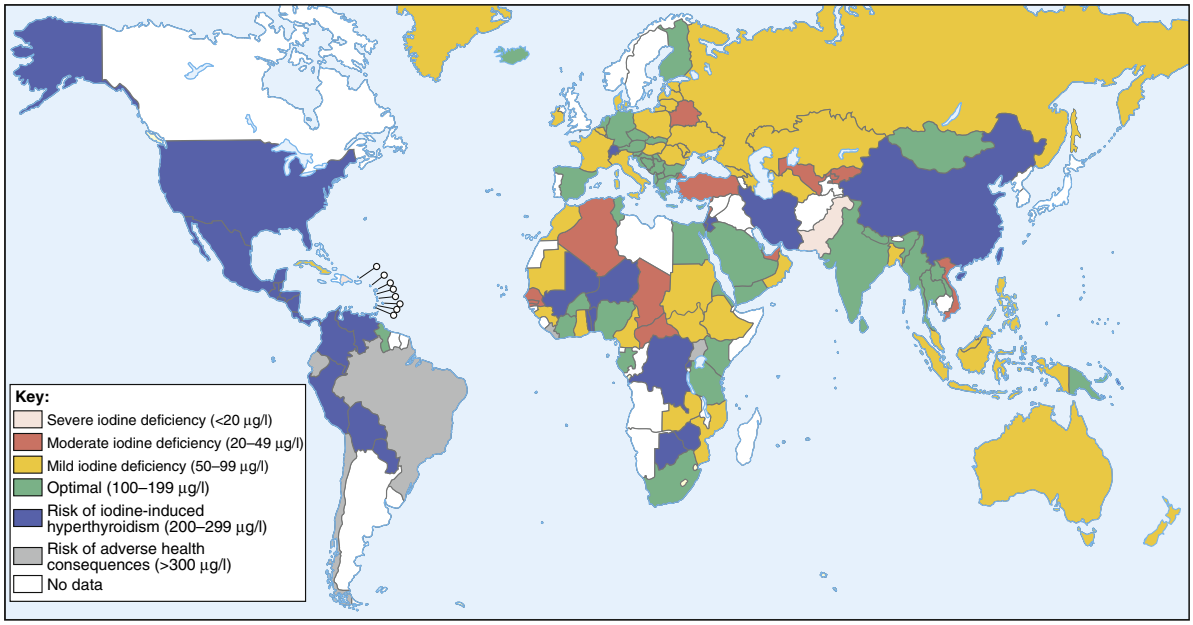


Fig. 7.23 Global iodine nutritional status based on median urinary iodine. (From WHO Global Database on Iodine Deficiency, Page 11, Figure 3.3. http://www.who.int/nutrition/publications/micronutrients/iodine_deficiency/9241592001/en/)



Fig. 7.24 Nepalese woman with 'endemic goitre'.
Total goitre prevalence (TGP), previously used as an indicator of iodine deficiency disorders (IDD), represents the tip of the iodine deficiency iceberg. Because TGP falls slowly after correction of iodine status (e.g. through salt iodization), and thus reflects a population's history of iodine nutrition, urinary iodine is now preferred as a monitor of current iodine status.

Downloaded From Vet-eBooks.com

TOXIN INGESTION

Konzo is a distinct form of spastic paraparesis, affecting mostly children and breast-feeding mothers, occurring exclusively in cassava-growing areas of sub-Saharan Africa and characterized by abrupt onset over hours or days of permanent but non-progressive spastic paralysis of the legs. It occurs mainly as epidemics, affecting up to 29/1000 during periods of food shortages or drought leading to overdependence on cassava; it also occurs less frequently as sporadic cases in endemic areas. Aetiology is attributed to months of ingestion of high cyanide from insufficiently processed cassava and low protein intake, in particular a lack of (protective) methionine and cysteine.



Fig. 7.25 Five siblings with konzo.
All five siblings have been affected during a period of food insecurity. (Courtesy, Dr W. Howlett.)

Downloaded from Vet-eBooks.com

8. Non-Communicable Disease

The growing importance of non-communicable disease in tropical regions of the world is highlighted by the 2015 Global Burden of Disease study with emerging prominence of diabetes, ischaemic heart disease, cardiovascular disease and cancer, whilst haemoglobinopathies contribute significant morbidity and mortality.

A number of genetic blood dyscrasias are especially common in some tropical areas. Some, such as sickle cell trait, may have afforded a positive selective advantage in areas highly endemic for falciparum malaria. However, as they are well documented elsewhere, only passing reference is made to these conditions here.



Fig. 8.1 African child with Burkitt's lymphoma of the maxilla.
Denis Burkitt originally described the endemic form of this high-grade B cell lymphoma in African children and young adults with facial swelling. The co-occurrence of immunosuppression due to falciparum malaria and persistent Epstein Barr virus (EBV) infection increases the risk of chromosomal translocation in replicating germinal centre B cells, explaining the geographical distribution of disease. Over 50% of cases present with mandibular or maxillary bone involvement. Sporadic forms outside malarial regions more often present with lymphadenopathy or intra-abdominal masses. (Courtesy, Professor O. Malik.)

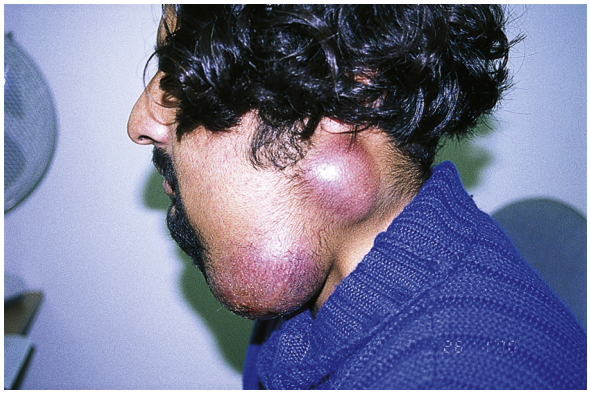


Fig. 8.2 Burkitt's lymphoma in an Asian adult.
The photograph shows enormous cervical lymphadenopathy, which was initially suggestive of tuberculous lymphadenitis but which biopsy revealed to be due to Burkitt's lymphoma.

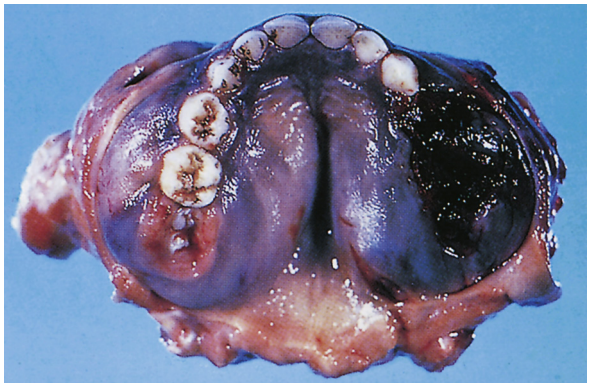


Fig. 8.3 Maxillary tumour at autopsy.
The extensive infiltration of both maxillae by Burkitt's lymphoma tissue is evident in this autopsy specimen. (Courtesy, Professor M. S. R. Hutt.)

Downloaded From Vet-eBooks.com

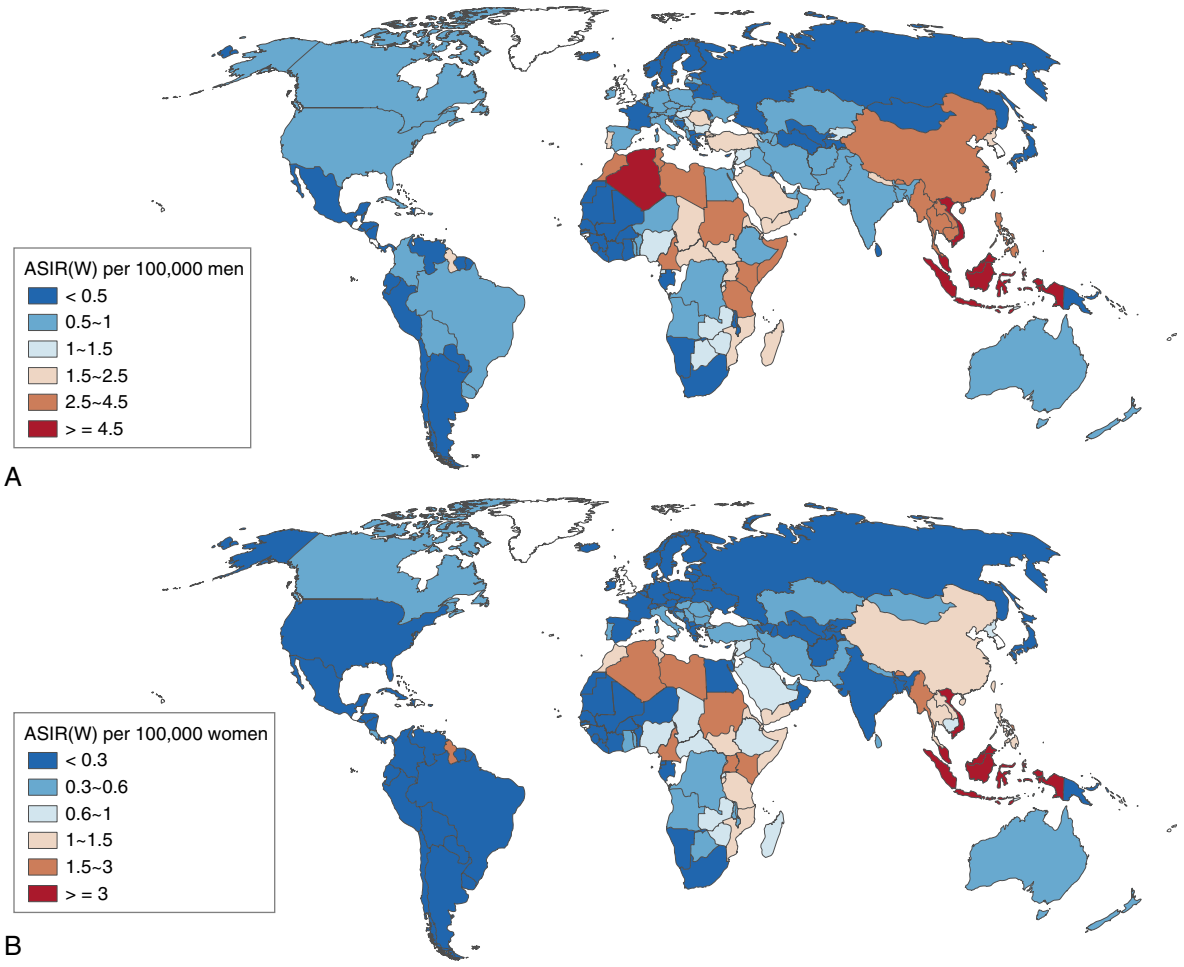


Fig. 8.4 Global estimates of age-standardized incidence of nasopharyngeal carcinoma in men (A) and women (B).
This condition, which is also associated with Epstein–Barr virus, has a high incidence in southern China, South East Asia and North Africa. Incidence is falling globally, believed to be due to reducing tobacco use and economic development, whilst drops in case fatality are attributed to diagnostic and therapeutic advances. (From Tang, L.-L. et al. Global trends in incidence and mortality of nasopharyngeal carcinoma. *Cancer Letters*, Volume 374, Issue 1, Pages 22–30, Figure 1. Copyright © 2016 Elsevier Ireland Ltd.)



Fig. 8.5 Endemic (non-AIDS) Kaposi's sarcoma of the hand and foot.
The sporadic form of this malignant spindle cell tumour was originally described in elderly eastern European men by Hungarian dermatologist Moritz Kaposi. A male preponderance also appears in the endemic form seen in Africa. Typical nodular lesions are seen on the hand and foot of this man from Lesotho; these may run a chronic, indolent course, though may sometimes be more aggressive with infiltrative lesions and associated gross limb swelling. Human herpesvirus 8 is causally associated with HIV-related Kaposi's sarcoma. (Courtesy, Professor S. Lucas.)

Downloaded From Vet-eBooks.com

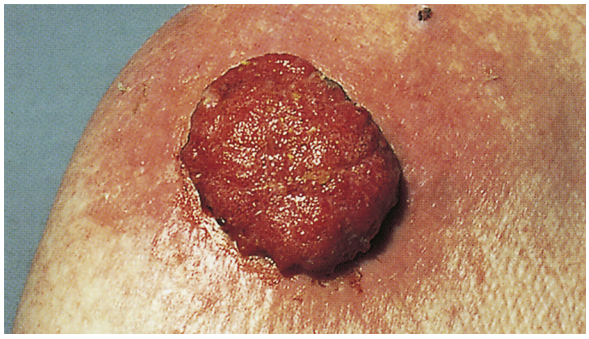


Fig. 8.6 Squamous cell carcinoma.
Chronic exposure to solar radiation, particularly in people with fair skin, can result in degenerative or neoplastic changes in the sun-exposed parts of the body. Thinning of the ozone layer is predicted to result in an increased frequency in conditions such as squamous cell carcinoma seen here on the shoulder of an albino patient. (Courtesy, Professor K. F. Schaller.)



Fig. 8.7 Malignant melanoma.
A sudden increase in pigmentation and enlargement of freckles following prolonged exposure to sunlight may be precursors to the development of a malignant melanoma in a fair-skinned individual. The large melanoma seen in this 54-year-old Caucasian woman shows marked local infiltration and carries a poor prognosis. (Courtesy, Dr W. A. D. Griffiths.)



Fig. 8.8 Malignant melanoma of the foot.
In dark-skinned people such as the African patient seen here the primary site of this condition is usually the non-pigmented sole, or occasionally the palmar surface of the hand. Similarly a malignant melanoma may occasionally occur in an area of vitiligo. (Courtesy, Professor K. F. Schaller.)



Fig. 8.9 Low-cost oral morphine solution.
A broader approach to palliative care is gradually gaining traction in many resource-limited settings. Morphine solution can be prepared locally and distributed at relatively low cost. (Courtesy, Dr K. Wakeham.)

Downloaded From Vet-eBooks.com

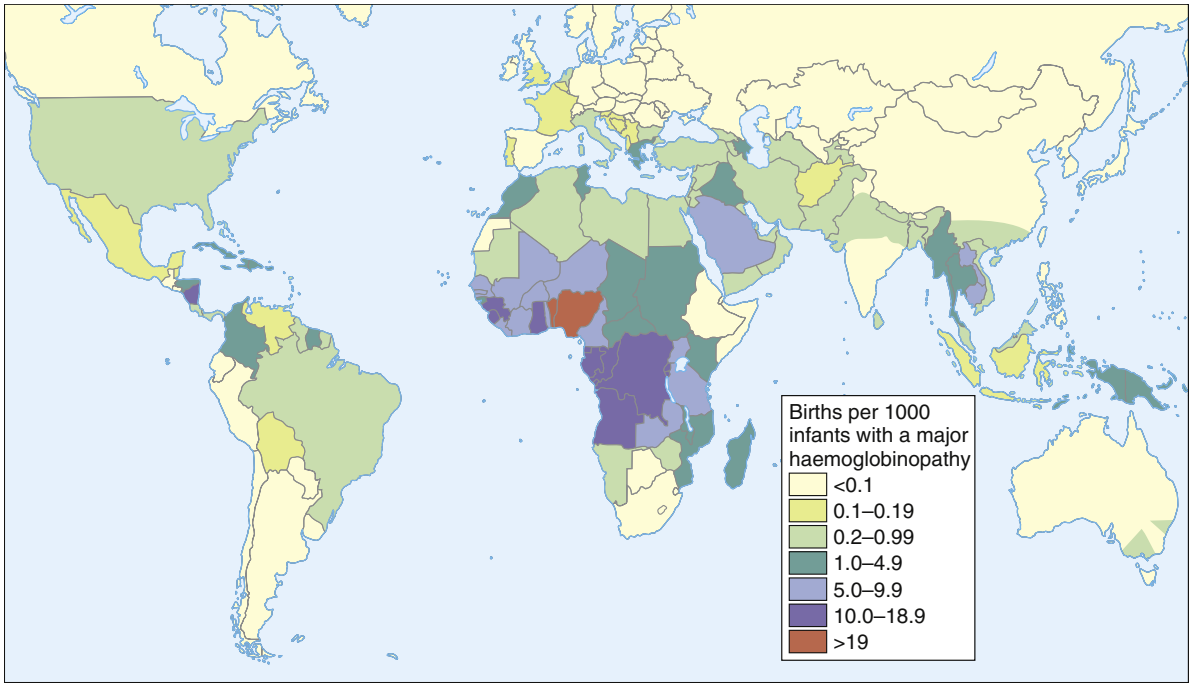


Fig. 8.10 Incidence of major haemoglobinopathies.
The map indicates the estimated numbers per 1000 births, of infants with major haemoglobinopathies. This can be compared with Fig. 8.11. (Courtesy of WHO GENOMIC RESOURCE CENTRE.)

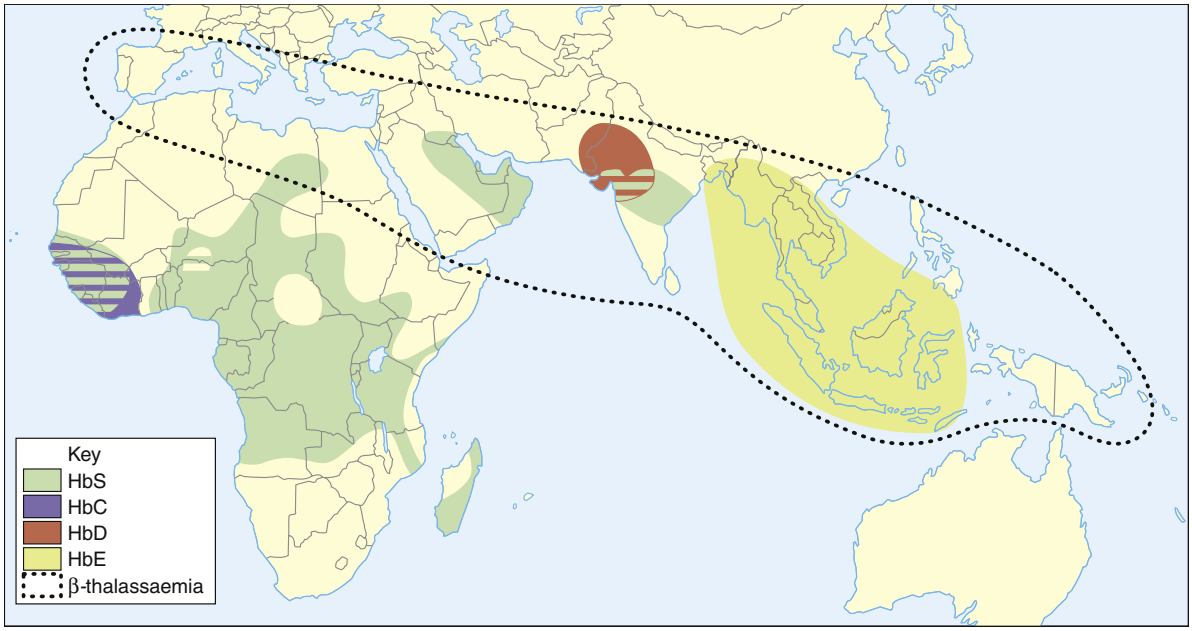


Fig. 8.11 Distribution map of haemoglobinopathies (excluding the Americas).
The most important abnormal haemoglobins (Hb) in the tropics are HbS, HbC and HbE. Thalassaemia, which is the result of decreased synthesis of one of the chains of haemoglobin (alpha or beta), is also widespread. HbD has a limited distribution and is clinically mild. The abnormal haemoglobins also occur in Central and South America (not shown) because of migration, and among African Americans in the United States. The haemoglobin AS phenotype in the same population, which renders the erythrocytes unfavourable to the development of *Plasmodium falciparum*, favours the survival of the gene in tropical Africa, where falciparum malaria is holoendemic, although the SS phenotype increases host mortality.

Downloaded from Vet-eBooks.com

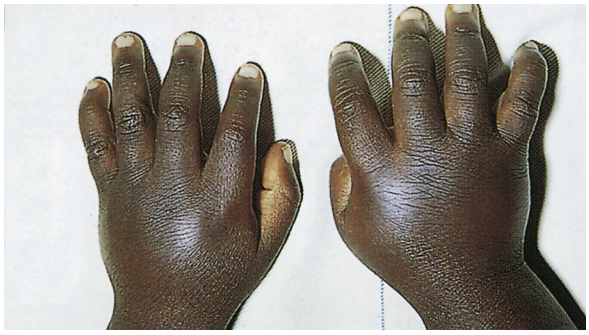


Fig. 8.12 Dactylitis due to sickle cell disease.
Severe bilateral dactylitis (hand-foot syndrome) is a common presentation of sickle cell disease in children, caused by vaso-occulsive bone infarction. (Courtesy, Professor P. Hamilton.)



Fig. 8.13 Bossing of the skull.
Bossing of the skull due to hyperplasia of the marrow is another feature of sickle cell disease; the skull height is increased with lateral indentations ('bosses'). Similar appearances may be seen in thalassaemia and in any other severe, congenital haemolytic anaemia. (Courtesy, Professor R. Hendrickse.)



Fig. 8.14 Radiograph of skull in thalassaemia.
Thalassaemia produces this typical 'hair-on-end' appearance of the skull in radiographs. (Courtesy, Dr G. D. Scarrow.)

Downloaded from Vet-eBooks.com



Fig. 8.15 'Mossy foot' in an Ethiopian.
Podoconiosis is a geo-genodermatosis caused by a genetically defective skin barrier permitting the passage of micro-particles from certain soils through the skin into the lymphatics. This sets up a destructive obliterative lymphangitis that leads to progressive debilitating lower limb lymphoedema. It is effectively restricted to barefoot farmers in highly fertile volcanic highlands such as Ethiopia.

Recurrent acute episodes (of presumed cellulitis) incapacitate the individual and worsen the lymphoedema. The surface of the skin becomes hyperkeratotic and 'mossy' in its appearance. (Courtesy, Dr C. Fuller.)



Fig. 8.16 Nodular appearance of long-standing podoconiosis.
As the limbs get larger, many patients additionally develop fibrotic nodules which restrict shoe-wearing. The condition can be prevented by the wearing of shoes before it has developed. In those with established disease, benefit can be achieved with simple washing, moisturizing, compression with socks and protection from further damage by wearing shoes. (Courtesy, Dr C. Fuller.)

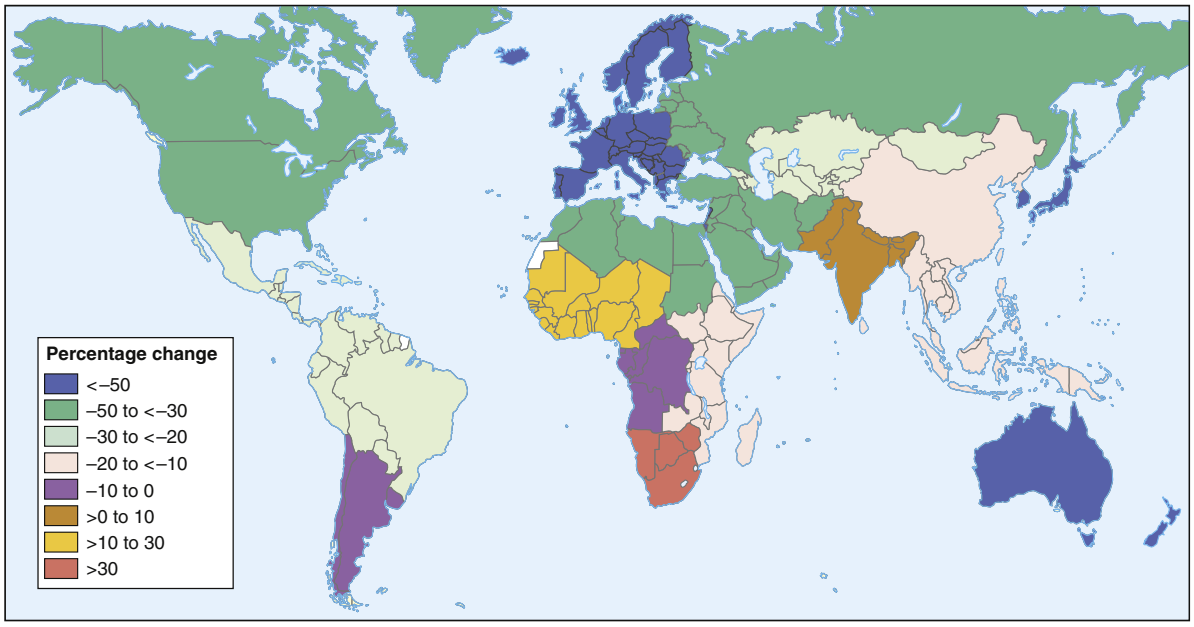


Fig. 8.17 Change in age-standardized road injury disability-adjusted life year (DALY) rates, 1990–2013.
Whilst road injury-attributable disability has been falling in high-income countries over the past 2 decades, rates have been increasing in South Asia and West and South sub-Saharan Africa. (From Haagsma, J.A., Graetz, N., Bolliger, I., et al. The global burden of injury: incidence, mortality, disability-adjusted life years and time trends from the Global Burden of Disease study 2013. *Injury Prevention*, 2016, Volume 22, Pages 3–18. Copyright © BMJ Publishing Group Limited.)

Downloaded from Vet-eBooks.com



Fig. 8.18 Mercury poisoning due to artisanal gold mining in Colombia.
There is growing recognition of the large public health burden of accidental domestic poisonings of children from household products and of larger-scale population poisonings arising from environmental degradation due to human activity, with poorer countries disproportionately affected. The use of mercury in artisanal gold mining is one example. (From Webster, P. C. Not all that glitters: mercury poisoning in Colombia. *The Lancet*, Volume 379, Issue 9824, Pages 1379–1380. Copyright © 2012 Elsevier.)



Fig. 8.19 Talipes equinovarus (clubfoot).
Clubfoot is twice as common amongst male as amongst female infants. The heel is rotated inward and the whole foot is deviated inward at the ankle. Untreated, this congenital deformity can cause significant lifelong impairment. (From Graham, J. M., Sanchez-Lara, P. A. Talipes equinovarus (clubfoot). In: *Smith's Recognizable Patterns of Human Deformation*. 2016, Pages 39–46, Figure 5-8 A.)



Fig. 8.20 Partial correction of talipes equinovarus with carefully directed pressure and taping.
There has been a major shift away from complex tendon release surgery and towards serial manipulations and weekly casts (the Ponseti method) of infants born with this condition. Taping and manipulation alone corrected this foot. (From Graham, J. M., Sanchez-Lara, P. A. Talipes equinovarus (clubfoot). In: *Smith's Recognizable Patterns of Human Deformation*. 2016, Pages 39–46, Figure 5-8 B.)



Fig. 8.21 Hand-pedalled locally built wheelchair in Sierra Leone.
Impaired mobility can be particularly challenging where terrain is uneven and wheelchair ramps are never seen. Innovative local solutions overcome supply chain hurdles, offer business opportunities and benefit from easily accessed maintenance know-how. (Courtesy, Dr V. Sawicki.)

Downloaded from Vet-eBooks.com



Fig. 8.22 Full-thickness burns.
Burn injuries are a major cause of morbidity in low-income settings, though disability can be substantially mitigated by simple early interventions and appropriate management. Training and capacity building by organizations such as Interburns enhance burns care in both the immediate aftermath and during recovery. Falling into the household fire due to undiagnosed or poorly controlled epilepsy remains an all-too-frequent cause of life-threatening burn injury. (From Kiser, M., Beijer, G., Mjuweni, S., et al. Photographic assessment of burn wounds: A simple strategy in a resource-poor setting. *Burns*, 2013, Volume 39, Issue 1, Pages 155–161, Figure 2. Copyright © 2012 Elsevier Ltd and ISBI.)



Fig. 8.23 Betel nut.
Chewing of a stimulant betel nut 'quid', variably containing the betel nut and/or leaf, slaked lime, tobacco and additional flavourings, is very common in Asia but is associated with high rates of oral cancer. Shown here is the commonest type of betel nut preparation in Taiwan called 'Ching-a', made by wrapping together an unripe betel fruit (1), inflorescence of Piper betle Linn slaked with lime paste (2), and a piece of betel leaf (3). All three parts are chewed together. (From Lin, C.-Y., Young, Y.-H. Effect of betel nut chewing on the otolithic reflex system. *Clinical Neurophysiology*, 2017, Volume 128, Issue 1, Pages 138–146, Figure 1. Copyright © 2016 International Federation of Clinical Neurophysiology.)

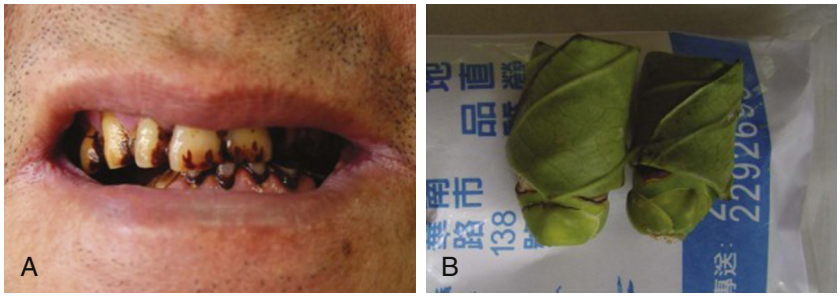


Fig. 8.24 Betel nut dental staining (A) and two betel nut 'quids' (B).
The characteristic red staining of the teeth reveals the habitual betel nut user. The nut is wrapped within its leaf in each of the quids seen here. (From Swartz, M. H. The oral cavity and pharynx. In: *Textbook of Physical Diagnosis*, 2014, Pages 278–314.e1, Figure 9–51 A.)



Fig. 8.25 Shackles used to restrain a patient with psychosis.
Mental health problems are hugely neglected in many countries. Ignorance and a lack of a suitably equipped healthcare system mean that approaches to management of disturbed behaviour are sometimes unacceptably violent. (Courtesy, Dr M. Wilkinson.)

Downloaded from Vet-eBooks.com

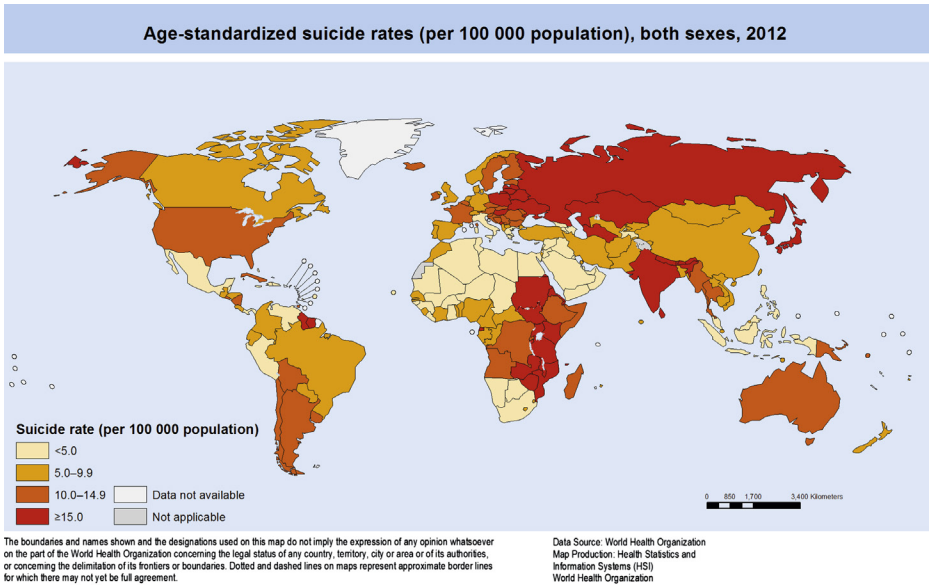


Fig. 8.26 Global suicide rates.
The age-standardized suicide rates (per 100,000 population) show considerable regional variation globally. Around 800,000 people die due to suicide each year, with almost 80% in low- and middle-income countries. It is the second leading cause of death in 15–29-year-olds worldwide. (Courtesy, © WHO, 2014. All rights reserved.)



Fig. 8.27 Distribution of sun protection products to children with albinism in Malawi.
The autosomal recessive condition of oculocutaneous albinism has long been associated with stigma and superstition often leading to social marginalization. The increased risk of skin cancer and other solar damage demands constant attention to sun protection. A sinister development in recent decades has been the emergence of the notion that albino body parts are imbued with magical powers, resulting in an increase in attacks and mutilating murders. (From Cruz-Inigo, A. E., Ladizinski, B., Sethi, A. Albinism in Africa: stigma, slaughter and awareness campaigns. *Dermatologic Clinics*, Volume 29, Issue 1, Pages 79–87, Figure 1. © Elsevier 2011.)

Downloaded From Vet-eBooks.com

9. Diseases of Unusual or Uncertain Aetiology

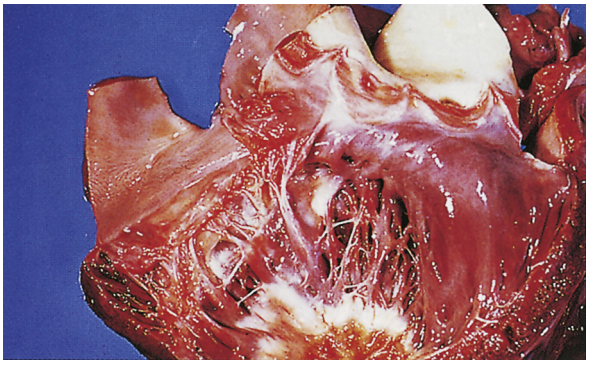


Fig. 9.1 Fibrotic changes in the heart of an African with endomyocardial fibrosis.
Endomyocardial fibrosis is an enigmatic and idiopathic cardiomyopathy that occurs primarily in subtropical Africa. Distribution is patchy, however, with a prevalence of less than 0.1% among cardiac patients in Nigeria contrasting with estimates of 20% in rural Mozambique. It presents in three clinical forms: mainly left-sided, as mitral incompetence; right-sided, with features suggestive of constrictive pericarditis; and a form involving both sides of the heart, presenting as congestive cardiac failure. Thromboembolic disease is an important risk.



Fig. 9.2 Ainhum of small toe.
This condition of unknown aetiology is a progressive encircling fibrosis of a toe, usually the fifth, sometimes leading to auto-amputation.

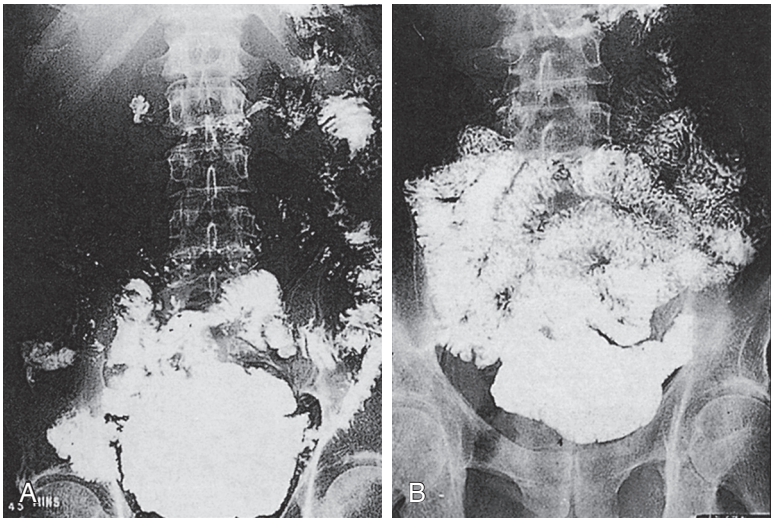


Fig. 9.3 Radiographs of patient with tropical sprue.
The postinfective malabsorption syndrome (also known as tropical sprue) is characterized by chronic steatorrhoea of unknown aetiology, with associated abdominal symptoms, weight loss, glossitis and megaloblastic anaemia. Fatty, bulky faeces are characteristic of this condition. The figures show loss of normal intestinal pattern before treatment (Fig. 9.3A), and then recovery after 3 months of treatment (Fig. 9.3B). (Courtesy, Professor M. S. R. Hutt (Fig. 9.3A); Courtesy, Dr J. Walters (Fig. 9.3B).)

Downloaded from Vet-e-Books.com

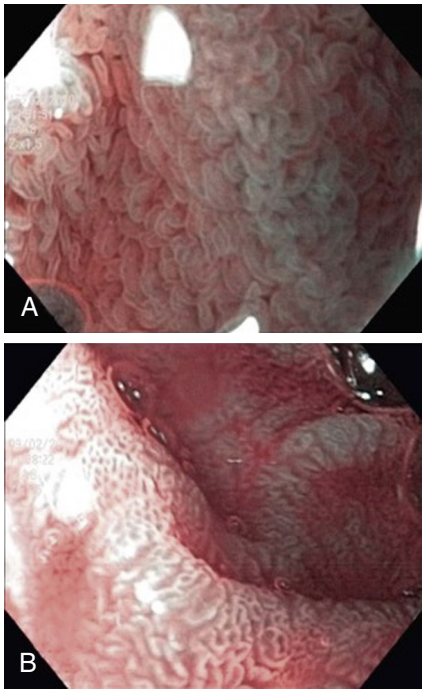


Fig 9.4 Endoscopic view of the second part of the duodenum in an Indian patient with tropical sprue using narrow-band imaging. (A) shows normal finger-like villi, and (B) shows areas of atrophic villi interspersed with areas of absent villi in a patient with tropical sprue. (Courtesy, Dr A. K. Dutta, Vellore, Tamil Nadu, India. From Ramakrishna, B. S. Tropical diarrhea and malabsorption. In: *Sleisenger and Fordtran's Gastrointestinal and Liver Disease*. Pages 1873–1885.e3, Figure 108-9. Copyright © 2016 Saunders, Elsevier Inc.)



Fig 9.6 Brazilian man with fogo selvagem.
The dermatological condition of pemphigus foliaceus occurs with high frequency in a number of endemic foci in rural areas of central and western Brazil, northern Argentina, Peru, Bolivia and Venezuela. The burning sensation in the skin gives rise to the name ("wild fire"). It was formerly believed to be caused by massive and repeated bites from the tiny blackfly *Simulium oyapockense* s.l. in the Amazon lowlands but is now recognized to be an autoimmune disease. The flaccid bullae are induced by IgG4 subclass antibodies. Another, more acute condition known as haemorrhagic syndrome of Altamira is probably caused by the bites of large numbers of *Simulium minusculum* in northern Brazil.



Fig 9.5 Collection of bladder stones.
Bladder stones are very common in children in Thailand, Indonesia and the Middle East. The aetiological factors involved include a low-milk–high-cereal diet, low urinary volume, high ambient temperature and ingestion of certain local vegetables and leaves of forest plants that have a high oxalate content. (Courtesy, Professor W. E. Farrar.)

Downloaded From Vet-eBooks.com





Fig 9.7 (A and B) Kanwa and peri-partum cardiac failure.
In northern Nigeria the practice of adding substantial quantities of sodium-rich lake salt ('kanwa') to food to promote the flow of breast milk (Fig. 9.7A), combined with the heating of the body by lying on a clay bed built over a fireplace to reduce susceptibility to infection (Fig. 9.7B), are believed to underlie the high rates of peri-partum cardiac failure reported. ((A) From Ford, L., Abdullahi, A., Anjorin, F. I. et al. The outcome of peripartum cardiac failure in Zaria, Nigeria. *The Quarterly Journal of Medicine*, 1998, Volume 91, Pages 93–103, Figure 1. Copyright © Oxford University Press. (B) Courtesy, Professor Sir E. Parry.)

Downloaded from Vet-eBooks.com

Index

A

Acanthamoeba keratitis, 122f
Acanthamoeba sp., trophozoite of, 122f
Achatina cantonensis, 199f–200f
Achatina fulica, 199f
Acrodermatitis chronica atrophicans, 35f
Acute hemorrhagic leukoencephalopathy, 58f
Acute meningococcemia, rash of, 252f
Acute pulmonary edema, in Hantavirus hemorrhagic fever with renal syndrome, 248f
Acute pulmonary tuberculosis, with cavitation, 261f
Acute renal failure, by *Vespa affinis*, 315f
Acute respiratory distress syndrome (ARDS)
  in scrub typhus, 27f
  in severe malaria, 43f
Acute rheumatic fever, 255f
Addison's disease, due to tuberculous adrenal involvement, gum hyperpigmentation in, 265f
Aedes, 2f–4f, 87f
Aerophobia, in rabies, 148f
Aflatoxin, 132f
African histoplasmosis, 277f
African 'killer bee,', 315
Age-standardized road injury disability-adjusted life year, change in, 338f
Age-standardized suicide rates, 341f
Ainhum, of small toe, 342f
Air bronchograms, right upper lobe consolidation with, 251f
Airborne infections, 244–281
Airway obstruction, diphtheria and, 254f
Albinism, sun protection for, 341f
Aleppo button. *see* Cutaneous leishmaniasis
Alveolar echinococcosis, 226–227, 226f–227f
Amastigotes, 63f, 66f, 79f
Amblyomma variegatum, 24f
Amnesic shellfish poisoning, 305f
Amoebae, 178f
Amoebiasis, of skin, 181f
Amoebic liver abscess, 180f
  aspiration of, 181f
Amoebic perforation, surgical resection and, 179f
'Anal lobes,', 297
Anaplasmosis, 22t
Ancylostoma caninum, in human ileum, 114f
Ancylostoma duodenale, 112f
  life cycle of, 113f
Ancylostoma spp. *see* Hookworms
Androctonus australis, 308f
Anemia
  due to hookworm, 114f
  malarial, 41f
  megaloblastic, 209f
  sickle cell, *Salmonella* osteomyelitis in, 171f
Aneurysm, apical, of heart, in Chagas disease, 65f
Angiostrongyliasis, 199–201
  ocular, 200f
Angiostrongylus cantonensis, 199f
Angiostrongylus costaricensis, 201f
Angular stomatitis, 328f
Anisakiasis, 192–193
  colonic, 193f
Anisakis, 192f
  larva of, 193f
Anisakis simplex, 192f
Anopheles, 2f–5f
Anthrax, cutaneous, 155f
  extensive erythema and hemorrhagic bullae in, 156f
Antibody-mediated immune complexes, 256f
Antitoxin, for diphtheria, 254f
Anus, squamous cell carcinoma of, HIV infection and, 136t–137t
Apis mellifera scutellata, 315f
Arboviruses. *see* Viral infections
Argemone mexicana, 321f
Ariboflavinosis, 328
Armillifer armillatus, 243f
Artemisia annua, 51f
Artesenal gold mining, mercury poisoning due to, 339f
Arthropod-borne diseases
  bacterial infections, 21–32
  parasitic infections, 35–108
  viral infections, 5–21, 6t
Ascariasis, 187
Ascaris lumbricoides, 187f–190f
Asian cobra, 319f
Atractaspididae, 317t
Atrax robustus, 309f
Auramine stain, 259f, 269f
Avian influenza infections, 244, 247f

B

Babesia
  B. divergens, 52f
  B. microti, 52f
Babesiosis, 52–53, 52f
Bacillary angiomatosis, 28f
  in HIV infection, 154f
Bacillary dysentery, due to shigellosis, 171f
Bacterial infections
  airborne, 253–256
  of gastrointestinal tract, 169–177

Note: Page numbers followed by "f" indicate figures, "t" indicate tables.

Downloaded From Vet-eBooks.com

Bacterial infections *(Continued)*
from sex, 137–143
from soil, 109–111
from water, 120–121
Bacterial pharyngitis, 255f
Bacterial pneumonias, 244
Baghdad boil. *see* Cutaneous leishmaniasis
Balamuthia, 122f
Balantidial ileitis, 184f
Balantidium coli, 178f, 184f
Bartonella, 28, 28f
Bartonella henselae
bacillary angiomatosis due to, 154f
HIV infection and, 136t–137t
Baylisascaris procyonis, 201, 201f
Bed bugs, 290
Beef tapeworm, 219–220
Bees, 315f
Bejel, 159f
Beri beri, 328f
infantile, 328
Betel nut, 340f
Bilateral dactylitis, 337f
Bilateral psoas abscess, 264f
Biomphalaria sp., as intermediate host of *Schistosoma mansoni*, 124f
Bites, 302–321
Bithynia funiculata, 231f
Bitot's spots, 326f
Bivalent oral polio vaccine, administration of, 166f
"Black enamel,", 325
Black flies. *see Simulium*
Black sickness. *see* Visceral leishmaniasis
Black widow spider, 311f
Blackwater fever, 43f
Bladder
Schistosoma haematobium, 128f
stones, 343f
Blindness, in trachoma, 157f
Blood film
babesiosis, 52f
Bartonella bacilliformis, 28f
Chagas disease, 63f
filariasis, 105f
human African trypanosomiasis, 56f
malaria, 39f–40f, 48f
preparation, 40f
tick-borne relapsing fever, 34f
Wuchereria bancrofti, 92f
Blood pathology
falciparum malaria, 43f
Lonomia achelous, 314f
viper bite, 319f
visceral leishmaniasis, 73f
Bone marrow aspirate, 74f
Borderline tuberculoid (BT) leprosy, 273f
Bordetella pertussis, 253f
Bossing, of skull, 337f
'Box' jellyfish, 302f
Brain pathology
Achatina cantonensis, 200f
alveolar echinococcosis, 227f
Baylisascaris procyonis, 201f
Chagas disease, 67f
Chikungunya, 13f
Congo-Crimean hemorrhagic fever, 21f
cystic echinococcosis, 225f
cysticercosis, 217f–219f
HIV infection, 135f
human African trypanosomiasis, 57f–59f
Japanese encephalitis, 18f
malaria, 41f–42f
paragonimiasis, 241f
rabies, 147f
toxoplasmosis, 183f–184f
tuberculosis, 266f–267f
West Nile virus, 16f
Zika virus, 14f
Brain stem, tuberculous involvement of, 267f
Brazilian wandering spiders, 312f
Brazilian yellow scorpion, 308f
Breast, tuberculosis of, 263f
Bronchioalveolar lavage specimen, middle east respiratory syndrome-coronavirus on, 246f
Brucella spondylitis, 177f
Brucella spp., 176f
Brucellosis
Rose Bengal test for, 176f
temperature chart in, 176f
Brugia
B. malayi, 84t–85t, 92f–93f
life cycle of, 88f
lymphedema in patient with, 91f
B. timori, 93f
abscess due to, 92f
Bubonic plague, 30f
Buffalo gnats. *see Simulium*
Bulinus sp., as intermediate host of *Schistosoma haematobium*, 124f
Bullae, hemorrhagic, in cutaneous anthrax, 156f
Burkholderia pseudomallei
melioidosis, 111f
suppurating parotid abscess due to, 111f
Burkitt's lymphoma, 333f
Burns
by *Epibolus pulchripes*, 313f
full thickness, 340f
Buruli ulcer, 154f
contractures from, 154f
plaque, 154f
Buthid scorpion, 308f
Butter clam, 305f

C

Calabar swelling, 97f
Calloselasma rhodostoma, 319f
Camels, 246f
Cancrum oris, 156f, 326f
Candida sp. infection, HIV infection and, 136t–137t
Candidiasis
esophageal, 160f
oral, white plaques of, 160f
Capillaria hepatica, 194f
Capillaria philippinensis, 193f–194f
Capillariasis, 193–194
Card agglutination test, for *Trypanosoma brucei gambiense*, 58f
Cardiac arrhythmias, diphtheria and, 254f
Cardiac failure, peri-partum, Kanwa and, 344f
Cardiomegaly, in Chagas disease, 65f
Carrión's disease, 28f
Carukia barnesii, 304f
Castleman's disease, multicentric, HIV infection and, 136t–137t
Cat scratch disease, 154f
Caterpillar, 313f
Cats, 183f, 213f, 231f
Centipedes, 312–316, 312f
Cercaria, 231f
Cercocyst, 211f
Cerebral atrophy, in HIV infection, 135f
Cerebral lymphoma, primary, HIV infection and, 136t–137t
Cerebral malaria, 41f–42f
Cerebral paragonimiasis, 241f
Cerebral toxoplasmosis, 184f
Cerebral tuberculosis, 267f
Cervical cancer
due to vaccine-preventable human papilloma virus infection, 134f
HIV infection and, 136t–137t
Cervical discharge, in gonorrhea, 141f
Cervical lymphadenopathy, 32f, 57f, 333f
Cervix, *Schistosoma haematobium* infection in, 129f
Cestodes, 207–227, 207t. *see also* Tapeworms
Chagas disease, 60–67, 63f
acquisition, risk factor for, 61f
distribution of, 60f
gastroesophageal manifestations of, 65f–66f

Downloaded From Vet-eBooks.com

Chagas disease *(Continued)*
heart block in, 64f
pericardial effusion in, 64f
reduction of, 67f
reservoir of, 61f
Chancre
primary, of syphilis, 138f
of *Trypanosoma brucei rhodesiense*, 56f
Chancroid
cutaneous, 160f
genital ulcers of, 137f
Cheilosis, 328f
Chemotherapy, lepromatous leprosy before, 269f
Cheyletiella parasitivorax, 287f
Chickenpox, primary manifestation of, 250f
Chiclero's ulcer, 82f
Chigger bites, to ankles, 288f
Chikungunya, 13, 13f
Chinese bamboo rat, 276f
'Ching-a,' 340
Chiracanthium lawrencei, 312f
Chironex fleckeri, 302f
geographic distribution of, 303f
Chlamydia trachomatis, pelvic inflammatory disease due to, 141f
Cholangiocarcinoma, *Clonorchis sinensis* causing, 234f
Cholera, 173f–175f
Cholera vibrios, 174f
Chromoblastomycosis, 162f
of hand, 163f
Chronic cryptococcal meningoencephalitis, 280f
Chronic eczematous scabies, 286f
Chronic rheumatic valvular disease, 255f
Chrysomya bezziana, 295f
Chrysops, 97f
Chyluria, 91f
Ciguatera poisoning, distribution map of, 306f
Ciguatoxin, 306
Cimex hemipterus, 290f
Cimex lectularius, 290f
Cinchona ledgeriana, 50f
Cirrhosis, liver, with *Schistosoma japonicum*, 130f
Clofazimine-induced discoloration, in leprosy, 272f
Clonorchis sinensis, 230f–234f
Clostridial necrotizing enteritis, 176f
Clostridium tetani, tetanus due to, 109f
Clubfoot, 339f
Cobra, 319f–320f
Cochliomyia hominivorax, 295f–296f
Coenurus cerebralis, 227f
Colon, *Oesophagostomum bifurcum* in, 119f
Colubridae, 317t
Community-based management of acute malnutrition (CMAM), 322
Condylomata lata, of secondary syphilis, 139f
Cone shells, 304f
Congenital toxoplasmosis
fundal changes in, 184f
hydrocephalus in, 183f–184f
Congo-Crimean hemorrhagic fever (CCHF), 19–21, 19f–21f
Conjunctiva
nodular disorder of, 261f
normal, 158f
Contractures, from Buruli ulcer, 154f
Conus marmoreus, 304f
Conus purpurascens, 304f
Cordylobia anthropophaga, 294, 297f–298f
Corneal opacity (CO), in trachomatous trichiasis, 158f
Corneal ulceration, 327f
Corona veneris, of secondary syphilis, 139f
Coronavirus, 245–246, 245f–246f
Corynebacterium diphtheriae, 254f
Coxiella burnetii, 256f
Cryptococcal antigen agglutination assays, 280f
Cryptococcal meningoencephalitis
in advanced HIV infection, 280f
chronic, 280f
Cryptococcosis, 276f
Cryptococcus gattii, 280f
Cryptococcus neoformans, 280f
in cerebrospinal fluid, 280f
Cryptococcus sp. infection, HIV infection and, 136t–137t
Cryptosporidium hominis, oocysts of, 182f
Cryptosporidium sp., 178f
HIV infection and, 136t–137t
CT scan
facial, of lepromatous leprosy, 270f
of tuberculosis, 263f
Ctenocephalides canis, 291f
Ctenocephalides felis, 214f, 291f
Ctenopharyngodon idella, 231f
Culex, 3f–4f, 86f
breeding grounds for, 87f
C. quinquefasciatus, 88f
Culicoides, 106f
Cutaneous diphtheria, healing, 255f
Cutaneous histoplasmosis, 277f
Cutaneous larva migrans ('creeping eruption'), due to larvae of animal hookworms, 114f
Cutaneous leishmaniasis, old world, 75–81
animal reservoirs of, 76f
distribution of, 75f, 81f
intralesional sodium stibogluconate for, 79f
invasive ulcerative lesion of, 78f
lymphatic spread of, 78f
mucocutaneous lesions in, 78f
multiple lesions in, 78f
noduloulcerative lesion of, 76f
punch biopsy for, 78f
spontaneous cure in, 77f
'wet' lesion of mouth in, 77f
Cutaneous streptococcal strains, 256f
Cutaneous talaromycosis, 276f
Cyclospora cayetanensis, 178f
oocysts of, 182f
Cyst
Pneumocystis, in bronchoalveolar lavage, 275f
protozoal, 178f
Cystic echinococcosis, 221f–225f
Cysticercosis, 216f–218f
in beef, 220f
fatal cerebral, 219f
subconjunctival, 218f
Cytomegalovirus (CMV) infection
esophagitis and, 144f
HIV infection and, 136t–137t
retinitis and, 144f

D

Dactylitis, 337f
Dapaong tumor, 119f
Dasypus novemcinctus, 61f
Deer mouse *(Peromyscus maniculatus)*, 248f
Demodex folliculorum, 287f
Dendrobates tinctorius, 316f
Dengue, 7–10, 7f–10f
Dental staining, Betel nut, 340f
Dermanyssus gallinae, 284f
Dermatitis
cercarial, 131f
onchocercal, 101f
Dermatobia hominis, 294, 298f–299f
Dermatophagoides, 284f
Dermatophagoides pteronyssinus, 284f
Descemetocele formation, 327f
Diarrhea, 169f. *see also* Cholera; Shigellosis
Dicrocoelium dendriticum, 237–238, 237f–238f
Didelphis species, 61f
Diffuse cutaneous leishmaniasis (DCL), 80f–82f
Diphtheria
healing cutaneous, 255f
patient with respiratory, pseudomembrane in, 254f

Downloaded From Vet-eBooks.com

Diphtheria, tetanus and pertussis (DTP), immunization coverage rates in infants, 254f
Diphyllobothriasis (fish tapeworm), 208–209
Diphyllobothrium latum, 208f–209f
Dipylidium caninum (dog tapeworm), 213–214, 213f–214f
Direct agglutination test (DAT), for visceral leishmaniasis, 75f
Direct microscopy with Gram stain, of cerebrospinal fluid, 253f
Dirofilaria
  D. immitis, 107f
  D. repens, 108f
Disability-adjusted life year (DALY), age-standardized road injury, change in, 338f
Diseases of unusual or uncertain etiology, 342–344
Disseminated intravascular coagulation, 31f, 43f
Disseminated visceral leishmaniasis, 73f
Dog tapeworm, 213–214
Dogs, 197f, 206f, 213f, 221f, 231f
  mass vaccination of, 147f
Domestic ducks, 246f
Donovan bodies, in exudate, 138f
Donovanosis, 138f
Dracunculiasis (Guinea worm), 204–206
Dracunculus medinensis, 206, 204f, 206f
  distribution of, 205f
  in dogs, 206f
Drug-resistant pulmonary tuberculosis, radiograph of, 261f
'Dry' beri beri, 328f
Dwarf tapeworm, 210–211
Dysentery. *see* Cholera; Shigellosis

E

Eastern equine encephalitis, 13f
Ebola virus disease (EVD)
  first documented outbreak of, 150f
  global chronology and scale of outbreaks of, 150f
  holding centre for, 151f
  ophthalmological complications of, 151f
  survivors of, 151f
  treatment centre for, 151f
Echinococcus granulosus, 221f–223f
Echinococcus vogeli, 227f
Echinostoma ilocanum, 230f
Echis ocellatus, 319f
Echocardiogram, of Q fever endocarditis, 256f
Ectoparasites, 282–301
  bed bugs, 290
  Cimex lectularius, 290f
  Cochliomyia hominivorax, 295f–296f
  Cordylobia anthropophaga, 298f
  Demodex folliculorum, 287f
  Dermanyssus gallinae, 284f
  Dermatobia hominis, 298f–299f
  fleas, 290–293
  lice, 288–289
  Lucilia sericata, 297f
  mites, 282t, 283–288
  myiasis, 294–301, 294t
  Neotrombicula autumnalis, 287, 287f
  papular urticaria, 291f
  Sarcoptes scabiei, 285f
  Thyreophagus entomophagus, 283f
  trombiculid mites, 283
  Tunga penetrans, 292f–293f. *see also* Mosquito vectors; *Simulium*
Eflornithine, for human African trypanosomiasis, 59f
Elapidae, 317t, 319f
Electron micrograph
  Ascaris lumbricoides, 188f
  Cholera vibrios, 174f
  Cimex hemipterus, 290f
  high-resolution scanning, of leptospires, 120f
  malaria, oocysts, 38f
  Plasmodium falciparum, 38f
    schizont rupture, 38f
  severe acute respiratory syndrome-coronavirus (SARS-CoV), 245f
Elephantiasis, 90f
Endemic goitre, 331f
Endemic mycoses, geographic distribution of, 276f
Endocarditis, Q fever, 256f
Endomyocardial fibrosis, 342f
Entamoeba histolytica, 178f–179f
  proctocolitis, 179f
Enteric fever
  multidrug resistant, source of, 170f
  rose spots in, 169f
Enteritis necrotica, 176f
Enterobiasis, 185–186
Enterobius vermicularis, 185f
  ovum of, 185f
Enterocytozoon bieneusi, 185f
Enterotoxigenic *Escherichia coli*, 172f
Enterovirus 71, 167f
Eosinophilia, helminthic migration associated with, 130f
Eosinophils, in cerebrospinal fluid, 200f
Epibolus pulchripes, 313f
Epidermophyton floccosum, tinea cruris due to, 161f
Epstein-Barr virus infection
  HIV infection and, 136t–137t
  incidence of, 334f
  oral hairy leukoplakia and, 143f
Erythema, 325f
  in cutaneous anthrax, 156f
Erythema chronicum migrans, 35f
Erythema nodosum leprosum (ENL), 274f
Escherichia coli, enterotoxigenic, 172f
Esophagitis
  candidal, 160f
  cytomegalovirus infection and, 144f
Espundia, 84f
Exanthem, of measles, 249f
Expanded programme of immunization (EPI), 322
Extensive pleuro-vertebral tuberculous disease, 263f
Eye pathology
  Acanthamoeba, 122f
  angiostrongyliasis, 200f
  Bordetella pertussis, 253f
  Chagas disease, 63f
  Congo-Crimean hemorrhagic fever, 21f
  cysticercosis, 218f
  cytomegalovirus, 144f
  Ebola virus disease, 151f
  Gnathostoma spinigerum, 203f
  Lassa fever, 152f
  leprosy, 272f
  Loa loa, 97f–98f
  malaria, 42f
  myiasis, 300f–301f
  Nairobi eye, 316f
  Neisseria meningitidis, 253f
  Oestrus ovis, 301f
  onchocerciasis, 104f
  phlyctenular conjunctivitis, 261f
  Rift Valley fever virus, 20f
  Taenia crassiceps, 227f
  tick-borne relapsing fever, 34f
  toxocariasis, 198f
  toxoplasmosis, 184f
  trachoma, 157f–158f
  trichinosis, 196f
  vitamin A deficiency, 326f–327f
Eyelids, papulo-pustular rash of monkeypox in, 146f

F

Facial lepromatous leprosy (LL), 270f
Facial muscle spasm, tetanus and, 110f
Facial nerve palsy, 200f
Facial swelling, in Lassa fever, 152f
Falciparum malaria, 40–44
Fasciola gigantica, 234f
Fasciola hepatica, 234f–236f

Downloaded From Vet-eBooks.com

Fasciola species, 234f, 237f
Fascioliasis, 234–237
Fasciolopsis buski, 228f–229f
'Feco-oral' transmission, 165
Filariases, 84–94
  microfilarial periodicity, 93f
  rapid serological diagnosis of, 94
  ultrasound of, 94f
Fire ant workers, 315f
Fish, poisonous, 306–307
Fish tapeworm, 208–209
Flagellates, 178f
Fleas, 290–293
Fluoroquinolone, resistance of *Mycobacterium tuberculosis* to, 261f
Fogo selvagem, 343f
Food security, 322
Foot
  Kaposi's sarcoma of, 334f
  malignant melanoma of, 335f
Formula milk feeding, perils of, 172f
Frank pneumonia, 253f
Frog, 209f
Full thickness burns, 340f
Fungal infections
  airborne, 275–281
  of gastrointestinal tract, 185
Fungi, environmental, universal distribution of, 245

G

Galba truncatula, 235f
Gambierdiscus toxicus, 306
Gangrene
  in septicemic plague, 31f
  in severe epidemic typhus, 23f
Gastrointestinal tract infections, 165–243
  bacterial, 169–177
  fungi, 185
  helminth, 185–242
  protozoal, 178–184, 178f
  viral, 165–169
Genetic blood dyscrasias, 333
Genital ulcers, of chancroid, 137f
Genital warts, due to human papilloma virus infection, 133f
Geohelminth infection, ecology of, 114f
Giardia intestinalis, 178f, 181f
  villous atrophy and, 181f
Gingivostomatitis, ulcerative, HSV-1 and, 143f
Global Trachoma Mapping Project (GTMP), 157f
Glomerular microscopy, for acute post-streptococcal glomerulonephritis, 256f
Glomerulonephritis, 255f–256f
  acute post-streptococcal, 256f
Glossina morsitans, 54f
Gnathostoma nipponicum, 201f
Gnathostoma spinigerum, 201f–203f
  periorbital larva migrans, 202f
Gnathostomiasis, 201–203
  intracerebral, 203f
Gold mining, artesenal, mercury poisoning due to, 339f
Gonorrhea
  cervical discharge in, 141f
  urethral discharge in, 140f
Granuloma inguinale, 138f
Greater blue-ringed octopus, 305f
Guinea worm, 204–206
Gum hyperpigmentation, in Addison's disease due to tuberculous adrenal involvement, 265f
Gynecomastia, in leprosy, 271f

H

Haemagogus, 11f
Haemophilus ducreyi, as cause of genital ulcers, 137f
Hairy leukoplakia, oral, 143f
Halzoun syndrome, 242f
Hand
  chromoblastomycosis of, 163f
  Kaposi's sarcoma in, 334f
Hand-foot syndrome, 337f
'Hanging groin,' 102
Hantavirus pulmonary syndrome (HPS), 248f
Hantaviruses, 248, 248f
Hapalochlaena fasciata, 305f
Hapalochlaena lunulata, 305f
'Harvest mites,' 287
Heart pathology
  Chagas disease, 64f–65f
  diphtheria, 254f
  endomyocardial fibrosis, 342f
  Kanwa, 344f
  Q fever, 256f
  rheumatic heart disease, 255f
  tuberculous pericarditis, 262f
Helicobacter pylori, 175f
Helminth infections
  ecology of, 114f
  of gastrointestinal tract, 185–242
  from soil, 112–119
  from water, 123–131
Helminthic migration, associated with eosinophilia, 130f
Hemiscorpius lepturus, 308f–309f
Hemoglobinopathies, 336f
Hemorrhagic fever with renal syndrome (HFRS), 248f
  hantavirus, acute pulmonary edema in, 248f
Henipaviruses, 247, 247f
Hepatitis A virus, 167f
  acute infection of, course of, 168f
  panlobular inflammation and lobular disarray due to, 168f
Hepatitis B
  chronic, hepatoma due to, 132f
  global epidemiology of, 133f
Hepatitis C infection
  global epidemiology of, 145f
  vasculitis in, 145f
Hepatitis E, brachial neuritis in, 168f
Hepatoma, due to chronic hepatitis B, 132f
Hepatosplenomegaly
  congenital syphilis, 140f
  paracoccidioidomycosis, 278
  schistosomiasis, 127f, 129f
  visceral leishmaniasis, 72f
Herpes B virus infection, 153f
Herpes simplex virus (HSV) infection
  HIV infection and, 136t–137t
  type 1 (HSV-1), ulcerative gingivostomatitis and, 143f
  type 2 (HSV-2), 132f
    in HIV infection, 132f
Histoplasma capsulatum, 277f
  HIV infection and, 136t–137t
Histoplasma duboisii, 277f
Histoplasmosis
  African, 277f
  cutaneous, 277f
  dissemination of, 276f
HIV infection, 135f
  acute, 135f
  bacillary angiomatosis in, 154f
  cerebral atrophy in, 135f
  cerebral toxoplasmosis in, 184f
  global epidemiology of, 134f
  herpes simplex virus type 2 in, 132f
  molluscum contagiosum in, 144f
  opportunistic infections and neoplastic disorders associated with, 136t–137t
  point of care lateral flow assay for, 140f
Holding centre, for Ebola virus disease, 151f
Hookworms
  anemia due to, 114f
  cutaneous larva migrans due to larvae, 114f
  eggs of, 118f
  estimated global burden of, 112f
Hornets, 315f
HTLV-1 infection
  global distribution of, 148f
  myelopathy associated with, 149f
  T cell lymphoma associated with, 149f
  uveitis associated with, 149f

Downloaded From Vet-eBooks.com

Human African trypanosomiasis, 53–60, 55f, 58f
control of, 60f
distribution of, 53f
life cycle of, 55f
morula cells, 59f
neurological dysfunction in, 57f
'Human flea,' 291
Human papilloma virus (HPV) infection
genital warts due to, 133f
vaccine-preventable, cervical cancer due to, 134f
Hunger map, 322f
Hyalomma marginatum rufipes, 20f
Hydrocele, 90f
Hydrophiidae, 317t
Hylesia metabus, 313f
Hylesia paulex, 313f
Hymenolepis diminuta (rat tapeworm), 212, 212f
cysticercoid of, 212f
Hymenolepis nana (dwarf tapeworm), 210–211, 210f–211f
Hyper-reactive malarial splenomegaly (HMS), 48f
Hyperkeratotic ('Norwegian') scabies, 286f
Hypersensitivity skin test for mites, 284f

I

Ileitis, balantidial, 184f
Ileum, adult *Ancylostoma caninum* in, 114f
Immunization, diphtheria, tetanus and pertussis (DTP), 254f
Inactivated polio vaccine, administration of, 166f
Indirect immunofluorescent antibody stain, 246f
Infantile beri beri, 328
Infantile rickets, 330f
Infants, DTP immunization coverage rates in, 254f
Infections acquired percutaneously, 109–164
Inflammatory disease, pelvic, due to *Chlamydia trachomatis* infection, 141f
Influenza viruses, 246–247, 246f–247f
Inoculation mycobacteriosis, at site of insulin injection, 155f
Insects, 312–316
Interburns, 340f
Interferon-gamma release assays (IGRAs), 259f
Intestinal flukes, 228–230
Intraabdominal hydatid, 225f
Invasive rhinocerebral mucormycosis, 281f
Invertebrates
marine, 302–305
terrestrial, 308–316
Iodine deficiency, 330–331, 331f
Irukandji syndrome, 304f
Isoniazid, resistance of *Mycobacterium tuberculosis* to, 261f
Isospora belli, 178f, 182f
Isospora sp. infection, HIV infection and, 136t–137t
Ivermectin, for onchocerciasis, 105f
Ixodes scapularis, 53f

J

Japanese encephalitis, 15–18, 15f, 17f–18f
Jaundice, 43f
JC virus, 169f
HIV infection and, 136t–137t
Jejunal mucosa, sections of parasitic female and eggs embedded in, 117f
Jigger flea, 292f–293f

K

K39 rapid diagnostic test, for visceral leishmaniasis, 75f
Kanwa, peri-partum cardiac failure and, 344f
Kaposi's sarcoma, 334f
HIV infection and, 136t–137t
Katayama fever, 130f
Keratitis, *Acanthamoeba*, 122f
Keratomalacia, 327f
to descemetocele formation, 327f
Kidney pathology
acute post-streptococcal glomerulonephritis, 256f
Quartan nephropathy, 47f–48f
Kitfo, 220f
Klebsiella granulomatis, donovanosis and, 138f
Koi pla, 193f
Konzo, 332, 332f
Koplik's spots, 249f
Kwashiorkor, 325f
skin changes in, 325f

L

Lanceolate (lancet-blade shaped) pneumococci, 252f
Langhans giant cells, 266f
Larva migrans, 198f, 201f–202f, 237f
Lassa fever
distribution of, 152f
facial swelling and subconjunctival hemorrhage in, 152f
rodent reservoir, 152f
Latrodectus mactans, 311f
Leishman-Donovan bodies. *see* Amastigotes
Leishmania
HIV infection and, 136t–137t
L. amazonensis, 82f
L. braziliensis, 83f
L. infantum, 74f
L. mexicana, 82f
L. tropica, 80f
life cycle of, 68f
Leishmaniasis, 68–84, 70f
mucocutaneous, 80f, 83f
destructive, 84f
nasal lesion, 83f
nasal septum, destruction of, 83f
old world cutaneous, 75–81
animal reservoirs of, 76f
distribution of, 75f, 81f
intralesional sodium stibogluconate for, 79f
invasive ulcerative lesion of, 78f
lymphatic spread of, 78f
mucocutaneous lesions in, 78f
multiple lesions in, 78f
noduloulcerative lesion of, 76f
punch biopsy for, 78f
spontaneous cure in, 77f
'wet' lesion of mouth in, 77f
pharyngeal involvement in, 84f
recidivans, 80f
reservoir of, 80f
visceral, 71–75
direct agglutination test for, 75f
distribution of, 71f
endemic area with, 71f–72f
HIV and, 73f
infantile, 72f
K39 rapid diagnostic test for, 75f
purpura in, 73f
reservoir of, 72f
'Leonine facies,' 103
in lepromatous leprosy, 270f
Leopard skin, 102f
Lepromatous leprosy (LL), 269f
before chemotherapy, 269f
cutaneous manifestations of, 270f
facial, 270f
histology of
nerve bundles in, 271f
skin in, 270f
Lucio's phenomenon, 274f
mucosal infiltration and septal destruction in, 270f
neuropathic pathology in, 271f
Ziehl-Neelsen staining of, 271f
Leprosy, 268, 268–274
clofazimine-induced discoloration in, 272f
global distribution of, 268f
gynecomastia in, 271f
ocular involvement in, 272f
spectrum of immunological response to, 269f

Downloaded From Vet-eBooks.com

Leptospires, high-resolution scanning electron microscopy of, 120f
Leptospirosis
environment characterized by hyperendemic, 120f
hepatic changes in, 121f
pulmonary involvement in, 121f
Leukoplakia, oral hairy, 143f
Lice, 288–289
Life cycles
Ancylostoma duodenale, 113f
Angiostrongylus cantonensis, 199f
Ascaris lumbricoides, 187f
Brugia malayi, 88f
Clonorchis sinensis, 231f
Dicrocoelium dendriticum, 237f
Diphyllobothrium latum, 208f
Dipylidium caninum, 213f
Dracunculus medinensis, 204f
Echinococcus granulosus, 221f
Fasciola species, 234f
Fasciolopsis buski, 228f
human African trypanosomiasis, 55f
Hymenolepis nana, 210f
Leishmania, 68f
Loa loa, 96f
malaria, 37f–38f
mosquito, 2f
Necator americanus, 113f
Onchocerca volvulus, 100f
Opisthorchis felineus, 231f
Opisthorchis viverrini, 231f
Paragonimus species, 239f
schistosomes, 123f
Strongyloides stercoralis, 116f
Taenia solium, 215f
Toxocara canis, 197f
Toxoplasma gondii, 183f
Trichinella spiralis, 195f
Trichuris trichiura, 190f
Trypanosoma cruzi, 62f
Wuchereria bancrofti, 88f
Linguatula serrata, 242f
Liponyssoides sanguineus, 26f
Lips, papulo-pustular rash of monkeypox in, 146f
Liver flukes, 230–238, 230f
Liver pathology
amoebic abscess, 180f–181f
ascariasis, 190f
Clonorchis sinensis, 233f–234f
cystic echinococcosis, 222f–224f
Echinococcus vogeli, 227f
fascioliasis, 236f
hepatitis, 168f
hepatoma, 132f
leishmaniasis, 72f
leptospirosis, 121f
malaria, 49f
Liver pathology *(Continued)*
schistosomiasis, 127f, 129f–130f
yellow fever, 12f
Loa loa, 95–98, 98f
distribution of, 95f
life cycle of, 96f
microfilaria of, 97f
subconjunctival, 97f–98f
Lobar pneumonia, 251f
Lobo's disease, 163f
Loeffler syndrome, 189f
Longstanding podoconiosis, nodular appearance of, 338f
Lonomia achelous, 314f
Low cost oral morphine solution, 335f
Lowenstein-Jensen medium, 260f
Loxosceles laeta, 310f
Loxosceles reclusa, 310f–311f
Loxoscelism, 310f
Lucilia sericata, 297f
Lucio's phenomenon, 274f
Lumbar puncture, 59f
Lung fluke, 239f
Lung pathology
ascariasis, 189f
avian influenza, 247f
cystic echinococcosis, 225f
lobar pneumonia, 251f
malaria, 43f
paracoccidioidomycosis, 279, 278f
paragonimiasis, 240f–241f
pneumonic plague, 31f–32f
Q fever, 256f
scrub typhus, 27f
severe acute respiratory syndrome, 245f
toxocariasis, 198f
tuberculosis, 261f–262f
Lutzomyia longipalpis, 69f
larvae of, 69f
male, 70f
pupa of, 69f
Lyme disease, 35, 35f
Bell's palsy lesion in, 35f
Lymphadenopathy
axillary and supraclavicular, 261f
inguinal and femoral, of monkeypox, 146f
Lymphangitis, in filariasis, 89f
Lymphatic filariasis
cellulitis in, 90f
distribution of, 85f
Lymphedema, filarial, 89f, 91f
Lymphogranuloma venereum (LGV), 142f
proctitis, 142f
Lymphoma, tuberculous cervical lymphadenitis *versus*, 262f

M

Macrolide, for diphtheria, 254f
Madura foot, 163f
Magnetic resonance imaging, of spondylodiscitis, 264f
Malaria, 36–52, 39f–40f
chronic complications of, 48–50, 48f–50f
distribution of, 36f
life cycle of, 37f–38f
treatment of, 50–52, 50f–52f
Malayan pit viper, 319f
Malignant melanoma, 335f
Malnutrition, 325–326, 325f–326f
Mammogram, filarial worms in, 91f
Mango fly. *see Cordylobia anthropophaga*
Mansonella, 105–108, 105f–107f
Mansonia, 86f–87f
Mantoux, 259f
Maps of distribution
alveolar echinococcosis, 226f
Chagas disease, 60f
Chironex fleckeri, 303f
ciguatera poisoning, 306f
Congo-Crimean hemorrhagic fever, 19f
cutaneous leishmaniasis, 75f, 81f
cystic echinococcosis, 221f
dengue, 7f
Dracunculus medinensis, 205f
endemic mycoses, 276f
hemoglobinopathies, 336f
HTLV-1 infection, 148f
human African trypanosomiasis, 53f
Japanese encephalitis, 15f
Lassa fever, 152f
leprosy, 268f
liver flukes, 230f
Loa loa, 95f
lymphatic filariasis, 85f
malaria, 36f
meningococcal meningitis belt, 252f
onchocerciasis, 98f
paragonimiasis, 238f
plague, 29f
Rift Valley fever virus, 19f
schistosomiasis, 126f
scrub typhus, 26f
strongyloidiasis, 115f
Taenia solium, 216f
tuberculosis, 258f
visceral leishmaniasis, 71f
West Nile virus, 15f
yellow fever, 11f
Marasmus, 325f
Marburg virus
rash from, 153f
transmission of, 153f

Downloaded From Vet-eBooks.com

Marine invertebrates, 302–305
Marine vertebrates, 306–307
Masked palm civet *(Panguma larvata)*, 245f
Mastomys natalensis, as reservoir of Lassa fever, 152f
Maxillary tumor, at autopsy, 333f
Measles, 249–250, 250f
  in twins, 249f
  typical exanthem of, 249f
Meat, inspection of, 220f
Megaloblastic anemia, 209f
Melioidosis
  Burkholderia pseudomallei as cause of, 111f
  pneumonia due to, 111f
Meningitis
  meningococcal, 253f
  pneumococcal, 252f
  tuberculous, 266f–267f
Meningococcal infection, 252–253
Meningococcal meningitis, 253f
Meningococcal meningitis belt, in Africa, 252f
Meningococcal septicemia, 252f
Meningococcemia, 253f
  acute, rash of, 252f
Meningoencephalitis
  cryptococcal
    in advanced HIV infection, 280f
    chronic, 280f
  primary amoebic, associated with bathing, warning signs indicating risk of, 122f
Mental health problems, 340f
Mercury poisoning, due to artesenal gold mining, 339f
Metacercaria, 229f, 232f, 240f
Metagonimus yokogawai, 229f
Mexican prickly poppy, 321f
Microfilaria, in skin biopsy, 101f
Microfilarial periodicity, 93f
Microsporidia, HIV infection and, 136t–137t
Mid-upper arm circumference (MUAC), measuring, 325f
Middle East respiratory syndrome-coronavirus (MERS-CoV), 246
  on bronchioalveolar lavage specimen, 246f
  reservoir of, 246f
Migratory waterfowl, 246f
Millipedes, 312–316
Miracidia, 235f
Mites, 282t, 283–288
Mitral valve, rheumatic heart disease of, 255f
Molluscum contagiosum, HIV infection and, 136t–137t, 144f
Monkeypox
  inguinal and femoral lymphadenopathy of, 146f
  papulo-pustular rash of, 146f
Morbilliform rash, 249f
Morphine solution, low cost oral, 335f
Morula cells, 59f
Mosquito vectors, 1–5, 2f
  Aedes, 2f–4f, 87f
  Anopheles, 2f–5f
  Culex, 3f–4f
  Haemagogus, 11f
  Mansonia, 86f–87f
  Stegomyia, 87f
'Mossy foot,' 338
Moths, 313f
Mucocutaneous leishmaniasis, 80f, 83f
  destructive, 84f
Mucocutaneous lesions, in paracoccidioidomycosis, 164f, 278f
Mucor, 281f
  surgical wound infection with, 281f
  typical appearance of, 281f
Mucosal infiltration, in lepromatous leprosy, 270f
Multi-dermatomal dissemination, 250f
Multi-drug-resistant tuberculosis, 258f, 261f
Multidrug treatment (MDT), 268
Murine typhus, 24f
Muscle spasm, facial, tetanus and, 110f
Mussels, 305f
Mycetoma, 163f
  fungal grains discharging in, 164f
Mycobacterium avium intracellulare infection, HIV infection and, 136t–137t
Mycobacterium leprae, 268f
  bacilli, 269f
  HIV infection and, 136t–137t
Mycobacterium marinum infection, 155f
Mycobacterium tuberculosis, 263f
  bacilli of, 267f
  culture of, 259f
    in liquid medium, 260f
  growing on solid medium, 260f
  HIV infection and, 136t–137t
  purulent necrotic material cultured, 263f
  rapid molecular testing for, 260f
  in sputum, 259f
  stereotactic biopsy confirmed, 267f
Mycobacterium ulcerans
  as causative agent of Buruli ulcer, 154f
  environment of, 155f
Mycotic aneurysm, salmonella, 171f
Myelopathy, HTLV-1 associated, 149f
Myiasis, 294–301, 294t
Myoglobinuria, by rattlesnake bite, 320f

N

Naegleria fowleri, trophozoite of, 121f
Nairobi eye, by *Paederus sabaeus*, 316f
Naja kaouthia, 319f
Nasal lesions, in paracoccidioidomycosis, 278
Nasopharyngeal carcinoma, incidence of, 334f
Necator americanus, life cycle of, 113f
Necrotizing cutaneous vasculitis, 274f
Necrotizing ulcerative stomatitis, 326f
Negri bodies, in rabies, 147f
Neisseria gonorrhoea
  as cause of urethral discharge, 140f
  congenital infection with, 141f
Neisseria meningitidis, 253f
Nematodes, 84–94
Neotricula aperta, as intermediate host of *Schistosoma mekongi*, 125f
Neotrombicula autumnalis, 287f
Nerve paralysis, diphtheria and, 254f
Nervous system
  beri beri, 328f
  leprosy, 271f, 273f
  polio, 167f
  rabies, 148f
  snake bite, 320f
Neurocysticercosis, 217f–218f
Neutrophil polymorphs, 252f
Niacin deficiency, 328–329, 329f
Nipah virus, reservoir of, 247f
Nodding syndrome, 105f
Noma, 326f
Non-communicable disease, 333
Non-Hodgkins lymphoma, HIV infection and, 136t–137t
North American hantavirus, 248f
Nutrition, 322–332
  malnutrition, 325–326, 325f–326f
  toxin ingestion and susceptibility, 332, 332f
  vitamin and mineral deficiencies, 326–331
    iodine deficiency, 330–331, 331f
    vitamin A deficiency, 326–327, 326f–327f
    vitamin B1 (thiamine) deficiency, 328, 328f
    vitamin B2 (riboflavin) deficiency, 328, 328f
    vitamin B3 (niacin) deficiency, 328–329, 329f
    vitamin C deficiency, 329, 329f
    vitamin D deficiency, 330, 330f

Downloaded From Vet-eBooks.com

O

Obesity map, 323f–324f
Octopus, 305f
Oculocutaneous albinism, 341f
Oesophagostomum bifurcum, in human colon, 119f
Oesophagostomum sp., in human appendix, 119f
Oestrus ovis (sheep nasal bot fly), 301f
Omental tuberculosis, 263f
Onchocerca volvulus, 100f–101f
  microfilariae of, 103f
Onchocercal dermatitis, 101f
Onchocerciasis, 98–105
  corneal involvement in, 104f
  distribution of, 98f
  nodules in, 104f
  social cost of, 104f
  transmission of, 99f
Oncomelania sp., as intermediate host of *Schistosoma japonicum*, 124f
Ophiocordyseps sinensis, 231f–232f
Ophthalmia neonatorum, 141f
Ophthalmomyiasis, 300f–301f
Opisthorchis felineus, 230f–232f
Opisthorchis viverrini, 230f–232f
Opisthotonos, in tetanus, 110f
Opportunistic infections and neoplastic disorders, HIV-associated, 136t–137t
Optic atrophy, in onchocerciasis, 104f
Oral hairy leukoplakia (OHL), 143f
Oriental sore. *see* Cutaneous leishmaniasis
Ornithodoros moubata, 33f–34f
Ornithonyssus bacoti, 283f
Ornithonyssus bursa, 284f
Oroya fever, 28f, 171f
Osteomalacia, 330f
Osteomyelitis, *Salmonella*, sickle cell anemia and, 171f

P

Paederus fusca, 316f
Pancytopenia, 73f
Panguma larvata, 245f
Papular urticaria, 291f
Paracoccidioides brasiliensis, 278f–280f
  paracoccidioidomycosis due to, 164f
  'pilot wheel' appearance of, 164
Paracoccidioidomycosis, 279f
  HIV infection and, 136t–137t
  mucocutaneous lesions in, 164f, 278f
  nasal lesions in
  pseudotumoral form of, 278f
  pulmonary, radiograph of, 278f
  pulmonary disease in
Paragonimiasis, 238–241, 238f, 240f–241f
Paragonimus heterotremus, 239f
Paragonimus kellicotti, 240f
Paragonimus pulmonalis, 240f
Paragonimus species, 239f
Paragonimus westermani, 240f
Paralytic shellfish poisoning, 305f
Pararama, 314f
Parotid abscess, suppurating, due to *Burkholderia pseudomallei*, 111f
Paucibacillary disease, 269f
Paucibacillary leprosy, 272f
Pediculus corporis, 23f
Pediculus humanus capitis infestation, 288f
Pediculus humanus corporis, 288, 289f
"Peeling paint" skin, 325f
Pellagra, 328, 329f
Pemphigus foliaceus, 343f
Penicillin, for diphtheria, 254f
Penicilliosis, in HIV, 276f
Penicillium, 276f
Pentastomiasis, 242–243
Peri-partum cardiac failure, Kanwa and, 344f
Pericardial effusion, in Chagas disease, 64f
Pericarditis, tuberculous, 262f
Peritoneal tuberculosis, 263f
Perleche, 328f
Pertussis, 253f
Petechiae, non-blanching, 252f
Peyer's patches, ulceration of, 170f
Pharyngitis, bacterial, 255f
Phlebotomus papatasi, 76f
Phlyctenular conjunctivitis, 261f
Phoneutria, 312f
Phrynoderma, 327f
Physalia physalis, 304f
Pian bois, 82f
Piedra
  black, 162f
  white, 162f
Piedraia hortae, black piedra due to, 162f
Pigbel, 176f
Pigs, 195f, 215f, 228f
'Pilot wheel' appearance, of *Paracoccidioides brasiliensis*, 279
Pinta, 160f
Pinworms, 186f
  sellotape test for, 186f
'Pipestem' fibrosis, periportal, 127f
Pityriasis versicolor, 161f
PKDL. *see* Post kala-azar dermal leishmaniasis
Placenta, malaria in, 50f
Plague, 29–32, 29f–30f, 32f
  bubonic, 30f
  pneumonic, 31f–32f
  septicemic, 31f
Plasmodium falciparum, 40–44, 40f–41f, 43f–44f
Plasmodium knowlesi, 48, 48f
Plasmodium malariae, 47–48, 47f–48f
Plasmodium ovale, 46, 46f
Plasmodium sp. infection, HIV infection and, 136t–137t
Plasmodium vivax, 45–46, 45f–46f
Plerocercoid, in fish, 209f
Plombage, left upper zone, chest radiograph with, 268f
Plumpynut, 325f
Pneumococcal infection, 251–252
Pneumococcal meningitis, 252f
Pneumocystis cysts, in bronchoalveolar lavage, 275f
Pneumocystis jirovecii, 275f
  HIV infection and, 136t–137t
Pneumocystis pneumonia, 275f
Pneumonia, 244
  due to melioidosis, 111f
  hemorrhagic, in disseminated *Strongyloides stercoralis* infection, 117f
  lobar, 251f
  Q fever, 256f
Pneumonic plague, 31f–32f
Pneumonitis, varicella zoster virus, 251f
Podoconiosis, 338f
Point of care (POC) lateral flow assay, for syphilis and HIV, 140f
Poisonous fish, 306–307
Polar bear, 196f
Polio
  flaccid paralysis due to, 167f
  shrinking global map of, 166f
Poliomyelitis virus, 165f
Polymerase chain reaction test, for *M. tuberculosis*, 260f
Pork tapeworm, 215–219
Porocephalus crotali, 242f
Post kala-azar dermal leishmaniasis (PKDL), 73f–74f
Post-streptococcal glomerulonephritis, acute, 256f
Postinfective malabsorption syndrome, 342f
Pott's disease, 265f
Poultry, raw, 246f
Premolis semirufa, 314f
Primary cerebral lymphoma, HIV infection and, 136t–137t
Proctitis, lymphogranuloma venereum, 142f
Proglottids
  of *Dipylidium caninum*, 214f
  of *Hymenolepis nana*, 211f
  of *Taenia saginata*, 219f
  of *Taenia solium*, 215f–216f

Downloaded From Vet-eBooks.com

Progressive multifocal leukoencephalopathy (PML), 169f
Promastigotes, 74f
Protein energy malnutrition (PEM), 325f
Protozoal infections
of gastrointestinal tract, 178–184, 178f
from sex, 142–143
from water, 121–123
Pseudomembrane, respiratory diphtheria and, 254f
Psoas abscess
bilateral, 264f
spondylodiscitis and, 264f
tuberculous, 264f
Psychosis, shackles for, 340f
Pteropus fruit bat (flying fox), 247f
Pthirus pubis, 289f
Ptosis, due to elapid bite, 320f
Puffer fish poisoning, 306, 307f
Pulex irritans, 291f
Pulmonary disease, in paracoccidioidomycosis
Pulmonary involvement, in leptospirosis, 121f
Pulmonary paracoccidioidomycosis, radiograph of, 278f
Pulmonary tuberculosis, acute, 261f
Purified protein derivative (PPD), 259f
Putzi fly. *see Cordylobia anthropophaga*
Pyomyositis, tropical, 156f

Q

Q fever
endocarditis, 256f
pneumonia, 256f
Quartan nephropathy, 47f–48f
Quinine, 50f

R

Rabies
aerophobia in, 148f
clinical, 147f
demonstration of, 147f
Negri bodies in, 147f
vaccination of dogs due to, 147f
Radiograph
chest
avian influenza, 247f
lobar pneumonia, 251f
Q fever pneumonia, 256f
tuberculosis, 261f–262f, 266f, 268f
Chrysomya bezziana, 294f
drug-resistant pulmonary tuberculosis, 261f
pulmonary paracoccidioidomycosis, 278f
Ranguna smithiana, 239f
Rapid molecular testing, for *Mycobacterium tuberculosis*, 260f
Rash
of acute meningococcemia, 252f
from Marburg virus disease, 153f
papulo-pustular, of monkeypox, 146f
of secondary syphilis, 139f
Rat bite fever, 156f
Rat tapeworm, 212
Rattlesnake bite, 320f
Ready-to-use therapeutic food (RUTF), 322
Redia, 235f
Relapsing fever, 33–35
tick-borne, 33–34
Respiratory diphtheria, patient with, pseudomembrane in, 254f
Retinitis, cytomegalovirus infection and, 144f
Rhabditiform larva, of *Strongyloides stercoralis*, 117f
Rhesus macaque, as carrier of herpes B virus, 153f
Rheumatic fever, 255f
Rheumatic heart disease, of mitral valve, 255f
Rhinosporidiosis, 123f
friable vascular polyp of *Rhinosporidis seeberi*, rhinosporidiosis due to, 123f
Riboflavin deficiency, 328, 328f
Rickets, 330, 330f
Rickettsia, 21, 22t
R. akari, 25f
R. prowazekii, 23f
R. sibirica, 25f
Rickettsia slovaca, 25f
Rickety rosary, 330f
Rifampicin resistance, tuberculosis and, 258f, 261f
Rift Valley fever virus (RFVF), 19–21, 19f–20f
Right lower zone consolidation, 262f
Risus sardonicus, in tetanus, 110f
Road injury disability-adjusted life year, changes in age-standardized, 338f
Rocky Mountain spotted fever, 24f
Romaña's sign, 63f
Rose spots, in enteric fever, 169f
Ross River virus, 13f
Rotavirus, 169f

S

Sac spiders, 312f
SAFE strategy, 157f
Salmonella
bacteremia, in malaria, 44f
mycotic aneurysm, 171f
Salmonella (Continued)
non-typhoidal, HIV infection and, 136t–137t
osteomyelitis, sickle cell anemia and, 171f
Sandfly bites, 70f
Sarcocyst, in human muscle, 182f
Sarcocystis, oocytes of, 181f
Sarcophaga species, 299f
Sarcoptes scabiei, 285f
SARS. *see* Severe acute respiratory syndrome
Saxidomus gigantea, 305f
Scabies, 285f–287f
lesions, 285f
mites, 285f
Schistosoma haematobium
in cervix, 129f
distribution of, 126f
ecology of, 128f
granulomatous inflammation in bladder wall, 128f
snail intermediate host of, 124f
Schistosoma intercalatum
distribution of, 126f
eggs of, 131f
Schistosoma japonicum
distribution of, 126f
ecology of, 130f
eggs of, 131f
liver cirrhosis with, 130f
snail intermediate host of, 124f
spinal involvement with, 129f
Schistosoma mansoni
adult, 124f
distribution of, 126f
ecology of, 126f
egg granuloma of, 127f
gastrointestinal disease due to, 128f
hepatosplenomegaly due to, 127f
male and female, 124f
snail intermediate host of, 124f
snail shedding bifurcate cercaria of, 125f
Schistosoma mekongi
distribution of, 126f
ecology of, 130f
eggs of, 131f
snail intermediate host of, 125f
Schistosomes, life cycle of, 123f
Schistosomiasis
hepatic, pathological lesion of, 127f
hepatosplenomegaly and, 129f
spinal, 129f
transmission of, 126f
Scolex
of *Dipylidium caninum*, 213f
of *Hymenolepis nana*, 211f
of *Taenia saginata*, 219f
of *Taenia solium*, 215f
Scombroid toxin poisoning, 306, 307f

Downloaded From Vet-eBooks.com

Scorpions, 308–309
Screw worm, 295f–296f
Scrotal elephantiasis, 102f
Scrub typhus, 22t, 26–28, 26f–28f
Scurvy, 329, 329f
'Sea wasp,' 302
  geographic distribution of, 303f
Secondary syphilis
  condylomata lata of, 139f
  corona veneris of, 139f
  extensive rash of, 139f
Segmentina hemisphaerula, 228f
Septal destruction, in lepromatous leprosy, 270f
Septicemia, meningococcal, 252f
Septicemic plague, 31f
Severe acute respiratory syndrome (SARS), 244
  lung changes in, 245f
Severe acute respiratory syndrome-coronavirus (SARS-CoV), 245f
  lung changes in, 245f
  reservoir of, 245f
Severe hemorrhagic syndrome, 314f
Sex, infections acquired percutaneously from, 132–135
  bacterial, 137–143
  protozoal, 142–143
  viral, 132–135
Shackles, for psychosis, 340f
Sheep nasal bot fly *(Oestrus ovis)*, 301f
Shellfish, 305f
Shigella dysenteriae, toxic megacolon due to, 171f
Shigellosis, 171f
  affecting sigmoid colon, 172f
Shingles, vesicular monodermatomal eruption of, 250f
Sickle cell anemia, *Salmonella* osteomyelitis in, 171f
Sickle-cell disease, 337f
Simulium, 99f, 105f
  larvae, 99f
  S. damnosum, 99f
Sin Nombre virus, 248f
Skin
  amoebiasis, 181f
  anthrax, 155f–156f
  Bartonella henselae, 154f
  bees, 315f
  biopsy, 78f
  chancroid, 160f
  chickenpox, 250f
  Chironex fleckeri, 302f
  Congo-Crimean hemorrhagic fever, 20f
  Epibolus pulchripes, 313f
  Fogo selvagem, 343f
  histoplasmosis, 277f
  hookworms, 114f
Skin *(Continued)*
  hornets, 315f
  kwashiorkor, 325f
  leishmaniasis, 76f, 78f
  lepromatous leprosy, 269f–270f
  lice, 288–289
  Lyme disease, 35f
  Marburg virus disease, 153f
  measles, 249f–250f
  meningococcemia, 252f
  mites, 284f
  molluscum contagiosum, 144f
  monkeypox, 146f
  onchocerciasis, 101f
  scabies, 285f–287f
  schistosomiasis, 131f
  scrub typhus, 27f
  smallpox, 145f–146f
  snake bite, 320f
  spider bite, 311f
  syphilis, 139f
  talaromycosis, 276f
  treponematoses, 159f–160f
  tuberculoid leprosy, 272f–273f
  vitamin A deficiency, 327f
  yaws, 159f
Skin-snip technique, 103f
Skull, bossing of, 337f
Skull MRI cranial tuberculosis, 266f
Slit-lamp examination, of eye, for onchocerciasis, 104f
Smallpox
  advanced hemorrhagic, 146f
  centrifugal development of, 145f
  residual scars ('pockmarks') of, 146f
Snakes, 316–321, 317t, 318f
Soil, infections acquired percutaneously from, 109–119
  bacterial, 109–111
  helminthic, 112–119
Solenopsis sp., 315f
Southern blue-ringed octopus, 305f
Sparganosis, 209–210, 210f
Spiders, 309–312, 311f
Spine, tuberculosis of, 265f
Spirometra, 209f
Spleen pathology
  congenital syphilis, 140f
  malaria, 44f, 48f–49f
  paracoccidioidomycosis
  schistosomiasis, 127f, 129f
  visceral leishmaniasis, 72f
Splenic rupture, in malaria, 44f
Splinter hemorrhages, 196f
Spondylitis, *Brucella*, 177f
Spondylodiscitis, psoas abscess and, 264f
Spontaneous systemic bleeding, after viper bite, 319f
'Sporotrichoid' dissemination, 82f
Sporotrichosis, 164f
  early lesions of, 164f
Spotted fever, 22t, 24–26, 24f
Sprue, tropical, 342f–343f
Sputum
  Mycobacterium tuberculosis in, 259f
  Streptococcus pneumoniae in, 251f
Squamous cell carcinoma, 335f
  anal, HIV infection and, 136t–137t
Stegomyia, 87f
Stings, 302–321
Stone fish, 307f
Streptococcus pneumoniae, 251f
  HIV infection and, 136t–137t
Streptococcus pyogenes, 255f
Streptococcus suis, subcutaneous hemorrhage due to, 177f
Strongyloides fülleborni, eggs of, 118f
Strongyloides stercoralis, 109
  disseminated infection
    hemorrhagic pneumonia in, 117f
    section of lung from a patient with, 118f
  eggs of, 119f
  life cycle of, 116f
  migrating larvae of, 117f
  rhabditiform larva of, 117f
  transmission of, 115f
Strongyloidiasis, distribution of, 115f
Subconjunctival petechial hemorrhages, 253f
Suicide rates, global, 341f
Sun protection, for albinism, 341f
'Swimmer's itch,' 131
Swollen belly sickness, 118f
Sydney funnel web spider, 309f
Synanceia horrida, 307f
Synanceia verrucosa, 307f
Syphilis
  congenital, 140f
  point of care lateral flow assay for, 140f
  primary chancre of, 138f
  secondary
    condylomata lata of, 139f
    corona veneris of, 139f
    extensive rash of, 139f

T

T cell lymphoma, HTLV-1 associated, 149f
Taenia crassiceps, 227f
Taenia saginata (beef tapeworm), 219–220, 219f–220f
Taenia solium (pork tapeworm), 215–219, 215f–218f
  proglottids of, 215f
Talaromyces marneffei, 276f
  in culture on Sabouraud agar, 277f
  HIV infection and, 136t–137t

Downloaded From Vet-eBooks.com

Talaromycosis, 276f
Talipes equinovarus, 339f
Tapeworms
  alveolar echinococcosis, 226–227
  diphyllobothriasis, 208–209
  Dipylidium caninum, 213–214
  Hymenolepis diminuta, 212
  Hymenolepis nana, 210–211
  sparganosis, 209–210
  Taenia saginata, 219–220
  Taenia solium, 215–219
Taping, for talipes equinovarus, 339f
Temperature chart
  brucellosis, 176f
  tick-borne relapsing fever, 34f
  typhoid, 170f
  visceral leishmaniasis, 72f
  yellow fever, 12f
Ternidens deminutus
  eggs of, 118f
  head capsule of adult, 118f
Terrestrial invertebrates, 308–316
Tetanus
  maternal, elimination of, progress towards, 110f
  neonatal, 109f
    elimination of, progress towards, 110f
  opisthotonos in, 110f
  risus sardonicus in, 110f
Thalassemia, 336f
  in skull, 337f
Thelazia callipaeda, 108f
Therapeutic food, for malnutrition, 325f
Thiamine deficiency, 328, 328f
Thoracic spine, of patient with Pott's disease, 265f
Thyreophagus entomophagus, 283f
Tick-borne relapsing fever, 33–34, 33f–34f
Tinea cruris, 161f
Tinea imbricata, 161f
Tityus serrulatus, 308f
Toxic megacolon, due to *Shigella dysenteriae*, 171f
Toxins, 302–321
  ingestion and susceptibility, 332, 332f
Toxocara canis, 197f–198f
Toxocariasis, 197–198
Toxoplasma gondii, 183f
  HIV infection and, 136t–137t
Trachoma
  active, 158f
  gradual slope towards blindness in, 157f
  trichiasis, 158f
Trachomatous scarring, 158f
Treatment centre, for Ebola virus disease, 151f
Trench fever, 288
Treponema carateum, as causative agent of pinta, 160f
Triatoma infestans, 61f
Tribolium confusum, 212f
Trichiasis, trachomatous, 158f
  corneal opacity in, 158f
Trichinella nativa, 196f
Trichinella spiralis, 195f
  larvae, 196f
Trichinellosis, 195–196
Trichinosis
  acute, 196f
  splinter hemorrhages and, 196f
  wild reservoir of, 195f
Trichomonas vaginalis
  cytoadherent amoeboid form of, 143f
  in vaginal discharge, 142f
Trichomoniasis, 142f
Trichophyton concentricum, tinea imbricata due to, 161f
Trichophyton rubrum, tinea cruris due to, 161f
Trichosporon sp., white piedra due to, 162f
Trichostrongylus
  adult male, 118f
  eggs of, 119f
Trichuriasis, 190–192
Trichuris trichiura, 190–192, 190f–192f
Trombiculid mites, 283
Trophozoite, 178f
  of *Acanthamoeba* sp., 122f
  of *Naegleria fowleri*, 121f
Tropical poison dart frog, 316f
Tropical pulmonary eosinophilia, chest radiograph of, 92f
Tropical splenomegaly syndrome, 48f
Tropical sprue, 342f–343f
Trypanosoma brucei gambiense, 54f, 56f–58f
Trypanosoma brucei rhodesiense, 54f, 56f–58f
Trypanosoma cruzi
  cerebral chagoma and, 67f
  HIV infection and, 136t–137t
  in human blood film, 63f
  life cycle of, 62f
  reservoir host of, 61f
Tsetse fly, 54f
Tuberculin skin test (TST), positive, 259f
Tuberculoid leprosy (TT), 269f
  borderline, 273f
  on buttock, lesion of, 272f
  loss of extremities in late, 273f
  nerve bundle in, 273f
  nerve thickening in, 273f
Tuberculomata, 267f
Tuberculosis (TB), 244–245, 256–268, 259f
  active, HIV prevalence in, 257f
  acute pulmonary, with cavitation, 261f
  base of brain, post-mortem appearance of, 267f
  of breast, 263f
  cerebral, 267f
  chest radiograph in miliary, 266f
  drug-resistant pulmonary, 261f
  global distribution of Gross National Income per capita, 258f
  incidence rates of, 257f
  multi-drug-resistant, 258f, 261f
  new, percentage of, 258f
  omental, 263f
  pathology of miliary, 266f
  peritoneal, 263f
  rifampicin-resistant, 258f
  skull MRI cranial, 266f
  of spine, 265f
  vertebral body destruction in, 265f
Tuberculous cervical lymphadenitis, 262f
Tuberculous chest wall collection, 263f
Tuberculous lymphadenitis, 333f
Tuberculous meningitis, 266f–267f
  cerebrospinal fluid, 267f
Tuberculous pericarditis, 262f
Tuberculous psoas abscess., 264f
Tuberculous supraclavicular abscess, aspiration of, 262f
Tularemia, 32, 32f
Tumbu fly
  lesions, 297f. *see also Cordylobia anthropophaga*
Tunga penetrans, 292f–293f
Tunga trimamillata, 293f
Tungiasis, 282
Twins, measles in, 249f
Type 1 reversal reaction, 274f
Type 2 reversal reaction, 274f
Typhoid, temperature chart in, 170f
Typhus, 22t, 23–24

U

Ulcerative gingivostomatitis, HSV-1 and, 143f
Ulcers
  Buruli, 154f
    contractures from, 154f
    plaque, 154f
  Chiclero's, 82f
  corneal, 327f
  cutaneous diphtheria, 255f
  genital, of chancroid, 137f
  leishmaniasis, 78f
  of Peyer's patches, 170f

Downloaded From Vet-eBooks.com

Ulnar nerve, in tuberculoid leprosy, 272f
Unilateral pleural effusion, 262f
Urethral discharge, in gonorrhea, 140f
Urine, blackwater fever, 43f
Uveitis, HTLV-1 associated, 149f

V

Vaccination, of dogs, 147f
Vampire bat bites, 148f
Varicella zoster virus (VZV), 250–251, 250f
  disseminated, 250f
  HIV infection and, 136t–137t
  pneumonitis, 251f
Vasculitis, in hepatitis C infection, 145f
Venoms, 302–321
Verruga peruana, 28f
Vertebral body destruction, in tuberculosis, 265f
Vertebrates, marine, 306–307
Vespa affinis, 315f
Vespa mandarinia, 315f
Vespa orientalis, 315f
Vibrios, 174f
Viperidae, 317t, 319f
Viral infections
  of gastrointestinal tract, 165–169
  from sex, 132–135
Visceral leishmaniasis, 71–75
  direct agglutination test for, 75f
  distribution of, 71f
  endemic area with, 71f–72f
  HIV and, 73f
  infantile, 72f
  K39 rapid diagnostic test for, 75f
  purpura in, 73f
  reservoir of, 72f
Vitamin A deficiency, 326–327, 326f–327f
Vitamin B1 (thiamine) deficiency, 328, 328f
Vitamin B2 (riboflavin) deficiency, 328, 328f
Vitamin B3 (niacin) deficiency, 328–329, 329f
Vitamin C deficiency, 329, 329f
Vitamin D deficiency, 330, 330f
Viverra civetta, 239f

W

Water
  filtration of, 206f
  infections acquired percutaneously from, 120–131
    bacterial, 120–121
    helminth, 123–131
    protozoal, 121–123
Water caltrop, 228f
Watercress, 235f
Weever fish, 307f
West Nile virus, 5, 6t, 15–18, 15f–16f
'Wet' beri beri, 328f
Wheelchair, 339f
White plaques, of oral candidiasis, 160f
Whole-blood clotting test, 321f
Whooping cough, subconjunctival hemorrhage in, 253f
Winterbottom's sign, 57f
Wohlfahrtia species, 299f
World Food Programme, 322
Wuchereria bancrofti, 84t–85t, 92f, 107f
  in blood vessel, 89f
  female, 89f
  life cycle of, 88f
  male, 89f

X

X-rays, tropical sprue, 342f
Xenodiagnosis, 67f
Xenopsylla cheopis, 29f–30f
Xerophthalmia, 326f

Y

Yambuku, 150f
Yaws, 159f
Yellow fever, 5, 6t, 11–12, 11f–12f

Z

Ziehl-Neelsen stain, 259f, 267f, 269f, 271f
Zika virus, 13–14, 13f–14f

Downloaded From Vet-eBooks.com